Simulation of Smoke Contamination in Upper Balcony by a Channelled Balcony Spill Plume in an Atrium

by

Chee Leong Ho

Supervised by

Dr Michael Spearpoint
Dr Kai Yuan Li

Fire Engineering Research Report 10/8
2010

A thesis submitted in partial fulfillment of the requirements for the degree of Master of Engineering in Fire Engineering

Department of Civil Engineering
University of Canterbury
Private Bag 4800
Christchurch, New Zealand

ABSTRACT

This research project has studied commercial building atrium upper balcony smoke contamination due to a balcony spill plume using computational fluid dynamics (CFD) software, Fire Dynamics Simulator (FDS) version 5.0. Simulation prediction on temperature and smoke contamination on small-scale model balcony configuration are compared with earlier researchers' work, Tan (2009) and Harrison (2009), who conducted a one-tenth small-scale experiment. Twelve experiments are selected for simulation.

Most of the temperature predictions are relatively within the range of the experiment's records. It is found that 10°C above ambient temperature (20°C ambient) slice files from FDS are also relatively matched to the photographic records of the experiment for smoke contamination. Hence, this shows that these FDS models are able to predict upper balcony smoke contamination fairly accurately.

Subsequently, the FDS small-scale models are extended to small and full-scale five balcony configuration, full-scale five balcony configuration without upstand and a seven balcony configuration for smoke contamination assessment. Full-scale fire size is up to 4.7MW, which is for sprinklered shop fire.

This study shows that full-scale configuration will have higher temperature within the balcony and more severe smoke contamination when compared to the small-scale model. The predictions are also highly sensitive to the boundary conditions.

This study also demonstrated that the upper balcony smoke contamination is also affected by the height of the atrium. Taller atria will have more severe smoke contamination on the lower balcony.

Finally, a new correlation is developed for the three to seven balcony with upstand configuration; this correlation has incorporated the atrium height parameter into the equation. This correlation will allow the designer to make the first order of assessment on upper balcony smoke contamination due to balcony spill plume.

ACKNOWLEDGEMENTS

I would like to thank my project supervisors Dr. Michael Spearpoint and Dr. Kai Yuan Li for their meticulous guidance throughout the course and research project. Both of them have shaped my perspective and fundamental understanding on small-scale experiment and FDS modelling.

Associate Professor Charley Fleischmann for engineering guidance during the course and sharing of personal invaluable experience in bringing up of children.

My family for their support in spending twelve months together with me in New Zealand.

Our good friends Mark and Clare with their family who have taken excellent care and support of my family during our stay in New Zealand.

My course mates Di, Jenny, Kevin, Marco, Peter and Tim for their company and mutual support during the course, especially Marco during the entire hot and quiet summer holidays at the university.

My course seniors Long and Fabian for their advice.

Last of all, I would like to thank the New Zealand Fire Service Commission for supporting the MEFE programme.

TABLE OF CONTENTS

LIST OF FIGURES

LIST OF TABLES

NOMENCLATURE

Symbol	Description
b	Balcony breadth (m)
C_d	Effective coefficient of discharge at opening
C_e	Constant for geometry
C_p	Specific heat (kJ/kgK) = 1.0kJ/kgK for ambient condition
D^*	Characteristic plume dimension (m)
d	Depth of smoke layer at the spill edge (m)
d_e	Depth of smoke layer below bottom of exhaust inlet (m)
f	Mass fraction (kg/kg)
g	Acceleration due to gravity (m/s^2)
H	Height of smoke contamination (m)
h	Height of the top of the opening above the floor (m)
L	Characteristic length of scale model (m)
$\dot{M}$	Mass flow rate (kg/s)
m_{max}	Maximum rate of exhaust without plugholing (kg/s)
n	Wall heat transfer function
P	Perimeter of fire (m)
$\dot{Q}$	Total heat release rate (kW)
$\dot{Q}_c$	Convective heat flow in the gas layer below the spill edge (kW)
T	Absolute gas temperature (K)

t	Time (sec)
u	Average velocity of smoke layer beneath edge of balcony (m/s)
$\dot{V}$	Volumetric flow rate (m^3/s)
w	Width of compartment opening or width of line plume (m)
z	Height of rise of plume from spill edge (m)
z^*	Characteristic length of modelling (m)
δx	Grid dimension in x-axis (m)
δy	Grid dimension in y-axis (m)
δz	Grid dimension in z-axis (m)
ΔP	Differential pressure (Pa)

Greek symbol	**Description**
β	Exhaust location factor (dimensionless)
θ	Temperature above ambient (°C) = 20°C
ρ	Density (kg/m^3) = 1.2 kg/m^3 for ambient condition

List of subscript	**Description**
3D	Three-dimensional spill plume
CO	Carbon monoxide
o	Ambient
p	Plume
s	Smoke

soot	Soot
spill	A property of a spill plume
trans	Transition in the rate of entrainment from a balcony spill plume to axi-symmetric

1. INTRODUCTION

It is common nowadays for atria to be openly connected to other levels through balcony in commercial shopping centre, hotel lobbies and office buildings. A typical atrium connected with five balconies of a shopping area is shown in Figure 1. Figure 2 shows the various forms of atria in building. The most critical of all the technical issues to be solved in a successful atrium design is life safety because atrium buildings break with orthodox concepts of fire safety (Gritch and Eason, 2009). The traditional ways of designing fire safe buildings use horizontal compartmentation and vertical separation of spaces (ECE, 2000). Gritch and Eason (2009) mentioned that the fire record has shown that smoke is the primary threat to life from fire in a building and proper smoke control in an atrium building is an absolute requirement. They also commented that the most comprehensive method of determining complex smoke management criteria is with computer fire modelling.

Morgan *et al* (1999) defines smoke as "liquid and /or solid particulates produced by combustion of fuel materials, suspended in a mixture of air and gaseous products of combustion, including steam" and gaseous combustion products usually include toxic gases. Smoke also lead to reduction in visibility, which will hamper evacuation, rescuing of disabled or injured occupants and the fire fighting operation.

Figure 1. Funan Shopping Centre in Singapore.

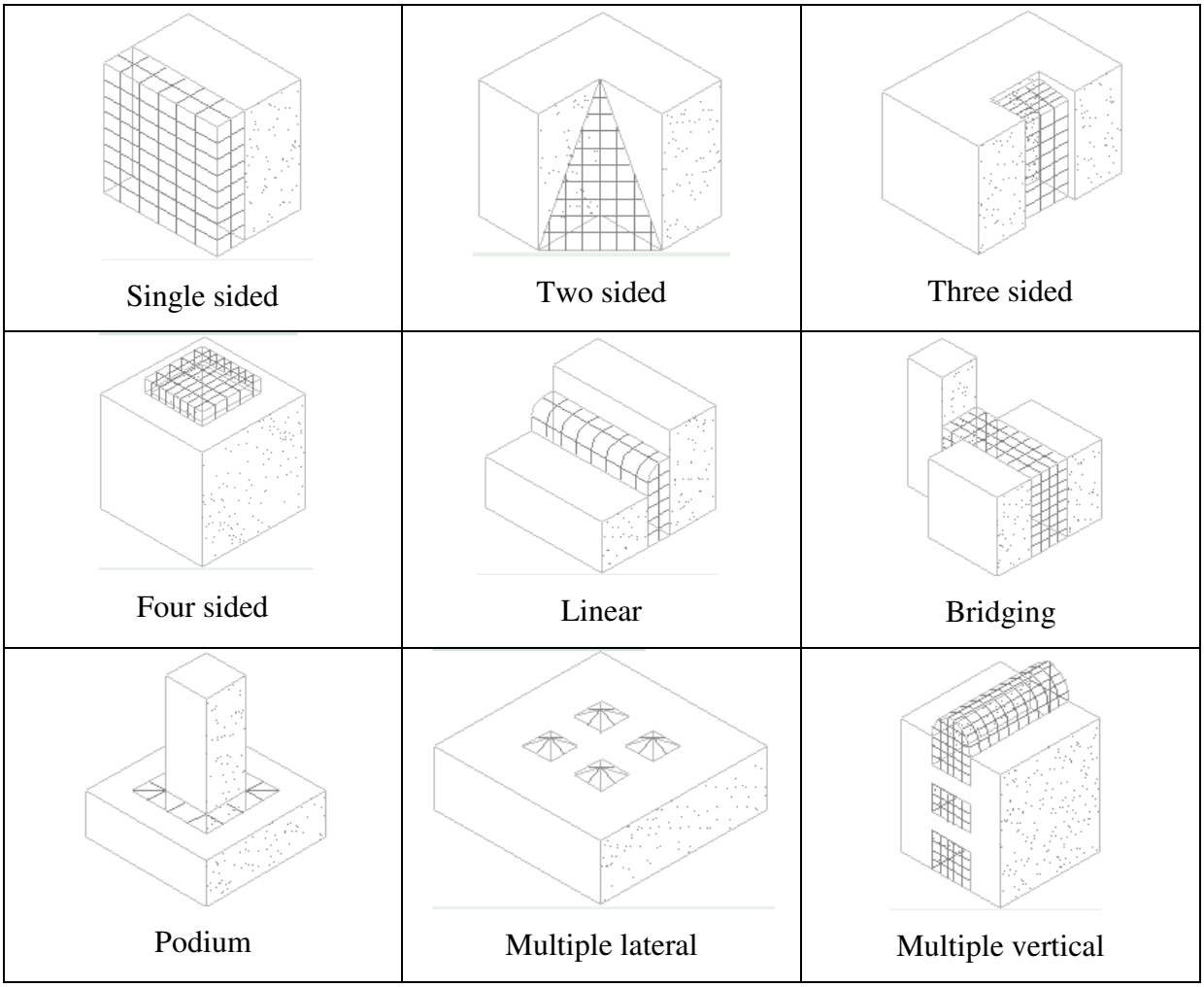

Figure 2. Various configuration of atrium space (Gritch and Eason, 2009)

1.1 Fire Location & Type of Smoke Plume in Atrium

Klote and Milke (2002) mentioned that depending on fire location in an atrium, it could result in different fire plumes. Fire in the atrium space could produce an axi-symmetric plume while fire in a space open to an atrium could produce a balcony spill plume. They further mentioned that North America usually designed for fire in atriums while Australia, United Kingdom (UK) and Europe usually designed for fire in spaces open to the atrium such as shops and offices.

Morgan *et al* (1999) mentioned that for a multi-storey shopping centre connected to an open atrium, the design of the smoke control system must be considered on a floor-by-floor basis. In general, the worst condition to be catered for an atrium fire was in an adjacent room on the lowest level, as this results in the most entrainment in the rising plume and hence the largest quantity of smoky gas entering the buoyant layer.

Lougheed (2000a) also stated that balcony spill plume could result in considerable air entrainment into the smoke flow, leading to high smoke production even for small fire.

Klote (2008) explained that for axi-symmetric plume, air is entrained into the plume from all sides and along the entire height of the plume. A balcony spill plume entrains air as it flows under and around the balcony and rises above the balcony. The balcony spill plume mass flow rate depends on the size of the fire, dimension of the balcony and the distance from the balcony edge to the smoke layer interface.

Harrison (2009) further explained there were two types of plume beyond the spill edge. When the plume could sufficiently project beyond any bounding walls (see Figure 3a), entrainment would occur on the full surface of the plume, which was referred to as balcony spill plume. When the plume nearer to the atrium was attached to it, it was referred as adhered spill plume (see Figure 3b). Adhered spill plume entrain less air than balcony spill plume as less surface area is involved.

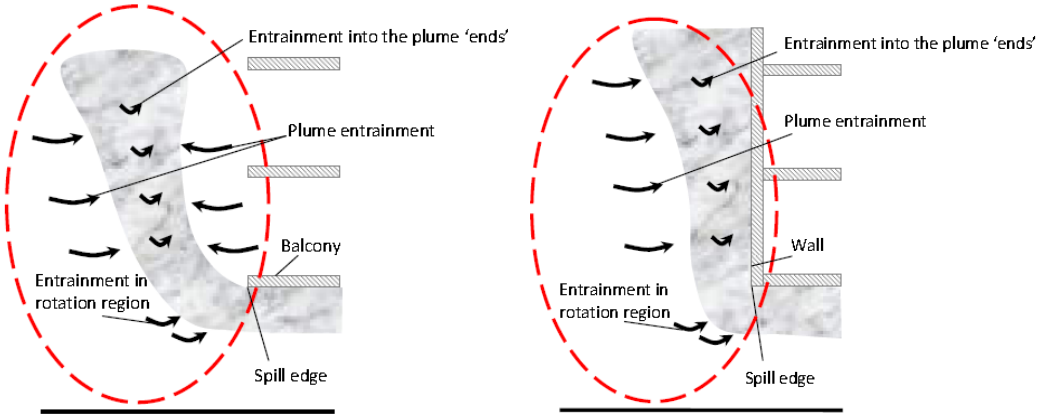

a. Balcony Spill Plume b. Adhered Spill Plume

Figure 3. Type of spill plume (Harrison, 2009).

1.2 Fire Size in Atrium

Law (1995a) reviewed the use of a 5MW fire size used in sprinklered shopping centres. Law concluded that statistical data indicated such a fire was likely to occur in less than 5% of fires in sprinklered shops, even in storage areas where stacked goods were more common than in the public areas. Where sprinklers operated, Law (1995a) assessment was heat output would unlikely to be sustained at 5MW. NFPA 92B (2009) further elaborated that the shop

mentioned by Law (1995a) has been described as 3.1m by 3.1m, resulting in an approximate heat release rate per unit area of 568 kW/m^2. Hence, fire assessment in shopping centres normally caps the most credible heat release rate at 5MW.

Chow (1999) mentioned that fire load density in an atrium was unlikely to be high, apart from using the atrium space for furniture exhibitions and there was more likely to be a fire in the retail shop in zone adjacent to the atrium.

Lougheed (2000a) suggested the most common approaches to the design of atrium smoke management systems assumes a steady-state design fire as shown in Table 1. The assumption being that the fire would only grow to a certain size because sprinklers were present to control the fire.

Fuel Loading	**Design Fire (MW)**
Low (minimum fire for fuel-restricted atrium)	2
Typical (minimum fire for atrium with combustibles)	5
High (large fire)	25

Table 1. Steady-state design fires for atria (Lougheed, 2000a).

Lougheed (2000a) also mentioned that most atrium smoke management systems assume a steady-state design fire as a system designed to deal with this fire would also be able to handle the fire as it grew.

Klote (2008) highlighted designers should not make the mistake of assumption that an atrium with almost no materials should have a very small design fire as there could be changes in space use or transient fuels. These fuels include holiday decorations, cardboard boxes waiting removal and upholstered furniture.

Morgan *et al* (1999) stated the steady state design fire for retail areas are 5MW and 2.5MW when the retails areas are fixed with standard response and quick response sprinklers respectively. The heat release rate density for both type of sprinkler is 625 kW/m^2.

1.3 North American Atrium Smoke Management

Ferreira (2008) provided an overall development history of atrium smoke management in America (NFPA 92B). In 1991, NFPA 92B introduced exhaust type systems to prescribe the maintenance of the smoke layer interface at a specified height in large-volume space. In 2005, NFPA 92B prescribed the smoke control system to maintain minimum smoke tenability levels rather than a prescribed smoke layer interface height. Hence, Ferreira (2008) commented that the use of CFD to analyse these types of systems became not only desirable, but in many cases necessary for tenability assessment.

Lougheed (2000b) explained that the National Building Code of Canada 1995 required "draft stops" to be installed at each floor level, immediately adjacent to and surrounding the opening to provide a smoke reservoir at the ceiling so that smoke can be detected. The minimum height of draft stop is 500mm, measured from the ceiling level to the bottom of the stop as shown in Figure 4. Lougheed (2000b) also commented the greater the opening between the atrium space and the adjacent spaces, the greater the possibility of smoke from a fire spreading through the atrium to other parts of the building. The complexity of the smoke management system design was directly related to the degree of interconnection of the spaces.

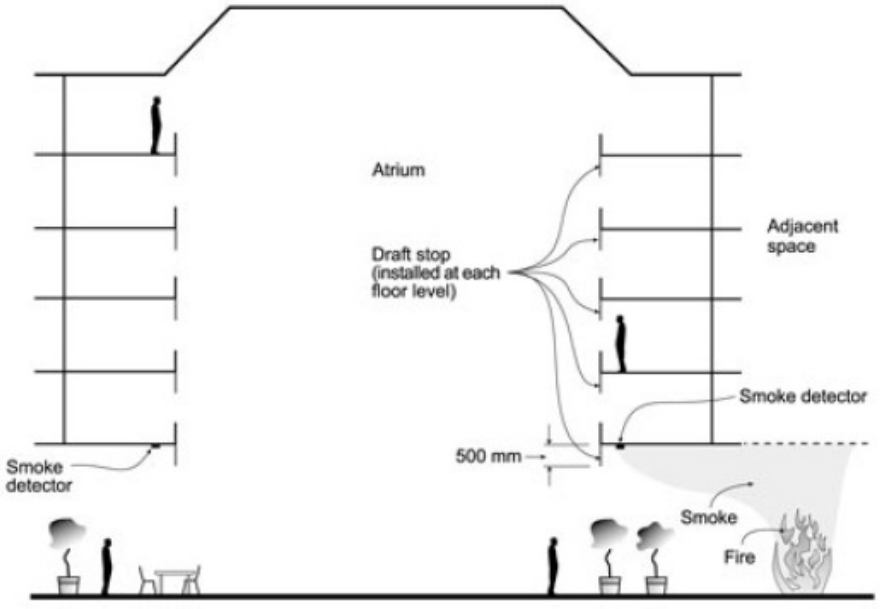

Figure 4. Atrium space with draft stop required by National Building Code of Canada (Lougheed, 2000b).

1.4 Smoke & Human Interaction

Klote (2009) has mentioned that most smoke management approaches were based on the idea that occupants need to be kept away from smoke. However, Klote (2009) added that NFPA 92B allowed a design system that provide tenable environment for occupants during evacuation, with some occupants coming in contact with diluted smoke.

Lougheed (2000a) reported that most engineers were reluctant to design systems that could expose occupants to any smoke at all for atrium smoke control. Lougheed suggested for complex atrium designs, numerical fire models might be required to assess the ability of the smoke management system to meet design objectives.

Harrison and Spearpoint (2005) suggested a smoke control system usually maintained the base of the smoke layer to remain above a pre-determined height, which is usually 2.5m above the highest floor open to the atrium. Morgan *et al* (1999) has provided the following possible requirement (see Table 2) for minimum clear height above escape routes.

Type of Building	Minimum Height (m)
Public buildings (e.g. single-storey malls, exhibition halls)	3.0
Non-public building (e.g. offices, apartments, prisons)	2.5
Car park	Smaller of 2.5m or 0.8 times ceiling height
Notes: These height apply to single-storey situations. Where smoke must rise through another storey before reaching the final smoke reservoir, it is usual to add another 0.5m to each value.	

Table 2. Minimum clear height above escape routes (Morgan *et al*, 1999).

1.5 Smoke Management System in Atrium from Adjacent Space Fire

Basically, there are two types of smoke management system (ECE, 2000) for atria which are as follows:

a. Smoke control on the floor of fire origin
b. Smoke ventilation within the atrium

Smoke control on the floor of fire origin could be achieved by a dedicated local smoke exhaust system with a downstand barrier at the atrium connection as shown in Figure 5a. Figure 5b shows a high-powered exhaust slot at the spill edge to extract the smoke without letting the smoke spill beyond the room. When there is balcony space for circulation, the space can be used as a smoke reservoir with a smoke screen around the balcony perimeter to prevent the smoke flowing into the atrium.

When the boundary between the room and the atrium is both imperforate and fire resisting, the solution is known as "sterile tube"; such design is often not favoured by designers due to restrictions on the atrium design and the use of atrium (Lougheed, 2000b).

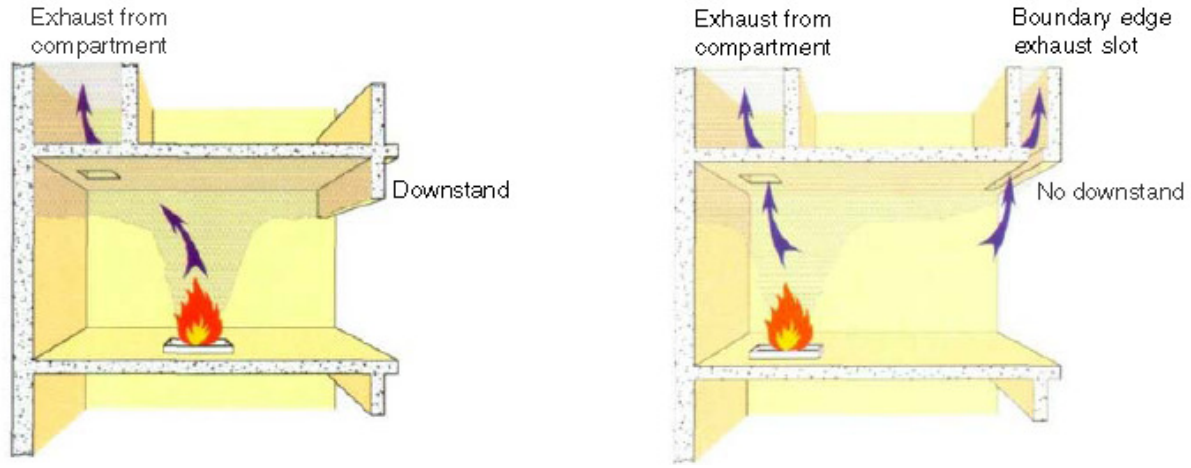

(a) (b)

Figure 5. Smoke control on the floor at the fire origin (Morgan *et al*, 1999).

Smoke ventilation within the atrium (as shown in Figure 6) was used when the smoke and heat could not be confined and removed from the room of origin. When smoke flows into the atrium, it will entrain air and increase in mass flow rate as it rises. A channelling screen could be used to channel the smoke the smoke into the atrium. Un-channelled or un-restricted smoke flow under a balcony would allow it to flow sideways towards the balcony and rise into the atrium space as a long line plume. Figure 7a and Figure 7b show un-channelled and channelled flow respectively. Such long line plume would have large air entrainment and resulted in large mass flow rate. This could lead to cooling of the smoke and reduce its buoyancy; this would also increase the likelihood of smoke contamination of the upper storey balconies. Figure 6 shows a combination of smoke management systems in building.

Morgan *et al* (1999) also mentioned that a channelling screen is commonly used to guide the smoke from the exit of the room to the balcony edge to reduce excessive entrainment. The depth of the channelling screen is dependent on the channel width and mass flow rate of smoke entering the smoke layer. For a 5MW fire, the screen depth could vary from one to six metres for a channel width of 4m to 12m for mass flow rate entering the smoke layer up to 200kg/s.

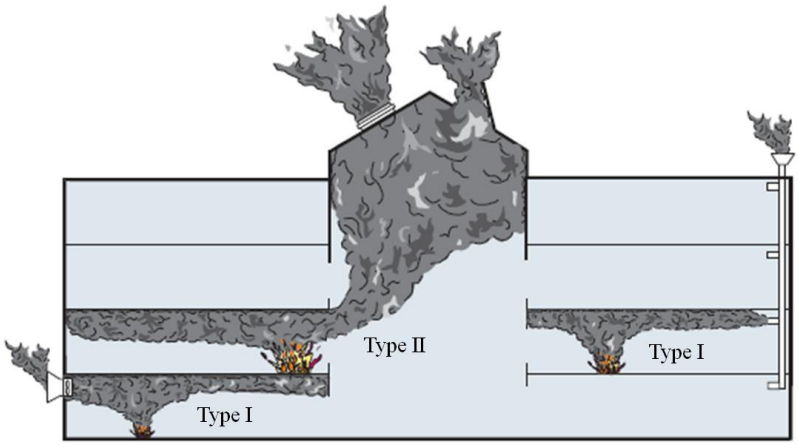

Figure 6. Combination of smoke management system in a building (Colt, 2007).

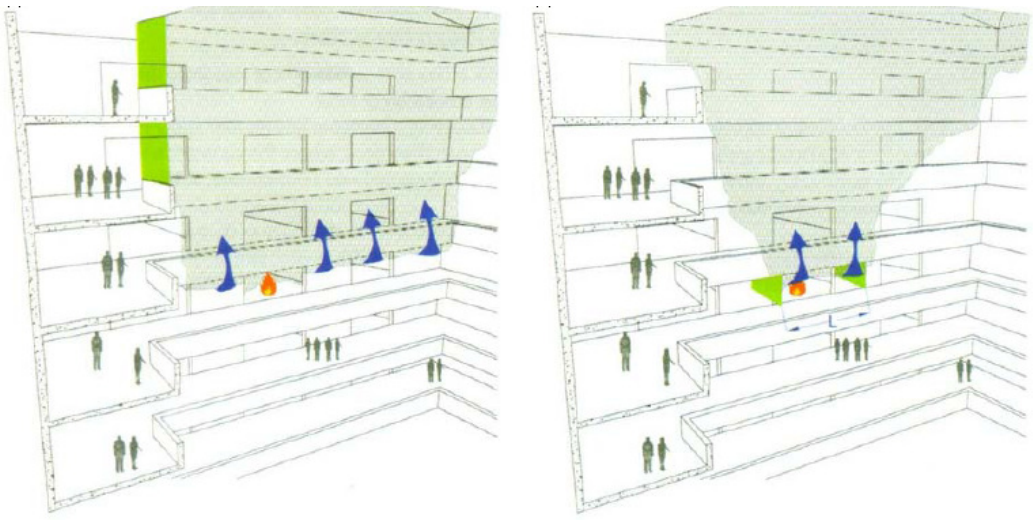

(a) Un-channelled flow (b) Channelled flow.

Figure 7. Smoke ventilation within an atrium (Morgan *et al*, 1999).

1.6 Practical Smoke Extraction Rate

Morgan *et al* (1999) suggested their experience found that a mass flow larger than 150 to 200kg/s was the limitation to the use of throughflow ventilation; this was economically impractical in terms of a smoke control system.

1.7 Upper Balcony Smoke Contamination from Balcony Spill Plume

Smoke management in atrium focus on removing the smoke from the atrium and avoid personnel coming into contact with the smoke. One of the concerns is that smoke may curl into the balconies from balcony spill plume as shown in Figure 8. Morgan *et al* (1999) mention that a balcony which was less than 2m would cause the rising plume to curl inwards towards the structure.

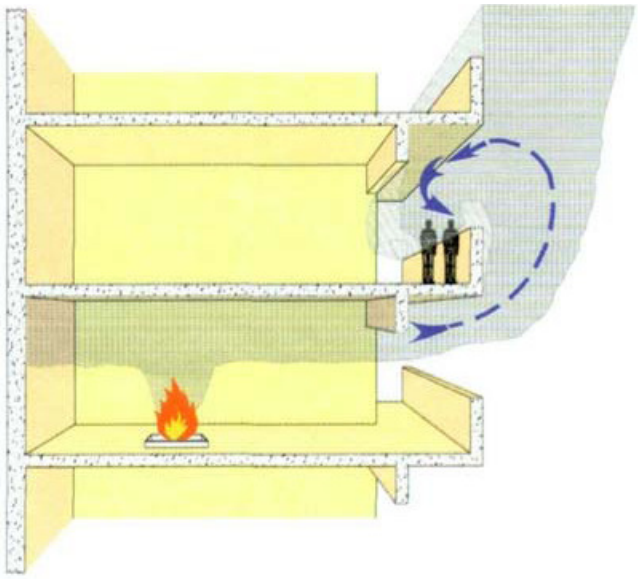

Figure 8. Smoke curl inwards on the above balcony (Morgan *et al*, 1999).

NFPA 92B (2009) does not specifically address the smoke contamination of an upper storey balcony. It mentions (clause 4.4.2.1) that to manage smoke spread to communicating spaces that connect to atrium, it is possible to provide a barrier to transform a communicating space into a separated space. An alternate method was to provide an opposed airflow through the opening to prohibit smoke spread into the communicating space as shown in Figure 9.

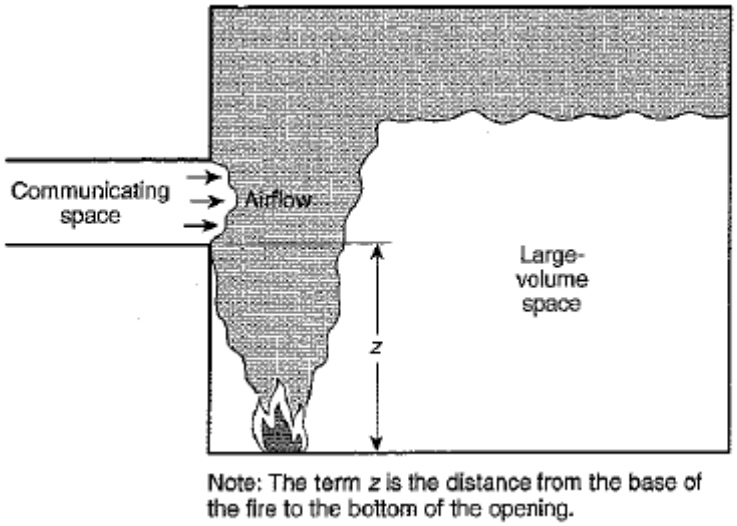

Figure 9. Use of airflow to prevent smoke propagation (NFPA 92B, 2009).

There has been limited research to determine the likelihood of smoke contamination on the upper balcony due to balcony spill plume. Tan (2009) studied upper balcony contamination due to spill plume by using a physical scale model at the University of Canterbury and systematically varied the balcony breadth, opening size and fire size. Tan (2009) developed an empirical correlation for designer to assess smoke contamination.

1.8 Use of CFD for Balcony Spill Plume

Morgan *et al* (1999) mentioned since the mid-1970s computational fluid dynamic (CFD) models have been developed to deduce how and at what rate smoke could fill an enclosure. The use of CFD solves the smoke movement using first principles to solve the basic laws of fluid flow and thermodynamics and can avoid the need to resort to experimental correlation during design. They highlighted the importance of prescribing appropriate boundary conditions, appropriateness of sub models used (heat transfer, radiation and turbulence) and adequate grid size for CFD modelling.

Lougheed (2000a) also mentioned that modern buildings with multiple atria and interconnected communication spaces or very large open space are often too complex for the use of empirical equations and zone models. For such buildings, numerical modelling such as CFD could allow detailed examination of smoke movement in the atrium.

1.9 Research Objective

The plan is to continue previous work by Tan (2009) in the upper balcony smoke contamination and conduct simulation analysis for full scale modelling with channelled balcony spill plume.

The aims of the research are as follows :

a. To verify FDS could model the experiment conducted by Tan (2009).

b. To determine the boundary effects on the smoke contamination in the upper balconies.

c. To extend and update Tan's (2009) balcony contamination correlation model for full-scale up to a five balcony configuration or the technical limitation of the computing resources.

d. To provide fire engineers a smoke contamination assessment model for upper balconies to use in commercial shopping centre buildings with large atria.

2. LITERATURE REVIEW

As previously noted in Section 1.1, plumes in atria might typically be axi-symmetric or balcony. Considerable work on axi-symmetric plumes has been undertaken by other researchers but will not be considered here. The literature review focus on study of balcony spill plume contamination on upper balconies by experiment and CFD modelling.

2.1 Balcony Spill Plume Contamination on Upper Balconies

Hansell *et al* (1993) pioneered the investigation of spill plume contamination of upper storey balconies using a one-tenth scale model atrium (see Figure 10) and the equivalent balcony breadths were 1.25m, 2.5m and 5m. There was no downstand from the room. Their findings were the extent of smoke contamination above the balcony was dependent on the balcony breadth and the result for channelled flow is shown in Table 3 and Figure 11. These results were adopted in the Design Methodologies for Smoke and Heat Exhaust Ventilation by Morgan *et al* (1999). This design document is a widely adopted design guide for smoke control in atrium and it recommends that balcony breadths wider than 2m would allow the plume to rise through the atrium space as a free plume. Hansell *et al* findings were as follows:

a. Found no plume reattachment to balcony breadth equivalent to 2.5m and 5.0m. They believed re-attachment to the wall was more likely as plumes widened.

b. A balcony narrower than 2m would likely become smoke-logged between the plume and the wall. Smoke logging on higher balconies would be more extensive.

c. The height at which the thermal plume contacted the wall increased with both decreasing length of plume and increasing heat release.

Law (1995b) reanalysed Hansell *et al*'s (1993) experimental data to develop a simple entrainment formula for balcony spill plume. The heat release in the scale model ranged from about 4kW to 15kW. The opening width and height were 0.4m and with channels at the opening. The balcony was 0.535m above the atrium floor, in other words, 0.135m above the spill edge. Law concluded that for 0.25m and 0.5m (equivalent to full size 2.5m and 5m) breadth balcony, there was balcony spill plume. A balcony with 0.125m (full size of 1.25m) breadth would have the plume attached to the wall above the balcony (adhered plume).

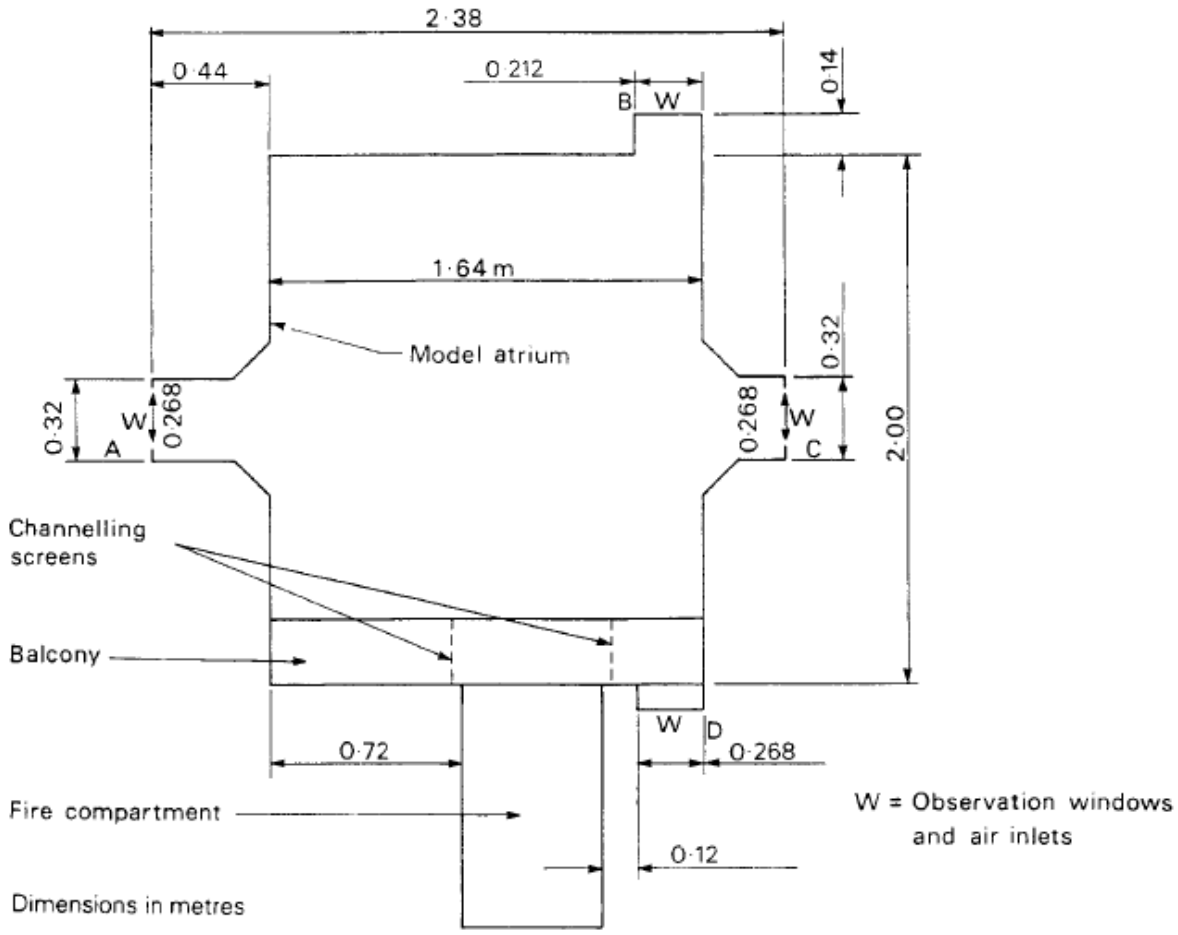

Figure 10. Plan of model atrium and fire compartment (Hansell *et al*, 1993).

Heat Flow (kW)	Balcony Breadth (m)	Channel Screen Separation (m)	Attachment Height (m)
2.9	0.125	0.525	0.25 to 0.3
6.0	0.125	0.525	0.6 to 0.7
8.2	0.125	0.525	0.9 to 1.0

Table 3. Plume re-attachment height for channelled screen experiment (Hansell *et al*, 1993).

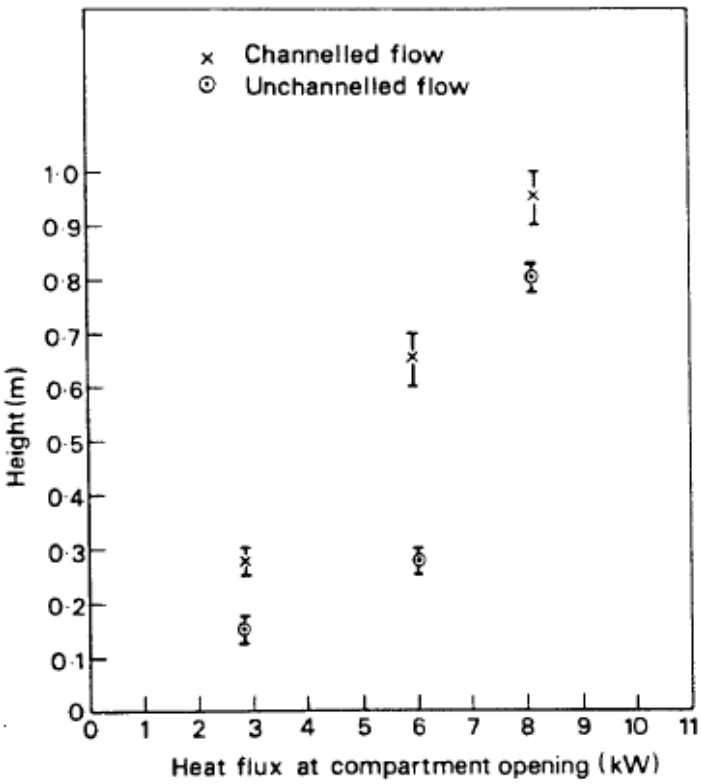

Figure 11. Above-balcony attachment height for plumes with 0.125m balcony (Hansell *et al*, 1993).

Cox (1995) has also explained that the effect of rising spill plume on the side nearest to the atrium structure caused the static pressure to fall in the region between the spill plume and atrium structure. This low pressure region could cause the spill plume to curl toward the atrium structure and contaminate the upper balcony as shown in Figure 12; this was generally known as Coanda effect. Cox (1995) mentioned how the heat transfer effect that was present when a window jet reattached to the wall above its source could have a dramatic effect on the spreading of a fire. The reattached flow could cause the windows above the floor of the fire origin to break and hot gas could enter the upper floor through this opening and ignite the floor above the fire, such as the Los Angeles Interstate Bank Building fire in 1989. Buildings with complete glass side walls or when the face of the building was made of combustible materials were particularly vulnerable to this fire spread mechanism.

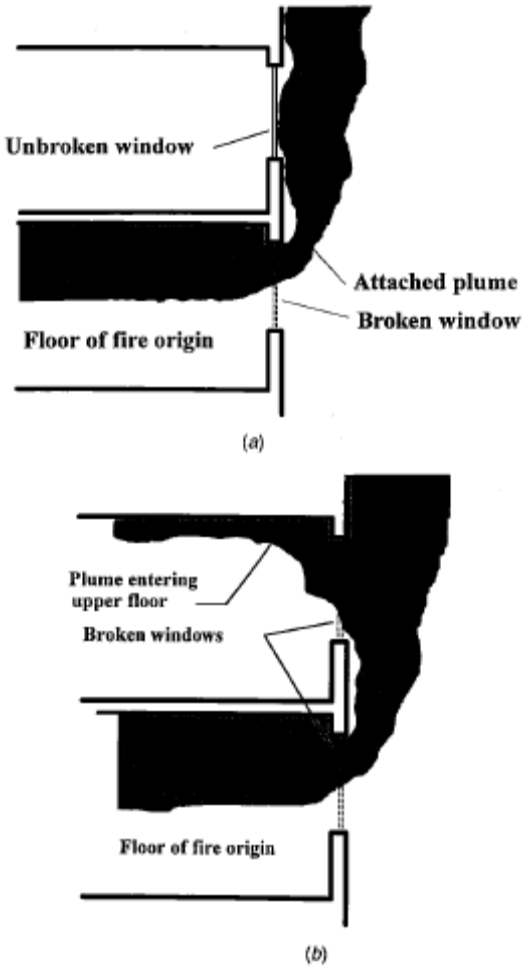

Figure 12. Plume before window was broken and (b) after window was broken (Cox, 1995).

Yii (1998) carried out a study of spill plumes using salt water modelling and Laser Induced Fluorescence (LIF) flow visualisation techniques. The experiment is shown in Figure 13 and Yii (1998) studied a single storey balcony with channelled flow. The figure shows a soffit (or downstand) at the "fire room" opening. The experiment was carried out using a $1/20^{th}$ scale model and the equivalent balcony widths were 2.5m and 5.0m. One of Yii's findings was smoke logging on an upper balcony was found to be more severe for a short breadth (2.5m) balcony compared to a long breath (5.0m) balcony as shown in Figure 14. Due to the experiment limitation, the equivalent fire size was not able to be determined. Yii (1998) concluded the salt water modelling could provide good flow visualisation.

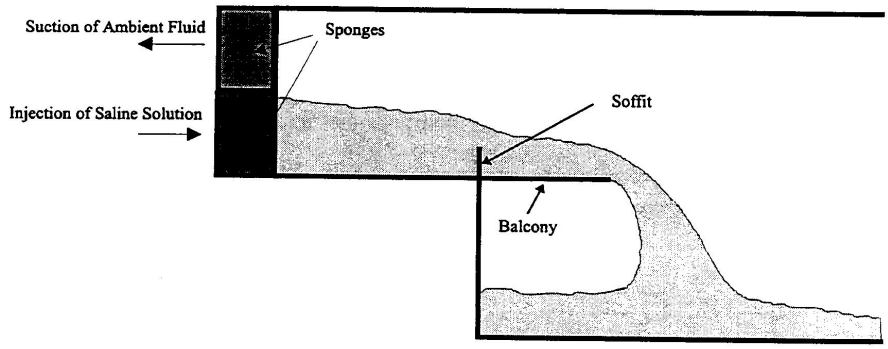

Figure 13. Generating "smoke layer" using saline solution (Yii, 1998).

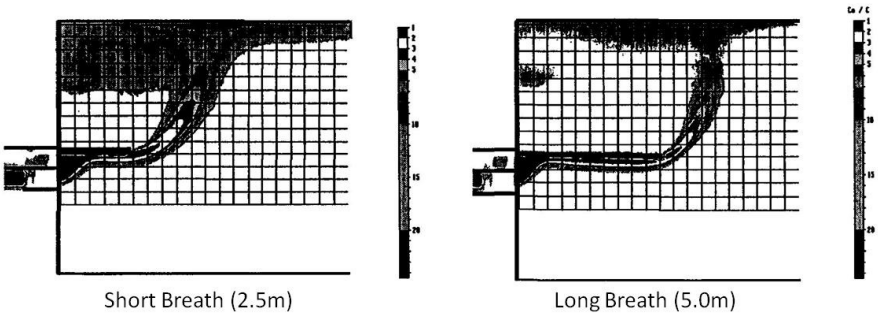

Figure 14. Flow image plots for short and long breath balcony (Yii, 1998).

Poreh *et at* (2008) conducted experiments to study how smoke flowed from fire room into a long corridor and then spill into a tall hall. The smoke in the hall adhered to the wall. Their experiment findings showed that when the Froude number of the horizontal layer was larger than 1, the rising plume would not adhere immediately to the wall of the hall as the flow from the horizontal layer was supercritical. An adhered plume very likely would cause upper storey balcony contamination.

Harrison (2004) found that the presence of downstand at the spill edge could cause plume leaving the fire compartment to rise vertically from the opening. Harrison (2004) believed such behaviour had significant implications for smoke logging on higher storey due to partial impingement of the plume with the upper balconies.

Harrison (2009) did his experiments on entrainment of air into thermal spill plumes using the configuration as shown in Figure 15. As shown in Figure 15, the model balcony breadth was 0.3m. Harrison's (2009) objective was to characterise thermal spill plume entrainment by conducting about 180 experiments. His findings showed that the entrainment was dependent

on gas flow below the spill edge, particularly in terms of the width and depth of the flow. In all his experiments Reynolds numbers ranged from 8100 to 20400, which exceeded the minimum turbulent requirement of 4000 for scale modelling. Figure 16 to Figure 18 shows the plume behaviour generated from a wide, intermediate and narrow width of compartment from Harrison's (2009) experiment. Harrison (2009) found that when the width of compartment opening decreases (and also when the fire size increases) the amount of horizontal projection and the breadth of the ends of the plume tended to increase. Harrison (2009) explained that this was most likely due to the increased amount of end entrainment occurring in the plume.

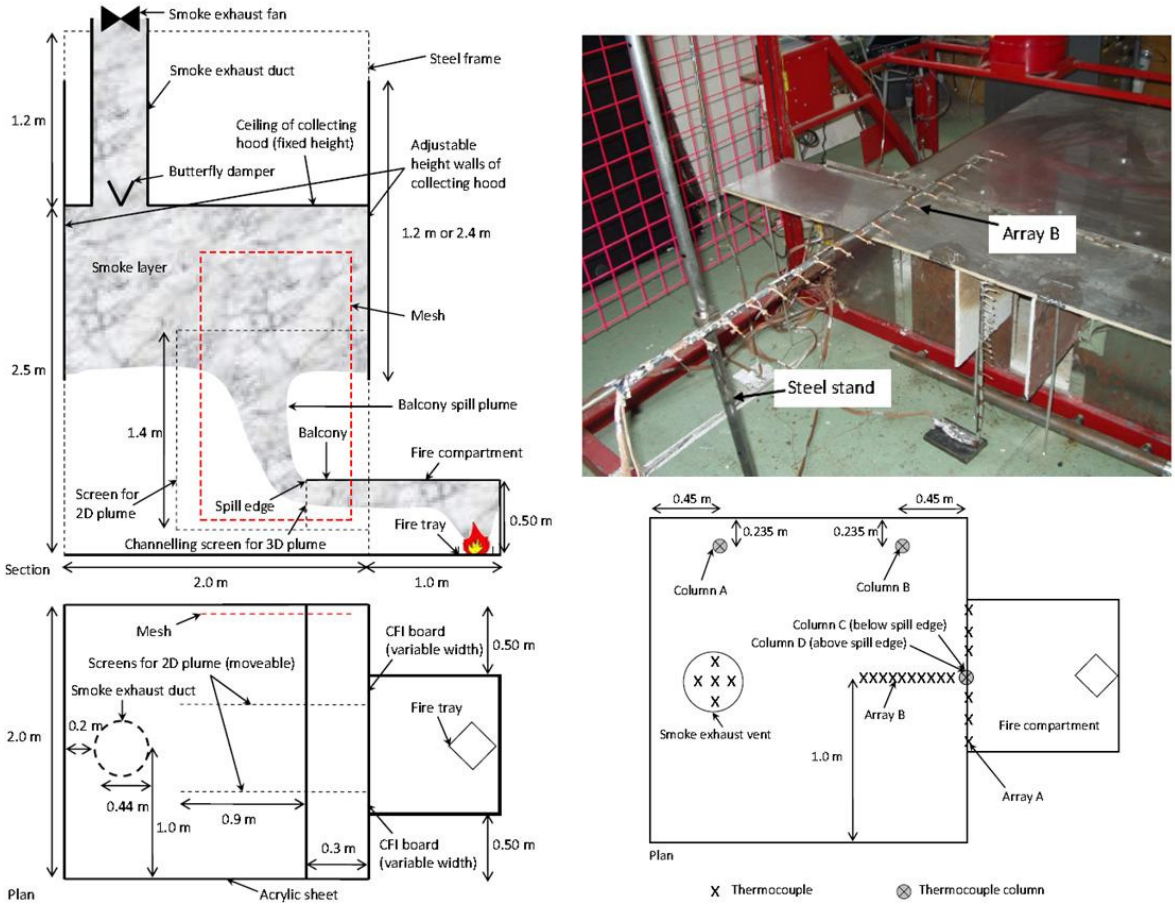

Figure 15. Harrison's experiment setup (Harrison, 2009).

a) Side view b) Front view

Figure 16. Plume behaviour for width of opening = 1.0m (Harrison, 2009).

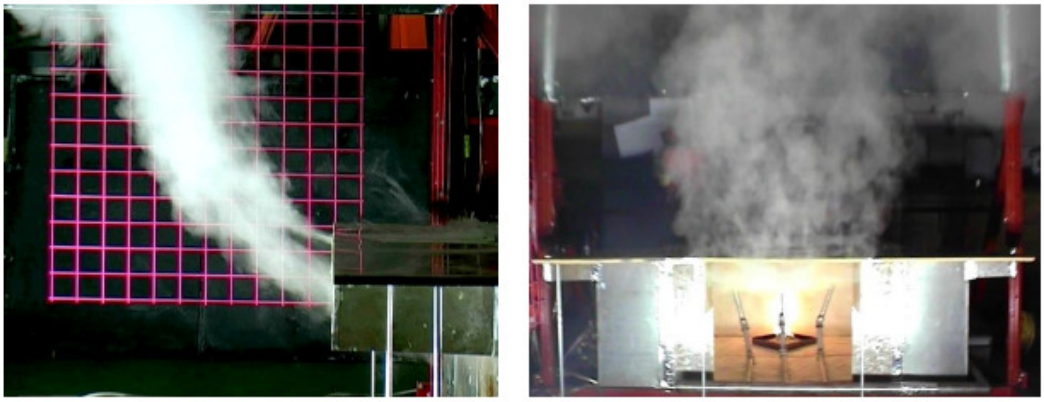

a) Side view b) Front view

Figure 17. Plume behaviour for width of opening = 0.6m (Harrison, 2009).

a) Side view b) Front view

Figure 18. Plume behaviour for width of opening = 0.2m (Harrison, 2009).

2.2 Recent Work

Tan (2009) has conducted experiments in a one-tenth physical scale model (Figure 19 and Figure 20) representing a six-storey atrium building to study the balcony spill plume smoke contamination on higher balconies. Tan (2009) modified the test rig from Harrison (2009) for the balcony experiment. Tan (2009) experiment numbers "16 to 30" had similar characteristics as Harrison's (2009) experiment. Due to safety considerations, only three balconies were used for his experiment. Tan devised sixty experiments for the study and he systematically varied the balcony breadths, plume widths and fire sizes to study smoke contamination. Tan has placed numerous thermocouples during the test, "column B" and "column C" as shown in Figure 21. In addition, Tan has provided the visual record (as shown in Figure 22) of the smoke logging. Tan used an upstand of 0.1m at the balcony edge, as shown in Figure 23.

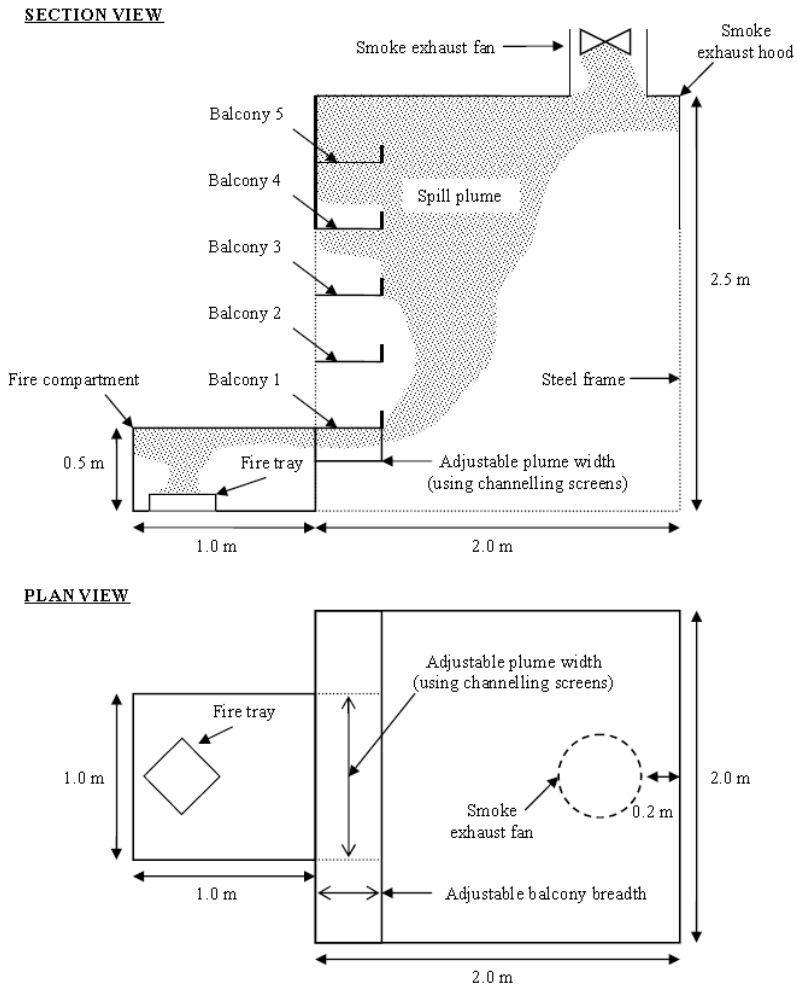

Figure 19. Schematic diagram and physical model for the Tan's experiment (Tan, 2009).

Figure 20. Physical model for the Tan's experiment (Tan, 2009).

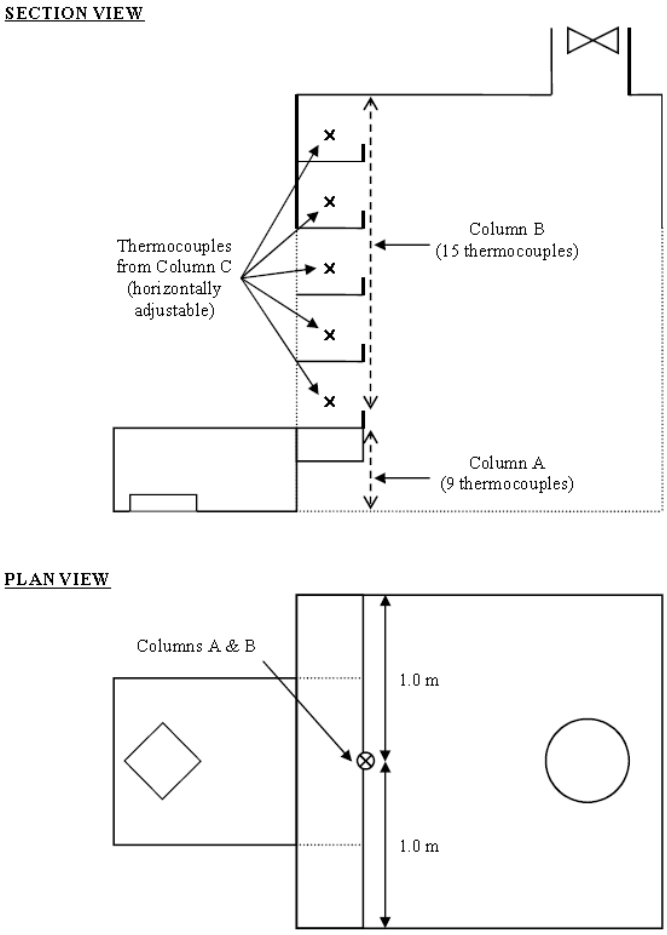

Figure 21. Location of Tan's experiment thermocouple (Tan, 2009).

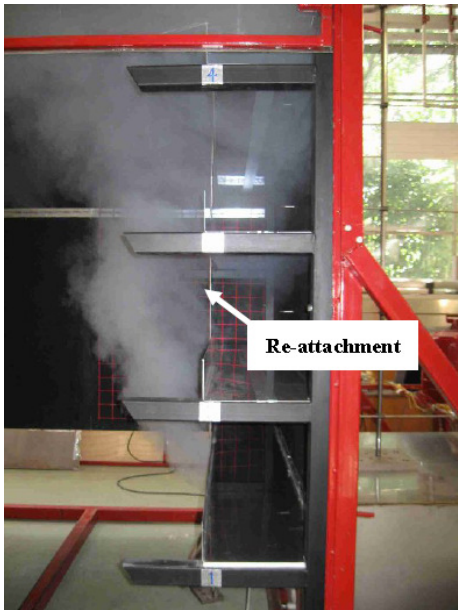

Figure 22. Visual record of Tan's experiment (Tan, 2009).

Figure 23. Upstand of 0.1m for Tan's experiment (Tan, 2009).

Finally Tan conducted fifty experiments as he inferred the remaining results from his earlier test data, as shown in Figure 24. Tan found that when the balcony thermocouple reading recorded 10°C above the ambient temperature of 20°C, smoke was also visually observed at the balcony. In other words, Tan used a temperature marker of 30°C to assess the balcony smoke contamination as it best-fitted the visual observations for the experiment.

One of Tan's major findings was that the aspect ratio of plume width (w) to balcony breadth (b) could be used to predict whether smoke contamination of upper balcony would occur. From his qualitative assessment data, he derived an empirical correlation for this smoke contamination assessment as shown in Figure 25. This correlation was used to determine the height of smoke contamination above the spill plume edge, which was valid for following situation:

a. $1.0 <$ Aspect Ratio (w/b) < 3.0

b. Height of upstand 0.1m, equivalent to full size of 1m

c. Vertical separation distance between balconies was 0.4m, equivalent to full size of 4m

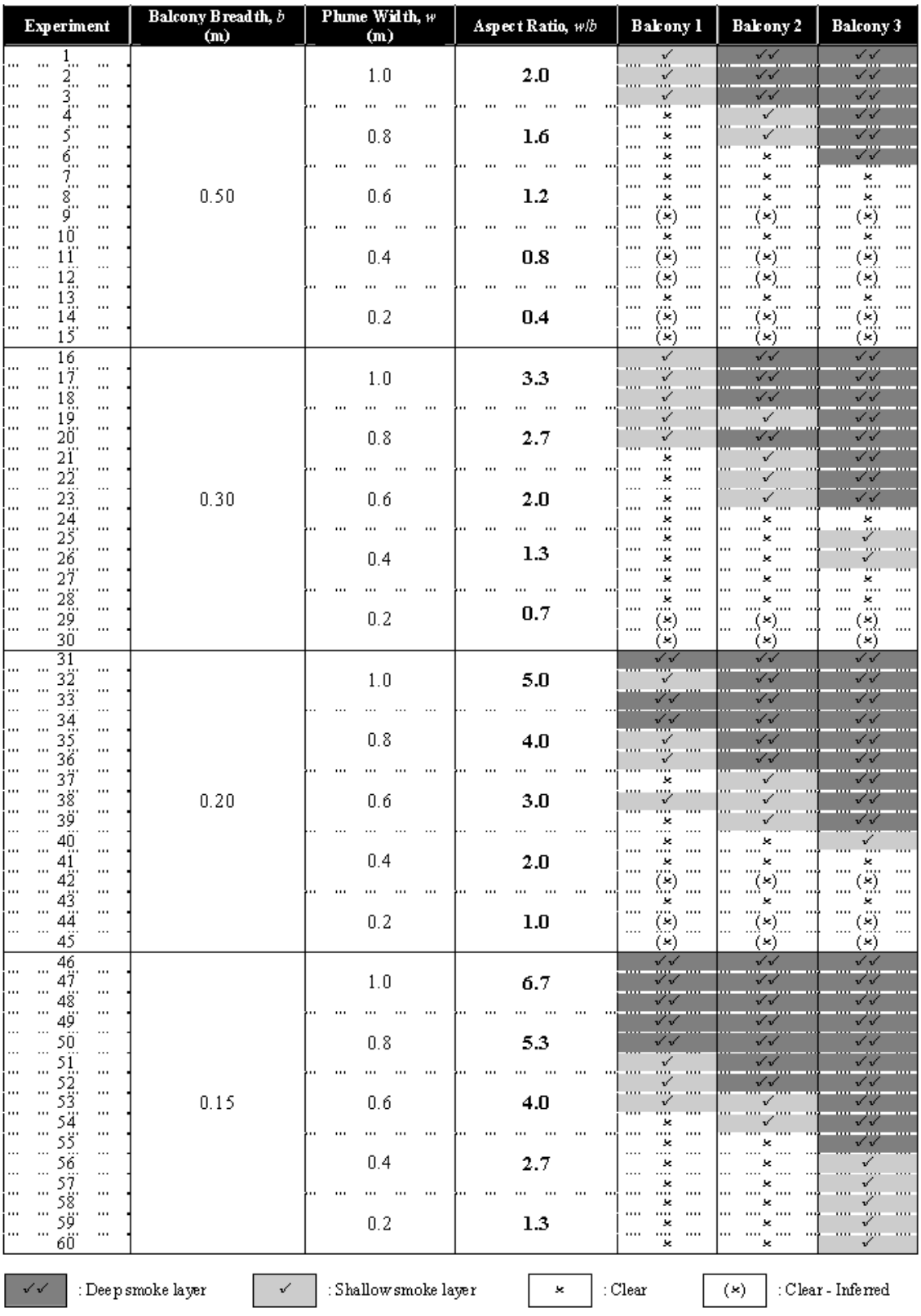

Figure 24. Summary of Tan's experiment result (Tan, 2009).

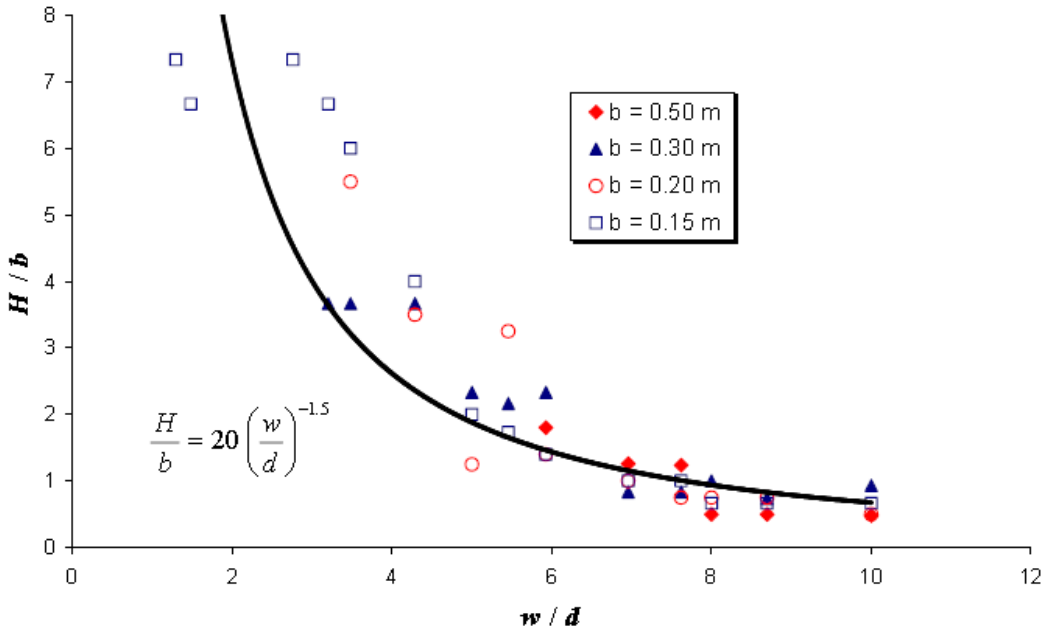

Figure 25. Tan's correlation for the contamination (Tan, 2009).

2.3 Computational Fluid Dynamic for Smoke Simulation

Gobeau *et al* (2002) mentioned that there were three approaches to predict smoke movement. The first approach was using empirical models, which were based on experiments. Empirical models were typically limited to geometrically very simple situations and should not extrapolate beyond the configuration in which the experiments were carried out.

The second approach was using zone models, which were simple mathematical models which divided the problem into small number of "zones", i.e. fire plume, a hot layer and cold air. Zone models were applicable to simple spaces such as regular-shaped rooms. They commented that zone models' basic assumption that the flow could be divided into zone for complex enclosed spaces and large modern warehousing would break down.

The third approach was using computational fluid dynamics (CFD) modelling without the constraints imposed by empirical models and zone models. Fire and smoke movement in complex spaces where turbulence and CFD modelling could be further classified into three categories:

a. Direct Numerical Simulation (DNS), which resolved by solving directly the Navier-Stokes equations that governed fluid flows.

b. Large Eddy Simulation (LES), which resolved by solving directly the Navier-Stokes equations except the smallest turbulent motions.

c. Reynolds-Averaged Navier-Stokes (RANS) models, which the Navier-Stokes equations was time-averaged to provide time-averaged characteristic quantities of the flow.

Among the three CFD modelling techniques, RANS grids need only to be fine enough to capture the important time-averaged features of the flow as it was not attempting to resolve the turbulent motions. Hence, Gobeau *et al* (2002) commented there was far less resource utilisation than DNS and LES. They further suggested that a CFD user should wherever possible check the predictions against spot measurements. In situation where these were not available, well established empirical correlations could sometimes be used in limited parts of the domain.

McGrattan (2005) also explained that DNS was still not practical for large-scale fire simulations. RANS models could handle well many industrial processes where the interest in some forms of "steady-state" solution and where the turbulence could be characterised as "homogeneous". LES techniques were for fire plumes, ceiling jets and other fire-driven flows. RANS models developed specifically for fire includes Jasmine, Kameleon, Smartfire and Sofie. However, regardless of the model type, for a prescribed heat release heat and yields, Mcgrattan (2005) mentioned that simulations could predict compartment temperatures to within 20% at worst and at best to within experimental accuracy.

McGratten *et al* (2009) mentioned that Fire Dynamics Simulator (FDS) had been under development for almost 25 years and the public version has been available since February 2000. FDS is a computational fluid dynamics model of fire-driven fluid flow. It solves the Navier-Stokes equations numerically for low-speed, thermally-driven flow and focuses on smoke and heat transport from fire. As a hydrodynamic model, FDS solved the Navier-Stokes equations using either a Large Eddy Simulation (LES) method or Direct Numerical Simulation (DNS) method for very fine mesh.

McCartney and Hadjisophocleous (2005) suggested guidelines for the use of CFD simulations for fire and smoke modelling. They suggested mesh resolutions in the order of 10^{-1}m could be used for plume models and non-isometric mesh elements should be applied carefully. Flows through doors and windows could be accurately predicted with addition of an exterior computational domain of small length. They also recommended when the fuel package is a single object consisting of multiple fuels, the package could be modelled as a block with fuel properties computed as a mass weighed average of the constituent fuel properties.

Chow (1999) who conducted numerical simulations on balcony spill plume cautioned that the free boundary conditions have to be specified carefully in carrying out CFD simulations, especially for cases where pressure distributions are important.

McCartney and Lougheed (2004) did a CFD (FDS version 3) investigation of balcony spill plumes in atria and the setup was one-tenth scale experiments. They explored various grid sizes in the order of 0.1m. Their finding was that FDS under predicted the flame and plume temperatures above the burner, resulting in low hot layer temperatures compared to the experimental data.

Ryder *et al* (2004) mentioned that for a well-defined situation with proper grid resolution and boundary condition, FDS results could match the experimental result, with less than 15% difference for temperature and velocity parameters (Figure 26). They also commented that their simulations did not have the ability to model ventilation limited fires at that time and FDS was highly dependent on the grid chosen to avoid skewing of the results.

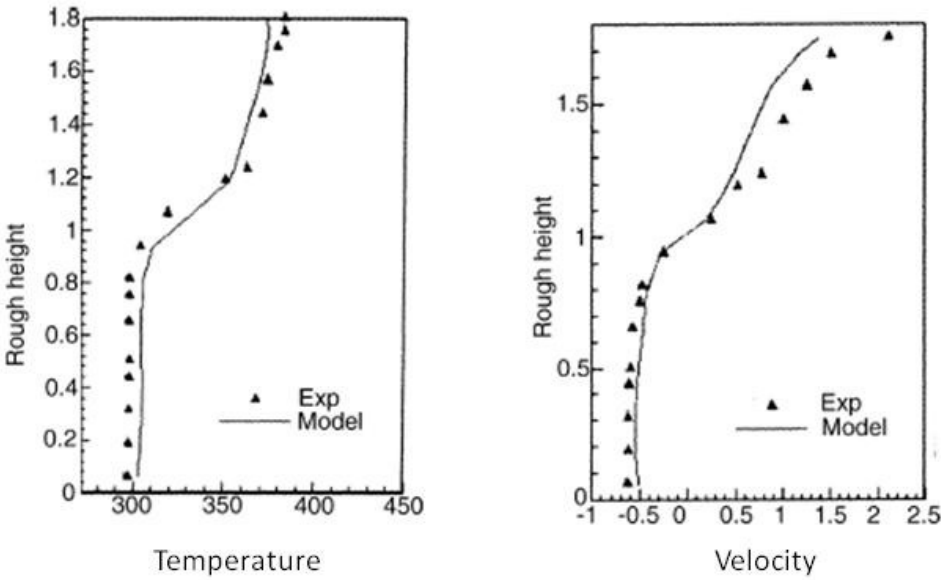

Figure 26. Doorway temperature and velocity from from FDS and experiment (Ryder *et al*, 2004).

Weckman, Lougheed and McCartney (2005) conducted CFD investigations of balcony spill plumes in atria for a parametric study. They found that accurate modelling of plume dynamics in atria required a grid size in the range of 0.1 to 1.0m. Their findings also included that the mass flow rate at various elevations converge around 0.25 to 0.5m as shown in Figure 27.

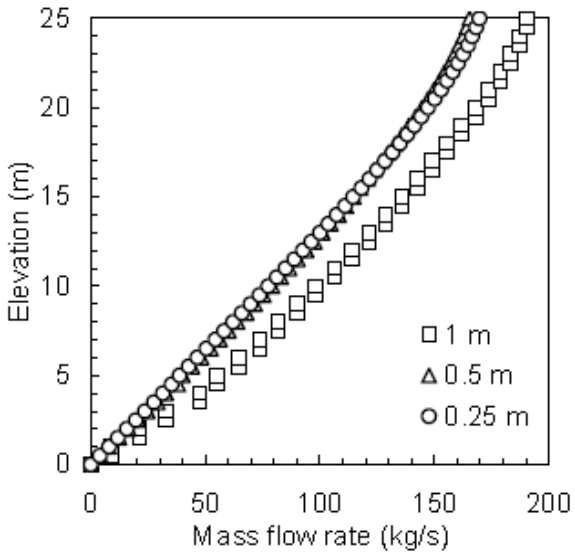

Figure 27. Mass flow rate profile variation with grid size (Weckman *et al*, 2005)

Tilley and Merci (2009) used FDS (version 4.0.7) to model adhered spill plumes in atria using small-scale experimental data from Poreh *et al* (2008). The distinction between adhered plumes and spill plumes was made on the basis of the Froude number. When the Froude number was larger than one, the plume would be a detached spill plume. Their objective was to investigate the adhered plume mass flow rate. Their heat release rate ranged from 2.9kW to 11.9kW and grid cell size was 50mm cube. Their finding was that the FDS simulation result agreed well with the experimental results on mass flow rate. Their large scale numerical simulation used a grid cell size of 100mm and 200mm for 4m and 7.2m wide atrium respectively. They observed that there were more dimensional effects occurring in the smoke layer; the smoke layer was not able to maintain a uniform depth over the entire width and length of the atrium.

Quintiere and Grove (1998) have provided the characteristic length of a line plume as shown in Equation 1. Quintiere and Ma (2003) discussed the important consideration of grid size on simulation results for CFD analysis. They defined the resolution of fire plume simulation as a dimensionless parameter (R) as shown in Equation 2. To simulate a fire correctly, a non-uniform grid was allowed and the aspect ratio of grid size should not exceed 2.0. They found that the plume dynamics could only be accurately simulated if the resolution limit was about R = 0.1 or smaller. Their findings on flame height simulation optimum resolution was R = 0.05; above this value, the flame height could be over-predicted.

$$z^* = \left(\frac{\dot{Q}_c / w}{\rho_o C_p T_o g^{1/2}} \right)^{2/3}$$ Equation 1

where

ρ_o is the density of ambient air = 1.21kg/m^3

C_p is the specific heat of ambient air = 1.01kJ/kgK

T_o is the ambient temperature = 293K

$$R = \frac{\max(\delta x, \delta y, \delta z)}{z^*}$$ Equation 2

where

R is the resolution of simulation, grid size / z^*

McGrattan *et al* (1998) recommended adequate resolution could be achieved when the characteristic length was spanned by roughly ten computational cells. However they commented given then computing capability, the number of cells could be incorporated in a given simulation was in the range of one to two million. They cautioned that for small fires, it must be studied in proportionately small domains if important features of the plume were to be captured.

Harrison (2004) used FDS to study thermal spill plume in a one-tenth scale model. Harrison found that the minimum grid size to achieve modelling results for the scale model experiment was 20mm. The modelling was for a flow from a compartment opening to a higher projecting balcony. It did not examine entrainment beyond the spill edge.

Harrison (2009) also conducted a comprehensive study on the *3-D* balcony spill plume using FDS modelling. He did a grid sensitivity study and found that FDS generally provided a good prediction of the flow from the fire compartment and subsequent spill plume behaviour and entrainment with grid size of 25mm on one-tenth scale model. In other words, this equated to a grid size of 0.25m for full scale flow. Harrison further elaborated that the chosen grid size must meet the following criteria for the grid size to be considered appropriate when $n^*_{spill} \geq 0.9$ for spill plume.

$$n^*_{spill} = \frac{D^*_{spill}}{\delta x}$$ Equation 3

and

$$D^*_{spill} = \left(\frac{\dot{Q}_c}{w \rho C_p T \sqrt{g}} \right)^{2/3} = z^*$$, similar to Equation 1

Figure 28 to Figure 30 show Harrison's (2009) simulation results on vertical velocity slice files compared with his experiment for adhered plume and spill plume. These demonstrated that the predicted behaviour close to the wall above the spill edge was very similar to the experiment for plumes generated from a wide, intermediate and narrow compartment opening width.

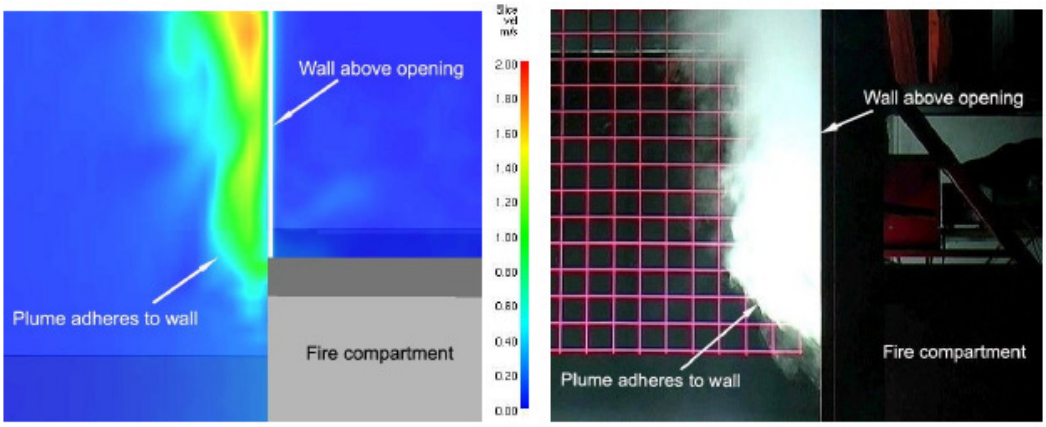

a) Simulation SE20 b) Experiment E209

Figure 28. Comparison of predicted plume behaviour with experiment for opening width = 1.0m (Harrison, 2009).

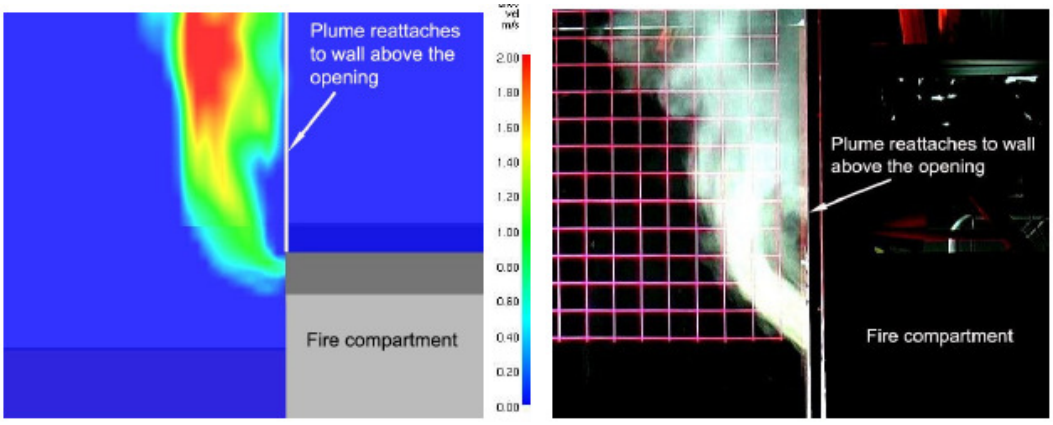

a) Simulation SE14 b) Experiment E215

Figure 29. Comparison of predicted plume behaviour with experiment for opening width = 0.6m (Harrison, 2009).

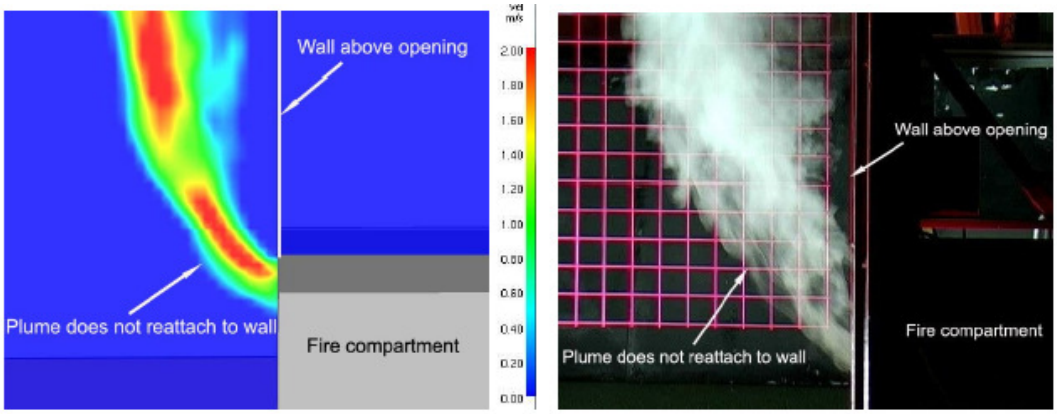

Figure 30. Comparison of predicted plume behaviour with experiment for opening width = 0.2m (Harrison, 2009).

Harrison (2009) also cautioned that the complex nature of the spill plume or the effect of the boundary layer close to the wall for rising plume velocity could be better dealt with a finer grid resolution.

Harrison (2009) commented on plumes that detach and then reattach to the wall, FDS tended to under predict the experiment mass flow rate by up to approximately 20%. For plumes that did not reattach to the wall above the spill edge, FDS could provide reasonably good mass flow rate prediction, and in some cases, there was a tendency to under predict entrainment by approximately 10% to 15%. Harrison (2008) concluded that although FDS provided an excellent prediction of *3-D* adhered plume behaviour, further work was desirable to provide improved guidance on the use of FDS to better quantify entrainment. Finally, Harrison (2009) recommended for design purposes, a grid size of 0.25m should be initially chosen for full-scale modelling until further work is carried out.

3. MODEL DEVELOPMENT & DATA INTERPRETATION

The overall approach for this simulation study is shown in Figure 31, which is a progressive methodology. The primary scope of work for this research project is from Step 1 to 7, which is to develop the smoke contamination correlation for a full scale model up to five upper balconies. Steps represented in a "dotted line" are studies for sensitivity analysis; all sensitivity studies are analyses with a reduced number of simulations. The scale model to simulate Tan's (2009) experiment scale model is referred to as "S*XX*E", where the "*XX*" refers to Tan's (2009) experiment number (see Figure 32a). The simulated scale and full-scale models for up to five balconies are referred to as"S*XX*E5" and "F*XX*E5" respectively (see Figure 32b and Figure 32c). Results from the experiment and simulation "S*XX*E" are compared to determine the confidence level to proceed to full-scale modelling. Critical dimensions for the scale model and full-scale model are shown in Figure 33 and Figure 34.

The simulations use a 32bit operating system personal computer as this is the commonly available resource at the University of Canterbury. Based on the experiment model geometry, it is found that the maximum number of balconies that could be simulated is seven. Hence, the full-scale modelling included simulation for this case, referred to as "F*XX*E7". For the practical smoke management system limit (Morgan *et al*, 1999), the five balcony configuration will be the main focus of this research project, hence, more simulations are conducted for this category.

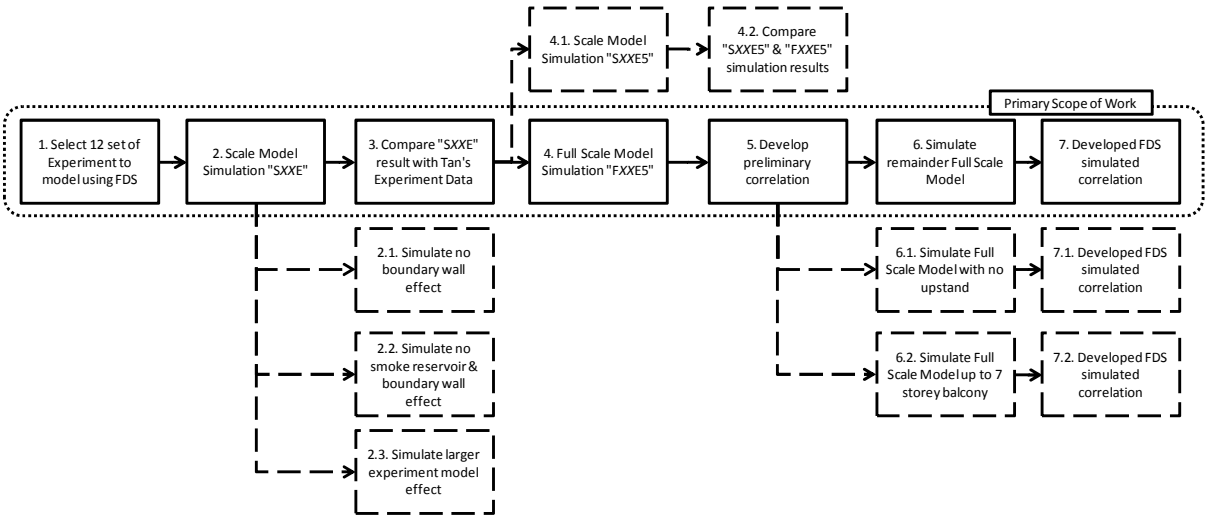

Figure 31. Overall approach for the simulation.

Steps 2.1 to 2.3 are to study the effect of different boundary conditions on the scale model. These include removal of the experiment boundary wall, removal of the smoke reservoir and a wider atrium. Steps 4.1 and 4.2 are to develop a small-scale five balcony configuration to compare with the full-scale five balcony configuration. This is to allow direct comparison with similar boundary condition, although conduction and radiation heat transfer are known to be not part of the scaling.

Steps 6.1 and 7.1 are to study the situation when there is no upstand. This is the situation where grills are provided as the physical barrier in the balcony. The simulation models have a suffix of "*NUS*" (i.e. no upstand).

Steps 6.2 and 7.2 are to study the effect of smoke contamination when there is seven balcony configuration (see Figure 32d).

3.1 Selection of Experiment Model

The simulation for the Tan's (2009) experiment starts with identifying twelve set of representative cases to develop the correlation equation. The selection is based on the following criteria:

a. Ensure a wide spread of aspect ratios (≤3.0) interpreted from Tan's (2009) experimental results

b. Ensure a wide spread of plume widths and different heat release rates

c. A mix of contamination and contamination-free models

The selected experiments for the modelling are shown in Table 4, which are referred to as the "twelve primary scenarios" in this report.

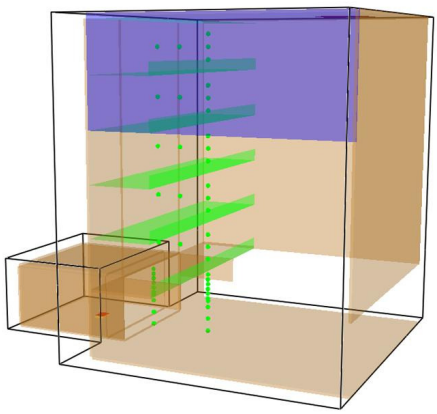

a. S*XX*E – Model to simulate Tan (2009) Experiment

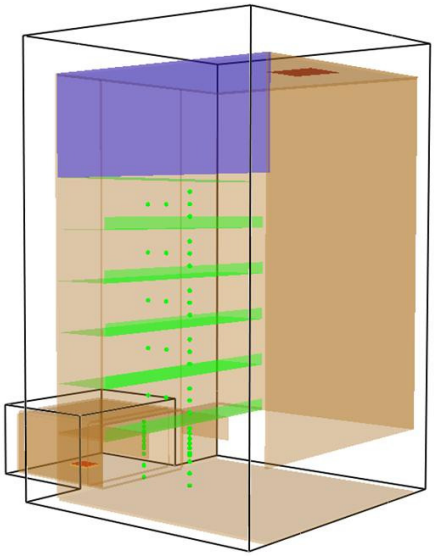

b. S*XX*E5 – Model extended to five balcony in scale model

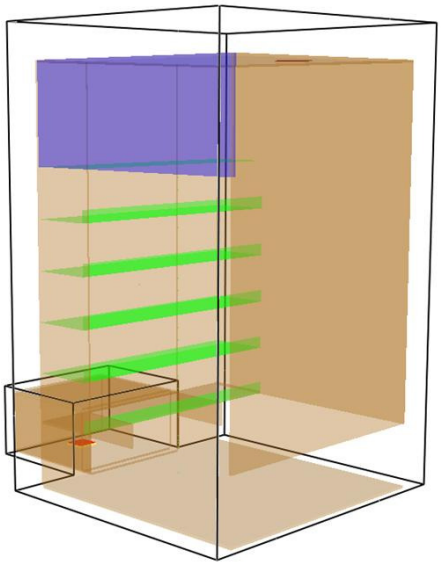

c. F*XX*E5 – Full scale model with five balcony

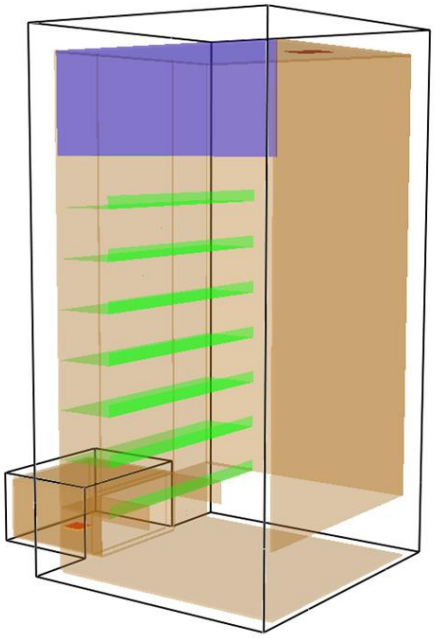

d. F*XX*E7 – Full scale model with seven balcony

Figure 32. Four main simulation models for assessment.

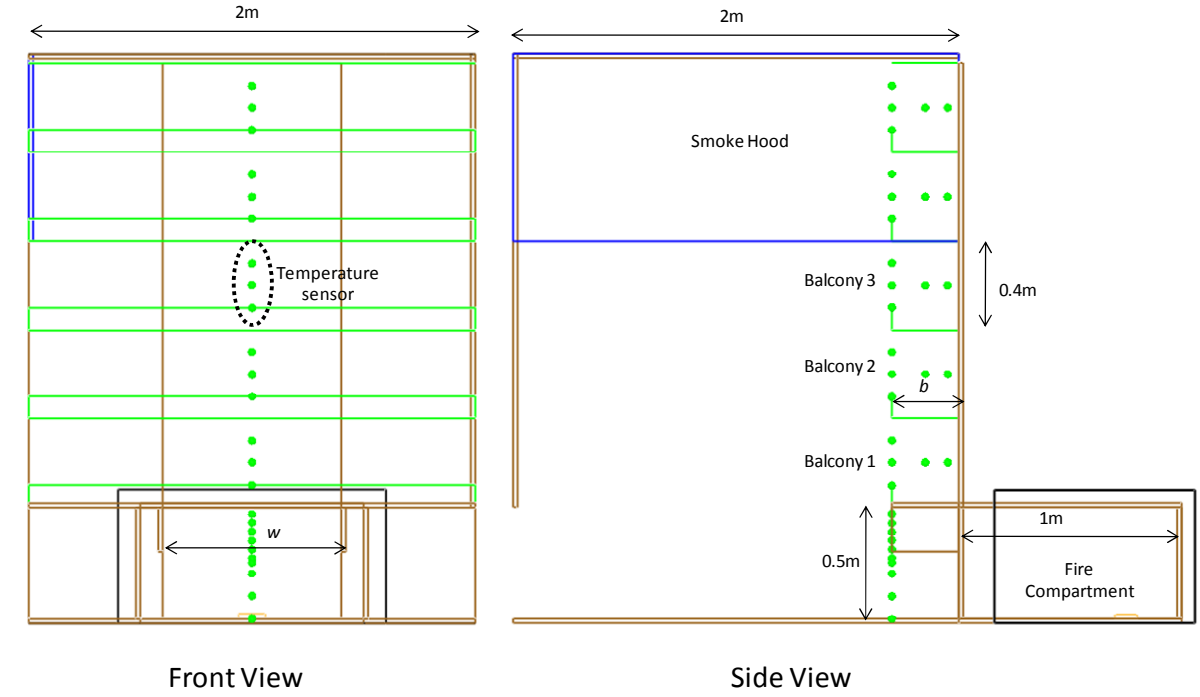

Figure 33. Dimension for scale model.

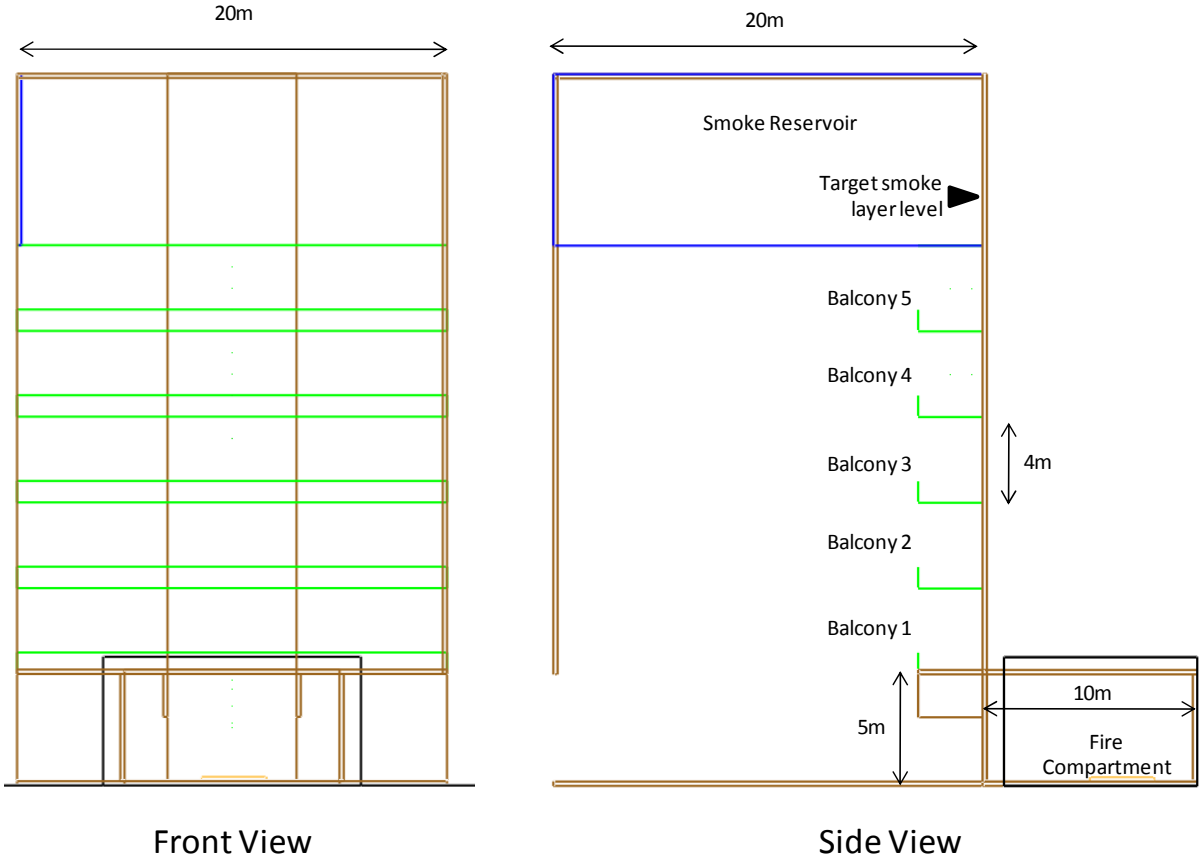

Figure 34. Dimension for full-scale model.

Experiment	Balcony Breath, b (m)	Plume Width, w (m)	Aspect Ratio, w/b	Heat Release Rate, Q_T (kW)	Balcony 1	Balcony 2	Balcony 3
1	0.5	1	2	5			
3	0.5	1	2	15			
8	0.5	0.6	1.2	10			
13	0.5	0.2	0.4	5			
19	0.3	0.8	2.7	5			
23	0.3	0.6	2	10			
27	0.3	0.4	1.3	15			
38	0.2	0.6	3	10			
41	0.2	0.4	2	10			
43	0.2	0.2	1	5			
56	0.15	0.4	2.7	10			
60	0.15	0.2	1.3	15			

	Clear
Experiment Result	Shallow smoke layer
	Deep smoke layer

Table 4. Selected experiments from Tan (2009) for simulation.

3.2 Smoke Contamination

For the scale model, Smokeview is unable to "present smoke movement effect" for smoke contamination as the volume of soot in the scale model is too little for visualisation. Hence, similar to Tan's (2009) approach, the 10°C above ambient temperature profile was used to determine whether it is similar to Tan's (2009) experimental visual record. The assumed ambient temperature was 20°C. The classification for the temperature profile observation adopts similar Tan's (2009) methodologies, which is shown in Figure 35 for the scale model; for full-scale model, each balcony height is 4m. Smokeview will be used to determine the 30°C temperature profile on each balcony to visually identify the deepest level of smoke contamination for the entire simulation period. Another approach was to consider using the FDS's smoke layer height device to determine the smoke layer height at each balcony.

As shown in Figure 35, a temperature profile of 30°C found within the balcony will be deemed as smoke in the balcony. When the 30°C temperature profile occupied more than 50% height from the balcony floor level, it is deemed as "deep smoke layer"; temperature profile less than 50% height is deemed as a "shallow smoke layer". This assessment is similar to Tan's (2009) methodology.

The slice file to identify the 30°C profile is taken at the mid position of the atrium, in line with the mid position of the burner as shown in Figure 36. It deliberately bound the temperature to a maximum of 100°C so that the 30°C profile could be easily identified.

Thermocouple devices were also placed in similar positions as Tan (2009) experiments as shown in Figure 37. The readings are compared with Tan (2009) experiment record. This is in line with the recommendation of Gobeau *et al* (2002) on using CFD mentioned in section 2.3.

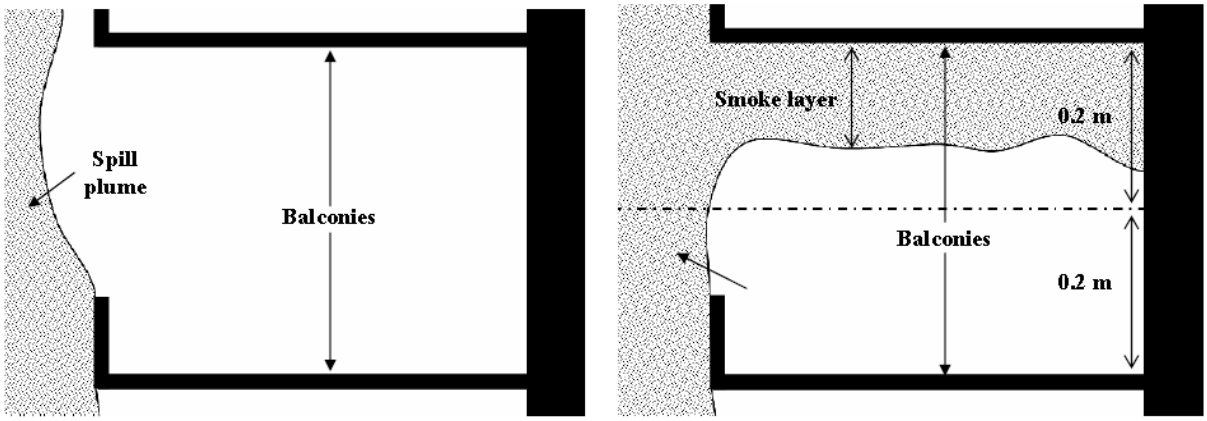

(a) Clear

(b) Shallow smoke layer (smoke level occupied less than 50% height)

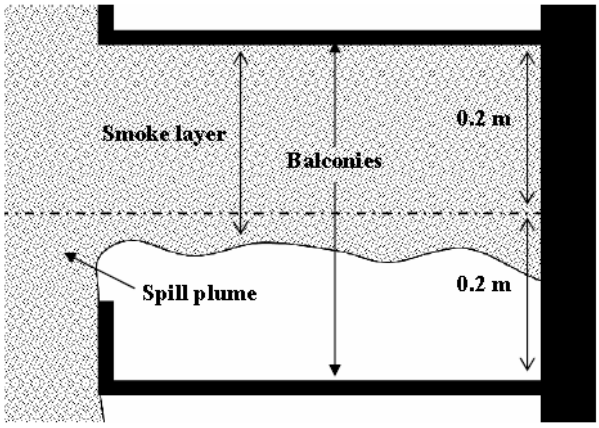

(c) Deep smoke layer (smoke level occupied more than 50% height)

Figure 35. Smoke contamination classification (Tan, 2009).

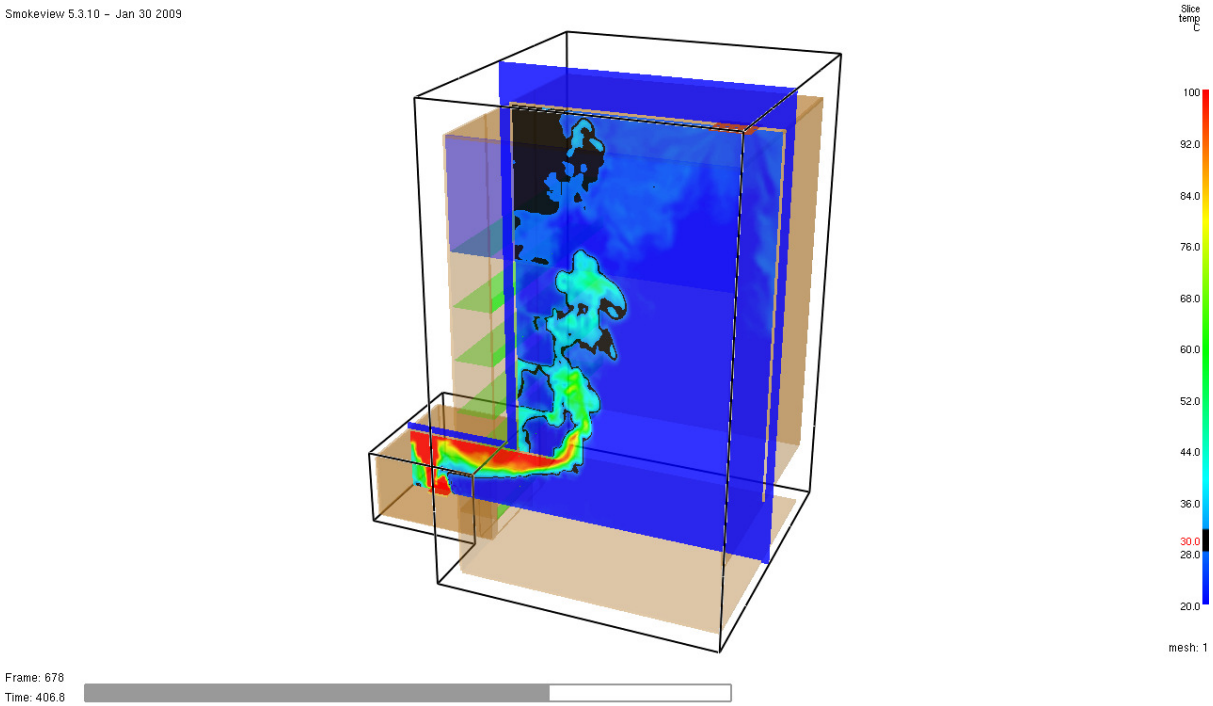

Figure 36. Position of slice file at mid position of the atrium using full-scale model.

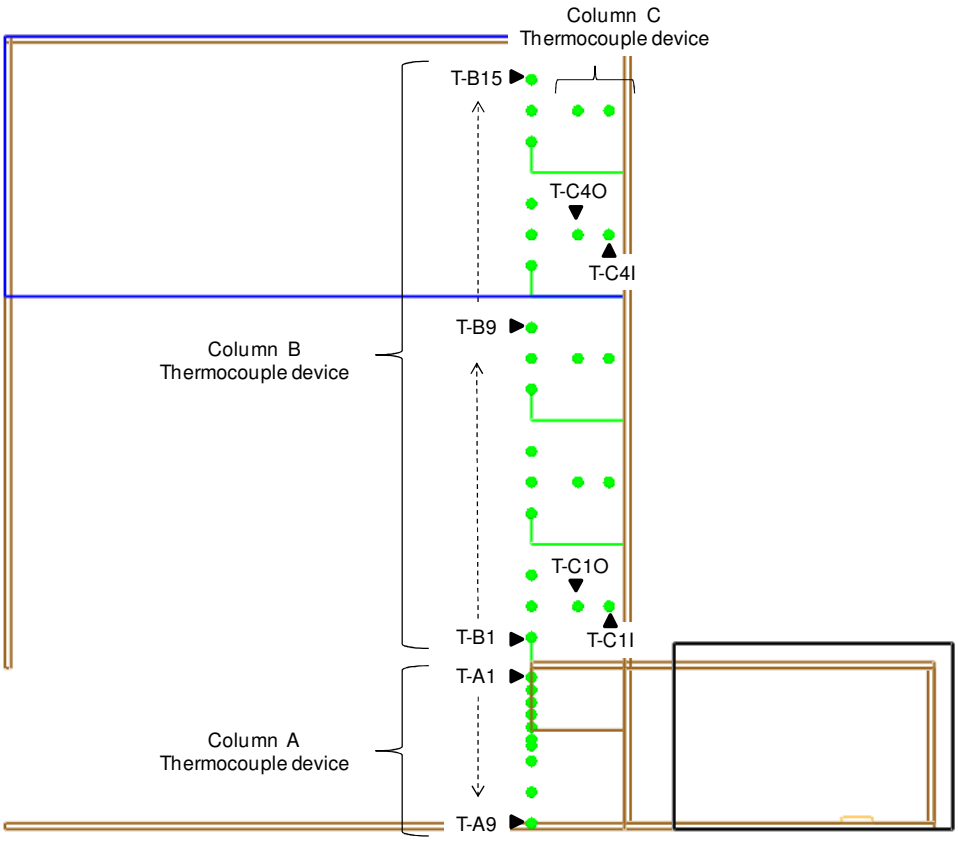

Figure 37. Position of thermocouple devices.

3.3 Height of Smoke Contamination

The determination for the height of smoke contamination adopts similar methodology as Tan (2009). A typical measurement is shown in Figure 38 and the measurement is always with reference from the spill edge. When the smoke layer reaches the floor, it is deemed to be full contamination, i.e. H = 0m. Smoke layer depth at the spill edge was determined using smoke layer height device in FDS and justification for use is demonstrated in Section 5.8. The FDS smoke layer height device predicts the location of the interface between the smoke-laden upper layer and the cooler lower layer in a burning compartment using Simpson's Rule on the continuous temperature height from the floor to the ceiling.

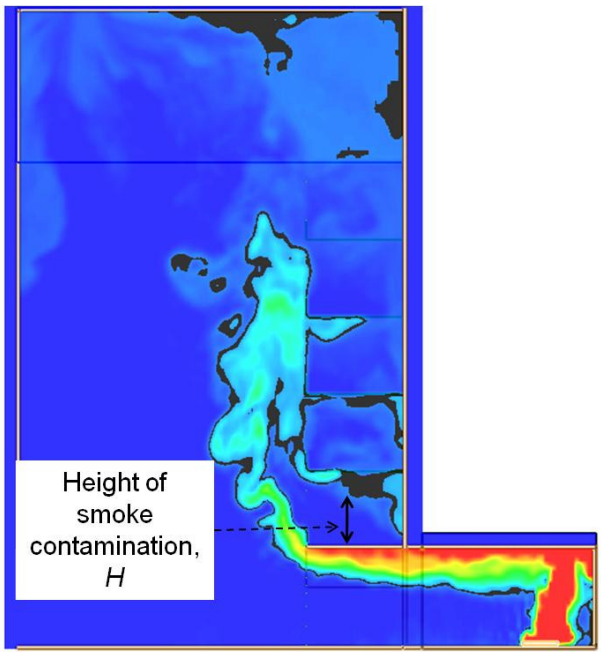

Figure 38. Determination for height of smoke contamination.

3.4 Theory

This section provides the formula used in the parts of the analysis. Tan (2009) did not record the rate of smoke extraction for the experiment, hence, it is necessary to estimate the smoke extraction rate for each simulation. Two different formulae are used. The first formula (Equation 5) is from Harrison and Spearpoint (2005) and using this has the limitation that the smoke reservoir depth increased and lead to a deep smoke layer at the highest balcony for those cases with a narrow discharge opening; in other words, Equation 5 does not work well for a narrow opening. The second formula (Equation 6) is an improvement from Harrison

(2009) which addressed those cases with a narrow discharge opening. Equation 6 was available at later stage of this project and hence, it is used for the simulation of the full-scale seven balcony configuration; all other simulations are based on the Equation 5.

Balcony Spill Plume

Morgan *et al* (1999) provide the mass flow of smoky gases passing through vertical opening as follows:

$$\dot{M}_w = \frac{C_e P w h^{3/2}}{\left[w^{2/3} + \frac{1}{C_d}\left(\frac{C_e P}{2}\right)^{2/3} \right]^{3/2}} \qquad \text{Equation 4}$$

where

$\dot{M}_w$ is the mass flow rate of gases at the compartment opening (kg/s)

C_e = 0.21kgs^{-1}m$^{-5/2}$ for large-area rooms where the ceiling is close to the fire, such as open-plan offices.

C_d = 0.65 for smoke spills past a deep downstand or 1.0 for no downstand.

Harrison and Spearpoint (2005) stated the mass flow due to the resulting 3-D spill plume could be found from the following equations:

$$M_p = 0.20 z \dot{Q}_c^{1/3} W^{2/3} + 0.0017 \dot{Q}_c + 1.5 \dot{M}_w \qquad \text{Equation 5}$$

Harrison (2009) used the 1/10th scale model and supported by numerical modelling using Computational Fluid Dynamics to characterise the thermal spill plume entrainment. Harrison (2009) found that the spill plume behaviour and subsequent entrainment were dependent on the characteristics of the layer flow below the spill edge. Plumes from narrow opening with deep layers would entrain air at higher rate with respect to height compared to plumes from wide and shallow layers. Harrison proposed the simplified design formula for *3-D* plume channelled by screen below the balcony as follows:

$$\dot{M}_{p,3D} = 0.16 \dot{Q}_c^{1/3} \left(w^{2/3} + 1.56 d^{2/3} \right) z + 1.34 \dot{M}_w \qquad \text{Equation 6}$$

Equation 6 is valid for $z \le z_{trans}$ and

$$z_{trans} = 3.4\left(w^{2/3} + 1.56d^{2/3}\right)^{3/2}$$ Equation 7

$$d \approx \frac{1}{C_d}\left[\frac{M_w}{2w}\right]^{2/3}$$ (Hansell, 1993) Equation 8

Plugholing

It is necessary to avoid plugholing at the extraction fan. This could be achieved by determining the smoke layer temperature followed by the maximum allowable extraction rate. All formulae are from Klote and Milke (2002).

The temperature of smoke layer can be expressed as:

$$T_s = T_o + \frac{\dot{Q}_c(1-n)}{\dot{M}_p C_p}$$ Equation 9

and n is the wall heat transfer fraction

In the absence of research about the wall heat transfer fraction, values of n are expected to be in the range of 0.3 to 0.7 for walls and ceilings of normal construction material (brick, concrete, glass, gypsum board, etc). Hence, an average value of 0.5 will be used.

The maximum mass flow rate that can be efficiency extracted using a single exhaust inlet is given as:

$$m_{\max} = C_{cp1}\beta d_e^{5/2}\left(\frac{T_s - T_o}{T_s}\right)^{1/2}\left(\frac{T_o}{T_s}\right)^{1/2}$$ Equation 10

where

d_e = 0.6m for scale model and 6m for full scale model

C_{ph1} is "3.13"

Based on limited information, suggested values of β are 2.0 for a ceiling exhaust inlet near a wall, 2.0 for a wall exhaust inlet near the ceiling, and 2.8 for a ceiling exhaust inlet far from any walls. The outlet is on the roof and uses 2.0 for conservativeness.

Scale Modelling

Harrison (2004) mentioned that the physical scale modelling is well established and was primarily developed at the Fire Research Station in the UK. This method is a modified Froude number scaling and requires the equivalent flows be fully turbulent on both the full and the model scale (Reynolds number ≥4000). Tan's (2009) research work was done using this methodology. This method requires keeping the temperature above ambient constant and the scaling laws are as follows:

$$\dot{Q}_c \propto L^{5/2};\ \dot{M} \propto L^{5/2};\ \dot{V} \propto L^{5/2} \text{ and } u \propto L^{1/2} \qquad \text{Equation 11}$$

NFPA 92B (2009) also includes the pressure difference and time for scaling as follows:

$$\Delta P \propto L;\ t \propto L^{1/2} \qquad \text{Equation 12}$$

3.5 Modelling Parameters

The assumption for the fire size is based on sprinklered design, hence, the fire size is capped at 5MW and the species for modelling uses pre-flashover conditions. Since the atrium balcony smoke contamination study is for shopping centres, the assumption will be using 50% polyurethane and 50% wood, i.e. f_{co} = 0.022kg/kg and f_{soot} = 0.11kg/kg (Wade *et al*, 2007). The inclusion of species in the modelling is to allow any future separate study to evaluate fractional effective dose (gaseous) in the balcony for future works.

This project is similar to another on-going research work that study un-channelled flow by Tiong (2010) using CFD simulation. Hence, similar materials properties are shown in Table 5. Tiong (2010) provided the specific heat of the CFI board from the supplier as shown in Figure 39. FDS 5.0 is used for the simulations and a typical FDS 5.0 input file for a five balcony configuration is shown in Appendix A.

Tan (2009) did not mention the ambient temperature for his experiments. As his experiments were conducted between Nov 2008 and Jan 2009, it was assumed ambient laboratory temperature of 20°C for this summer period.

CFI Board		
Conductivity (W/mk)	0.041	(Drysdale, 1998)
Density (kg/m^3)	229	
Specific heat (kJ/kgK)	0.82	see Figure 39
Thickness (mm)	16 (scale model) / 160 (full-scale)	
Steel		
Conductivity (W/mk)	45.8	(Buchanan, 2002)
Specific heat (kJ/kgK)	0.46	
Density (kg/m^3)	7850	
Thickness (mm)	1 (scale model) / 10 (full-scale)	
Acrylic Glass		
Conductivity (W/mk)	0.19	(Drysdale, 1998)
Specific heat (kJ/kgK)	1.42	
Density (kg/m^3)	1190	
Thickness (mm)	12 (scale model) / 120 (full-scale)	
Ethanol		
Carbon	2	
Hydrogen	6	
Oxygen	1	
Heat of combustion (kJ/kg)	2680	(Karlsson & Quintiere, 2000)
Radiative Fraction	0.2	(Drysdale, 1998)

Table 5. Typical material properties used in simulation.

The scale model fire sizes simulated are 5kW, 10kW and 15kW, which are similar to Tan's (2009) experiment parameters. Using Equation 11, the full-scale fire sizes simulated are 1581kW, 3162kW and 4743kW. Table 6 shows the dimensions and heat release rates for the

small-scale model and full-scale model simulations. Small scale model and full-scale model balcony heights are 0.4m and 4.0m respectively. The dimensions for the full-scale model are determined using Equation 11.

The smoke extraction rate for each simulation plays a critical role as an incorrect exhaust could lead to plugholing or smoke spilling to the highest balcony. Equation 4 to Equation 10 are used to size the exhaust fan extraction rate. Appendix B shows the extraction rates for all the models. Calculation shows that smoke mass flow rate from a 10m opening fire compartment and a rise of 20m is in the region of 200 kg/s, which is system limitation as mentioned in Section 1.6 by Morgan *et al* (1999).

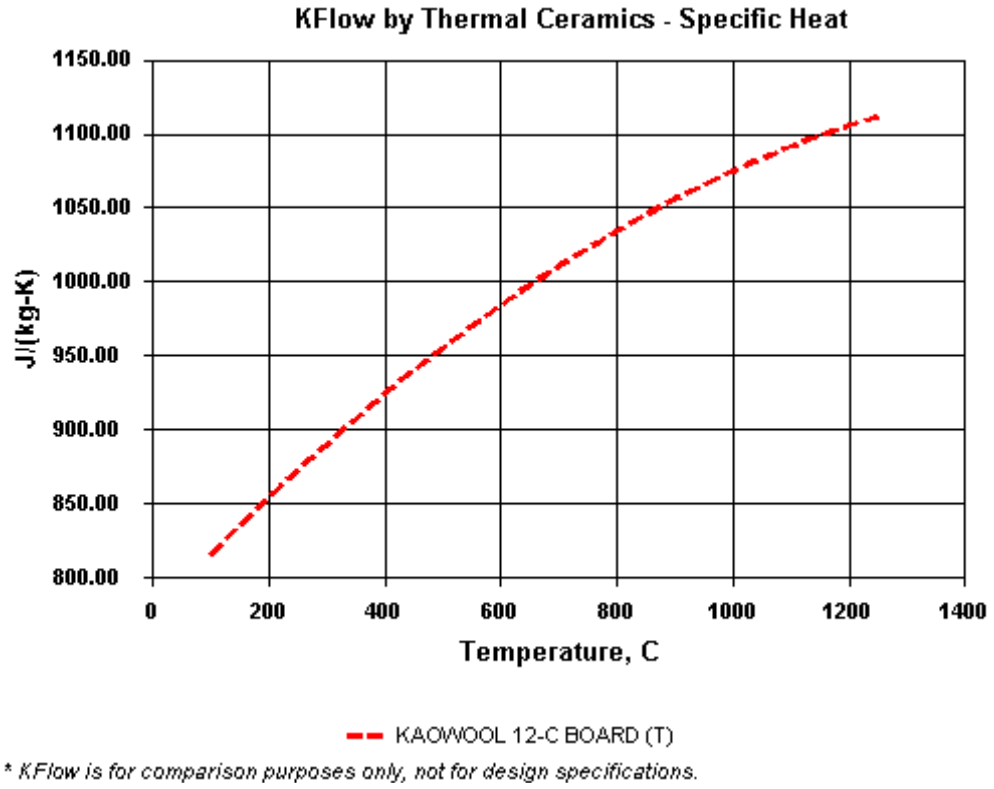

Figure 39. Supplier information on specific heat for CFI board.

	Tan (2009) Experiment and Scale Model Simulation Dimension & Heat Release Rate				Full-scale Simulation Dimension & Heat Release Rate			
Experiment or Simulation	Balcony Breath, b (m)	Plume Width, w (m)	Aspect Ratio, w/b	Heat Release Rate, Q_T (kW)	Balcony Breath, b (m)	Plume Width, w (m)	Aspect Ratio, w/b	Heat Release Rate, Q_T (kW)
1	0.5	1	2	5	5	10	2	1581
2				10				3162
3				15				4743
4		0.8	1.6	5		8	1.6	1581
5				10				3162
6				15				4743
7		0.6	1.2	5		6	1.2	1581
8				10				3162
9				15				4743
10		0.4	0.8	5		4	0.8	1581
11				10				3162
12				15				4743
13		0.2	0.4	5		2	0.4	1581
14				10				3162
15				15				4743
16		1	1.3	5	4	10	1.3	1581
17				10				3162
18				15				4743
19	0.3	0.8	2.7	5	3	8	2.7	1581
20				10				3162
21				15				4743
22		0.6	2	5		6	2	1581
23				10				3162
24				15				4743
25		0.4	1.3	5		4	1.3	1581
26				10				3162
27				15				4743
28		0.2	0.7	5		2	0.7	1581
29				10				3162
30				15				4743
31		1	5	5		10	5	1581
32				10				3162
33				15				4743
34		0.8	4	5		8	4	1581
35				10				3162
36				15				4743
37	0.2	0.6	3	5	2	6	3	1581
38				10				3162
39				15				4743
40		0.4	2	5		4	2	1581
41				10				3162
42				15				4743
43		0.2	1	5		2	1	1581
44				10				3162
45				15				4743
46		1	6.7	5	1.5	10	6.7	1581
47				10				3162
48				15				4743
49		0.8	5.3	5		8	5.3	1581
50				10				3162
51				15				4743
52		0.6	4	5		6	4	1581
53				10				3162
54				15				4743
55	0.15	0.4	2.7	5	1.5	4	2.7	1581
56				10				3162
57				15				4743
58		0.2	1.3	5		2	1.3	1581
59				10				3162
60				15				4743

Not within scope

Table 6. Dimension and heat release rate for scale model and full-scale simulation.

3.6 Modelling Grid Size

Tan's (2009) experimental model characteristic length is as shown in Table 7, calculated using Equation 1. Table 7 shows the tabulation of various characteristic lengths for scale model and full-scale model. As shown in Table 7, using 20mm and 200mm grid for scale model and full-scale model respectively meet the requirement of Equation 3. Using modelling size of 25mm as recommended by Harrison (2009) mentioned in Section 2.3 would unable to meet the criterion stated in Equation 3 for the most stringent case.

$\dot{Q}$ (kW)	5	10	15	1581	3162	4743
$\dot{Q}_c$ (kW)	4	8	12	1264.8	2529.6	3794.4
	Width = 1m			Width = 10m		
z^* (m)	0.02	0.04	0.05	0.24	0.38	0.49
	Width = 0.8m			Width = 8m		
z^* (m)	0.03	0.04	0.06	0.27	0.44	0.57
	Width = 0.6m			Width = 6m		
z^* (m)	0.03	0.05	0.07	0.33	0.53	0.69
	Width = 0.4m			Width = 4m		
z^* (m)	0.04	0.07	0.09	0.44	0.69	0.91
	Width = 0.2m			Width = 2m		
z^* (m)	0.07	0.11	0.14	0.69	1.10	1.44

Table 7. Characteristic length (m) of the scale model and full-scale model.

4. RESULTS

This chapter shows when the temperature readings reached stability so that average values could be computed for comparison with experimental record from Tan (2009). The simulated temperature at the spill edge was also compared with Harrison's (2009) experimental records to determine whether the grid size is optimal to model the spill plume.

Subsequently, the FDS output was compared with Tan's (2009) experimental records. Results from full-scale models with and without upstand configurations are presented. Finally, the full-scale model with seven balcony configuration is presented.

4.1 Stability of Temperature Reading

Figure 40 and Figure 41 show the temperature-time history from FDS for small-scale models S03E and S19E, which represent the small-scale experiments from Tan (2009). One temperature reading from each balcony is selected for demonstration and the temperatures are from the balcony edge. From these figures, they show that temperature stability is achieved after 100s. Hence, average temperatures and peak temperatures are determined after 100s for all scale model simulation.

Figure 42 and Figure 43 show the temperature-time history from FDS for full-scale models F03E5 and F19E5. Similarly, one temperature reading from each balcony is selected for demonstration and the temperatures are from the balcony edge. From these figures, they show that temperature stability is achieved after 200s.

Equation 12 states the time relationship between scale and full-scale models. Using this equation, the equivalent time for full-scale model to achieve stability is three times of scale model, which is 300s. However using the temperature prediction from FDS, the full-scale model achieves temperature stability after 200s; this could be due to the subjective assessment of time to reach temperature stability. Hence, average temperature and peak temperature are determined after 200s for all full-scale model simulation.

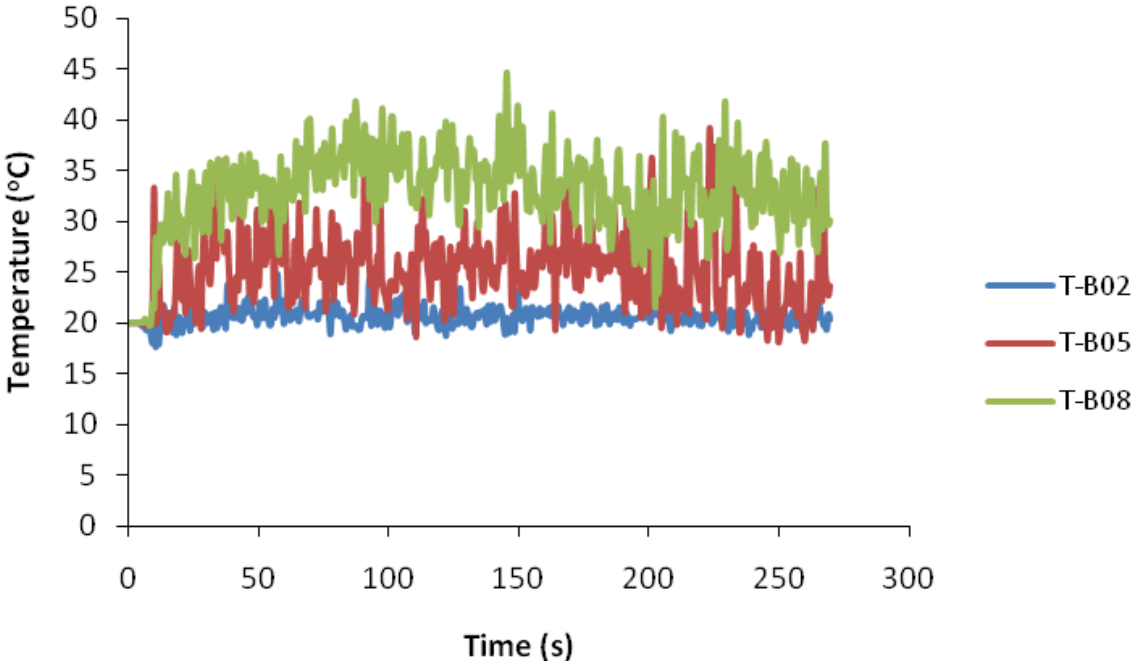

Figure 40. Temperature prediction from FDS on scale model S03E.

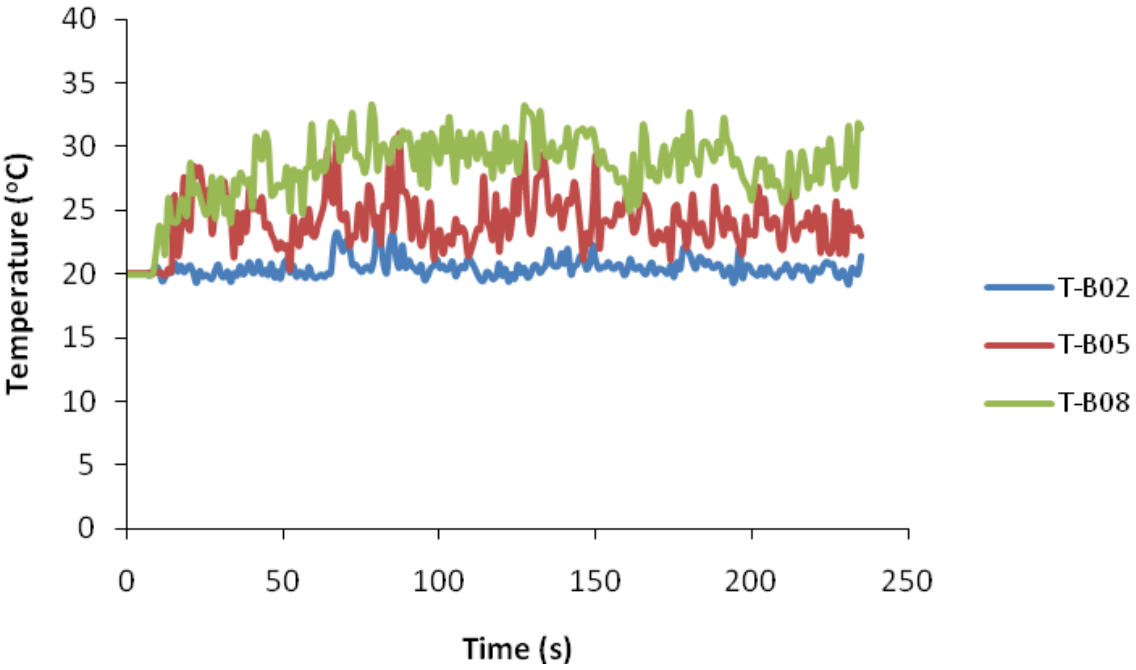

Figure 41. Temperature prediction from FDS on scale model S19E.

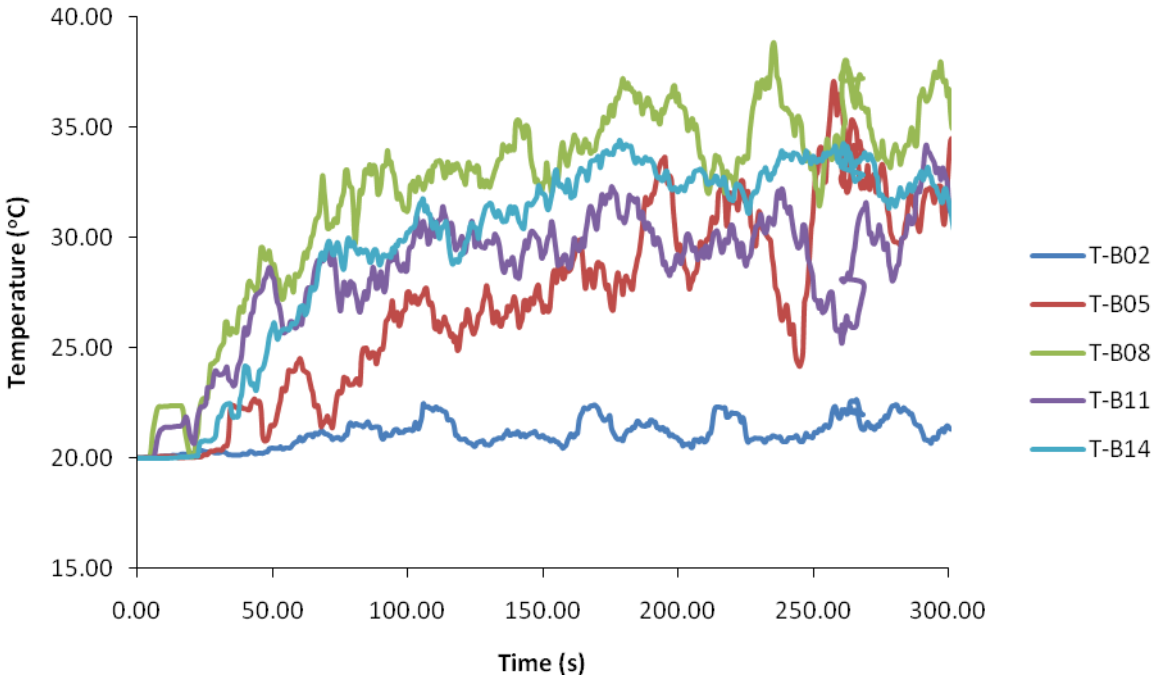

Figure 42. Temperature prediction from FDS on full-scale model F03E5.

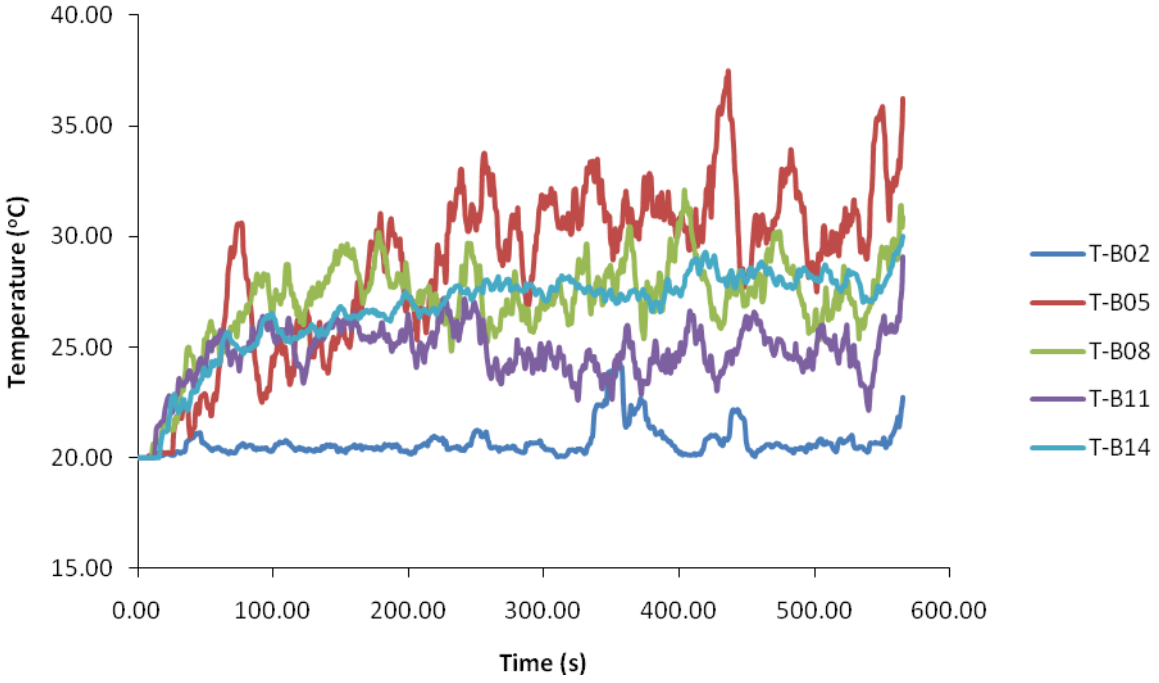

Figure 43. Temperature prediction from FDS on full-scale model F19E5.

4.2 Comparing with Harrison's (2009) Experimental Record

Three scale-model FDS outputs are analysed and compared with Harrison's (2009) experiments records of the temperature profile below the spill edge. The model's grid size is 20mm as Harrison (2009) suggested 25mm for his modelling of the experiment and the comparison are shown in Figure 44 to Figure 46. The comparison shows that the simulated results closely resemble the experimental data, hence, the simulation resolution is in the right order of magnitude, i.e. 20mm and 200mm grid size will be used for scale model and full-scale model respectively.

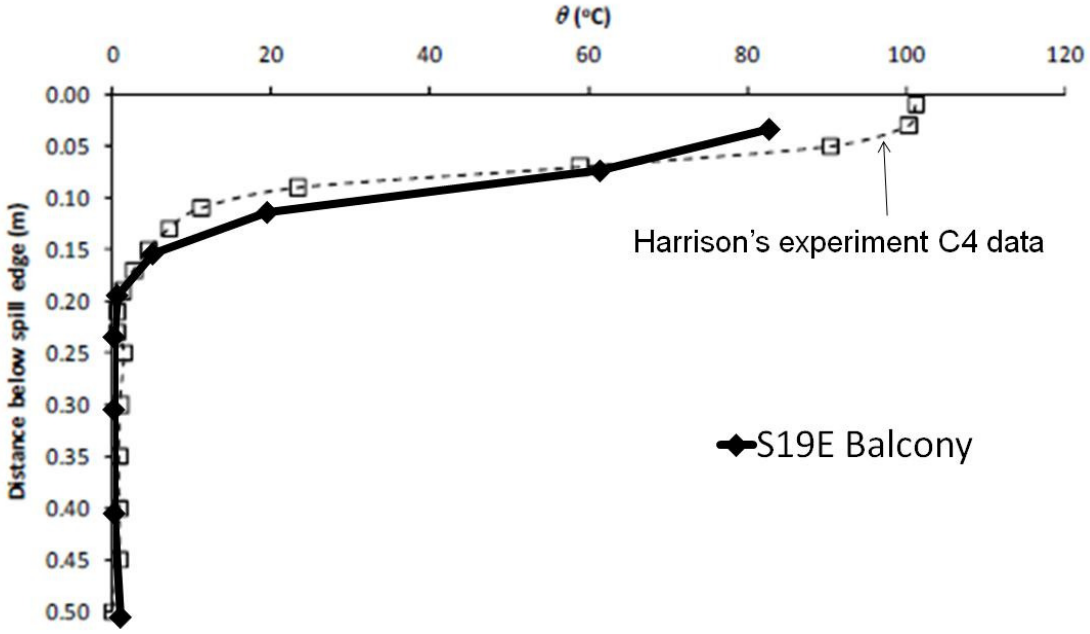

Figure 44. FDS output compared with Harrison's experimental data.

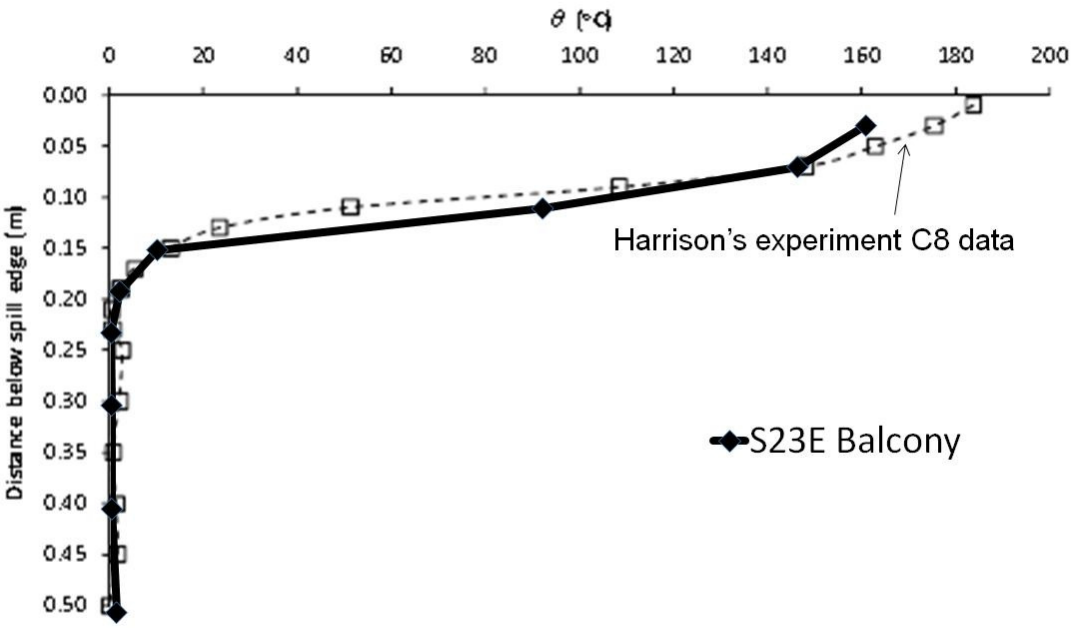

Figure 45. FDS output compared with Harrison's experimental data.

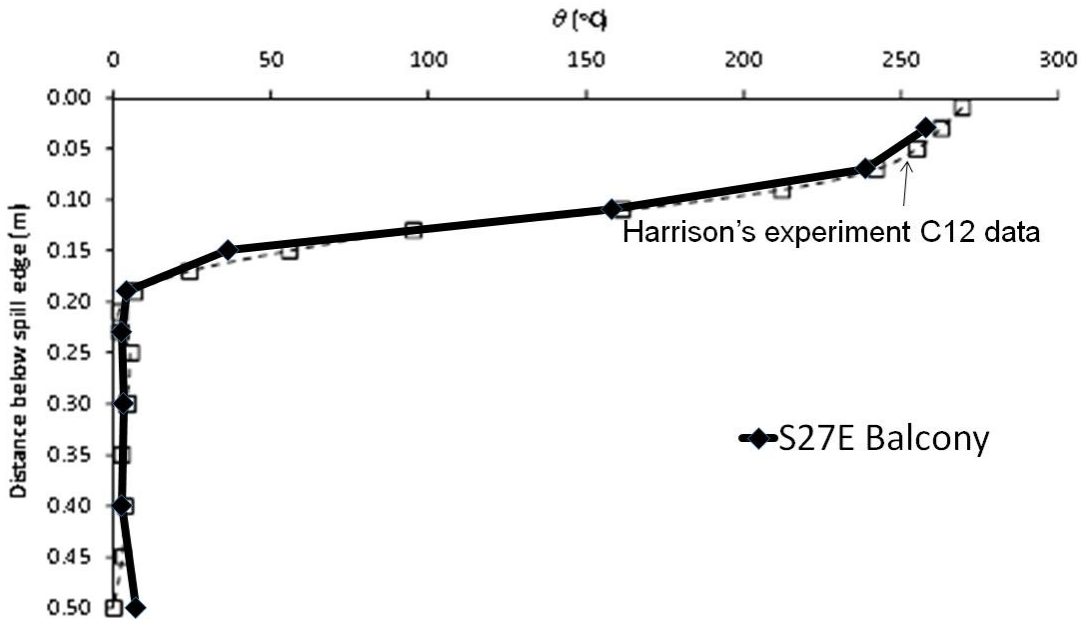

Figure 46. FDS output compared with Harrison's experimental data.

4.3 Comparing with Tan's (2009) Experimental Record

The twelve primary scenarios were simulated and compared with Tan's (2009) experimental record. In general, the predicted temperatures are lower as compared with the experimental record. Two scenarios (S01E and S03E) out of twelve primary scenarios predicted temperatures are much lower than the experimental record. A typical temperature profile (comparing with Experiment 19) across balcony edge is shown in Figure 47. As shown in Figure 47, the experiment result is bounded by the simulation average and simulation maximum (or peak) temperature. Figure 48 shows the temperature profile along the balcony breadth which also demonstrated a similar profile and the average simulated temperature is lower than the experimental record.

Tan (2009) used a 10°C above ambient condition (i.e. 30°C) as one of the criteria to assess smoke contamination; this approach was investigated to evaluate the FDS simulation. Figure 49 compares the simulation temperature profile (FDS slice file) at 25°C and 30°C, compared with Tan's (2009) photographic record. It shows that the 30°C profile closely resembles the photographic record. In other words, it is possible to use the 30°C temperature profile to determine the amount of smoke contamination in the balcony. Out of the twelve primary scenarios, two models (S01E and S03E) have a 25°C temperature profile closer to the photographic records. Using this approach, the simulation shows more contamination than Tan's (2009) experiment findings. Hence, the conclusion is that 30°C profile (slice file) in lieu of the temperature profiles across the balcony edge and along the balcony breadth can be used to determine the smoke contamination at the various levels. All twelve primary scenarios simulation results are shown in Appendix C. The summary result is shown in Table 8 and the parameters in "brackets" are for the equivalent full-scale simulation.

These twelve primary scenarios simulation results have shown that FDS could reasonably model the smoke contamination, although predicted temperatures are usually lower, in line with Harrison's (2009) findings. Hence, with the assessment of smoke contamination using FDS slice file for 30°C, the simulation was extended to a full-scale five balcony configuration. For direct comparison with the full-scale five balcony configuration, the small-scale model was also extended to five balcony configuration.

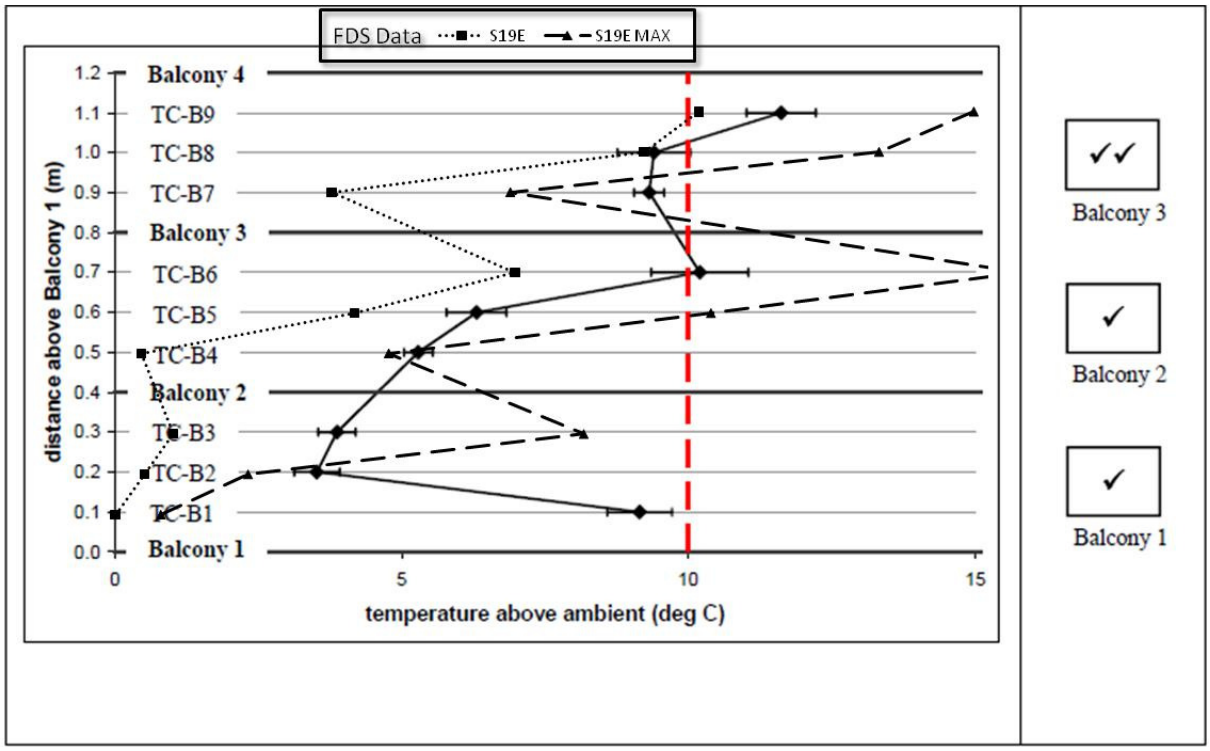

Figure 47. Temperature profiles across balcony edge from FDS and Tan's experiment 19.

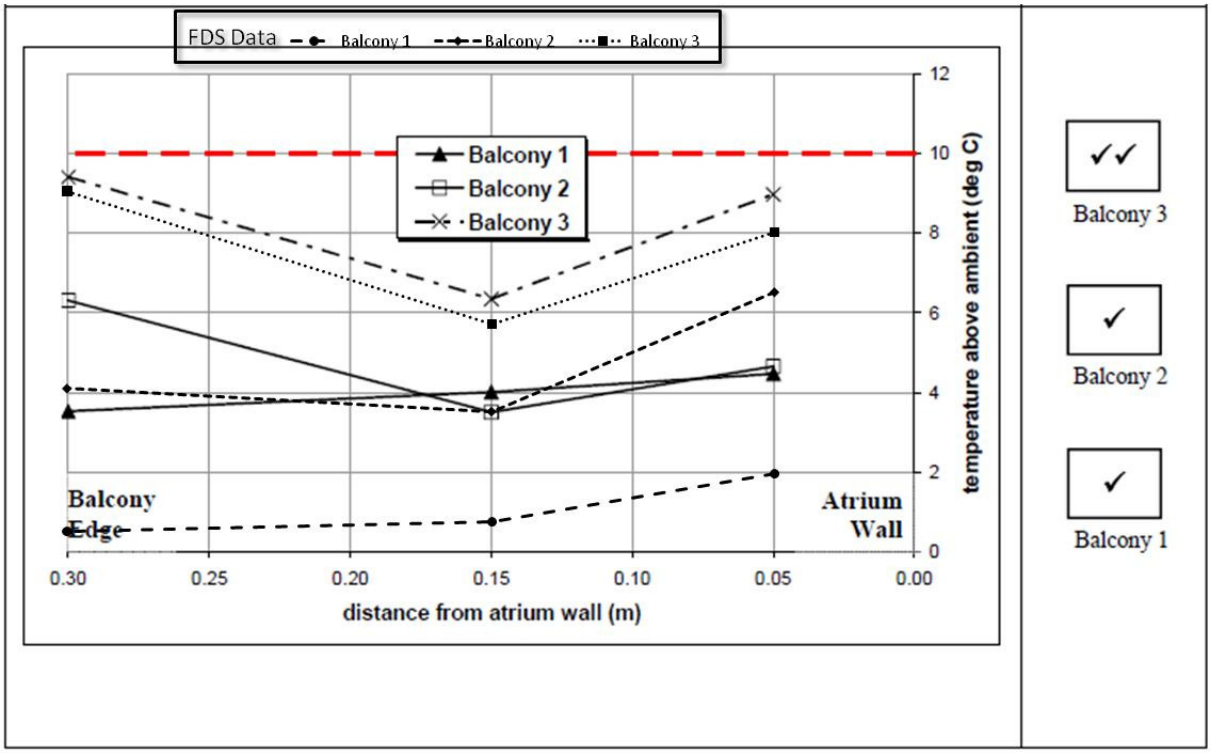

Figure 48. Temperature profiles along balcony breadth from FDS and Tan's experiment 19.

Experiment No.	=	19	
Balcony Breadth	=	300	mm
Plume Width	=	800	mm
Heat Release Rate	=	5	kW

Balcony Level	Photograph
3	
2	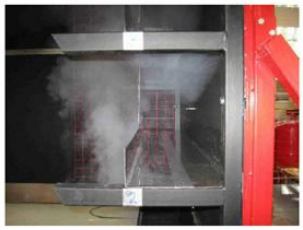
1	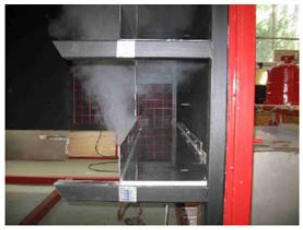

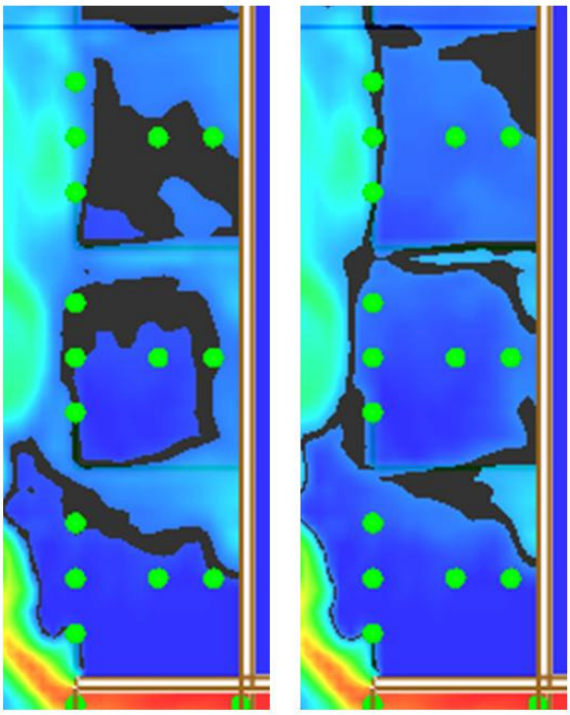

Figure 49. Temperature profile and Tan's experiment 19 photographic records.

					Full-Scale Simulation				
					Tan (2009) Experiment & Small Scale Simulation				
Experiment or Simulation	Balcony Breath, b (m)	Plume Width, w (m)	Aspect Ratio, w/b	Heat Release Rate, Q_T (kW)	Balcony 1	Balcony 2	Balcony 3	Balcony 4	Balcony 5
1	0.5 (5)	1 (10)	2	5 (1581)	▪•	■●	■●	●	●
2				10 (3162)	•	●	●	●	●
3				15 (4746)	▪•	■●	■●	●	●
4		0.8 (8)	1.6	5 (1581)	•	●	●	●	●
5				10 (3162)	•	●	●	●	●
6				15 (4746)	•	●	●	●	●
7		0.6 (6)	1.2	5 (1581)	•	●	●	●	●
8				10 (3162)	□•	□•	▪●	●	●
9				15 (4746)	•	•	•	•	●
10		0.4 (4)	0.8	5 (1581)	○	•	•	•	●
11				10 (3162)	○	○	•	•	●
12				15 (4746)	○	•	•	•	●
13		0.2 (2)	0.4	5 (1581)	□○	□○	□○	○	•
14				10 (3162)	○	○	○	○	●
15				15 (4746)	○	○	•	•	●
16	0.3 (3)	1 (10)	3.3	5 (1581)					
17				10 (3162)					
18				15 (4746)					
19		0.8 (8)	2.7	5 (1581)	▪●	▪●	■●	●	●
20				10 (3162)	●	●	●	●	●
21				15 (4746)	●	●	●	●	●
22		0.6 (6)	2	5 (1581)	•	●	●	●	●
23				10 (3162)	□•	▪●	■●	●	●
24				15 (4746)	•	●	●	●	●
25		0.4 (4)	1.3	5 (1581)	•	•	●	●	●
26				10 (3162)	•	•	●	●	●
27				15 (4746)	□○	□•	▪•	●	●
28		0.2 (2)	0.7	5 (1581)	○	○	○	•	●
29				10 (3162)	○	○	•	•	●
30				15 (4746)	○	•	•	•	●
31	0.2 (2)	1 (10)	5	5 (1581)					
32				10 (3162)					
33				15 (4746)					
34		0.8 (8)	4	5 (1581)					
35				10 (3162)					
36				15 (4746)					
37		0.6 (6)	3	5 (1581)	●	●	●	●	●
38				10 (3162)	▪•	▪●	■●	●	●
39				15 (4746)	●	●	●	●	●
40		0.4 (4)	2	5 (1581)	•	●	●	●	●
41				10 (3162)	□•	□•	▪●	●	●
42				15 (4746)	•	●	●	●	●
43		0.2 (2)	1	5 (1581)	□○	□○	▪•	•	●
44				10 (3162)	○	•	•	●	●
45				15 (4746)	○	•	•	●	●
46	0.15 (1.5)	1 (10)	6.7	5 (1581)					
47				10 (3162)					
48				15 (4746)					
49		0.8 (8)	5.3	5 (1581)					
50				10 (3162)					
51				15 (4746)					
52		0.6 (6)	4	5 (1581)					
53				10 (3162)					
54				15 (4746)					
55		0.4 (4)	2.7	5 (1581)	•	●	●	●	●
56				10 (3162)	▪•	■●	■●	●	●
57				15 (4746)	•	●	●	●	●
58		0.2 (2)	1.3	5 (1581)	○	○	•	•	●
59				10 (3162)	○	○	•	•	●
60				15 (4746)	□○	□○	▪•	●	●
					Experiment Result	Small Scale Simulation	Full-scale Simulation		
		Not within scope		Clear		□	○		
				Shallow smoke layer		▪	•		
				Deep smoke layer		■	●		

Table 8. Smoke contamination assessment from FDS and comparison with Tan's (2009) experimental result.

4.4 Smoke Layer Depth at Spill Edge

Tan (2009) has assessed smoke layer depth at the spill edge using Harrison's (2009) data as the fire size and fire compartment were similar. Table 9 shows the tabulation of the smoke layer depth from FDS prediction and Tan's (2009) data. It shows that the prediction and experimental data are relatively close.

Experiment			**FDS's Depth Prediction (m)**
Plume Width, w (m)	Heat Release Rate, $\dot{Q}$ (kW)	Depth, d (m)	
1	5	0.100	S01E (0.07)
	10	0.155	
	15	0.125	S03E (0.09)
0.8	5	0.105	S19E (0.10)
	10	0.115	
	15	0.135	
0.6	5	0.110	
	10	0.120	S08E (0.10), S23E (0.11) & S38E (0.13)
	15	0.140	
0.4	5	0.115	
	10	0.125	S41E (0.13) & S56E (0.14)
	15	0.145	S27E (0.11)
0.2	5	0.135	S13E (0.12) & S43E (0.13)
	10	0.155	
	15	0.170	S60E (0.15)

Table 9. Depth of smoke layer at spill edge.

4.5 Full-scale Five Balcony Configuration

A two phase approach was used to model the full-scale five balcony configuration. The first phase used the twelve primary scenarios (described previously) for assessment. The second phase attempted to model as many as possible configurations similar to Tan's (2009) work. Figure 50 and Figure 51 show the same experiment model mentioned in the Section 4.3 for

the full-scale model. Figure 50 shows the full-scale model has predicted a higher peak temperature value. Figure 50 shows the peak temperature is much higher than ambient, hence, heavy contamination could be expected at the balcony immediately above the spill edge. Figure 51 also demonstrated a “V” shape temperature profile along the balcony breadth. It could be implied that the model predicted the smoke reached the atrium wall and slid downward, which has a similar profile as Figure 52. Appendix D shows the simulation result for all full-scale five balcony configuration. Moreover, the full-scale simulation models also show more balcony contaminations, as shown in Table 8. The higher peak temperature of the full-scale model could also lead to more smoke contamination.

The height of contamination assessment is carried out by estimation of smoke level using the 30°C slice file as shown in Figure 52. Each storey is 4m, using a "ruler" for visual assessment, the smoke level height above the spill edge is determined.

Figure 53 shows a direct comparison of the temperature prediction for small-scale and full-scale five balcony configuration. The vertical axis of Figure 53 has been normalised to the maximum height so that both graphs could be plotted together for comparison. The profile for the average temperature and peak temperatures value are similar. The variation between the small-scale and full-scale simulation could be due to the limitation of scale modelling, i.e. the radiation and conduction effects are different. Another reason could be the higher turbulence flow of the full-scale model, which has higher velocity prediction and hence, higher Reynolds number. Appendix E shows the comparison of the twelve primary scenarios simulation temperature predictions for small-scale and full-scale models. The Appendix also includes the smoke layer height measurement for the small-scale five balcony configuration.

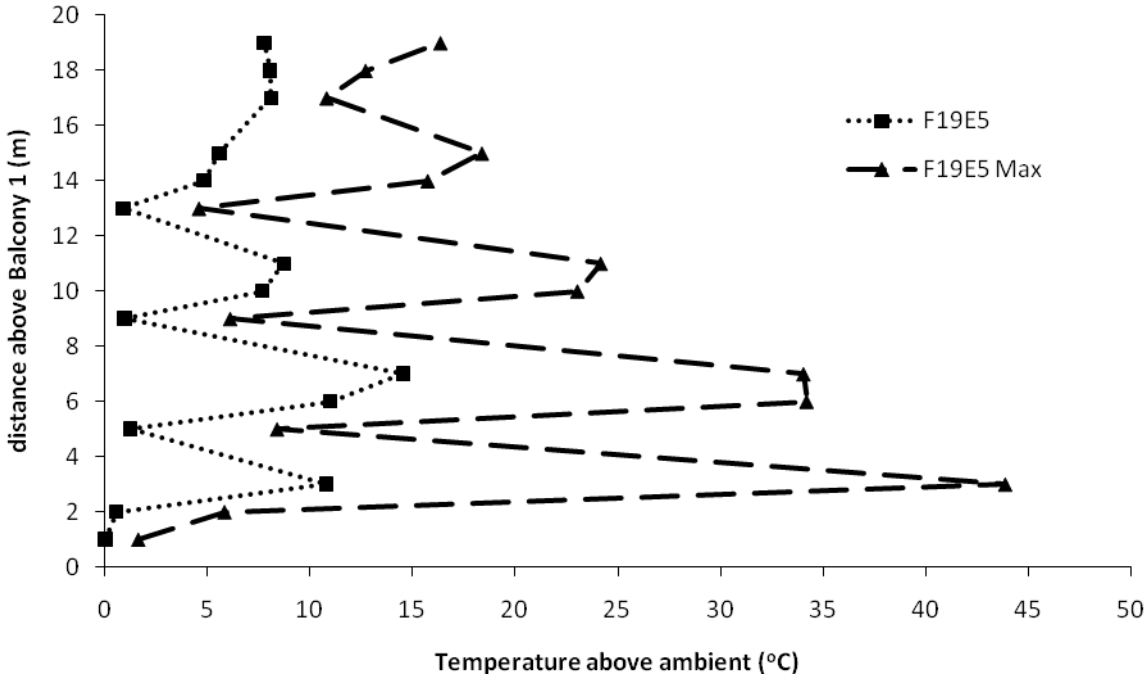

Figure 50. Temperature profiles across balcony edge.

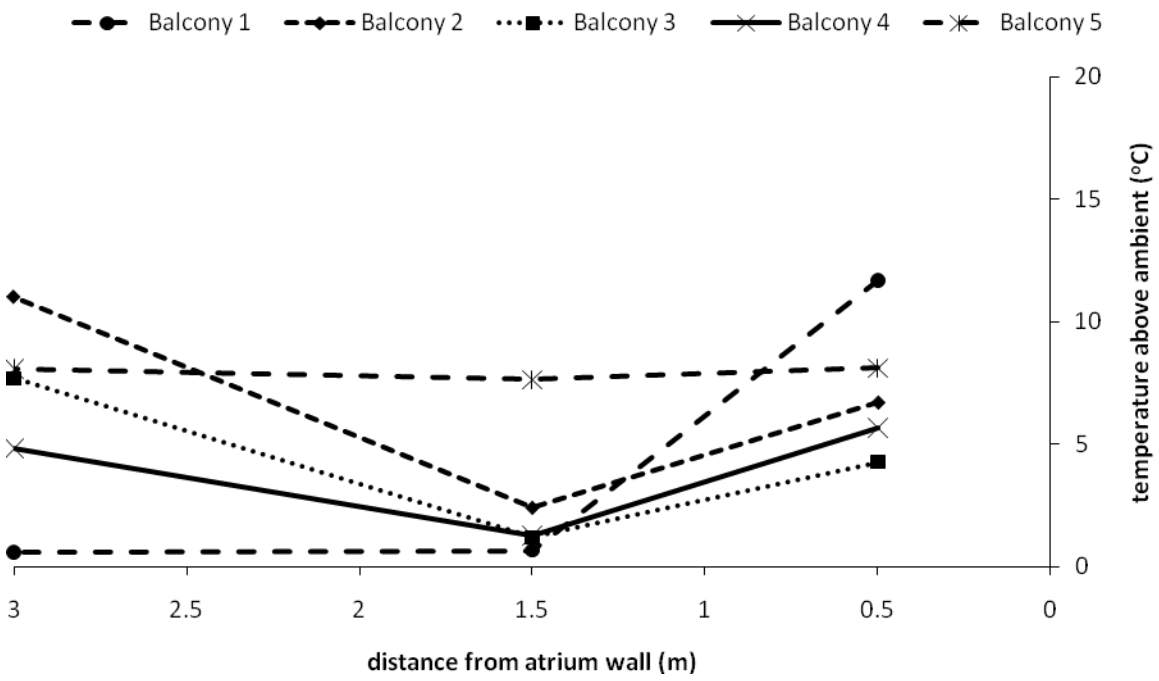

Figure 51. Temperature profiles along balcony breadth.

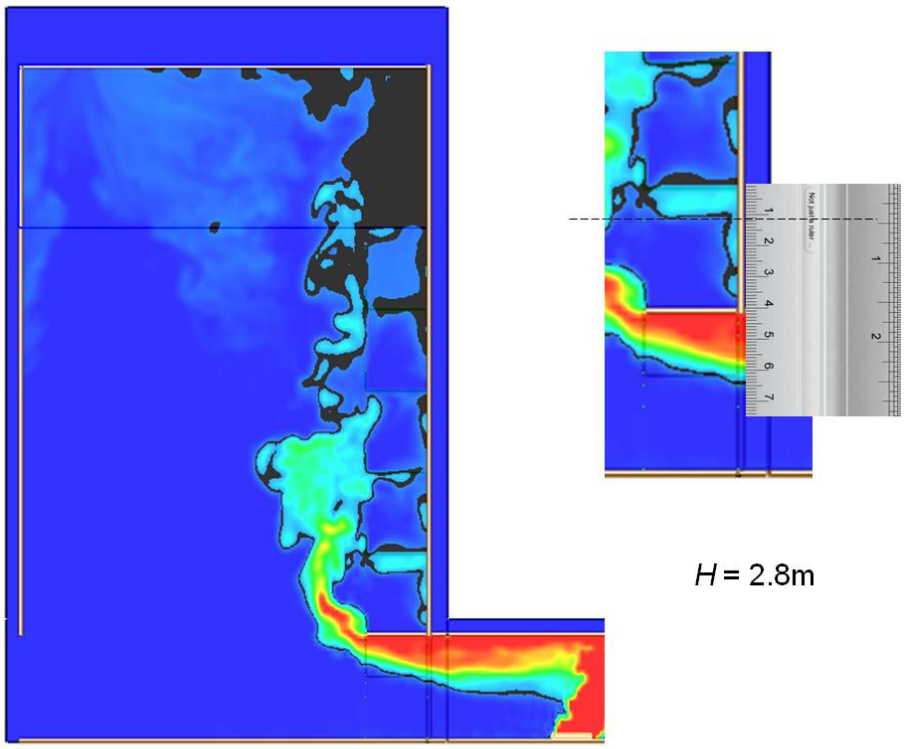

Figure 52. Smoke layer height measurement.

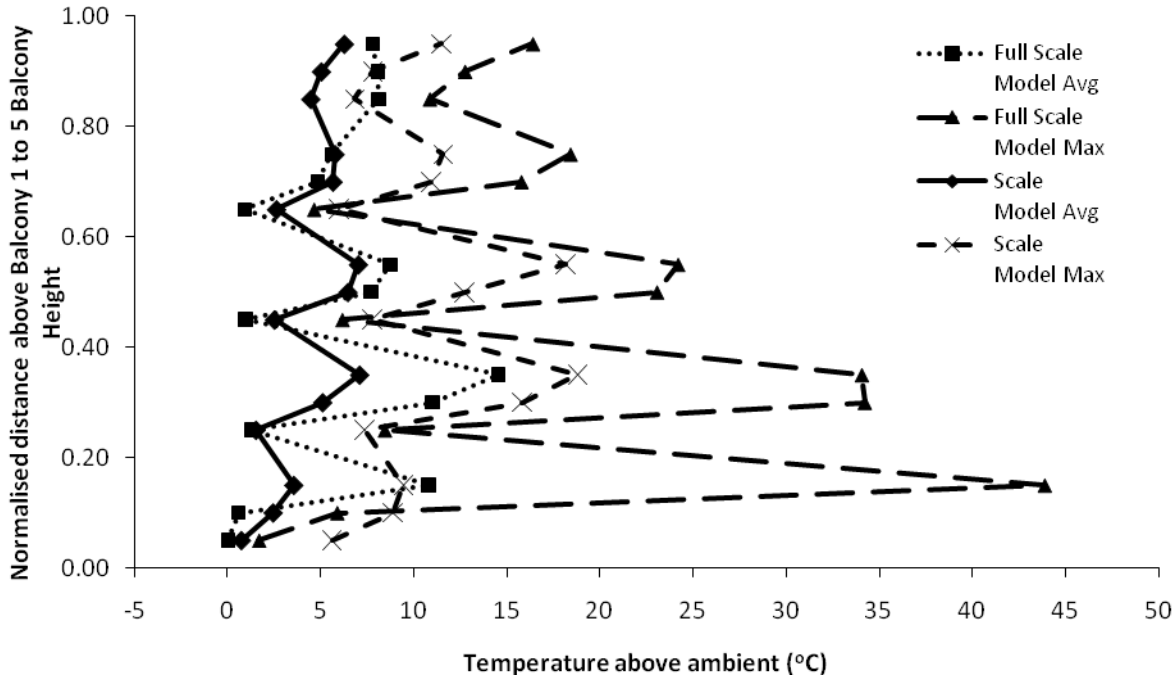

Figure 53. Comparing small scale (S19E5) and full scale (F19E5) simulation results.

4.6 Smokeview's Smoke Visualisation and Temperature Profile

Forney (2007) has stated that Smokeview could visualise smoke realistically by converting soot density to smoke opacity. Forney explained the goal of Smokeview was to display smoke as it actually appears to an observer. For the five balcony configuration twelve primary scenarios full-scale models, Smokeview's smoke output are compared with the temperature profile from the slice files using the same or a similar time frame. Three temperature profiles are selected, 25°C, 30°C and 35°C. Figure 54 shows the comparison for F19E5 and it shows that the 30°C temperature profile resembles the Smokeview's smoke. All the twelve primary scenarios results comparisons are shown in Appendix F and all of them show that the 30°C temperature profile resemble the smoke. This also reinforced the methodology of using 30°C temperature profile to assess the smoke layer height for the full-scale model.

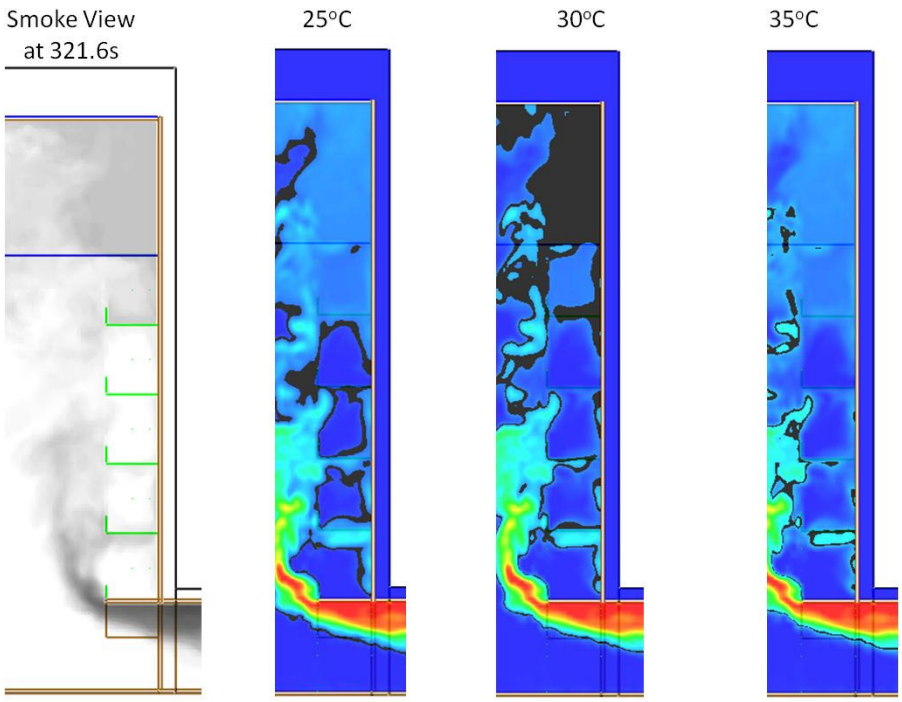

Figure 54. Smokeview and temperature profile for F19E5.

4.7 Model with No Upstand Configuration

It is generally observed there is more smoke contamination within the balcony for model with no upstand. Figure 55 to Figure 57 show the simulation result for model F19E5NUS. All results for the twelve primary scenarios are shown in Appendix G. Comparing Figure 52 and

Figure 57, it is obvious that the model without upstand has deeper smoke contamination. Figure 58 shows the average temperature across the balcony edge shows some difference for model with and without upstand. Out of the twelve primary scenarios models selected for study, most of them have similar average temperature across the balcony edge as shown in Figure 59. All comparisons for the simulations are shown in Appendix H. Table 10 shows the summary of smoke contamination for models without upstand. Table 11 is re-produced to show the twelve primary scenarios models selected for comparison on smoke contamination. Comparing Table 10 and Table 11, it is obvious that models without upstand will have lower smoke contamination height and more severe smoke contamination.

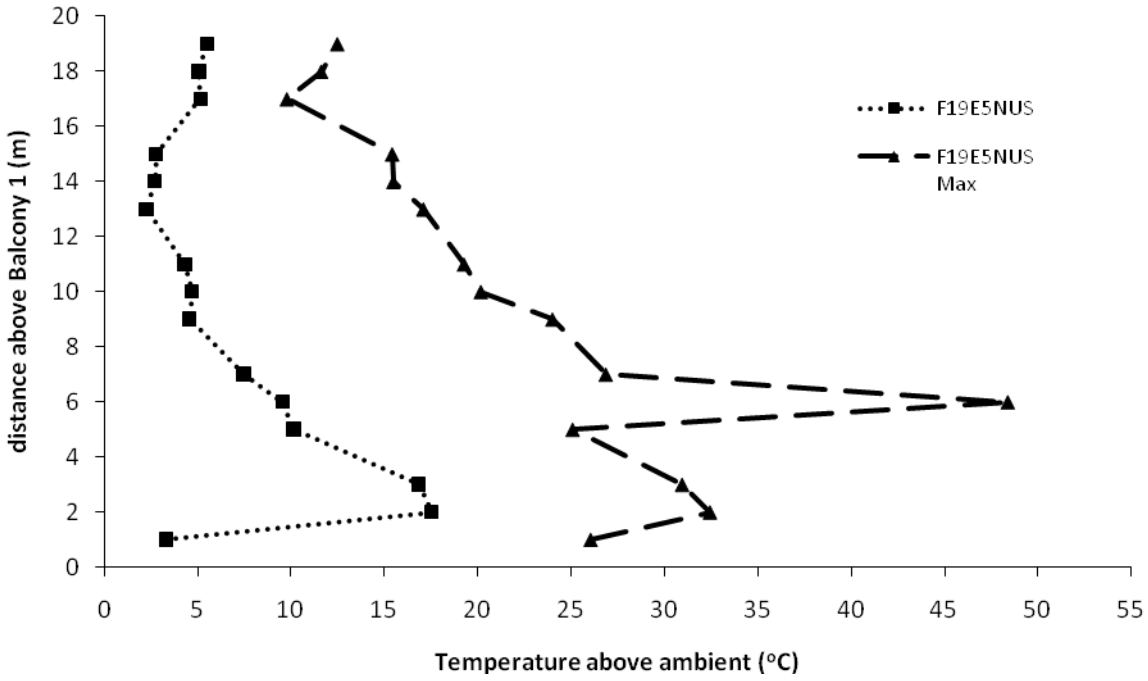

Figure 55. Temperature profiles across balcony edge.

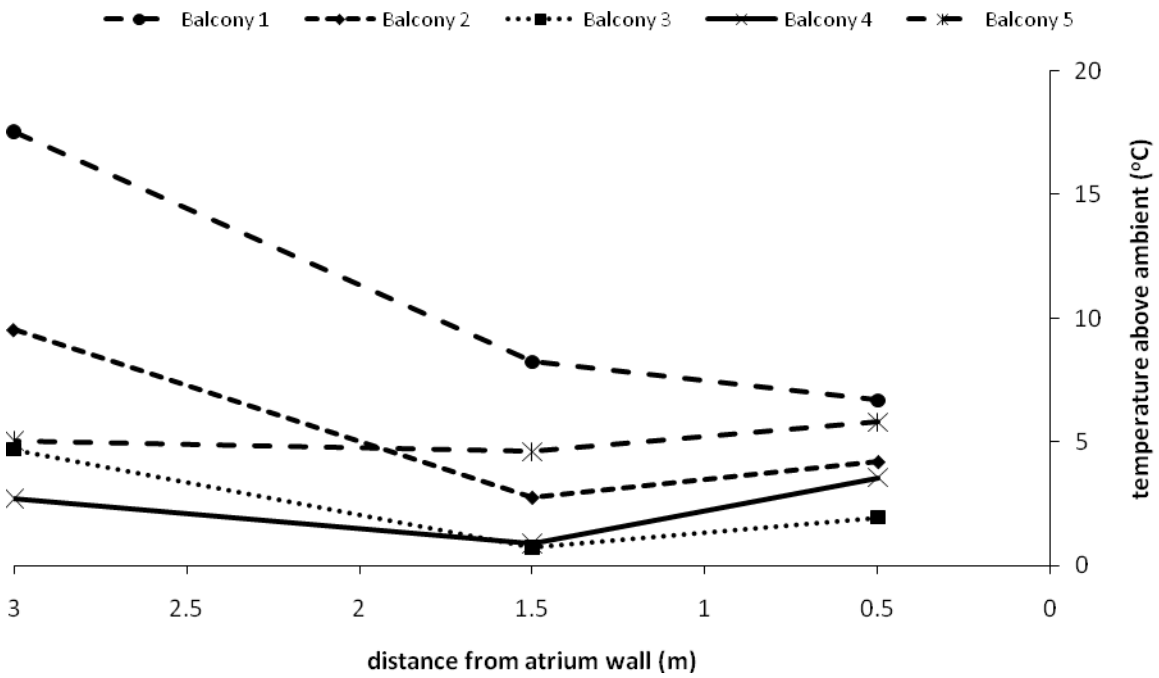

Figure 56. Temperature profiles along balcony breadth.

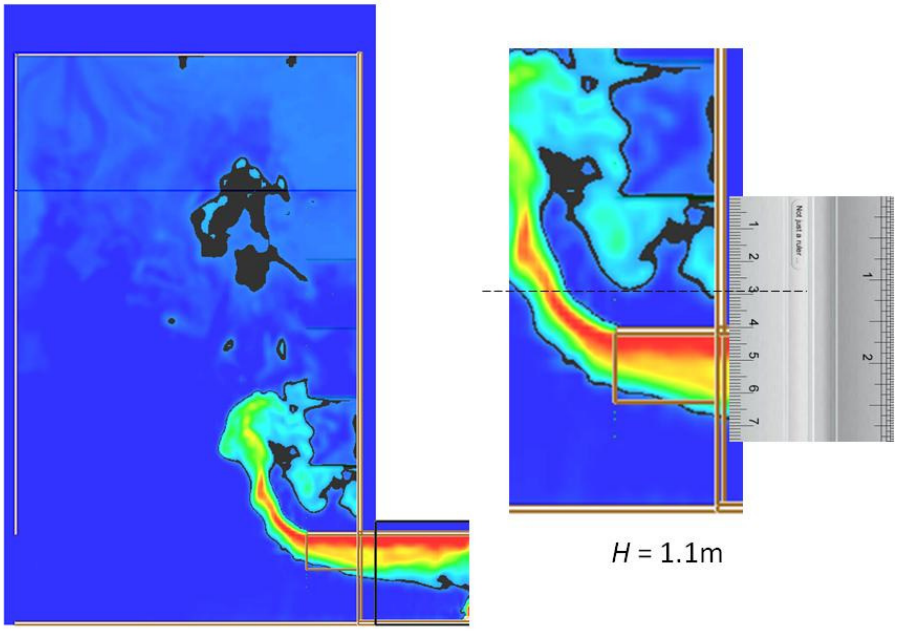

Figure 57. Smoke layer height measurement.

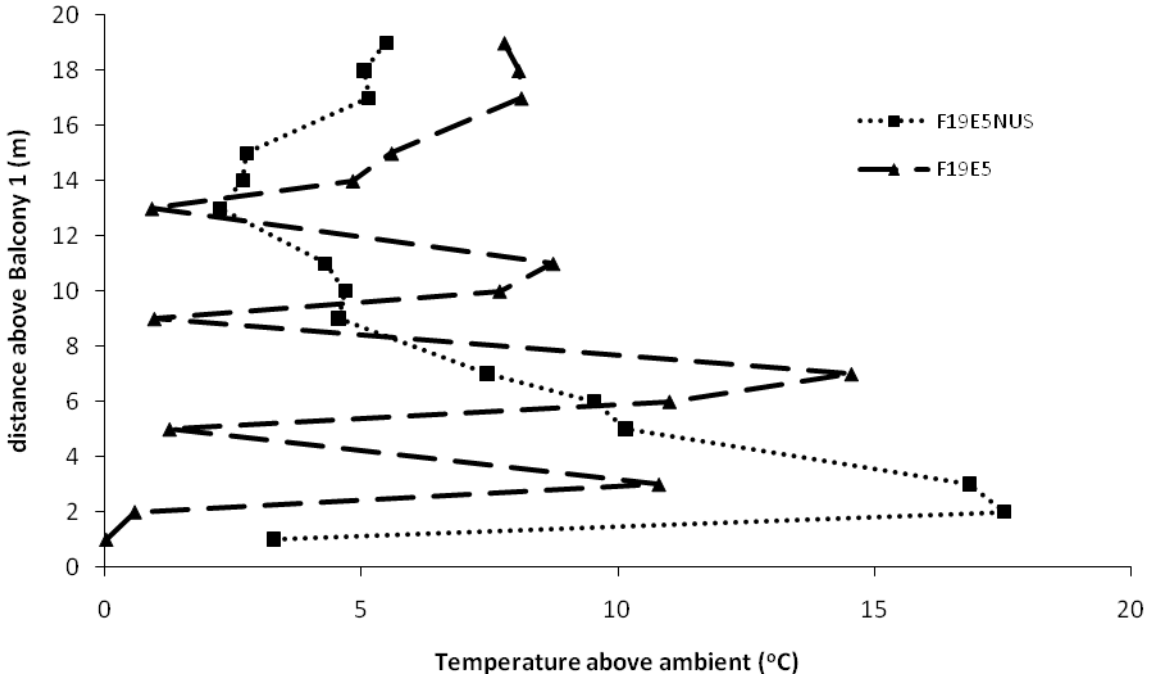

Figure 58. Comparing of F19E5 and F19E5NUS for temperature profile across balcony edge.

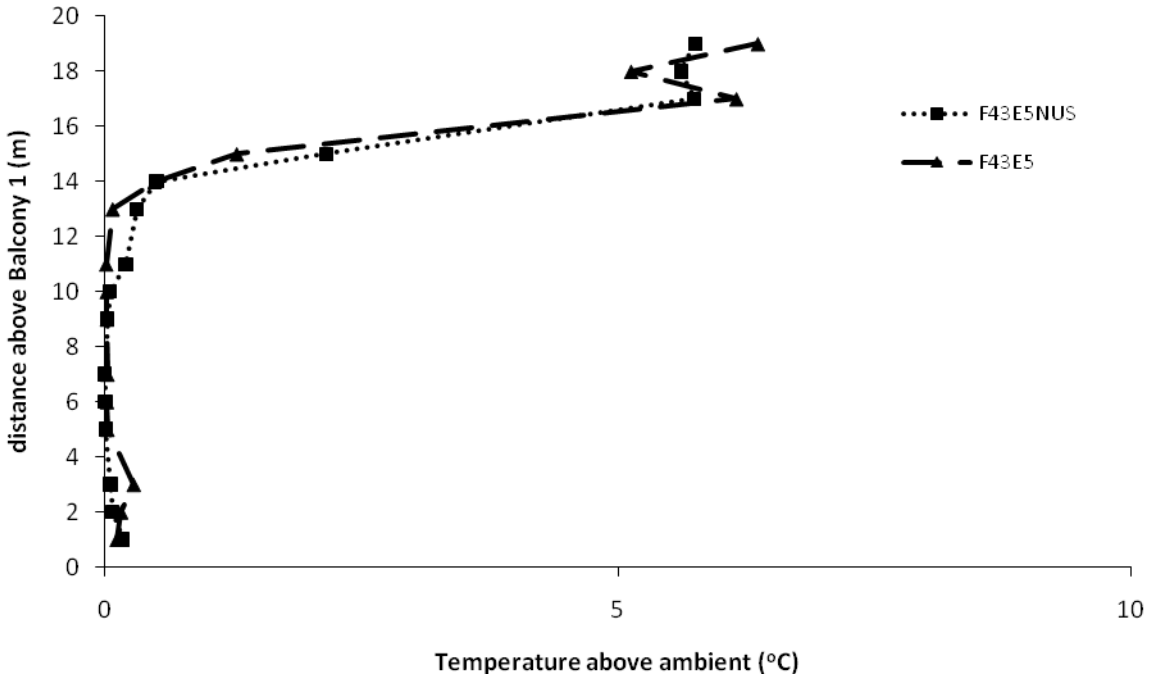

Figure 59. Comparing of F43E5 and F43E5NUS for temperature profile across balcony edge.

Simulation	Balcony Breath, b (m)	Plume Width, w (m)	Aspect Ratio, w/b	Heat Release Rate, Q_T (kW)	Balcony 1	Balcony 2	Balcony 3	Balcony 4	Balcony 5
1	5	10	2	1581	●	●	●	●	●
3	5	10	2	3162	●	●	●	●	●
8	5	6	1.2	4746	●	●	●	●	●
13	5	2	0.4	1581	○	○	○	○	•
19	3	8	2.7	1581	●	●	●	●	●
23	3	6	2	3162	●	●	●	●	●
27	3	4	1.3	4746	•	●	●	●	●
38	2	6	3	3162	●	●	●	●	●
41	2	4	2	3162	●	●	●	●	●
43	2	2	1	1581	○	○	●	●	●
56	1.5	4	2.7	3162	●	●	●	●	●
60	1.5	2	1.3	4746	○	•	●	●	●
					Full-scale Simulation				
				Clear	○				
				Shallow smoke layer	•				
				Deep smoke layer	●				

Table 10. Summary of smoke contamination for simulation without upstand.

Simulation	Balcony Breath, b (m)	Plume Width, w (m)	Aspect Ratio, w/b	Heat Release Rate, Q_T (kW)	Balcony 1	Balcony 2	Balcony 3	Balcony 4	Balcony 5
1	5	10	2	1581	•	●	●	●	●
3	5	10	2	3162	•	●	●	●	●
8	5	6	1.2	4746	•	•	●	●	●
13	5	2	0.4	1581	○	○	○	○	•
19	3	8	2.7	1581	●	●	●	●	●
23	3	6	2	3162	•	●	●	●	●
27	3	4	1.3	4746	○	•	•	●	●
38	2	6	3	3162	•	●	●	●	●
41	2	4	2	3162	•	•	●	●	●
43	2	2	1	1581	○	○	•	•	●
56	1.5	4	2.7	3162	•	●	●	●	●
60	1.5	2	1.3	4746	○	○	•	●	●
					Full-scale Simulation				
				Clear	○				
				Shallow smoke layer	•				
				Deep smoke layer	●				

Table 11. Re-produced summary of smoke contamination for full-scaled model with upstands.

4.8 Model for Seven Balcony Configuration

The simulation results show that the balcony smoke contamination for full-scale seven balcony configuration is more severe than the full-scale five balcony configuration at a low level. The twelve primary scenarios models simulation results are shown in Appendix I. Figure 60 shows the similarity of temperature profile across the balcony edge for the full-scale five and seven balcony configurations. Table 12 shows the summary of smoke contamination for the full-scale seven balcony configuration. Comparing Table 11 and Table 12, the smoke contamination heights are lower and more severe for the seven balcony configuration.

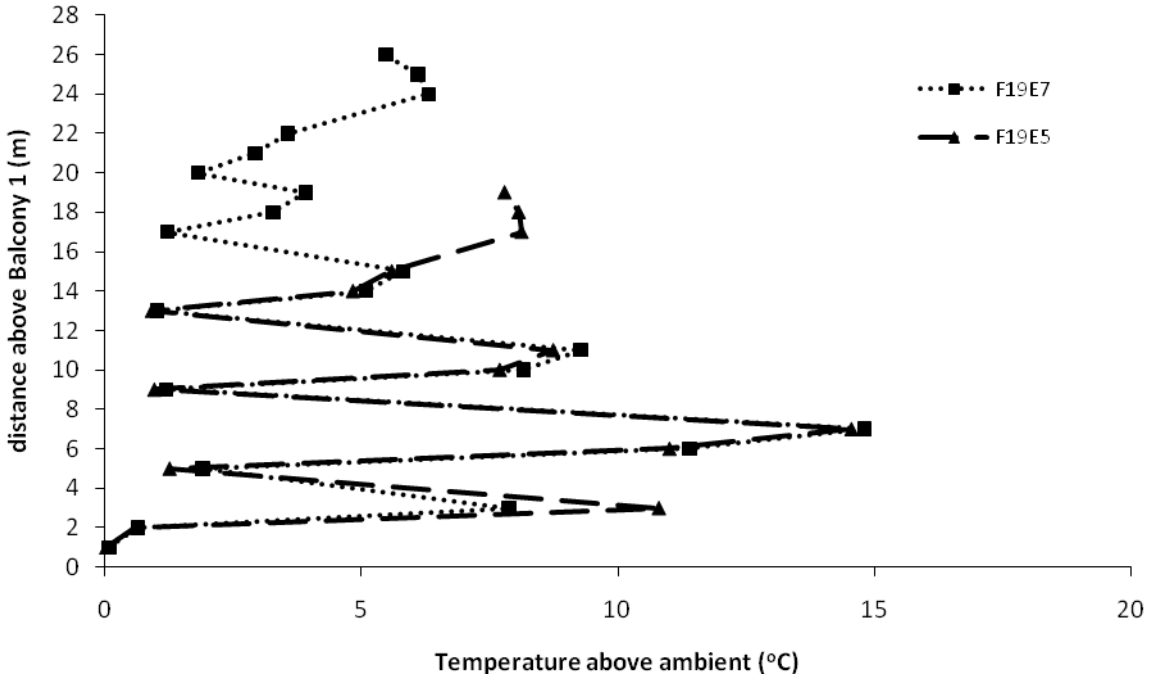

Figure 60. Comparing of F19E5 and F19E7 for temperature profile across balcony edge.

Case	Balcony Breath, b (m)	Plume Width, w (m)	Aspect Ratio, w/b	Heat Release Rate, Q_T (kW)	Balcony 1	Balcony 2	Balcony 3	Balcony 4	Balcony 5	Balcony 6	Balcony 7
1	5	10	2	1581	●	●	●	●	●	●	●
3	5	10	2	3162	●	●	●	●	●	●	●
8	5	6	1.2	4746	•	•	●	●	●	●	●
13	5	2	0.4	1581	○	○	○	○	○	○	○
19	3	8	2.7	1581	●	●	●	●	●	●	●
23	3	6	2	3162	•	●	●	●	●	●	●
27	3	4	1.3	4746	•	●	●	●	●	●	●
38	2	6	3	3162	●	●	●	●	●	●	●
41	2	4	2	3162	•	●	●	●	●	●	●
43	2	2	1	1581	○	○	•	•	●	●	●
56	1.5	4	2.7	3162	●	●	●	●	●	●	●
60	1.5	2	1.3	4746	○	•	●	●	●	●	●

	Full-scale Simulation
Clear	○
Shallow smoke layer	•
Deep smoke layer	●

Table 12. Summary of smoke contamination for simulation on full-scale seven balcony configuration.

4.9 Comparing Scaled Three Storey and Scaled Five Balcony Configuration

The previous section highlighted there are smoke contamination differences between five and seven balcony configurations. Hence, the contamination for the small-scale three and five balcony configurations should be compared. Table 13 and Table 14 show the simulation results for the scaled three and five balcony configurations respectively. From both figures, they show more contamination and the severity also increased when the model became taller, and this is consistent with observation in the previous section.

Simulation	Balcony Breath, b (m)	Plume Width, w (m)	Aspect Ratio, w/b	Heat Release Rate, Q_T (kW)	Balcony 1	Balcony 2	Balcony 3	Balcony 4	Balcony 5
1	5	10	2	1581	▪	■	■		
3	5	10	2	3162	▪	■	■		
8	5	6	1.2	4746	□	□	▪		
13	5	2	0.4	1581	□	□	□		
19	3	8	2.7	1581	▪	▪	■		
23	3	6	2	3162	□	▪	■		
27	3	4	1.3	4746	□	□	▪		
38	2	6	3	3162	▪	▪	■		
41	2	4	2	3162	□	□	▪		
43	2	2	1	1581	□	□	▪		
56	1.5	4	2.7	3162	▪	■	■		
60	1.5	2	1.3	4746	□	□	▪		
					Small Scale Simulation				
				Clear	□				
				Shallow smoke layer	▪				
				Deep smoke layer	■				

Table 13. Simulation result for scaled three balcony configuration (from models "S*XX*E").

Simulation	Balcony Breath, b (m)	Plume Width, w (m)	Aspect Ratio, w/b	Heat Release Rate, Q_T (kW)	Balcony 1	Balcony 2	Balcony 3	Balcony 4	Balcony 5
1	5	10	2	1581	•	●	●	●	●
3	5	10	2	3162	●	●	●	●	●
8	5	6	1.2	4746	○	•	•	●	●
13	5	2	0.4	1581	○	○	○	○	○
19	3	8	2.7	1581	●	●	●	●	●
23	3	6	2	3162	•	●	●	●	●
27	3	4	1.3	4746	○	•	•	●	●
38	2	6	3	3162	●	●	●	●	●
41	2	4	2	3162	•	•	●	●	●
43	2	2	1	1581	○	○	•	•	•
56	1.5	4	2.7	3162	•	●	●	●	●
60	1.5	2	1.3	4746	○	•	•	●	●
					Small Scale Simulation				
				Clear	○				
				Shallow smoke layer	•				
				Deep smoke layer	●				

Table 14. Simulation result for scaled five balcony configuration (from models "S*XX*E5").

5. DISCUSSION ON SIMULATION RESULT

Two sensitivity analyses were performed to demonstrate the models were optimum. The first analysis attempted to increase the number of grid cells (reducing the grid size) of the model to run on a 32bit Operating System (OS) personal computer to determine the sensitivity of simulation predictions. The second analysis changed the boundary conditions and assessed the effect on the temperature prediction.

The discussion also includes the plume re-attachment to the balcony, using the FDS smoke layer height devices and explains why there is more smoke contamination for balcony without an upstand.

5.1 Grid Sensitivity

For a small-scale model to simulate Tan's (2009) experiment, attempts were made to model it with a finer grid size using personal computers in the University of Canterbury Civil Computer Suite. The area where the plume leaves the spill edge was modelled with a 10mm grid as shown in Figure 61 where the other areas used a 20mm grid. Such a configuration had already reached the limit of a 32bit OS. The difficulty in modelling this configuration is that once run is interrupted, a restart is not possible and it is necessary to start from time zero. It was not possible to apply this grid size beyond three balconies for a 32bit OS system.

Figure 62 shows the comparison of the two models for S19E with a 20mm grid or a 10mm grid at the core. The average temperatures of both models are reasonably close, except the peak temperature for the finer grid is higher. Comparison of all twelve primary scenarios is shown in Appendix J.

Out of the twelve primary scenarios, only simulations 01 and 03 showed significant difference for the two grid sizes. In other words, these two models are preferably simulated with higher resolution grid, but this will push the simulation to a 64bit OS. As mentioned in the Section 4.3, the temperature slice files are able to simulate experiment's photographic records. Hence, a 20mm grid was adequate for the present study. For study of other effects, it might require a higher resolution grid size, which is beyond present scope of this work.

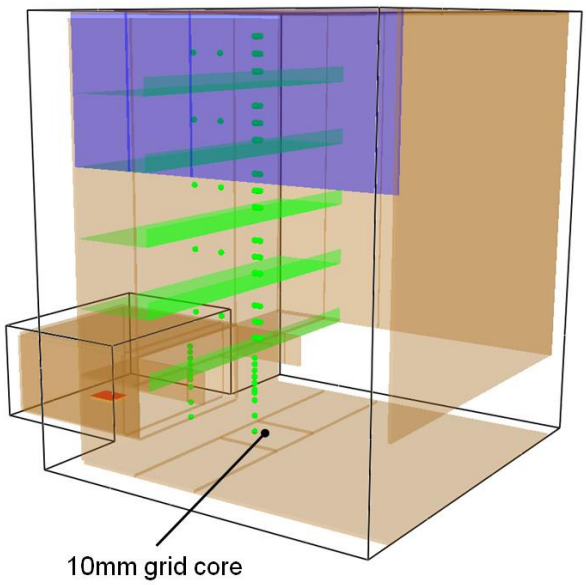

Figure 61. Model with inner "core" 10mm grid.

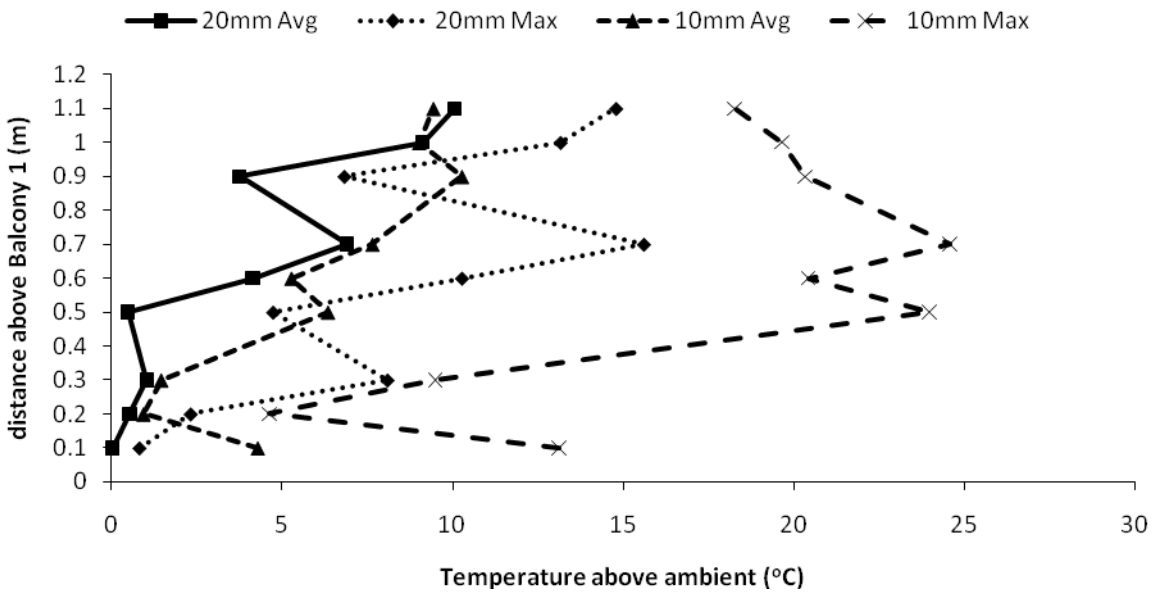

Figure 62. Comparison of 20mm grid with 10mm grid at the core for S19E.

5.2 Boundary Condition Sensitivity

Three additional models were developed to compare the effect of the boundary condition on the FDS prediction. The various models are shown in Figure 63 and they are variants of the small-scale model S01E.

FDS predictions for the various models are shown in Figure 64. "Model 4-O" has the lowest temperature profile as heat is lost from four directions. "Model 3-O" result implies that the smoke reservoir has significant effect on the temperature profile; this is probably due to radiation from the smoke layer. Widening the simulated atrium space also causes a lower temperature profile as more cool air is available for cooling. This study shows the significant effect of the boundary conditions for the smoke contamination study. Hence, it is critical to model a similar boundary condition to the experiment to derive useful findings.

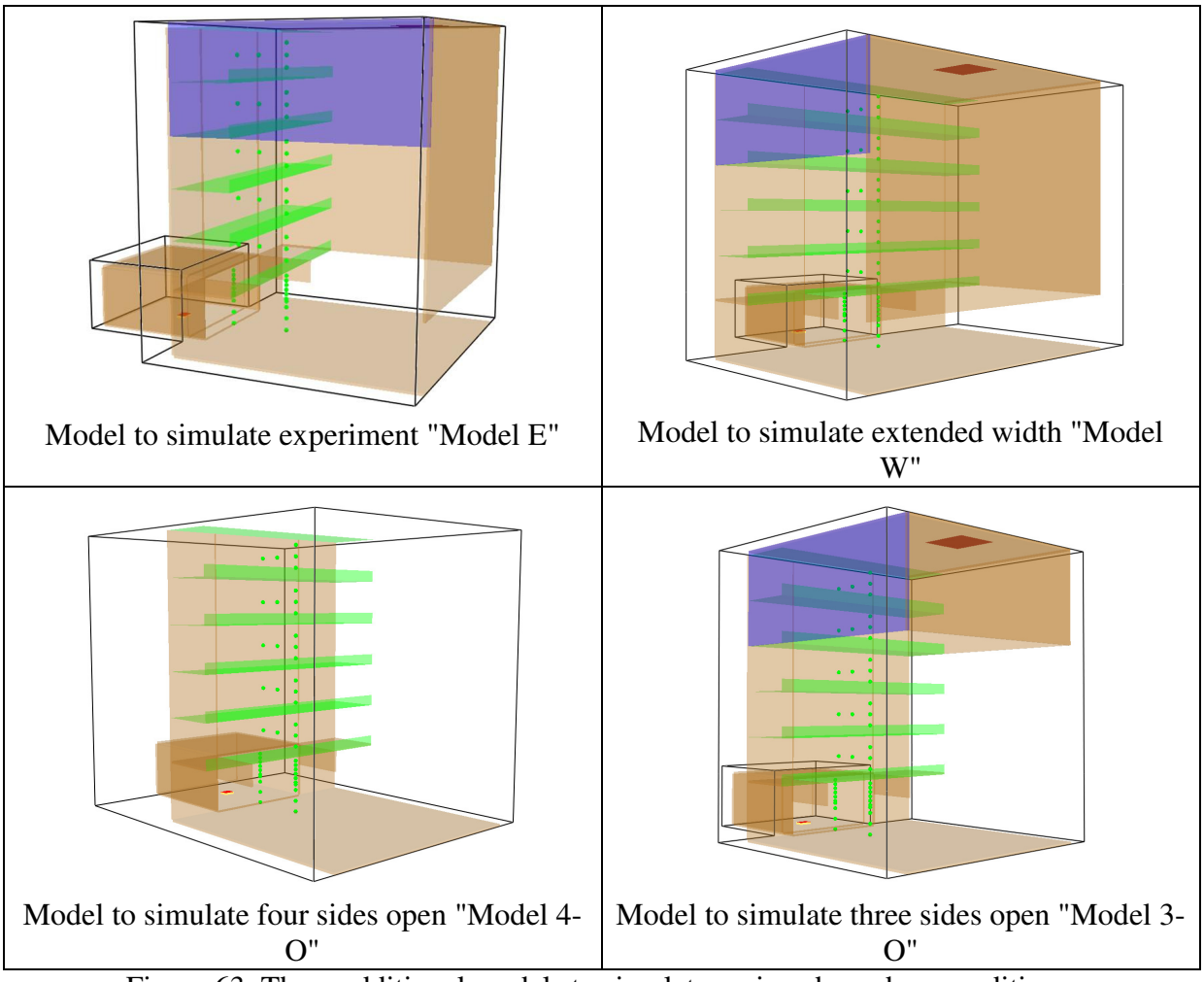

Model to simulate experiment "Model E"

Model to simulate extended width "Model W"

Model to simulate four sides open "Model 4-O"

Model to simulate three sides open "Model 3-O"

Figure 63. Three additional models to simulate various boundary conditions.

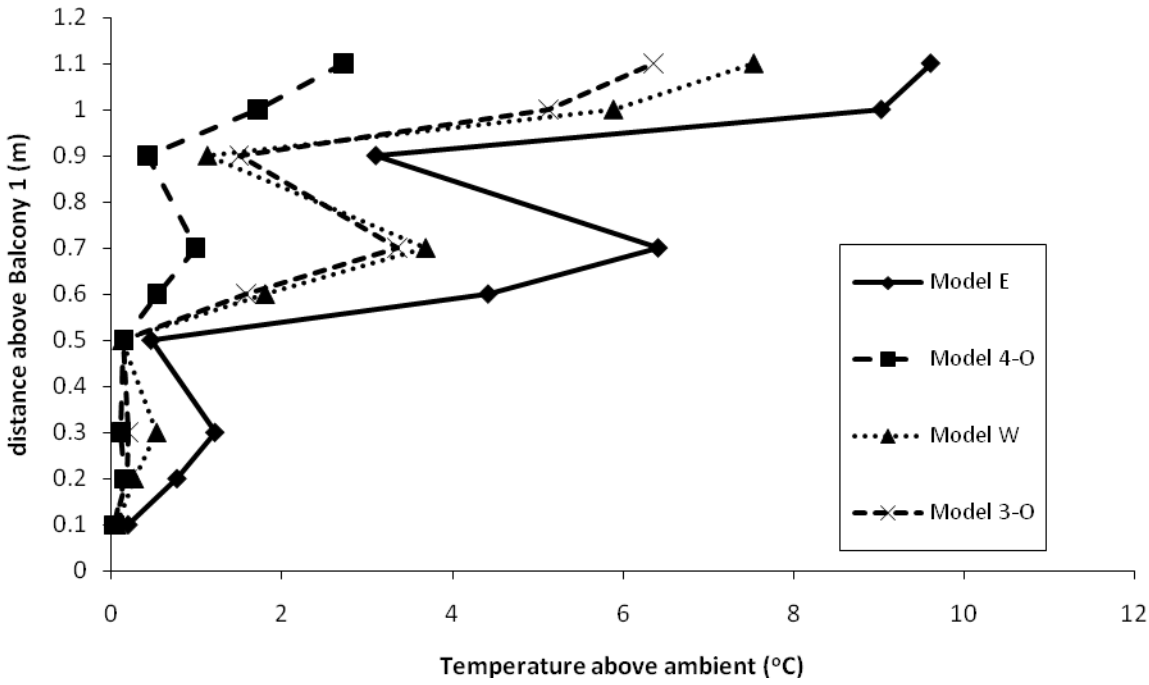

Figure 64. Temperature profiles across balcony edge for a different boundary condition.

5.3 Delay of Smoke Contamination at Upper Balcony

From the simulations, it was observed that the rising spill plume does not contaminate the upper balcony immediately. There is a time lag as the rising plume moves toward the balcony as shown in Figure 65 and Figure 66. Simulation F01E5 has a large opening width (10m) with a fire size of 1581kW and simulation F39E5 has a smaller opening (6m) and larger fire (4743kW) as compared to F01E5. Hence, the F39E5 spill plume will have larger trajectory discharge velocity and temperature at the spill edge as compared to F01E5. In other words, F39E5's spill plume could discharge further away from the balcony and take a longer time for it to re-attach to the balcony and cause smoke contamination.

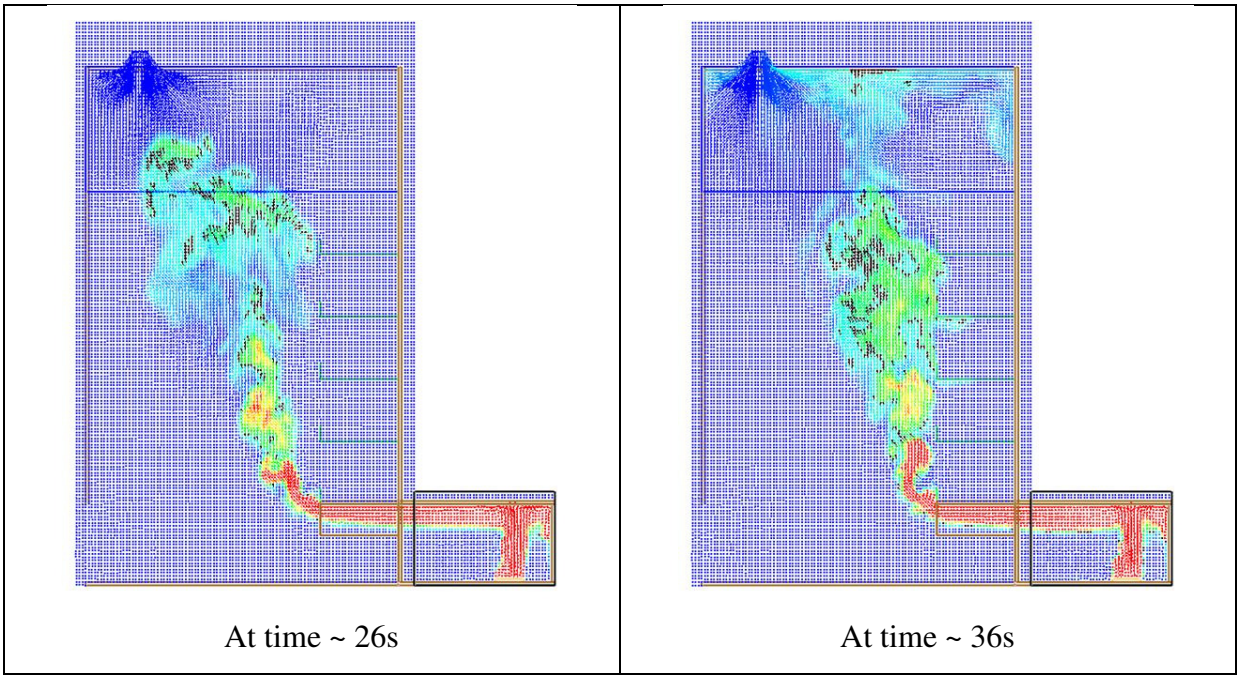

At time ~ 26s | At time ~ 36s

Figure 65. Simulation F01E5 shows the plume moving toward the balcony within 10s.

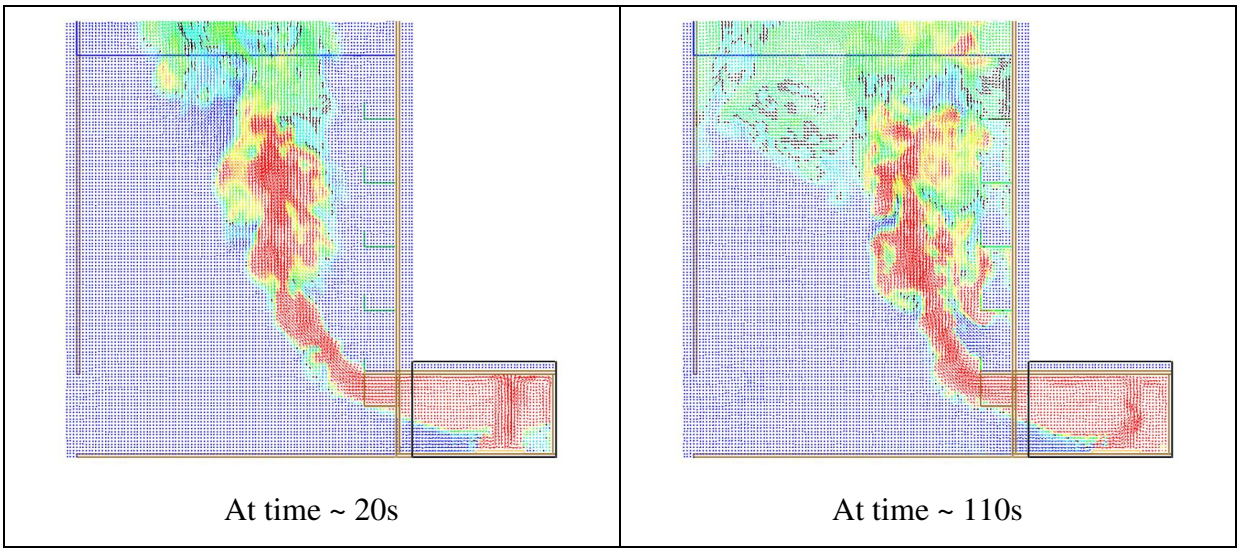

At time ~ 20s | At time ~ 110s

Figure 66. Simulation F39E5 shows the plume moving toward the balcony within 90s.

5.4 Mechanism for Re-attachment

Figure 67 to Figure 72 show the pressure on the region around the plume changes with time over 140s. These figures are plotted using velocity vectors and the velocity allows visualisation of churning air around the plume. At early stage (time = 20s), the pressure region on the left of the plume (away from balcony) and on the right of the plume (nearer to balcony) is fairly evenly distributed. As time progresses to 60s, (Figure 68), there are more

regions having a pressure below ambient condition nearer to the balcony. This is apparently due to less replacement air from the balcony area as compared to the open side that is on the left of the plume. This caused a larger area to have lower pressure as time develops (see Figure 69 to Figure 72). As time approaches 160s (Figure 72), the 2nd balcony above the spill edge has almost the entire balcony with a pressure below ambient condition and the velocity vector also shows a churning action, which is the smoke movement within the balcony. The unequal distribution of a lower pressure region surrounding the plume could have caused the plume to move toward the balcony and lead to smoke contamination. The simulation observation closely matched Cox's (1995) comment on the plume re-attachment mentioned in the Section 2.1.

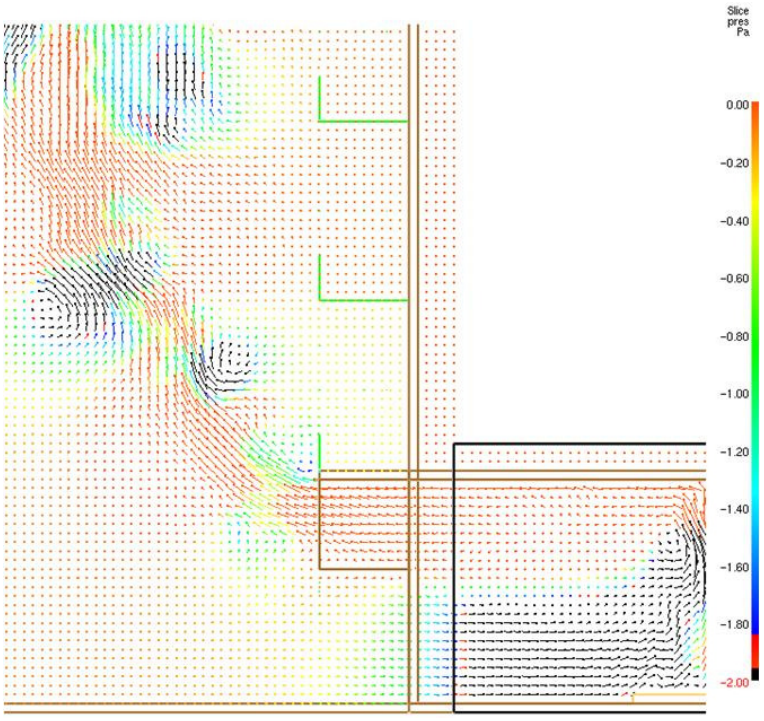

Figure 67. F39E5 pressure at time = 20s.

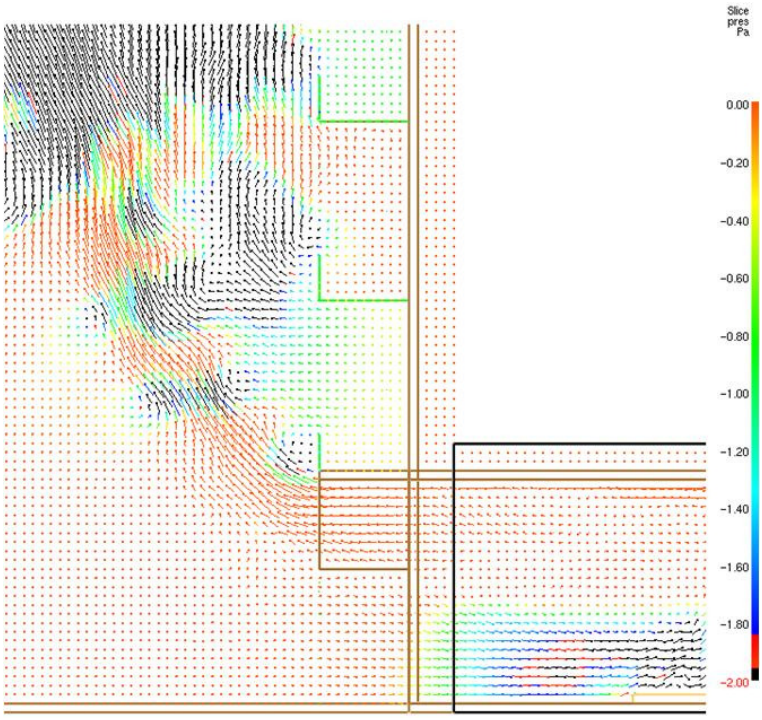

Figure 68. F39E5 pressure at time = 60s.

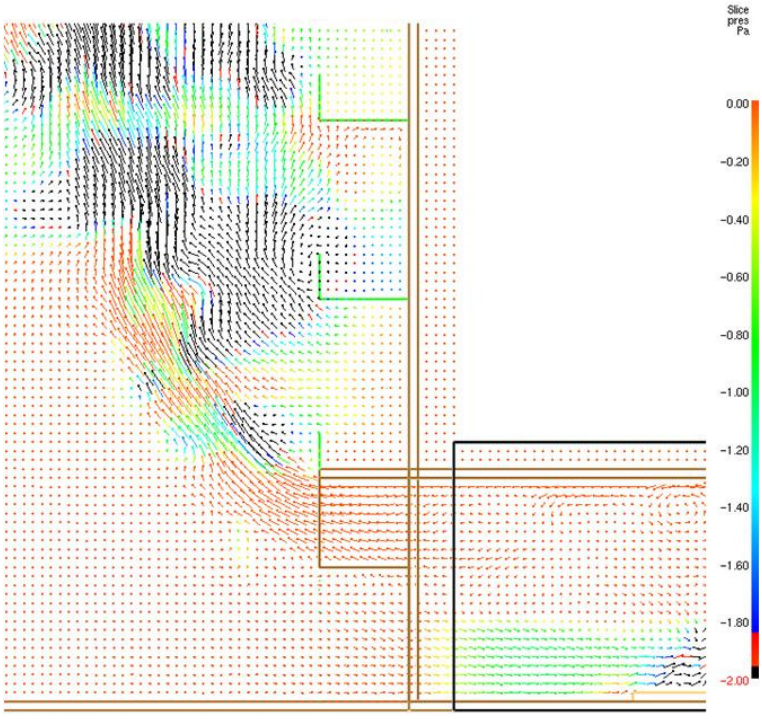

Figure 69. F39E5 pressure at time = 80s.

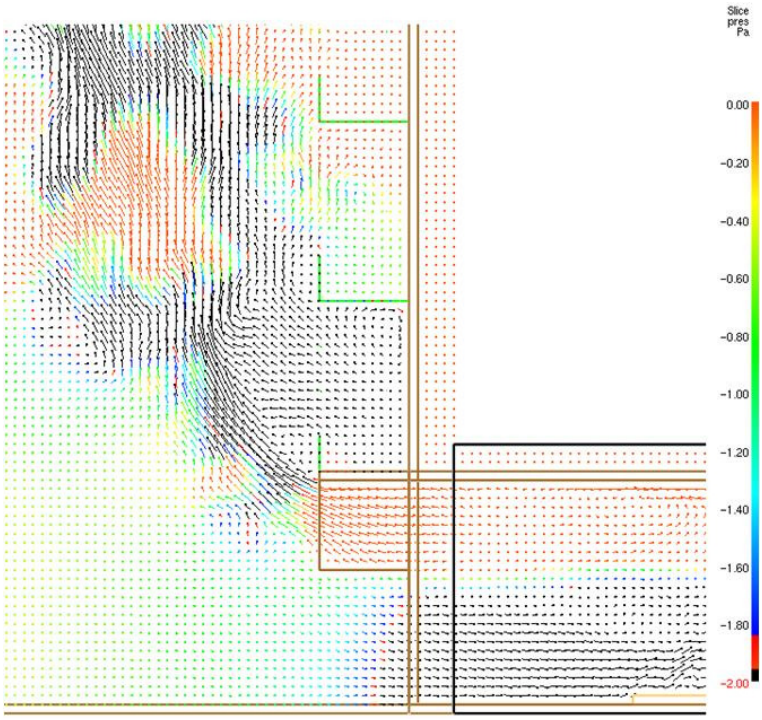

Figure 70. F39E5 pressure at time = 100s.

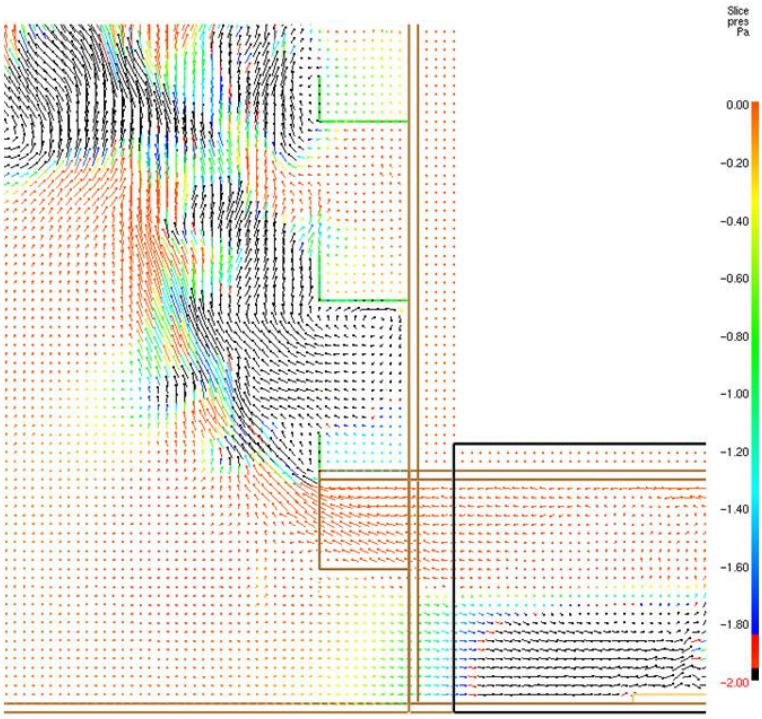

Figure 71. F39E5 pressure at time = 120s.

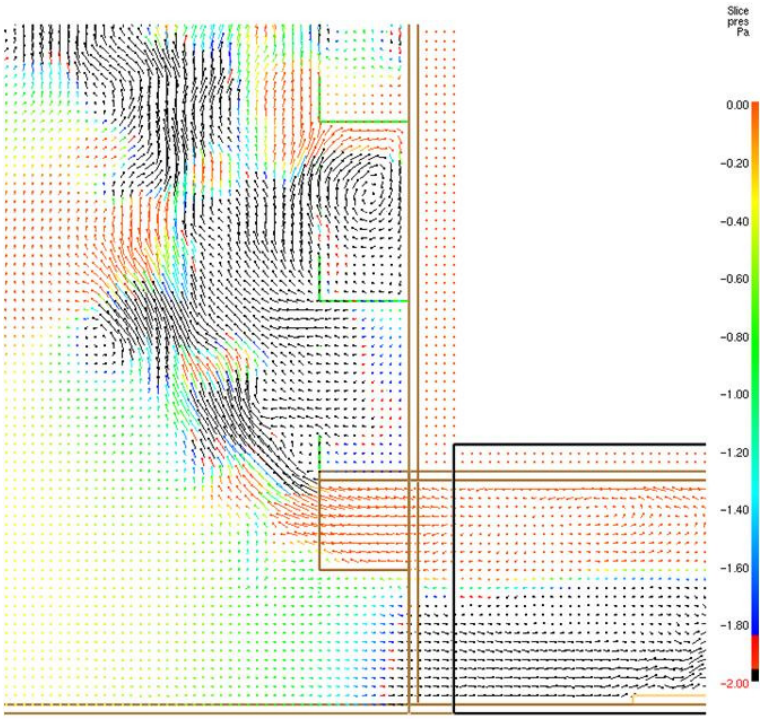

Figure 72. F39E5 pressure at time = 160s.

5.5 Smoke Contamination Starts from the Highest Balcony

It was also observed that the smoke contamination begins from the highest balcony and progressively move downwards towards the spill edge. This could have been due to increasing air entrainment as the spill plume rises and causing more velocity vortices on higher balconies which created a lower pressure region to induce smoke into the balcony. Figure 73 shows the temperature and velocity vector plot at the highest balcony. As seen in the figure, the lower balcony starts to exhibit air vortex formation, which also generates a low pressure and further induces the plume toward the balcony. The effect of plume broadening with height probably also contributed to contamination on higher levels.

Figure 73 also shows the two forms of smoke movement into the balcony. On the higher balcony a vortex is seen to form within the balcony. Due to the formation of the vortex, it leads to a lower pressure on the balcony (by conservation of energy) and the smoke is induced into the balcony. On the lower balcony, the velocity is seen to move into the balcony. This could be due to smoke expansion pushing itself into the balcony.

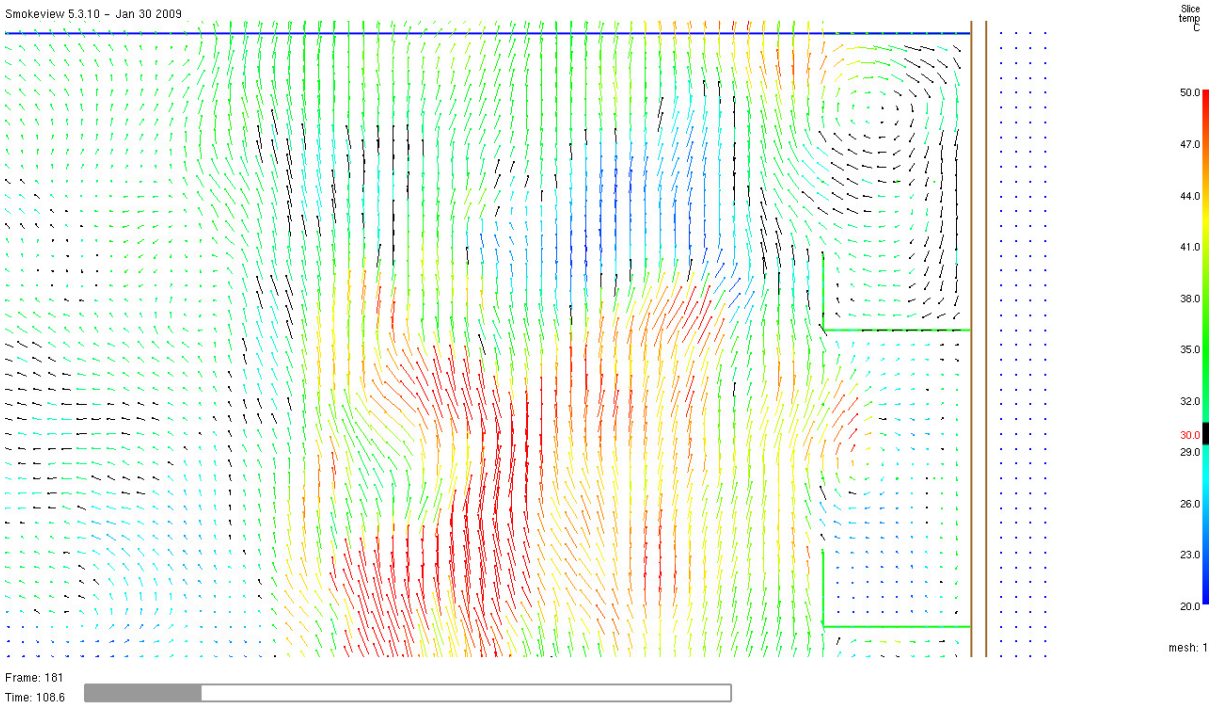

Figure 73. Smoke contamination begins from highest balcony and progress download.

5.6 Simulation Result on Balcony Contamination

Tan (2009) believed that when there is no smoke contamination in the balconies in one set of experiments, there should not be any smoke contamination in the balcony for similar configuration using higher heat release rate. This was because Tan (2009) suggested that the greater momentum from the larger fire would propel the plume further and lead to lower contamination. With this argument, Table 8 has some irregularities as some cases of a higher heat release rate lead to more contamination on the balcony. Hence, a detailed analysis is warranted to review the simulation results.

Upon close examination, there are four categories that lead to the assignment of more contamination:

(1) Smoke only enters the balcony once. This is due to the visual assessment that selected the worst case contamination.

(2) Inadequate smoke extraction rate, but this mainly affects the highest balcony.

(3) Smoke only occasionally enters the balcony.

(4) Smoke is always present in the balcony.

Category (2) does not affect the correlation as it affects the highest balcony. Categories (3) and (4) are genuine case of smoke contamination. From this review, it appears that besides a fire with a higher heat release rate generating greater momentum, it also leads to more entrainment and could cause a higher pressure differential around the spill plume (between the free surface and near the balcony); there could be a critical momentum when this occurred. This could have caused the spill plume to re-attach to the balcony and lead to smoke contamination. It could be argued that Category (1) could be downgraded to no contamination for the three simulations. However, three points out of the total simulation runs would not significantly affect the correlation development. The summary of findings is shown in Table 15.

Simulation	Balcony Breath, b (m)	Plume Width, w (m)	Aspect Ratio, w/b	Heat Release Rate, Q_T (kW)	Full-Scale Simulation				
					Balcony 1	Balcony 2	Balcony 3	Balcony 4	Balcony 5
1	5	10	2	1581	•	●	●	●	●
2				3162	•	●	●	●	●
3				4746	•	●	●	●	●
4		8	1.6	1581	•	●	●	●	●
5				3162	•	●	●	●	●
6				4746	•	●	●	●	●
7		6	1.2	1581	•	●	●	●	●
8				3162	•	•	●	●	●
9				4746	•	•	•	•	●
10		4	0.8	1581	○	•	•	•	●
11				3162	○	○	•	•	●
12				4746	○	• (1)	•	•	●
13		2	0.4	1581	○	○	○	○	•
14				3162	○	○	○	○	●
15				4746	○	○	• (1)	• (2)	●
16	3	10	3.3	1581					
17				3162					
18				4746					
19		8	2.7	1581	●	●	●	●	●
20				3162	●	●	●	●	●
21				4746	●	●	●	●	●
22		6	2	1581	•	●	●	●	●
23				3162	•	●	●	●	●
24				4746	•	●	●	●	●
25		4	1.3	1581	•	•	●	●	●
26				3162	•	•	●	●	●
27				4746	○	•	•	●	●
28		2	0.7	1581	○	○	○	•	●
29				3162	○	○	• (3)	•	●
30				4746	○	• (1)	• (3)	•	●
31	2	10	5	1581					
32				3162					
33				4746					
34		8	4	1581					
35				3162					
36				4746					
37		6	3	1581	●	●	●	●	●
38				3162	•	●	●	●	●
39				4746	● (4)	●	●	●	●
40		4	2	1581	•	●	●	●	●
41				3162	•	•	●	●	●
42				4746	•	● (4)	●	●	●
43		2	1	1581	○	○	•	•	●
44				3162	○	• (3)	•	● (3)	●
45				4746	○	• (3)	•	● (3)	●
46	1.5	10	6.7	1581					
47				3162					
48				4746					
49		8	5.3	1581					
50				3162					
51				4746					
52		6	4	1581					
53				3162					
54				4746					
55		4	2.7	1581	•	●	●	●	●
56				3162	•	●	●	●	●
57				4746	•	●	●	●	●
58		2	1.3	1581	○	○	•	•	●
59				3162	○	○	•	•	●
60				4746	○	○	•	● (2)	●

Not within scope

(1) Smoke goes in once
(2) Inadequate exhaust
(3) Occasionally smoke goes in
(4) Smoke always present

Table 15. Review of smoke contamination caused by higher heat release rate.

5.7 Changing Parameters to Identify Upper Balcony Contamination Trends

Table 8 can be rearranged to study the effect of upper balcony smoke contamination by changing one variable. Table 16 shows that for each group of same balcony breadth and heat release rate, a reduction of plume width will lead to a reduction in smoke contamination on the upper balcony. As shown in the Table 16, the "pattern" is consistent for each group of balcony breadth, either experimental or simulation results.

Table 17 shows that for each heat release rate and plume width, a reduction in balcony breadth in general will have higher level of smoke contamination. However, for higher heat release rate (3162kW and 4743kW) and narrow plume width (2m), the trend seems to change; the smoke contamination reduces. Tan (2009) believed this trend should be linear, i.e. more contamination as the balcony breadth was reduced. This concept has led Tan (2009) not to carry out all his planned experiments and inferred some of the result. Hence, there is no comparison available for this study.

					Full-Scale Simulation				
					Tan (2009) Experiment & Small Scale Simulation				
Experiment or Simulation	Balcony Breath, b (m)	Plume Width, w (m)	Aspect Ratio, w/b	Heat Release Rate, Q_T (kW)	Balcony 1	Balcony 2	Balcony 3	Balcony 4	Balcony 5
1	0.5	1 (10)	2	5 (1581)	▪•	■●	■●	●	●
4		0.8 (8)	1.6		•	●	●	●	●
7		0.6 (6)	1.2		•	●	●	●	●
10		0.4 (4)	0.8		○	•	•	•	●
13		0.2 (2)	0.4		□○	□○	□○	○	•
2		1 (10)	2	10 (3162)	•	●	●	●	●
5		0.8 (8)	1.6		•	●	●	●	●
8		0.6 (6)	1.2		□•	□•	▪●	●	●
11		0.4 (4)	0.8		○	○	•	•	●
14		0.2 (2)	0.4		○	○	○	○	●
3		1 (10)	2	15 (4746)	▪•	■●	■●	●	●
6		0.8 (8)	1.6		•	●	●	●	●
9		0.6 (6)	1.2		•	•	•	•	●
12		0.4 (4)	0.8		○	•	•	•	●
15		0.2 (2)	0.4		○	○	•	•	●
16	0.3	1 (10)	3.3	5 (1581)					
19		0.8 (8)	2.7		▪●	▪●	■●	●	●
22		0.6 (6)	2		•	●	●	●	●
25		0.4 (4)	1.3		•	•	●	●	●
28		0.2 (2)	0.7		○	○	○	•	●
17		1 (10)	3.3	10 (3162)					
20		0.8 (8)	2.7		●	●	●	●	●
23		0.6 (6)	2		□•	▪●	■●	●	●
26		0.4 (4)	1.3		•	•	●	●	●
29		0.2 (2)	0.7		○	○	•	•	●
18		1 (10)	3.3						
21		0.8 (8)	2.7		●	●	●	●	●
24		0.6 (6)	2	15 (4746)	•	●	●	●	●
27		0.4 (4)	1.3		□○	□•	▪•	●	●
30		0.2 (2)	0.7		○	•	•	•	●
31	0.2	1 (10)	5						
34		0.8 (8)	4						
37		0.6 (6)	3		●	●	●	●	●
40		0.4 (4)	2	5 (1581)	•	●	●	●	●
43		0.2 (2)	1		□○	□○	▪•	•	●
32		1 (10)	5						
35		0.8 (8)	4						
38		0.6 (6)	3		▪•	▪●	■●	●	●
41		0.4 (4)	2	10 (3162)	□•	□•	▪●	●	●
44		0.2 (2)	1		○	•	•	●	●
33		1 (10)	5						
36		0.8 (8)	4						
39		0.6 (6)	3		●	●	●	●	●
42		0.4 (4)	2	15 (4746)	•	●	●	●	●
45		0.2 (2)	1		○	•	•	●	●
46	0.15	1 (10)	6.7						
49		0.8 (8)	5.3						
52		0.6 (6)	4						
55		0.4 (4)	2.7	5 (1581)	•	●	●	●	●
58		0.2 (2)	1.3		○	○	•	•	●
47		1 (10)	6.7						
50		0.8 (8)	5.3						
53		0.6 (6)	4						
56		0.4 (4)	2.7	10 (3162)	▪•	■●	■●	●	●
59		0.2 (2)	1.3		○	○	•	•	●
48		1 (10)	6.7						
51		0.8 (8)	5.3						
54		0.6 (6)	4						
57		0.4 (4)	2.7	15 (4746)	•	●	●	●	●
60		0.2 (2)	1.3		□○	□○	▪•	●	●
					Experiment Result	Small Scale Simulation	Full-scale Simulation		
		Not within scope		Clear		□	○		
				Shallow smoke layer		▪	•		
				Deep smoke layer		■	●		

Table 16. Effect of reducing plume width.

					Full-Scale Simulation				
					Tan (2009) Experiment & Small Scale Simulation				
Experiment or Simulation	Balcony Breath, b (m)	Plume Width, w (m)	Aspect Ratio, w/b	Heat Release Rate, Q_T (kW)	Balcony 1	Balcony 2	Balcony 3	Balcony 4	Balcony 5
1	0.5 (5)	1 (10)	2	5 (1581)	▪•	■●	■●	●	●
16	0.3 (3)		3.3						
31	0.2 (2)		5						
46	0.15 (1.5)		6.7						
4	0.5 (5)	0.8 (0.8)	1.6	5 (1581)	•	●	●	●	●
19	0.3 (3)		2.7		▪●	▪●	■●	●	●
34	0.2 (2)		4						
49	0.15 (1.5)		5.3						
7	0.5 (5)	0.6 (6)	1.2	5 (1581)	•	●	●	●	●
22	0.3 (3)		2		•	●	●	●	●
37	0.2 (2)		3		●	●	●	●	●
52	0.15 (1.5)		4						
10	0.5 (5)	0.4 (4)	0.8	5 (1581)	○	•	•	•	●
25	0.3 (3)		1.3		•	•	●	●	●
40	0.2 (2)		2		•	●	●	●	●
55	0.15 (1.5)		2.7		•	●	●	●	●
13	0.5 (5)	0.2 (2)	0.4	5 (1581)	□○	□○	□○	○	•
28	0.3 (3)		0.7		○	○	○	•	●
43	0.2 (2)		1		□○	□○	▪•	•	●
58	0.15 (1.5)		1.3		○	○	•	•	●
2	0.5 (5)	1 (10)	2	10 (3162)	•	●	●	●	●
17	0.3 (3)		3.3						
32	0.2 (2)		5						
47	0.15 (1.5)		6.7						
5	0.5 (5)	0.8 (0.8)	1.6	10 (3162)	•	●	●	●	●
20	0.3 (3)		2.7		●	●	●	●	●
35	0.2 (2)		4						
50	0.15 (1.5)		5.3						
8	0.5 (5)	0.6 (6)	1.2	10 (3162)	□•	□•	▪●	●	●
23	0.3 (3)		2		□•	▪●	■●	●	●
38	0.2 (2)		3		▪•	▪●	■●	●	●
53	0.15 (1.5)		4						
11	0.5 (5)	0.4 (4)	0.8	10 (3162)	○	○	•	•	●
26	0.3 (3)		1.3		•	•	●	●	●
41	0.2 (2)		2		□•	□•	▪●	●	●
56	0.15 (1.5)		2.7		▪•	■●	■●	●	●
14	0.5 (5)	0.2 (2)	0.4	10 (3162)	○	○	○	○	●
29	0.3 (3)		0.7		○	○	•	•	●
44	0.2 (2)		1		○	•	•	●	●
59	0.15 (1.5)		1.3		○	○	•	•	●
3	0.5 (5)	1 (10)	2	15 (4746)	▪•	■●	■●	●	●
18	0.3 (3)		3.3						
33	0.2 (2)		5						
48	0.15 (1.5)		6.7						
6	0.5 (5)	0.8 (0.8)	1.6	15 (4746)	•	●	●	●	●
21	0.3 (3)		2.7		●	●	●	●	●
36	0.2 (2)		4						
51	0.15 (1.5)		5.3						
9	0.5 (5)	0.6 (6)	1.2	15 (4746)	•	•	•	•	●
24	0.3 (3)		2		•	●	●	●	●
39	0.2 (2)		3		●	●	●	●	●
54	0.15 (1.5)		4						
12	0.5 (5)	0.4 (4)	0.8	15 (4746)	○	•	•	•	●
27	0.3 (3)		1.3		□○	□•	▪•	●	●
42	0.2 (2)		2		•	●	●	●	●
57	0.15 (1.5)		2.7		•	●	●	●	●
15	0.5 (5)	0.2 (2)	0.4	15 (4746)	○	○	•	•	●
30	0.3 (3)		0.7		○	•	•	•	●
45	0.2 (2)		1		○	•	•	●	●
60	0.15 (1.5)		1.3		□○	□○	▪•	●	●

	Experiment Result	Small Scale Simulation	Full-scale Simulation
Not within scope			
Clear		□	○
Shallow smoke layer		▪	•
Deep smoke layer		■	●

Table 17. Effect of reducing balcony breadth.

5.8 Using the FDS Layer Height Device in Balconies and at the Spill Edge

Two simulation models F24E5 and F57E5 were simulated with the FDS smoke layer height device in each balcony and at the spill edge as shown in Figure 74. In the balcony, the smoke layer devices are positioned in the mid position. The smoke layer device at the spill edge is located similarly to Harrison's (2009) experiment. Figure 75 and Figure 76 show the devices' output for F24E5 and F57E5. The upper graph uses the direct output from FDS and the lower graph is using a 30 point for average. Both 30°C temperature profiles show that the balcony temperature already reached 30°C on the floor but the smoke layer device output still showed a layer 0.5m above floor. Furthermore, the device output also showed a wide range of layer height readings within the balcony. Table 18 shows a tabulation of "worst case" smoke layer height in each balcony based on observations using Smokeview. This shows that the smoke layer height device is not viable in the balcony due to the dynamic movement of smoke within the balcony. There is also a situation as shown in Figure 77 where smoke appears simultaneously on the balcony ceiling and floor, which might complicate the computation of smoke layer height in FDS.

On the other hand, Figure 78 and Figure 79 show the smoke layer height at the spill edge for F24E5 and F57E5. The variations of the smoke layer height reading range are not wide and they also corresponded closely with Figure 75 and Figure 76 respectively. Hence, the smoke layer height device usage at the spill edge is viable.

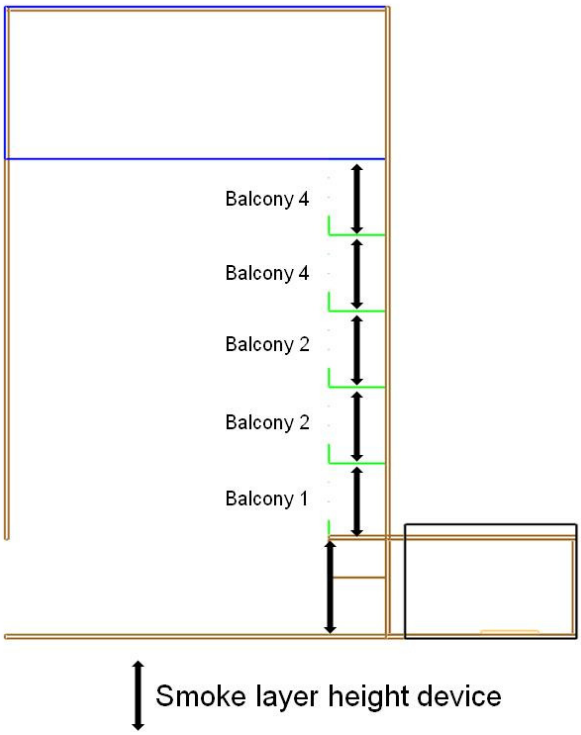

Figure 74. Position of smoke layer height sensors.

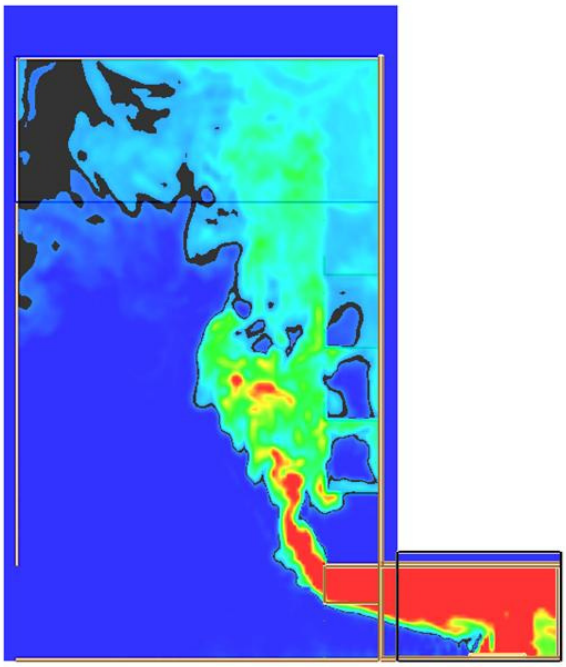

30°C temperature profile

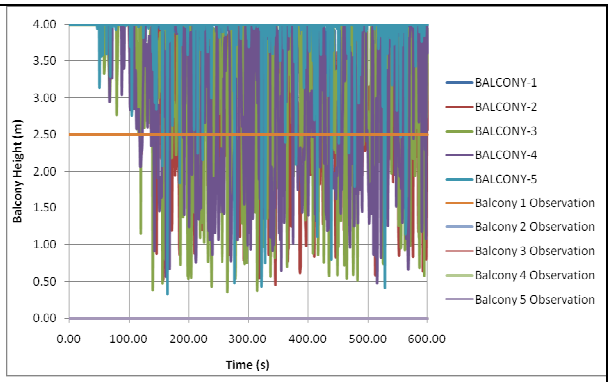

Direct output from FDS

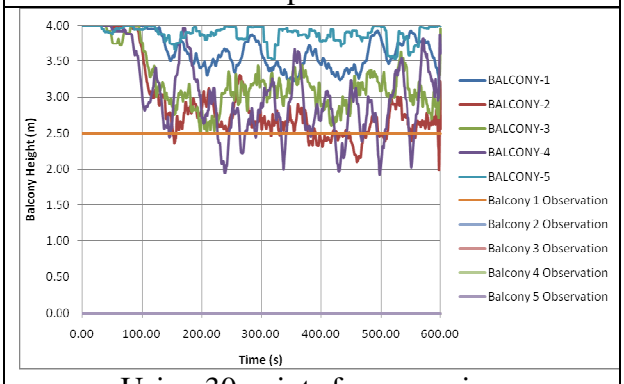

Using 30 points for averaging

Figure 75. For simulation F24E5.

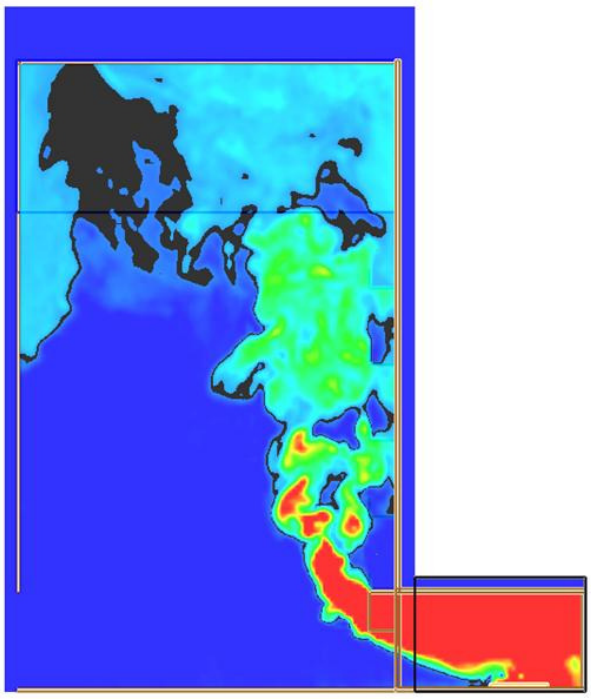

30°C temperature profile

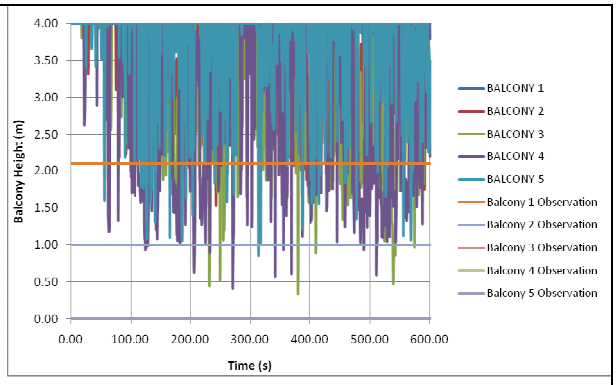

Direct output from FDS

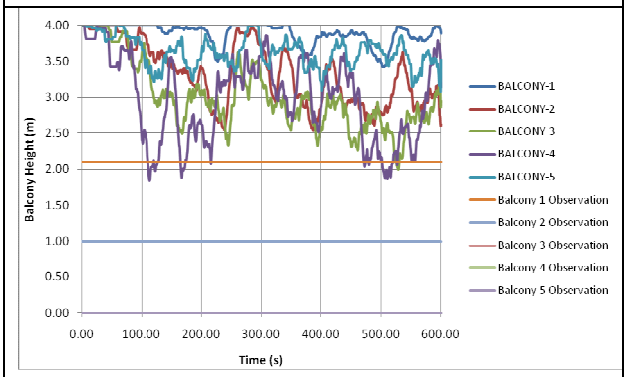

Using 30 points for averaging

Figure 76. For simulation F57E5.

	Smoke Layer Height(m)	
	F24E5	F57E5
Balcony 1 Observation	2.5	2.1
Balcony 2 Observation	0	1
Balcony 3 Observation	0	0
Balcony 4 Observation	0	0
Balcony 5 Observation	0	0

Table 18. Observation of smoke layer in each balcony.

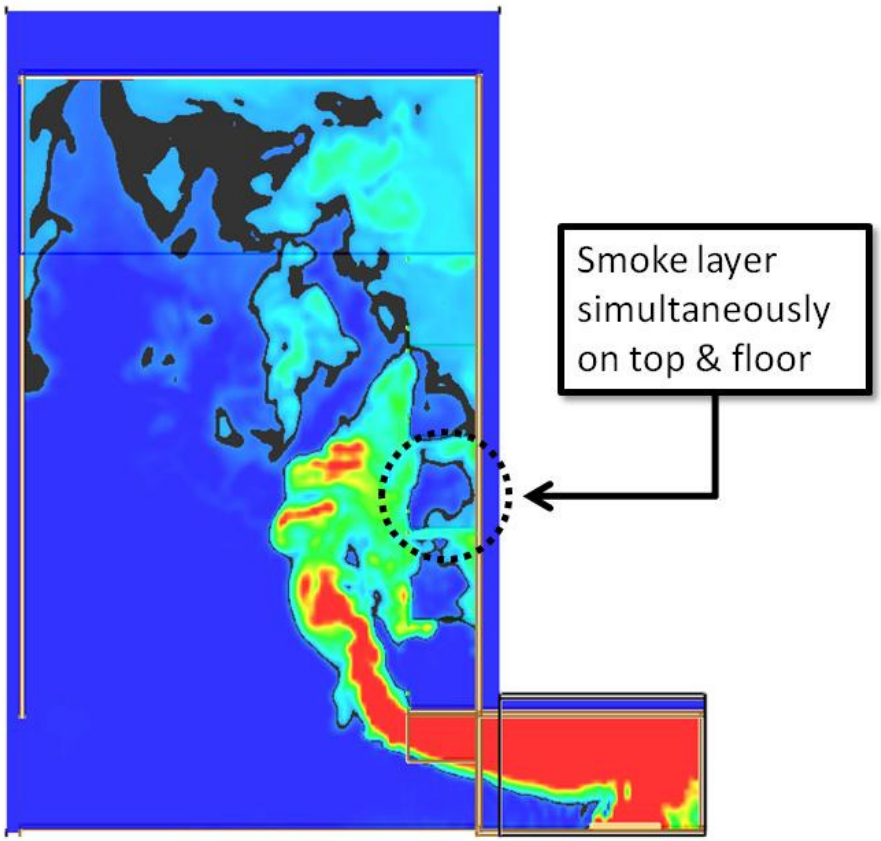

Figure 77. Smoke appears simultaneously on ceiling and floor of balcony.

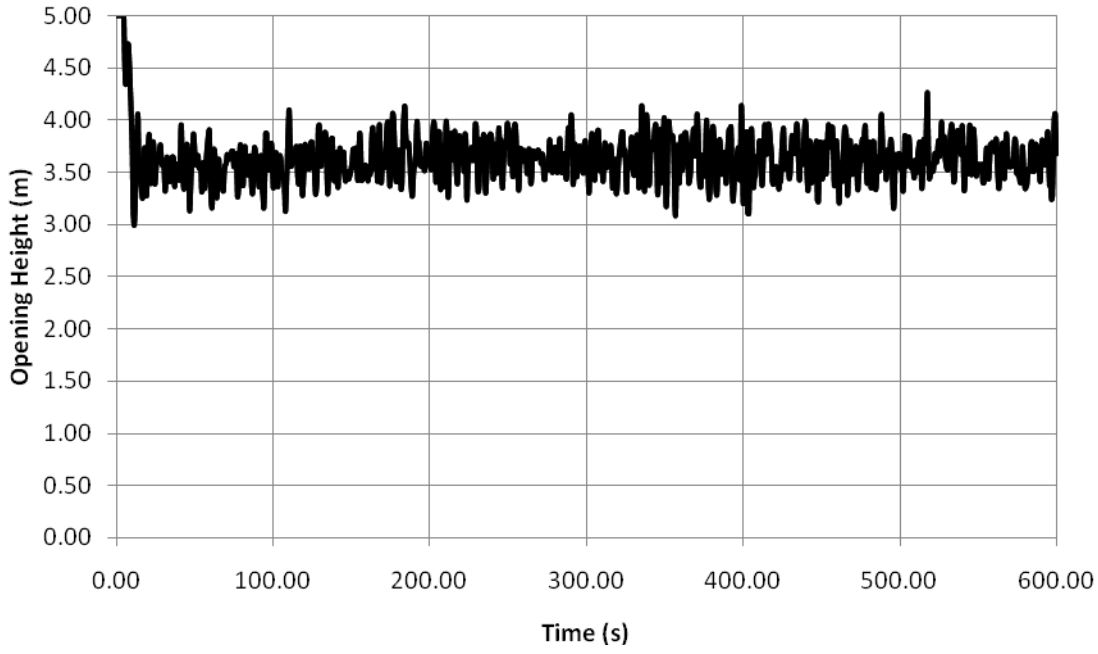

Figure 78. Smoke layer height device output at the spill edge for simulation F24E5.

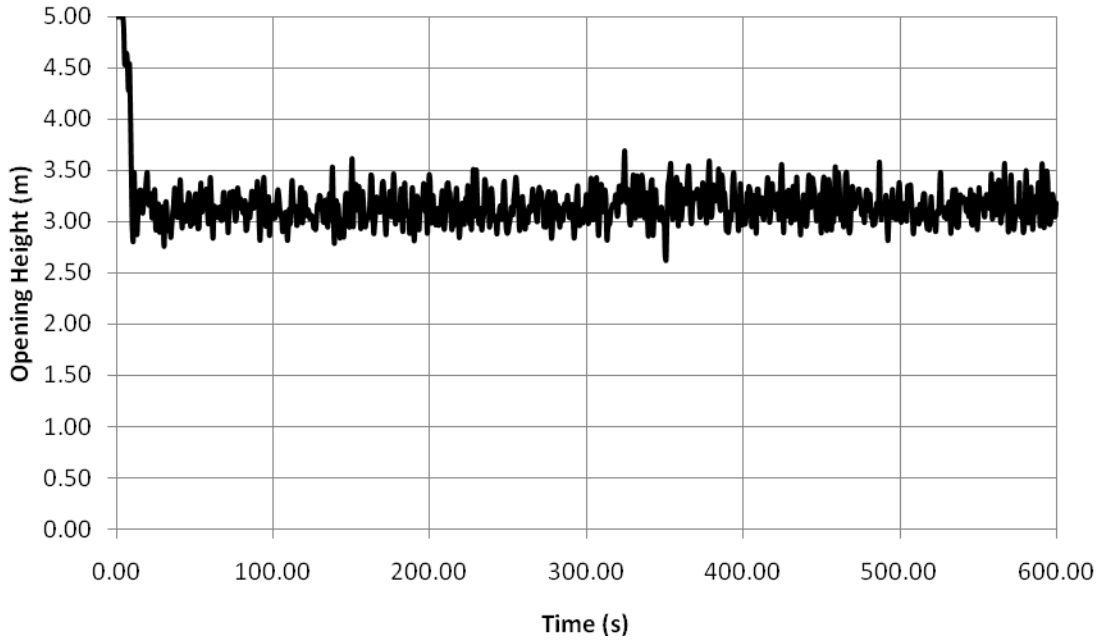

Figure 79. Smoke layer height device output at the spill edge for simulation F57E5.

5.9 Cause of Increased Smoke Contamination in Configuration without Upstand

Figure 80 shows the velocity diagram for a typical case without upstand. From the figure, it can be observed that air is easily dragged into the spill plume. For a configuration with an upstand, it will act as an obstacle to the air flow. In other words, without an upstand the air within the balcony is able to make a complete churning action and more easily circulates the smoke from the ceiling to the floor level. Hence, this could be one of the reasons for more contamination at lower balcony for a configuration without an upstand as compared to the configuration with an upstand.

5.10 Cause of Increased Smoke Contamination in Higher Atrium

As spill plume rises with height, it entrains more air and the cross-section of the plume will also increase with height. At high level, the plume will cause higher differential pressure around the spill plume. There will be higher pressure differential between the free side and the plume surface near the balcony. As discussed in the Section 5.4, this could be why the plume leans towards the balcony. This leaning force should be increasing with height as the plume size also increases with height.

Hence for taller atria, the plume will experience higher pressures which push it towards the balcony. When the plume top portion re-attaches to the balcony, the re-attachment will proceed downwards as explained in the Section 5.5. This momentum action of the plume re-attachment would have caused more smoke contamination on the lower balcony as a taller plume also has higher momentum force.

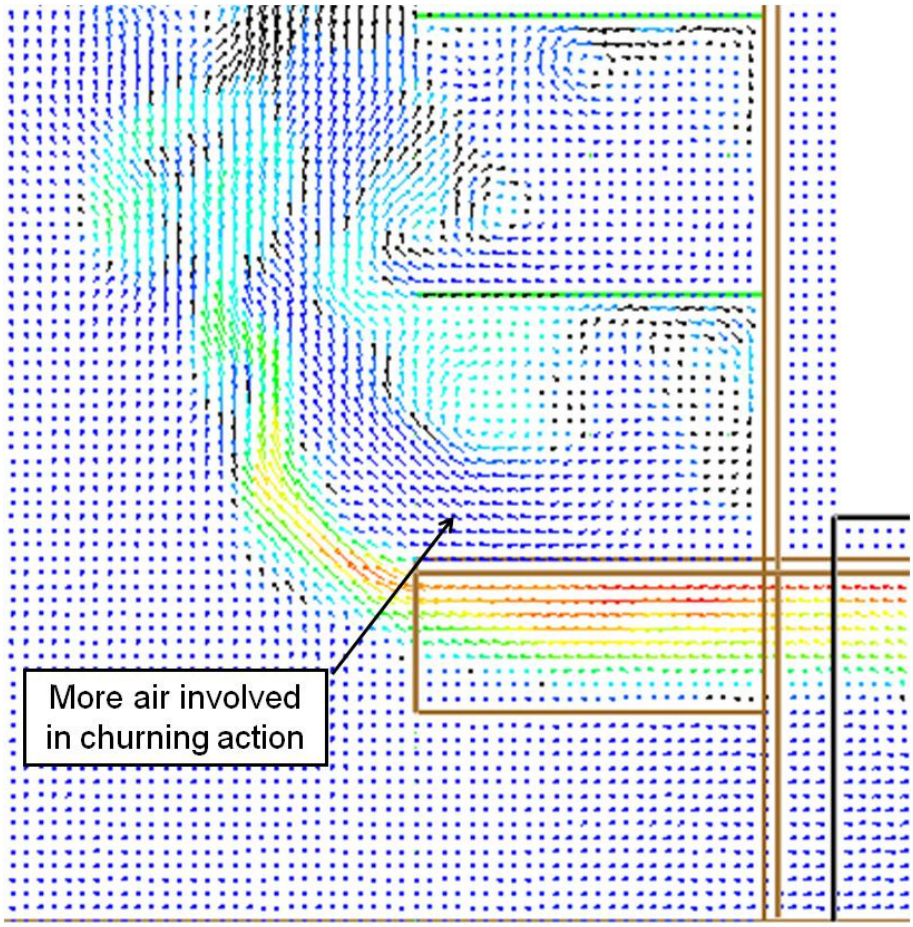

Figure 80. More air dragged into the spill plume.

5.11 Simulation with Larger Fire

Eight scenarios were simulated with larger fire of 9486kW. This was to determine whether a higher heat release rate will cause more smoke contamination on upper balconies. However, results from five of the scenarios were unable to be determined as the channelling screen was too shallow and lead to the smoke spilling under it and directly contaminated the Balcony 1. The result is shown in Table 19 and those highlighted are these selected simulations. For the remaining three simulations, two simulations show that larger fire will cause more upper balcony smoke contamination. Although with similar plume width, a higher heat release rate

fire will propel the plume a further distance as there is more energy within the plume, the larger entrainment due to larger fire size also caused more smoke contamination.

Appendix K shows the smoke contamination height and smoke layer depth at the spill edge for the three successfully modelled scenarios.

Simulation	Balcony Breath, b (m)	Plume Width, w (m)	Aspect Ratio, w/b	Heat Release Rate, Q_T (kW)	Full-Scale Simulation				
					Balcony 1	Balcony 2	Balcony 3	Balcony 4	Balcony 5
1	5	10	2	1581	•	●	●	●	●
2				3162	•	●	●	●	●
3				4746	■●	●	●	●	●
3a				9486	●	●	●	●	●
4		8	1.6	1581	•	●	●	●	●
5				3162	•	●	●	●	●
6				4746	•	●	●	●	●
7		6	1.2	1581	•	●	●	●	●
8				3162	•	•	●	●	●
9				4746	•	•	•	•	●
10		4	0.8	1581	○	•	•	•	●
11				3162	○	○	•	•	●
12				4746	○	•	•	•	●
12a				9486	Spilled Smoke				
13		2	0.4	1581	○	○	○	○	•
14				3162	○	○	○	○	●
15				4746	○	○	•	•	●
15a				9486	Spilled Smoke				
16	3	10	3.3	1581					
17				3162					
18				4746					
19		8	2.7	1581	●	●	●	●	●
20				3162	●	●	●	●	●
21				4746	●	●	●	●	●
22		6	2	1581	•	●	●	●	●
23				3162	•	●	●	●	●
24				4746	•	●	●	●	●
24a				9486	●	●	●	●	●
25		4	1.3	1581	•	•	●	●	●
26				3162	•	•	●	●	●
27				4746	○	•	•	●	●
28		2	0.7	1581	○	○	○	•	●
29				3162	○	○	•	•	●
30				4746	○	•	•	•	●
30a				9486	Spilled Smoke				
31	2	10	5	1581					
32				3162					
33				4746					
34		8	4	1581					
35				3162					
36				4746					
37		6	3	1581	●	●	●	●	●
38				3162	•	●	●	●	●
39				4746	●	●	●	●	●
40		4	2	1581	•	●	●	●	●
41				3162	•	•	●	●	●
42				4746	•	●	●	●	●
42a				9486	•	●	●	●	●
43		2	1	1581	○	○	•	•	●
44				3162	○	•	•	●	●
45				4746	○	•	•	●	●
45a				9486	Spilled Smoke				
46	1.5	10	6.7	1581					
47				3162					
48				4746					
49		8	5.3	1581					
50				3162					
51				4746					
52		6	4	1581					
53				3162					
54				4746					
55		4	2.7	1581	•	●	●	●	●
56				3162	•	●	●	●	●
57				4746	•	●	●	●	●
58		2	1.3	1581	○	○	•	•	●
59				3162	○	○	•	•	●
60				4746	○	○	•	●	●
60a				9486	Spilled Smoke				

	Full-scale Simulation
Clear	○
Shallow smoke layer	•
Deep smoke layer	●

Not within scope

Table 19. Simulation result for larger fire (9486kW).

6. CORRELATION

Two equations are presented for the balcony with and without upstand configurations. The first correlation equation is for three to seven balconies with upstand configuration; the development of this equation is shown in the subsequent sections, which was the primary objective of this research project. The second equation is for the full-scale five balcony model without upstand configuration. Results are primarily plotted using the same non-dimensional parameters suggested by Tan (2009).

6.1 Correlation Equation for Small-scale Three Balcony Configuration

The small-scale three balcony configuration was to simulate the experiments conducted by Tan (2009). Figure 81 and Table 20 show the correlation and summary for the small-scale three balcony configuration. Figure 82 shows the simulated correlation superimposed onto the experimental correlation from Tan (2009). The figure shows that the simulated result could emulate the experiment well. This also demonstrated the grid size recommended by Harrison (2009) and the assessment methodology of using the FDS temperature slice file of 30°C profiles are adequate for this research project.

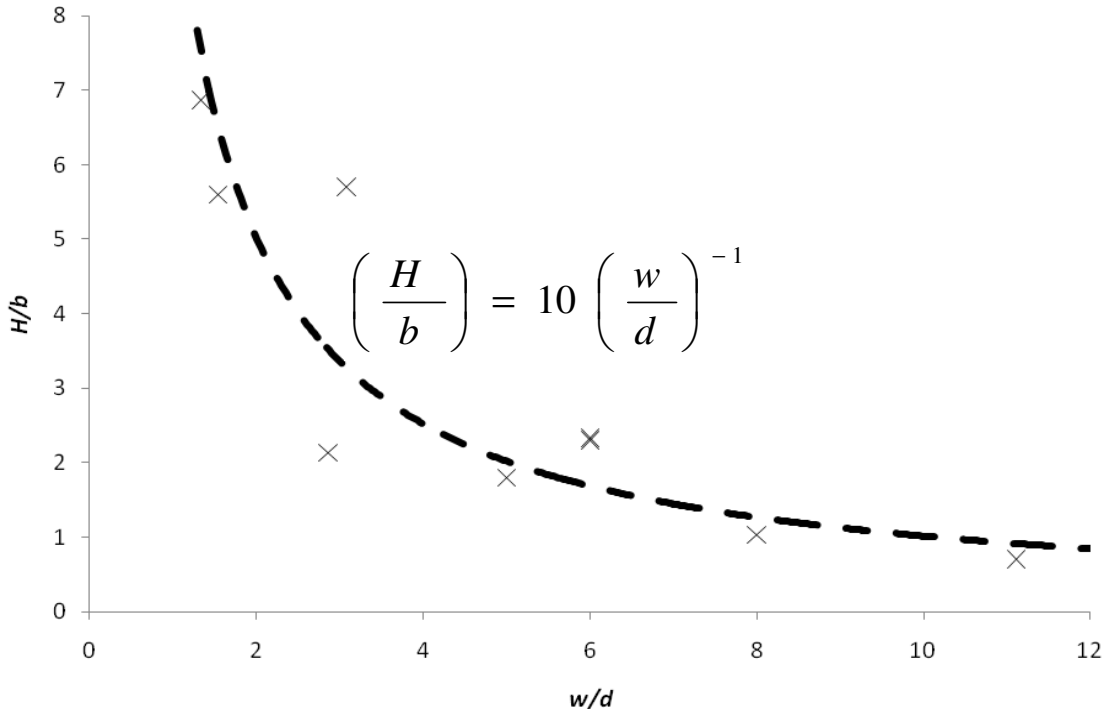

Figure 81. Correlation for simulated small-scale three balcony configuration.

Small-scale 3 Balconies Simulation	*H* (m)	*b* (m)	*w* (m)	*d* (m)	*H/b*	*w/d*
1	0.34	0.50	1.0	0.07	0.68	14.29
3	0.35	0.50	1.0	0.09	0.70	11.11
8	1.15	0.50	0.6	0.10	2.30	6.00
13	>1.60	0.50	0.1	0.12	-	-
19	0.31	0.30	0.8	0.10	1.03	8.00
23	0.70	0.30	0.6	0.10	2.33	6.00
27	1.09	0.30	0.4	0.12	3.63	3.33
38	0.36	0.20	0.6	0.12	1.80	5.00
41	1.14	0.20	0.4	0.13	5.70	3.08
43	1.12	0.20	0.2	0.13	5.60	1.54
56	0.32	0.15	0.4	0.14	2.13	2.86
60	1.03	0.15	0.2	0.15	6.87	1.33

Table 20. Summary of result for simulated small-scale three balcony configuration

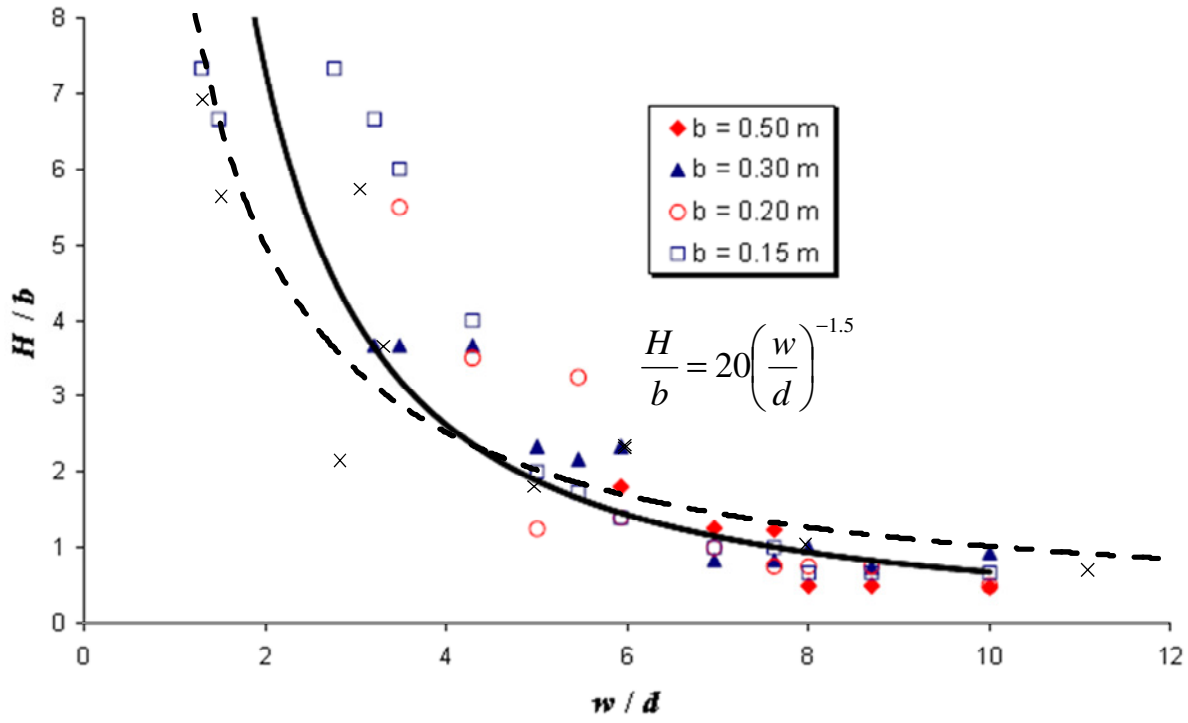

Figure 82. Superimposed of FDS small-scale simulation and experimental result from Tan (2009).

6.2 Correlation Equation for Full-scale and Small-scale Five Balcony Configuration

In this case, a two phase approach was adopted. The first step was to use the twelve primary scenarios predictions to develop the correlation as shown Figure 83. The second step developed the correlation using more simulations (total forty-two) as shown in Figure 84.

As shown in Figure 85, there is no significant difference when the number of simulation increased. Table 21 shows the summary of data points from the simulation.

Figure 86 and Table 22 show the correlation and summary result for the small-scale five balcony configuration; the two "zero" points on the *x-axis* are not consider when developing the correlation. Figure 87 shows the comparison of correlations for small-scale and full-scale five balcony configurations. The figure shows that the simulations for small-scale and full-scale yield similar prediction as would be expected from the appropriate application of the scaling laws.

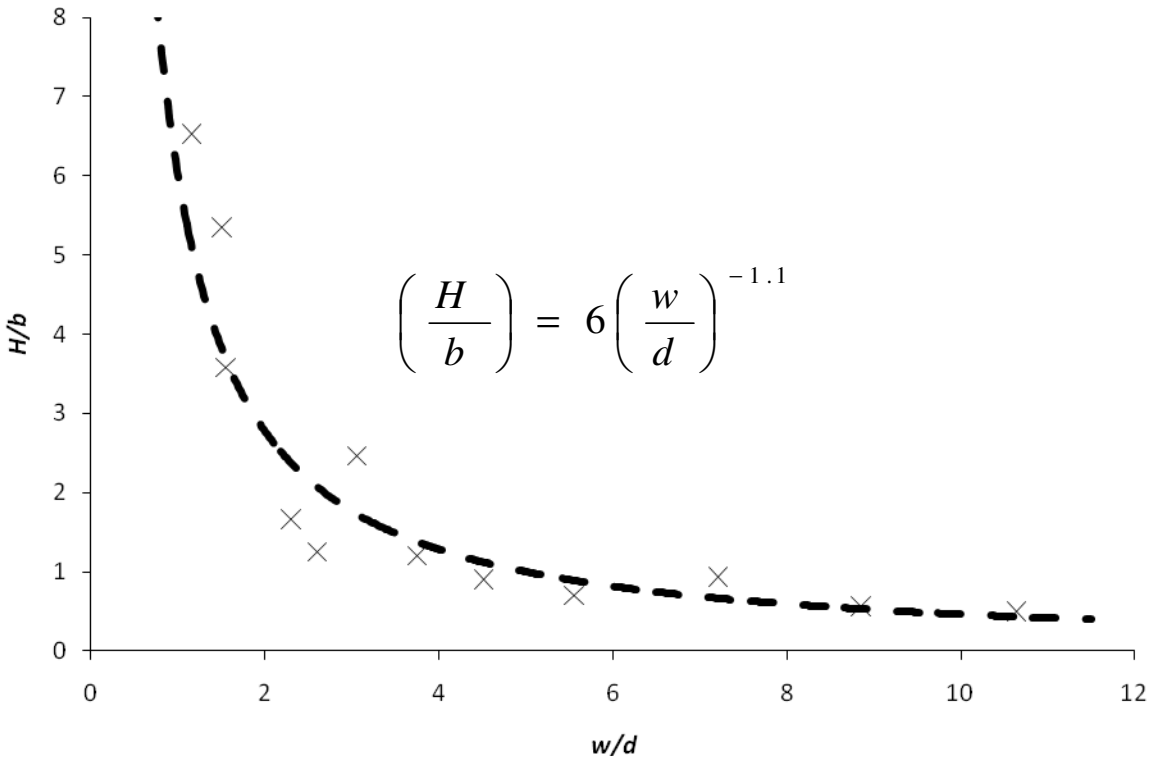

Figure 83. Correlation developed using twelve primary scenarios.

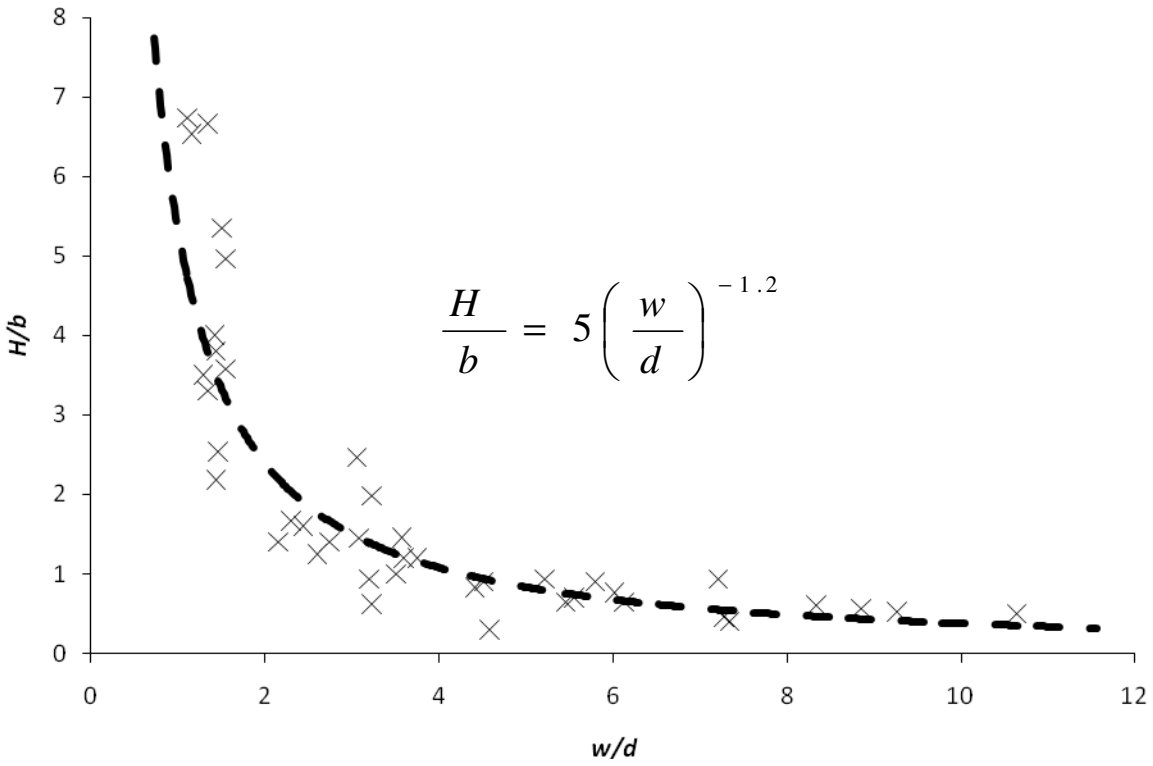

Figure 84. Correlation developed using forty-two simulation models.

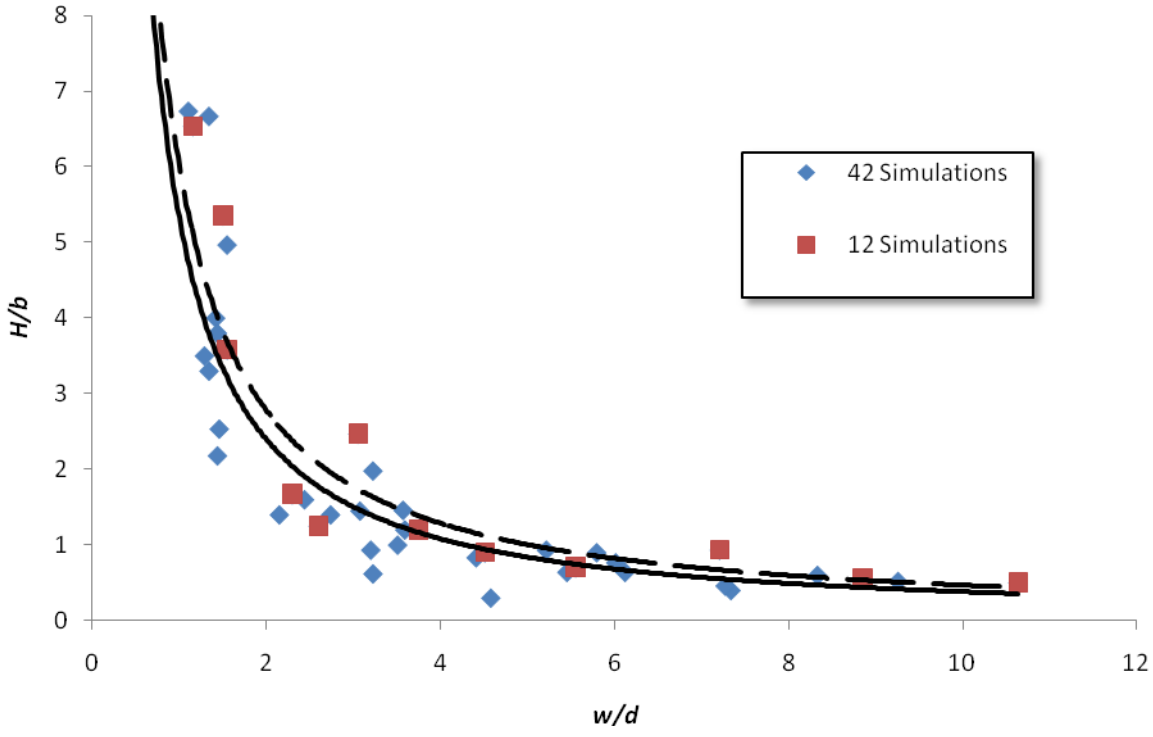

Figure 85. Comparison of the effect of simulation models on correlations.

Full-scale 5 Balconies Simulation	*H* (m)	*b* (m)	*w* (m)	*d* (m)	*H/b*	*w/d*
1	2.5	5.0	10	0.94	0.50	10.64
2	2.6	5.0	10	1.08	0.52	9.26
3	2.8	5.0	10	1.13	0.56	8.85
4	3.0	5.0	8	0.96	0.60	8.33
5	2.0	5.0	8	1.09	0.40	7.34
6	2.3	5.0	8	1.10	0.46	7.27
7	3.2	5.0	6	0.98	0.64	6.12
8	3.5	5.0	6	1.08	0.70	5.56
9	3.2	5.0	6	1.10	0.64	5.45
10	7.3	5.0	4	1.12	1.46	3.57
11	9.9	5.0	4	1.24	1.98	3.23
12	3.1	5.0	4	1.24	0.62	3.23
13	17.9	5.0	2	1.29	3.58	1.55
14	20.0	5.0	2	1.41	4.00	1.42
15	10.9	5.0	2	1.39	2.18	1.44
19	2.8	3.0	8	1.11	0.93	7.21
20	2.3	3.0	8	1.33	0.77	6.02
21	2.7	3.0	8	1.38	0.90	5.80
22	2.8	3.0	6	1.15	0.93	5.22
23	2.7	3.0	6	1.33	0.90	4.51
24	2.5	3.0	6	1.36	0.83	4.41
25	3.0	3.0	4	1.14	1.00	3.51
26	2.8	3.0	4	1.25	0.93	3.20
27	7.4	3.0	4	1.31	2.47	3.05
28	14.9	3.0	2	1.29	4.97	1.55
29	11.4	3.0	2	1.39	3.80	1.44
30	7.6	3.0	2	1.37	2.53	1.46
37	0.6	2.0	6	1.31	0.30	4.58
38	2.4	2.0	6	1.60	1.20	3.75
39	2.4	2.0	6	1.67	1.20	3.59
40	2.9	2.0	4	1.30	1.45	3.08
41	2.5	2.0	4	1.54	1.25	2.60
42	3.2	2.0	4	1.64	1.60	2.44
43	10.7	2.0	2	1.33	5.35	1.50
44	6.6	2.0	2	1.49	3.30	1.34
45	7.0	2.0	2	1.55	3.50	1.29
55	2.1	1.5	4	1.46	1.40	2.74
56	2.5	1.5	4	1.74	1.67	2.30
57	2.1	1.5	4	1.86	1.40	2.15
58	10.0	1.5	2	1.49	6.67	1.34
59	9.8	1.5	2	1.73	6.53	1.16
60	10.1	1.5	2	1.81	6.73	1.10

Table 21. Summary of result for full-scale five balcony configuration.

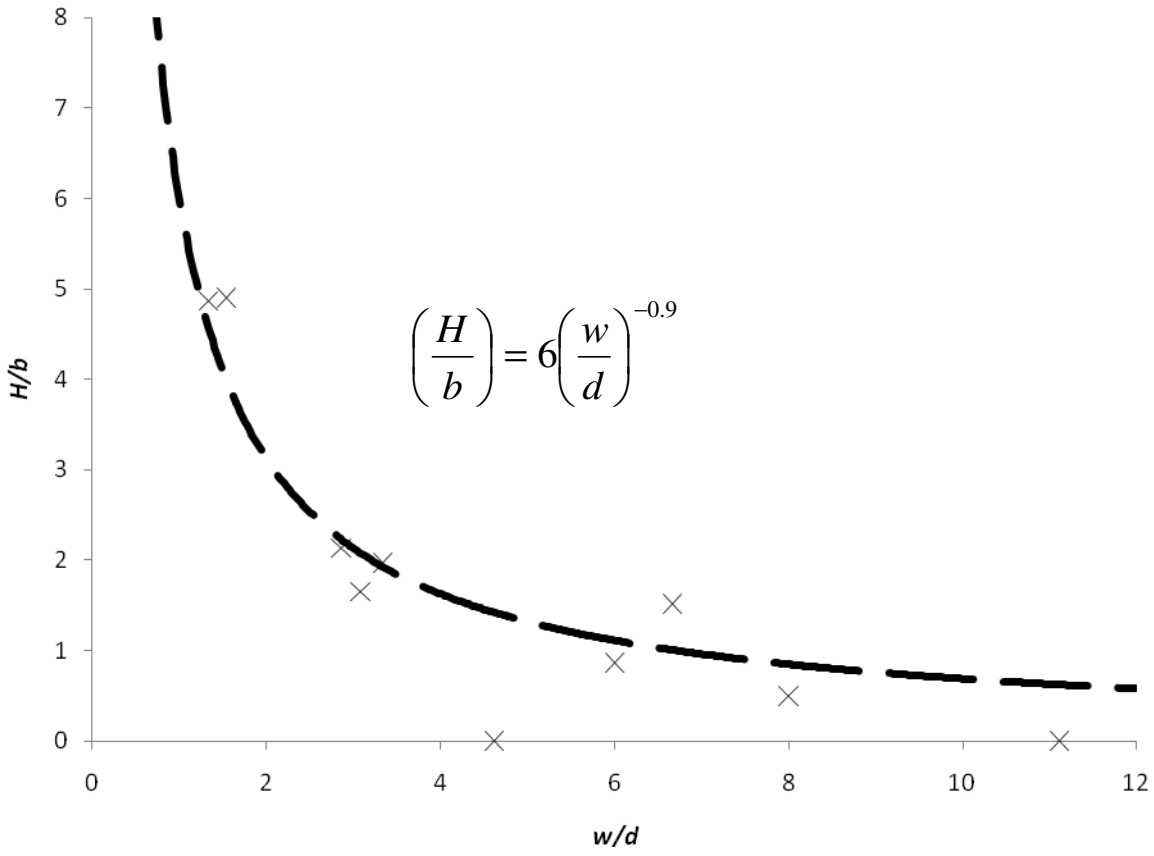

Figure 86. Correlation for small-scale five balcony configuration.

Small-scale 5 Balconies Simulation	*H* (m)	*b* (m)	*w* (m)	*d* (m)	*H/b*	*w/d*
1	0.35	0.50	1.0	0.07	0.70	14.29
3	0.00	0.50	1.0	0.09	0.00	11.11
8	0.76	0.50	0.6	0.09	1.52	6.67
13	>2.00	0.50	0.1	0.13	-	-
19	0.15	0.30	0.8	0.10	0.50	8.00
23	0.26	0.30	0.6	0.10	0.87	6.00
27	0.59	0.30	0.4	0.12	1.97	3.33
38	0.00	0.20	0.6	0.13	0.00	4.62
41	0.33	0.20	0.4	0.13	1.65	3.08
43	0.98	0.20	0.2	0.13	4.90	1.54
56	0.32	0.15	0.4	0.14	2.13	2.86
60	0.73	0.15	0.2	0.15	4.87	1.33

Table 22. Summary of result from small-scale five balcony configuration.

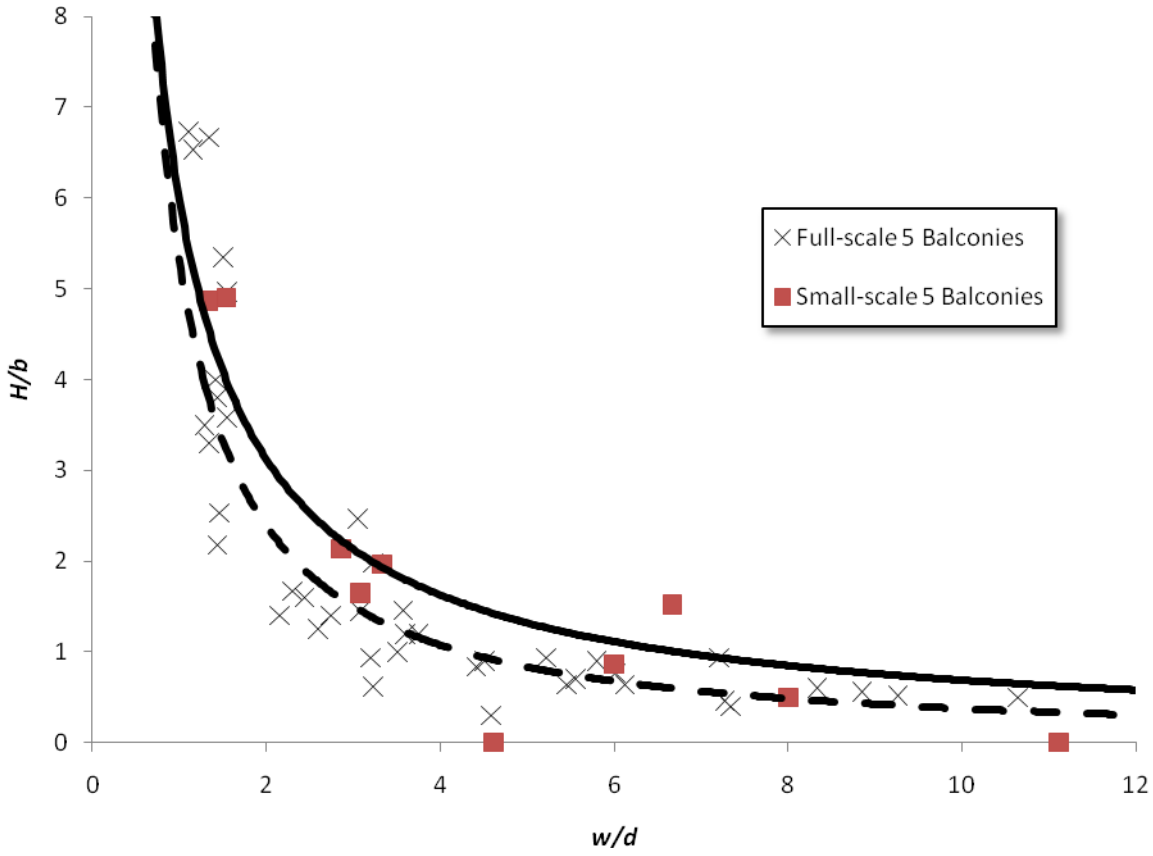

Figure 87. Comparison of small-scale and full-scale for five balcony configurations.

6.3 Correlation Equation for Full-scale Five Balcony Configuration without Upstand

Figure 88 and Table 23 show the correlation and summary from FDS on the full-scale five balcony with no upstand configuration.

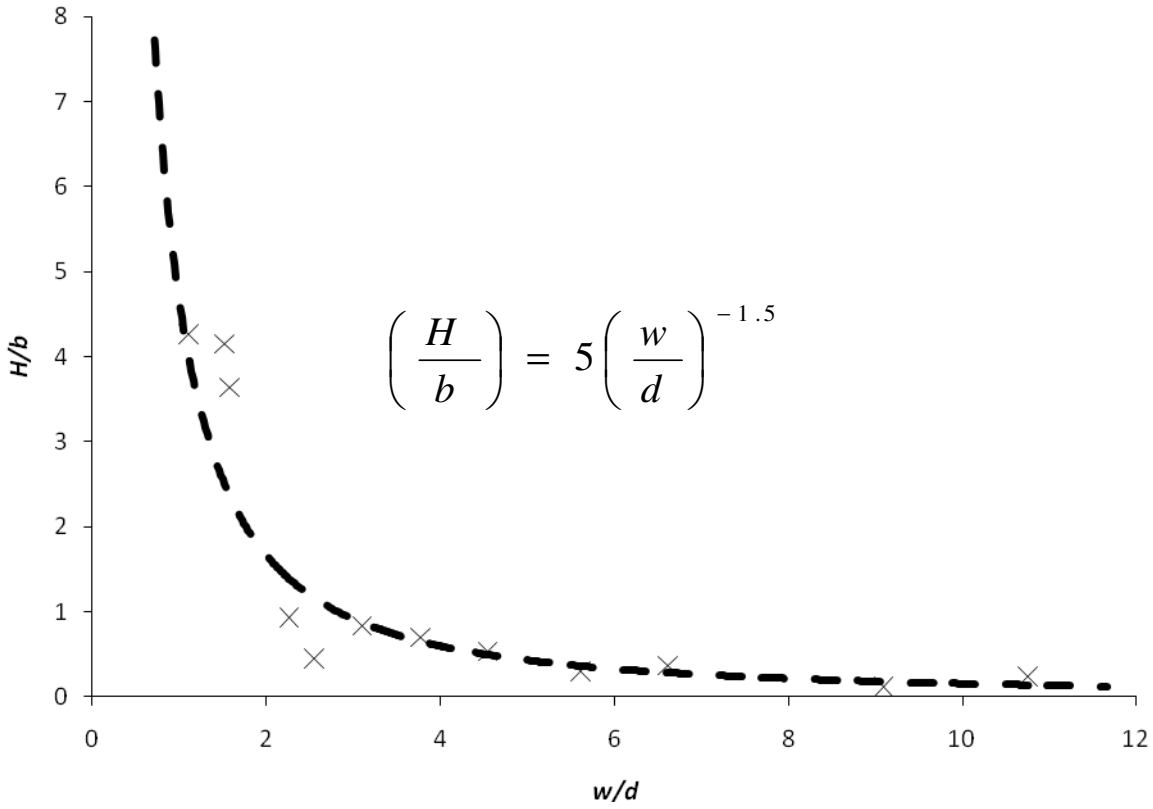

Figure 88. Correlation for full-scale five balcony with no upstand configuration.

Full-scale 5 Balconies No Upstand Simulation	*H* (m)	*b* (m)	*w* (m)	*d* (m)	*H/b*	*w/d*
1	1.2	5.0	10	0.93	0.24	10.75
3	0.6	5.0	10	1.10	0.12	9.09
8	1.5	5.0	6	1.07	0.30	5.61
13	18.2	5.0	2	1.27	3.64	1.57
19	1.1	3.0	8	1.21	0.37	6.61
23	1.6	3.0	6	1.32	0.53	4.55
27	2.5	3.0	4	1.29	0.83	3.10
38	1.4	2.0	6	1.59	0.70	3.77
41	0.9	2.0	4	1.57	0.45	2.55
43	8.3	2.0	2	1.32	4.15	1.52
56	1.4	1.5	4	1.77	0.93	2.26
60	6.4	1.5	2	1.81	4.27	1.10

Table 23. Summary of result for full-scale five balcony with no upstand configuration.

6.4 Correlation Equation for Full-scale Seven Balcony Configuration

Figure 89 and Table 24 show the correlation and summary from FDS on the full-scale seven balcony configuration. The three data points which have zero value on the vertical axis (*H/b*) are not taken into consideration for the correlation. This methodology is applied to all subsequent correlations when this data is used.

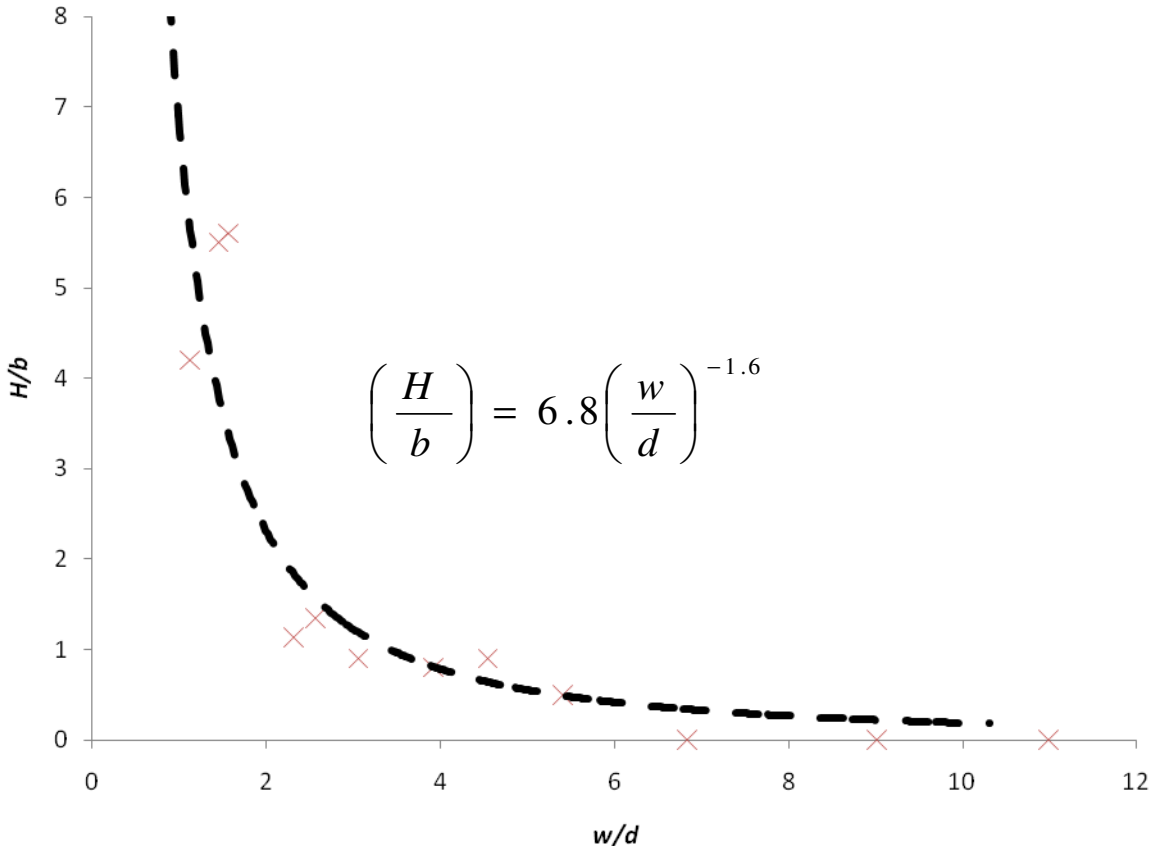

Figure 89. Correlation for full-scale seven balcony configuration.

Full-scale 7 Balconies Simulation	*H* (m)	*b* (m)	*w* (m)	*d* (m)	*H/b*	*w/d*
1	0.0	5.0	10	0.91	0.00	10.99
3	0.0	5.0	10	1.11	0.00	9.01
8	2.5	5.0	6	1.11	0.50	5.41
13	28.0	5.0	2	1.28	5.60	1.56
19	0.0	3.0	8	1.17	0.00	6.84
23	2.7	3.0	6	1.32	0.90	4.55
27	2.7	3.0	4	1.31	0.90	3.05
38	1.6	2.0	6	1.53	0.80	3.92
41	2.7	2.0	4	1.56	1.35	2.56
43	11.0	2.0	2	1.38	5.50	1.45
56	1.7	1.5	4	1.73	1.13	2.31
60	6.3	1.5	2	1.79	4.20	1.12

Table 24. Summary of result for full-scale seven balcony configuration.

6.5 Comparison of Full-scale Five Balcony with and without Upstand Simulations

Figure 90 shows the comparison of the earlier two correlation equations for full-scale five balcony with and without upstand configurations. As shown in the figure, when there is no upstand (such as using grill as balcony barricade), it will have lower height of smoke contamination. These comparisons demonstrate the effect of the balcony configuration condition on the correlation.

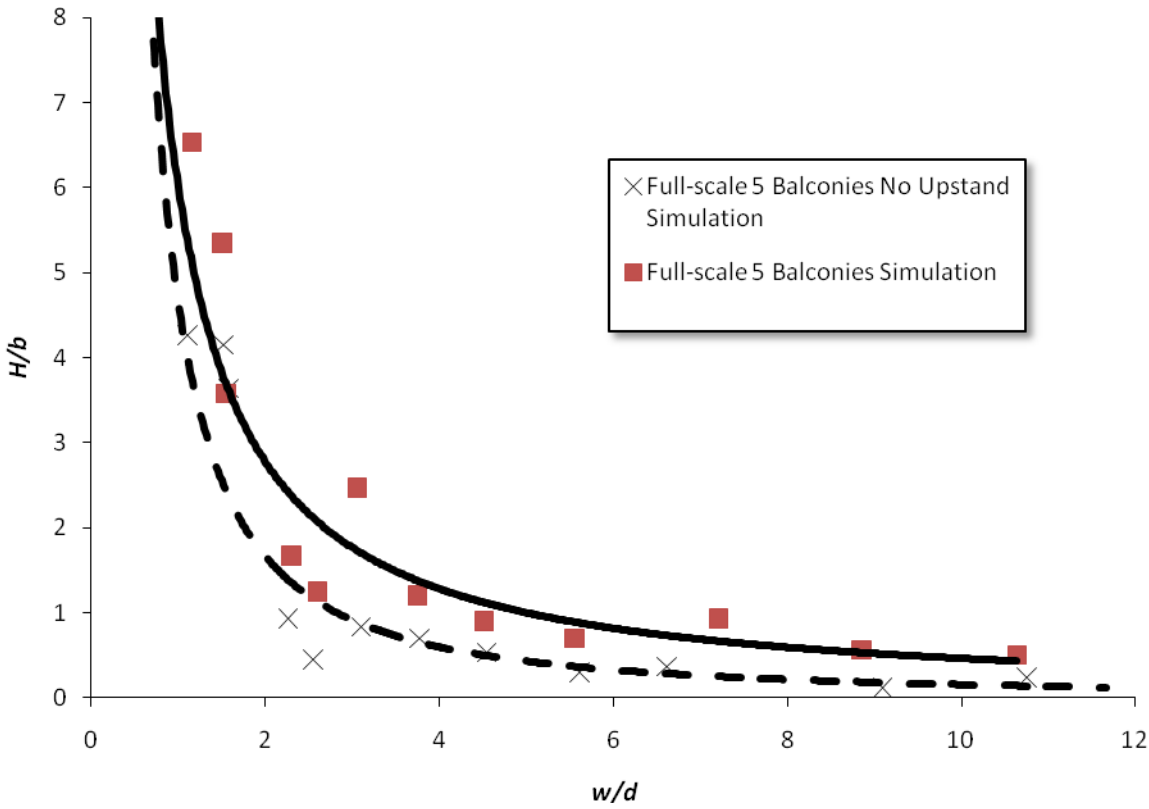

Figure 90. Comparison of full-scale five balcony with and without upstand.

6.6 Comparing the Effect of Number of Balcony on Correlations

Figure 91 shows the three correlations for small-scale three balcony, full-scale five and seven balcony configurations plotted together. From the figure, it shows that the correlation curves are well separated, and the trend of the correlation curve bent toward the origin with the increased number of balconies. Hence, it could conclude the atrium height has an effect on the smoke contamination correlation.

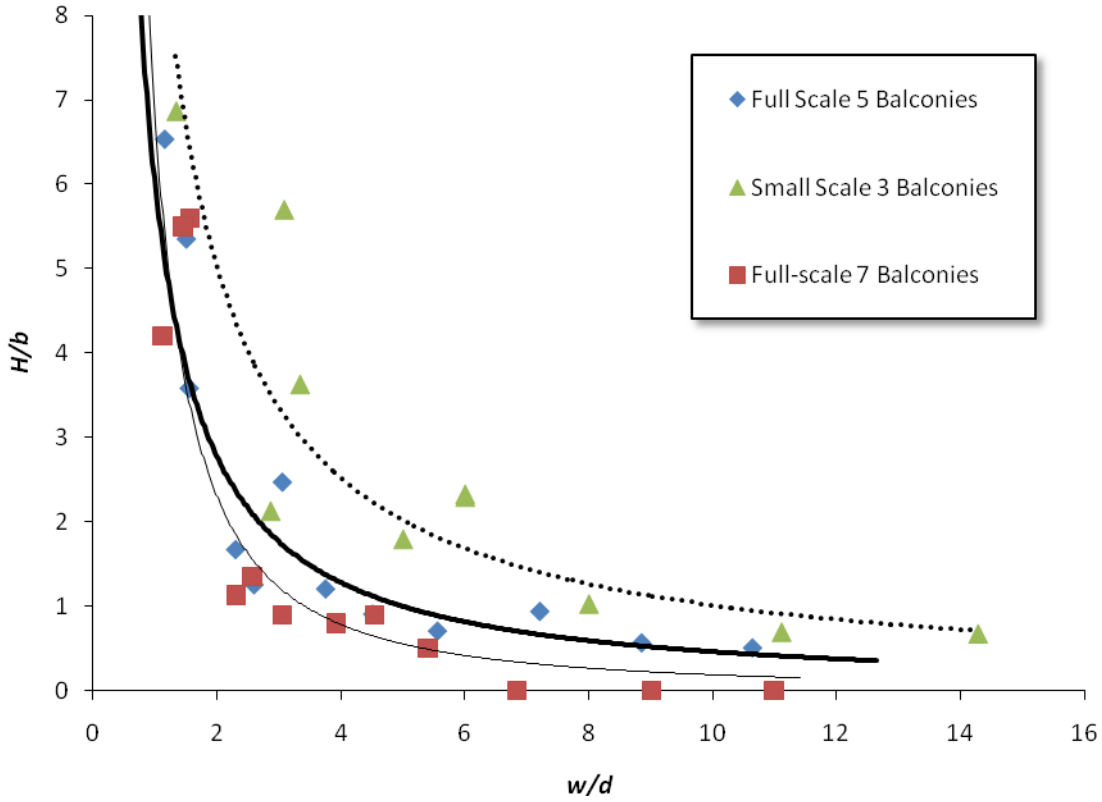

Figure 91. Comparison of number of balcony on correlations.

6.7 Proposed Revised Correlation

Since the height of the atrium has an effect on the smoke contamination correlation, it is proposed to revise the vertical axis of the graph. The graph is based on dimensionless axes so that all scale of configurations could be compared. The horizontal axis catered for the trajectory of the spill plume leaving the fire compartment. It is suggested that the vertical axis is suggested be revised as follows:

$$\text{Vertical Axis} = \frac{H}{b} * \frac{z}{b}$$

where

z is height of rise to the base of the layer (m)

The revised correlation for the configuration with upstand for three balcony to seven balcony is shown in Figure 92. Table 25 to Table 28 show the updated summary for small-scale three balcony and full-scale five and seven balcony configurations using this revised correlation.

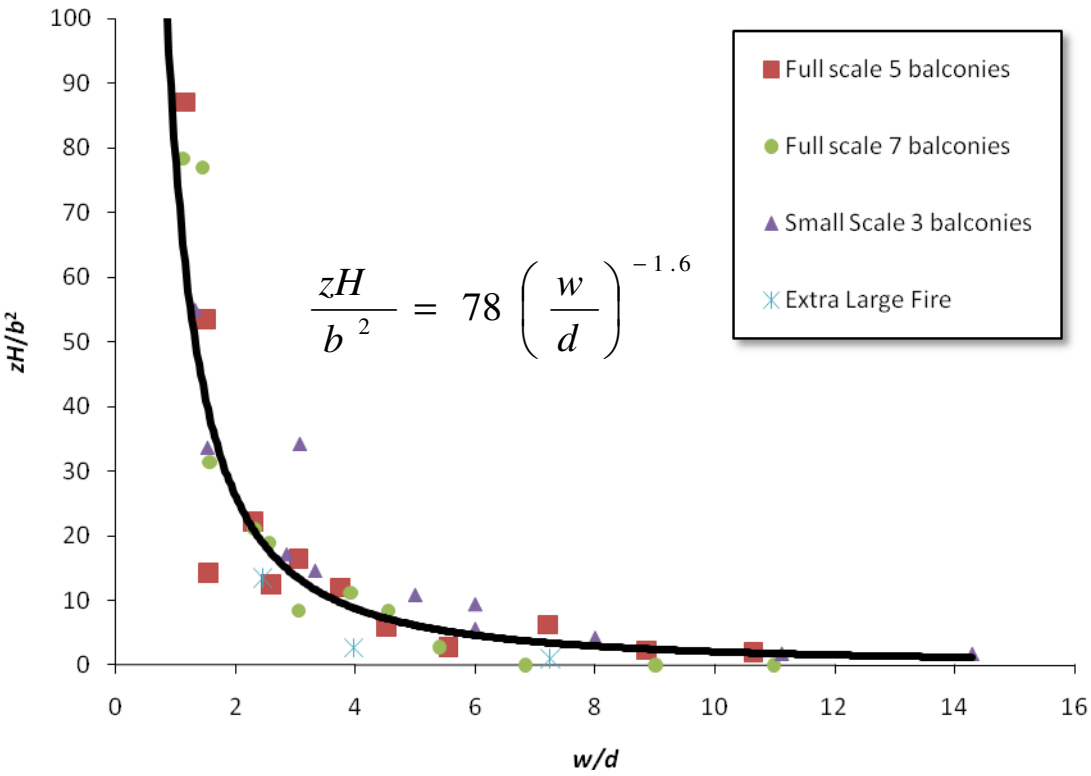

Figure 92. Proposed correlation for three to seven balcony with upstand configuration.

Full Scale 5 Balconies Simulation	*H* (m)	*b* (m)	*w* (m)	*d* (m)	zH/b^2	*w/d*
1	2.5	5.0	10	0.94	2.00	10.64
3	2.8	5.0	10	1.13	2.24	8.85
8	3.5	5.0	6	1.08	2.80	5.56
13	17.9	5.0	2	1.29	14.32	1.55
19	2.8	3.0	8	1.11	6.22	7.21
23	2.7	3.0	6	1.33	6.00	4.51
27	7.4	3.0	4	1.31	16.44	3.05
38	2.4	2.0	6	1.60	12.00	3.75
41	2.5	2.0	4	1.54	12.50	2.60
43	10.7	2.0	2	1.33	53.50	1.50
56	2.5	1.5	4	1.74	22.22	2.30
60	9.8	1.5	2	1.73	87.11	1.16

Table 25. Summary for full-scale five balcony simulation using revised vertical axis.

Full-scale 7 Balconies Simulation	H (m)	b (m)	w (m)	d (m)	$z H/b^2$	w/d
1	0.0	5.0	10	0.91	0.00	10.99
3	0.0	5.0	10	1.11	0.00	9.01
8	2.5	5.0	6	1.11	2.80	5.41
13	28.0	5.0	2	1.28	31.36	1.56
19	0.0	3.0	8	1.17	0.00	6.84
23	2.7	3.0	6	1.32	8.40	4.55
27	2.7	3.0	4	1.31	8.40	3.05
38	1.6	2.0	6	1.53	11.20	3.92
41	2.7	2.0	4	1.56	18.90	2.56
43	11.0	2.0	2	1.38	77.00	1.45
56	1.7	1.5	4	1.73	21.16	2.31
60	6.3	1.5	2	1.79	78.40	1.12

Table 26. Summary for full-scale seven balcony simulation using revised vertical axis.

Small-scale 3 Balconies Simulation	H (m)	b (m)	w (m)	d (m)	$z H/b^2$	w/d
1	0.34	0.5	1	0.07	1.63	14.29
3	0.35	0.5	1	0.09	1.68	11.11
8	1.15	0.5	0.6	0.1	5.52	6.00
13	>1.6	0.5	0.1	0.12	-	-
19	0.31	0.3	0.8	0.1	4.13	8.00
23	0.7	0.3	0.6	0.1	9.33	6.00
27	1.09	0.3	0.4	0.12	14.53	3.33
38	0.36	0.2	0.6	0.12	10.80	5.00
41	1.14	0.2	0.4	0.13	34.20	3.08
43	1.12	0.2	0.2	0.13	33.60	1.54
56	0.32	0.15	0.4	0.14	17.07	2.86
60	1.03	0.15	0.2	0.15	54.93	1.33

Table 27. Summary for small-scale three balcony simulation using revised vertical axis.

Extra Large Fire Simulation	H (m)	b (m)	w (m)	d (m)	$z H/b^2$	w/d
3a	1.3	5	10	1.38	1.04	7.25
24a	1.2	3	6	1.51	2.67	3.97
42a	2.7	2	4	1.63	13.50	2.45

Table 28. Summary for extra large fire simulation using revised vertical axis.

6.8 Applying the New Correlation on the Various Configurations with Upstand

The proposed correlation is applied to the experimental correlation and full-scale five and seven balcony configurations with an upstand. Figure 93 to Figure 95 show that the proposed correlation could better represent the full-scale five and seven balcony configurations than the small-scale three balcony configuration. The "solid" line in each figure is the original correlation developed for each configuration.

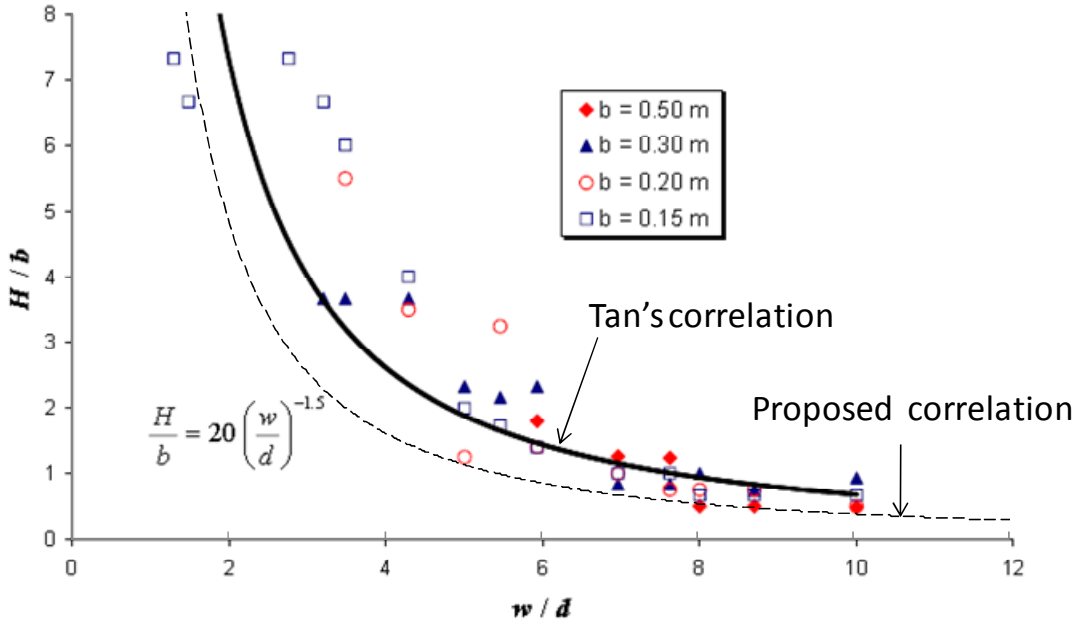

Figure 93. Application of proposed correlation onto Tan's (2009) experimental correlation.

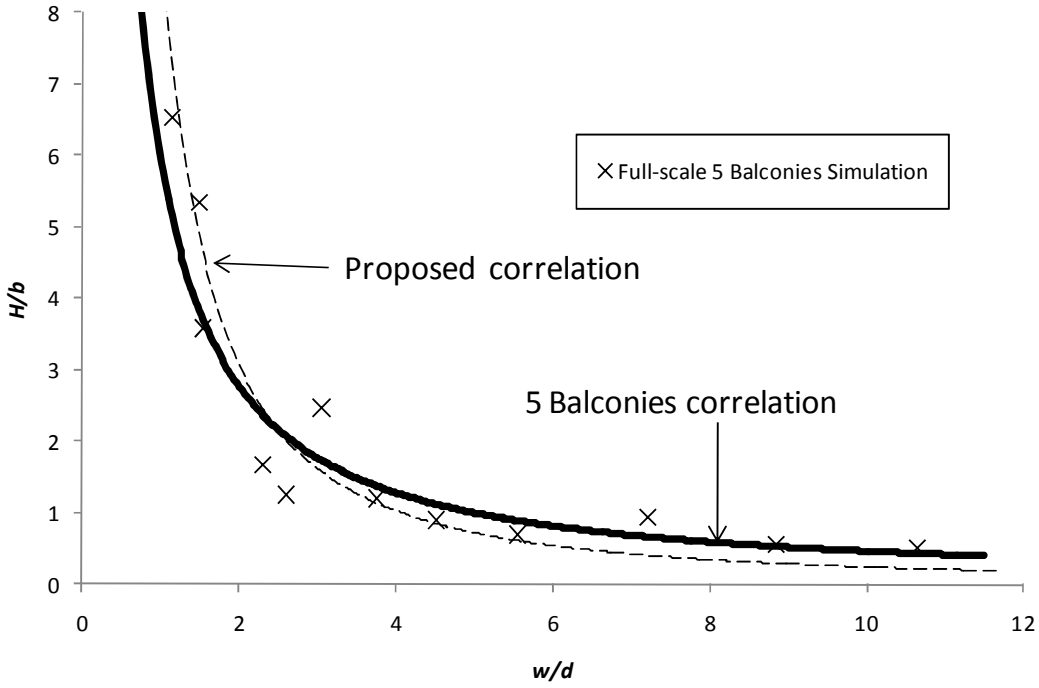

Figure 94. Application of proposed correlation onto full-scale five balcony configuration.

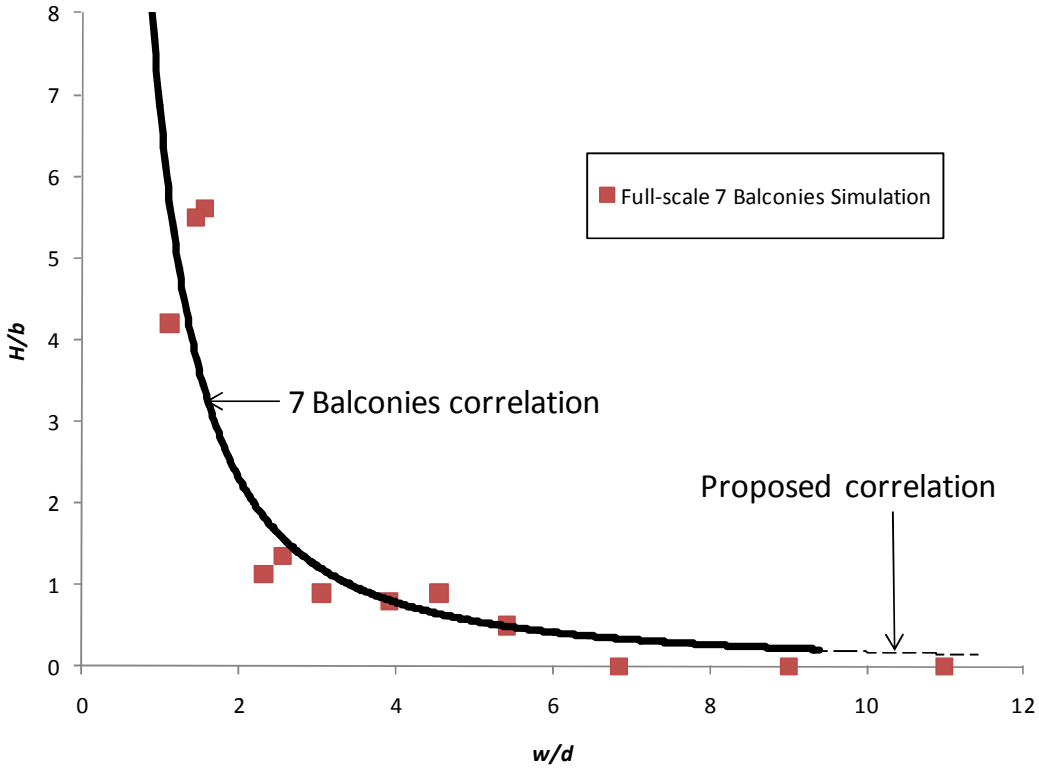

Figure 95. Application of proposed correlation onto full-scale seven balcony configuration.

7. FURTHER WORK

Further work is recommended in the following areas:

a. Use the Harrison (2009) formula to predict the smoke extraction rate and determine the smoke contamination at the highest balcony level.

b. Vary the separation height between the balconies to determine the effect on the correlation.

c. Morgan *et al* (1999) have mentioned that smoke contamination at each balcony should be studied independently. NFPA 92B (2005) also states minimum smoke tenability level instead of prescribed smoke layer interface height. Hence, it is suggested studying the fractional effective dose (FED) of toxic gases and thermal conditions at the balcony occupied height.

d. Vary the height of the upstand to study the effect on balcony contamination.

e. Determine the factors that cause different smoke contamination for balconies with and without upstand.

f. To study the effect of height of an atrium on balcony smoke contamination.

g. To study the effects of growing fires on balcony smoke contamination.

h. To conduct scale experiments to study the smoke contamination for balcony breadth of 0.15m and 0.2m.

i. To conduct small-scale experiments to verify the temperature and smoke contamination for balconies without an upstand.

8. CONCLUSION

Based on the modelling fundamentals established by Harrison (2009) and experimental results from Tan (2009), the correlation for upper balcony smoke contamination caused by a balcony spill plume has been developed for three to seven balconies with upstand configuration. The conclusions to this research project are as follows:

a. FDS is able to successfully simulate well the experiments conducted by Tan (2009) using the grid size recommended by Harrison (2009). It is viable to use the FDS slice file of temperature 30°C profiles to identify the level of smoke contamination in the balcony caused by the spill plume.

b. Similar configurations of small scale and full scale have similar smoke contamination characteristics.

c. Peak temperatures on full-scale configurations are higher than on the scale model.

d. The boundary conditions such as side walls, smoke reservoir, upstand and atrium height have significant effect on the smoke contamination characteristics.

e. As the atrium height increases, the smoke contamination on balconies, including the balcony immediately above the spill edge, is more severe.

f. For a balcony without upstand, smoke contamination on lower balcony could be more severe than a configuration with an upstand.

g. With constant fire size and plume width, the general belief that smoke contamination increases with reduction of balcony breadth is not consistent for breadth between full-scale 2.0m to 1.5m. More investigation is required to understand the smoke behaviour at these dimensions.

h. Based on the simulations, the revised correlation to predict the height of smoke contamination in the upper balcony for three to seven balconies with upstand configuration is as follows:

$$\frac{zH}{b^2} = 78\left(\frac{w}{d}\right)^{-1.6} \quad \text{or} \quad H = 78\frac{b^2}{z}\left(\frac{w}{d}\right)^{-1.6}$$

i. This correlation is valid for the following conditions:

   i. Between three to seven balconies.
   ii. Each balcony height is 4.0m.
   iii. The upstand height is 1.0m.
   iv. Aspect ratio $\left(\frac{w}{b}\right)$ is from 1.0 to 3.0.
   v. Steady heat release rate from 1.6 to 4.7 MW
   vi. There is no draft stop at the spill edge.

j. The correlations could allow the design engineer to conduct preliminary assessment of atrium upper balcony smoke contamination.

k. This study found that the boundary conditions beyond the spill edge are crucial and that the effect of time on the flow region above the balconies is important. Hence, each specific "real" design is recommended be modelled during detail design.

9. REFERENCES

Buchanan A. H. 2002. Structural Design for Fire Safety. John Wiley & Sons, Ltd. England.

Chow W.K. 1999. *Numerical simulations on balcony spill plume*. Fire and Materials (23). Page 91 to 99.

Colt. 2007. Smoke Control in Shopping Centres. Colt International Limited. United Kingdom.

Cox G. 1995. Combustion Fundamentals of Fire. Academic Press. UK London.

Drysdale D. 1998. An Introduction to Fire Dynamics. 2nd Edition. John Wiley & Sons. England.

ECE. 2000. *Fire safety in atria*. Energy Comfort 2000 Information Dossier. Esbensen Consulting Engineers.

Ferreira M. J. 2008. *Development in the design of smoke control systems*. Fire Protection Engineering. Society of the Protection Engineers. Bethesda, USA.

Forney G. P. 2007. Visualisation, A Tool for Understanding Fire Dynamics. National Institute of Standards and Technology. Gaithersburg, Maryland.

Gobeau N., Ledin H. S. and Lea C. J. 2002. Guidance for HSE Inspectors: Smoke movement in complex enclosed spaces – Assessment of Computational Fluid Dynamics. Health & Safety Laboratory. UK, Buxton.

Gritch T and Eason B. 2009. *Building envelope design guide – atria system*. Whole Building Design Guide. National Institute of Building Sciences. Washington, USA.

Hansell G. O. 1993. Heat and Mass Transfer Process Affecting Smoke Control in Atrium Buildings. PhD thesis. South Bank University.

Hansell G. O. Morgan H. P. and Marshall N. R. 1993. Smoke flow experiments in a model atrium. BRE Occasional Paper OP55, BRE.

Harrison R. 2004. Smoke Control in Atrium Buildings: A Study of the Thermal Spill Plume. Master thesis. University of Canterbury. Christchurch, New Zealand.

Harrison R. 2009. Entrainment of Air into Thermal Spill Plumes. PhD thesis. University of Canterbury. Christchurch, New Zealand.

Harrison R. and Spearpoint M. 2005. *Spill Over*. Fire Engineering Journal and Fire Protection. Page 33 to 35.

Karlsson B. and Quintiere J G 2000. Enclosure Fire Dynamics. CRC Press. Washington DC.

Klote J. H. 2008. *State-of-the-art atrium smoke control*. HPAC Engineering. Cleveland, USA.

Klote J. H. 2009. *Minimum smoke-layer depth in atrium smoke control*. HPAC Engineering. Cleveland, USA.

Klote J. H. and Milke J. A. 2002. Principles of Smoke Management. American Society of Heating, Refrigerating and Air-conditioning Engineers. Atlanta.

Law M. 1995a. *The origins of the 5MW design fire*. Fire Safety Engineering. Page 17 to 20.

Law M. 1995b. *Measurement of balcony smoke flow*. Fire Safety Journal (24). Page 189 to 195.

Lougheed G. D. 2000a. *Considerations in the design of smoke management systems for atriums*. Construction Technology Update. No. 48. National Research Council Canada.

Lougheed G. D. 2000b. *Basic principles of smoke management for atriums*. Construction Technology Update. No. 47. National Research Council Canada.

McCartney C.J. and Hadjisophocleous G. V. 2005. *Guidelines for the use of CFD simulations for fire and smoke modelling*. ASHRAE Transactions. Volume 111 No. 2 Page 583 to 594.

McCartney C. J. and Lougheed G. D. 2004. *CFD investigation of balcony spill plumes in atria*. 12th Annual Conference of the CFD Society of Canada, Combustion and Smoke Management. Page 823 to 830. Ottawa, Canada.

McGrattan K. 2005. *Fire modeling: Where are we? Where are we going?* 8th International Association for Fire Safety Science. PRC Beijing.

McGrattan K. B., Rehm R. G. and Baum H. R. 1998. *Large eddy simulations of smoke movement*. Fire Safety Journal. Volume 30. Page 161 to 178.

McGrattan K., Klein B., Hostikka S. and Floyd J. 2009. Fire Dynamics Simulator (Version 5) User's Guide. NIST Special Publication 1019-5. National Institute of Standards and Technology. Gaithersburg, Maryland, USA.

Morgan H. P., Ghosh B. K., Garrad G., Pamlitschka R., Smedt J. C. D. and Schoonbaert L. R. 1999. Design Methodologies for Smoke and Heat Exhaust Ventilation. Building Research Establishment. Watford, UK.

NFPA 92B. 2009. Smoke Management Systems in Malls, Atria, and Large Spaces. National Fire Protection Association. USA.

Poreh M, Regev A. and Marshall N. R. 2008. *Entrainment by adhered two-dimensional plumes*. Fire Safety Journal (43). Page 344-350.

Quintiere J. G. and Grove B. S. 1998. *A unified analysis for fire plumes. Twenty-Seventh Symposium (International) on Combustion*. The Combustion Institute. Page 2757 to 2766.

Quintiere J. G. and Ma T. G. 2003. *Numerical simulation of axi-symmetric fire plumes: accuracy and limitations*. Fire Safety Journal Volume 38. Page 467 to 492.

Ryder N. L., Sutula J. A., Schemel C. F., Hamer A. J. and Brunt. V. V. 2004. *Consequence modeling using the fire dynamics simulator*. Journal of Hazardous Materials. Volume 115. Page 149 to 154.

Tan F. 2009. Physical Scale Modelling of Smoke Contamination in Upper Balcony by a Balcony Spill Plume in an Atrium. University of Canterbury. New Zealand, Christchurch.

Yii E. H. 1998. Exploratory Salt Water Experiments of Balcony Spill Plume using Laser Induced Fluorescence Technique. Fire Engineering Research Report, University of Canterbury.

Tilley N. and Merci B. 2009. *Application of FDS to adhered spill plumes in atria*. Fire Technology. Volume 45. Springer Science + Business Media, LLC. USA.

Tiong H. Y. 2010. Numerical Simulation of Unchannelled Balcony Spill Plume (Ongoing). University of Canterbury. Christchurch, New Zealand.

Wade C., Beever P., Fleischmann C., Lester J., Lloydd D., Moule A., Saunders N. and Thory P. 2007. *Developing fire performance criteria for New Zealand's performance based building code*. Fire Safety Engineering International Seminar. 26 and 27 April 2007. Paris, France.

Weckman E. J., Lougheed G. D. and McCartney C. J. 2005. *CFD investigation of balcony spill plmes in atria (Part II)*. 13th Annual Conference of the Computational Fluid Dynamics Society of Canada. 31 July to 3 Aug 2005.

Sample FDS 5.0 Code for Full-Scale Model

```
&HEAD CHID='F01E5', TITLE='F01E5'/
&MESH IJK = 120, 108, 180, XB = -2.0, 22.0, -0.6, 21.0, -0.2, 35.8/ Mesh Size 200mm for Atrium
&MESH IJK = 60, 45, 30, XB = 4.0, 16.0, 21.0, 30.0, -0.2, 5.8/ Mesh Size 200mm for Fire Room

&TIME T_END = 600.0/

&DUMP DT_RESTART = 10/ Backup Interval
/&MISC RESTART = .TRUE./ RESUME

&VENT MB='XMIN', SURF_ID='OPEN'/
&VENT MB='XMAX', SURF_ID='OPEN'/
&VENT MB='YMIN', SURF_ID='OPEN'/
&VENT MB='YMAX', SURF_ID='OPEN'/
&VENT MB='ZMIN', SURF_ID='OPEN'/
&VENT MB='ZMAX', SURF_ID='OPEN'/

&MISC SURF_DEFAULT='CFI board'/

&MATL ID='CFI board'
        CONDUCTIVITY    = 0.041
        SPECIFIC_HEAT   = 0.82
        DENSITY         = 229.0/

&SURF ID='CFI board'
        MATL_ID         = 'CFI board'
        COLOR           = 'BRICK'
        TRANSPARENCY    = 0.4
        BACKING                 = 'VOID'
        THICKNESS       = 0.16 /  wall properties

&SURF ID = 'STEEL SHEET'
        MATL_ID = 'STEEL'
        COLOR = 'GREEN'
        BACKING = 'VOID'
        THICKNESS = 0.01
        TRANSPARENCY = 0.4/ STRUCTURAL DESIGN FOR FIRE SAFETY TABLE 3.4

&MATL ID = 'STEEL'
        CONDUCTIVITY = 45.8
        SPECIFIC_HEAT =0.46
        DENSITY = 7850.0/

/DEFINING A BURNING OBJECT

REAC ID='Ethanol'
        C       = 2
        H       = 6
        O       = 1
        HEAT_OF_COMBUSTION = 26800
        CO_YIELD = 0.022
        SOOT_YIELD = 0.11/ Ethanol properties

/FIRE SIZE
&SURF ID = 'BURNER', HRRPUA = 488, COLOR = 'RED'/ To use with 1581kW
/&SURF ID = 'BURNER', HRRPUA = 468, COLOR = 'RED'/ To use with 3162kW
/&SURF ID = 'BURNER', HRRPUA = 522, COLOR = 'RED'/ To use with 4743kW
&RADI RADIATIVE_FRACTION = 0.20/

&OBST XB = 9.1, 10.9, 26.2, 28.0, 0.0, 0.2, SURF_IDS = 'BURNER', 'INERT', 'INERT'/  1581kW (5kW)
/&OBST XB = 8.7, 11.3, 25.4, 28.0, 0.0, 0.2, SURF_IDS = 'BURNER', 'INERT', 'INERT'/  3162kW (10kW)
/&OBST XB = 8.5, 11.5, 25.0, 28.0, 0.0, 0.2, SURF_IDS = 'BURNER', 'INERT', 'INERT'/  4743kW(15kW)

/FIRE COMPARTMENT & ATRIUM WALL
&OBST XB = 0.0, 20.0, 20.0, 20.16, 0.0, 33.0/ ATRIUM WALL
&OBST XB = 4.84, 5.0, 20.0, 30.0, 0.0, 5.0/ BURNER S WALL
&OBST XB = 15.0, 15.16, 20.0, 30.0, 0.0, 5.0/ BURNER N WALL
```

```
&OBST XB = 5.0, 15.0, 29.84, 30.0, 0.0, 5.0/ BURNER W WALL
&OBST XB = 5.0, 15.0, 20.0, 30.0, 5.0, 5.16/ BURNER CEILING

&OBST XB = 5.0, 15.0, 20.0, 30.0, -0.16, 0.0/ BURNER ROOM FLOOR
&OBST XB = 0.0, 20.0, 0.0, 20.0, -0.16, 0.0/ ROOM FLOOR

/CHANNEL SCREEN WIDTH & OPENING = 10.0M
&OBST XB = 4.84, 5.0, 15.0, 20.0, 3.0, 5.0/ S CHANNEL
&OBST XB = 15.0, 15.16, 15.0, 20.0, 3.0, 5.0/ S CHANNEL
&HOLE XB = 5.0, 15.0, 18.0, 22.0, 0.0, 5.0/ FRONT OPENING

/BREATH 5.0M
/BALCONY 1 FLOOR
&OBST XB = 0.0, 20.0, 15.0, 20.0, 5.0, 5.16/ BALCONY 1 FLOOR
&OBST XB = 0.0, 20.0, 15.0, 15.01, 5.0, 6.0, SURF_ID = 'STEEL SHEET'/ UPSTAND

/BALCONY 2 FLOOR
&OBST XB = 0.0, 20.0, 15.0, 20.0, 9.0, 9.01, SURF_ID = 'STEEL SHEET'/ FLOOR
&OBST XB = 0.0, 20.0, 15.0, 15.01, 9.0, 10.0, SURF_ID = 'STEEL SHEET'/ UPSTAND

/BALCONY 3 FLOOR
&OBST XB = 0.0, 20.0, 15.0, 20.0, 13.0, 13.01, SURF_ID = 'STEEL SHEET'/ FLOOR
&OBST XB = 0.0, 20.0, 15.0, 15.01, 13.0, 14.0, SURF_ID = 'STEEL SHEET'/ UPSTAND

/BALCONY 4 FLOOR
&OBST XB = 0.0, 20.0, 15.0, 20.0, 17.0, 17.01, SURF_ID = 'STEEL SHEET'/ FLOOR
&OBST XB = 0.0, 20.0, 15.0, 15.01, 17.0, 18.0, SURF_ID = 'STEEL SHEET'/ UPSTAND

/BALCONY 5 FLOOR
&OBST XB = 0.0, 20.0, 15.0, 20.0, 21.0, 21.01, SURF_ID = 'STEEL SHEET'/ FLOOR
&OBST XB = 0.0, 20.0, 15.0, 15.01, 21.0, 22.0, SURF_ID = 'STEEL SHEET'/ UPSTAND

&OBST XB = 0.0, 20.0, 15.0, 20.0, 24.99, 25.0, SURF_ID = 'STEEL SHEET'/ CEILING FOR BALCONY 5

&SURF ID = 'PERSPEX SHEET'
        MATL_ID = 'PERSPEX'
        COLOR = 'BLUE'
        BACKING = 'VOID'
        THICKNESS = 0.12
        TRANSPARENCY = 0.4/ FROM HARRISON (2009)

&MATL ID = 'PERSPEX'
        CONDUCTIVITY = 0.19
        SPECIFIC_HEAT =1.42
        DENSITY = 1190.0/

/Additional Walls to Emulate the Experiment Setup
&OBST XB = 19.84, 20.0, 0.0, 20.0, 5.0, 33.0/ ATRIUM NORTH WALL
&OBST XB = 0.0, 20.0, 0.0, 0.16, 5.0, 33.0/ ATRIUM EAST WALL
&OBST XB = 0.0, 20.0, 0.0, 20.0, 32.8, 33.0/ ATRIUM CEILING
&OBST XB = 0.0, 0.12, 0.0, 20.0, 25.0, 33.0, SURF_ID = 'PERSPEX SHEET'/ ATRIUM WEST WALL

/EXHAUST Fan
&SURF ID = 'FAN', MASS_FLUX_TOTAL = 28.0, COLOR='BROWN'/ MASS FLOW RATE IN KG PER SEC PER M2 ASSUME
MASS FLOW = 252.0KG/S
&VENT XB = 8.5, 11.5, 2.0, 5.0, 32.8 ,32.8, SURF_ID='FAN' / FAN OPENING ASSUMED 3.0M BY 3.0M

/To see the Flame
&ISOF QUANTITY = 'MIXTURE_FRACTION', VALUE(1) = 0.06, VALUE(2) = 0.001/
&ISOF QUANTITY = 'TEMPERATURE', VALUE(1) = 25.0, VALUE(2) = 30.0/
&ISOF QUANTITY = 'carbon monoxide', VALUE(1) = 0.0014/
&ISOF QUANTITY = 'carbon dioxide', VALUE(1) = 0.05/
&ISOF QUANTITY = 'oxygen', VALUE(1) = 0.12/

/Slice File
&SLCF PBX = 10.0, QUANTITY = 'VISIBILITY'/
&SLCF PBY = 15.0, QUANTITY = 'VISIBILITY'/
&SLCF PBX = 10.0, QUANTITY = 'TEMPERATURE'/
&SLCF PBX = 10.0, QUANTITY = 'carbon dioxide'/
&SLCF PBX = 10.0, QUANTITY = 'carbon monoxide'/
&SLCF PBX = 10.0, QUANTITY = 'PRESSURE'/
&SLCF PBX = 10.0, QUANTITY = 'oxygen'/
&SLCF PBX = 10.0, QUANTITY = 'VELOCITY', VECTOR=.TRUE./
```

```
&SLCF PBY = 17.5, QUANTITY = 'VISIBILITY'/
&SLCF PBY = 17.5, QUANTITY = 'TEMPERATURE'/
&SLCF PBY = 17.5, QUANTITY = 'carbon dioxide'/
&SLCF PBY = 17.5, QUANTITY = 'carbon monoxide'/
&SLCF PBY = 17.5, QUANTITY = 'PRESSURE'/
&SLCF PBX = 17.5, QUANTITY = 'oxygen'/

/EXTRA SLCF TO SEE THE PRESSURE DISTRIBUTION AT 2M ABOVE EACH BALCONY
&SLCF PBZ = 7.0, QUANTITY = 'PRESSURE'/
&SLCF PBZ = 11.0, QUANTITY = 'PRESSURE'/
&SLCF PBZ = 15.0, QUANTITY = 'PRESSURE'/
&SLCF PBZ = 19.0, QUANTITY = 'PRESSURE'/
&SLCF PBZ = 23.0, QUANTITY = 'PRESSURE'/

&SLCF PBZ = 7.0, QUANTITY = 'VISIBILITY'/
&SLCF PBZ = 11.0, QUANTITY = 'VISIBILITY'/
&SLCF PBZ = 15.0, QUANTITY = 'VISIBILITY'/
&SLCF PBZ = 19.0, QUANTITY = 'VISIBILITY'/
&SLCF PBZ = 23.0, QUANTITY = 'VISIBILITY'/

&SLCF PBZ = 7.0, QUANTITY = 'TEMPERATURE'/
&SLCF PBZ = 11.0, QUANTITY = 'TEMPERATURE'/
&SLCF PBZ = 15.0, QUANTITY = 'TEMPERATURE'/
&SLCF PBZ = 19.0, QUANTITY = 'TEMPERATURE'/
&SLCF PBZ = 23.0, QUANTITY = 'TEMPERATURE'/

&SLCF PBZ = 7.0, QUANTITY = 'carbon dioxide'/
&SLCF PBZ = 11.0, QUANTITY = 'carbon dioxide'/
&SLCF PBZ = 15.0, QUANTITY = 'carbon dioxide'/
&SLCF PBZ = 19.0, QUANTITY = 'carbon dioxide'/
&SLCF PBZ = 23.0, QUANTITY = 'carbon dioxide'/

&SLCF PBZ = 7.0, QUANTITY = 'carbon monoxide'/
&SLCF PBZ = 11.0, QUANTITY = 'carbon monoxide'/
&SLCF PBZ = 15.0, QUANTITY = 'carbon monoxide'/
&SLCF PBZ = 19.0, QUANTITY = 'carbon monoxide'/
&SLCF PBZ = 23.0, QUANTITY = 'carbon monoxide'/

&SLCF PBZ = 7.0, QUANTITY = 'oxygen'/
&SLCF PBZ = 11.0, QUANTITY = 'oxygen'/
&SLCF PBZ = 15.0, QUANTITY = 'oxygen'/
&SLCF PBZ = 19.0, QUANTITY = 'oxygen'/
&SLCF PBZ = 23.0, QUANTITY = 'oxygen'/

/TEMPERATURE SENSOR FOR COLUMN A, IMMEDIATELY OUTSIDE THE FIRE CELL
&DEVC XYZ = 10.0, 15.0, 4.7, QUANTITY = 'TEMPERATURE', ID = 'T-A1'/ 0.3M BELOW BALCONY 1
&DEVC XYZ = 10.0, 15.0, 4.3, QUANTITY = 'TEMPERATURE', ID = 'T-A2'/ 0.7M BELOW BALCONY 1
&DEVC XYZ = 10.0, 15.0, 3.9, QUANTITY = 'TEMPERATURE', ID = 'T-A3'/ 1.1M BELOW BALCONY 1
&DEVC XYZ = 10.0, 15.0, 3.5, QUANTITY = 'TEMPERATURE', ID = 'T-A4'/ 1.5M BELOW BALCONY 1
&DEVC XYZ = 10.0, 15.0, 3.1, QUANTITY = 'TEMPERATURE', ID = 'T-A5'/ 1.9M BELOW BALCONY 1
&DEVC XYZ = 10.0, 15.0, 2.7, QUANTITY = 'TEMPERATURE', ID = 'T-A6'/ 2.3M BELOW BALCONY 1
&DEVC XYZ = 10.0, 15.0, 2.0, QUANTITY = 'TEMPERATURE', ID = 'T-A7'/ 3.0M BELOW BALCONY 1
&DEVC XYZ = 10.0, 15.0, 1.0, QUANTITY = 'TEMPERATURE', ID = 'T-A8'/ 4.0M BELOW BALCONY 1
&DEVC XYZ = 10.0, 15.0, 0.0, QUANTITY = 'TEMPERATURE', ID = 'T-A9'/ 5.0M BELOW BALCONY 1

/CHECK LAYER HEIGHT
&DEVC XB = 10.0, 10.0, 15.0, 15.0, 0.0, 5.0, QUANTITY = 'LAYER HEIGHT', ID = 'LAY-A1'/

/TEMPERATURE SENSOR FOR COLUMN B, IMMEDIATELY OUTSIDE THE BALCONY
&DEVC XYZ = 10.0, 15.0, 6.0, QUANTITY = 'TEMPERATURE', ID = 'T-B01'/  1.0M ABOVE BALCONY 1
&DEVC XYZ = 10.0, 15.0, 7.0, QUANTITY = 'TEMPERATURE', ID = 'T-B02'/  2.0M ABOVE BALCONY 1
&DEVC XYZ = 10.0, 15.0, 8.0, QUANTITY = 'TEMPERATURE', ID = 'T-B03'/  3.0M ABOVE BALCONY 1
&DEVC XYZ = 10.0, 15.0, 10.0, QUANTITY = 'TEMPERATURE', ID = 'T-B04'/ 5.0M ABOVE BALCONY 1
&DEVC XYZ = 10.0, 15.0, 11.0, QUANTITY = 'TEMPERATURE', ID = 'T-B05'/ 6.0M ABOVE BALCONY 1
&DEVC XYZ = 10.0, 15.0, 12.0, QUANTITY = 'TEMPERATURE', ID = 'T-B06'/ 7.0M ABOVE BALCONY 1
&DEVC XYZ = 10.0, 15.0, 14.0, QUANTITY = 'TEMPERATURE', ID = 'T-B07'/ 9.0M ABOVE BALCONY 1
&DEVC XYZ = 10.0, 15.0, 15.0, QUANTITY = 'TEMPERATURE', ID = 'T-B08'/ 10.0M ABOVE BALCONY 1
&DEVC XYZ = 10.0, 15.0, 16.0, QUANTITY = 'TEMPERATURE', ID = 'T-B09'/ 11.0M ABOVE BALCONY 1
&DEVC XYZ = 10.0, 15.0, 18.0, QUANTITY = 'TEMPERATURE', ID = 'T-B10'/ 13.0M ABOVE BALCONY 1
&DEVC XYZ = 10.0, 15.0, 19.0, QUANTITY = 'TEMPERATURE', ID = 'T-B11'/ 14.0M ABOVE BALCONY 1
&DEVC XYZ = 10.0, 15.0, 20.0, QUANTITY = 'TEMPERATURE', ID = 'T-B12'/ 15.0M ABOVE BALCONY 1
&DEVC XYZ = 10.0, 15.0, 22.0, QUANTITY = 'TEMPERATURE', ID = 'T-B13'/ 17.0M ABOVE BALCONY 1
```

```
&DEVC XYZ = 10.0, 15.0, 23.0, QUANTITY = 'TEMPERATURE', ID = 'T-B14'/ 18.0M ABOVE BALCONY 1
&DEVC XYZ = 10.0, 15.0, 24.0, QUANTITY = 'TEMPERATURE', ID = 'T-B15'/ 19.0M ABOVE BALCONY 1

/VISIBILITY SENSOR FOR COLUMN B, IMMEDIATELY OUTSIDE THE BALCONY
&DEVC XYZ = 10.0, 15.0, 6.0, QUANTITY = 'VISIBILITY', ID = 'V-B01'/  1.0M ABOVE BALCONY 1
&DEVC XYZ = 10.0, 15.0, 7.0, QUANTITY = 'VISIBILITY', ID = 'V-B02'/  2.0M ABOVE BALCONY 1
&DEVC XYZ = 10.0, 15.0, 8.0, QUANTITY = 'VISIBILITY', ID = 'V-B03'/  3.0M ABOVE BALCONY 1
&DEVC XYZ = 10.0, 15.0, 10.0, QUANTITY = 'VISIBILITY', ID = 'V-B04'/ 5.0M ABOVE BALCONY 1
&DEVC XYZ = 10.0, 15.0, 11.0, QUANTITY = 'VISIBILITY', ID = 'V-B05'/ 6.0M ABOVE BALCONY 1
&DEVC XYZ = 10.0, 15.0, 12.0, QUANTITY = 'VISIBILITY', ID = 'V-B06'/ 7.0M ABOVE BALCONY 1
&DEVC XYZ = 10.0, 15.0, 14.0, QUANTITY = 'VISIBILITY', ID = 'V-B07'/ 9.0M ABOVE BALCONY 1
&DEVC XYZ = 10.0, 15.0, 15.0, QUANTITY = 'VISIBILITY', ID = 'V-B08'/ 10.0M ABOVE BALCONY 1
&DEVC XYZ = 10.0, 15.0, 16.0, QUANTITY = 'VISIBILITY', ID = 'V-B09'/ 11.0M ABOVE BALCONY 1
&DEVC XYZ = 10.0, 15.0, 18.0, QUANTITY = 'VISIBILITY', ID = 'V-B10'/ 13.0M ABOVE BALCONY 1
&DEVC XYZ = 10.0, 15.0, 19.0, QUANTITY = 'VISIBILITY', ID = 'V-B11'/ 14.0M ABOVE BALCONY 1
&DEVC XYZ = 10.0, 15.0, 20.0, QUANTITY = 'VISIBILITY', ID = 'V-B12'/ 15.0M ABOVE BALCONY 1
&DEVC XYZ = 10.0, 15.0, 22.0, QUANTITY = 'VISIBILITY', ID = 'V-B13'/ 17.0M ABOVE BALCONY 1
&DEVC XYZ = 10.0, 15.0, 23.0, QUANTITY = 'VISIBILITY', ID = 'V-B14'/ 18.0M ABOVE BALCONY 1
&DEVC XYZ = 10.0, 15.0, 24.0, QUANTITY = 'VISIBILITY', ID = 'V-B15'/ 19.0M ABOVE BALCONY 1

/TEMPERATURE SENSOR FOR COLUMN C, INSIDE THE BALCONY
&DEVC XYZ = 10.0, 17.5, 7.0, QUANTITY = 'TEMPERATURE', ID = 'T-C1O'/  2.0M ABOVE BALCONY 1
&DEVC XYZ = 10.0, 19.5, 7.0, QUANTITY = 'TEMPERATURE', ID = 'T-C1I'/  2.0M ABOVE BALCONY 1
&DEVC XYZ = 10.0, 17.5, 11.0, QUANTITY = 'TEMPERATURE', ID = 'T-C2O'/ 2.0M ABOVE BALCONY 2
&DEVC XYZ = 10.0, 19.5, 11.0, QUANTITY = 'TEMPERATURE', ID = 'T-C2I'/ 2.0M ABOVE BALCONY 2
&DEVC XYZ = 10.0, 17.5, 15.0, QUANTITY = 'TEMPERATURE', ID = 'T-C3O'/ 2.0M ABOVE BALCONY 3
&DEVC XYZ = 10.0, 19.5, 15.0, QUANTITY = 'TEMPERATURE', ID = 'T-C3I'/ 2.0M ABOVE BALCONY 3
&DEVC XYZ = 10.0, 17.5, 19.0, QUANTITY = 'TEMPERATURE', ID = 'T-C4O'/ 2.0M ABOVE BALCONY 4
&DEVC XYZ = 10.0, 19.5, 19.0, QUANTITY = 'TEMPERATURE', ID = 'T-C4I'/ 2.0M ABOVE BALCONY 4
&DEVC XYZ = 10.0, 17.5, 23.0, QUANTITY = 'TEMPERATURE', ID = 'T-C5O'/ 2.0M ABOVE BALCONY 5
&DEVC XYZ = 10.0, 19.5, 23.0, QUANTITY = 'TEMPERATURE', ID = 'T-C5I'/ 2.0M ABOVE BALCONY 5


/VISIBILITY SENSOR FOR COLUMN C, INSIDE THE BALCONY
&DEVC XYZ = 10.0, 17.5, 7.0, QUANTITY = 'VISIBILITY', ID = 'V-C1O'/  2.0M ABOVE BALCONY 1
&DEVC XYZ = 10.0, 19.5, 7.0, QUANTITY = 'VISIBILITY', ID = 'V-C1I'/  2.0M ABOVE BALCONY 1
&DEVC XYZ = 10.0, 17.5, 11.0, QUANTITY = 'VISIBILITY', ID = 'V-C2O'/ 2.0M ABOVE BALCONY 2
&DEVC XYZ = 10.0, 19.5, 11.0, QUANTITY = 'VISIBILITY', ID = 'V-C2I'/ 2.0M ABOVE BALCONY 2
&DEVC XYZ = 10.0, 17.5, 15.0, QUANTITY = 'VISIBILITY', ID = 'V-C3O'/ 2.0M ABOVE BALCONY 3
&DEVC XYZ = 10.0, 19.5, 15.0, QUANTITY = 'VISIBILITY', ID = 'V-C3I'/ 2.0M ABOVE BALCONY 3
&DEVC XYZ = 10.0, 17.5, 19.0, QUANTITY = 'VISIBILITY', ID = 'V-C4O'/ 2.0M ABOVE BALCONY 4
&DEVC XYZ = 10.0, 19.5, 19.0, QUANTITY = 'VISIBILITY', ID = 'V-C4I'/ 2.0M ABOVE BALCONY 4
&DEVC XYZ = 10.0, 17.5, 23.0, QUANTITY = 'VISIBILITY', ID = 'V-C5O'/ 2.0M ABOVE BALCONY 5
&DEVC XYZ = 10.0, 19.5, 23.0, QUANTITY = 'VISIBILITY', ID = 'V-C5I'/ 2.0M ABOVE BALCONY 5

/CARBON MONOXIDE SENSOR, INSIDE THE BALCONY
&DEVC XYZ = 10.0, 17.5, 7.0, QUANTITY = 'carbon monoxide', ID = 'CO-1'/  2.0M ABOVE BALCONY 1
&DEVC XYZ = 10.0, 17.5, 11.0, QUANTITY = 'carbon monoxide', ID = 'CO-2'/ 2.0M ABOVE BALCONY 2
&DEVC XYZ = 10.0, 17.5, 15.0, QUANTITY = 'carbon monoxide', ID = 'CO-3'/ 2.0M ABOVE BALCONY 3
&DEVC XYZ = 10.0, 17.5, 19.0, QUANTITY = 'carbon monoxide', ID = 'CO-4'/ 2.0M ABOVE BALCONY 4
&DEVC XYZ = 10.0, 17.5, 23.0, QUANTITY = 'carbon monoxide', ID = 'CO-5'/ 2.0M ABOVE BALCONY 5

/CARBON DIOXIDE SENSOR, INSIDE THE BALCONY
&DEVC XYZ = 10.0, 17.5, 7.0, QUANTITY = 'carbon dioxide', ID = 'CO2-1'/  2.0M ABOVE BALCONY 1
&DEVC XYZ = 10.0, 17.5, 11.0, QUANTITY = 'carbon dioxide', ID = 'CO2-2'/ 2.0M ABOVE BALCONY 2
&DEVC XYZ = 10.0, 17.5, 15.0, QUANTITY = 'carbon dioxide', ID = 'CO2-3'/ 2.0M ABOVE BALCONY 3
&DEVC XYZ = 10.0, 17.5, 19.0, QUANTITY = 'carbon dioxide', ID = 'CO2-4'/ 2.0M ABOVE BALCONY 4
&DEVC XYZ = 10.0, 17.5, 23.0, QUANTITY = 'carbon dioxide', ID = 'CO2-5'/ 2.0M ABOVE BALCONY 5

/OXYGEN SENSOR, INSIDE THE BALCONY
&DEVC XYZ = 10.0, 17.5, 7.0, QUANTITY = 'oxygen', ID = 'O2-1'/  2.0M ABOVE BALCONY 1
&DEVC XYZ = 10.0, 17.5, 11.0, QUANTITY = 'oxygen', ID = 'O2-2'/ 2.0M ABOVE BALCONY 2
&DEVC XYZ = 10.0, 17.5, 15.0, QUANTITY = 'oxygen', ID = 'O2-3'/ 2.0M ABOVE BALCONY 3
&DEVC XYZ = 10.0, 17.5, 19.0, QUANTITY = 'oxygen', ID = 'O2-4'/ 2.0M ABOVE BALCONY 4
&DEVC XYZ = 10.0, 17.5, 23.0, QUANTITY = 'oxygen', ID = 'O2-5'/ 2.0M ABOVE BALCONY 5

/FED SENSOR, INSIDE THE BALCONY
&DEVC XYZ = 10.0, 17.5, 7.0, QUANTITY = 'FED', ID = 'FED-1'/  2.0M ABOVE BALCONY 1
&DEVC XYZ = 10.0, 17.5, 11.0, QUANTITY = 'FED', ID = 'FED-2'/ 2.0M ABOVE BALCONY 2
&DEVC XYZ = 10.0, 17.5, 15.0, QUANTITY = 'FED', ID = 'FED-3'/ 2.0M ABOVE BALCONY 3
&DEVC XYZ = 10.0, 17.5, 19.0, QUANTITY = 'FED', ID = 'FED-4'/ 2.0M ABOVE BALCONY 4
&DEVC XYZ = 10.0, 17.5, 23.0, QUANTITY = 'FED', ID = 'FED-5'/ 2.0M ABOVE BALCONY 5
```

```
&DUMP DT_PL3D = 5.0, PLOT3D_QUANTITY(1:5) ='TEMPERATURE','U-VELOCITY','V-VELOCITY','W-
VELOCITY','PRESSURE'/

&TAIL/ END OF FILE
```

Calculation for Smoke Extraction Rate

For the scale model, the fan size is assumed as 0.4m by 0.4m and this is estimated from Tan (2009) experiment. For the full scale model, the fan size is assumed as 3.0m by 3.0m. The input to FDS 5.0 is $kgs^{-1}m^{-2}$. This calculation is to prevent plugholing. Table B1 shows the smoke extraction using Equation 5 and Equation 6. For all cases, Equation 6 predicts higher smoke extraction rate requirement. Formula used in the simulation is highlighted in "grey".

Model	Equation 5 (kg/s)	Equation 6 (kg/s)	Plugholing (kg/s)		Model	Equation 5 (kg/s)	Equation 6 (kg/s)	Plugholing (kg/s)
S01E	0.45	0.44	0.44		F01E5	253	261	51
S03E	0.66	0.66	0.61		F02B5	322	341	63
S08E	0.43	0.48	0.62		F03E5	369	394	72
S13E	0.18	0.28	0.68		F04E5	221	241	54
S19E	0.39	0.4	0.47		F05E5	281	314	67
S23E	0.43	0.48	0.62		F06E5	322	364	77
S27E	0.39	0.5	0.78		F07E5	186	218	59
S38E	0.43	0.48	0.62		F08E5	236	288	73
S41E	0.34	0.43	0.69		F09E5	271	332	83
S43E	0.18	0.28	0.68		F10E5	145	196	66
S56E	0.34	0.43	0.69		F11E5	185	259	82
S60E	0.26	0.44	0.92		F12E5	212	300	94
					F13E5	96	173	81
S01E5	0.76	0.76	0.34		F14E5	122	229	100
S03E5	1.12	1.15	0.48		F15E5	139	266	114
S08E5	0.71	0.83	0.49		F19E5	221	240	54
S13E5	0.29	0.48	0.34		F20E5	281	315	67
S19E5	0.66	0.69	0.36		F21E5	322	364	77
S23E5	0.71	0.83	0.49		F22E5	186	219	59
S27E5	0.64	0.86	0.62		F23E5	236	288	73
S38E5	0.71	0.83	0.49		F24E5	271	333	83
S41E5	0.56	0.74	0.55		F25E5	145	196	66
S43E5	0.29	0.49	0.54		F26E5	185	259	82
S56E5	0.56	0.74	0.55		F27E5	212	300	94
S60E5	0.42	0.76	0.75		F28E5	96	173	81
					F29E5	122	229	100
F01E7	333	347	44		F30E5	139	266	114
F03E7	484	524	63		F37E5	186	219	59
F08E7	308	381	64		F38E5	236	288	73
F13E7	123	231	72		F39E5	271	333	83
F19E7	290	319	47		F40E5	145	196	66
F23E7	308	381	64		F41E5	185	259	82
F27E7	275	399	83		F42E5	212	300	94
F38E7	308	381	64		F43E5	96	173	81
F41E7	240	344	73		F44E5	122	229	100
F43E7	123	231	72		F45E5	139	266	114
F56E7	240	343	73		F55E5	145	196	66
F60E7	139	266	114		F56E5	185	259	82
					F57E5	212	300	94
					F58E5	96	173	81
					F59E5	121	229	100
					F60E5	139	266	114

Table B1. Smoke extraction rate basing on Equation 5 and Equation 6.

Scale Model (S01E) and Tan's Experiment 1 Data Comparison

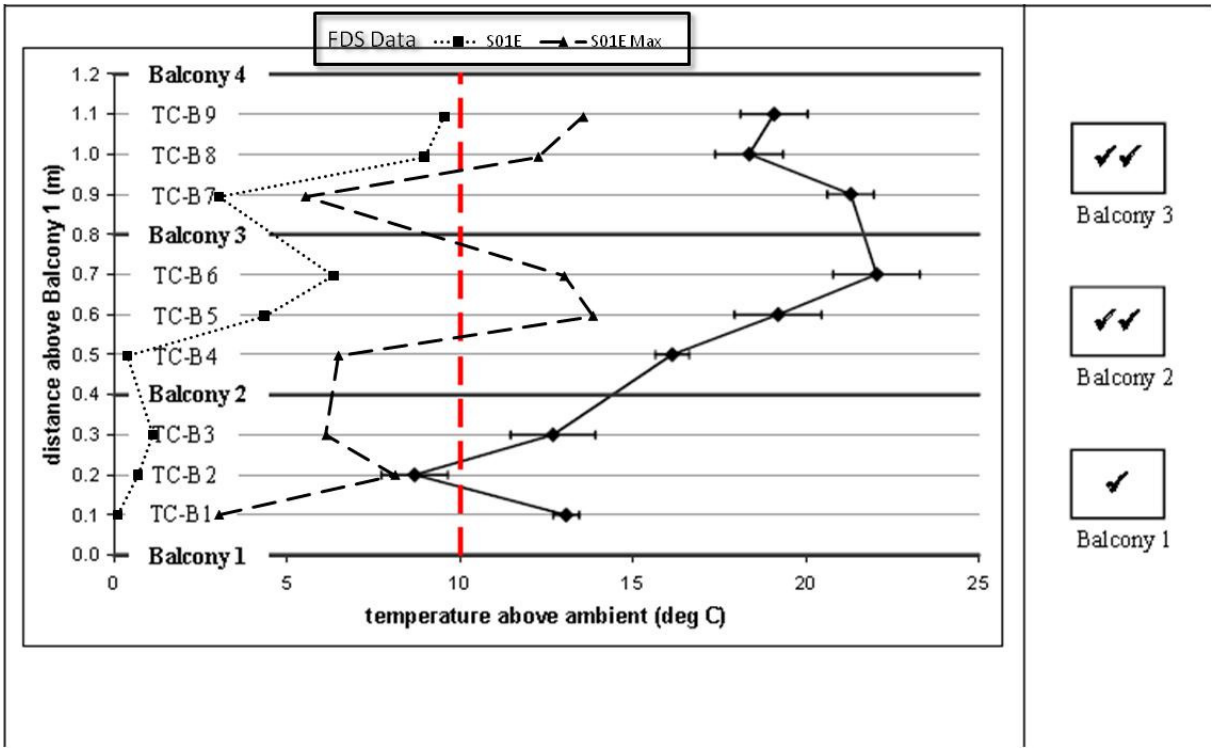

Figure C1. Temperature profiles across balcony edge from FDS and Tan's experiment.

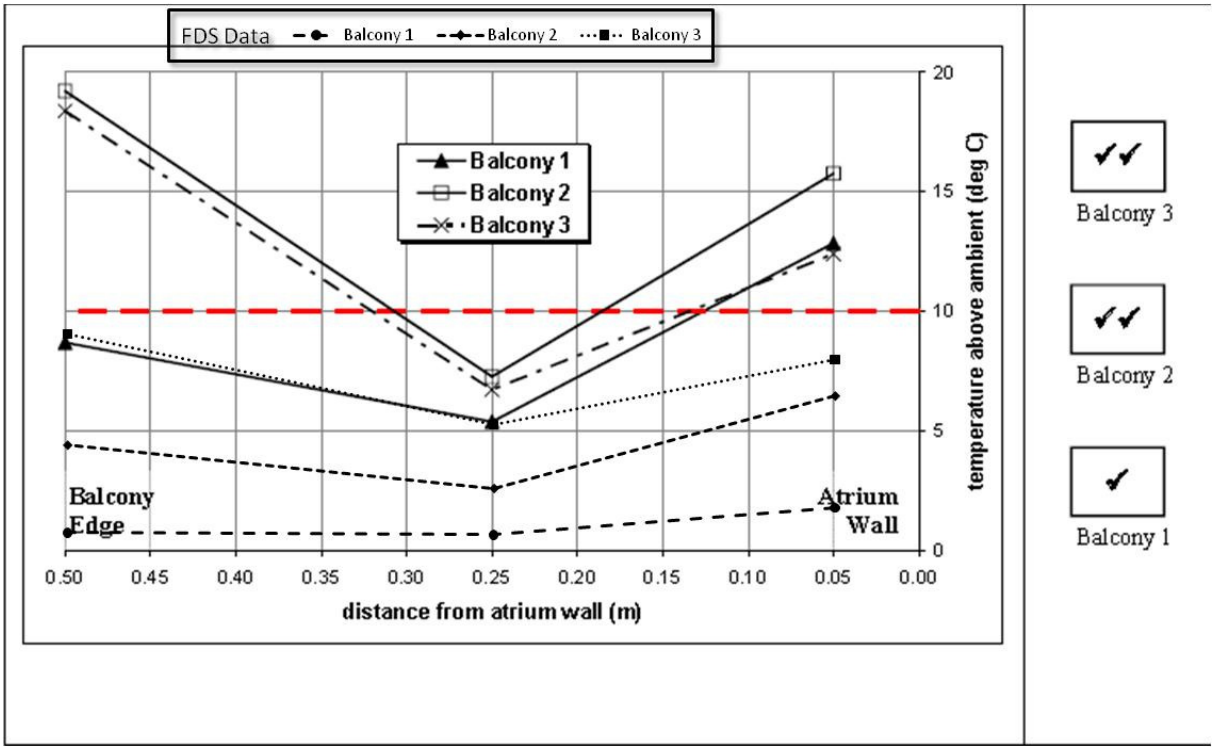

Figure C2. Temperature profiles along balcony breadth from FDS and Tan's experiment.

Experiment No. = 1
Balcony Breadth = 500 mm
Plume Width = 1000 mm
Heat Release Rate = 5 kW

Balcony Level	Photograph
3	
2	
1	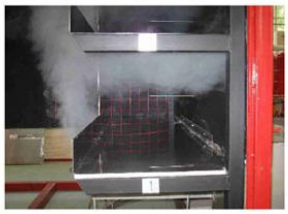

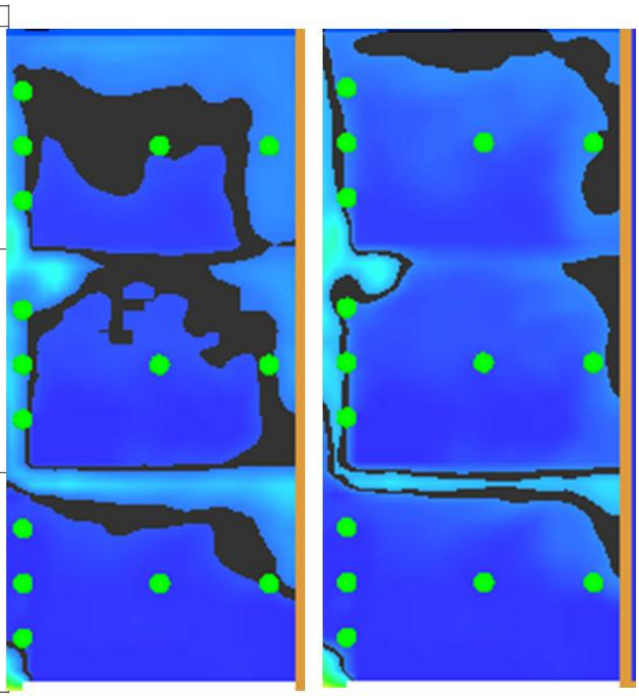

Figure C3. Temperature profile and Tan's experiment photographic records.

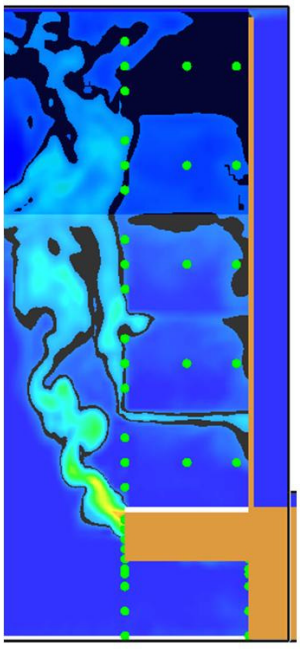

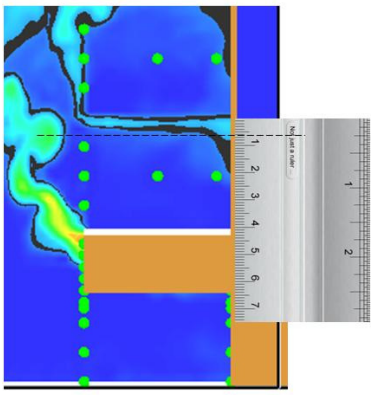

Figure C4. Smoke layer height measurement.

Scale Model (S03E) and Tan's Experiment 3 Data Comparison

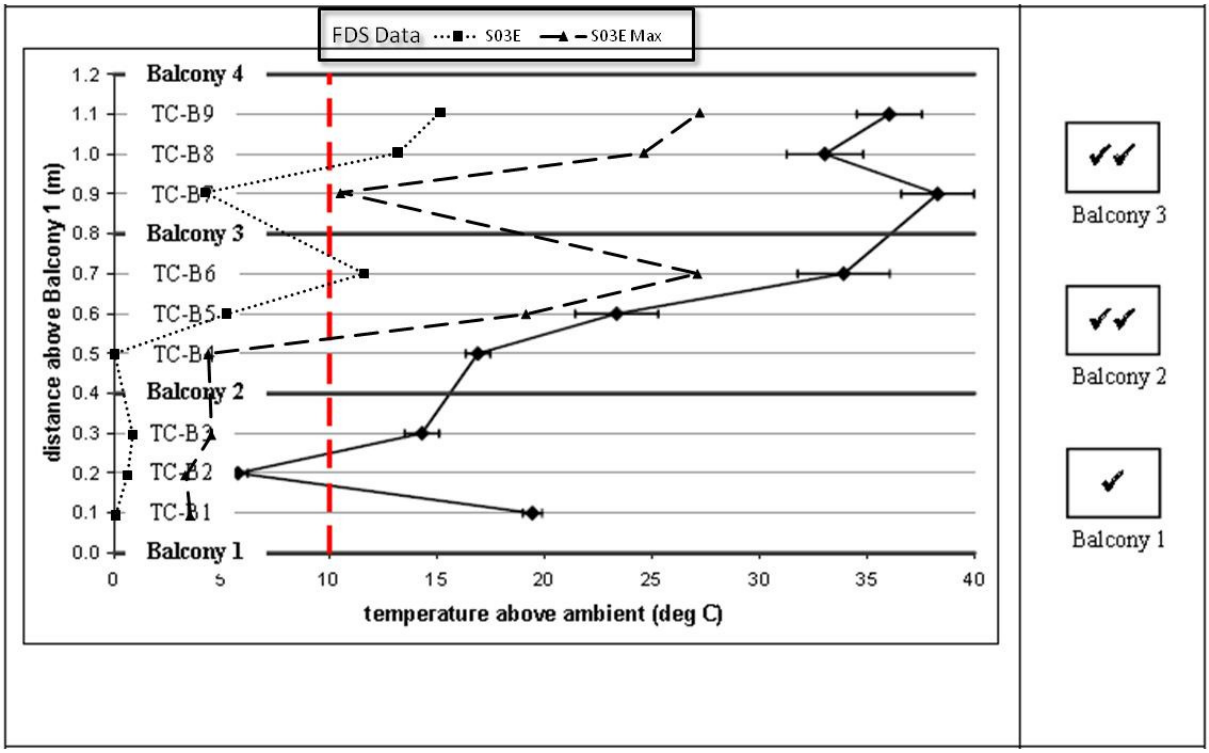

Figure C5. Temperature profiles across balcony edge from FDS and Tan's experiment.

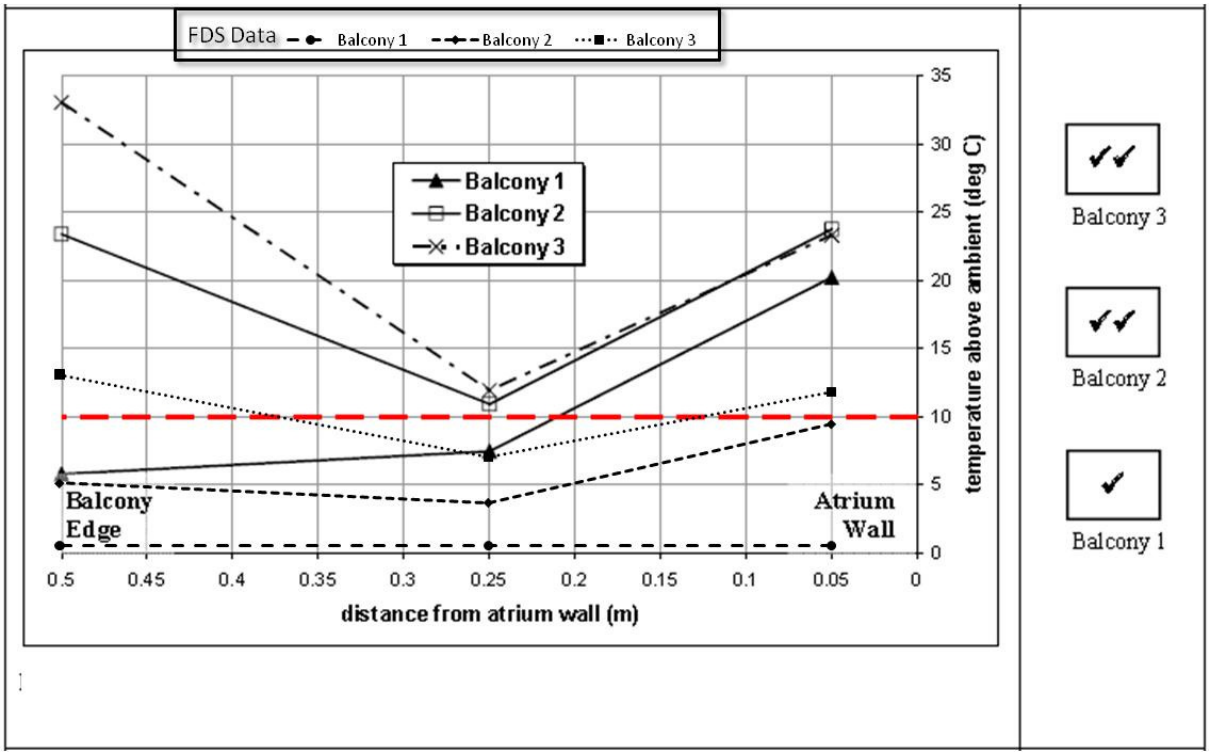

Figure C6. Temperature profiles along balcony breadth from FDS and Tan's experiment.

Experiment No. = 3
Balcony Breadth = 500 mm
Plume Width = 1000 mm
Heat Release Rate = 15 kW

Balcony Level	Photograph
3	
2	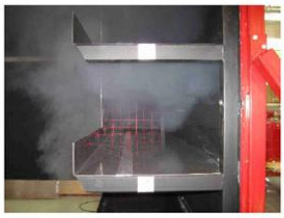
1	

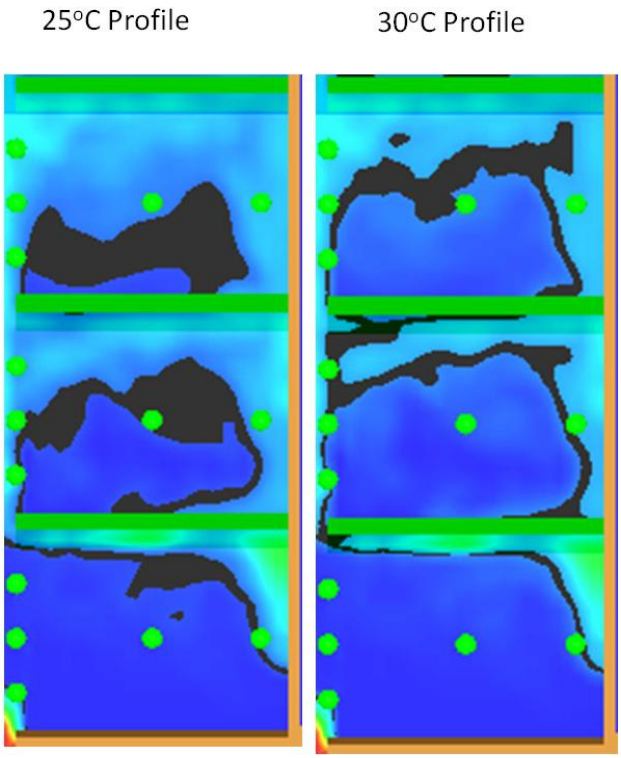

Figure C7. Temperature profile and Tan's experiment photographic records.

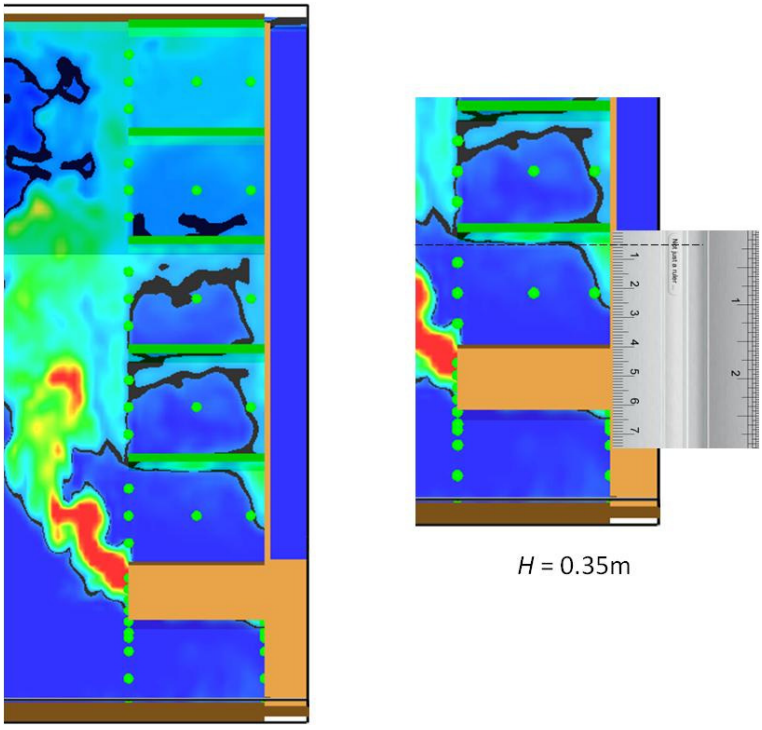

Figure C8. Smoke layer height measurement.

Scale Model (S08E) and Tan's Experiment 8 Data Comparison

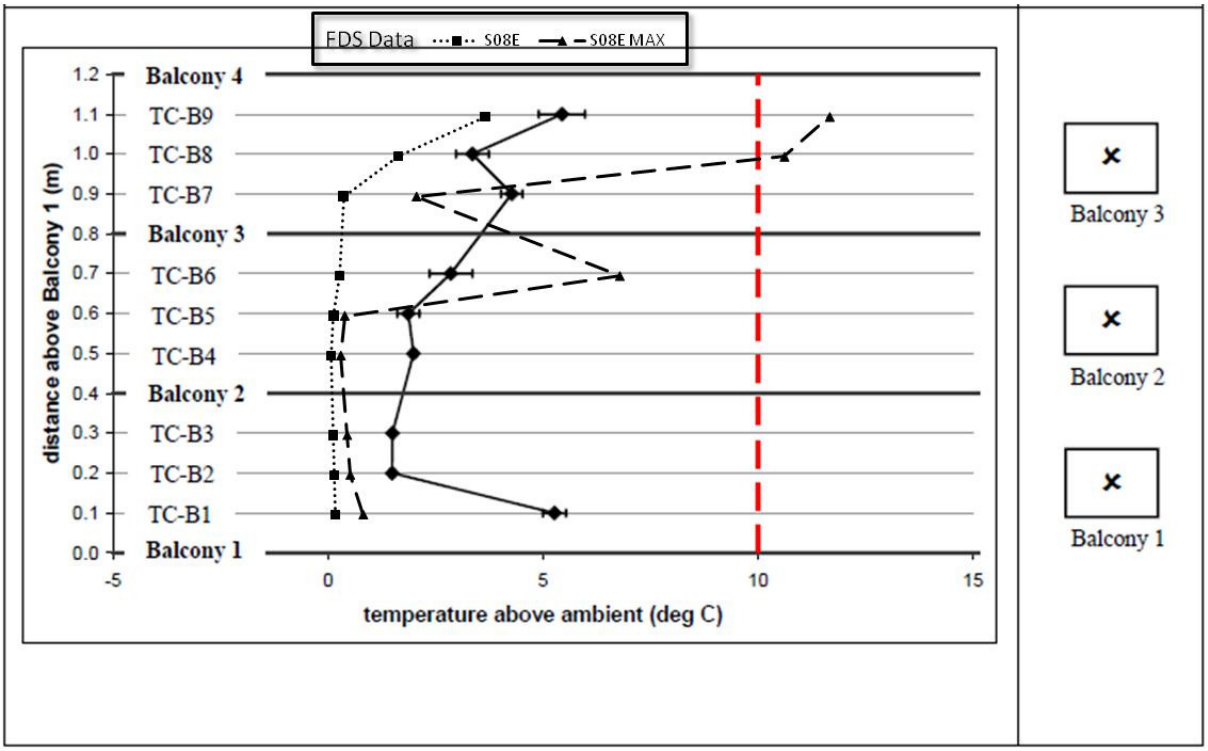

Figure C9. Temperature profiles across balcony edge from FDS and Tan's experiment.

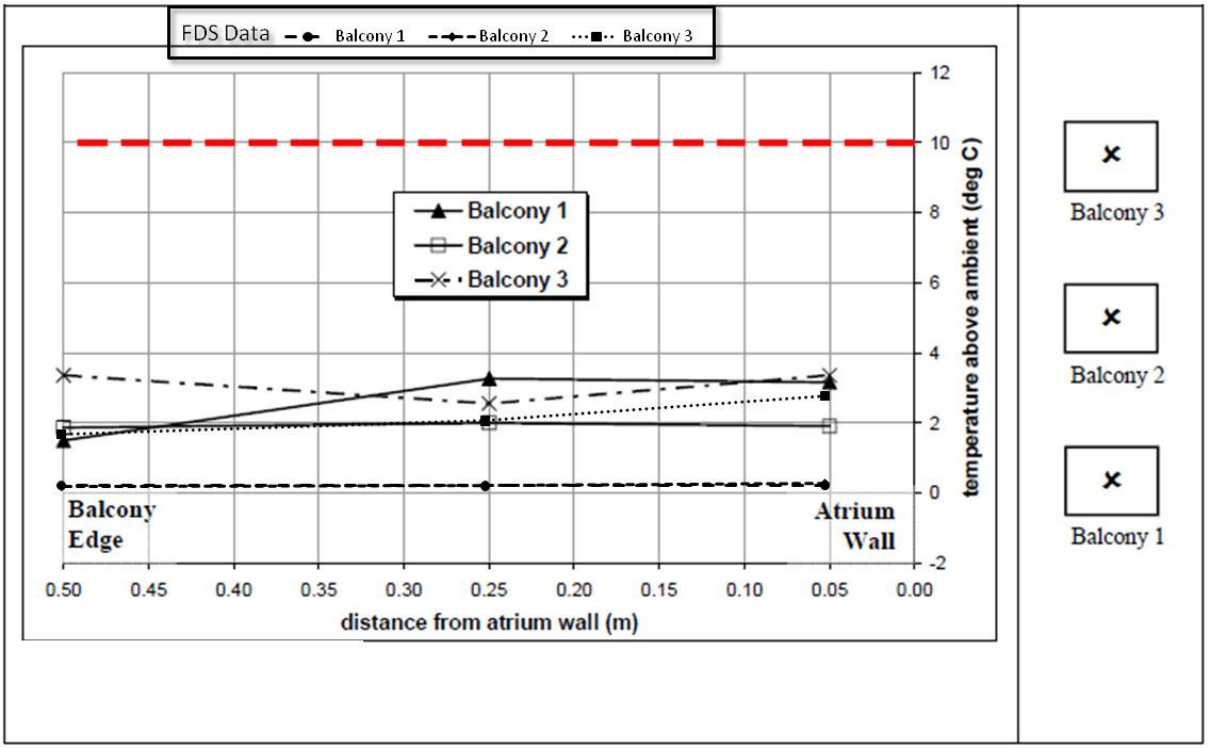

Figure C10. Temperature profiles along balcony breadth from FDS and Tan's experiment.

Experiment No. = 8
Balcony Breadth = 500 mm
Plume Width = 600 mm
Heat Release Rate = 10 kW

Balcony Level	Photograph
3	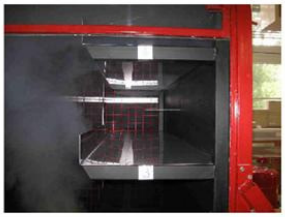
2	
1	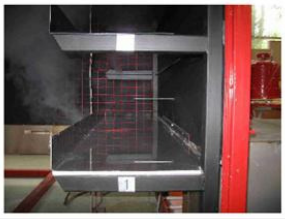

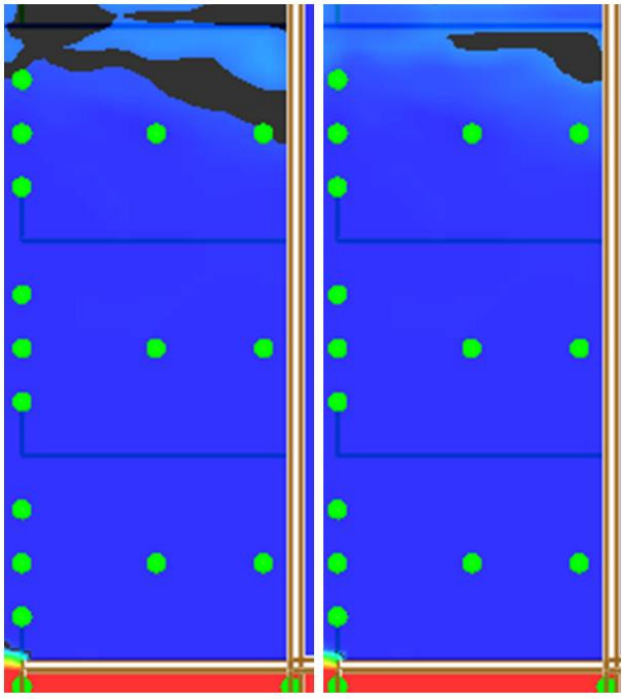

Figure C11. Temperature profile and Tan's experiment photographic records.

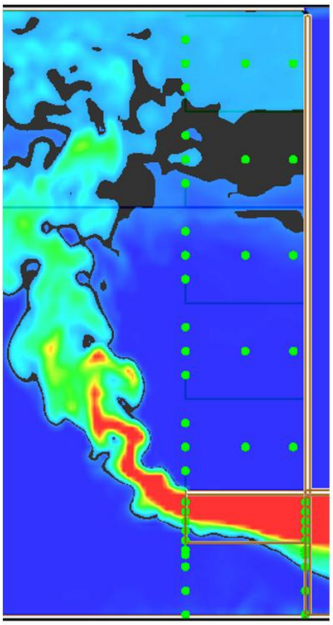

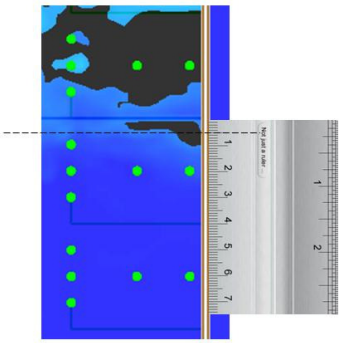

Figure C12. Smoke layer height measurement.

Scale Model (S13E) and Tan's Experiment 13 Data Comparison

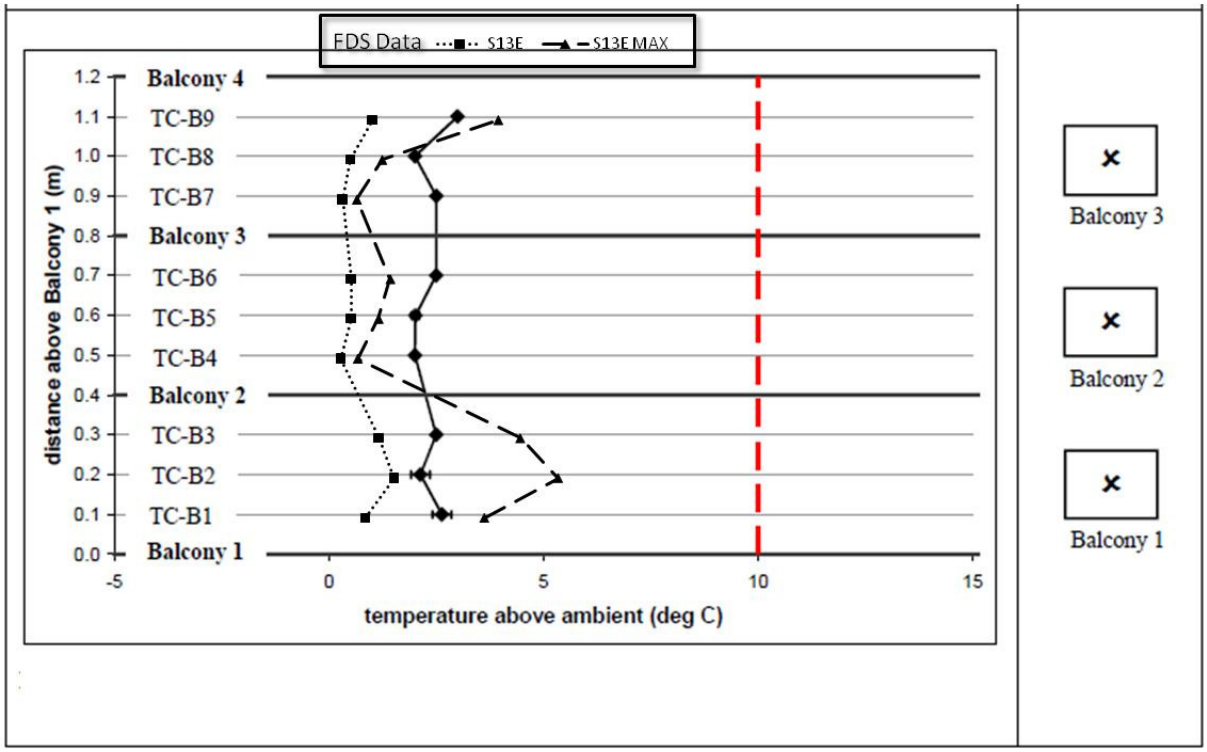

Figure C13. Temperature profiles across balcony edge from FDS and Tan's experiment.

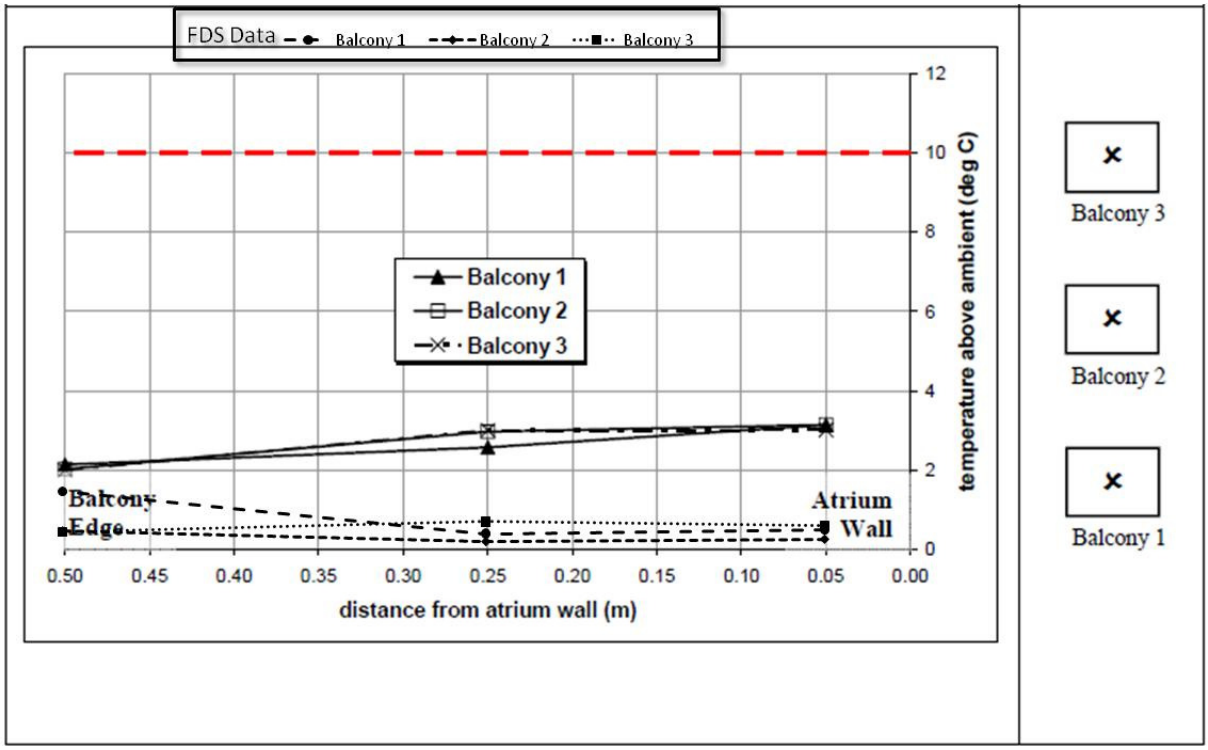

Figure C14. Temperature profiles along balcony breadth from FDS and Tan's experiment.

Experiment No.	=	13	
Balcony Breadth	=	500	mm
Plume Width	=	200	mm
Heat Release Rate	=	5	kW

Balcony Level	Photograph
3	
2	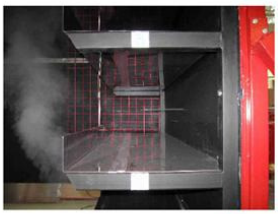
1	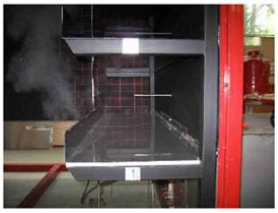

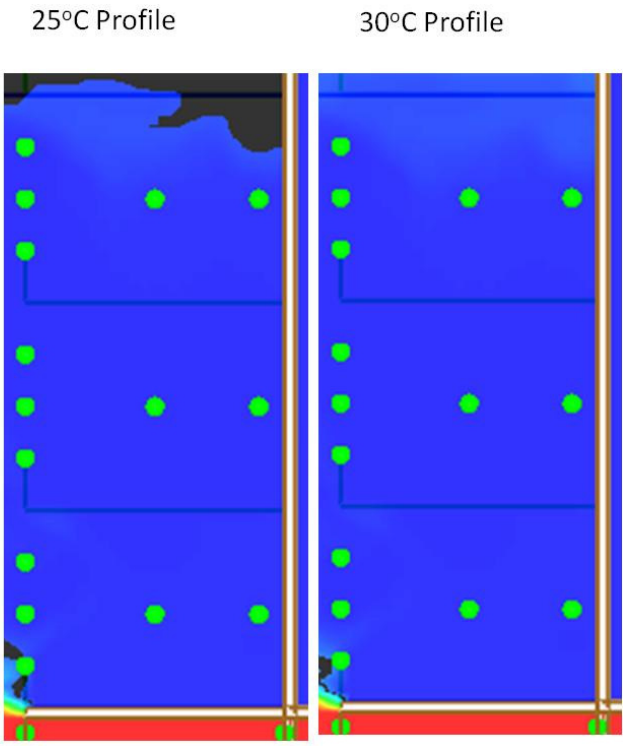

Figure C15. Temperature profile and Tan's experiment photographic records.

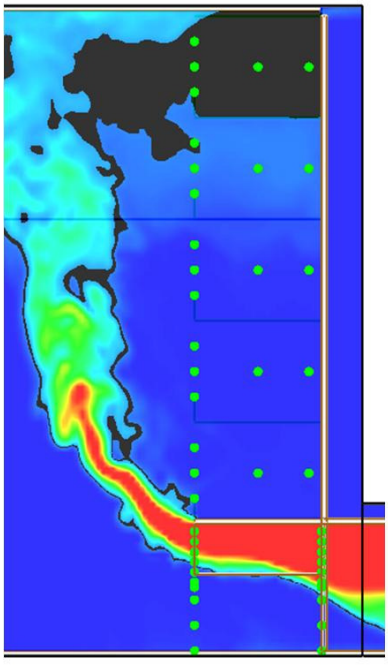

No smoke contamination

Figure C16. Smoke layer height measurement.

Scale Model (S19E) and Tan's Experiment 19 Data Comparison

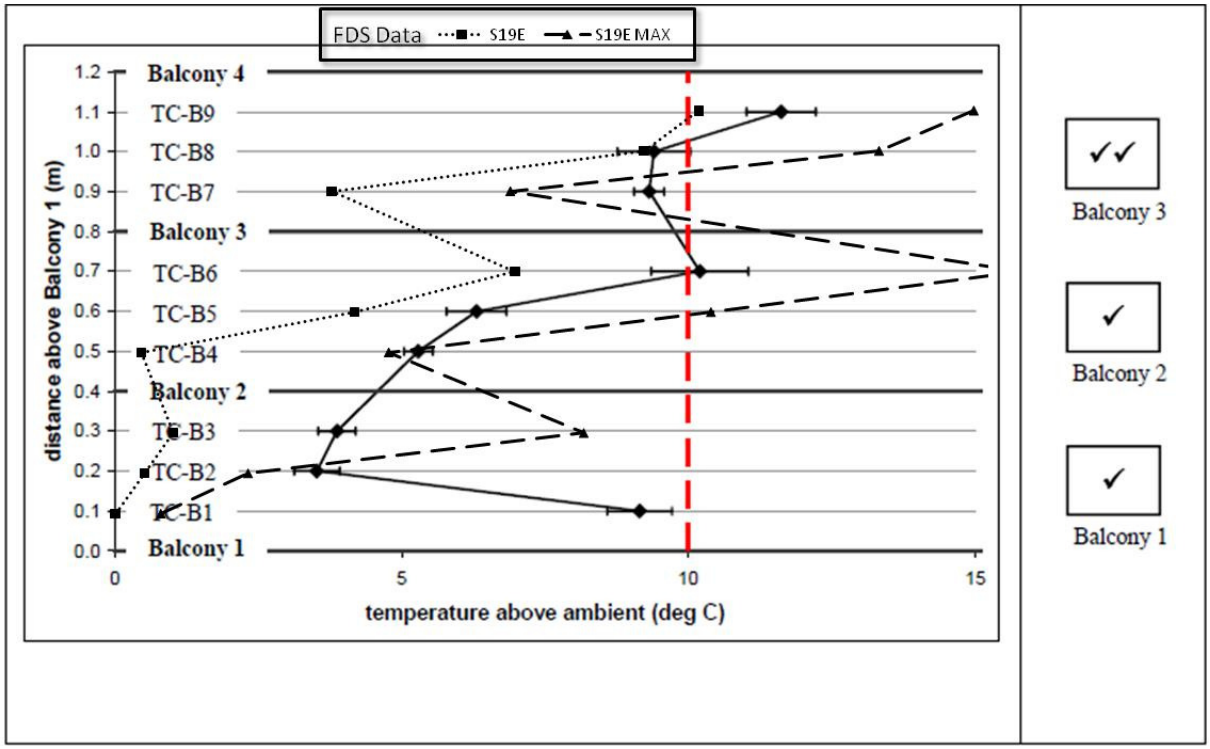

Figure C17. Temperature profiles across balcony edge from FDS and Tan's experiment.

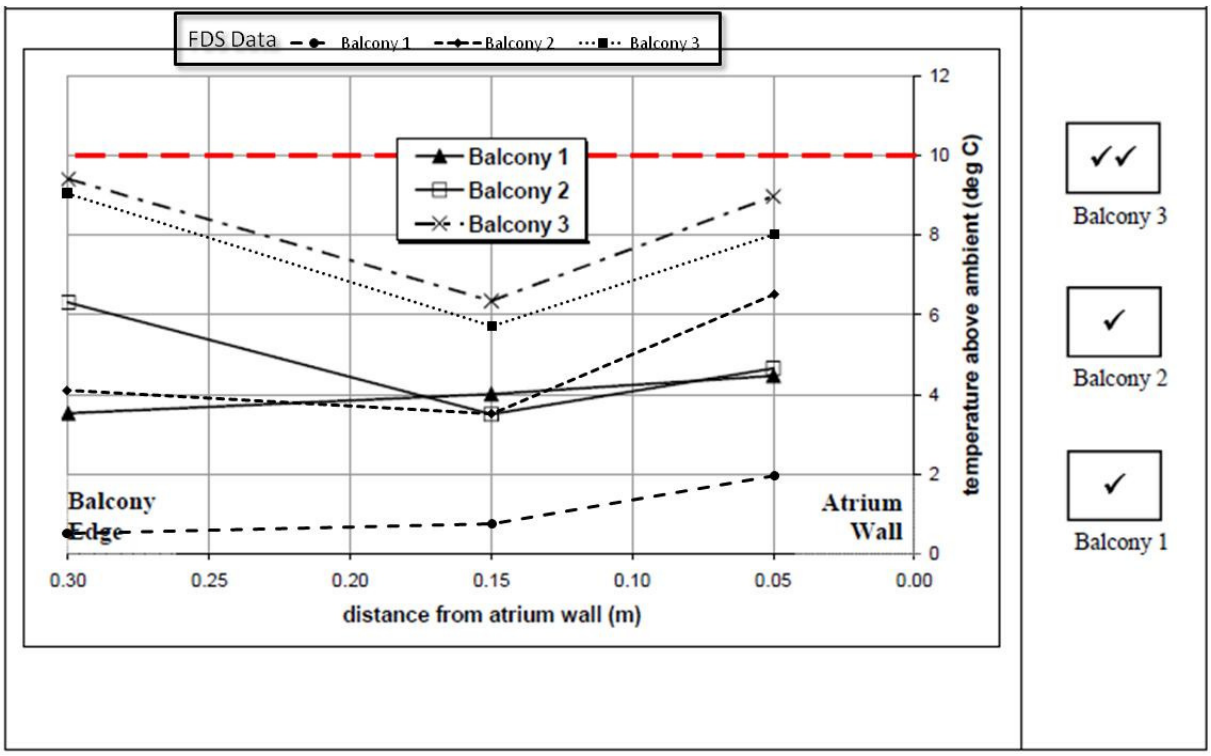

Figure C18. Temperature profiles along balcony breadth from FDS and Tan's experiment.

Experiment No.	=	19	
Balcony Breadth	=	300	mm
Plume Width	=	800	mm
Heat Release Rate	=	5	kW

Balcony Level	Photograph
3	
2	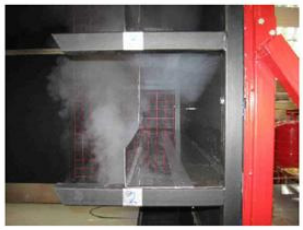
1	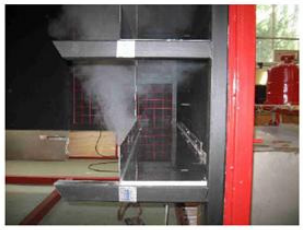

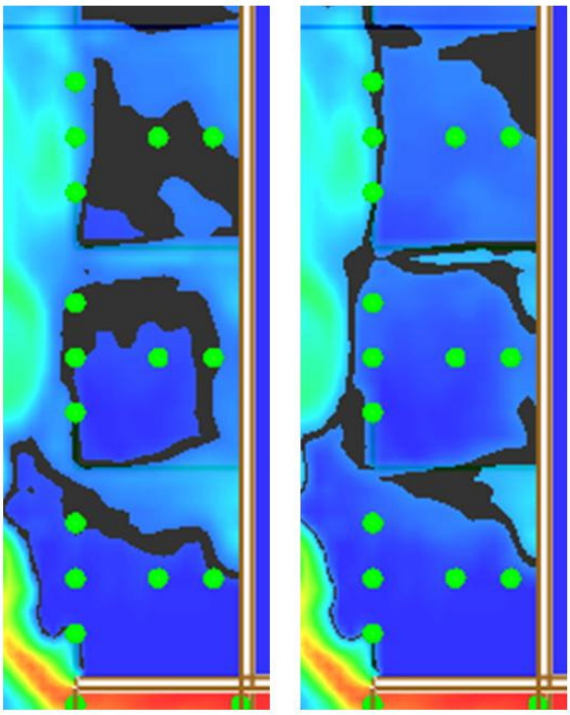

Figure C19. Temperature profile and Tan's experiment photographic records.

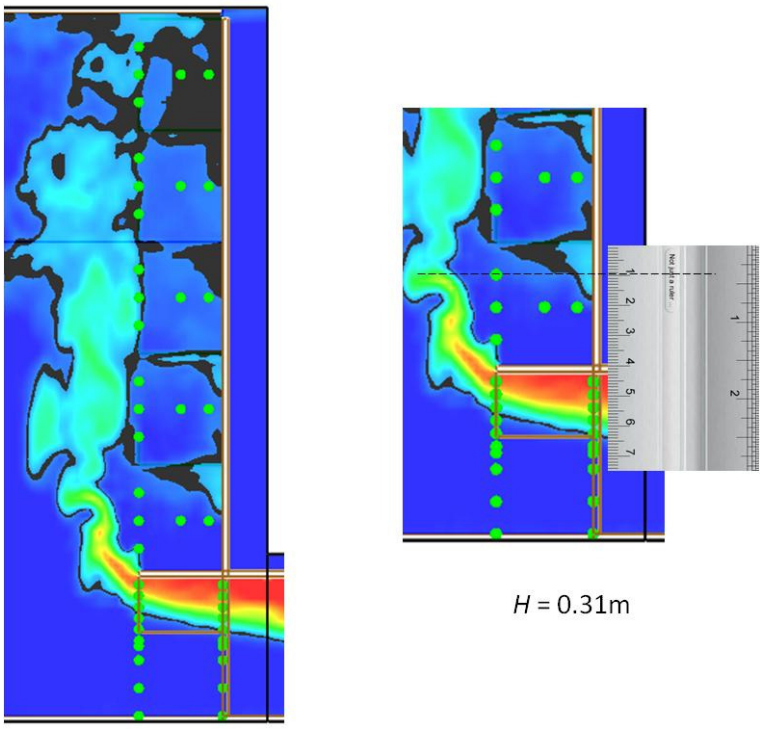

Figure C20. Smoke layer height measurement.

Scale Model (S23E) and Tan's Experiment 23 Data Comparison

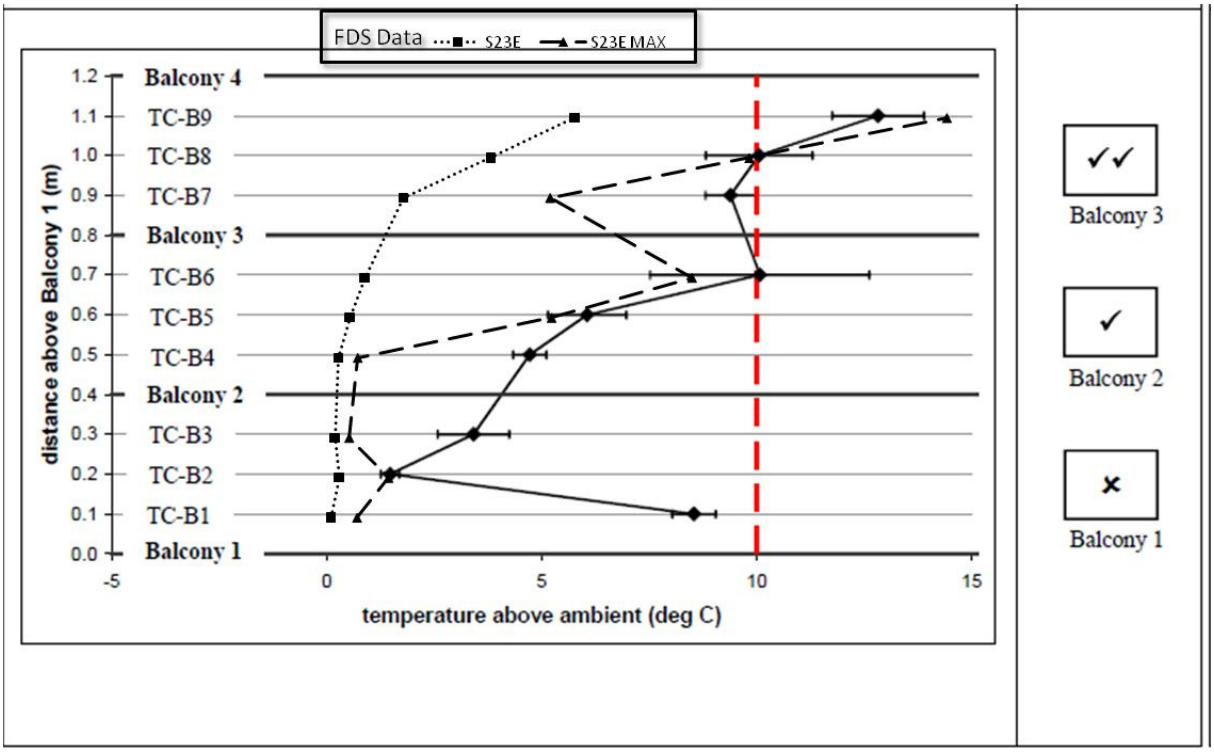

Figure C21. Temperature profiles across balcony edge from FDS and Tan's experiment.

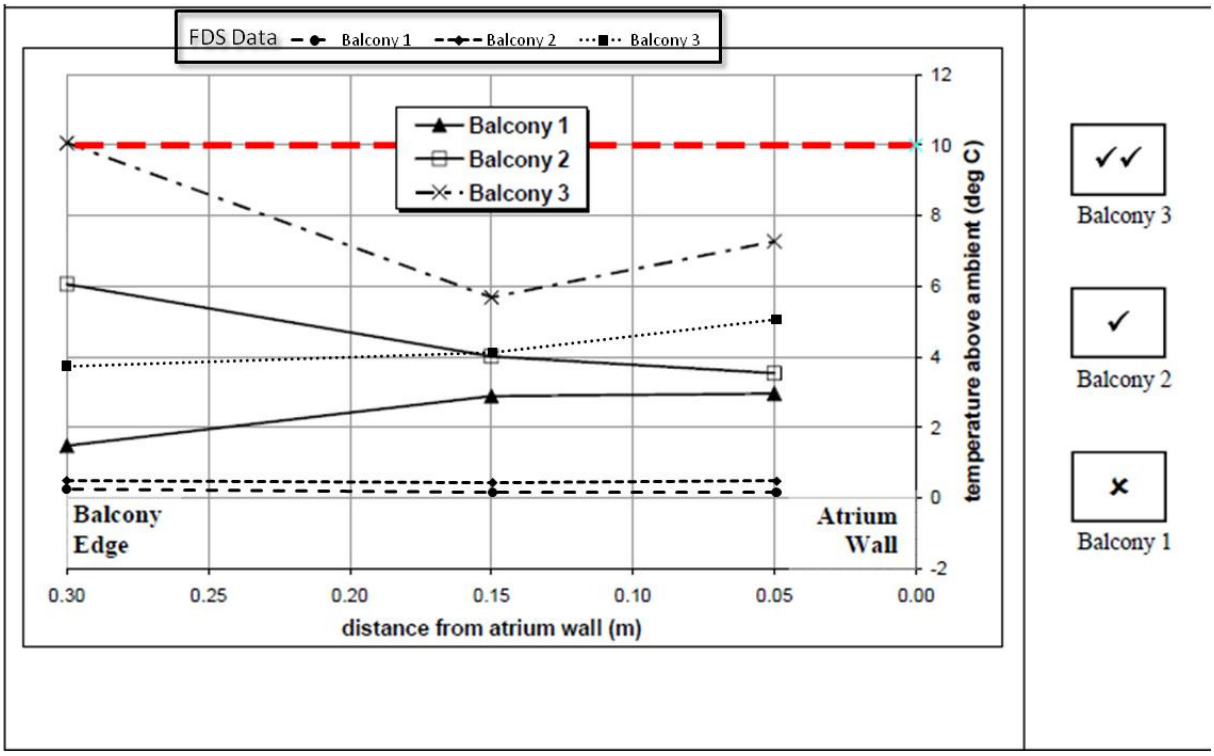

Figure C22. Temperature profiles along balcony breadth from FDS and Tan's experiment.

Experiment No.	=	23	
Balcony Breadth	=	300	mm
Plume Width	=	600	mm
Heat Release Rate	=	10	kW

Balcony Level	Photograph
3	
2	
1	

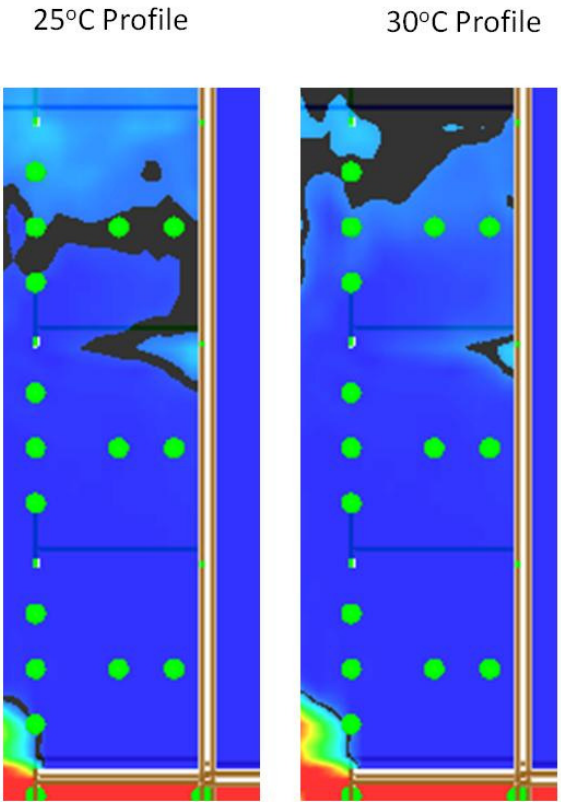

Figure C23. Temperature profile and Tan's experiment photographic records.

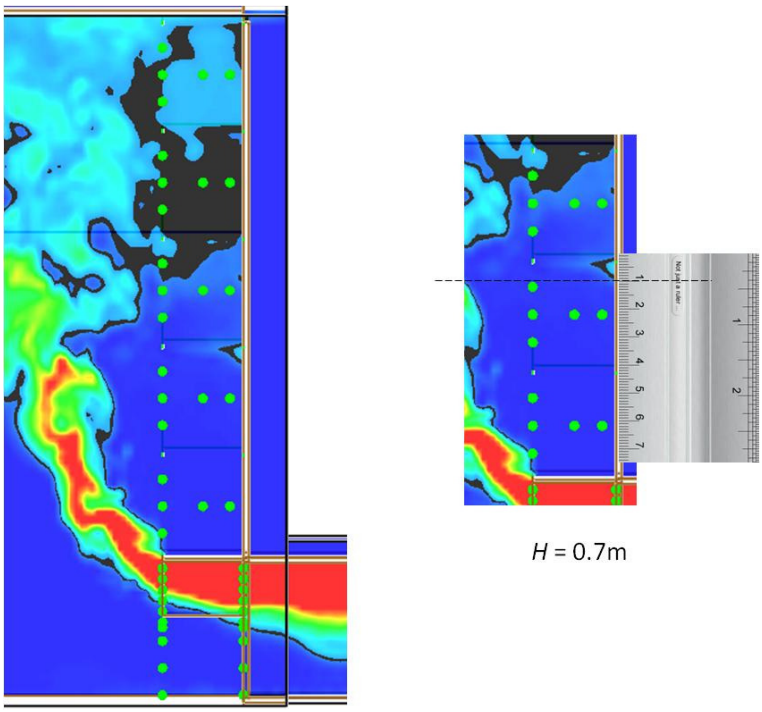

Figure C24. Smoke layer height measurement.

Scale Model (S27E) and Tan's Experiment 27 Data Comparison

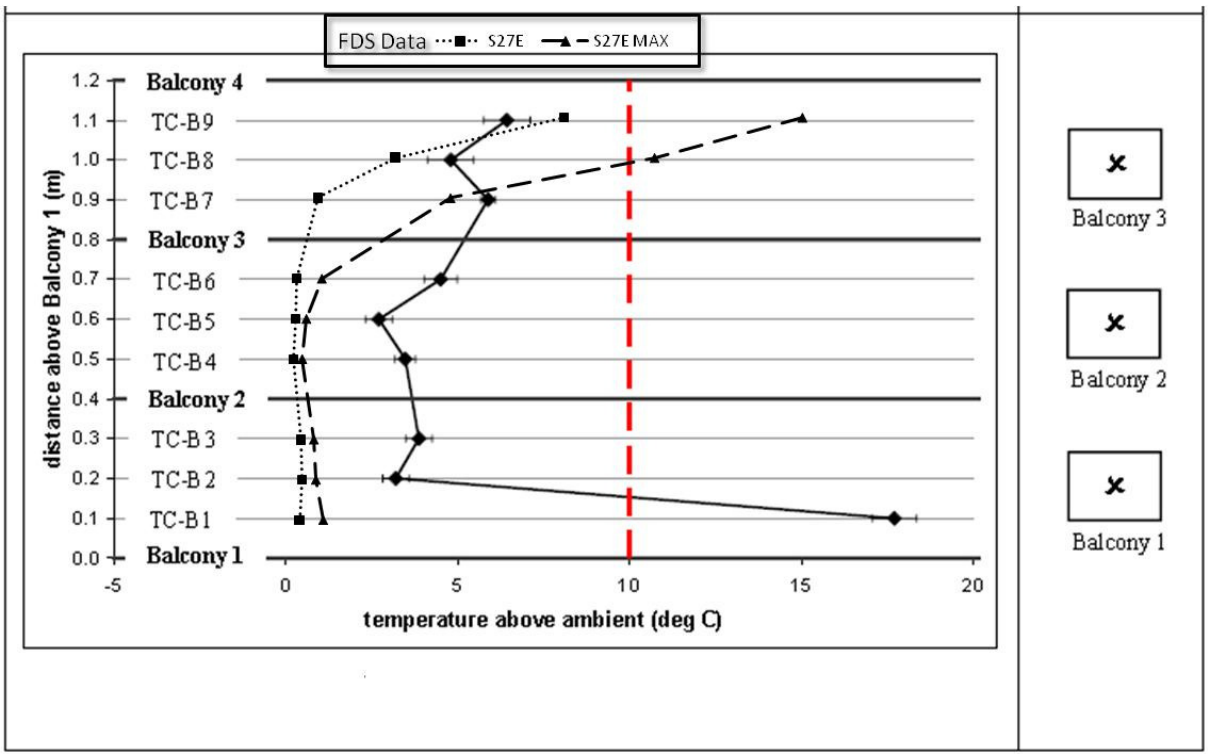

Figure C25. Temperature profiles across balcony edge from FDS and Tan's experiment.

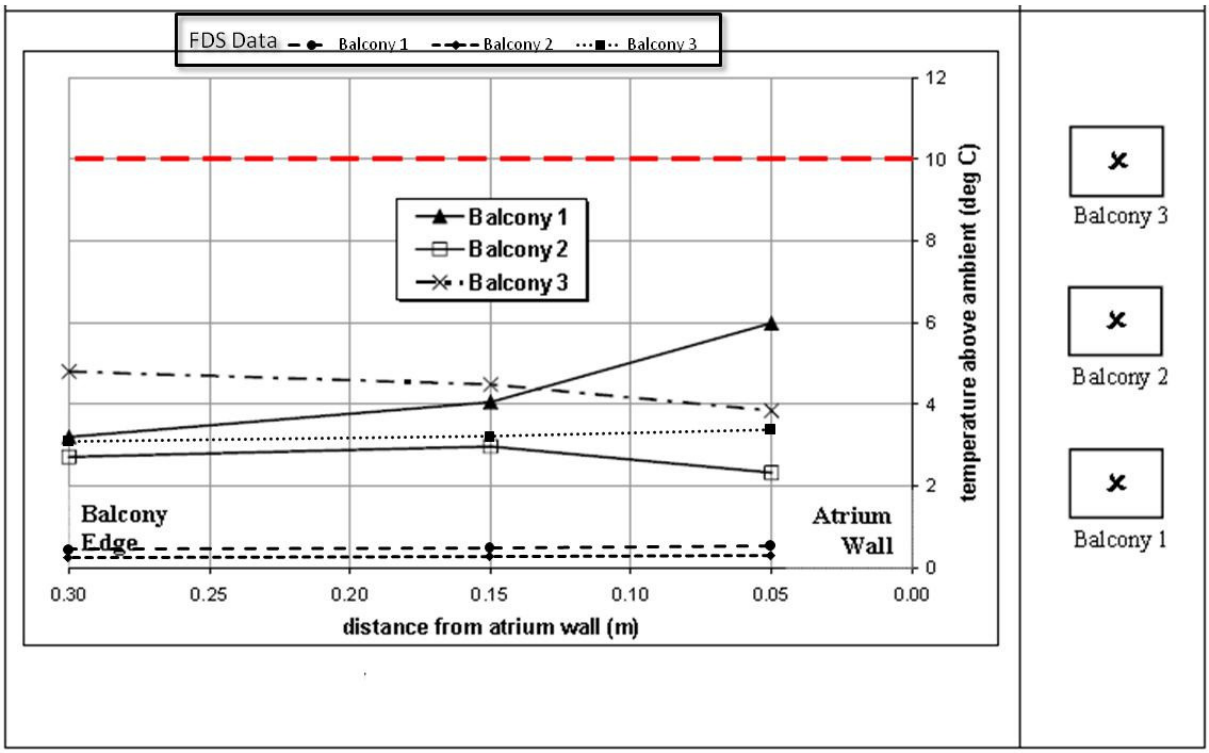

Figure C26. Temperature profiles along balcony breadth from FDS and Tan's experiment.

Experiment No. = 27
Balcony Breadth = 300 mm
Plume Width = 400 mm
Heat Release Rate = 15 kW

Balcony Level	Photograph
3	
2	
1	

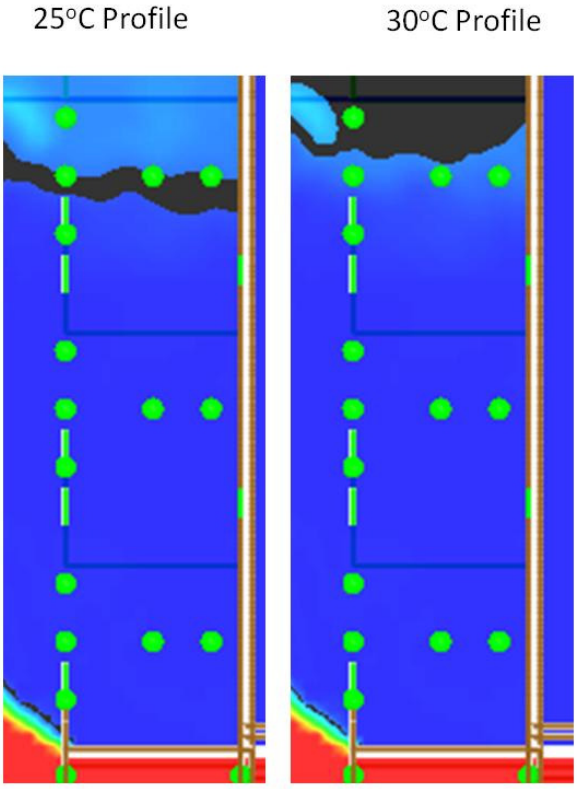

Figure C27. Temperature profile and Tan's experiment photographic records.

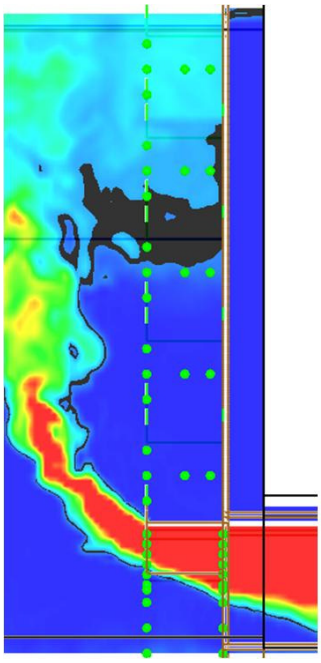

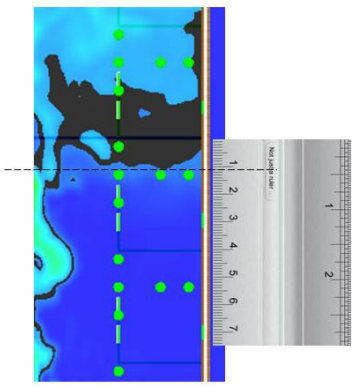

Figure C28. Smoke layer height measurement.

Scale Model (S38E) and Tan's Experiment 38 Data Comparison

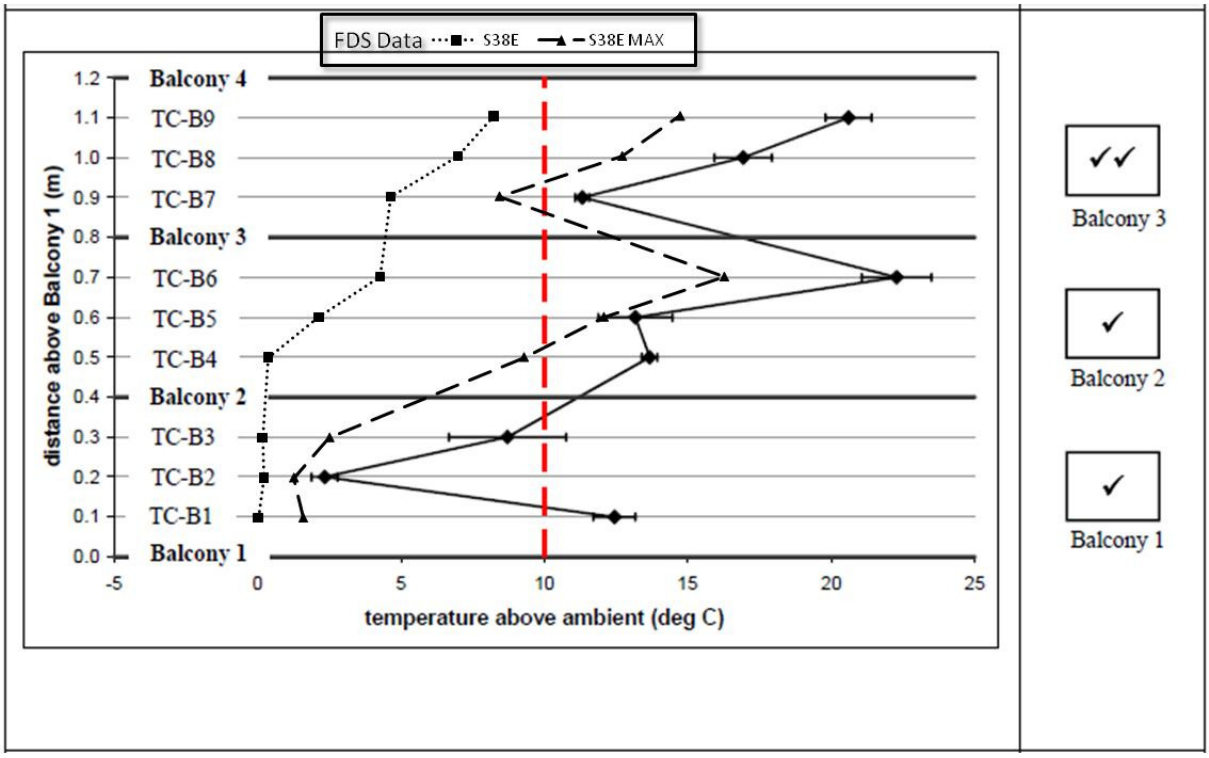

Figure C29. Temperature profiles across balcony edge from FDS and Tan's experiment.

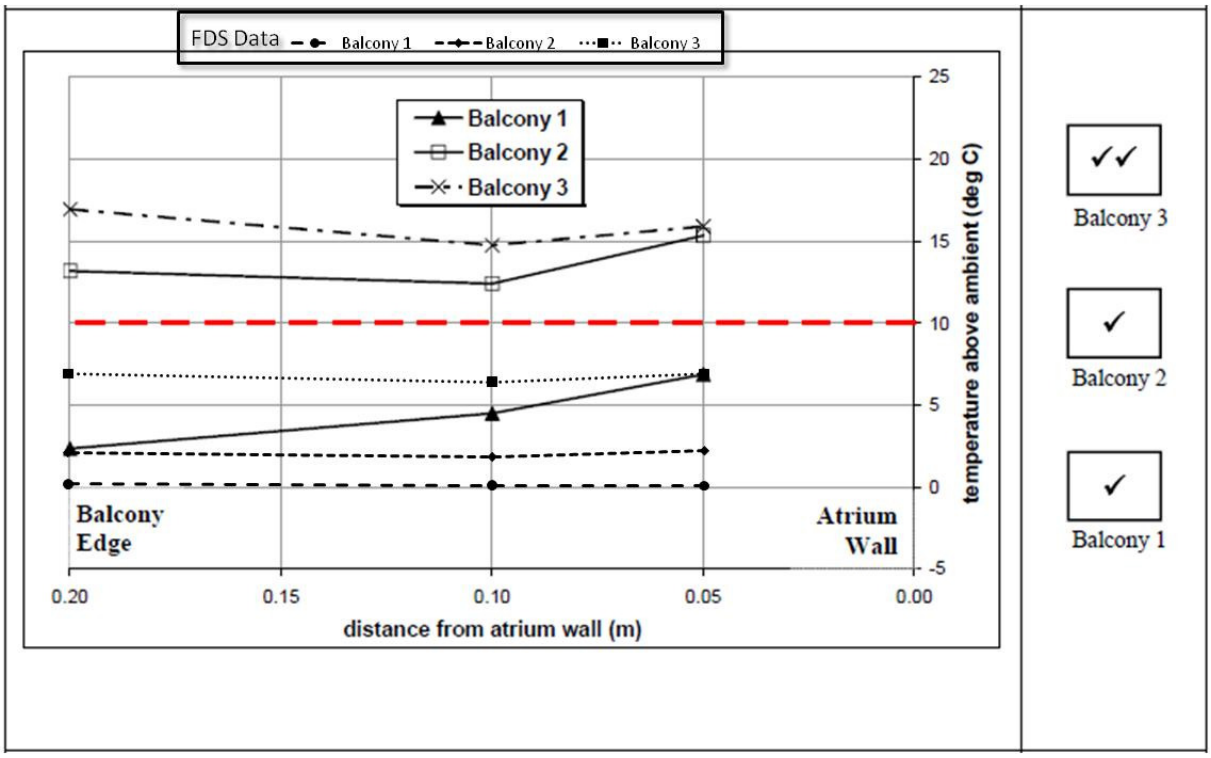

Figure C30. Temperature profiles along balcony breadth from FDS and Tan's experiment.

Experiment No.	=	38	
Balcony Breadth	=	200	mm
Plume Width	=	600	mm
Heat Release Rate	=	10	kW

Balcony Level	Photograph
3	
2	
1	

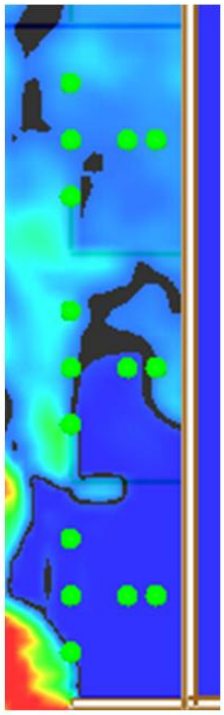

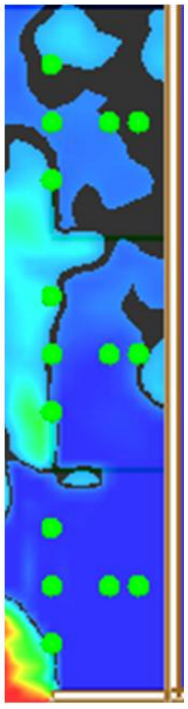

Figure C31. Temperature profile and Tan's experiment photographic records.

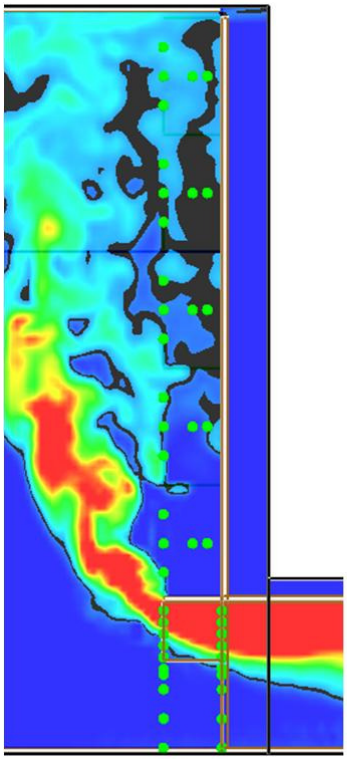

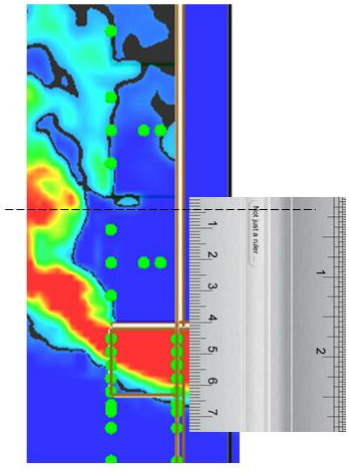

H = 0.36m

Figure C32. Smoke layer height measurement.

Scale Model (S41E) and Tan's Experiment 41 Data Comparison

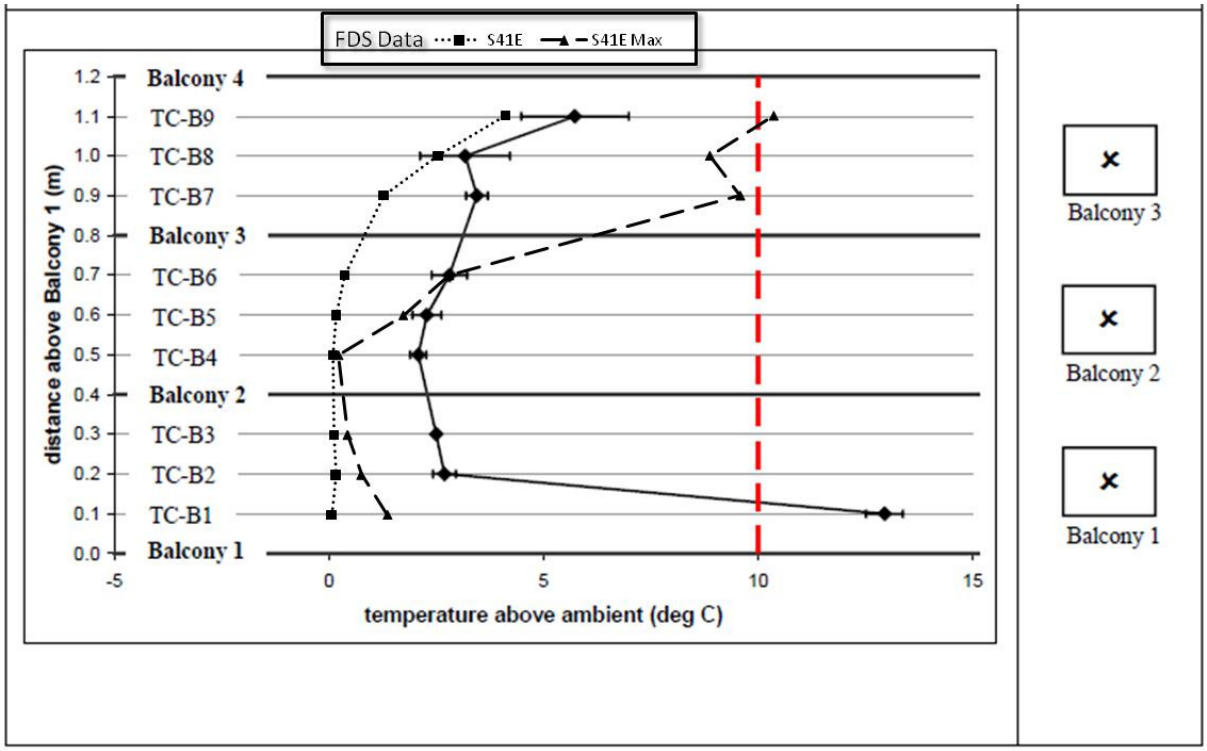

Figure C33. Temperature profiles across balcony edge from FDS and Tan's experiment.

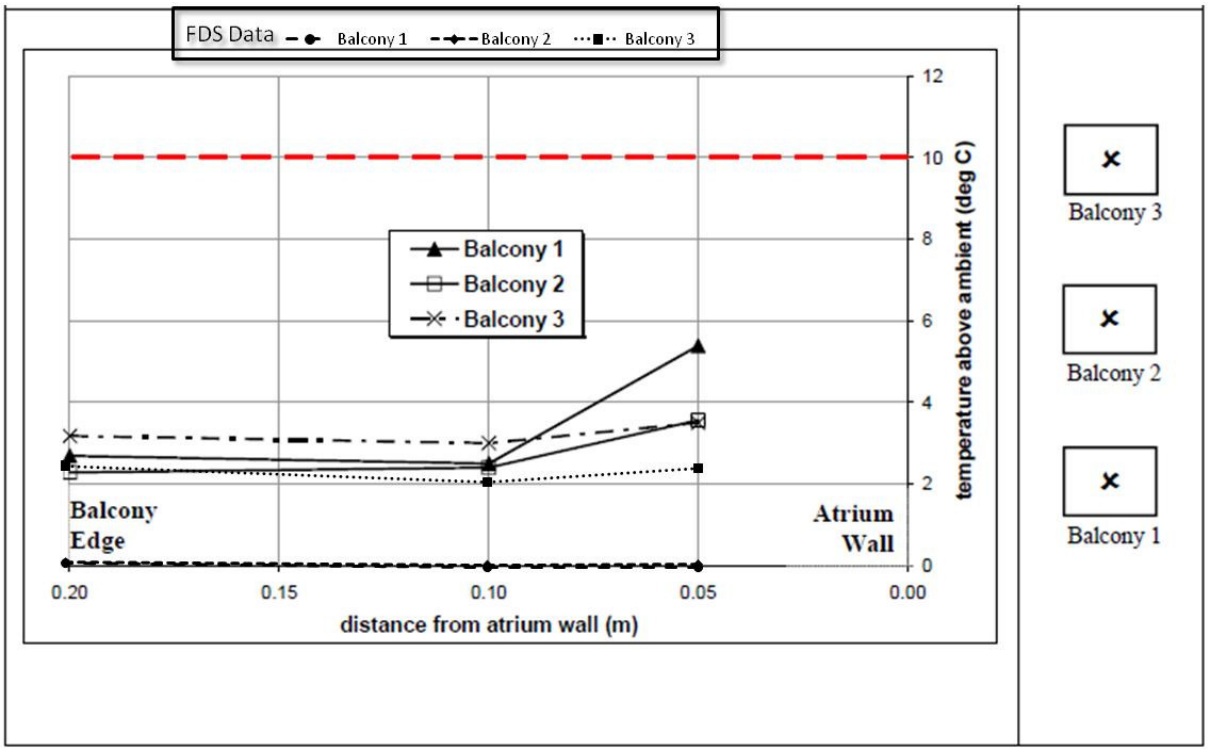

Figure C34. Temperature profiles along balcony breadth from FDS and Tan's experiment.

Experiment No.	=	41	
Balcony Breadth	=	200	mm
Plume Width	=	400	mm
Heat Release Rate	=	10	kW

Balcony Level	Photograph
3	
2	
1	

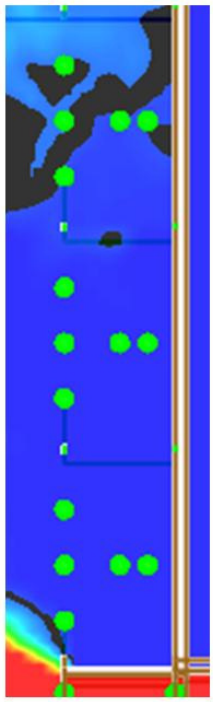

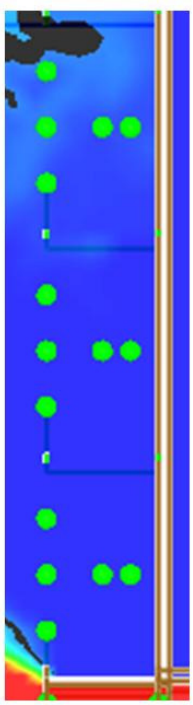

Figure C35. Temperature profile and Tan's experiment photographic records.

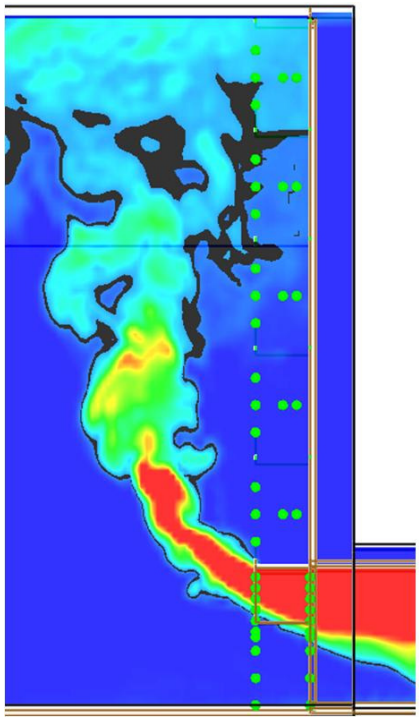

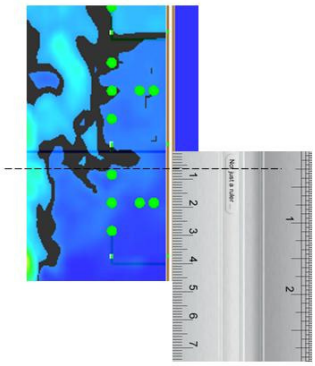

H = 1.14m

Figure C36. Smoke layer height measurement.

Scale Model (S43E) and Tan's Experiment 43 Data Comparison

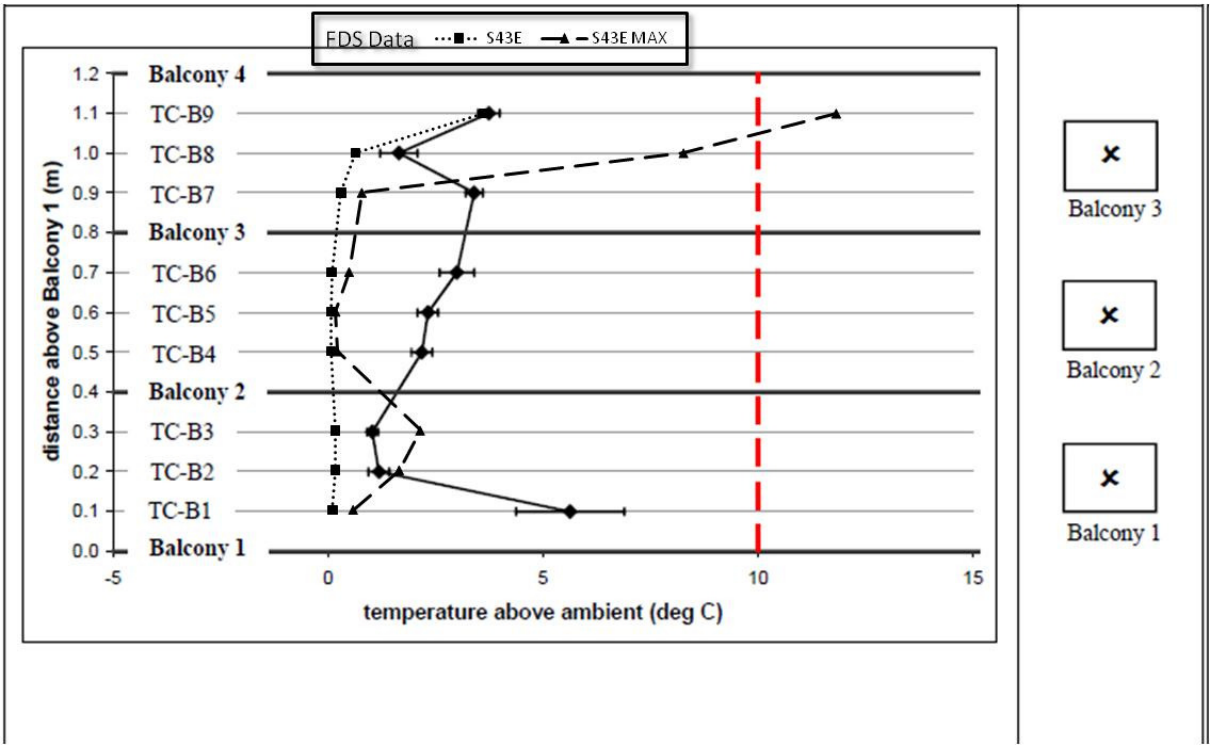

Figure C37. Temperature profiles across balcony edge from FDS and Tan's experiment.

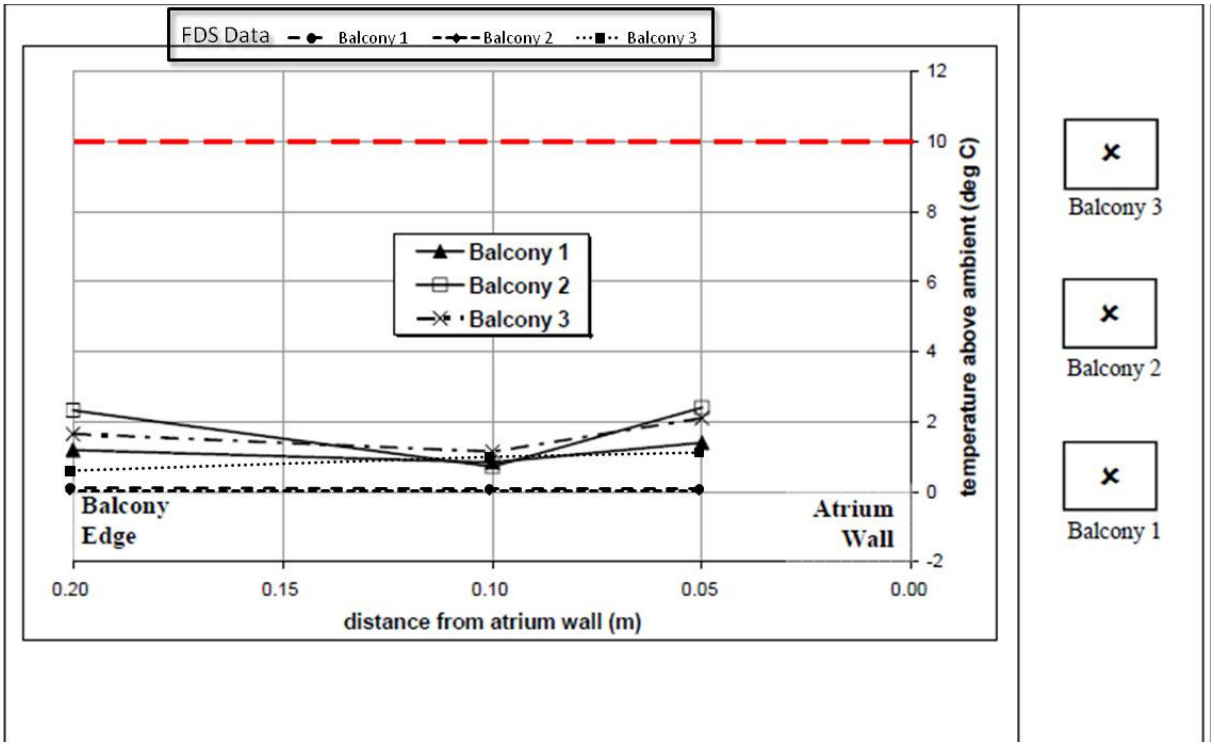

Figure C38. Temperature profiles along balcony breadth from FDS and Tan's experiment.

Experiment No. = 43
Balcony Breadth = 200 mm
Plume Width = 200 mm
Heat Release Rate = 5 kW

Balcony Level	Photograph
3	
2	
1	

25°C Profile

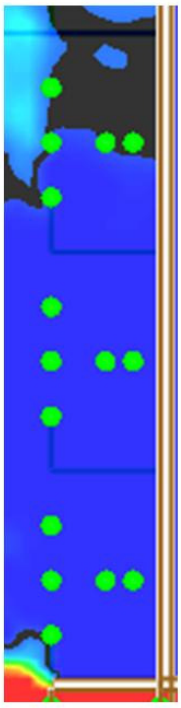

30°C Profile

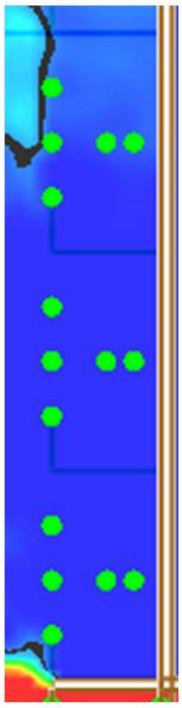

Figure C39. Temperature profile and Tan's experiment photographic records.

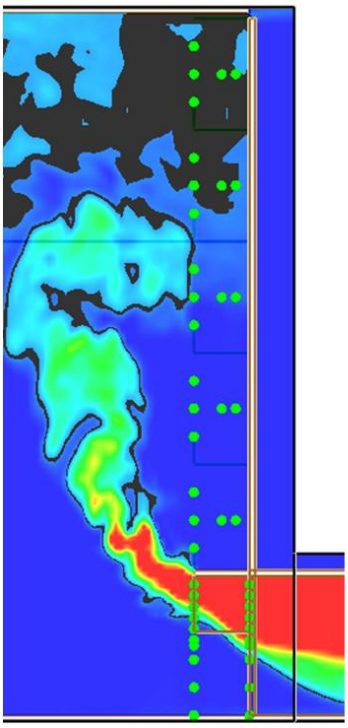

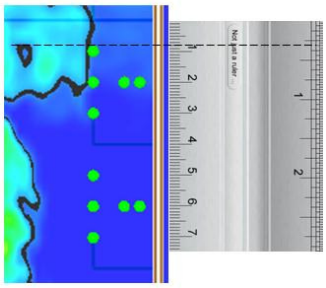

H = 1.12m

Figure C40. Smoke layer height measurement.

Scale Model (S56E) and Tan's Experiment 56 Data Comparison

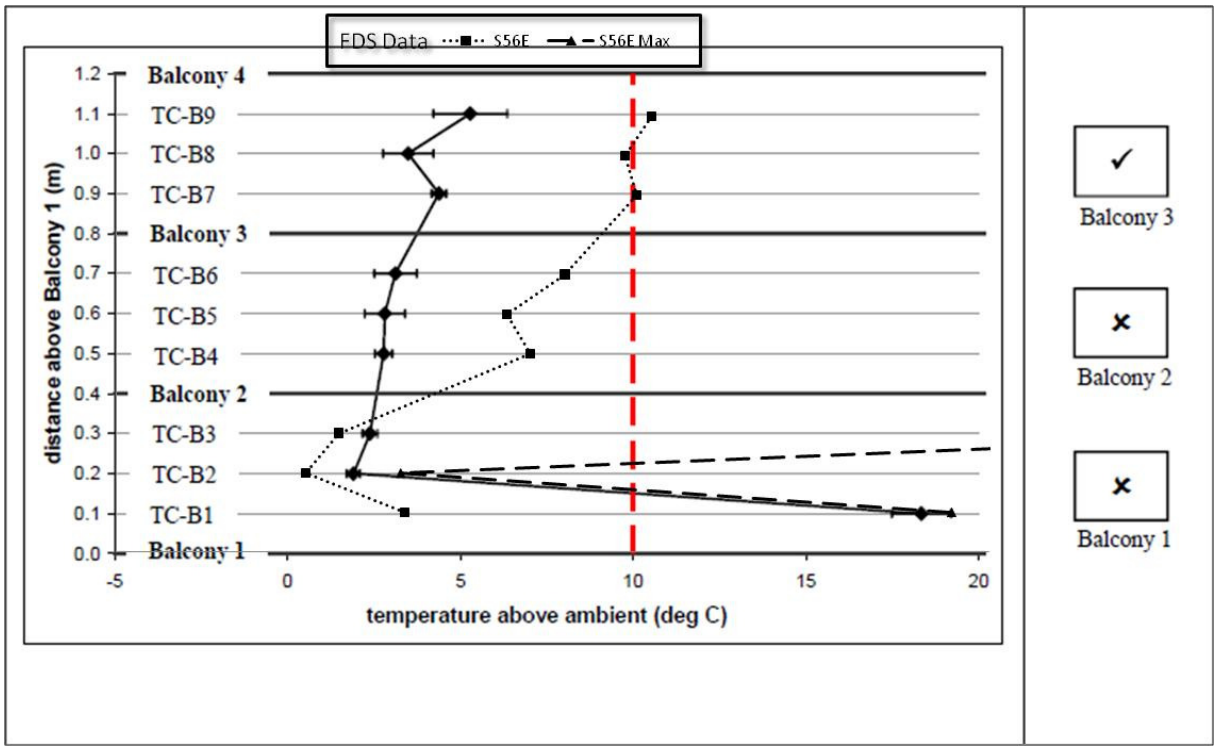

Figure C41. Temperature profiles across balcony edge from FDS and Tan's experiment.

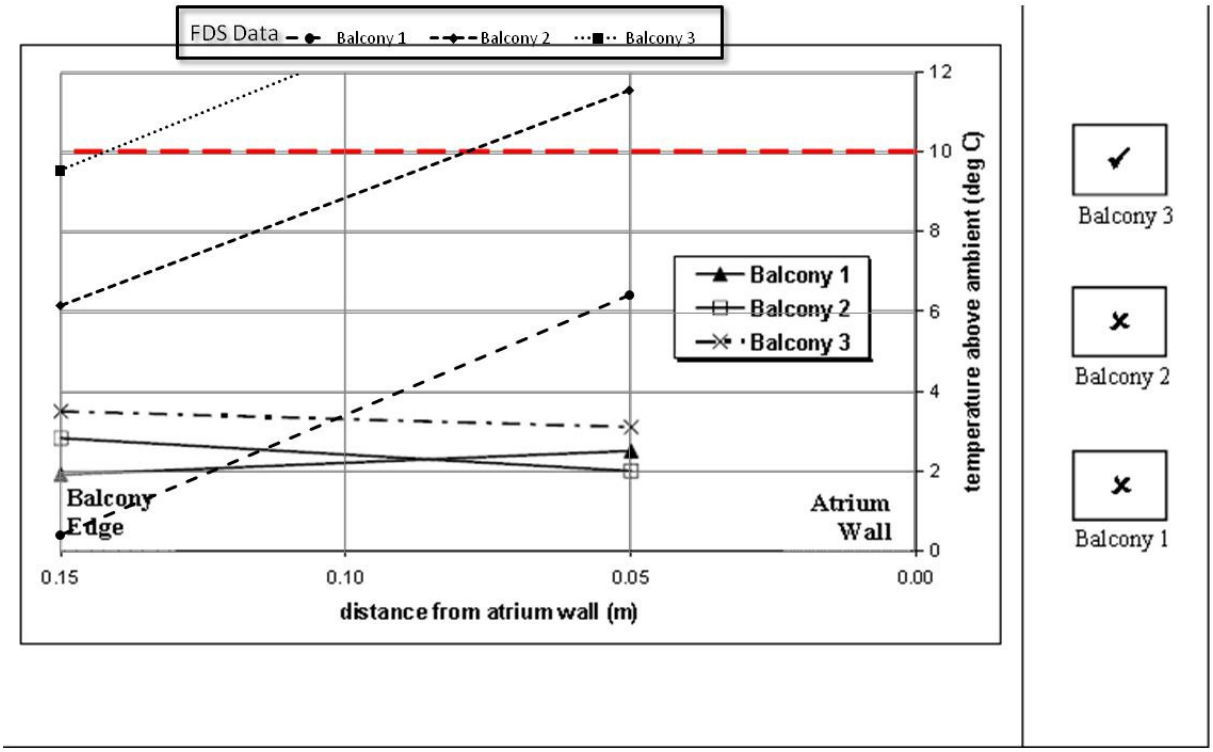

Figure C42. Temperature profiles along balcony breadth from FDS and Tan's experiment.

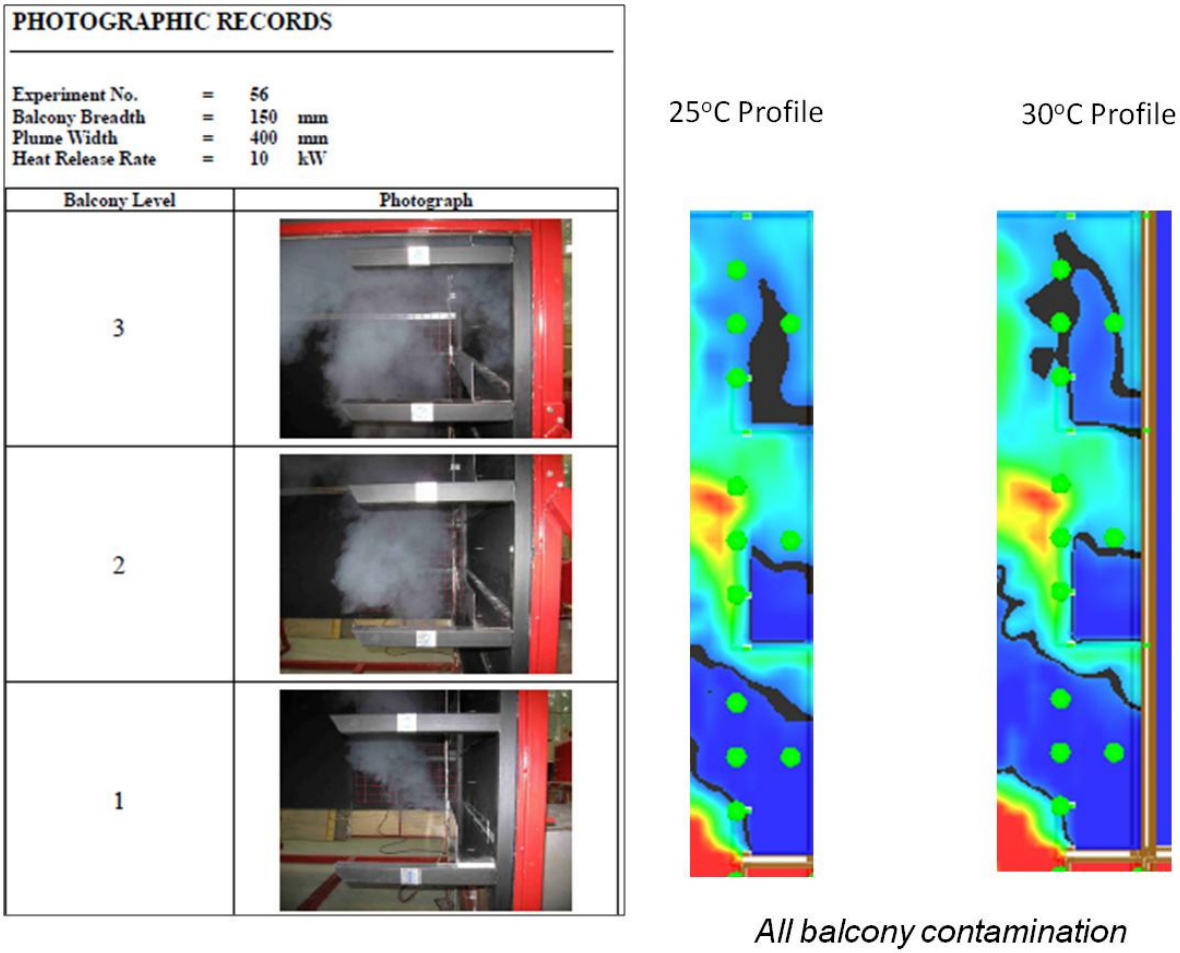

Figure C43. Temperature profile and Tan's experiment photographic records.

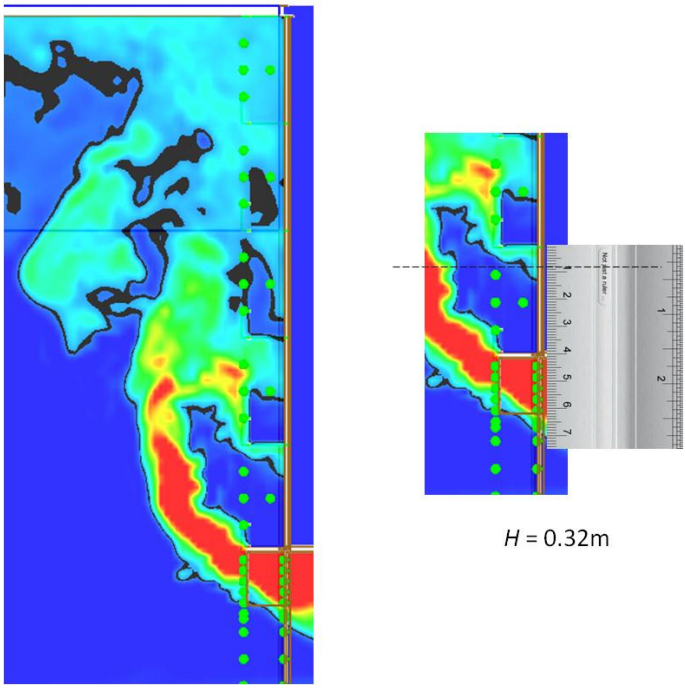

Figure C44. Smoke layer height measurement.

Scale Model (S60E) and Tan's Experiment 60 Data Comparison

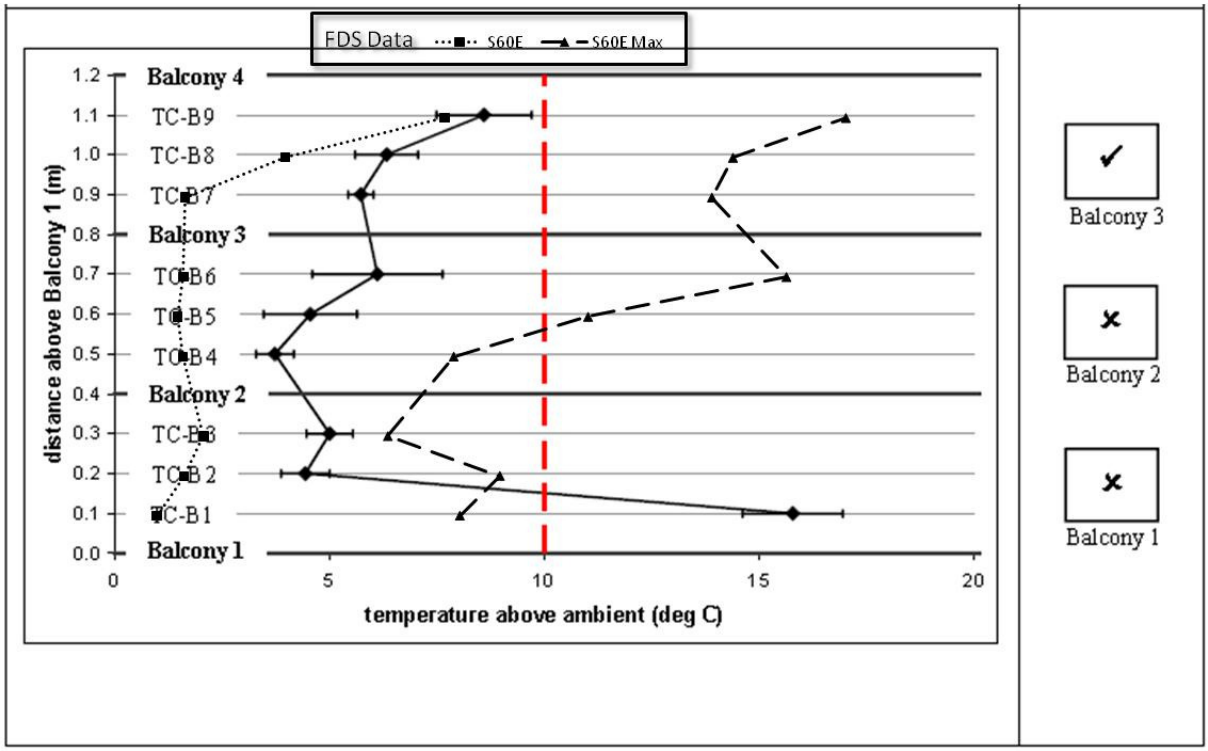

Figure C45. Temperature profiles across balcony edge from FDS and Tan's experiment.

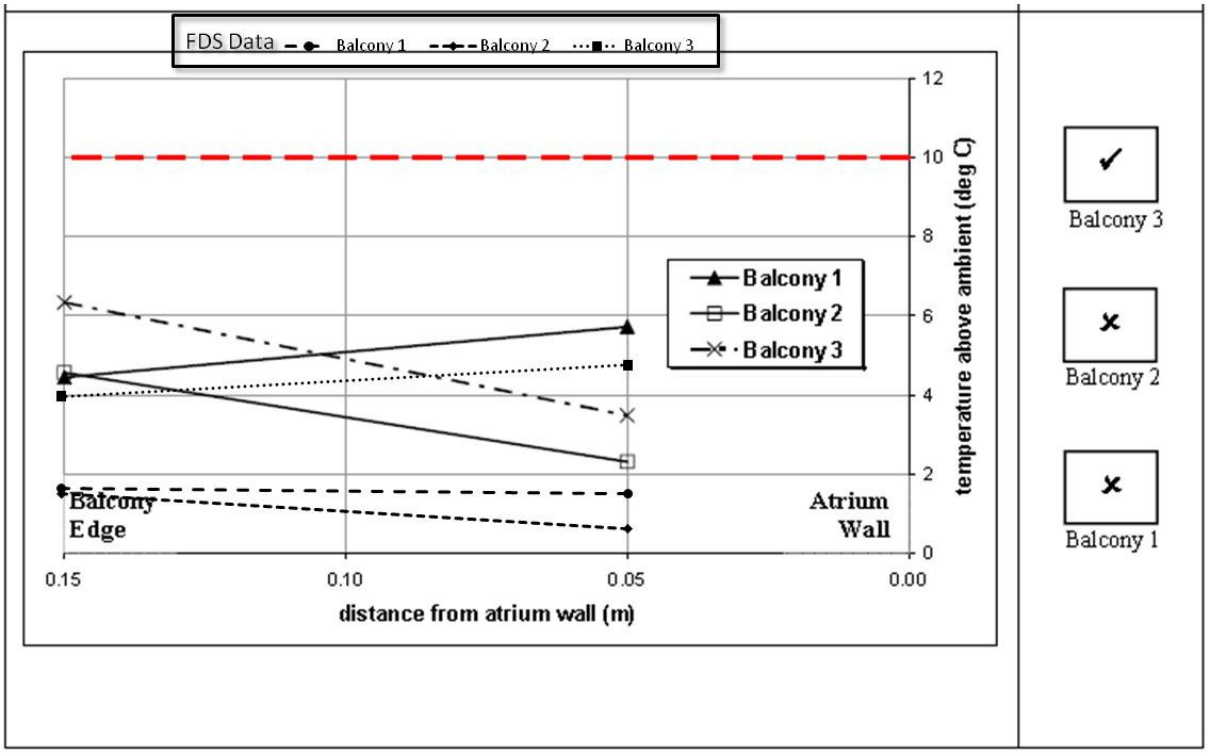

Figure C46. Temperature profiles along balcony breadth from FDS and Tan's experiment.

Experiment No.	=	60	
Balcony Breadth	=	150	mm
Plume Width	=	200	mm
Heat Release Rate	=	15	kW

Balcony Level	Photograph
3	
2	
1	

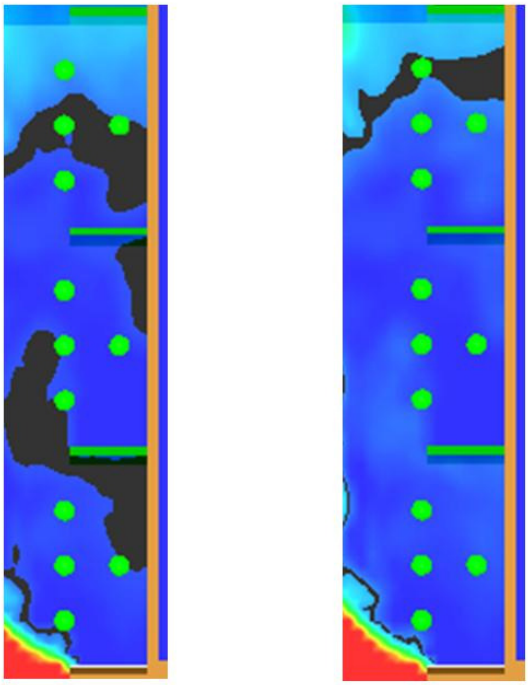

Figure C47. Temperature profile and Tan's experiment photographic records.

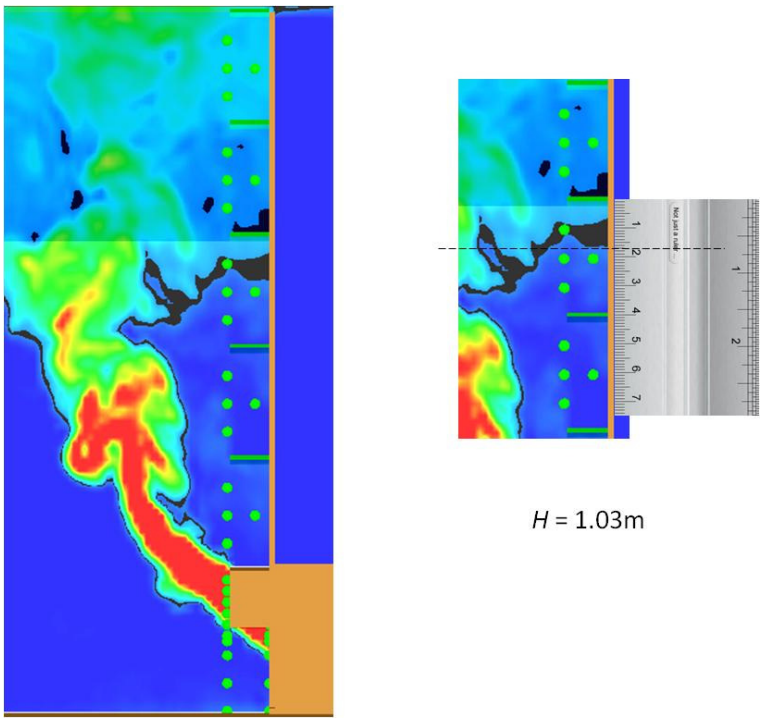

Figure C48. Smoke layer height measurement.

Simulation Result for Full Scale Five Balcony Configuration

Full scale for 5 storey balcony (F01E5)

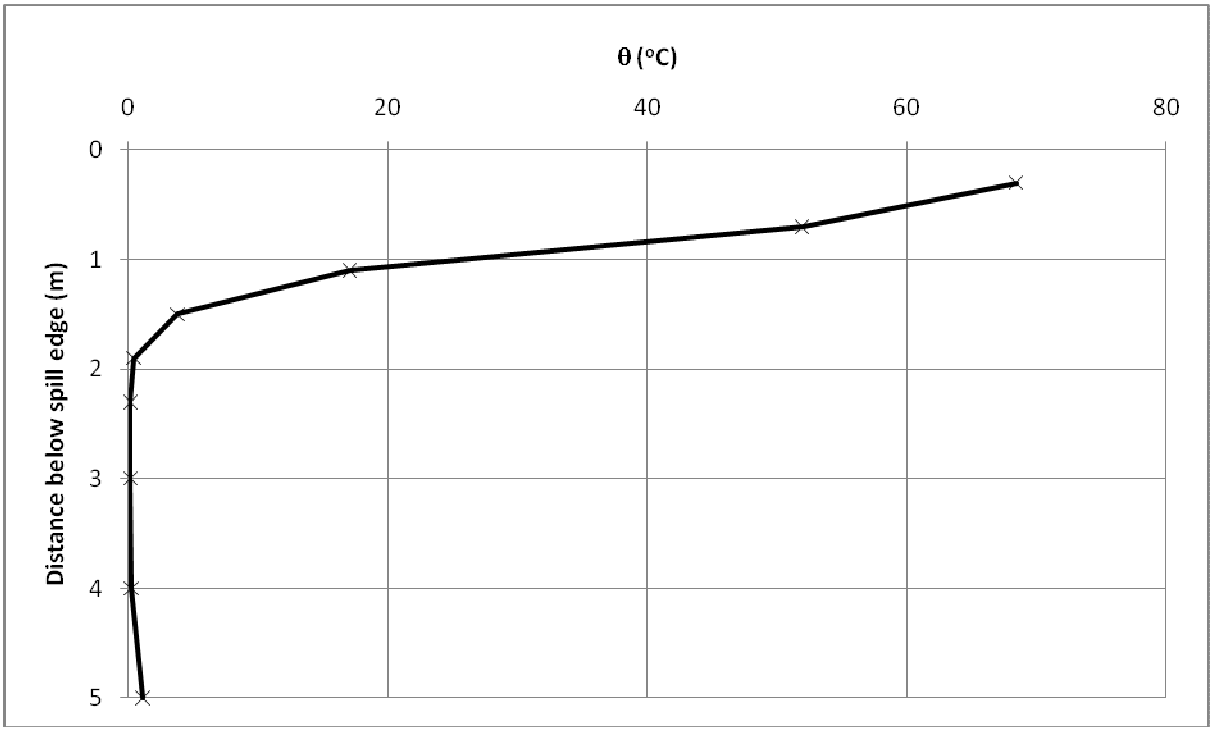

Figure D1. Temperature above ambient at the spill edge.

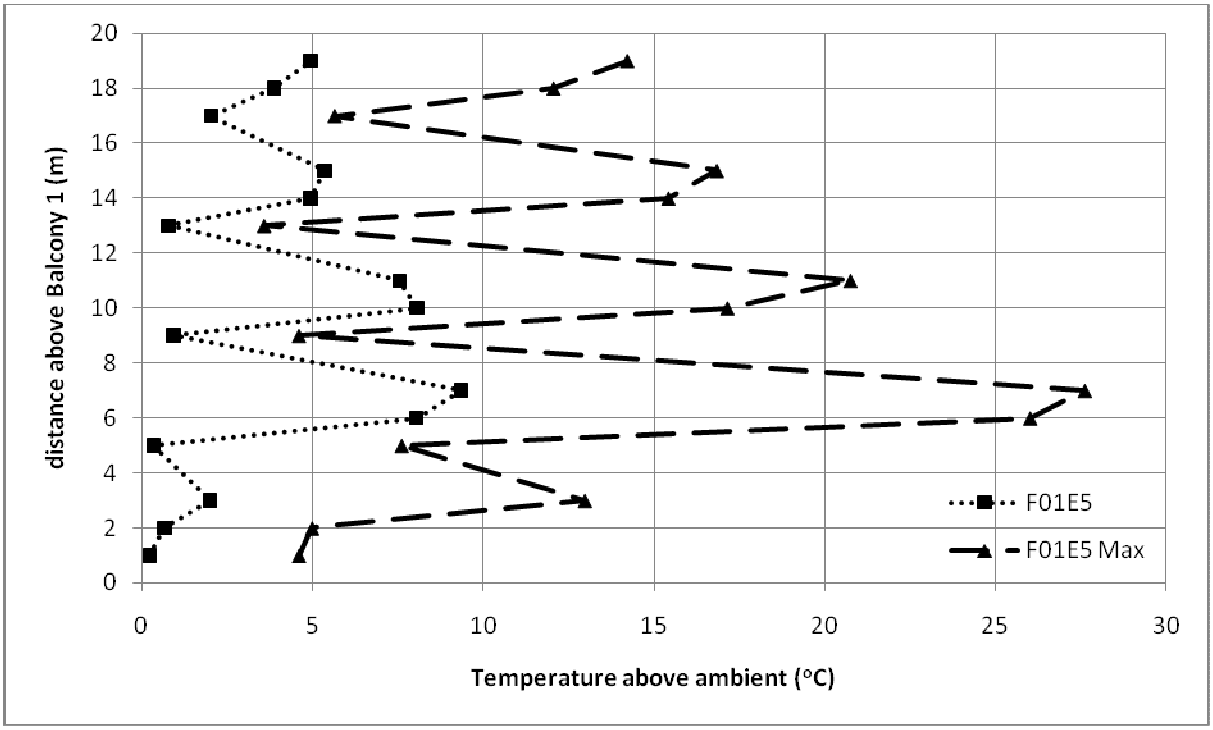

Figure D2. Temperature profiles across balcony edge.

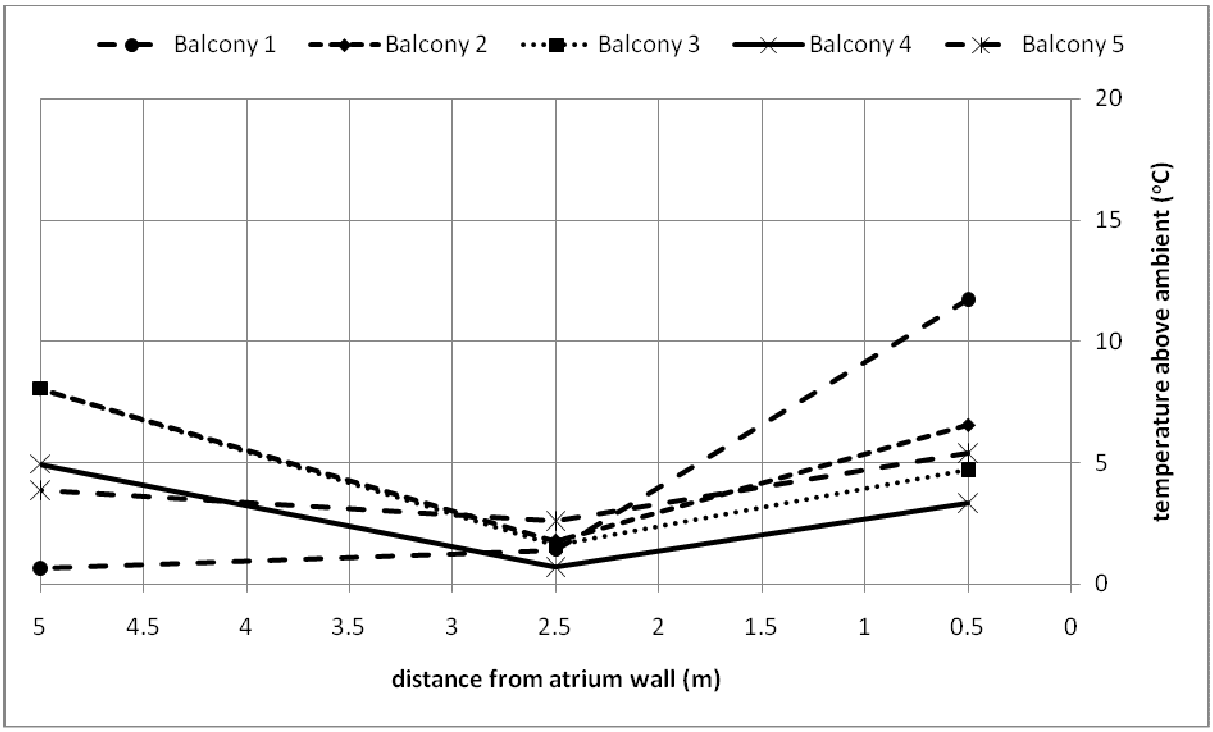

Figure D3. Temperature profiles along balcony breadth.

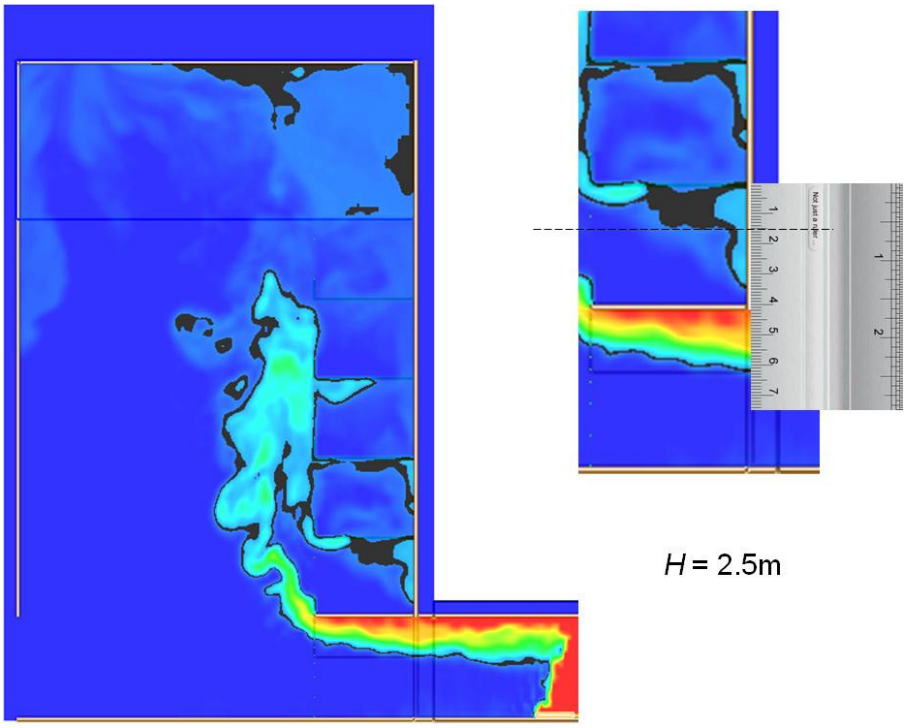

Figure D4. Smoke layer height measurement.

Full scale for 5 balcony (F02E5)

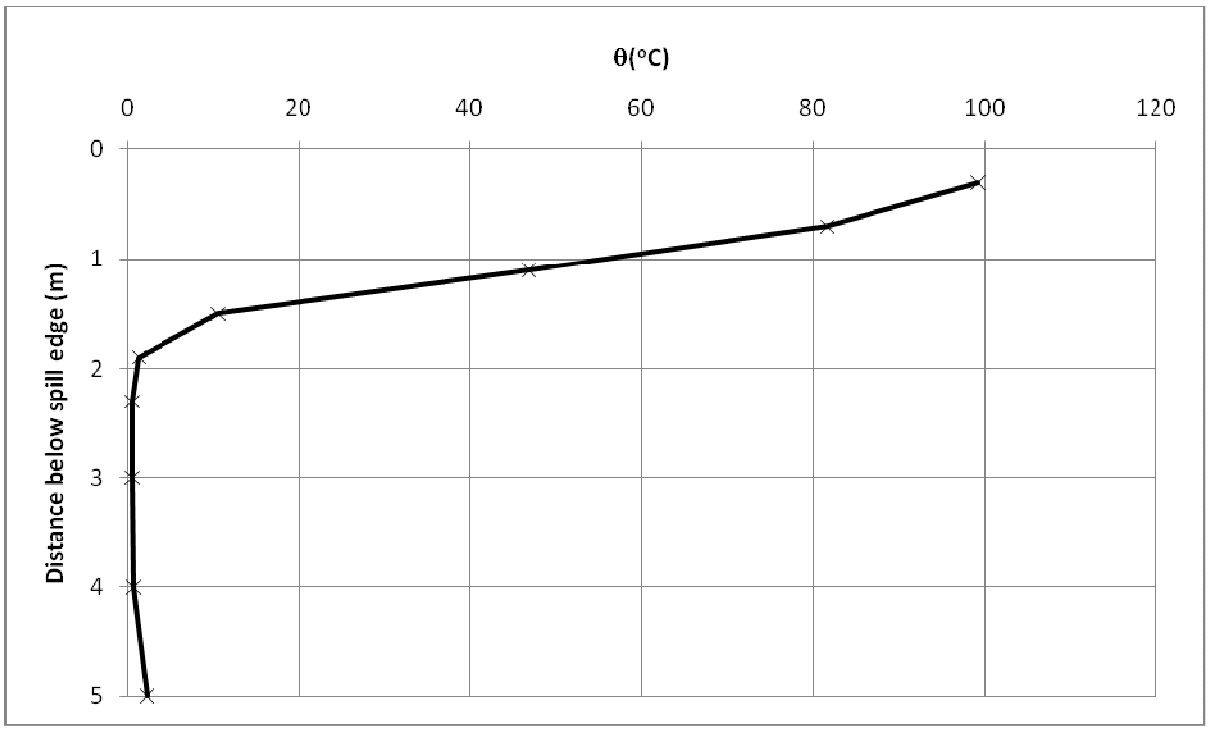

Figure D5. Temperature above ambient at the spill edge.

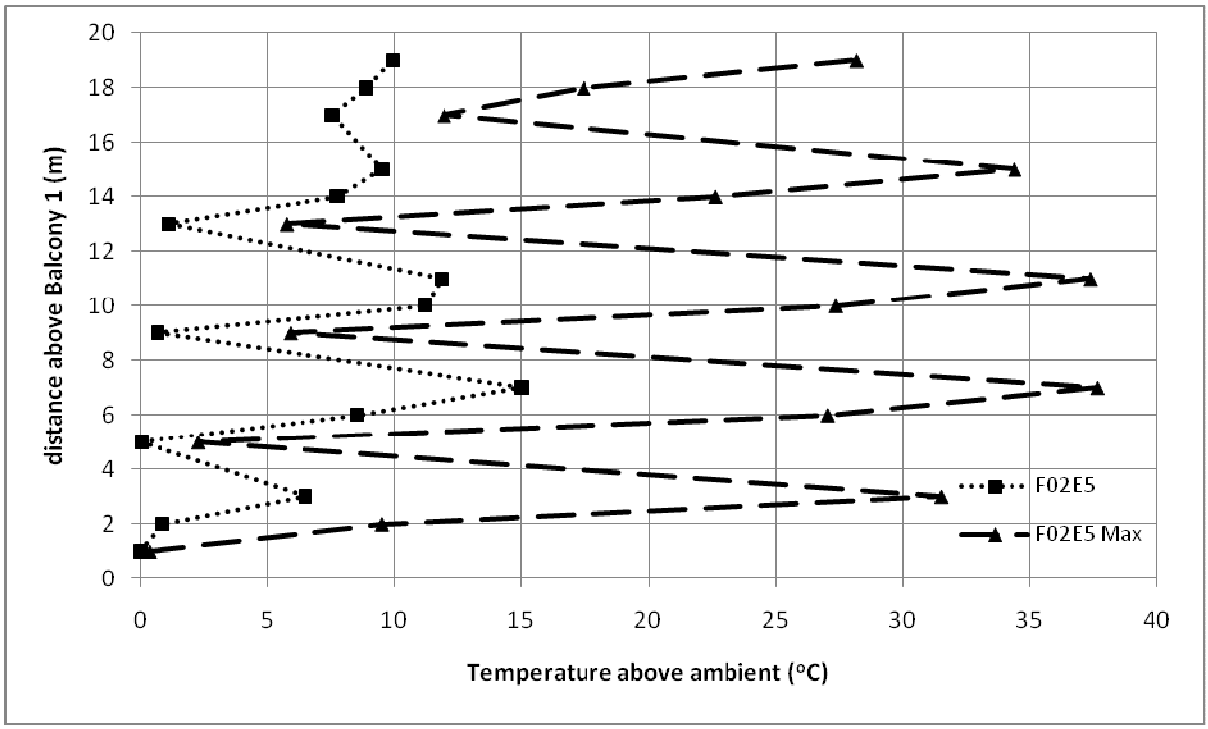

Figure D6. Temperature profiles across balcony edge.

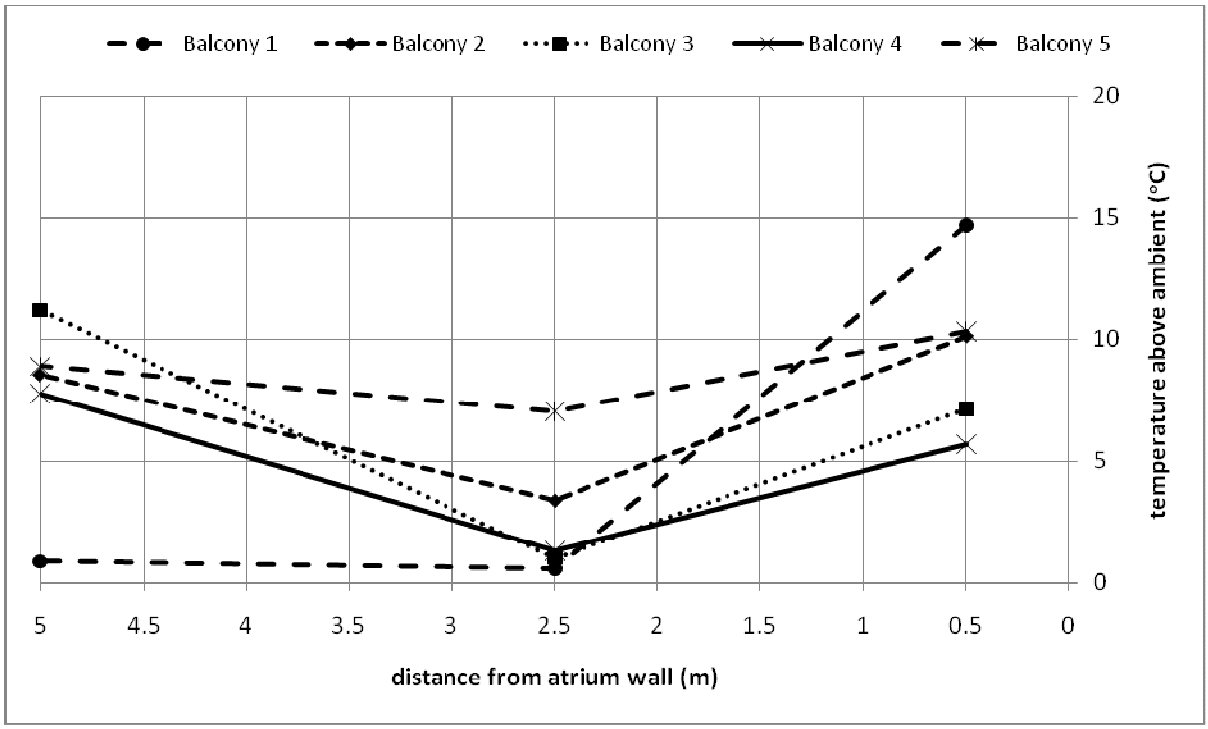

Figure D7. Temperature profiles along balcony breadth.

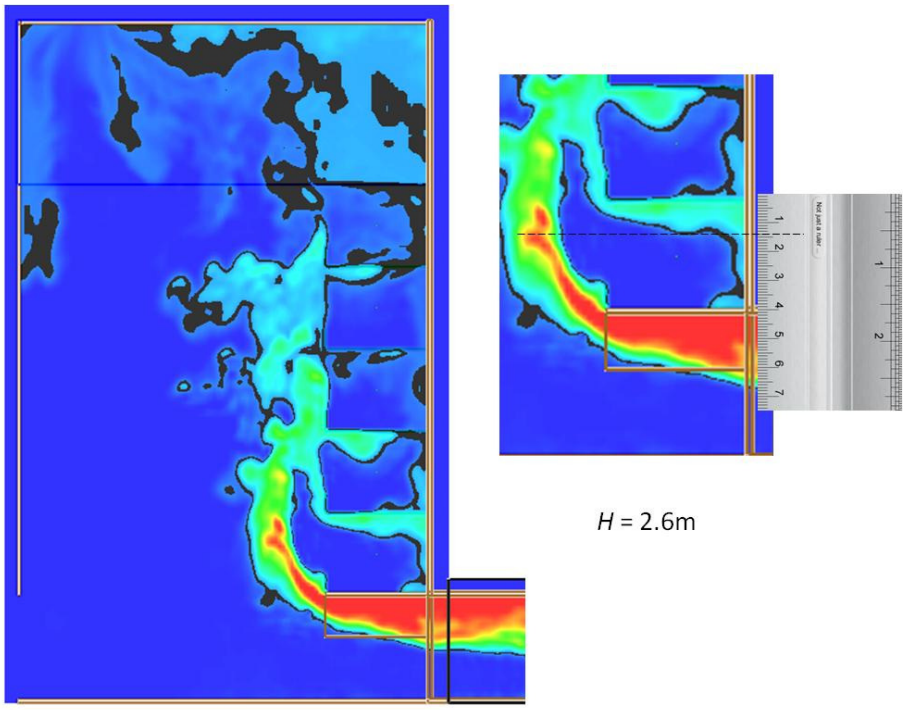

Figure D8. Smoke layer height measurement.

Full scale for 5 balcony (F03E5)

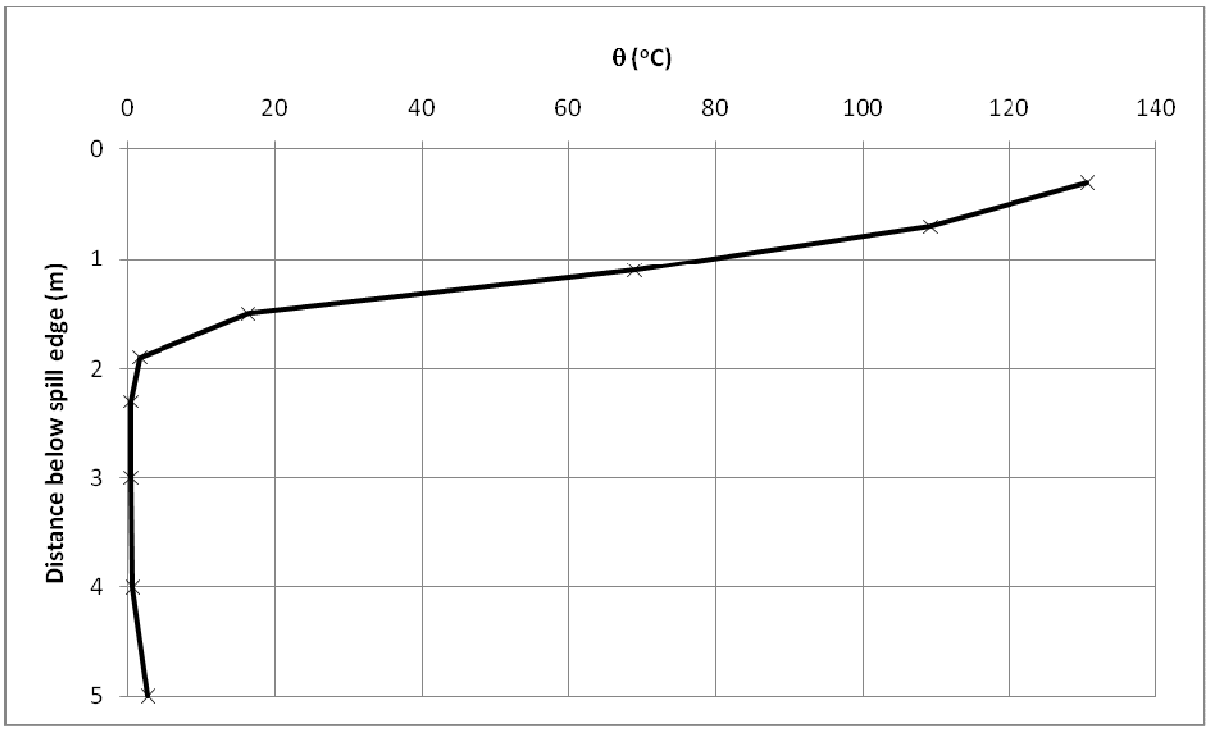

Figure D9. Temperature above ambient at the spill edge.

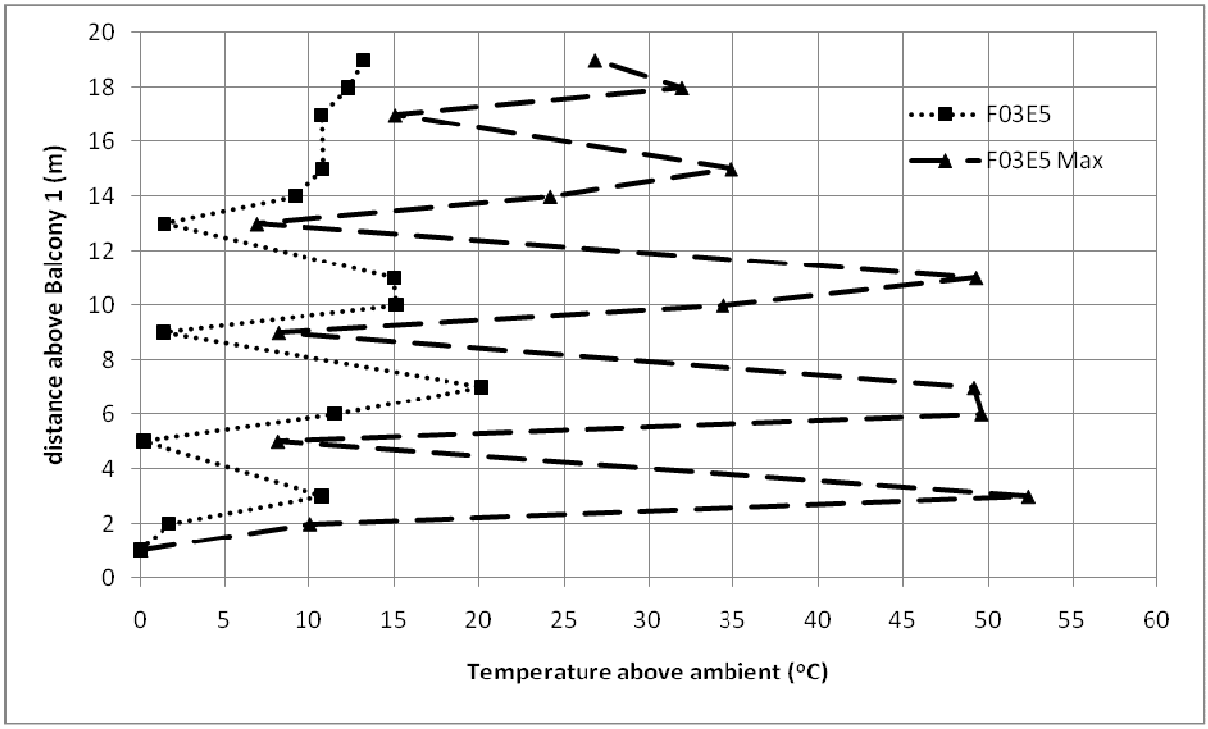

Figure D10. Temperature profiles across balcony edge.

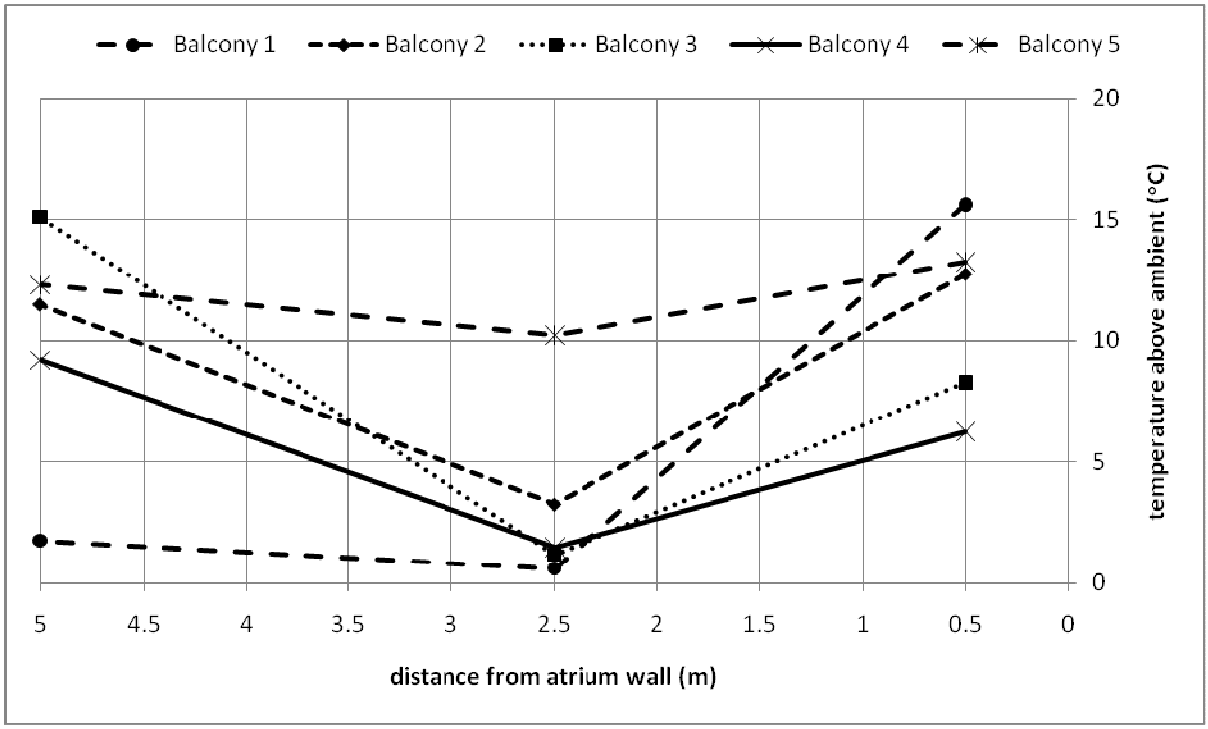

Figure D11. Temperature profiles along balcony breadth.

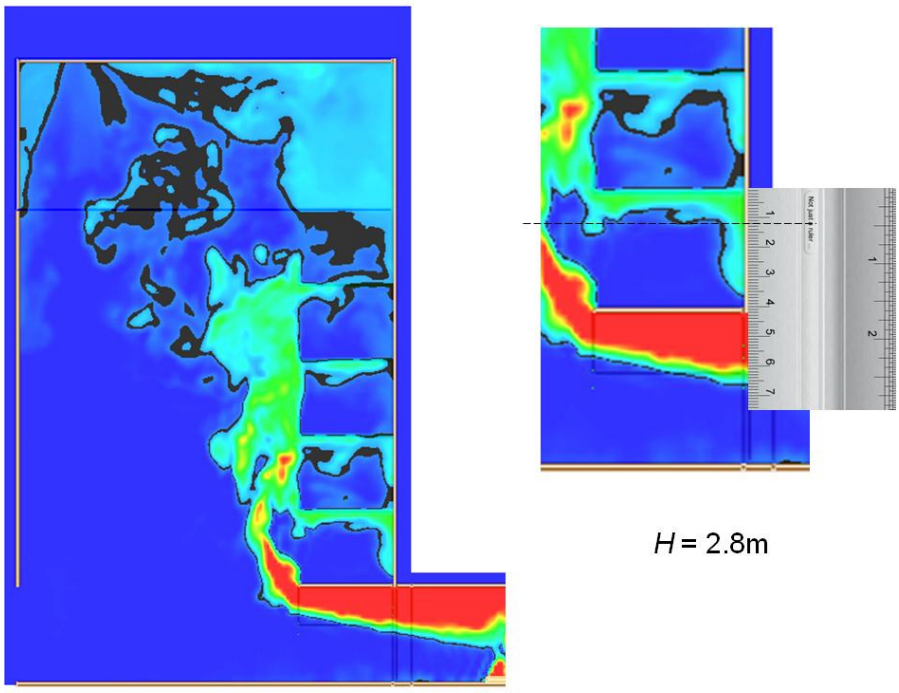

Figure D12. Smoke layer height measurement.

Full scale for 5 balcony (F04E5)

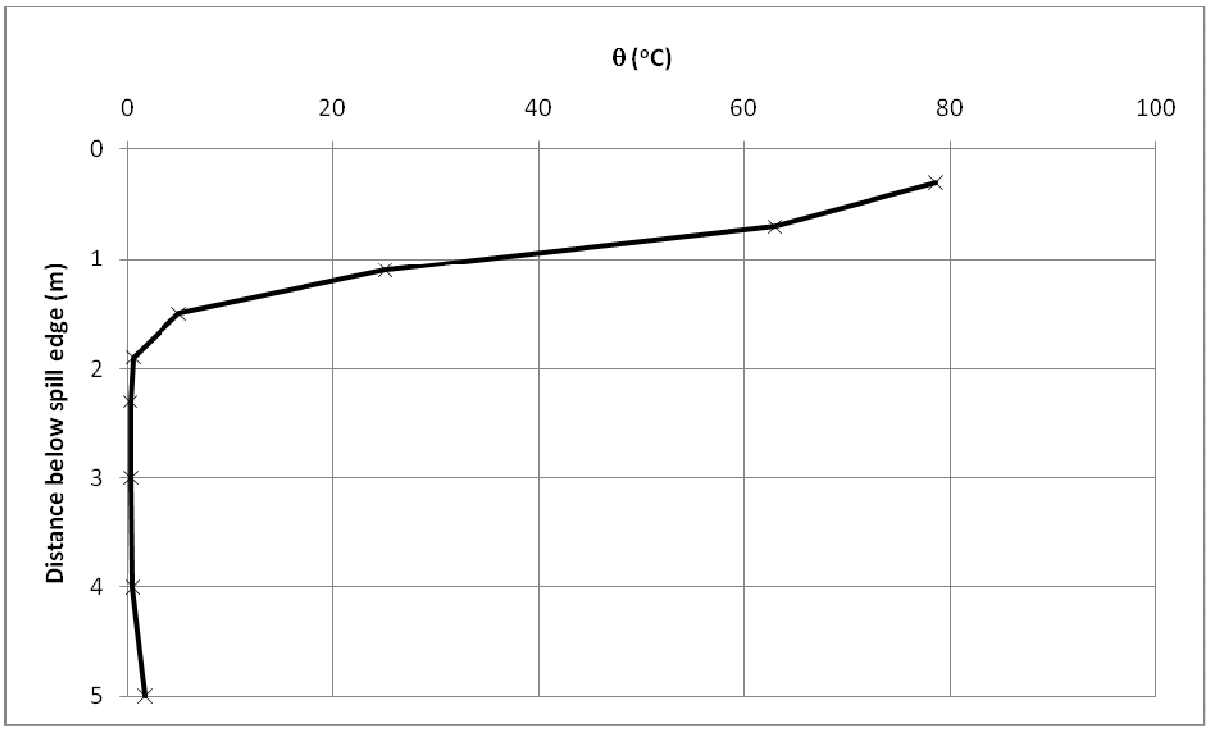

Figure D13. Temperature above ambient at the spill edge.

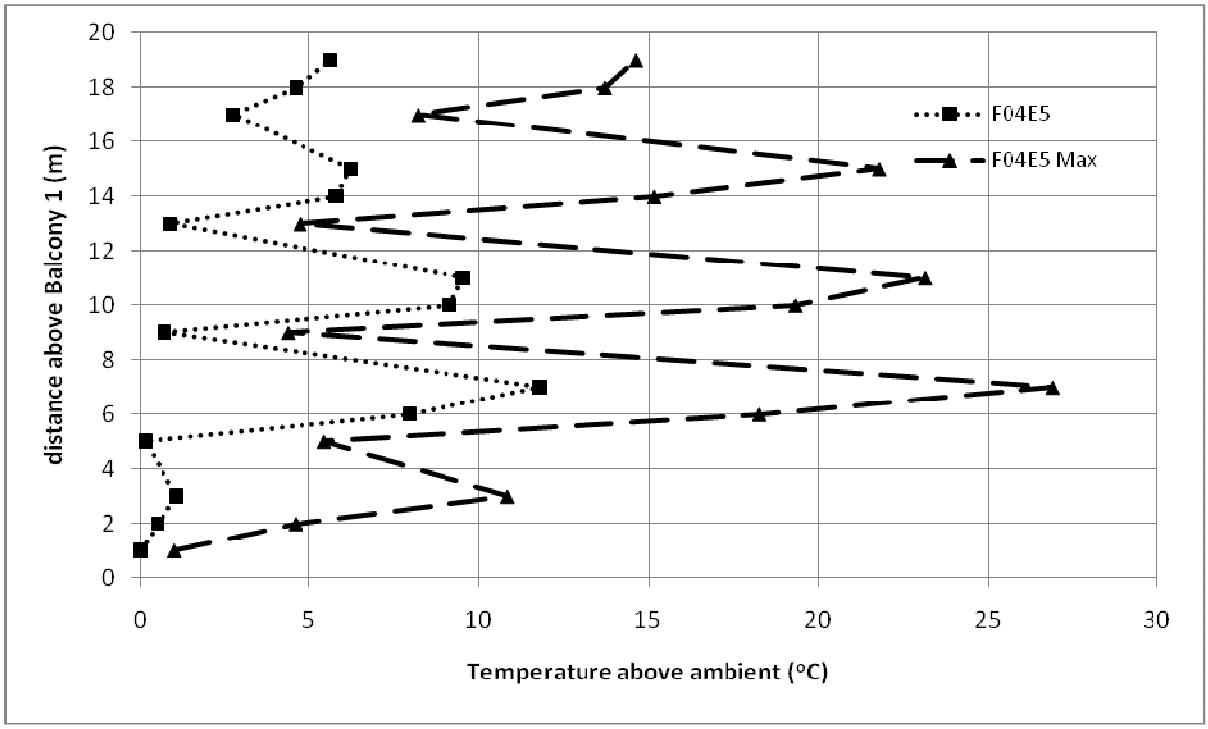

Figure D14. Temperature profiles across balcony edge.

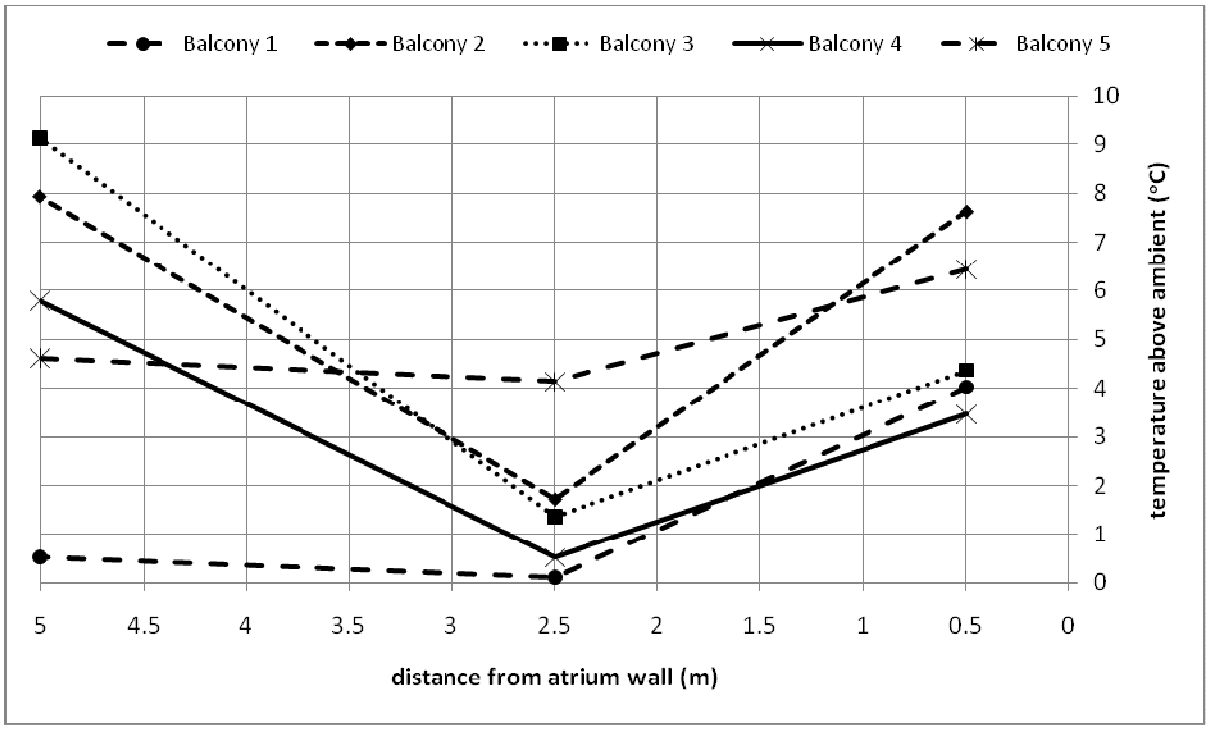

Figure D15. Temperature profiles along balcony breadth.

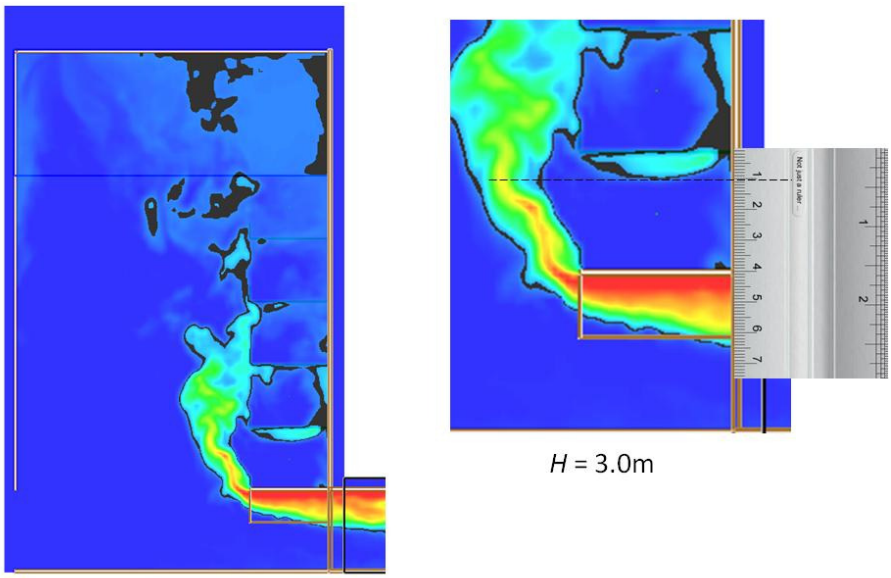

Figure D16. Smoke layer height measurement.

Full scale for 5 balcony (F05E5)

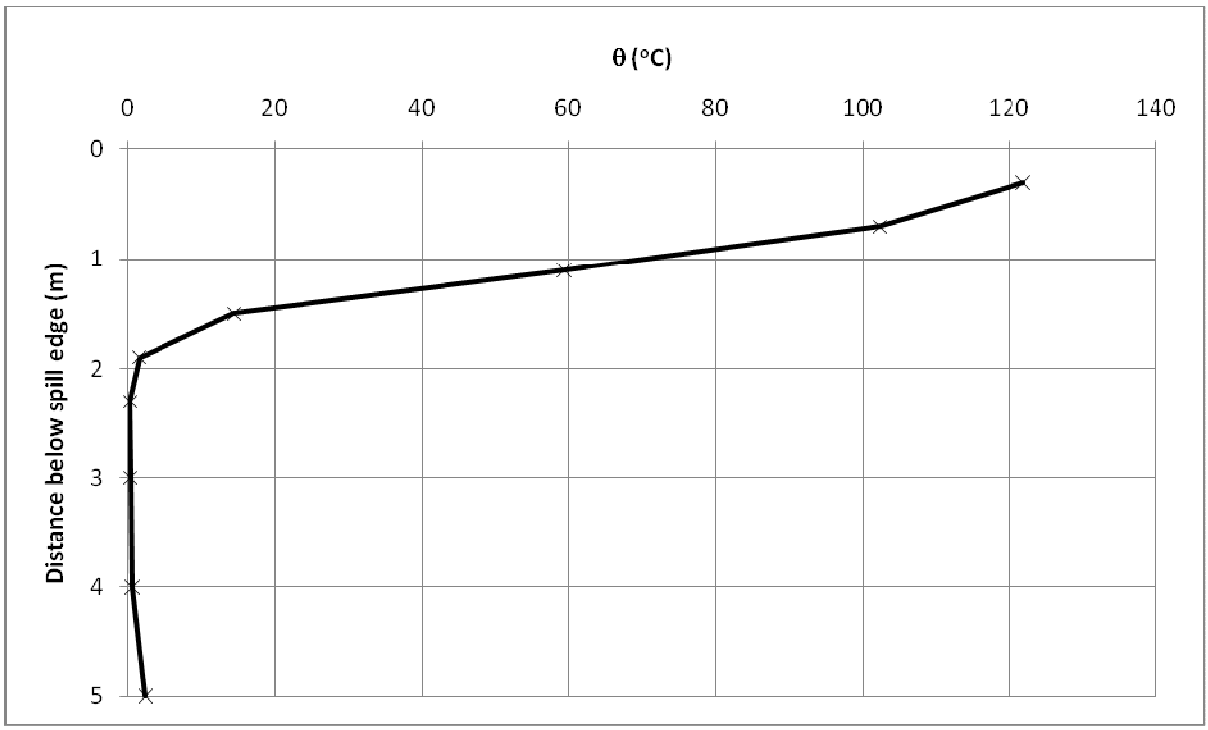

Figure D17. Temperature above ambient at the spill edge.

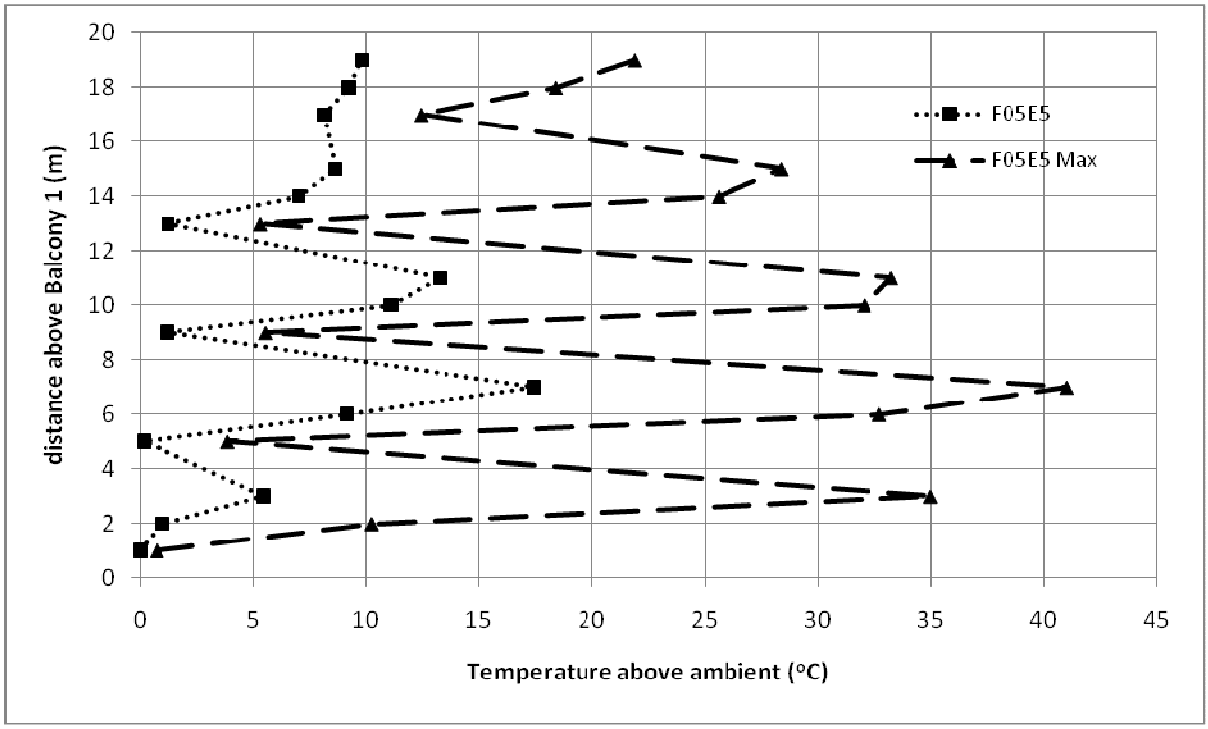

Figure D18. Temperature profiles across balcony edge.

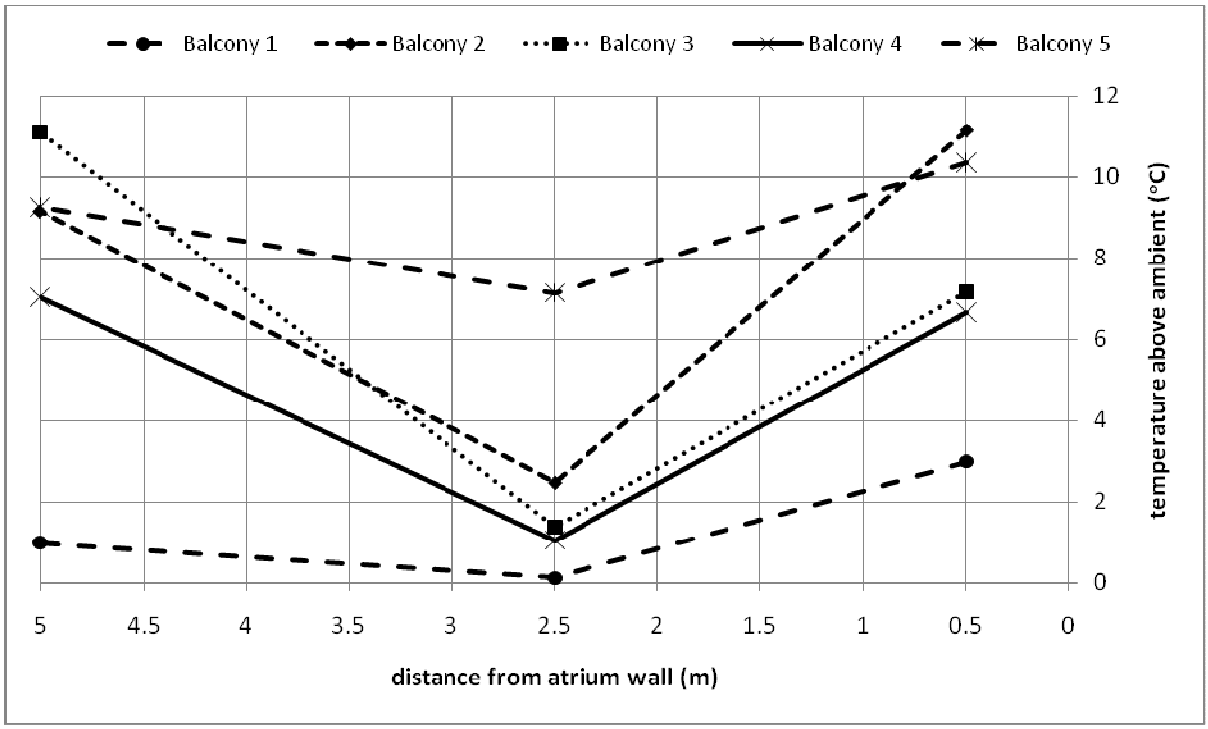

Figure D19. Temperature profiles along balcony breadth.

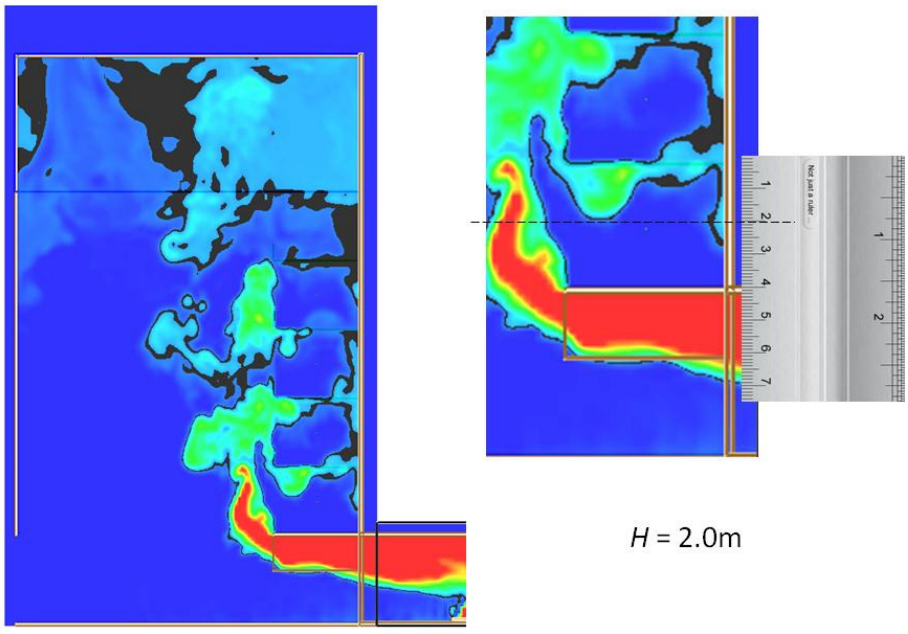

Figure D20. Smoke layer height measurement.

Full scale for 5 balcony (F06E5)

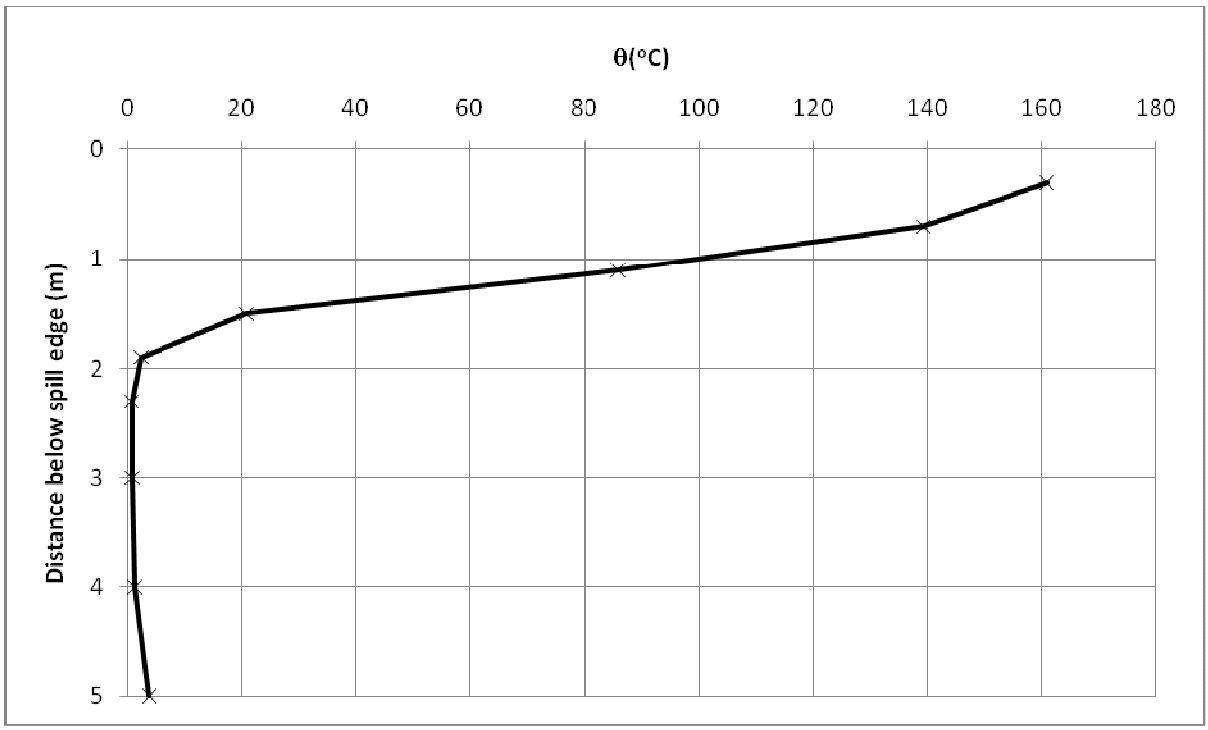

Figure D21. Temperature above ambient at the spill edge.

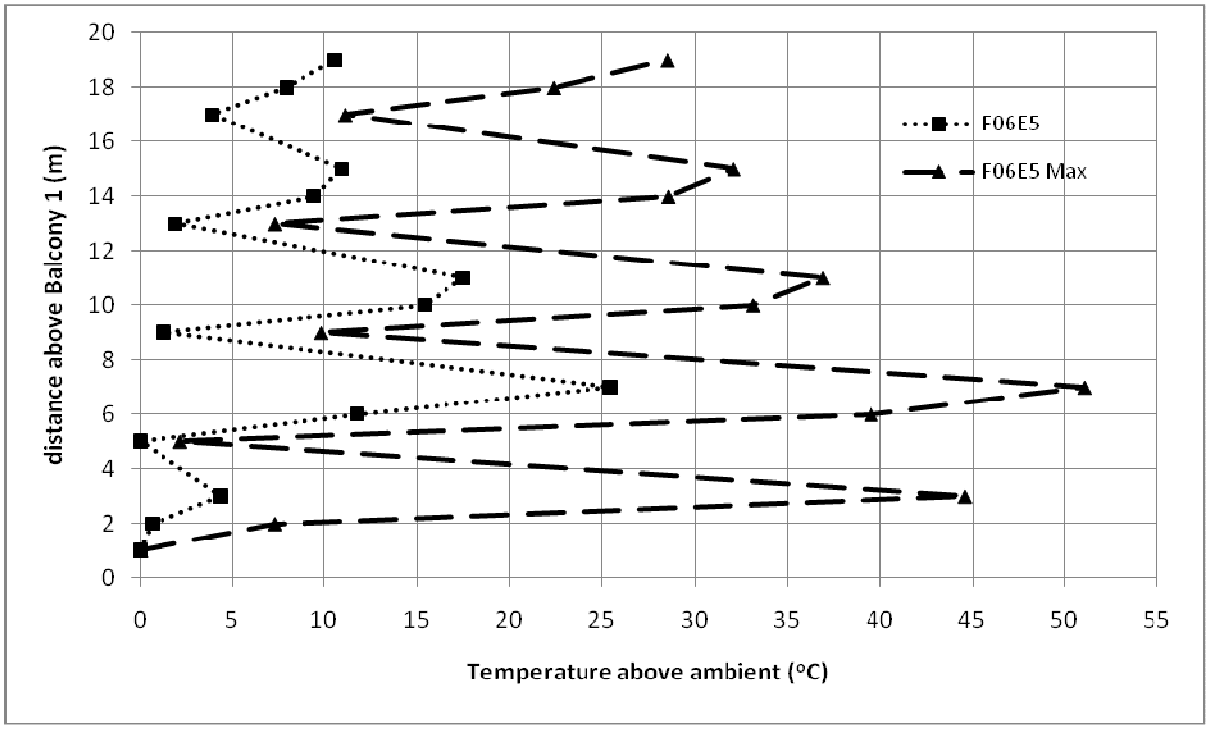

Figure D22. Temperature profiles across balcony edge.

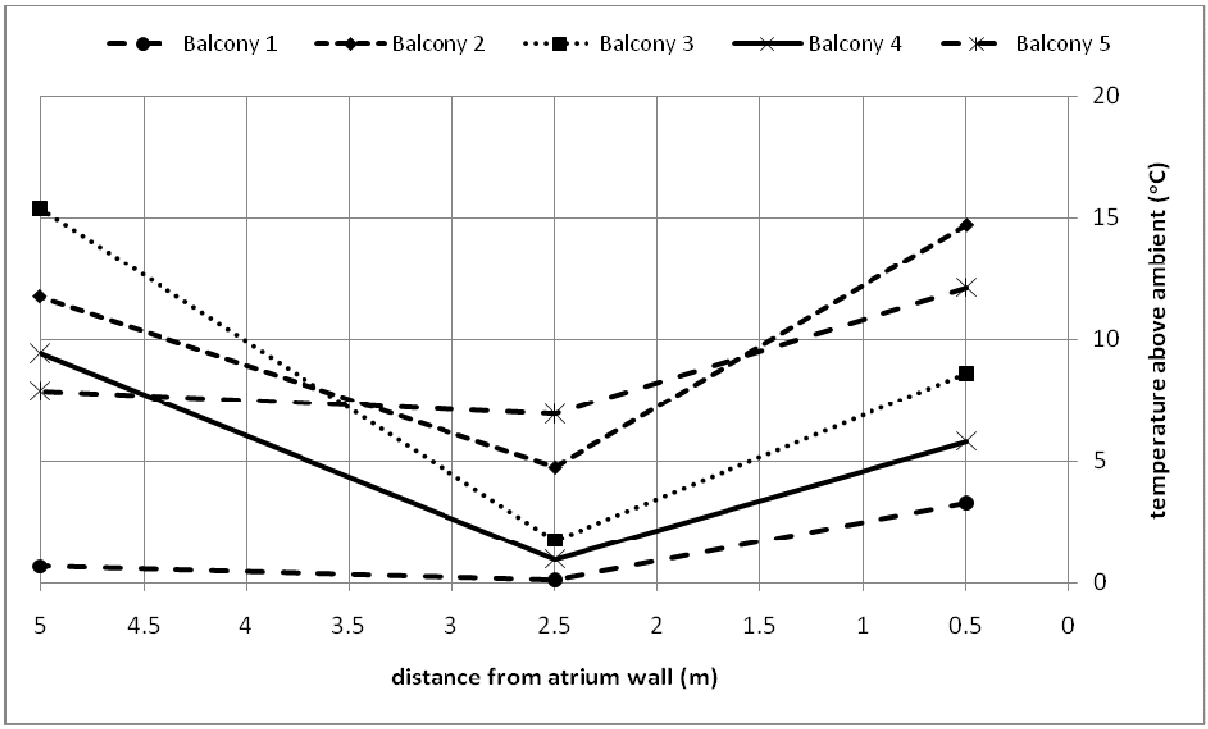

Figure D23. Temperature profiles along balcony breadth.

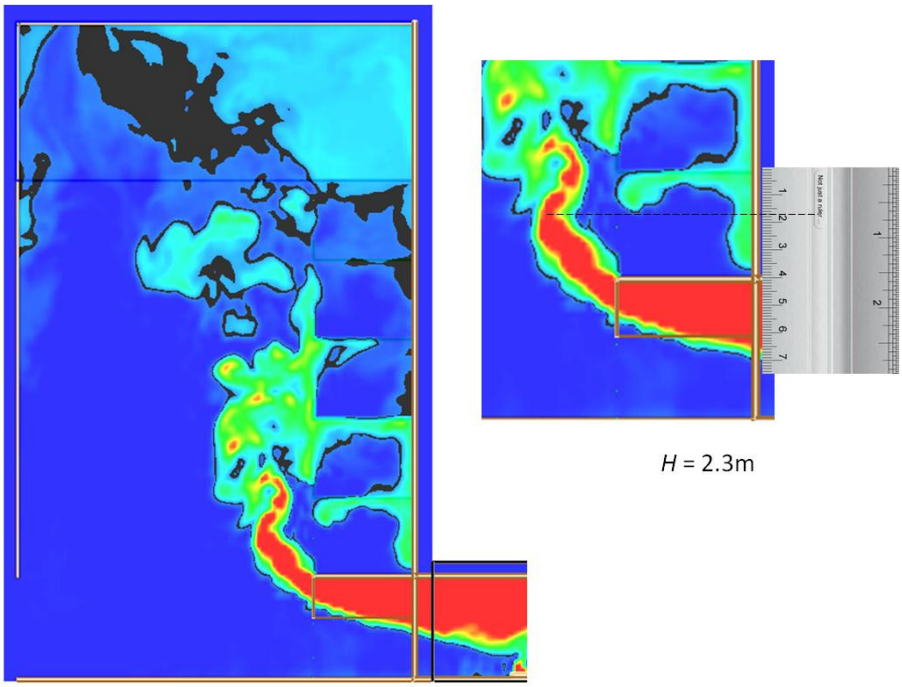

Figure D24. Smoke layer height measurement.

Full scale for 5 balcony (F07E5)

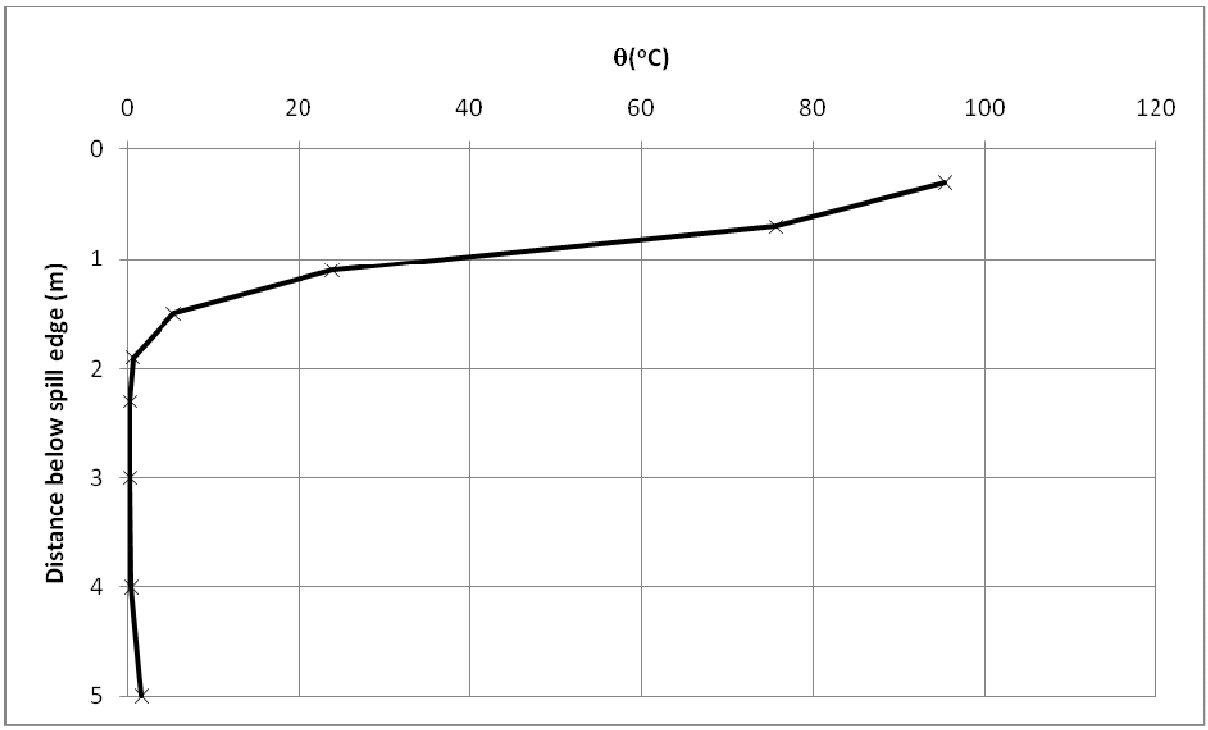

Figure D25. Temperature above ambient at the spill edge.

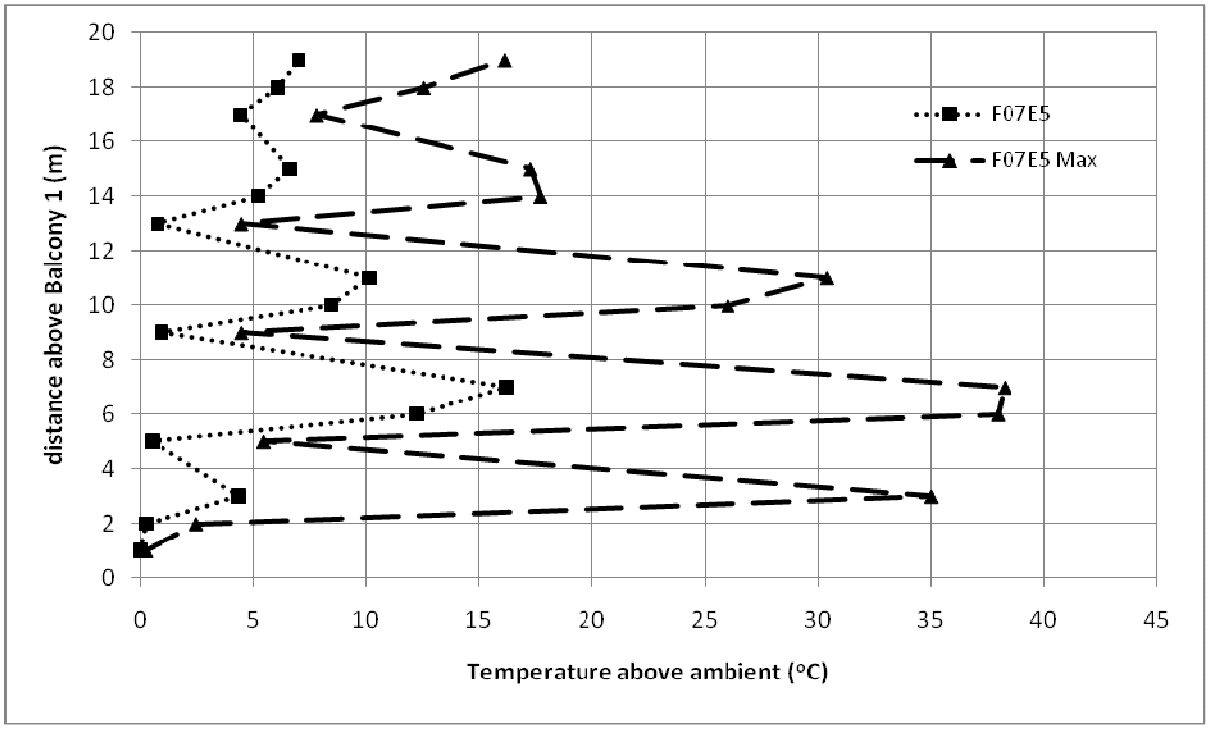

Figure D26. Temperature profiles across balcony edge.

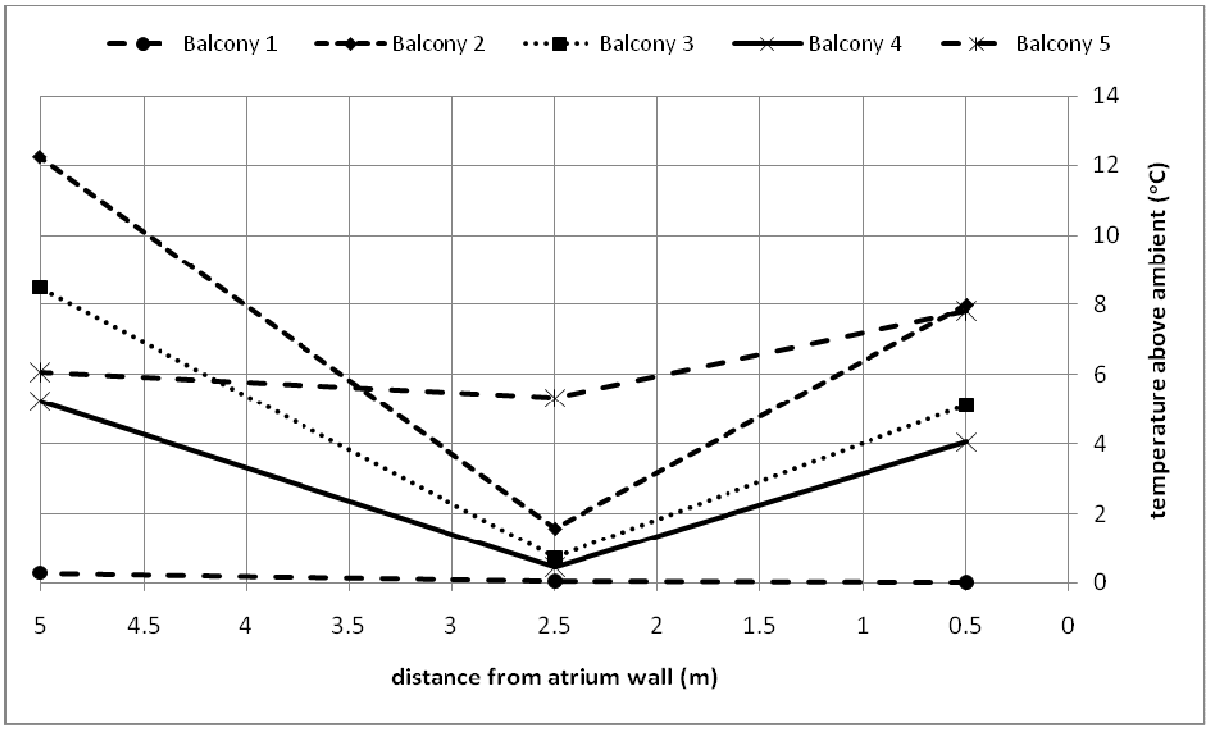

Figure D27. Temperature profiles along balcony breadth.

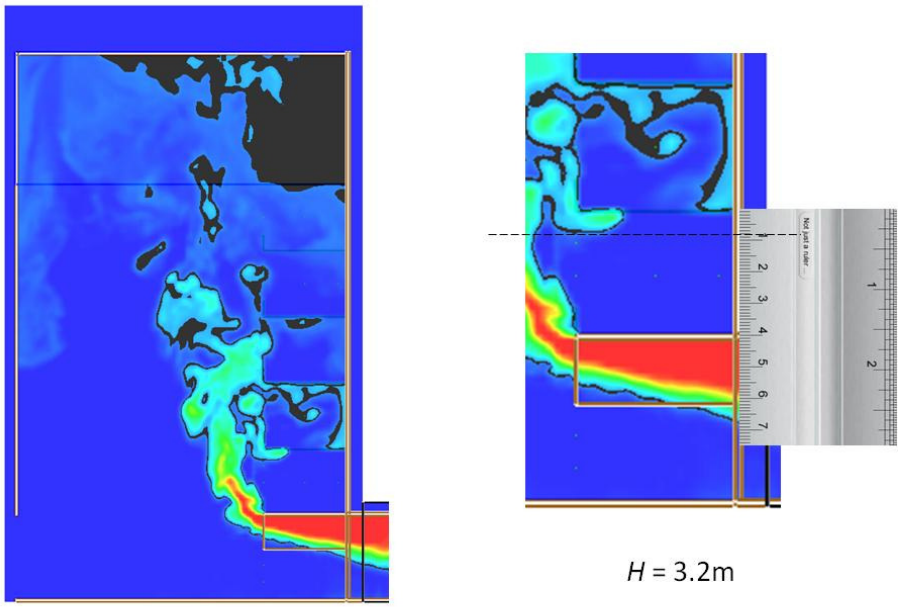

Figure D28. Smoke layer height measurement.

Full scale for 5 balcony (F08E5)

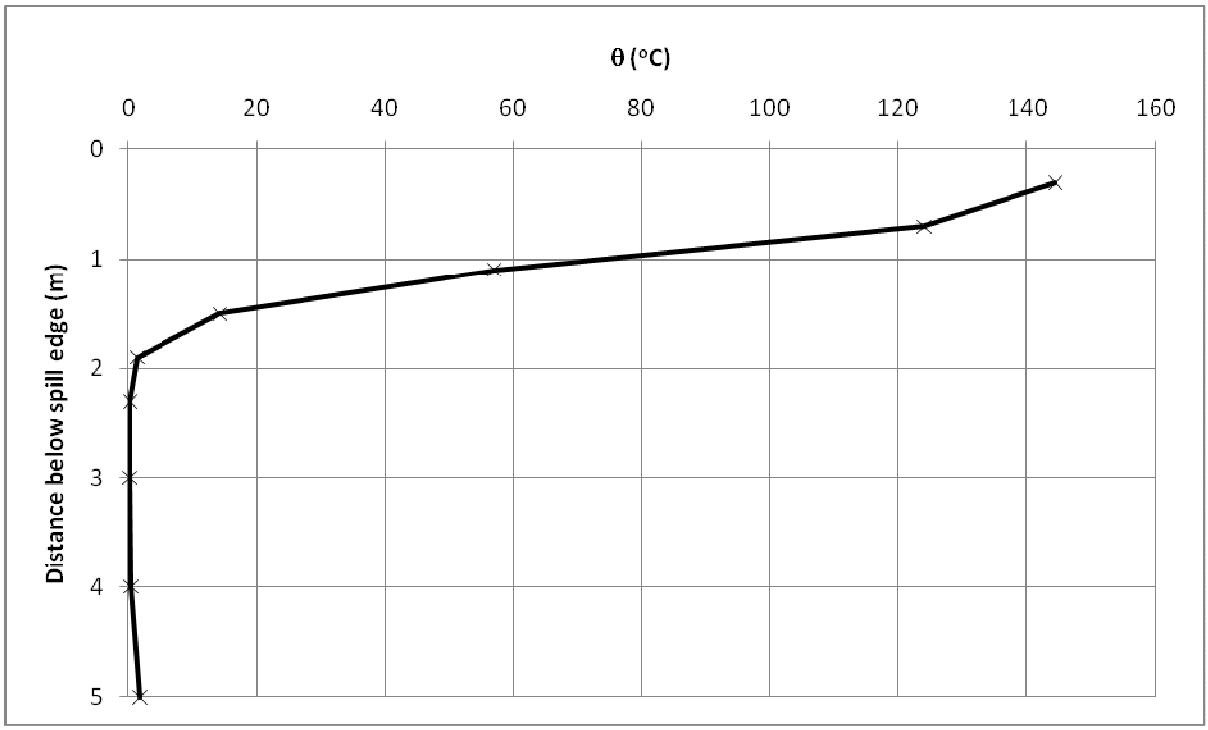

Figure D29. Temperature above ambient at the spill edge.

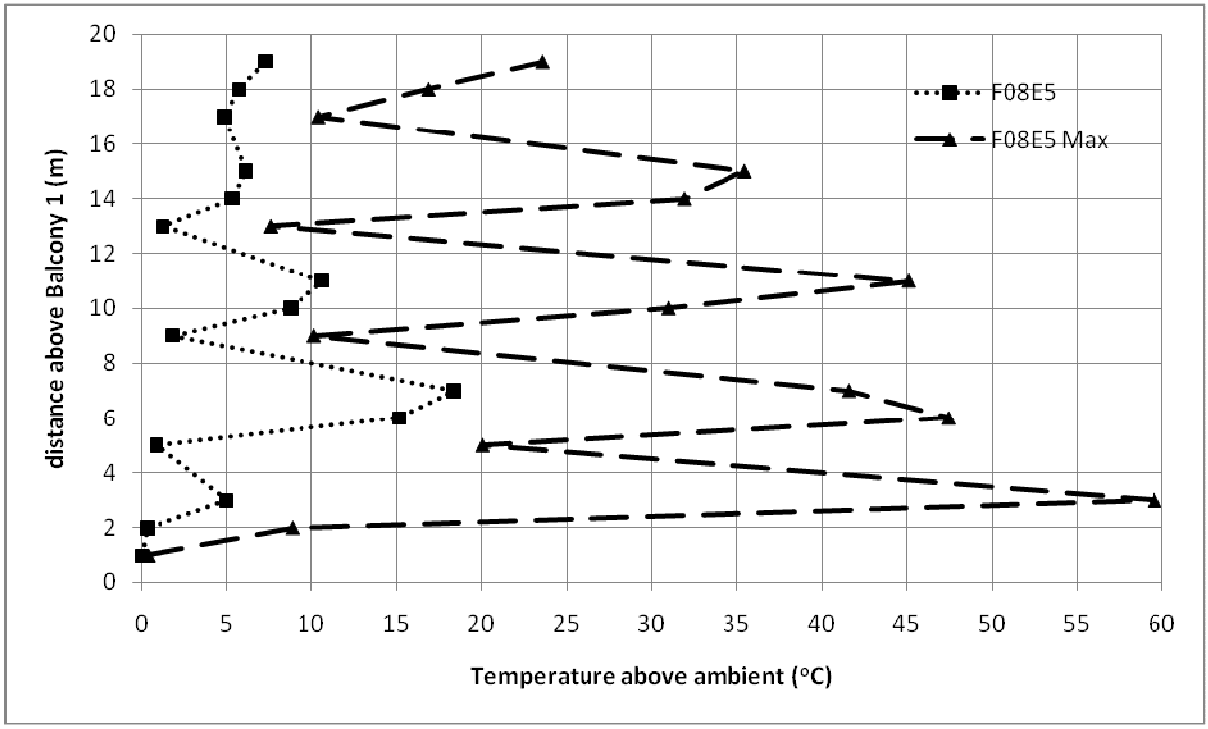

Figure D30. Temperature profiles across balcony edge.

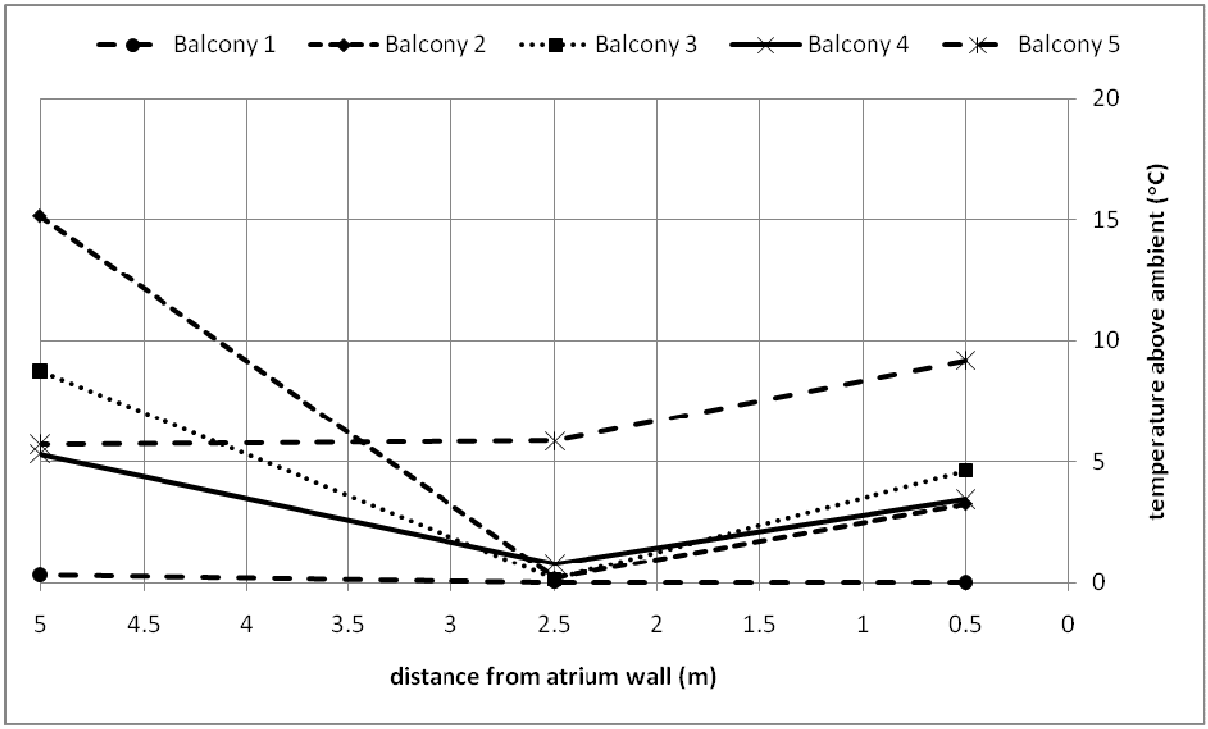

Figure D31. Temperature profiles along balcony breadth.

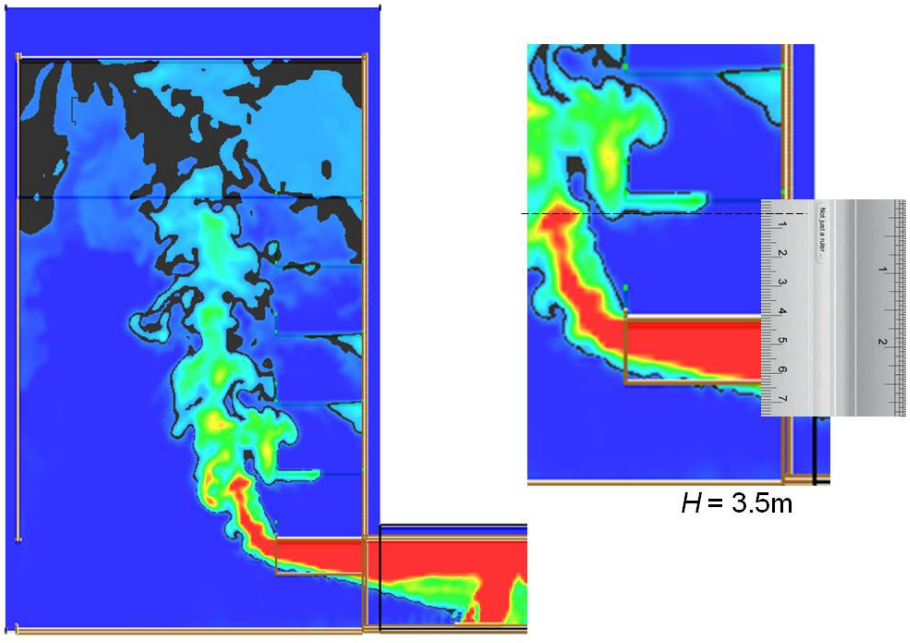

Figure D32. Smoke layer height measurement.

Full scale for 5 balcony (F09E5)

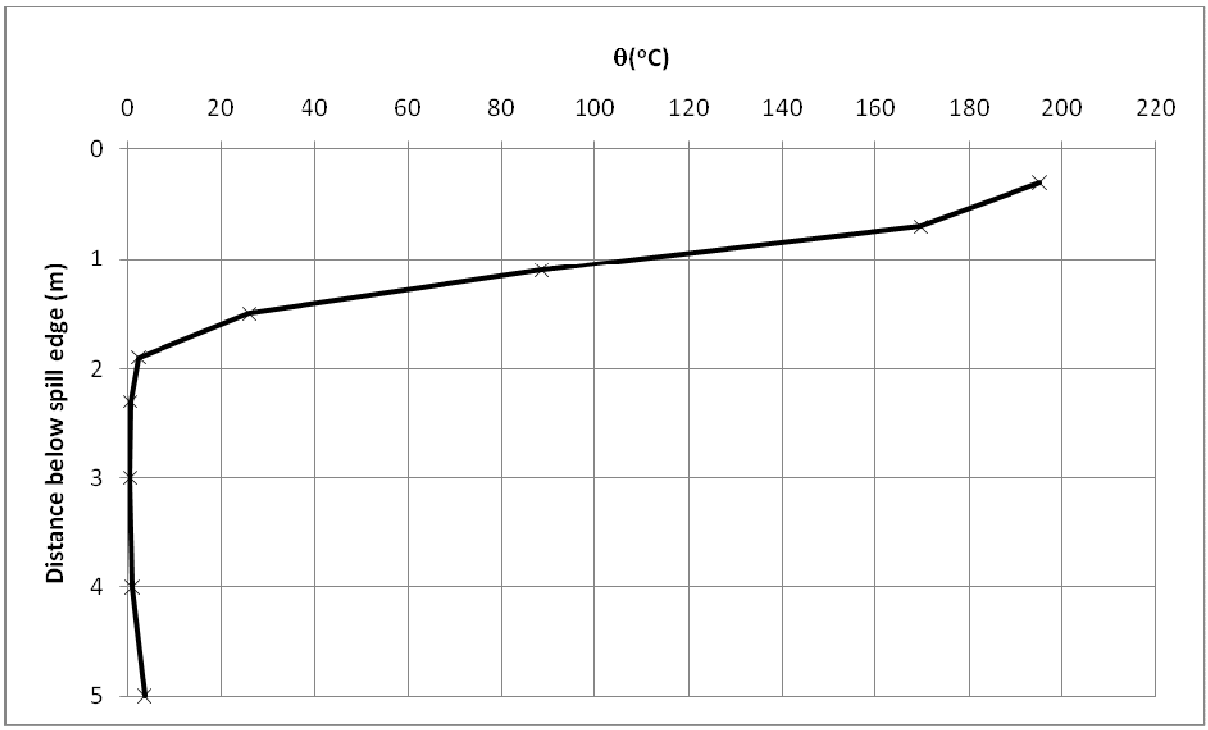

Figure D33. Temperature above ambient at the spill edge.

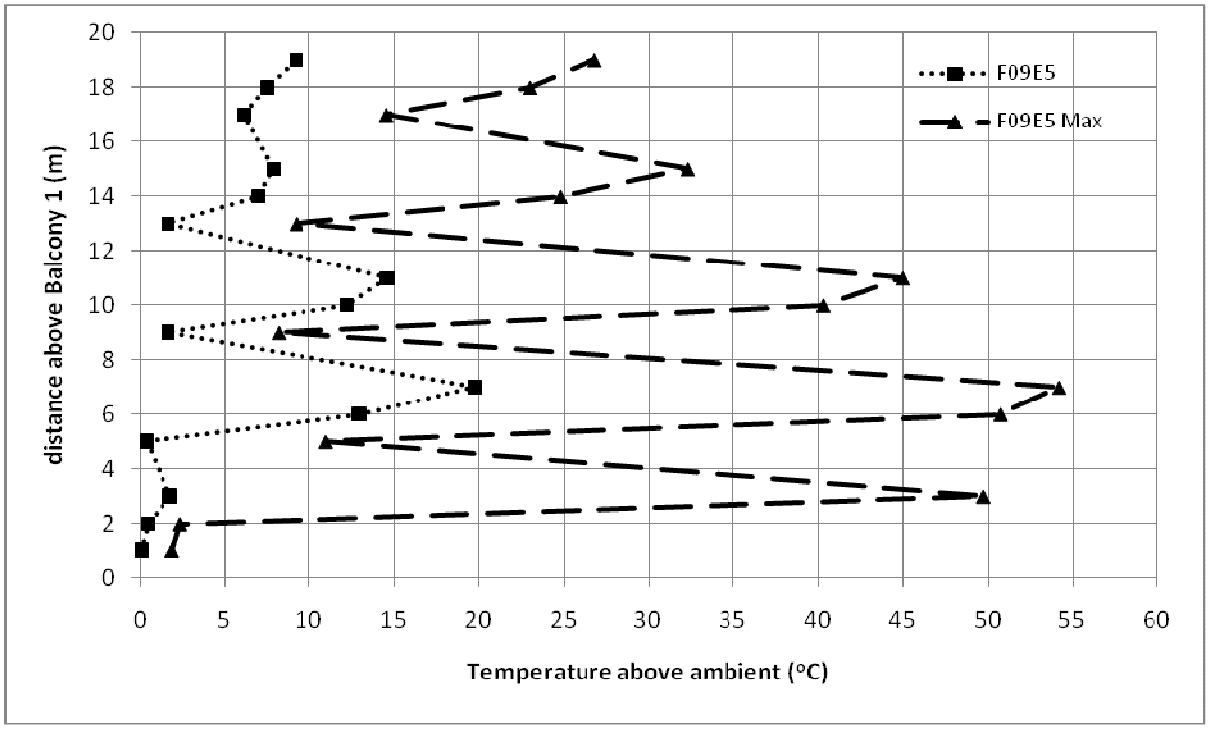

Figure D34. Temperature profiles across balcony edge.

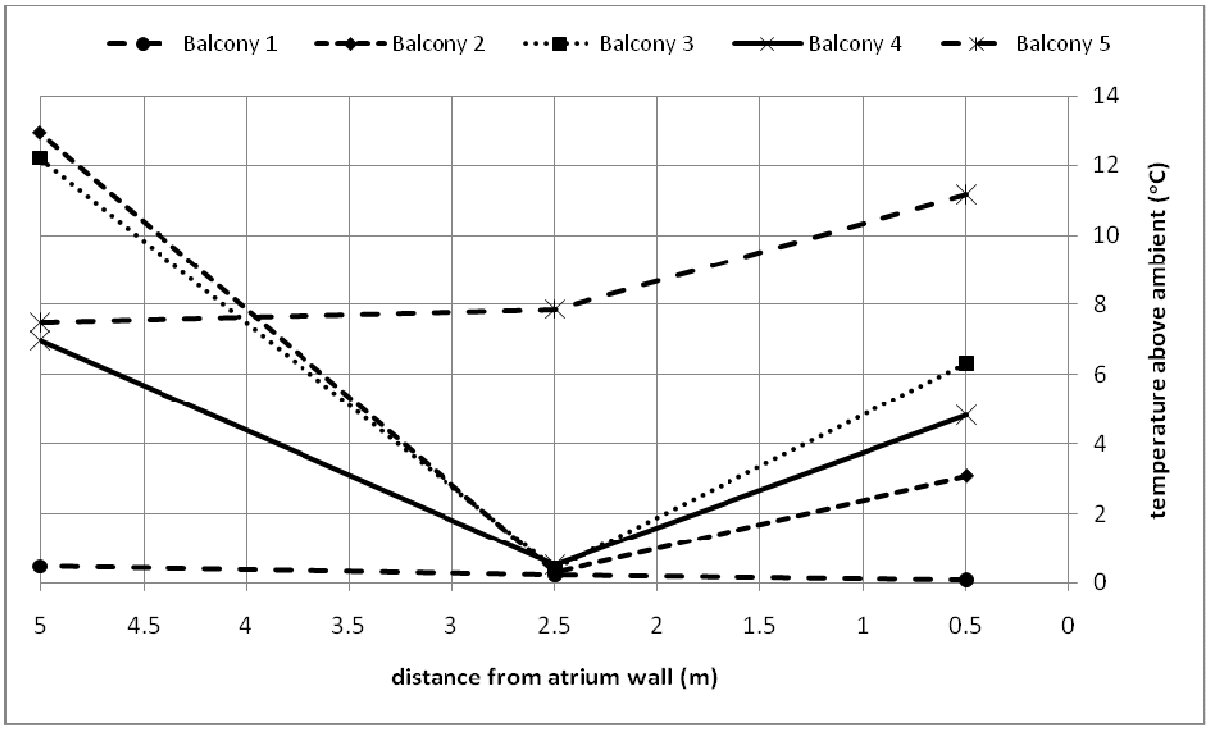

Figure D35. Temperature profiles along balcony breadth.

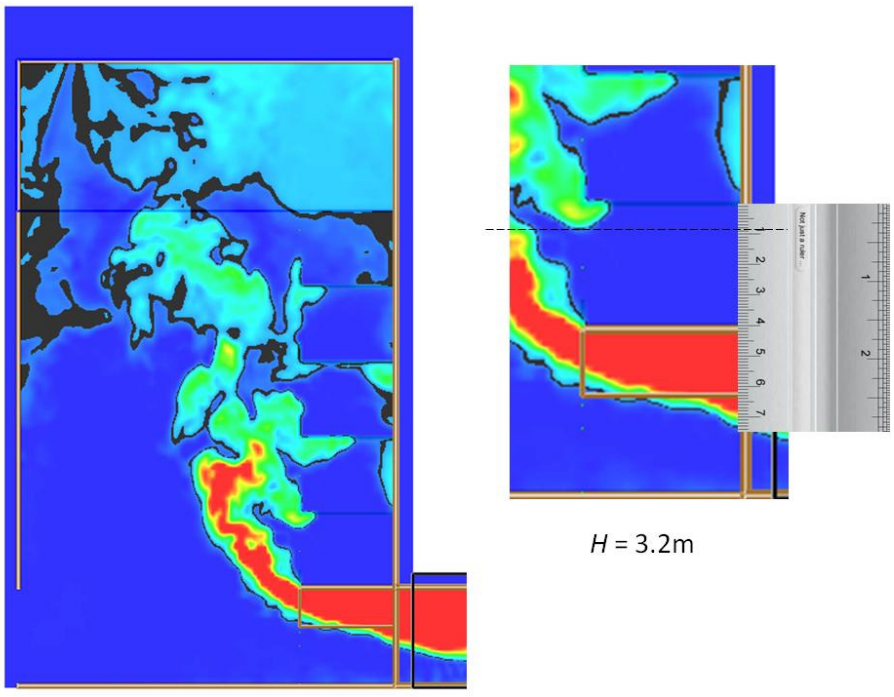

Figure D36. Smoke layer height measurement.

Full scale for 5 balcony (F10E5)

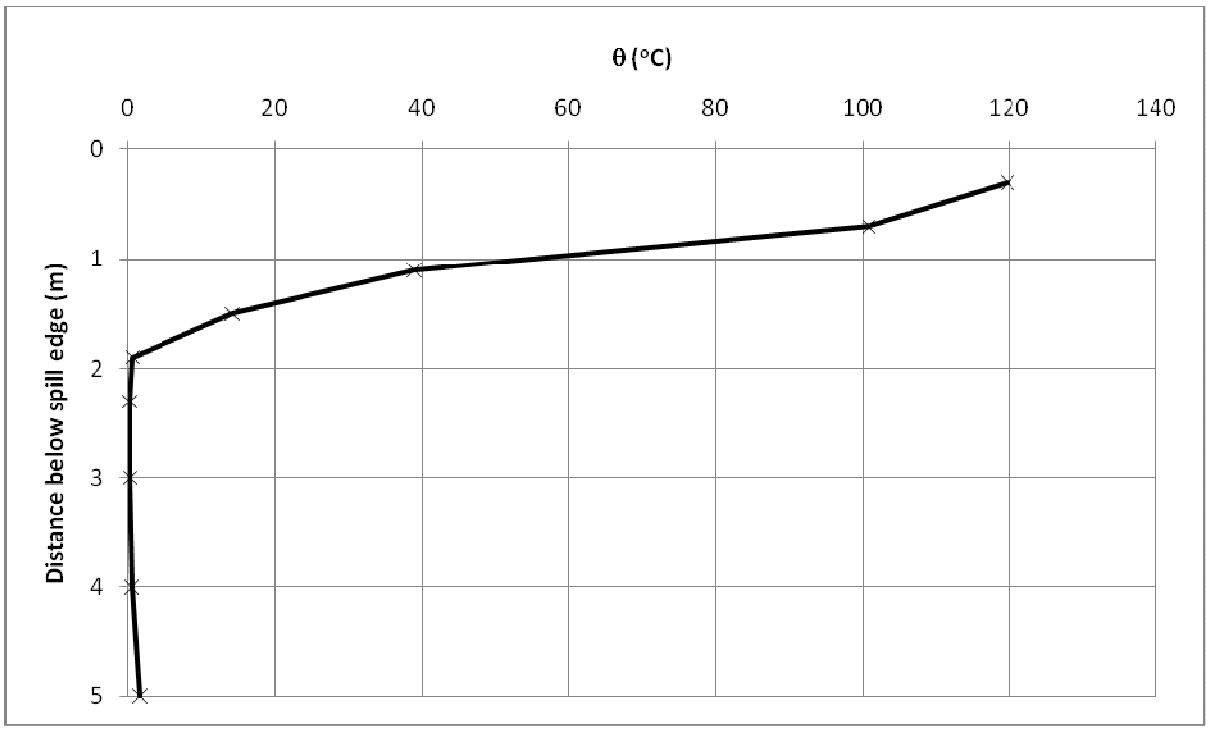

Figure D37. Temperature above ambient at the spill edge.

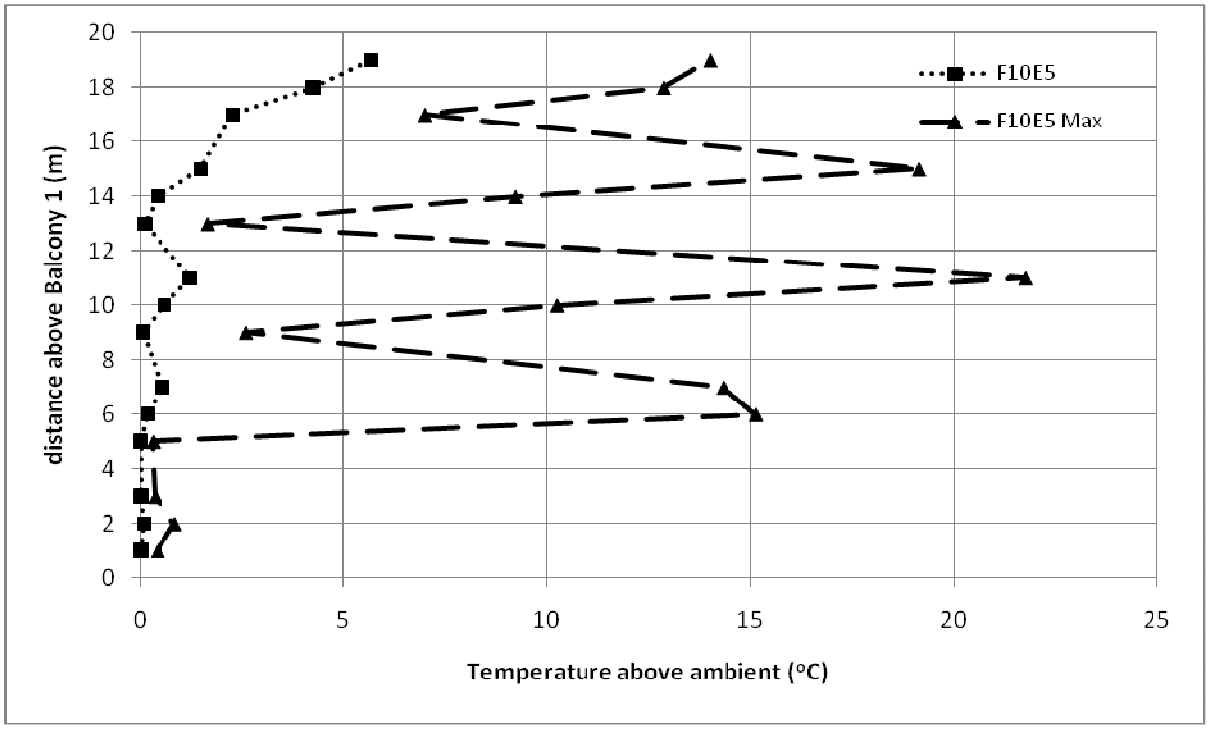

Figure D38. Temperature profiles across balcony edge.

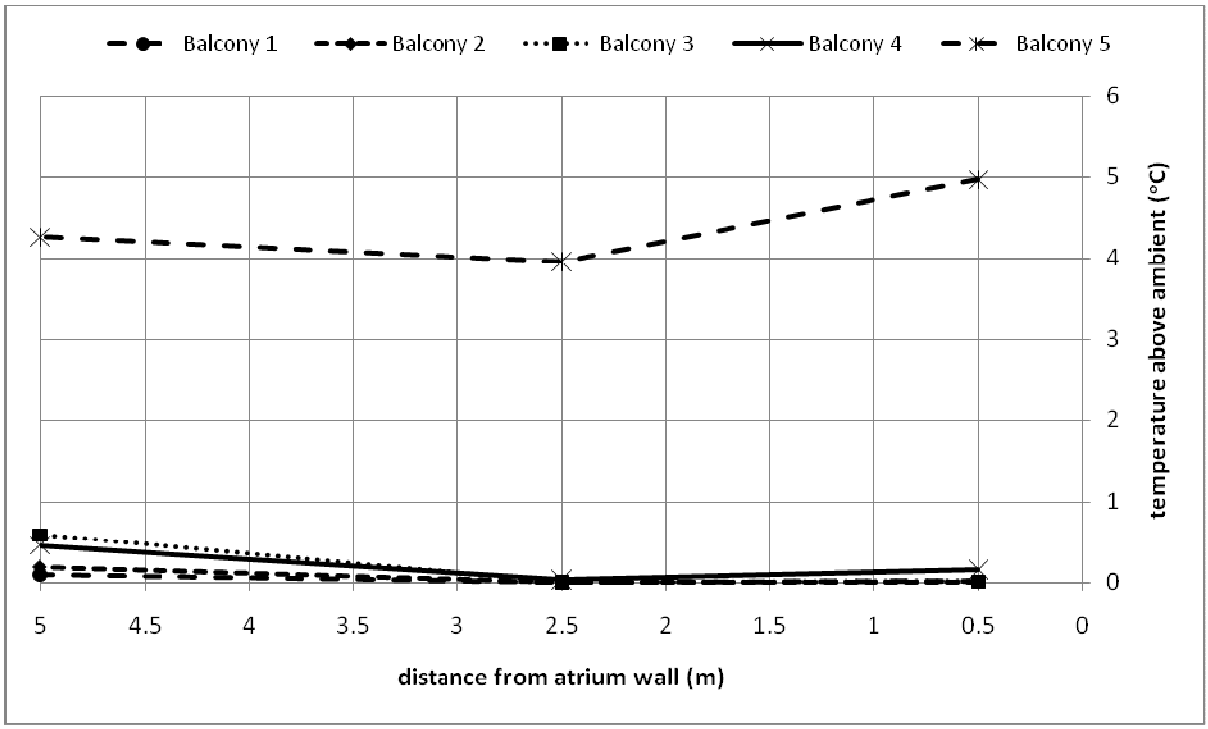

Figure D39. Temperature profiles along balcony breadth.

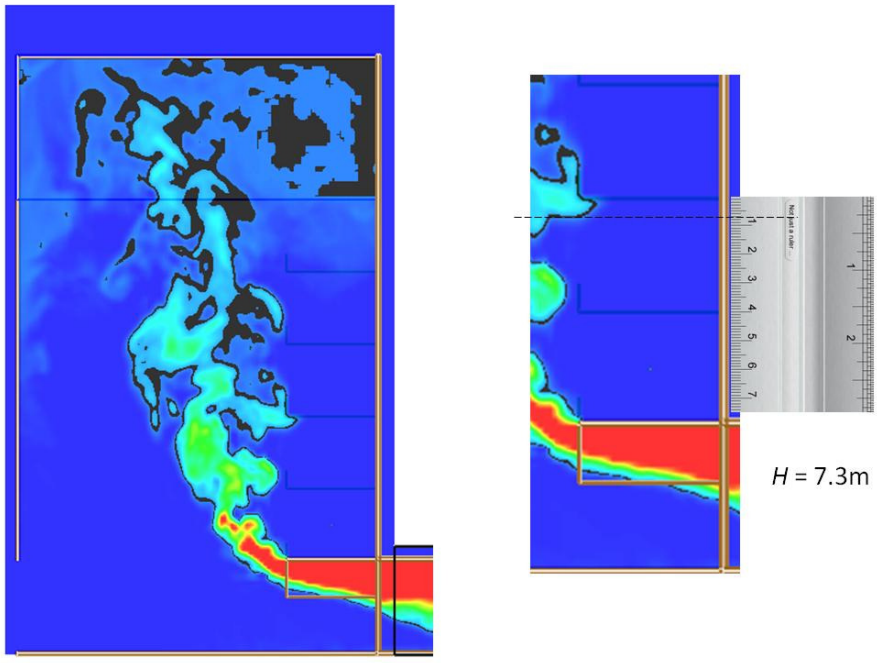

Figure D40. Smoke layer height measurement.

Full scale for 5 balcony (F11E5)

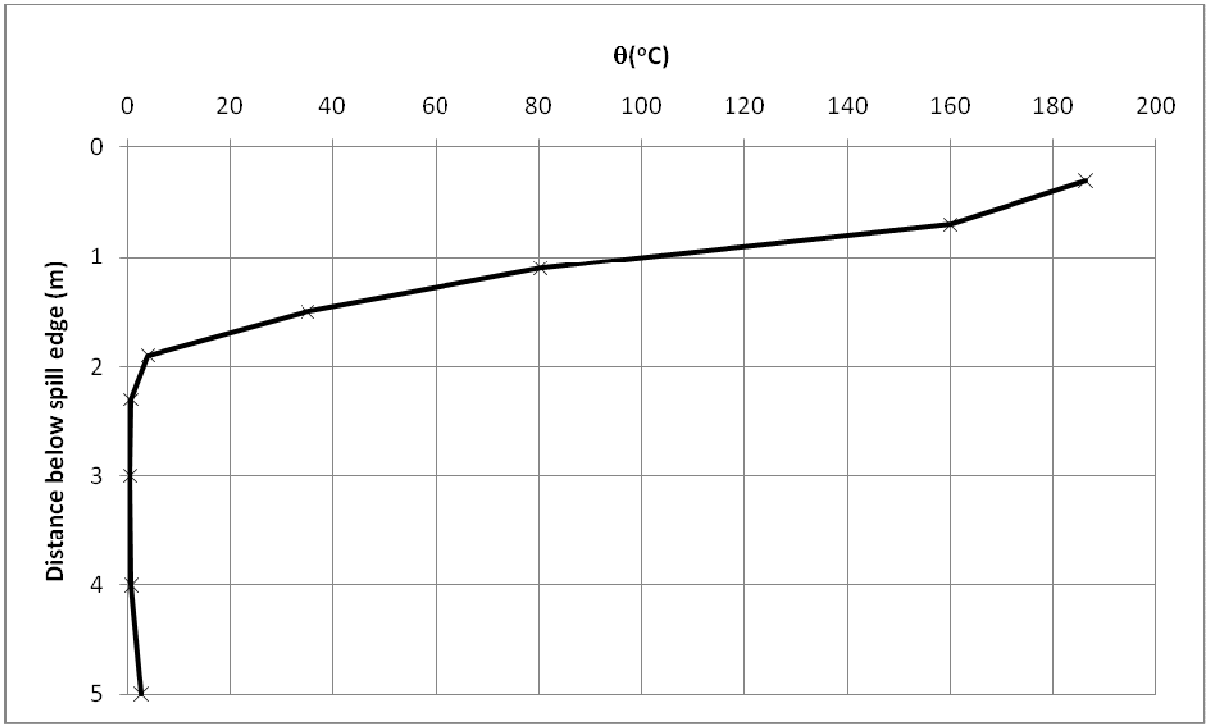

Figure 41. Temperature above ambient at the spill edge.

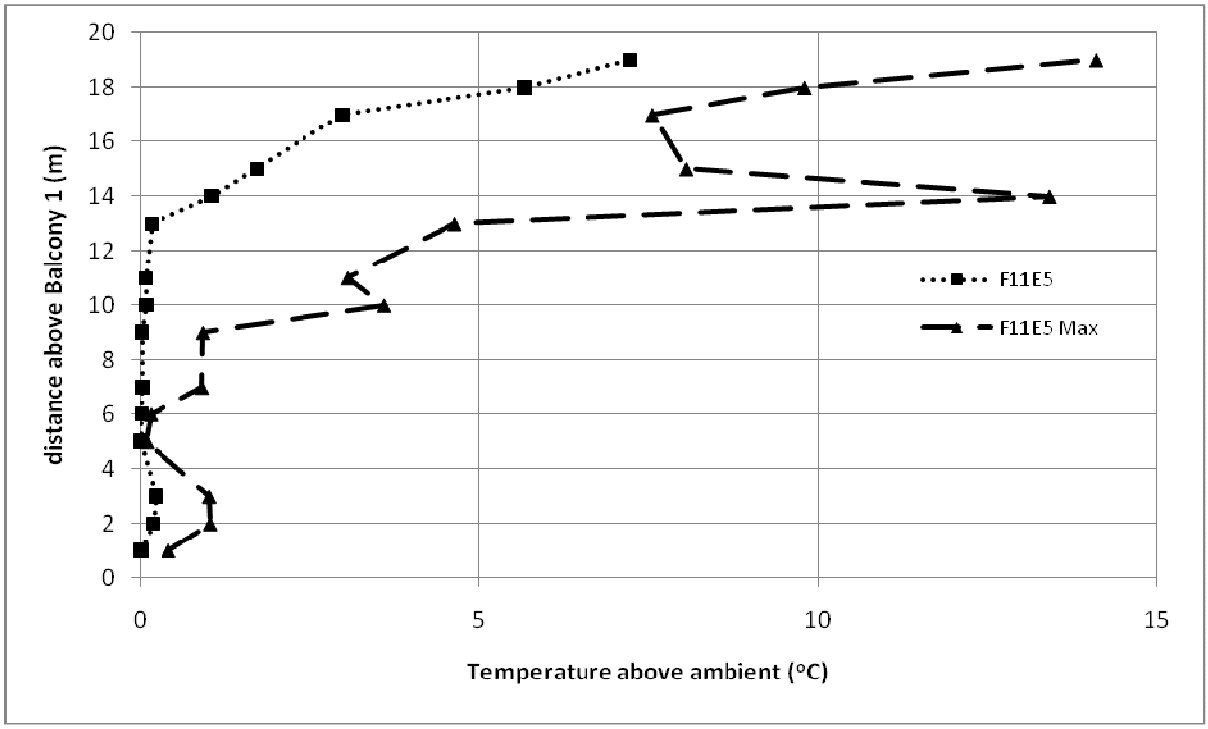

Figure D42. Temperature profiles across balcony edge.

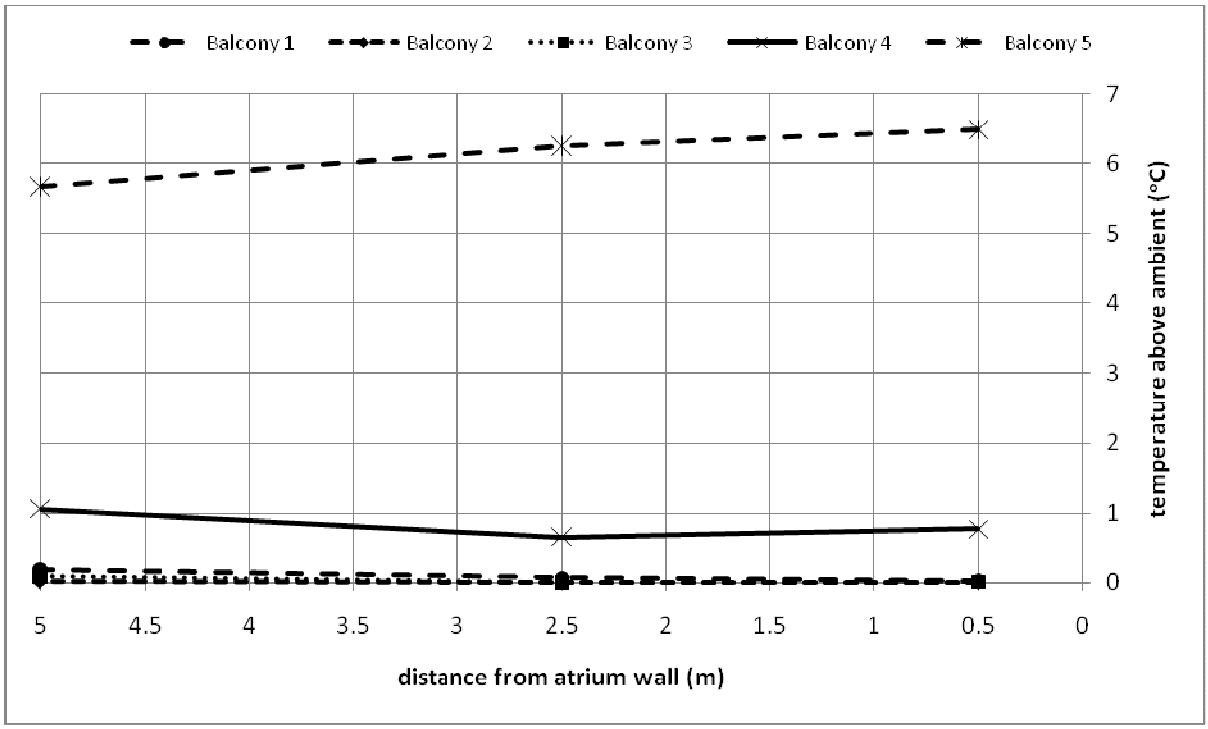

Figure D43. Temperature profiles along balcony breadth.

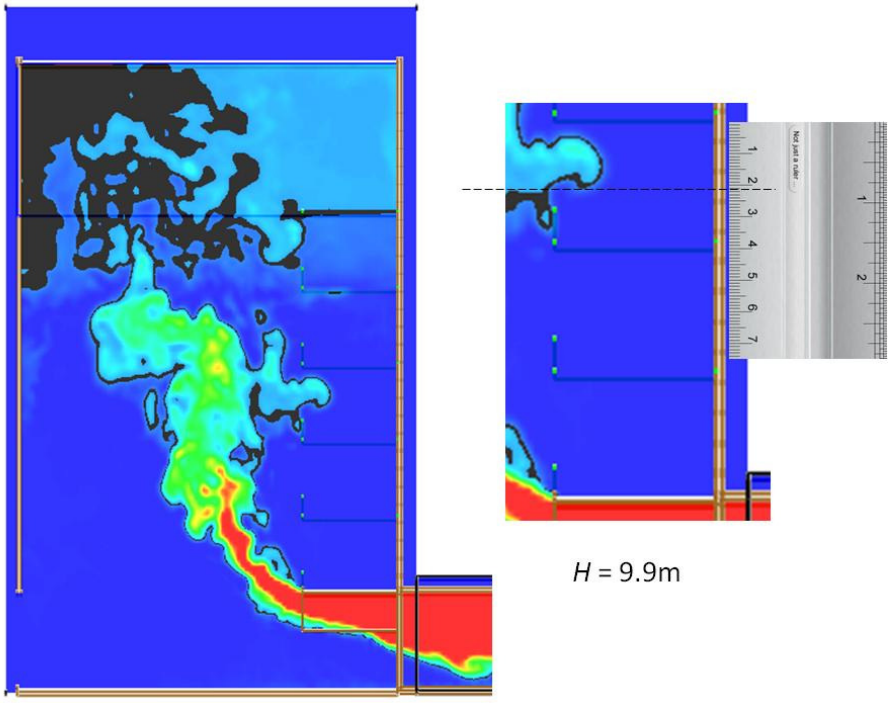

Figure D44. Smoke layer height measurement.

Full scale for 5 balcony (F12E5)

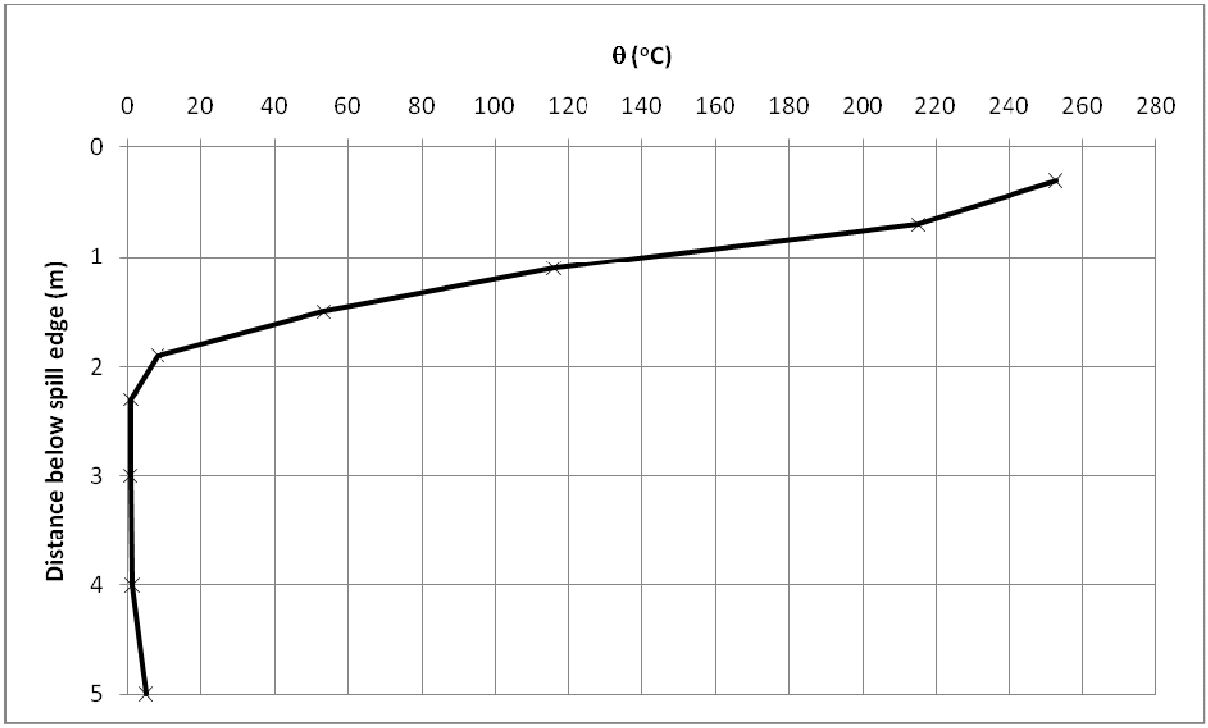

Figure D45. Temperature above ambient at the spill edge.

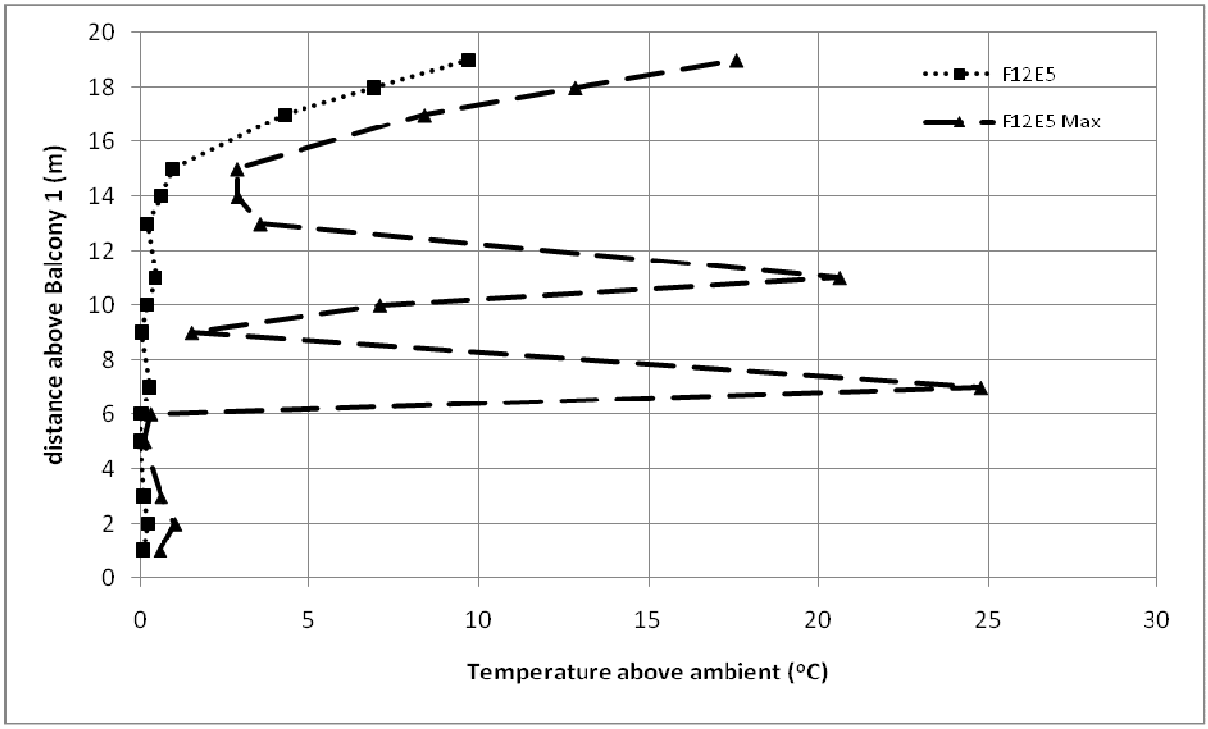

Figure D46. Temperature profiles across balcony edge.

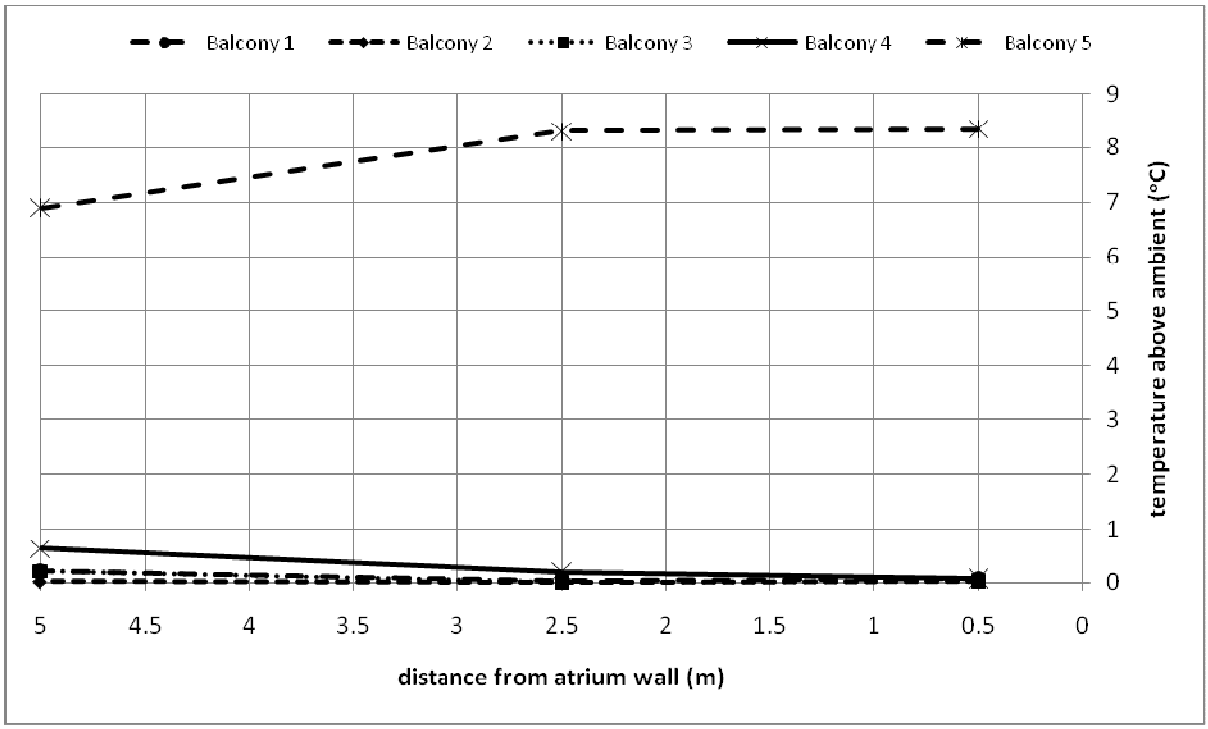

Figure D47. Temperature profiles along balcony breadth.

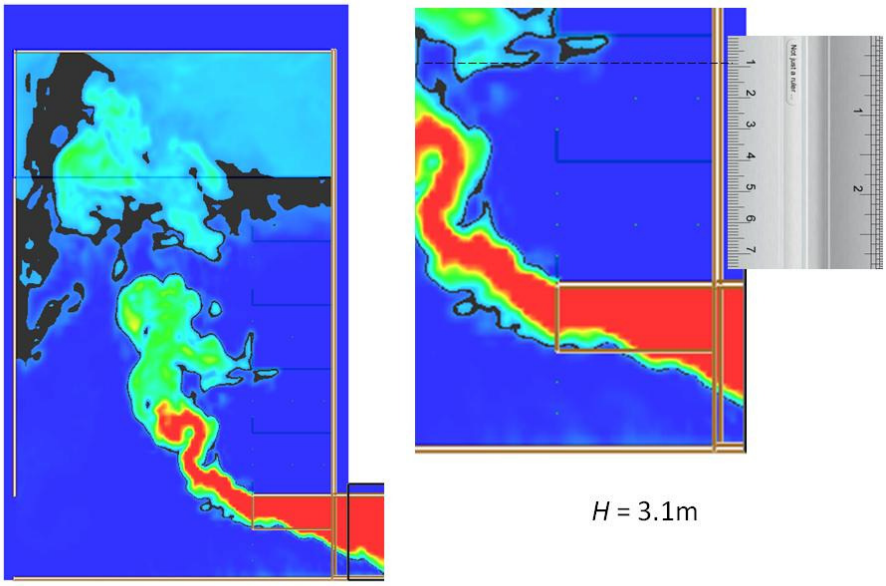

Figure D48. Smoke layer height measurement.

Full scale for 5 balcony (F13E5)

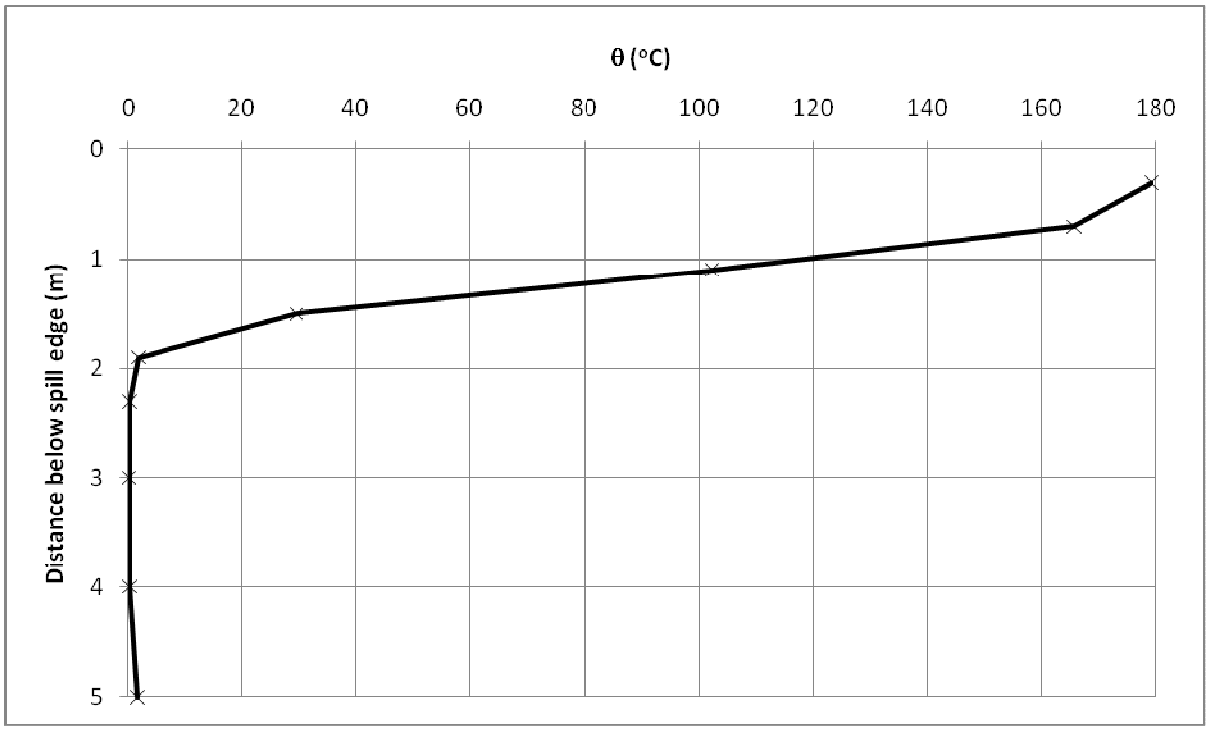

Figure D49. Temperature above ambient at the spill edge.

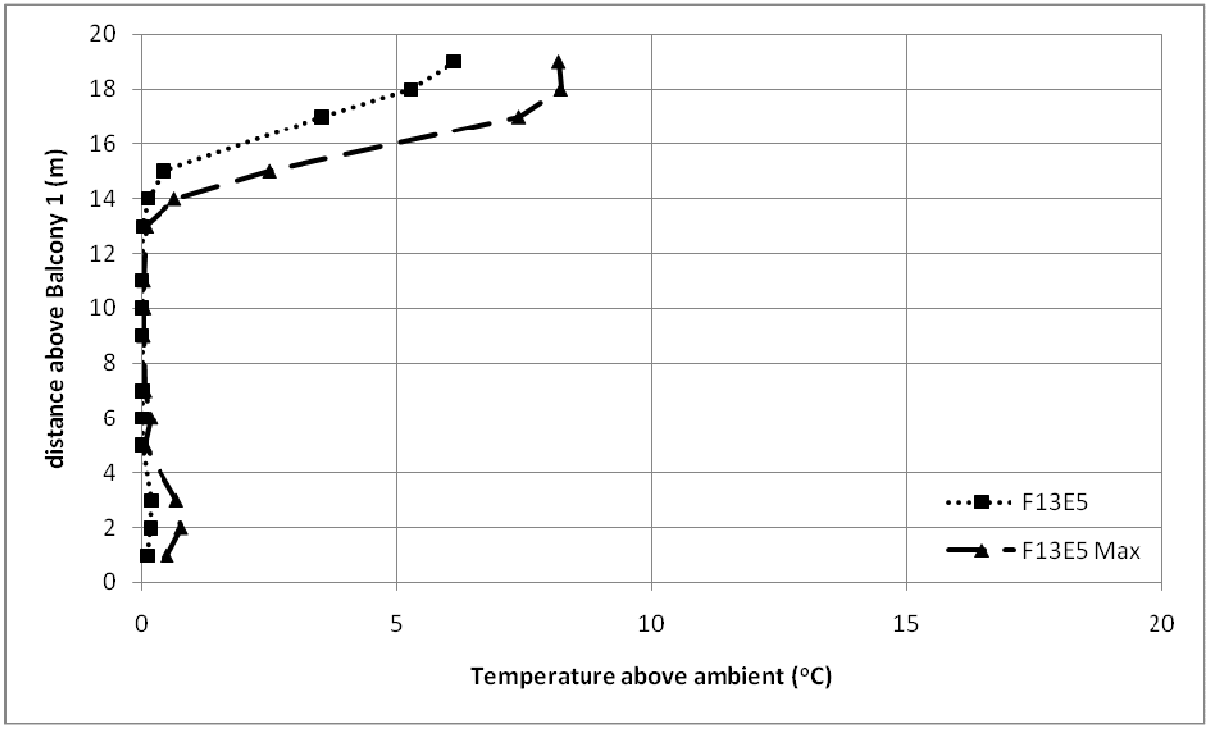

Figure D50. Temperature profiles across balcony edge.

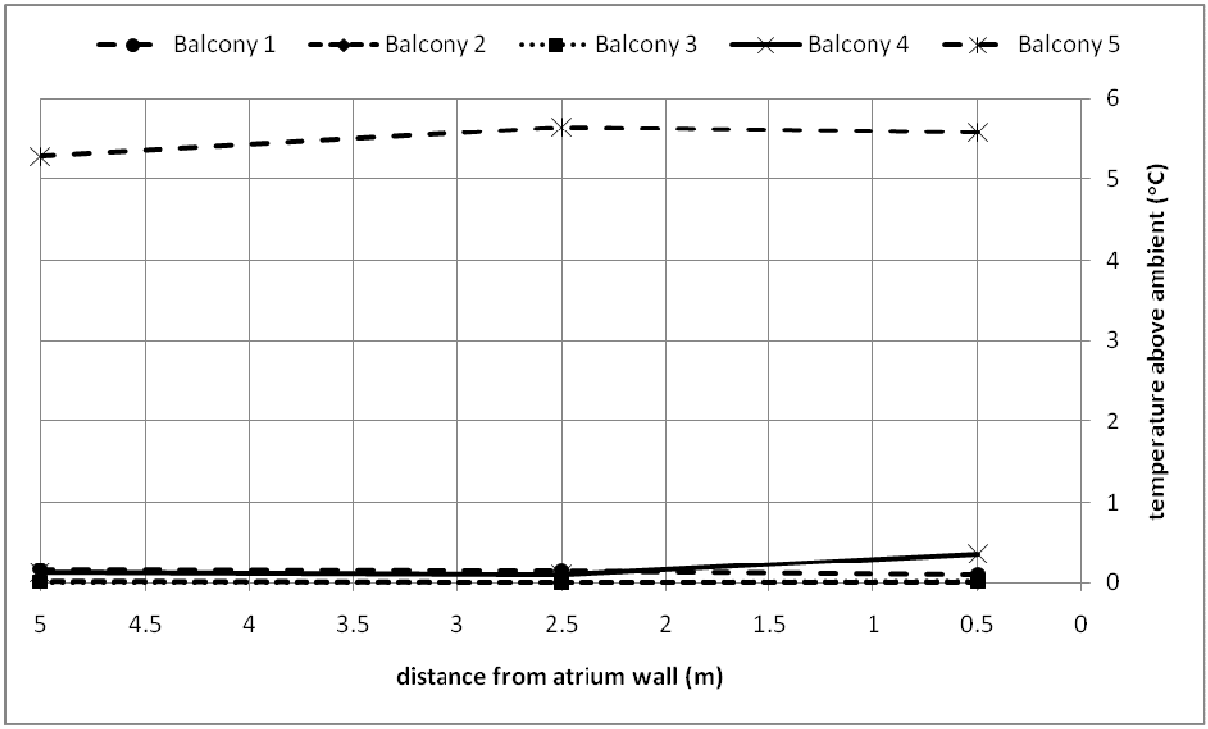

Figure D51. Temperature profiles along balcony breadth.

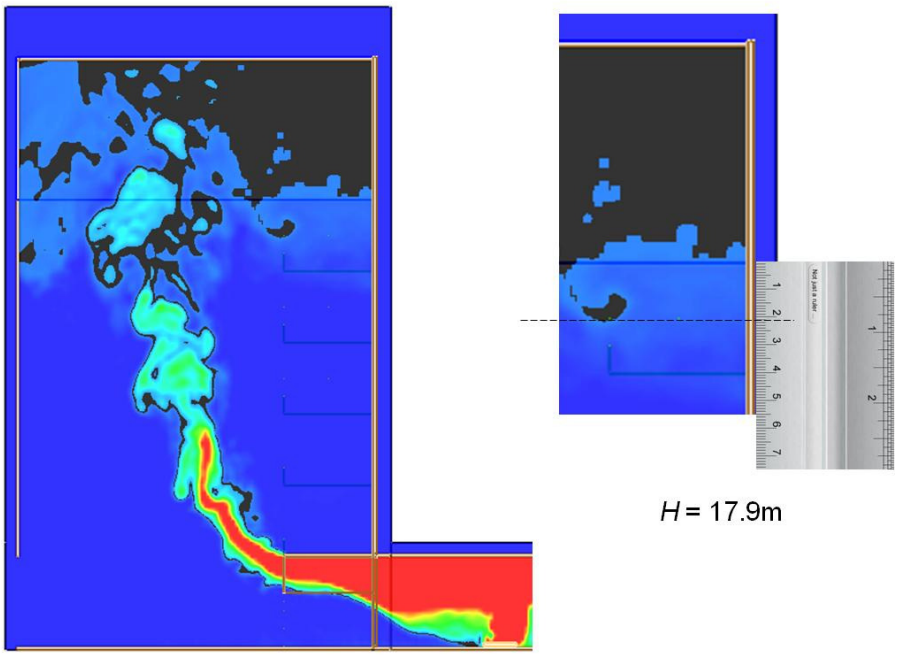

Figure D52. Smoke layer height measurement.

Full scale for 5 balcony (F14E5)

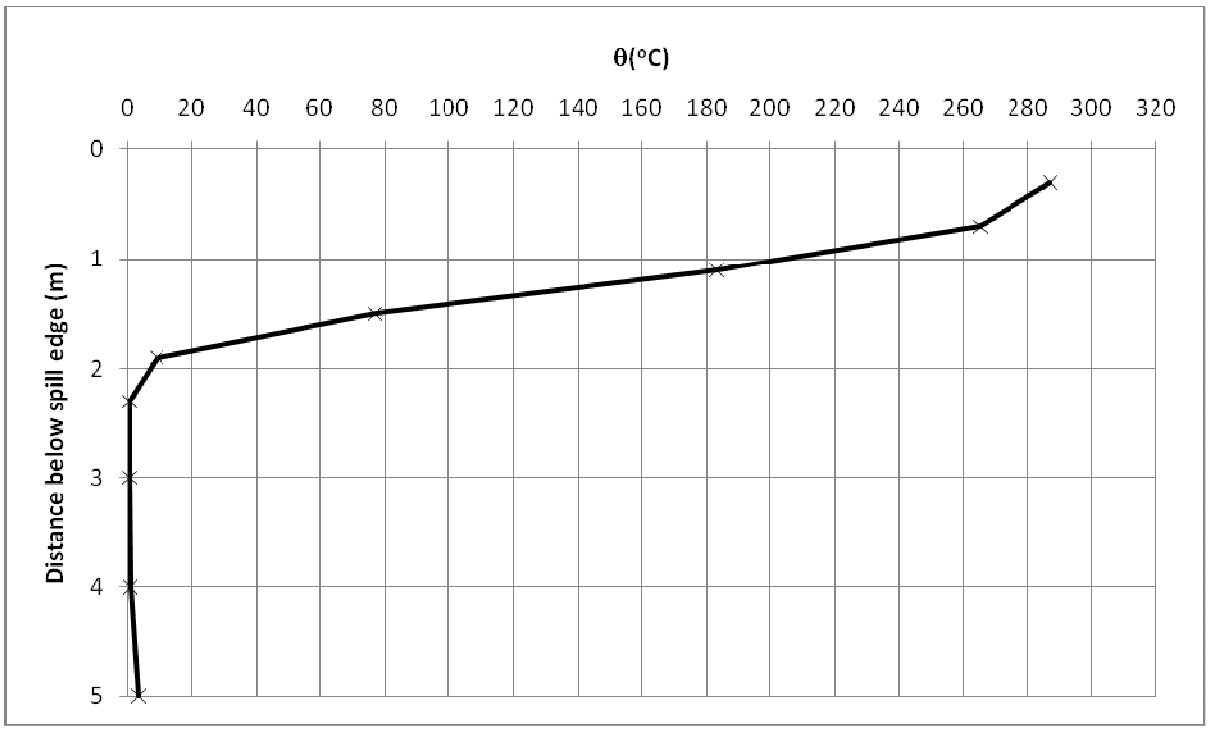

Figure D53. Temperature above ambient at the spill edge.

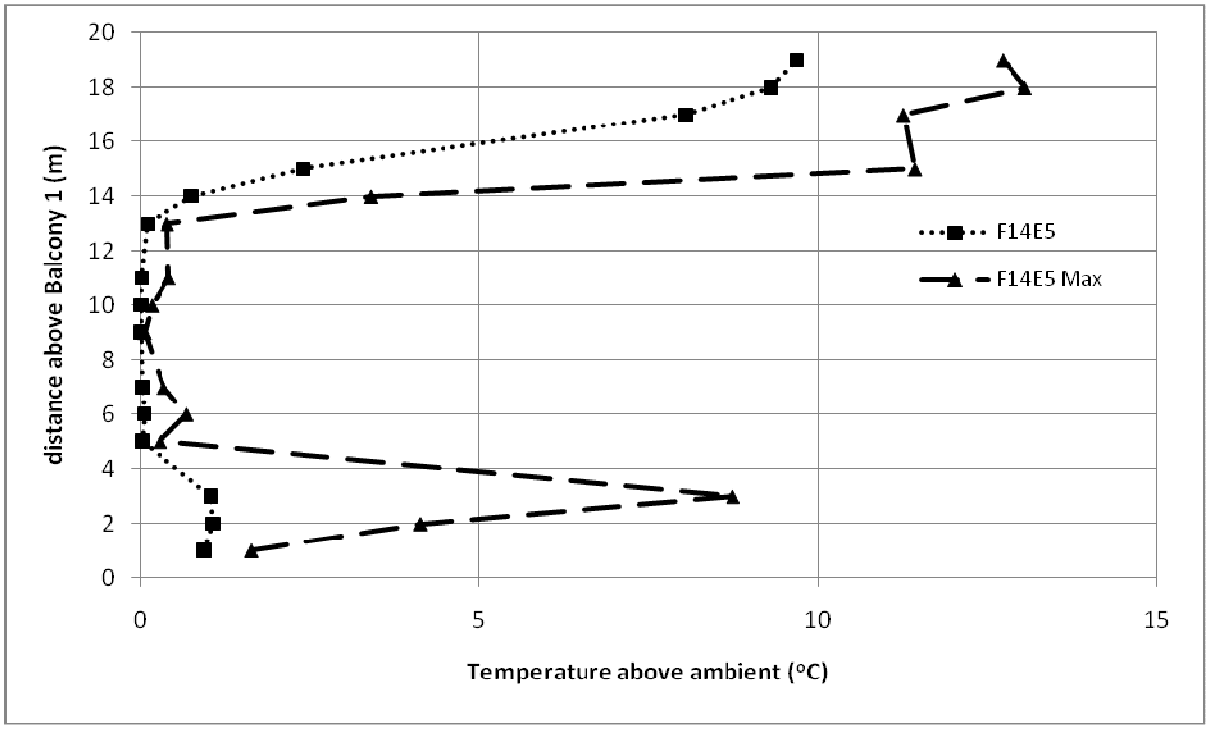

Figure D54. Temperature profiles across balcony edge.

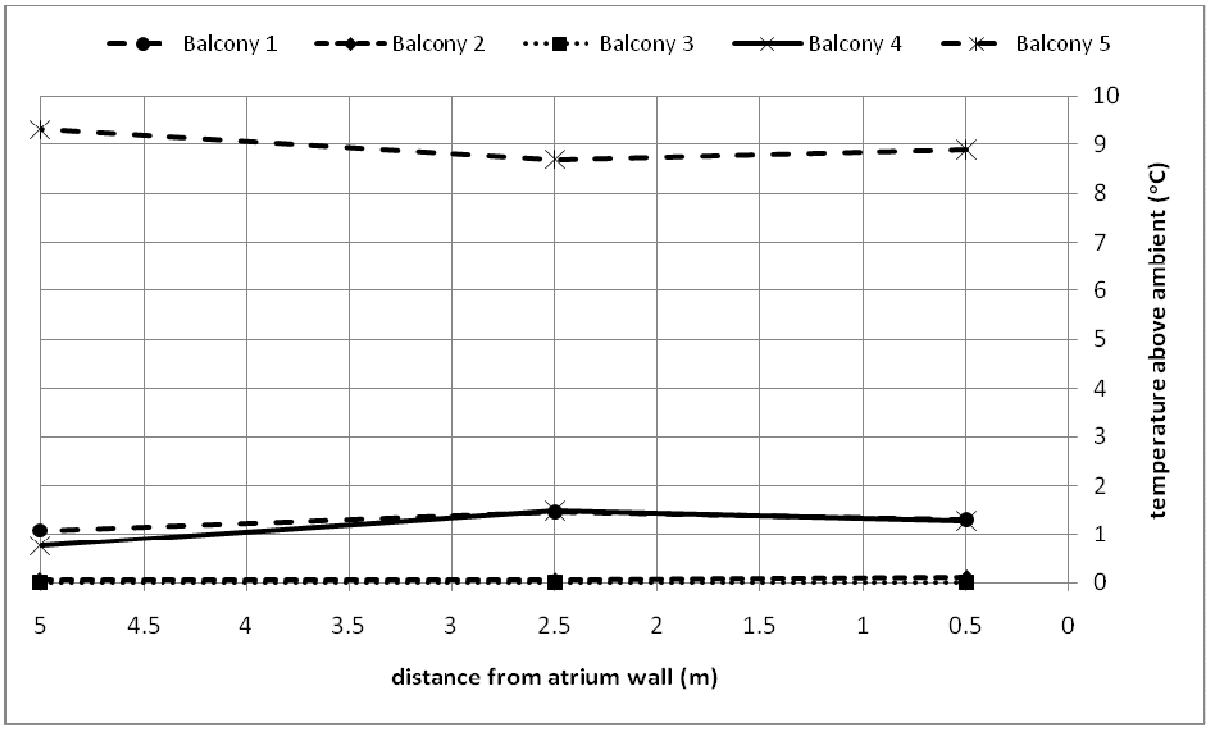

Figure D55. Temperature profiles along balcony breadth.

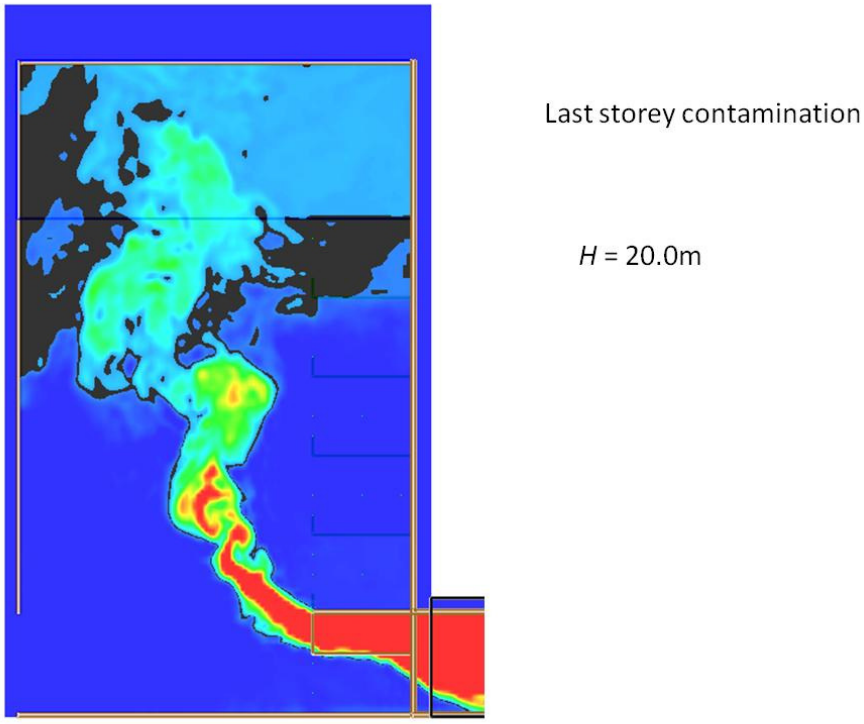

Figure D56. Smoke layer height measurement.

Full scale for 5 balcony (F15E5)

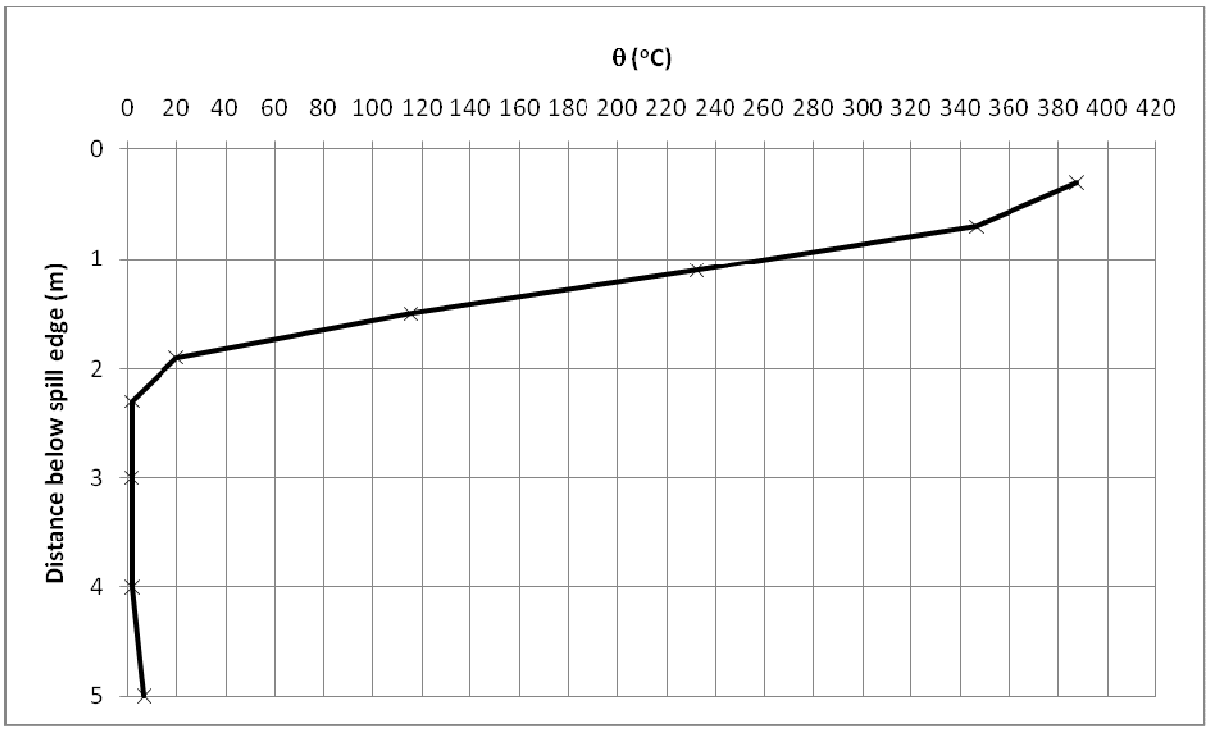

Figure D57. Temperature above ambient at the spill edge.

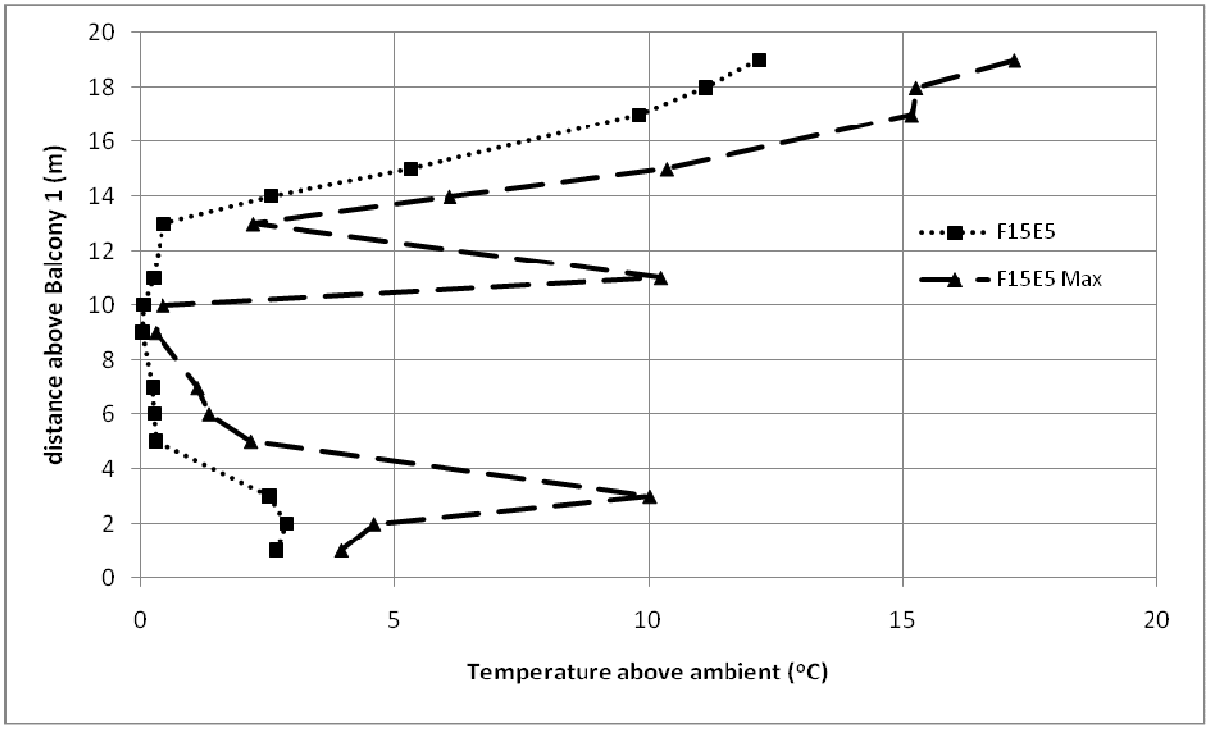

Figure D58. Temperature profiles across balcony edge.

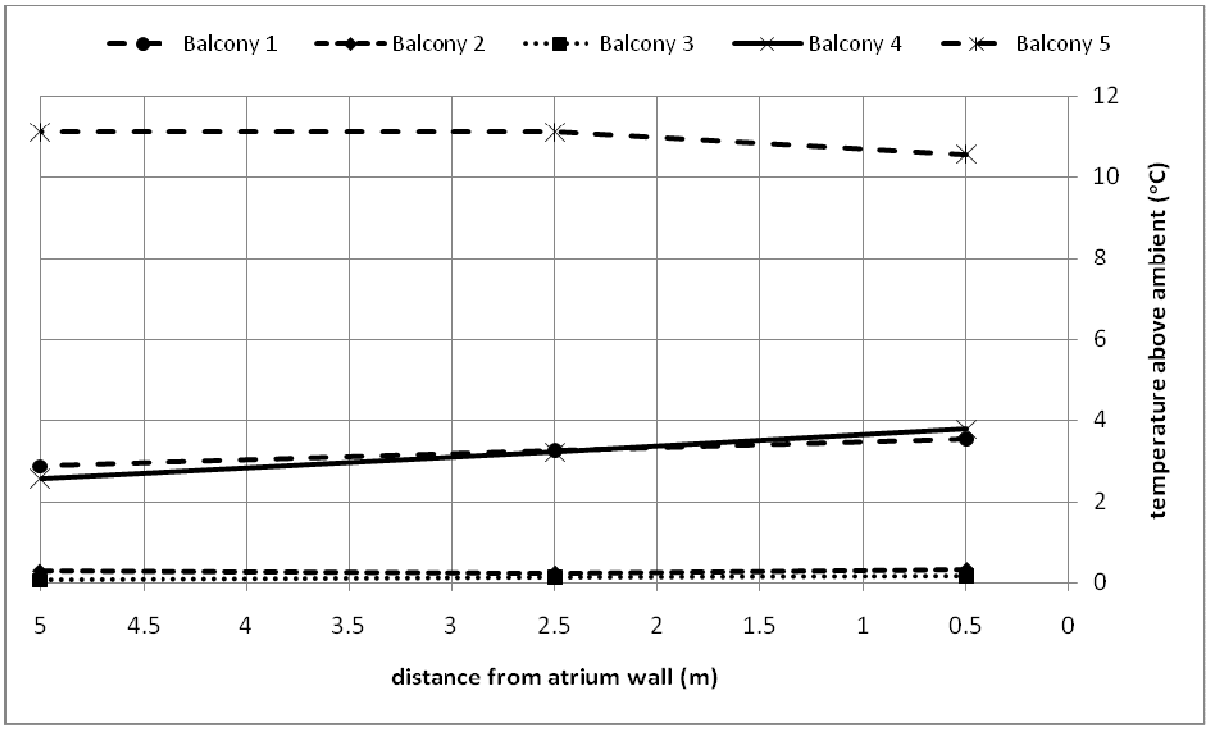

Figure D59. Temperature profiles along balcony breadth.

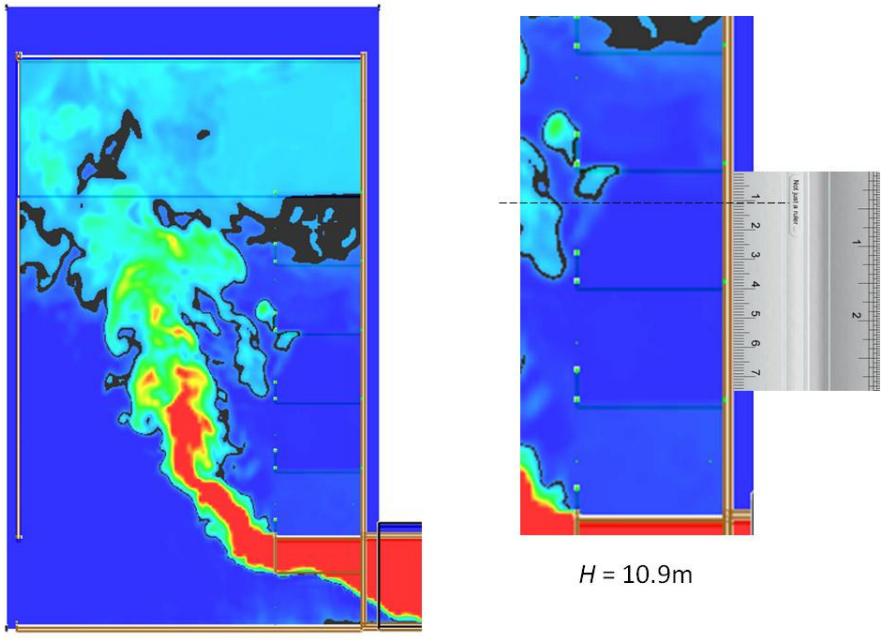

Figure D60. Smoke layer height measurement.

Full scale for 5 balcony (F19E5)

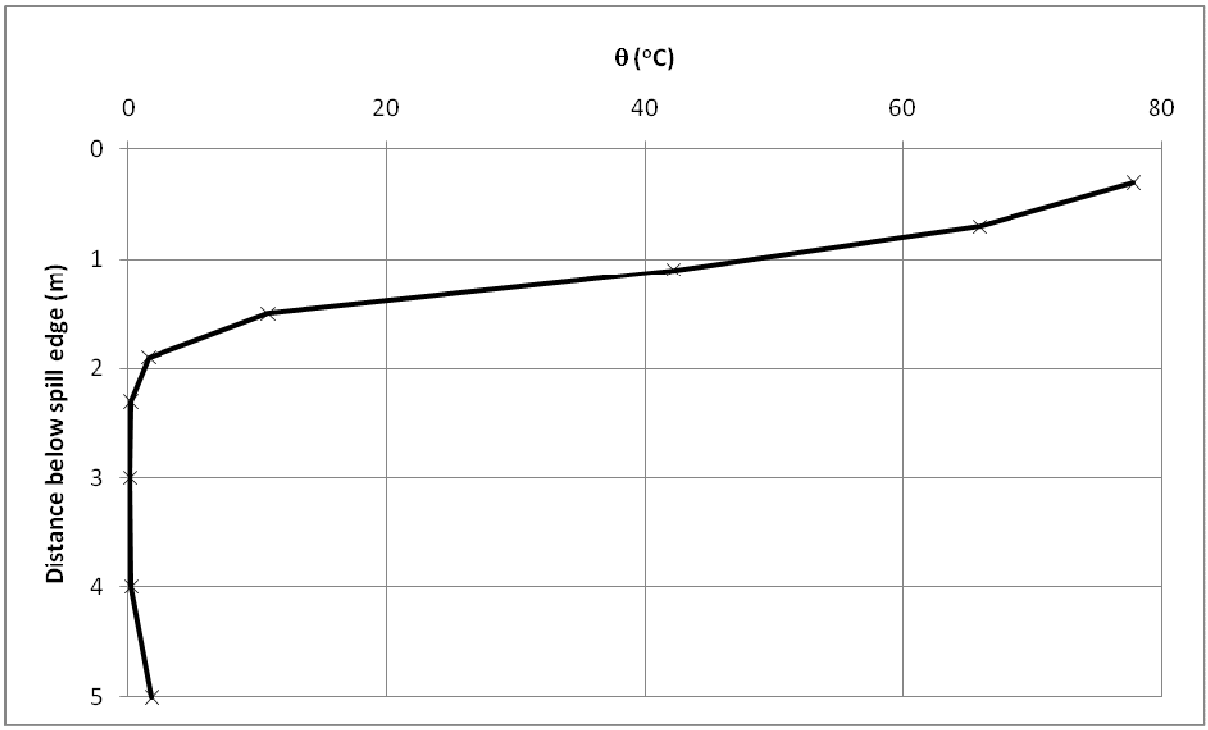

Figure D61. Temperature above ambient at the spill edge.

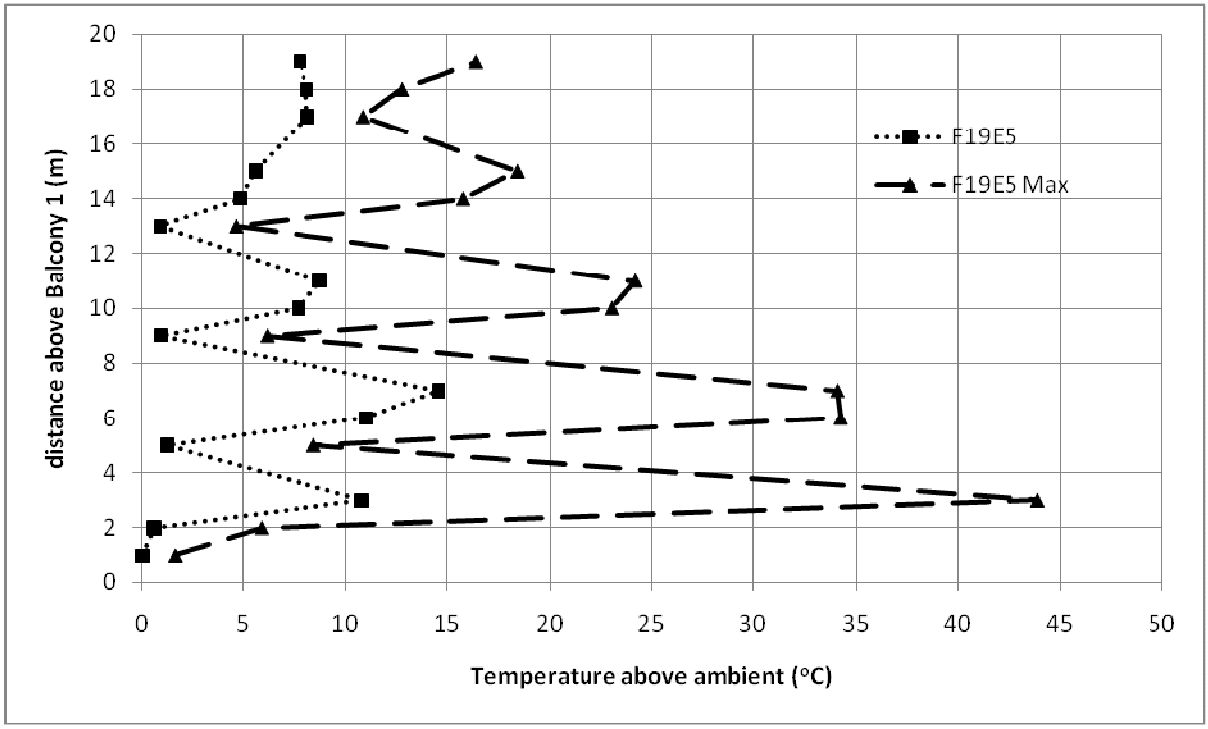

Figure D62. Temperature profiles across balcony edge.

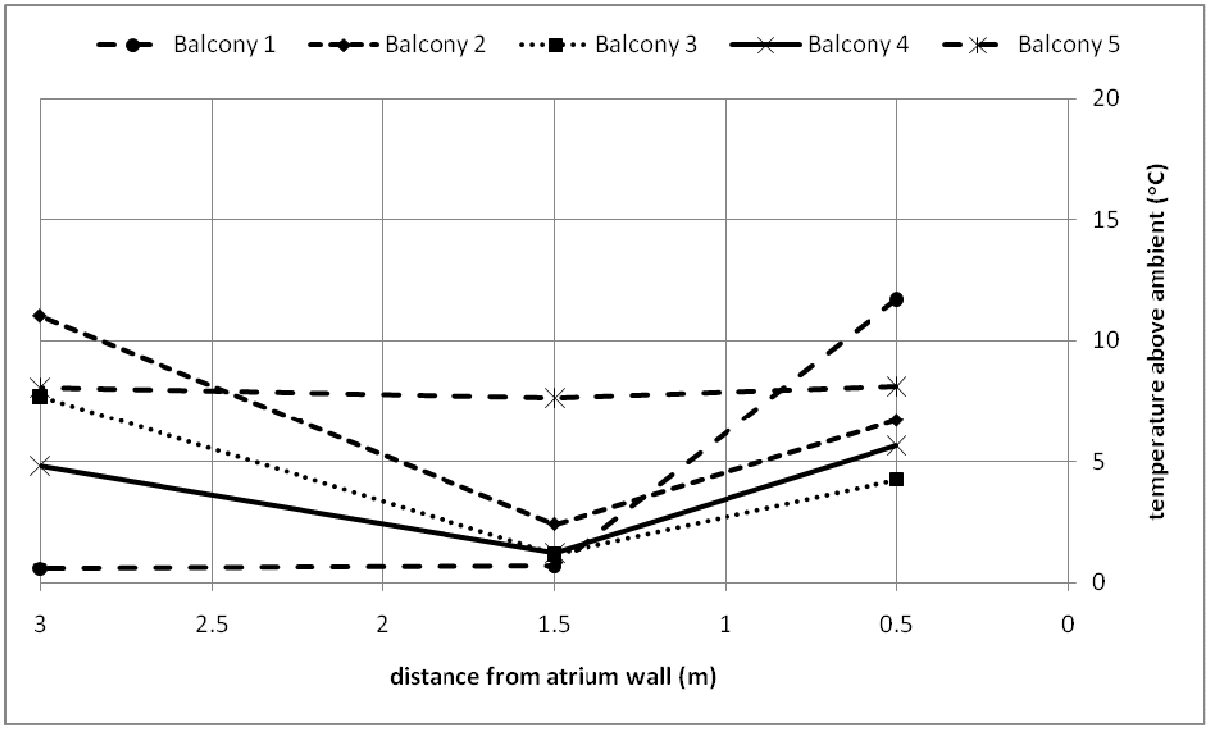

Figure D63. Temperature profiles along balcony breadth.

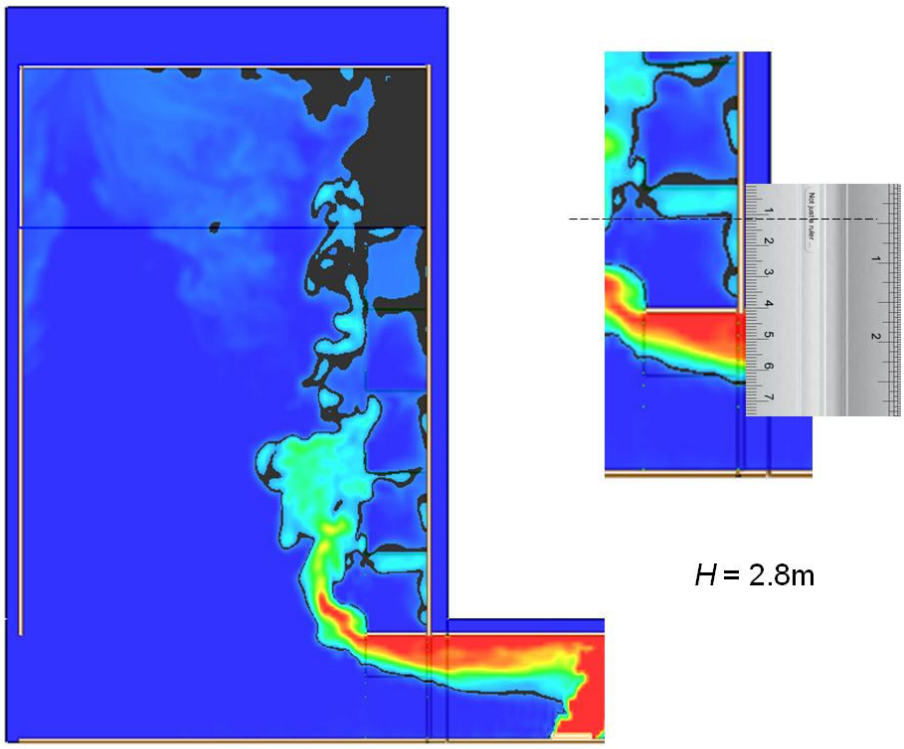

Figure D64. Smoke layer height measurement.

Full scale for 5 balcony (F20E5)

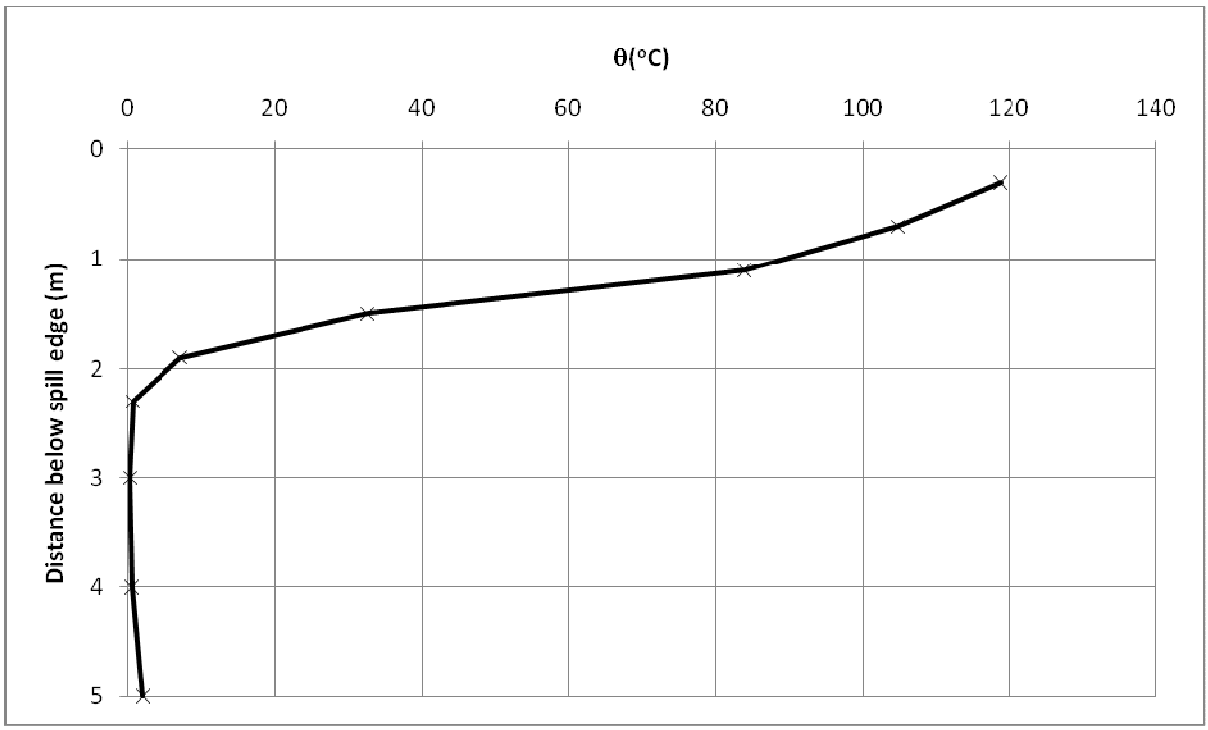

Figure D65. Temperature above ambient at the spill edge.

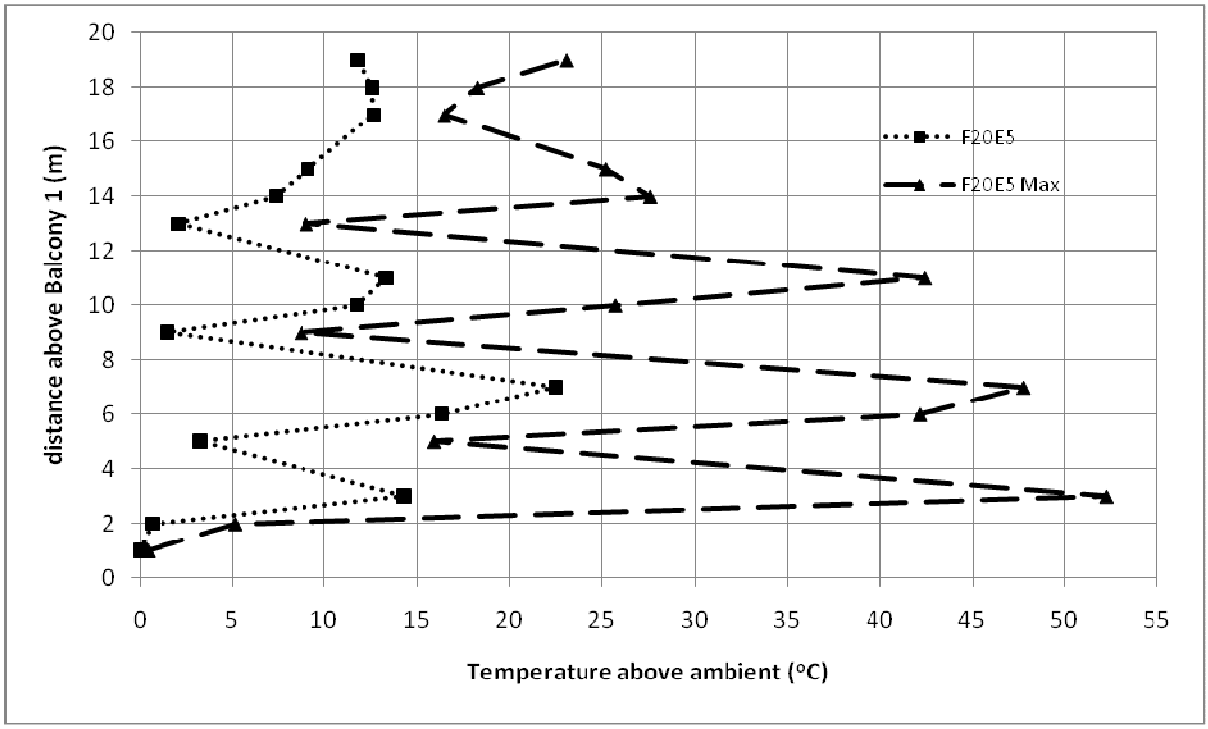

Figure D66. Temperature profiles across balcony edge.

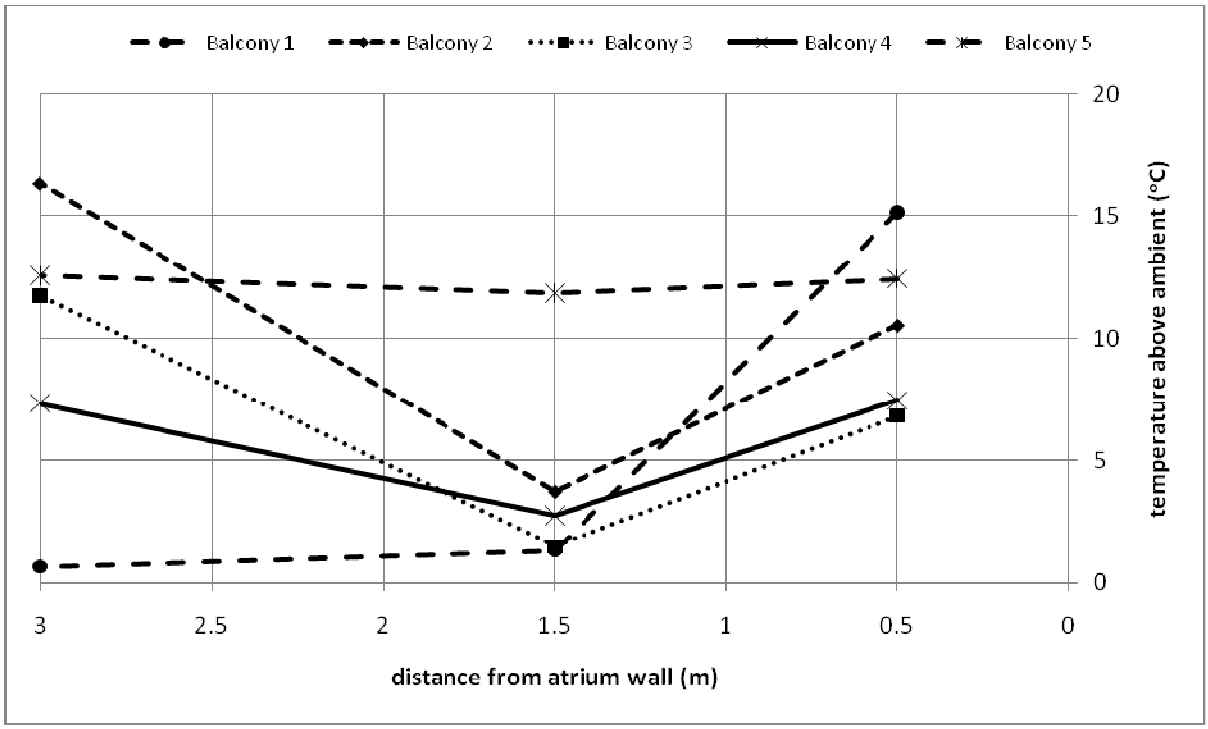

Figure D67. Temperature profiles along balcony breadth.

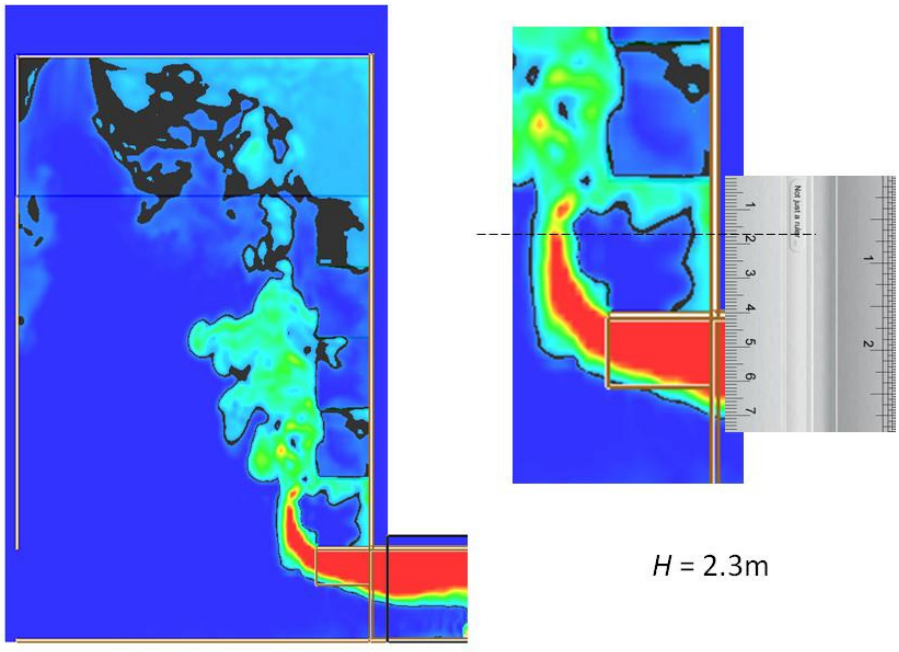

Figure D68. Smoke layer height measurement.

Full scale for 5 balcony (F21E5)

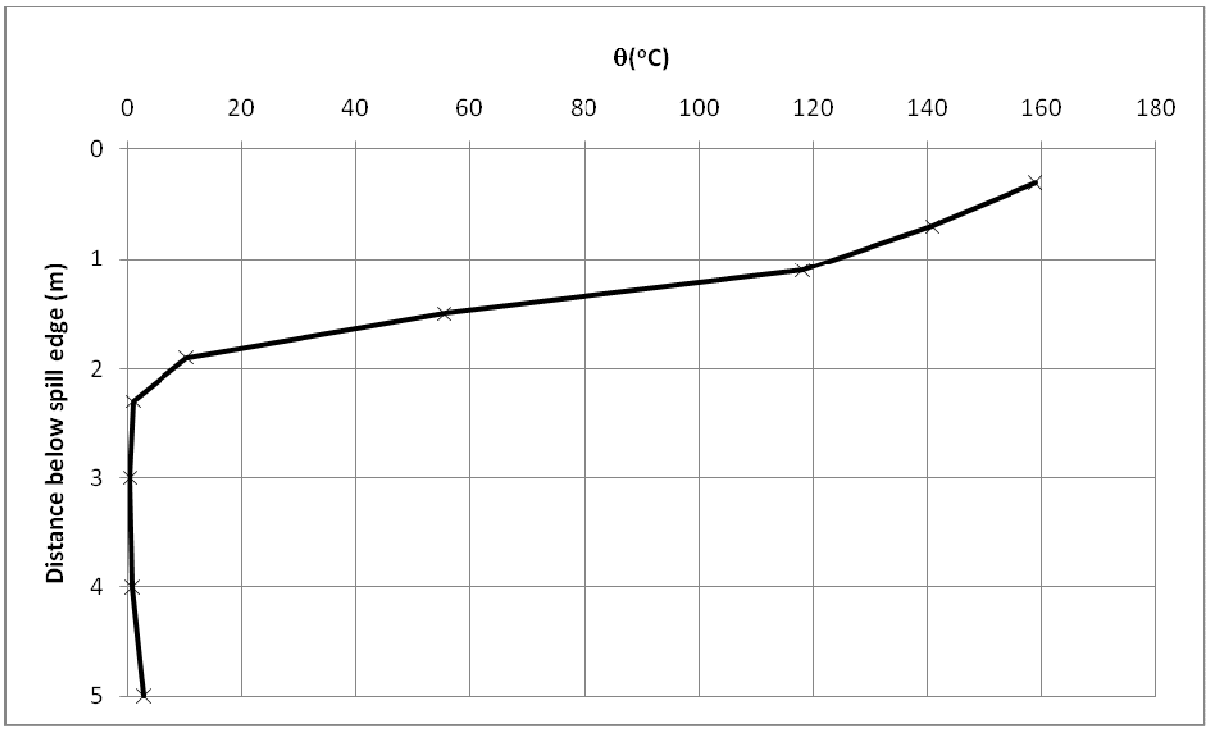

Figure D69. Temperature above ambient at the spill edge.

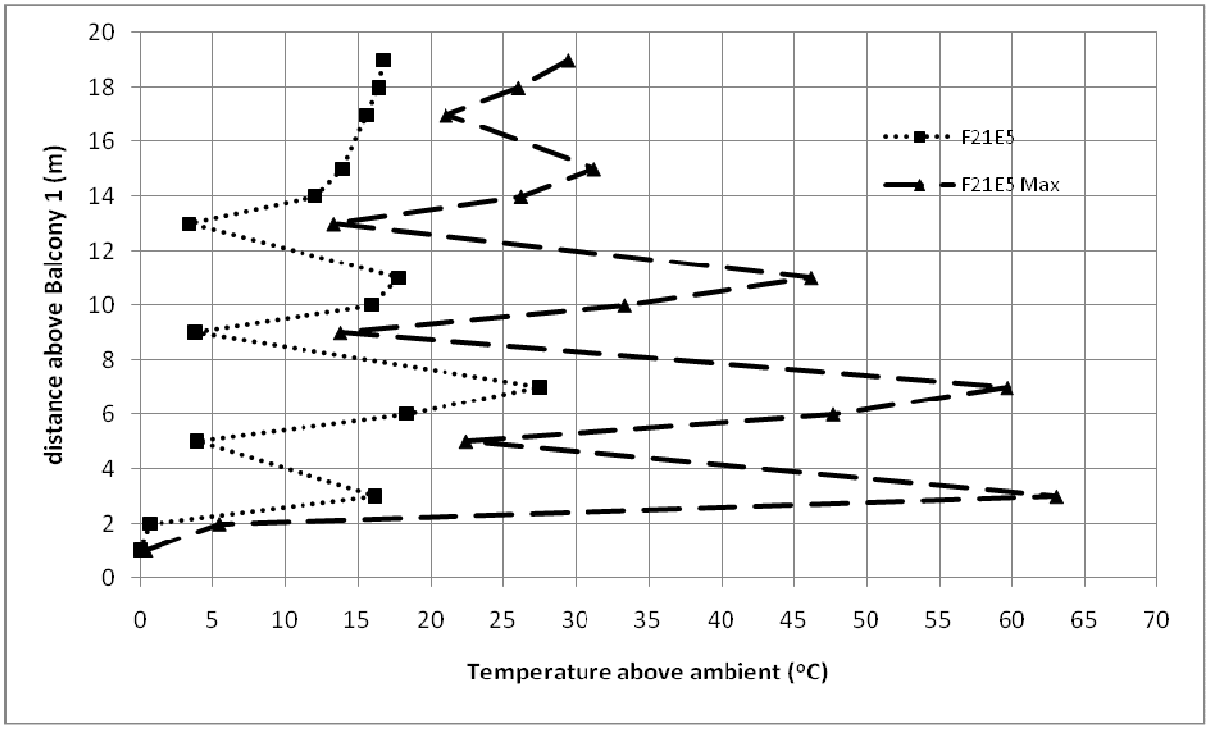

Figure D70. Temperature profiles across balcony edge.

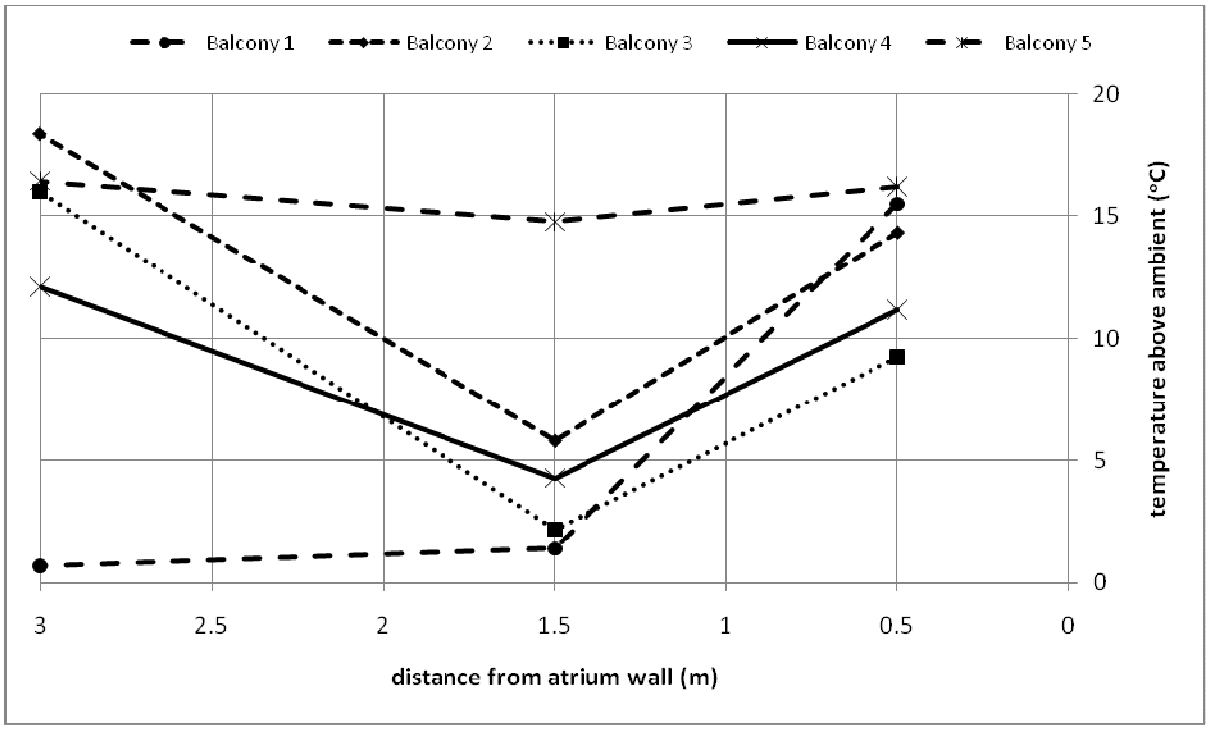

Figure D71. Temperature profiles along balcony breadth.

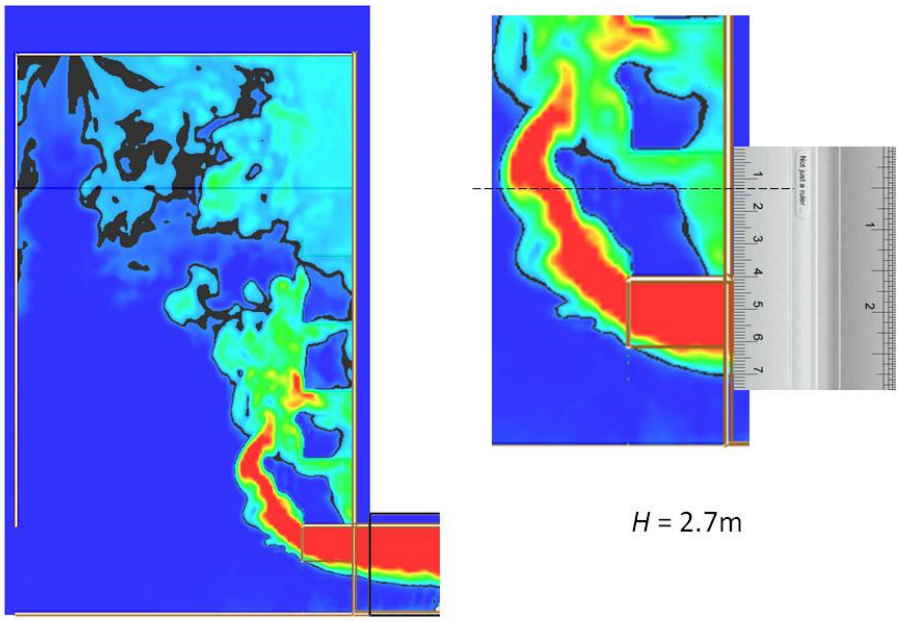

Figure D72. Smoke layer height measurement.

Full scale for 5 balcony (F22E5)

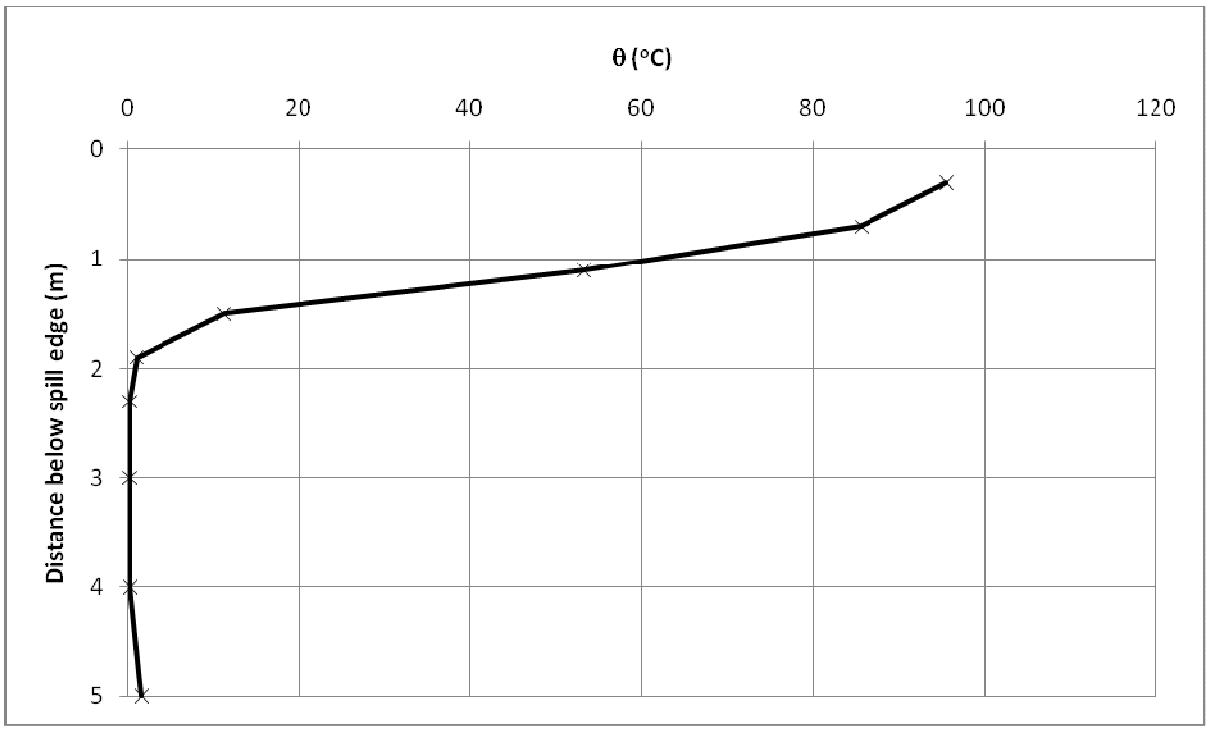

Figure D73. Temperature above ambient at the spill edge.

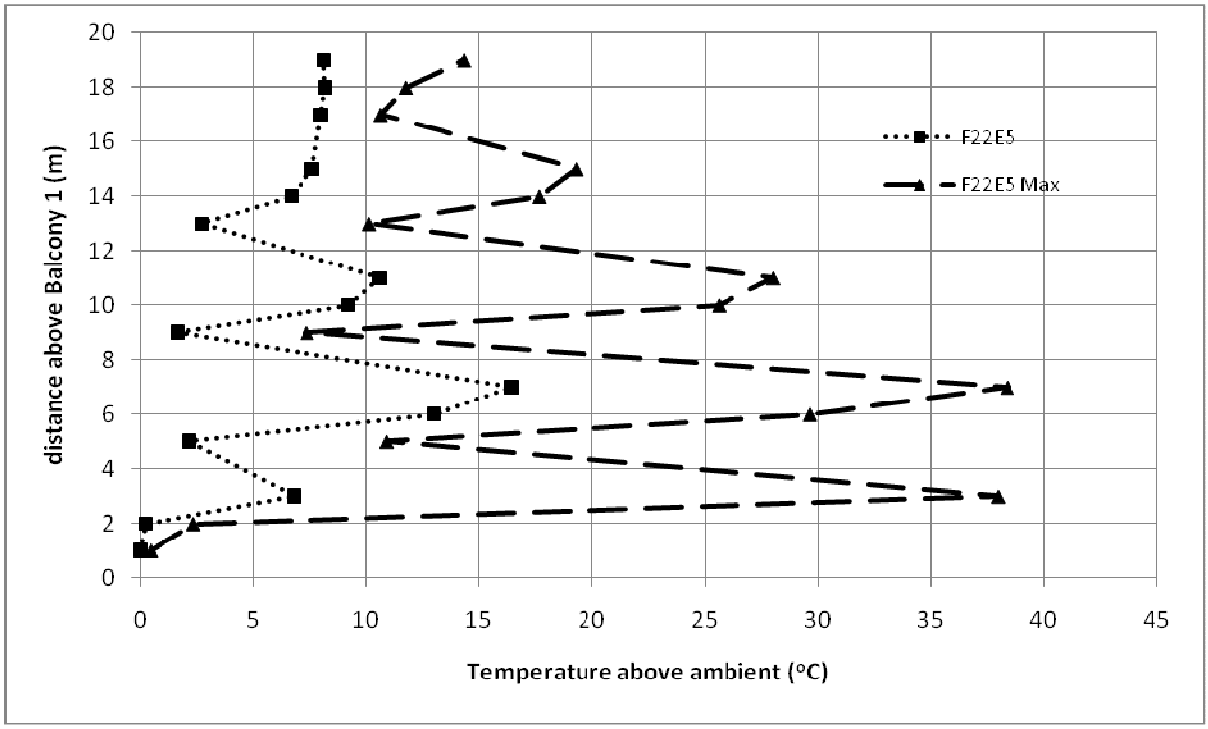

Figure D74. Temperature profiles across balcony edge.

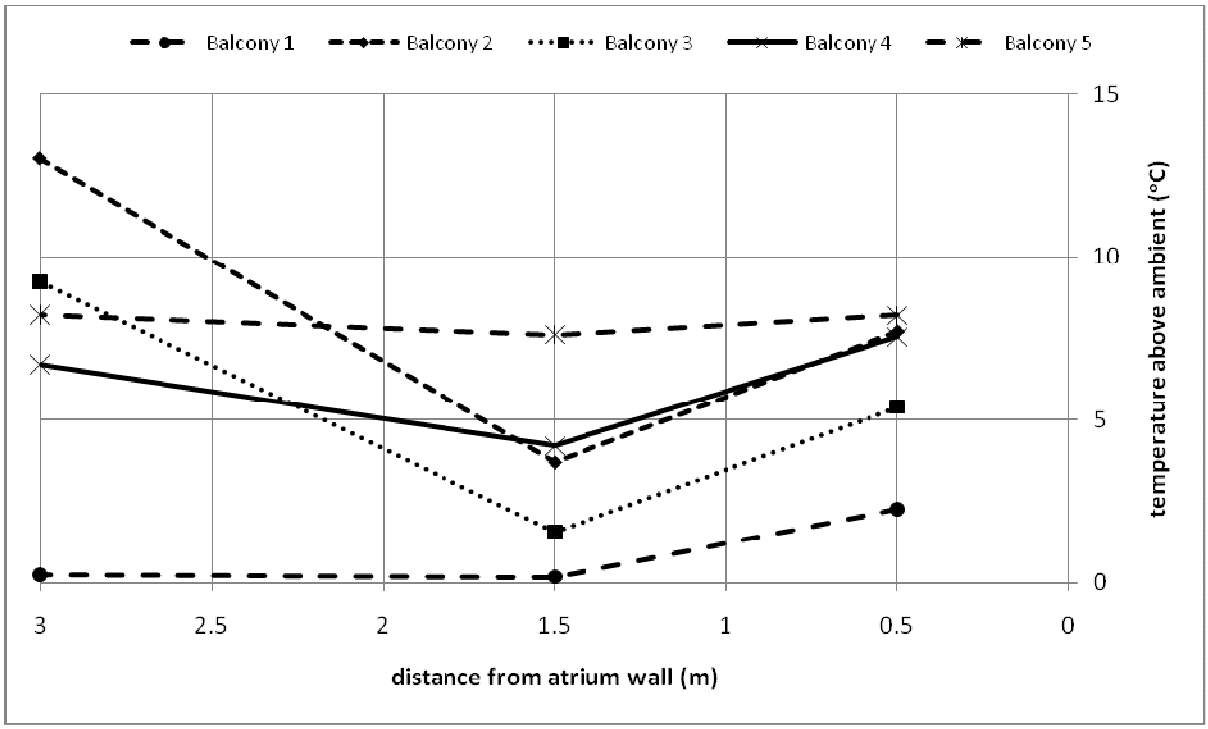

Figure D75. Temperature profiles along balcony breadth.

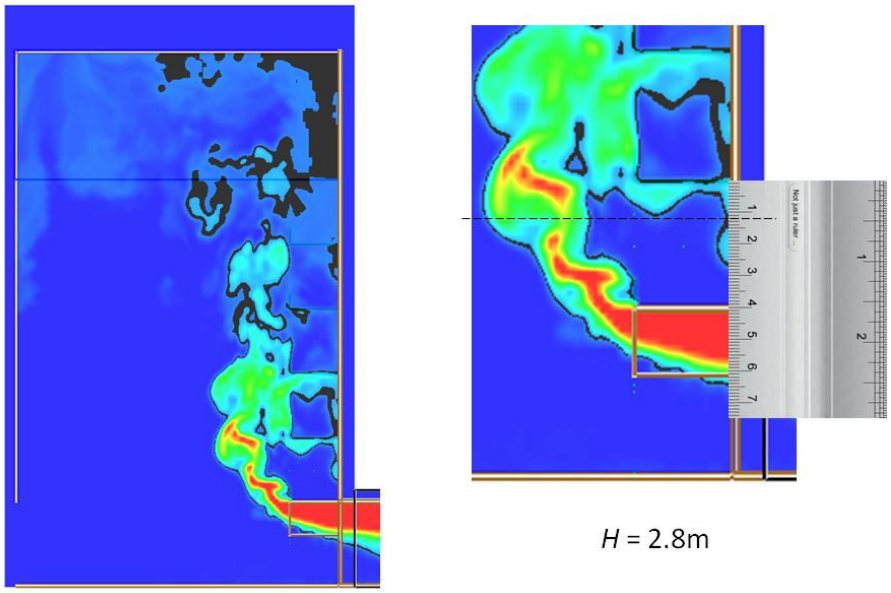

Figure D76. Smoke layer height measurement.

Full scale for 5 balcony (F23E5)

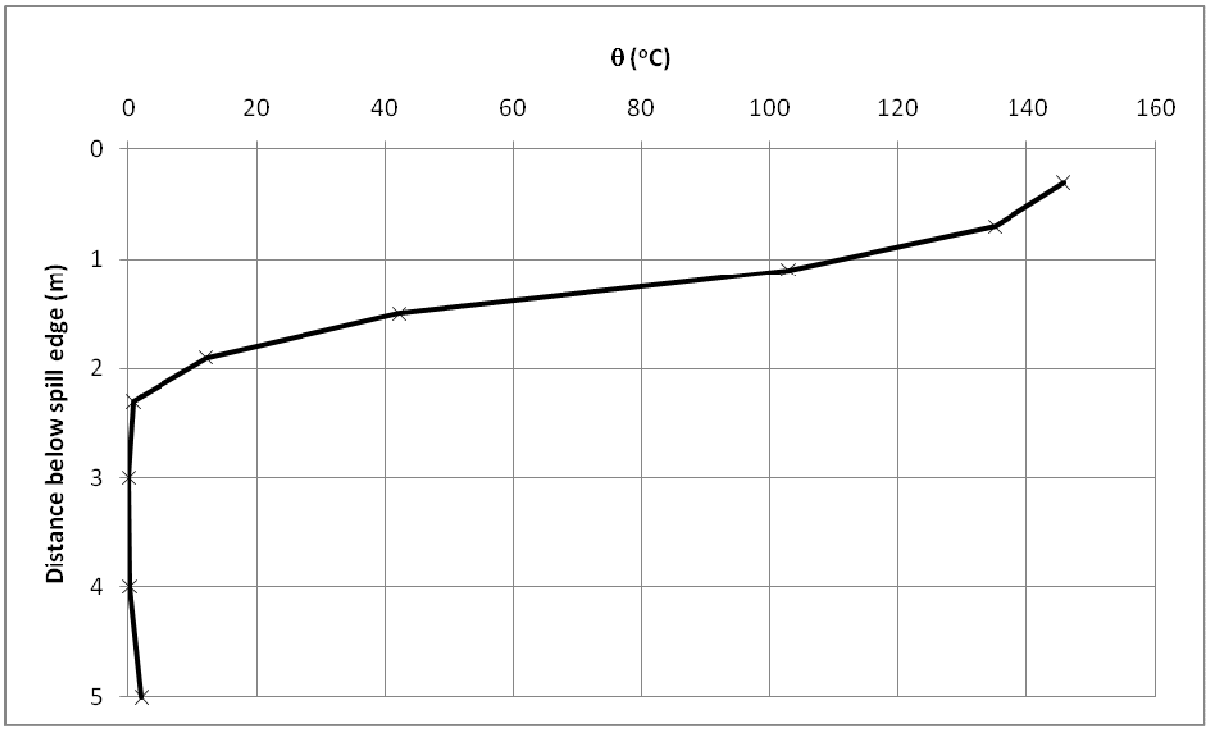

Figure D77. Temperature above ambient at the spill edge.

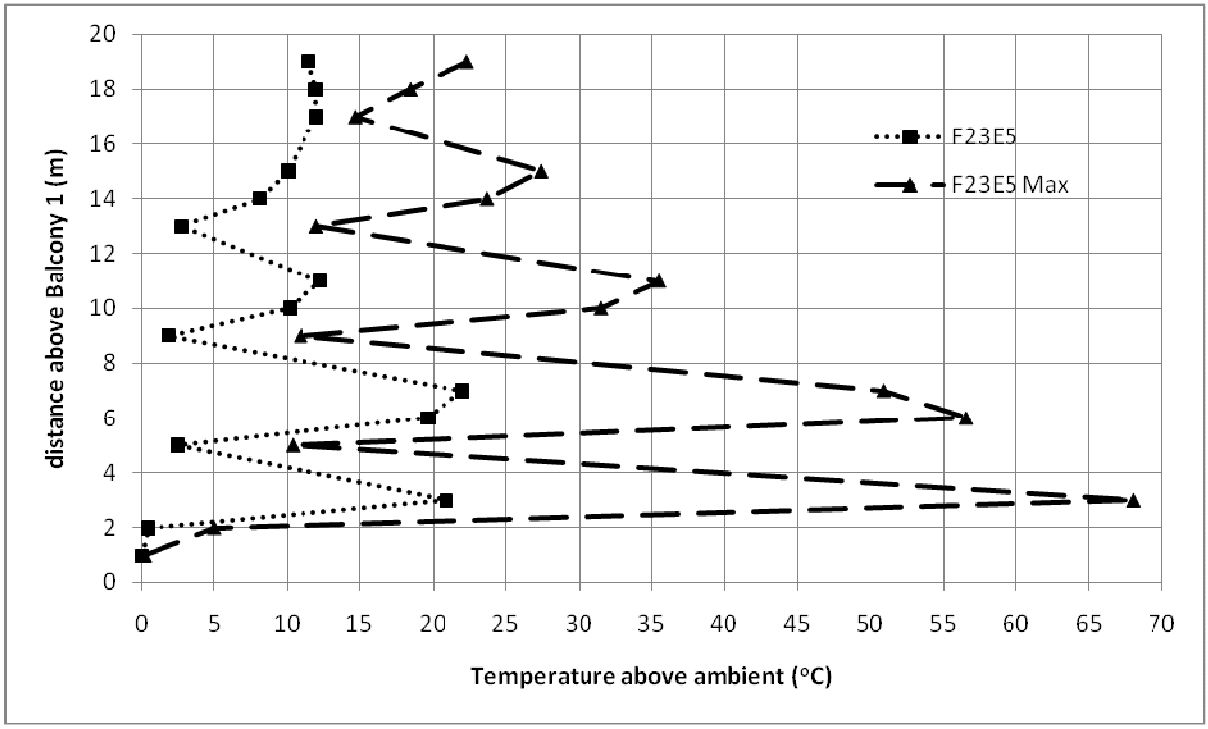

Figure D78. Temperature profiles across balcony edge.

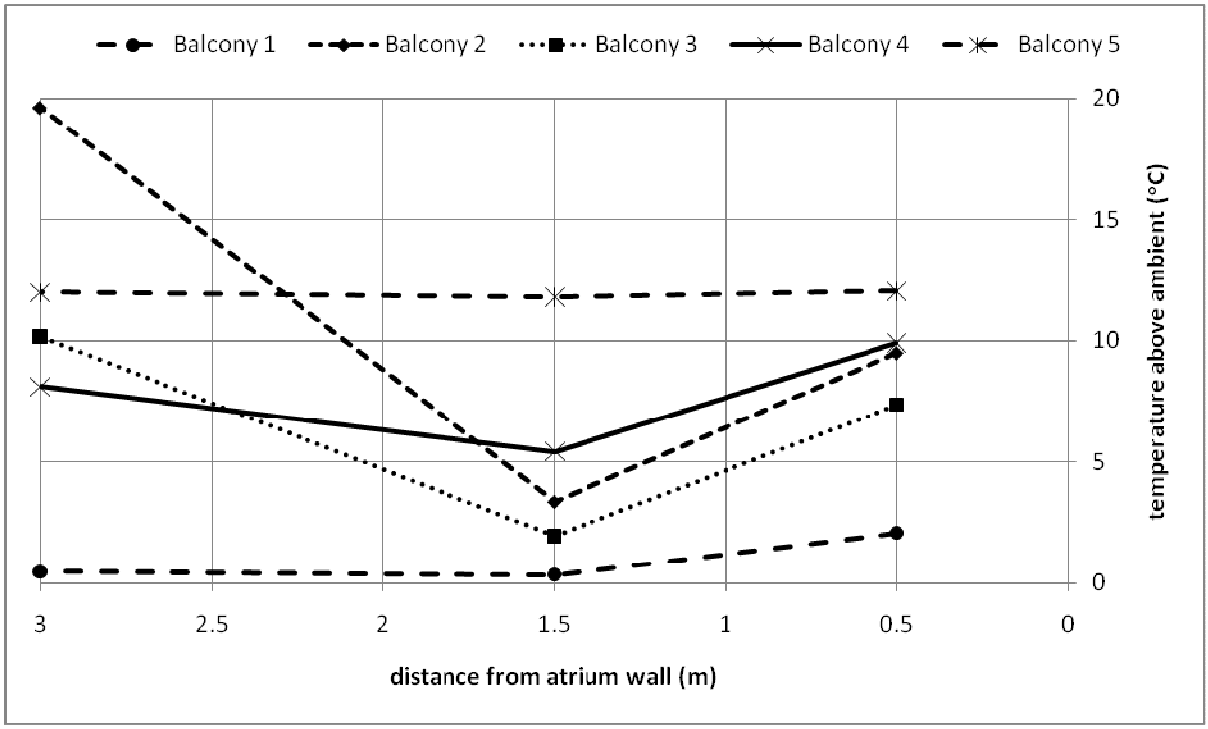

Figure D79. Temperature profiles along balcony breadth.

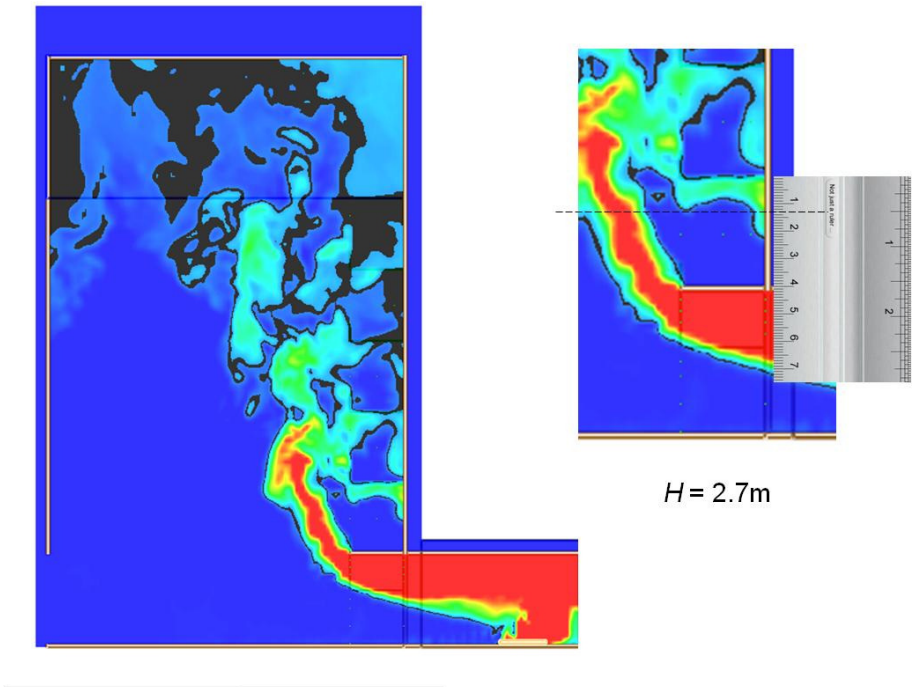

Figure D80. Smoke layer height measurement.

Full scale for 5 balcony (F24E5)

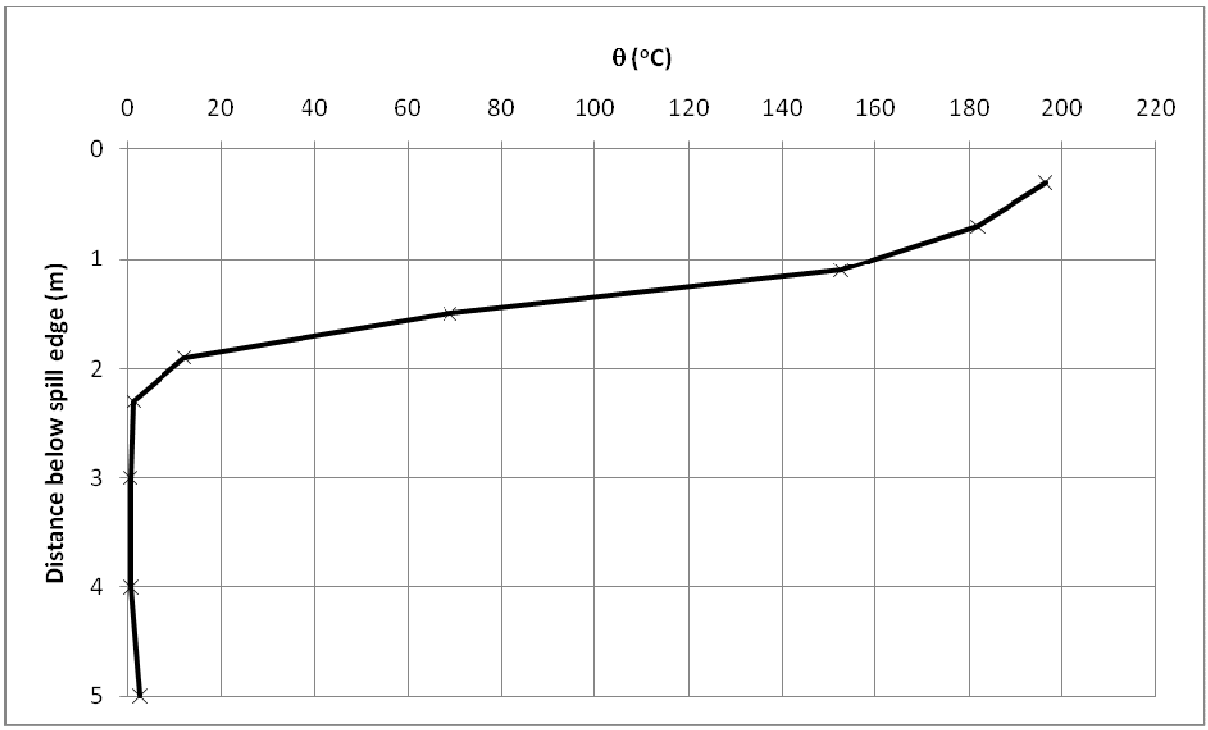

Figure D81. Temperature above ambient at the spill edge.

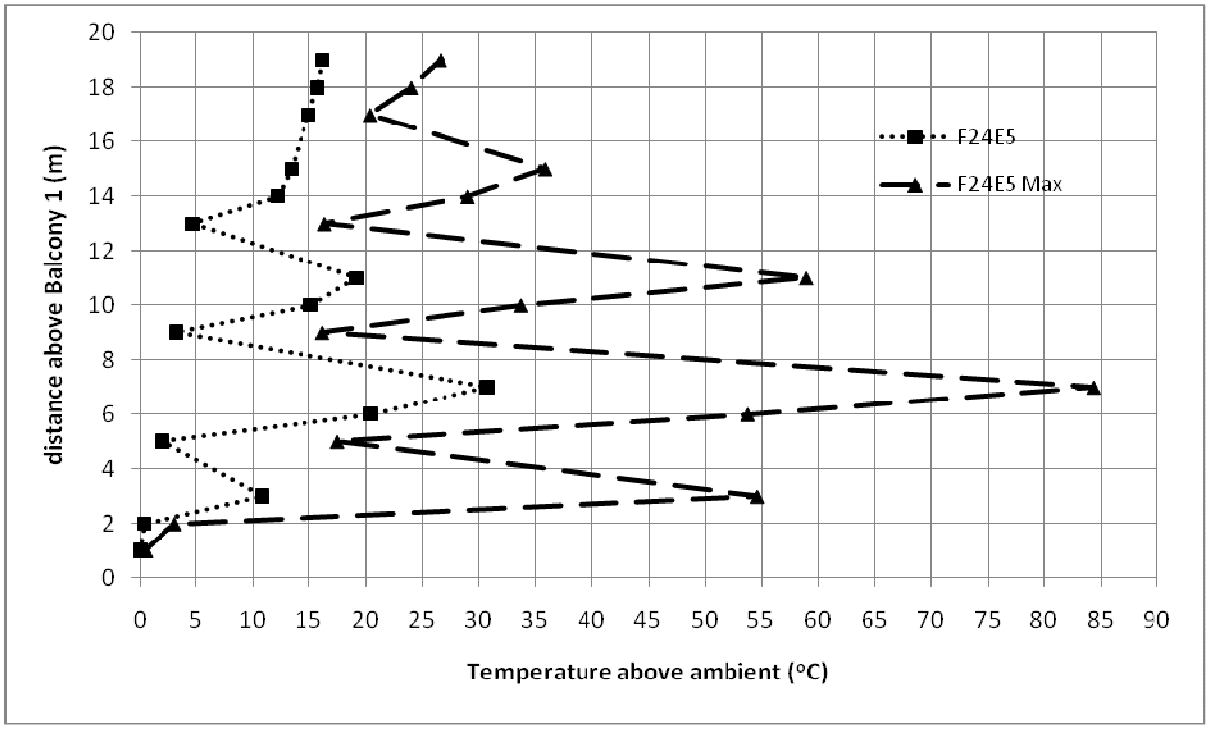

Figure D82. Temperature profiles across balcony edge.

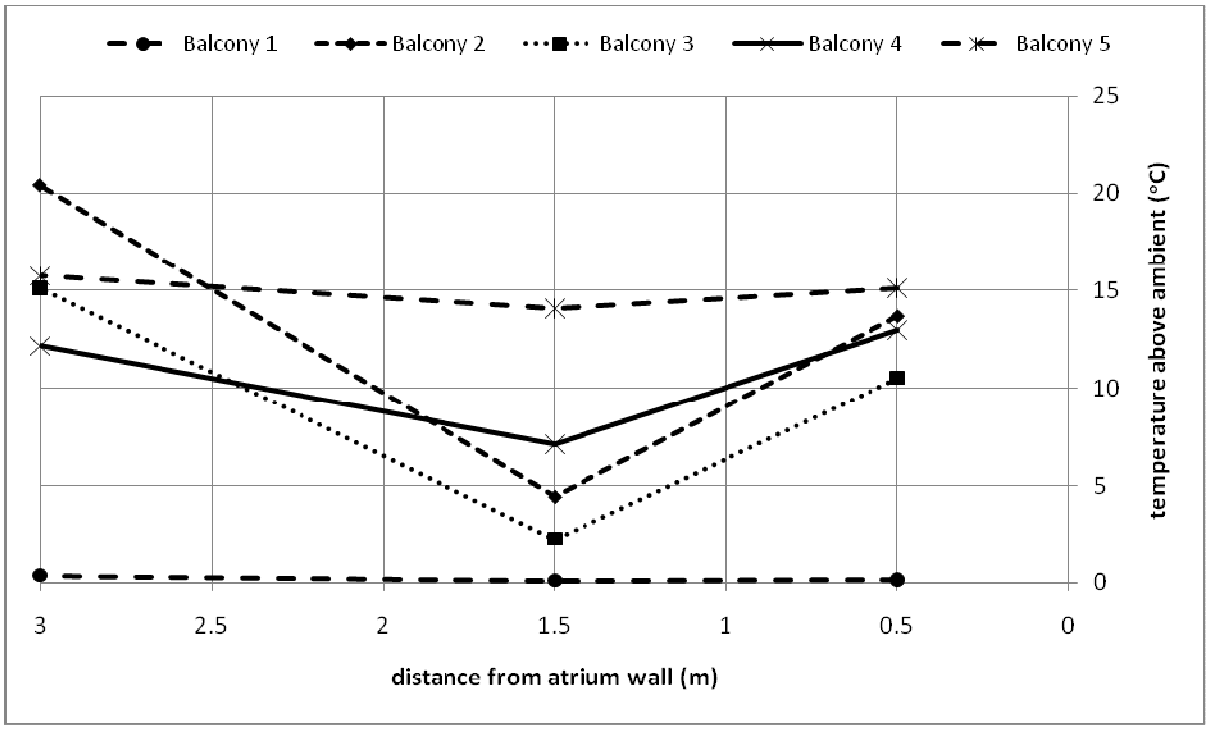

Figure D83. Temperature profiles along balcony breadth.

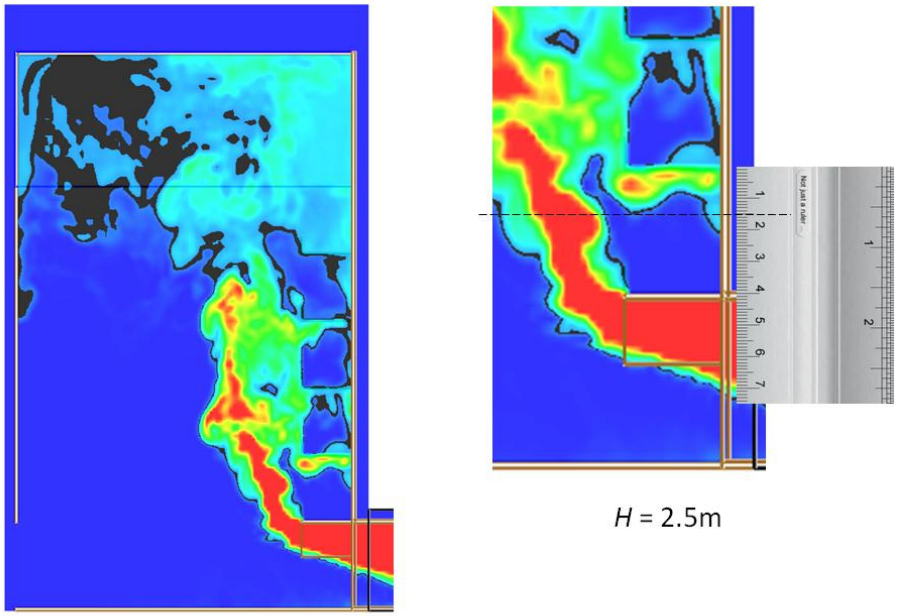

Figure D84. Smoke layer height measurement.

Full scale for 5 balcony (F25E5)

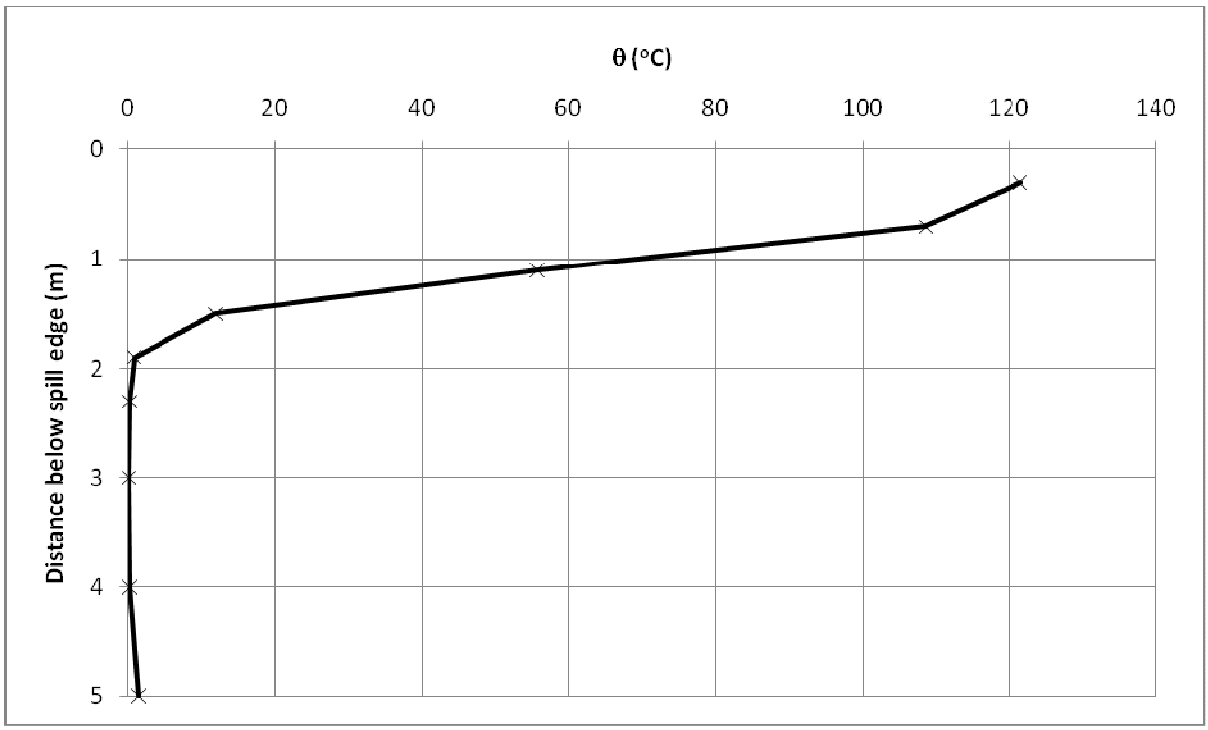

Figure D85. Temperature above ambient at the spill edge.

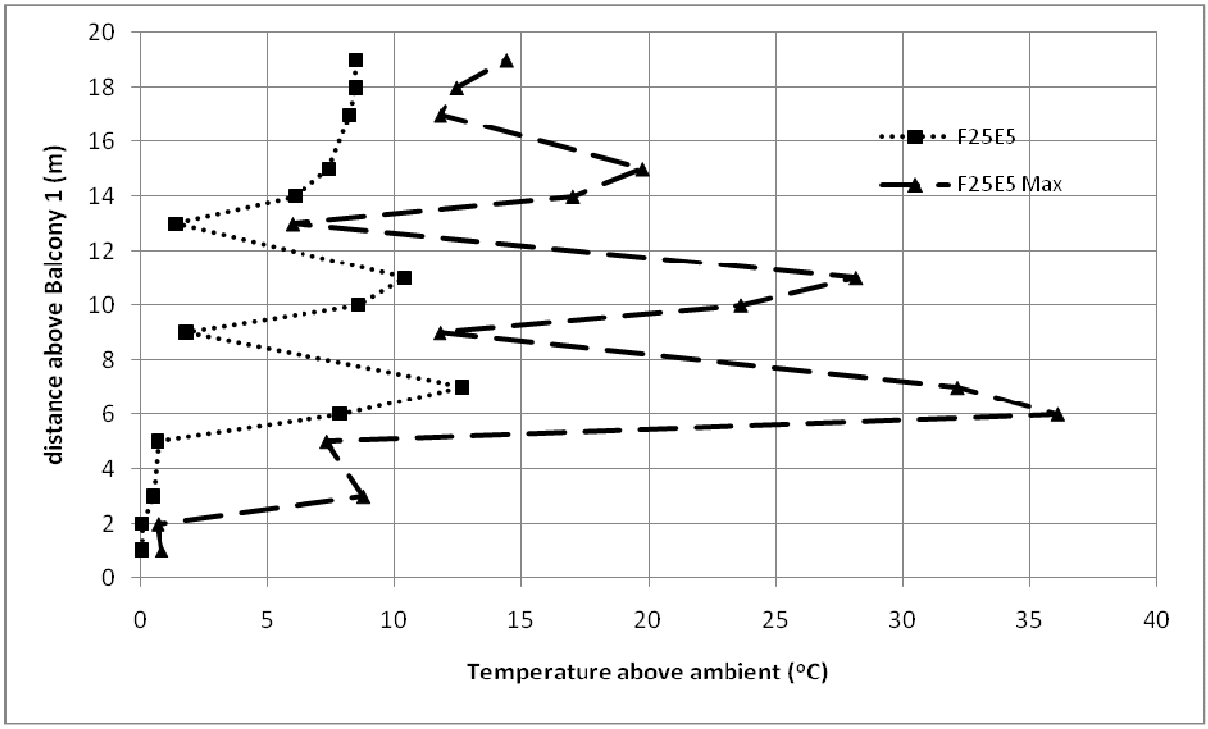

Figure D86. Temperature profiles across balcony edge.

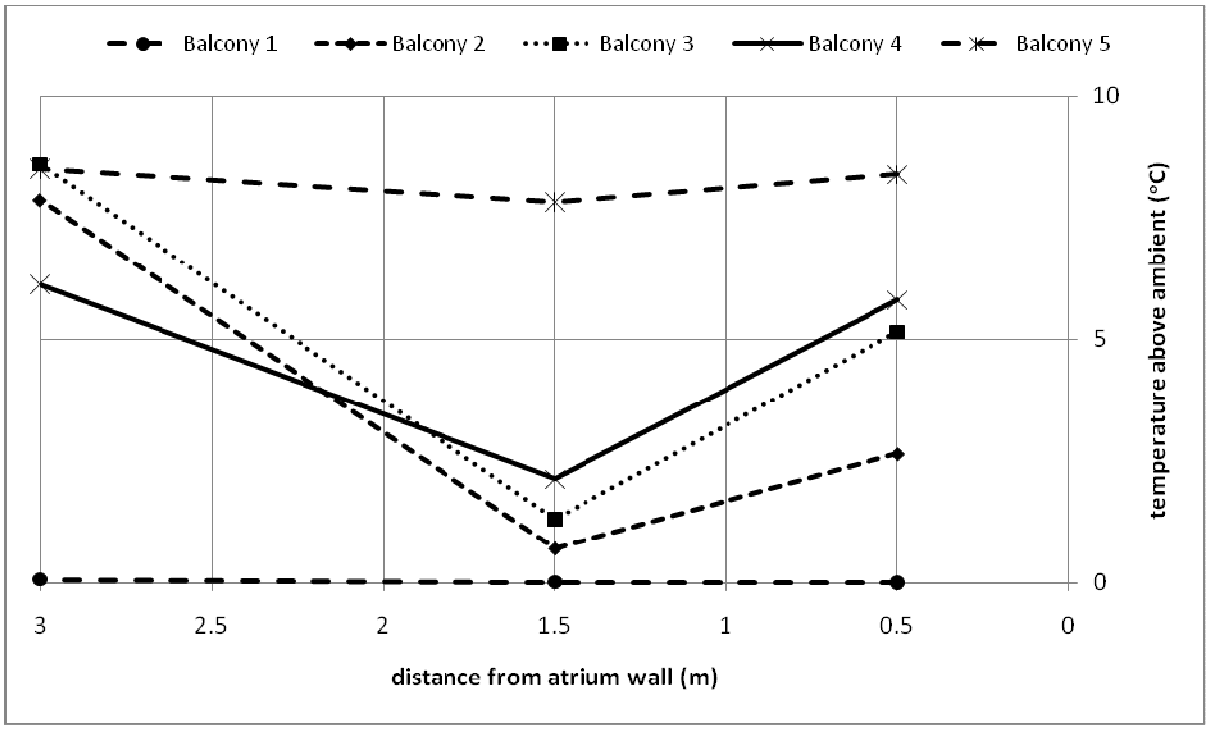

Figure D87. Temperature profiles along balcony breadth.

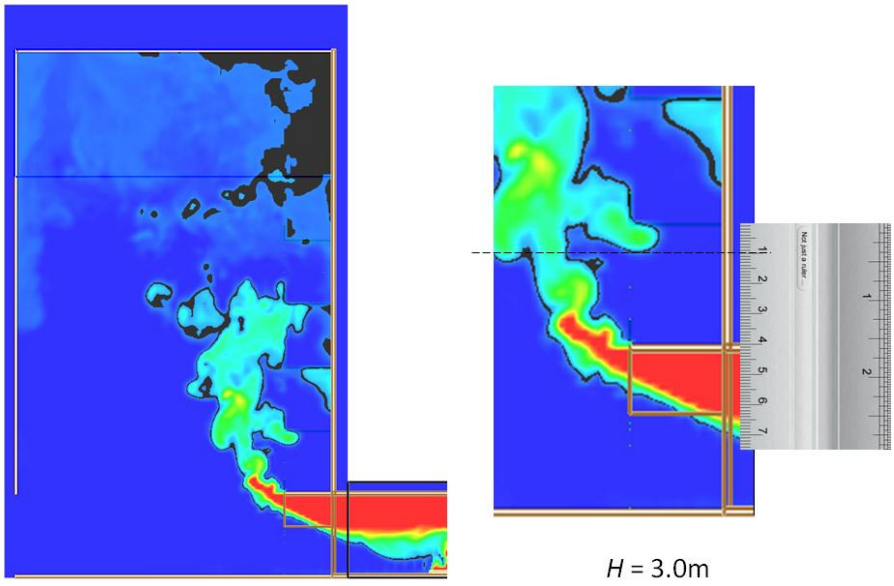

Figure D88. Smoke layer height measurement.

Full scale for 5 balcony (F26E5)

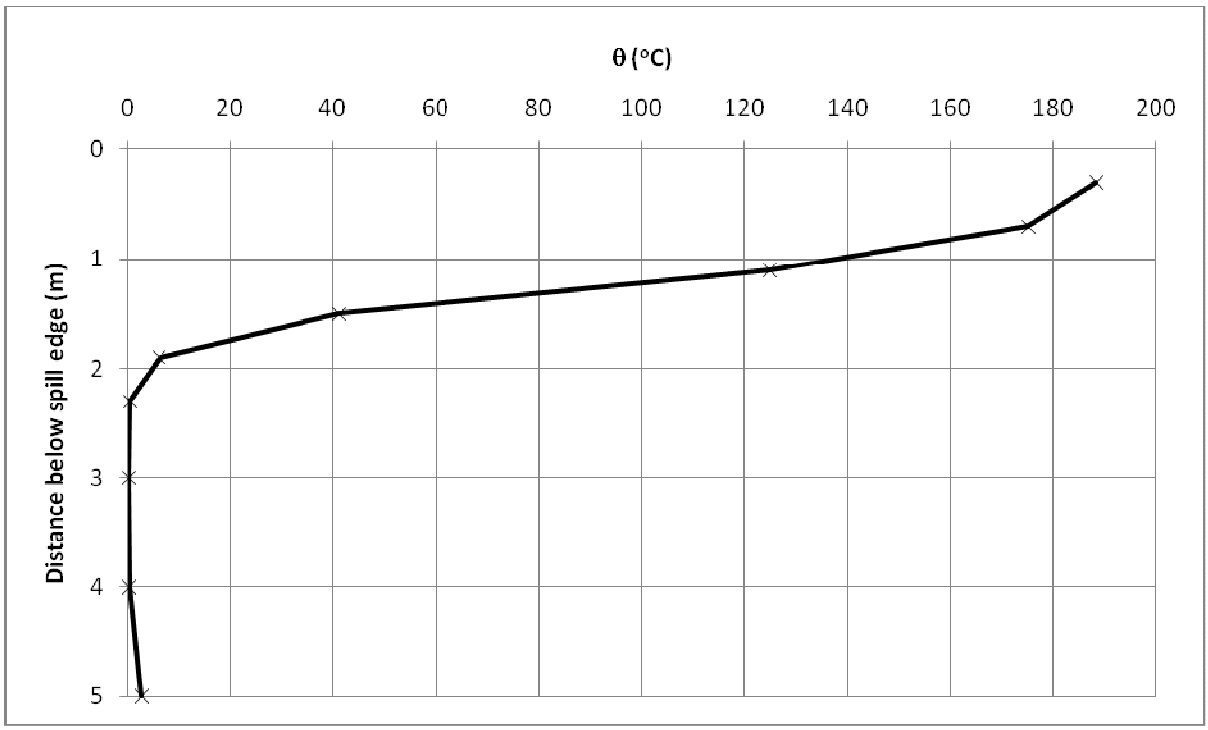

Figure D89. Temperature above ambient at the spill edge.

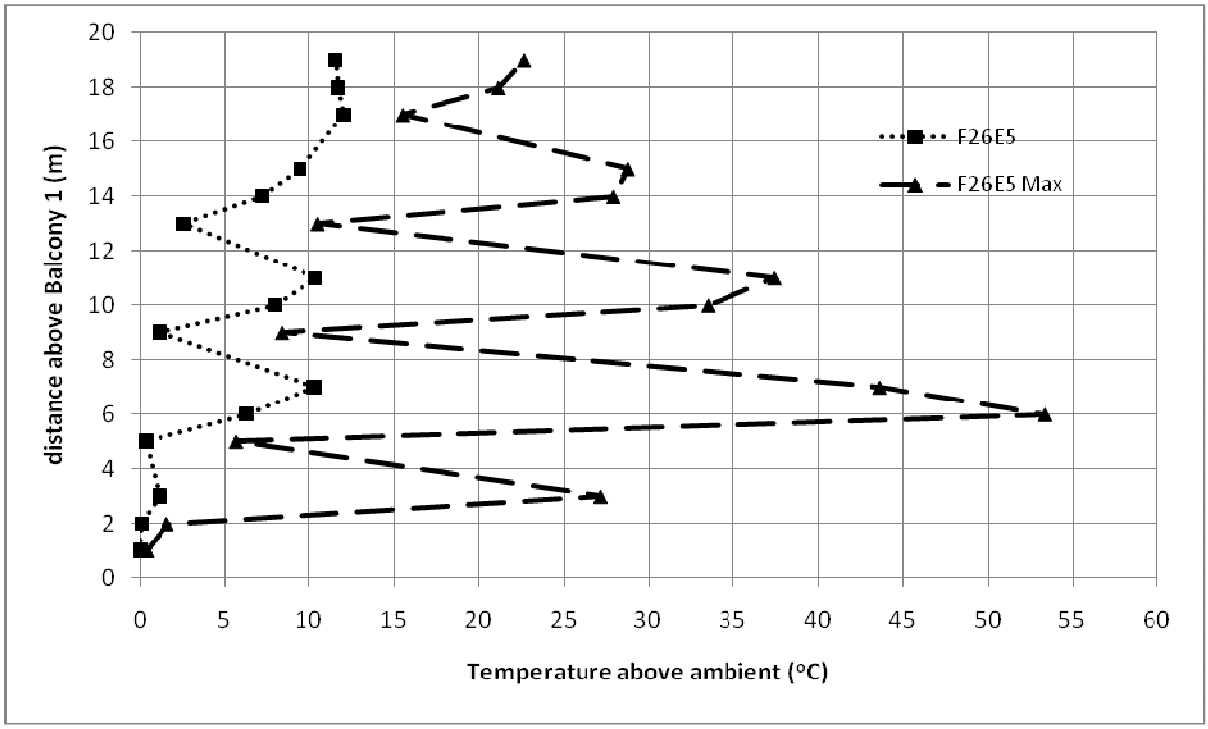

Figure D90. Temperature profiles across balcony edge.

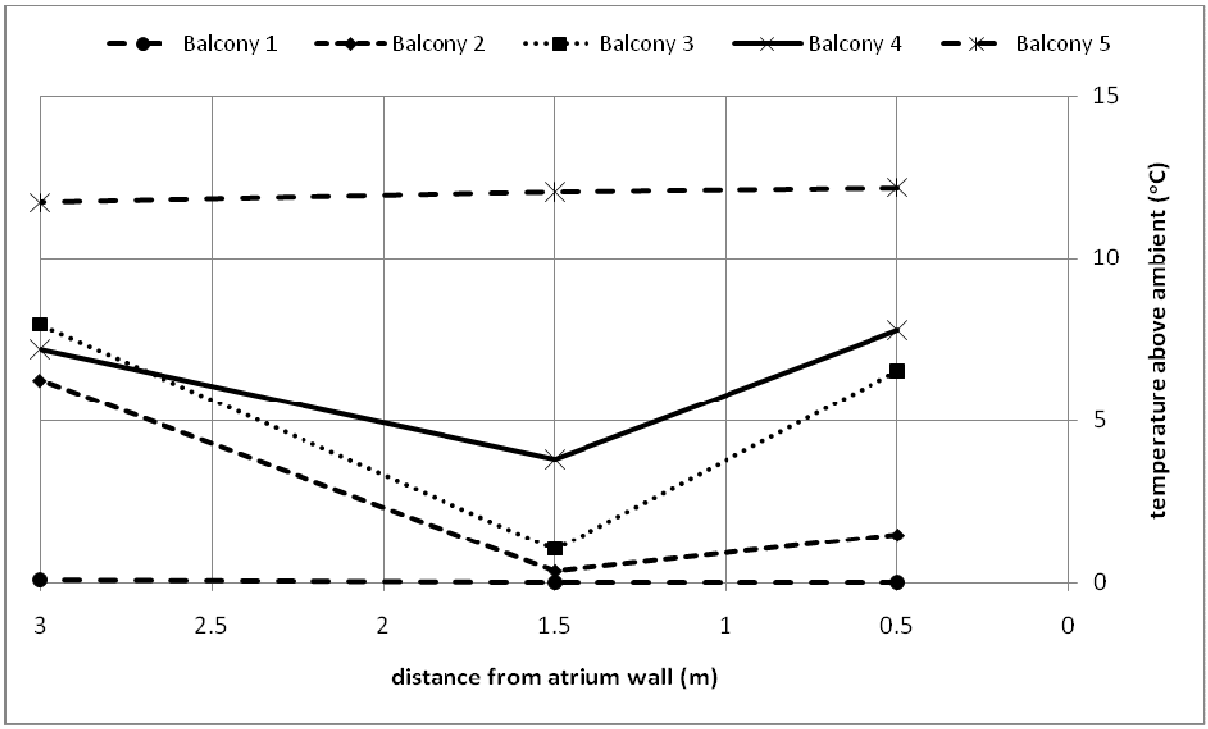

Figure D91. Temperature profiles along balcony breadth.

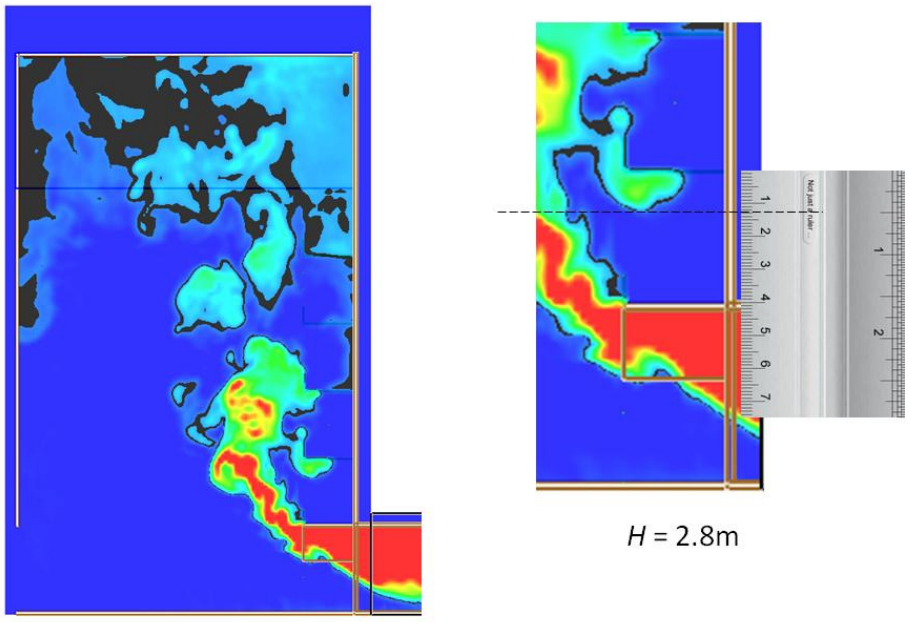

Figure D92. Smoke layer height measurement.

Full scale for 5 balcony (F27E5)

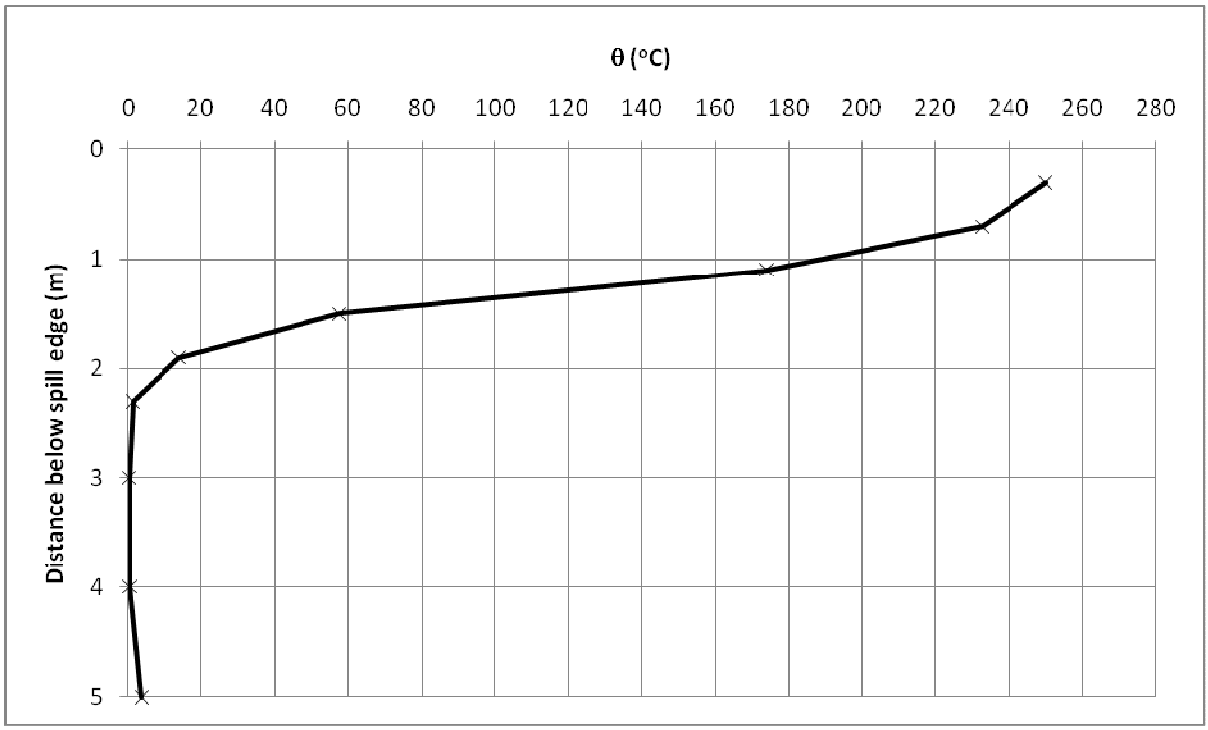

Figure D93. Temperature above ambient at the spill edge.

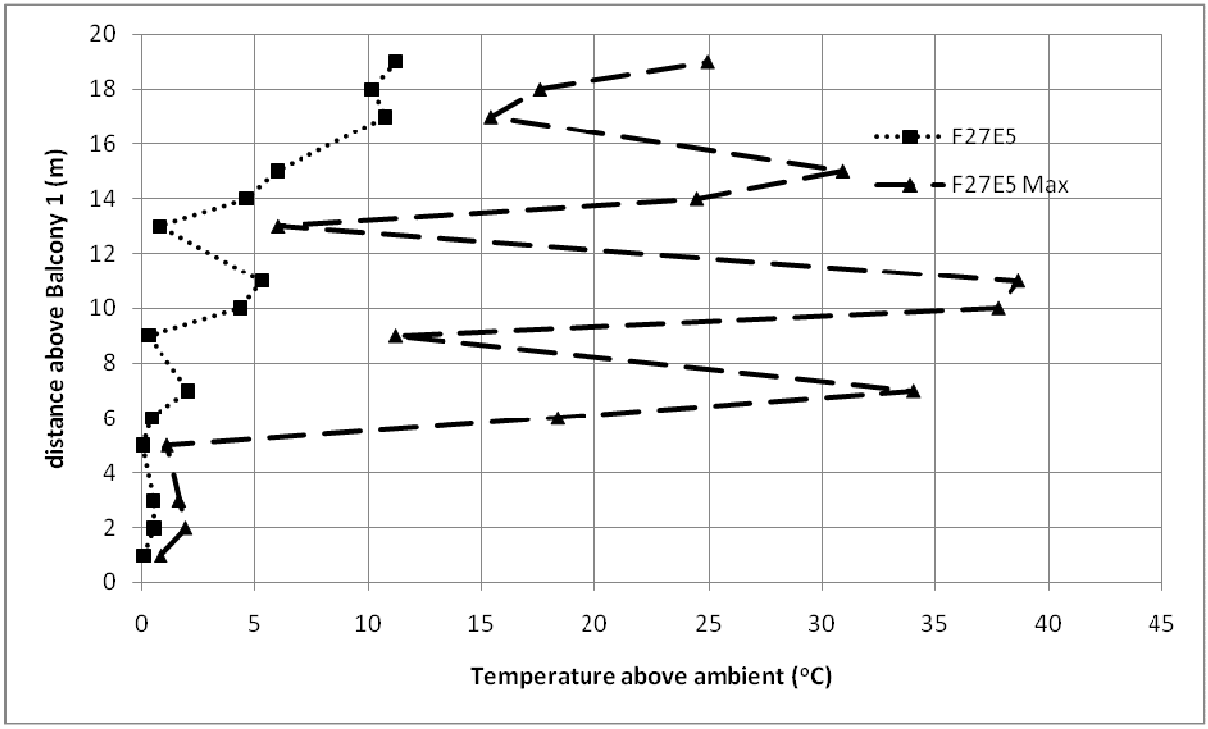

Figure D94. Temperature profiles across balcony edge.

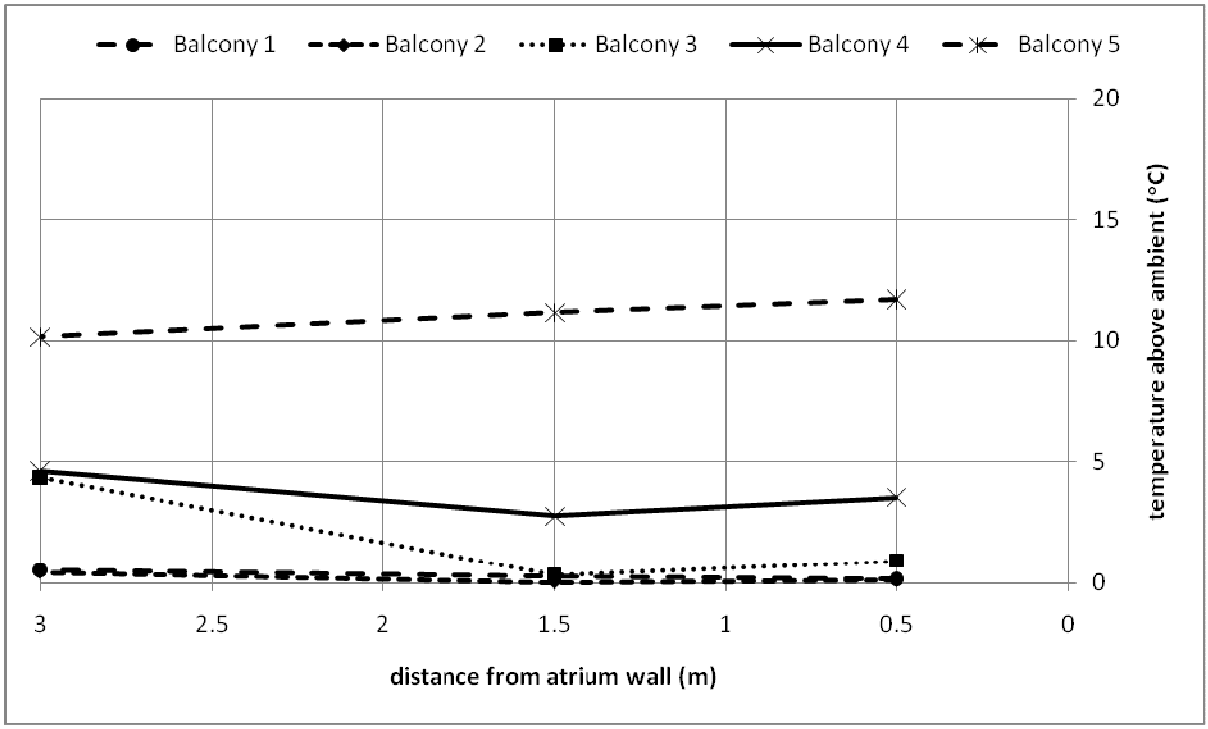

Figure D95. Temperature profiles along balcony breadth.

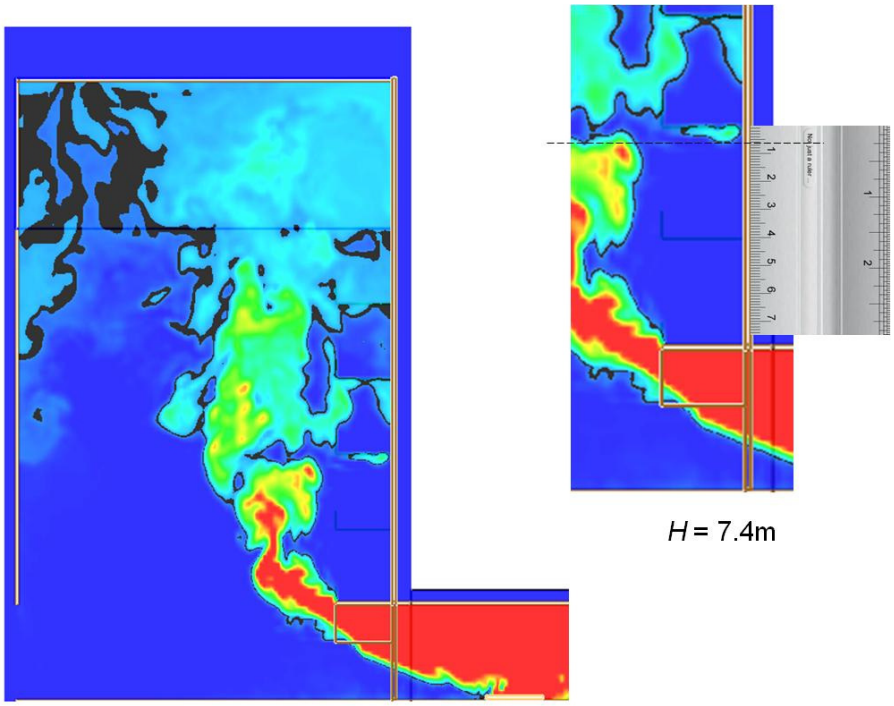

Figure D96. Smoke layer height measurement.

Full scale for 5 balcony (F28E5)

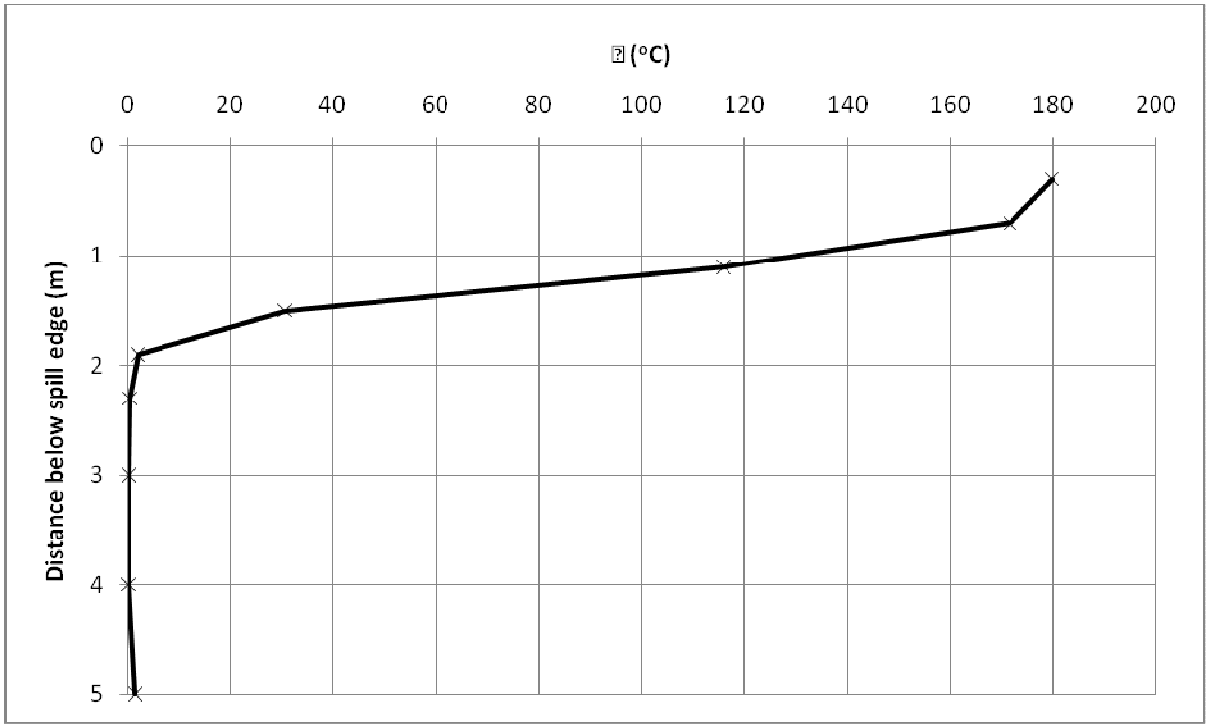

Figure D97. Temperature above ambient at the spill edge.

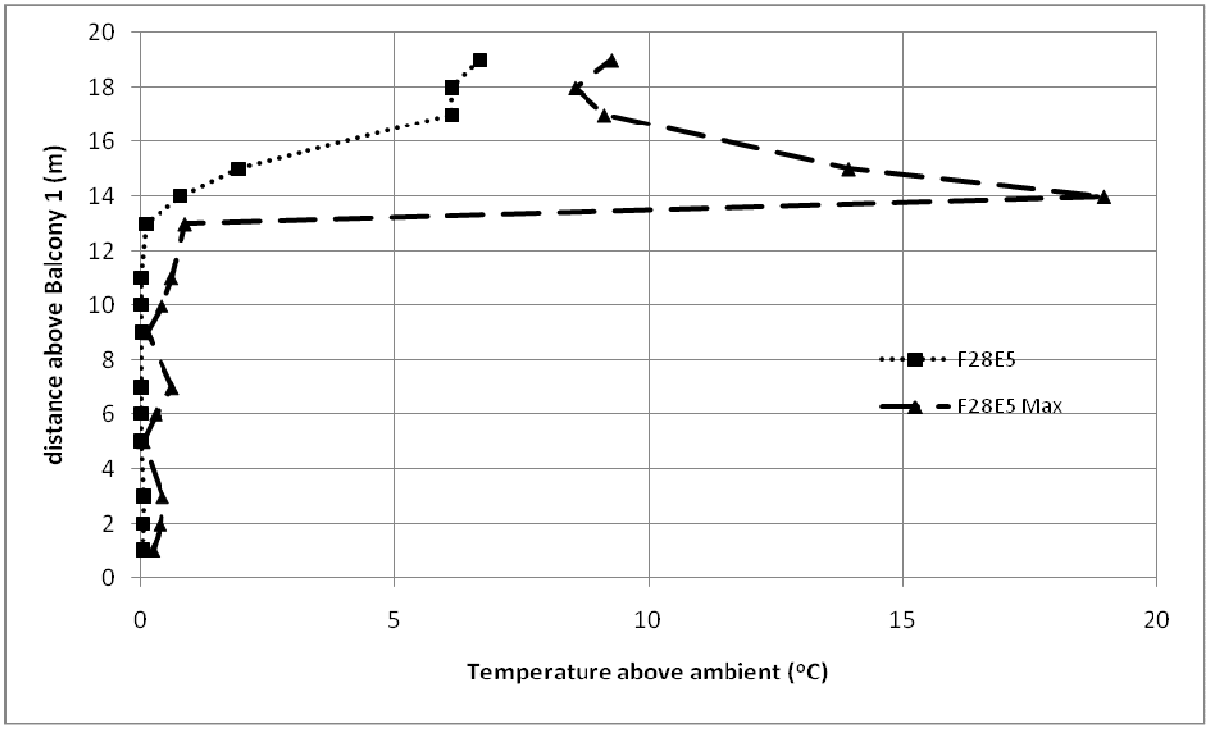

Figure D98. Temperature profiles across balcony edge.

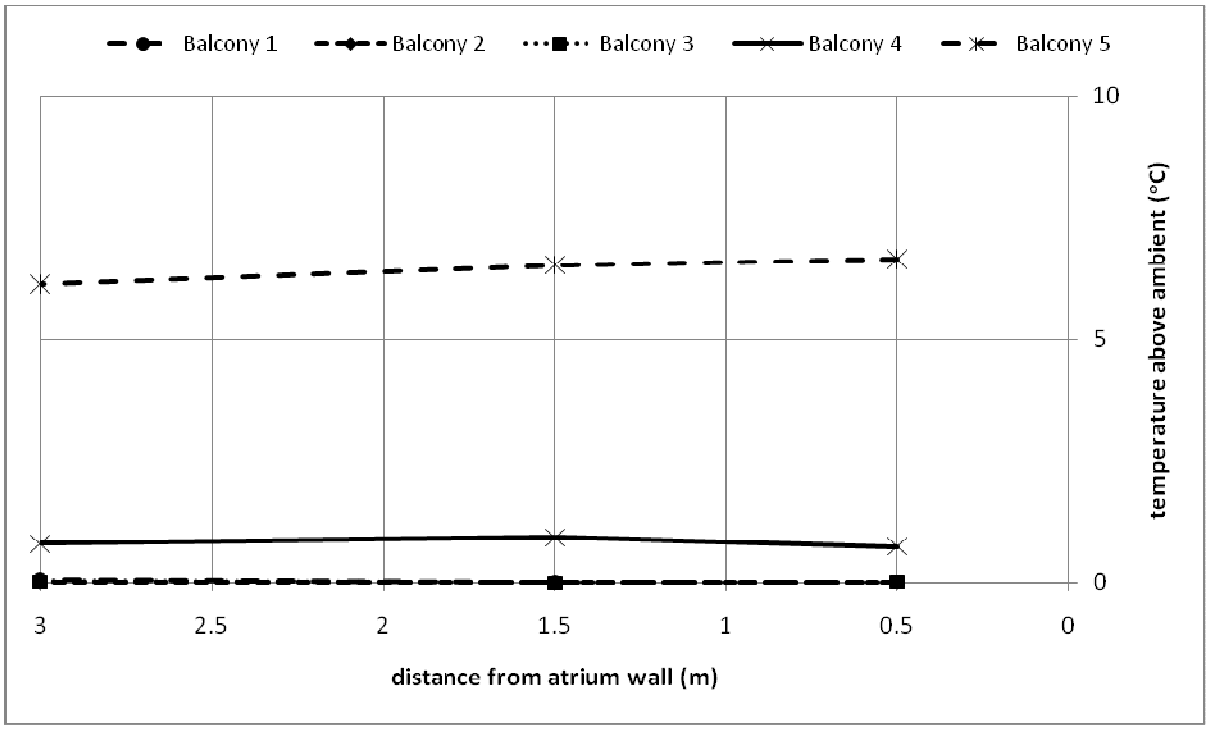

Figure D99. Temperature profiles along balcony breadth.

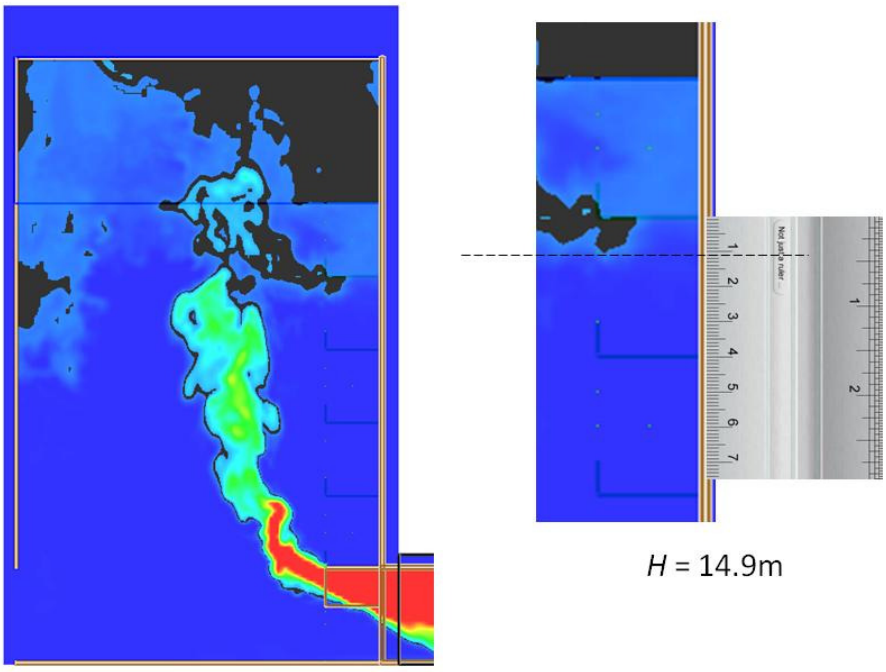

Figure D100. Smoke layer height measurement.

Full scale for 5 balcony (F29E5)

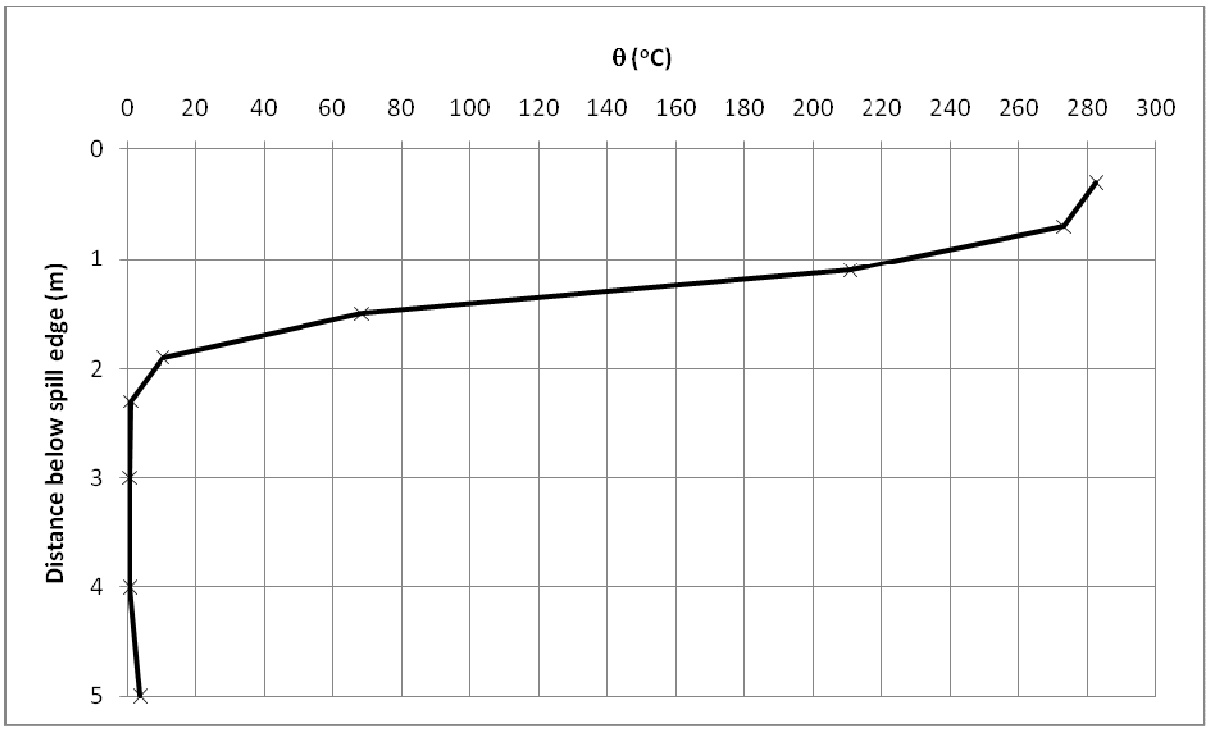

Figure D101. Temperature above ambient at the spill edge.

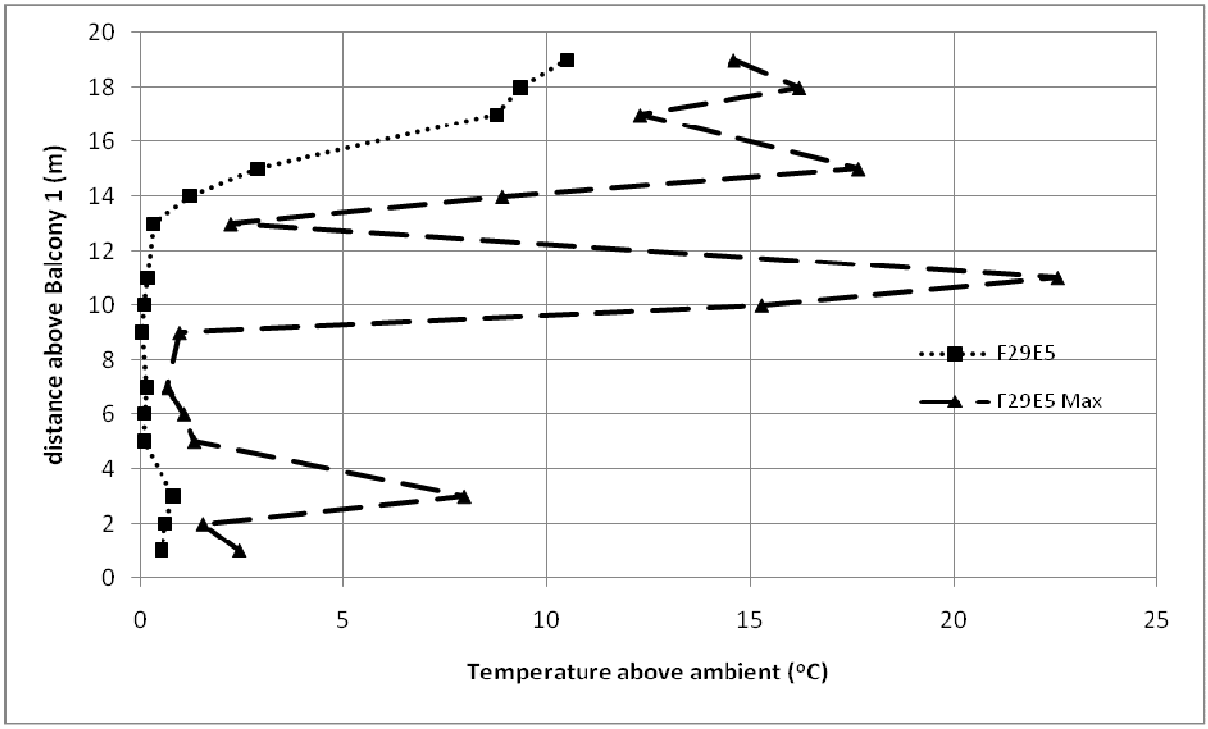

Figure D102. Temperature profiles across balcony edge.

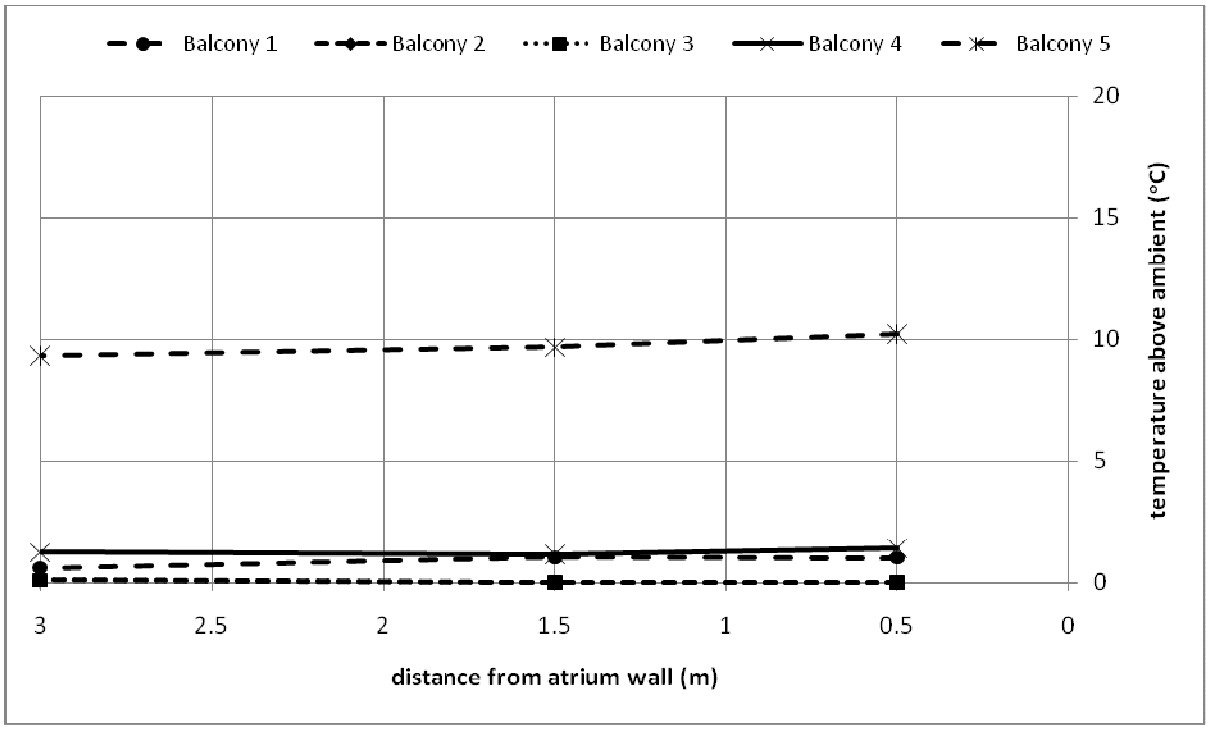

Figure D103. Temperature profiles along balcony breadth.

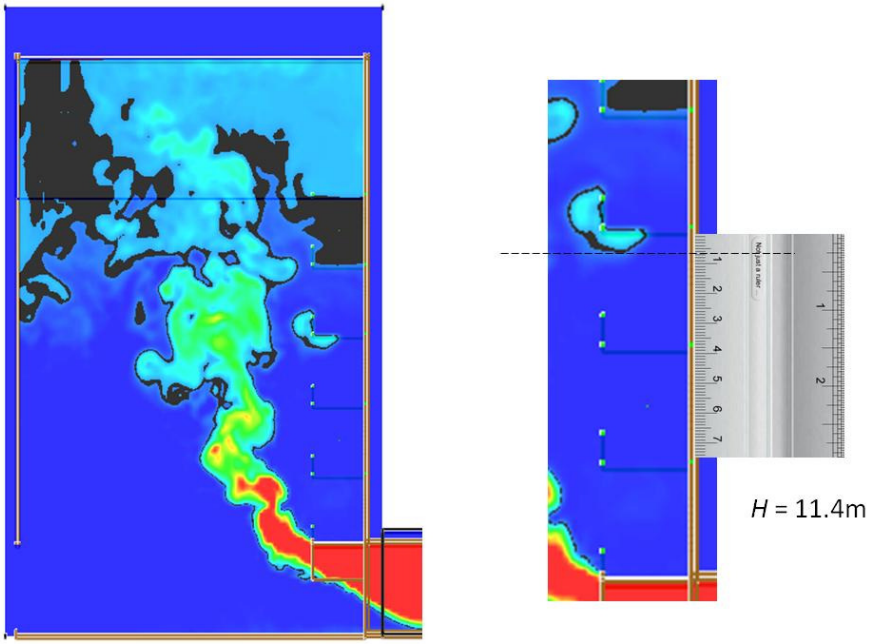

Figure D104. Smoke layer height measurement.

Full scale for 5 balcony (F30E5)

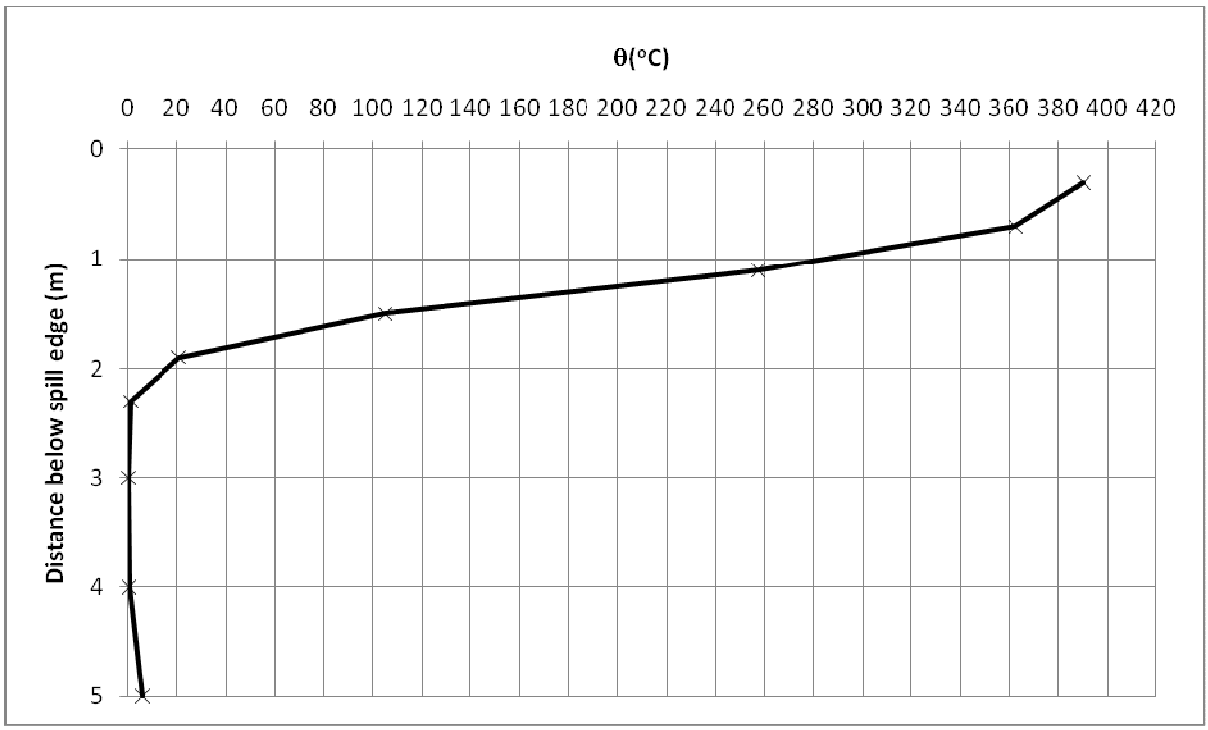

Figure D105. Temperature above ambient at the spill edge.

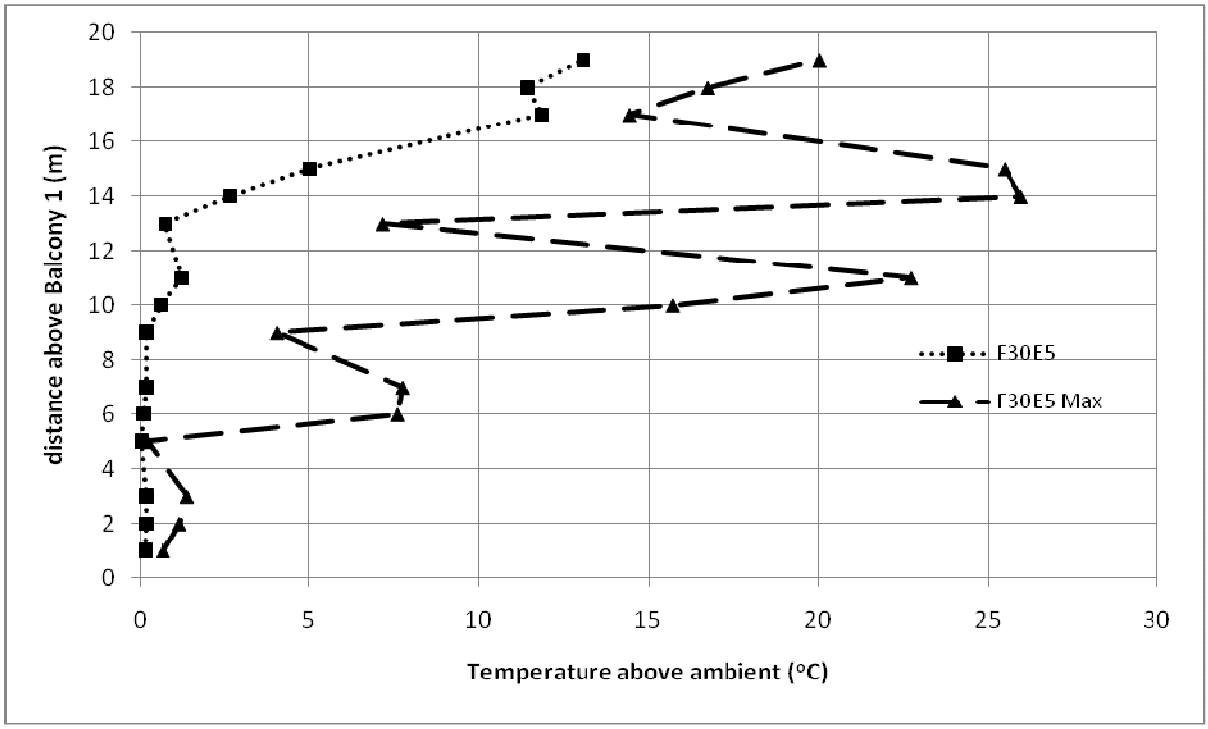

Figure D106. Temperature profiles across balcony edge.

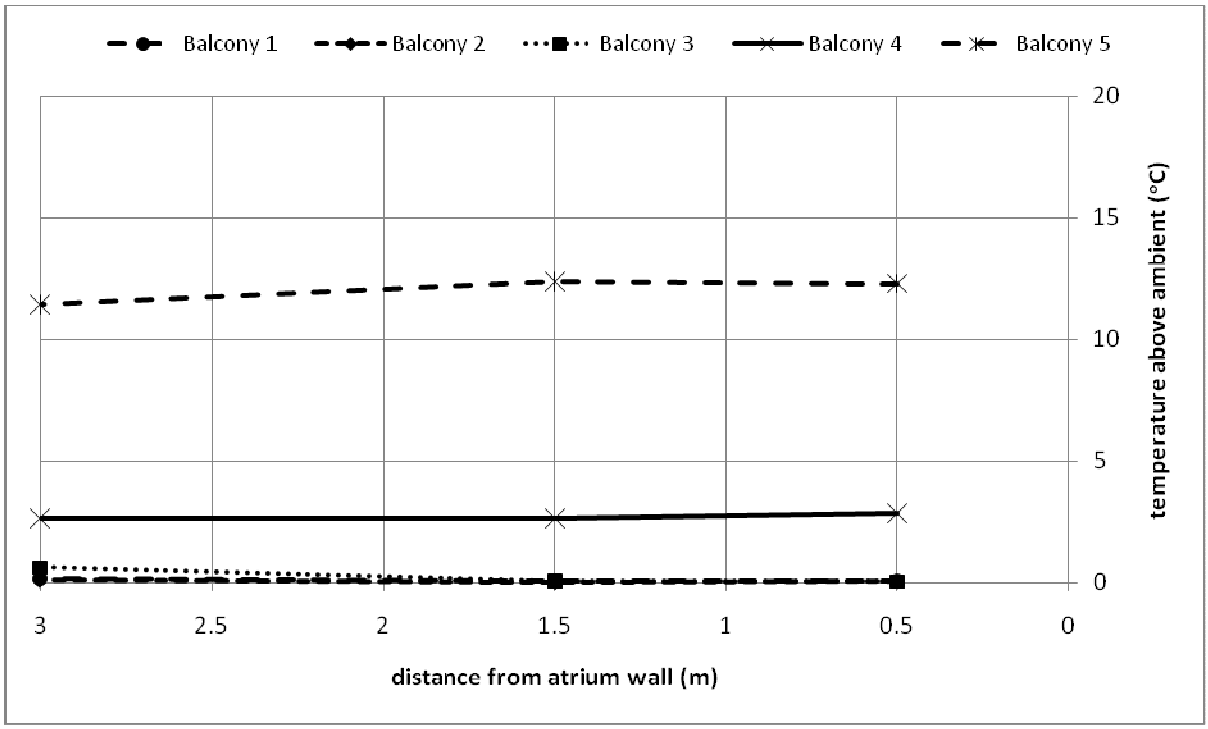

Figure D107. Temperature profiles along balcony breadth.

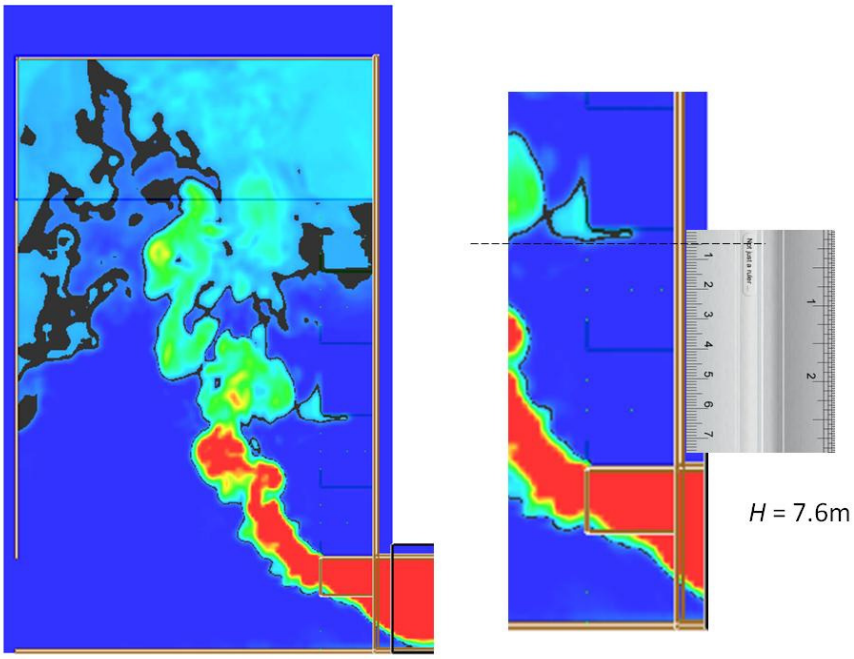

Figure D108. Smoke layer height measurement.

Full scale for 5 balcony (F37E5)

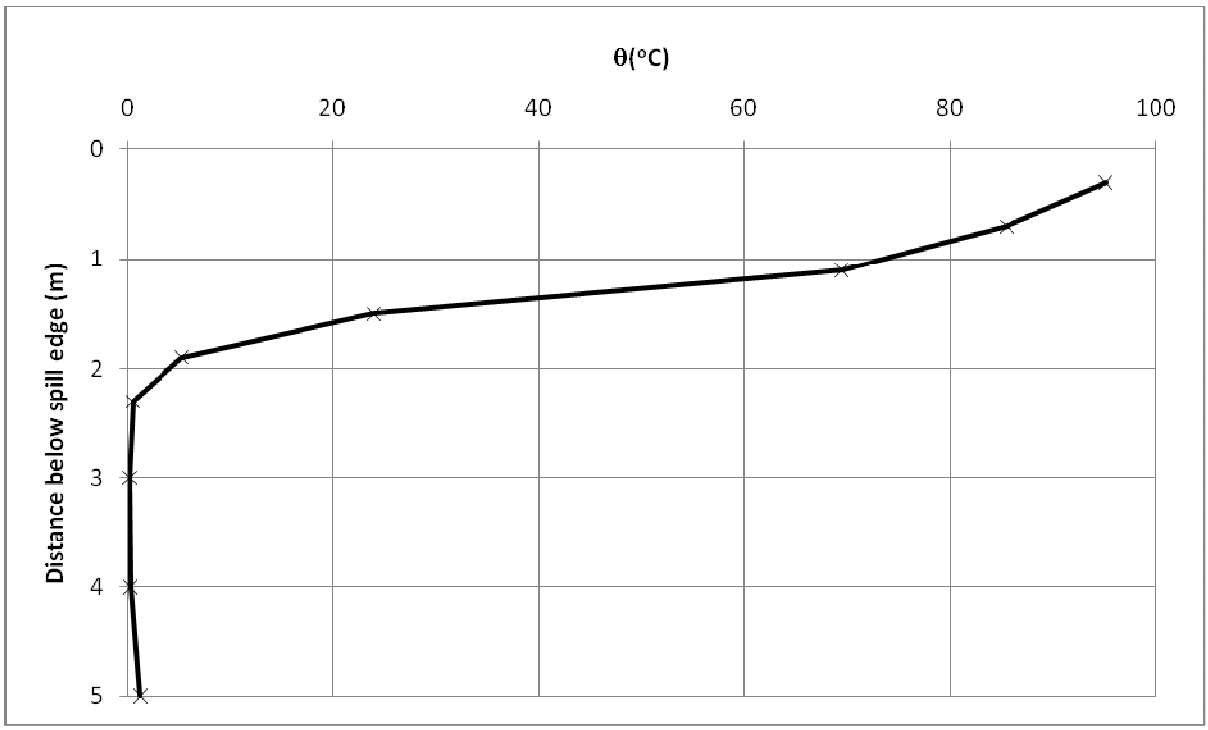

Figure D109. Temperature above ambient at the spill edge.

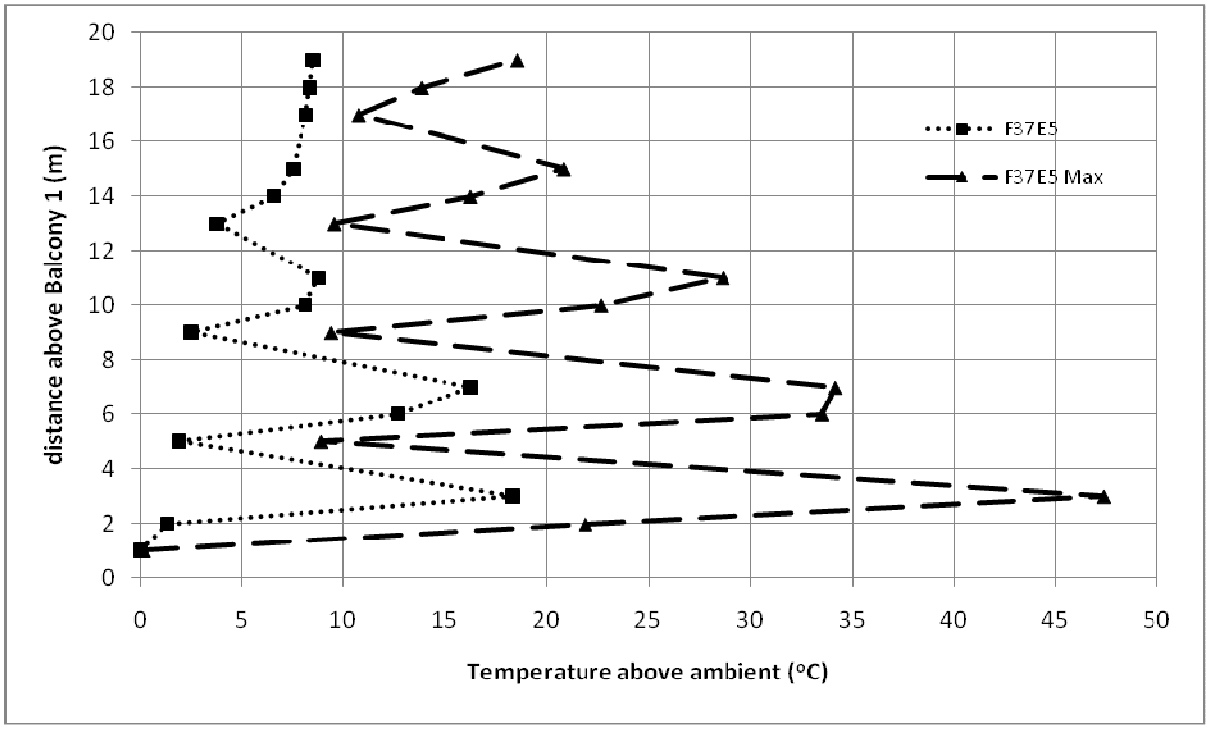

Figure D110. Temperature profiles across balcony edge.

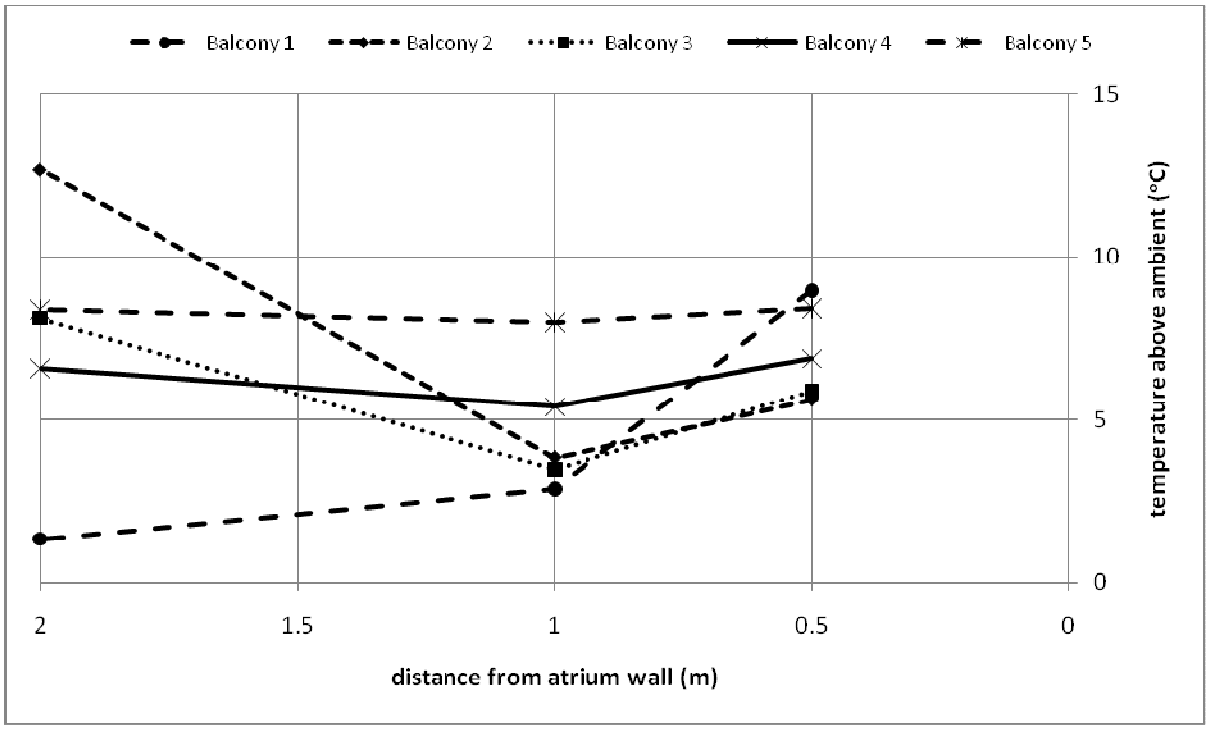

Figure D111. Temperature profiles along balcony breadth.

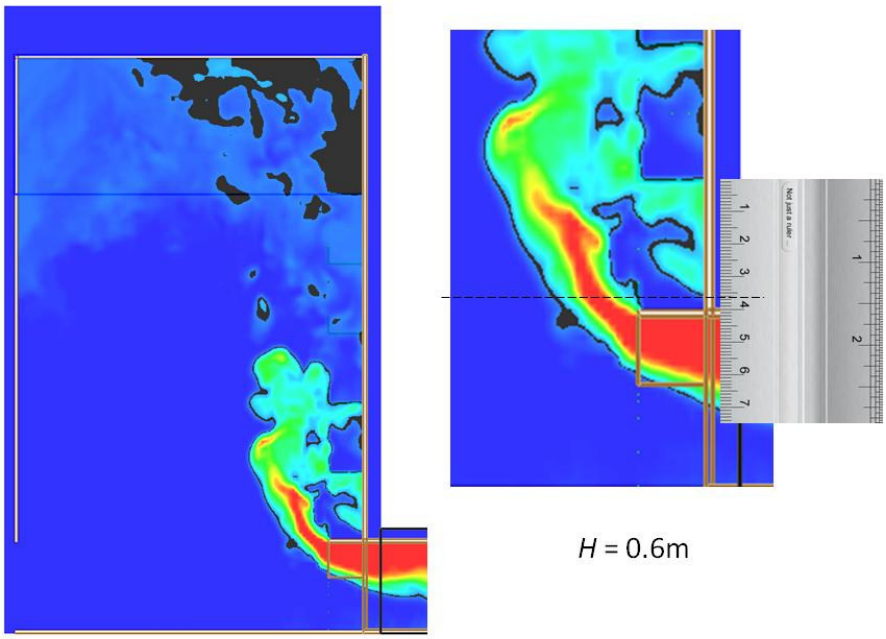

Figure D112. Smoke layer height measurement.

Full scale for 5 balcony (F38E5)

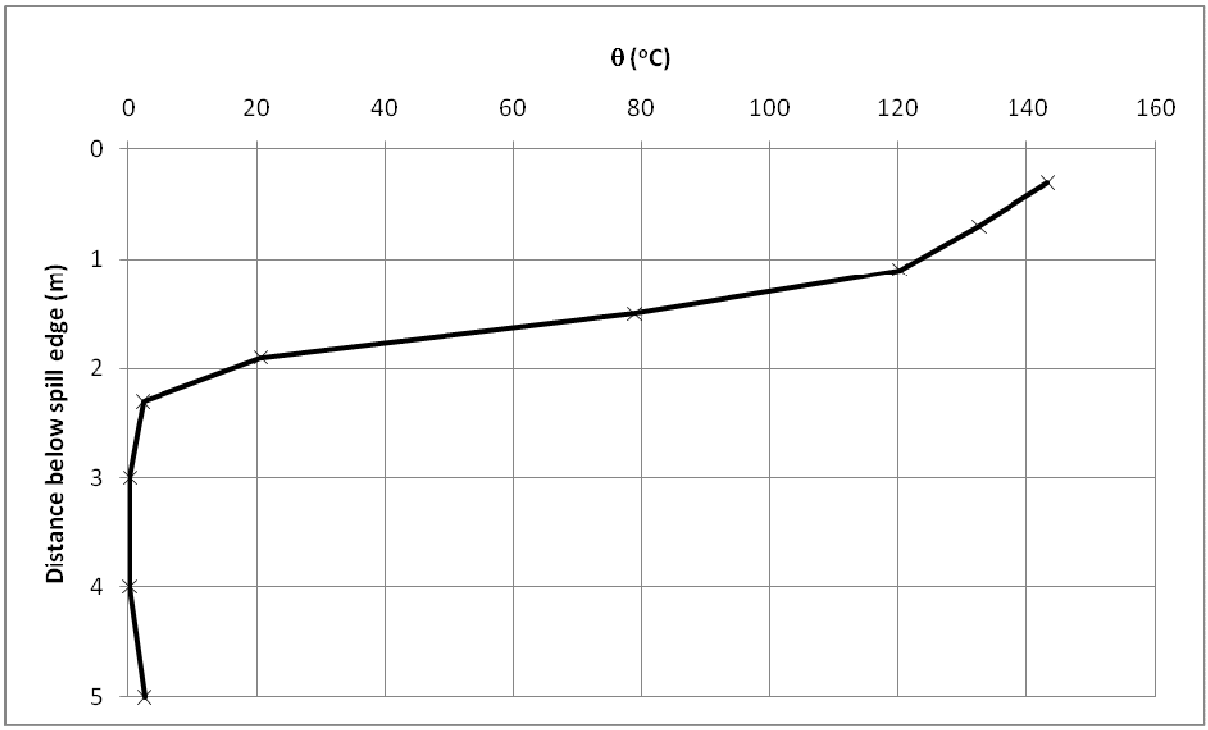

Figure D113. Temperature above ambient at the spill edge.

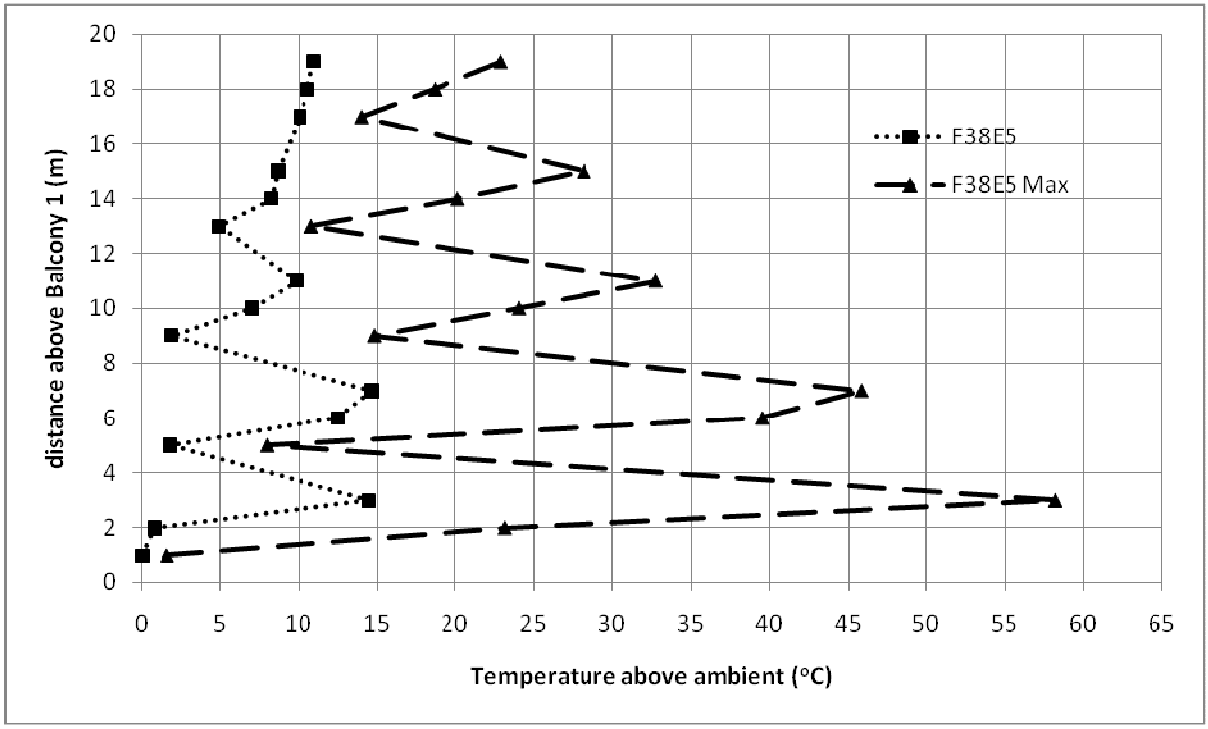

Figure D114. Temperature profiles across balcony edge.

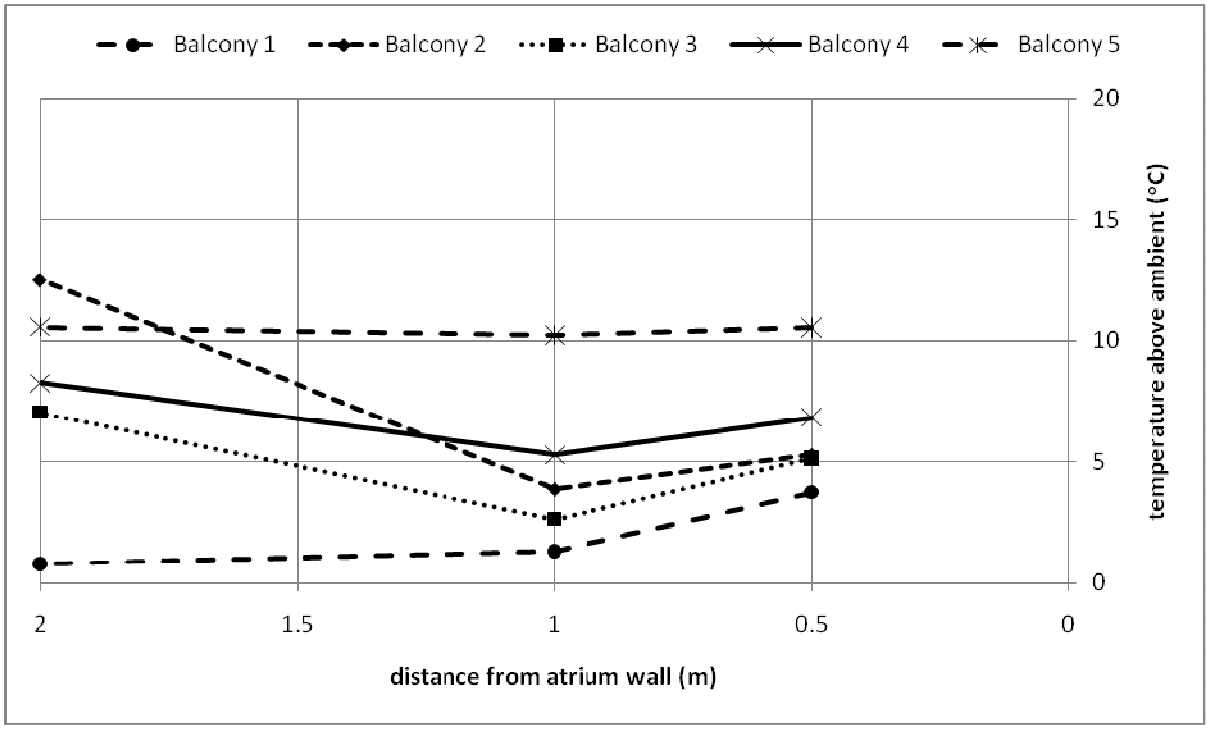

Figure D115. Temperature profiles along balcony breadth.

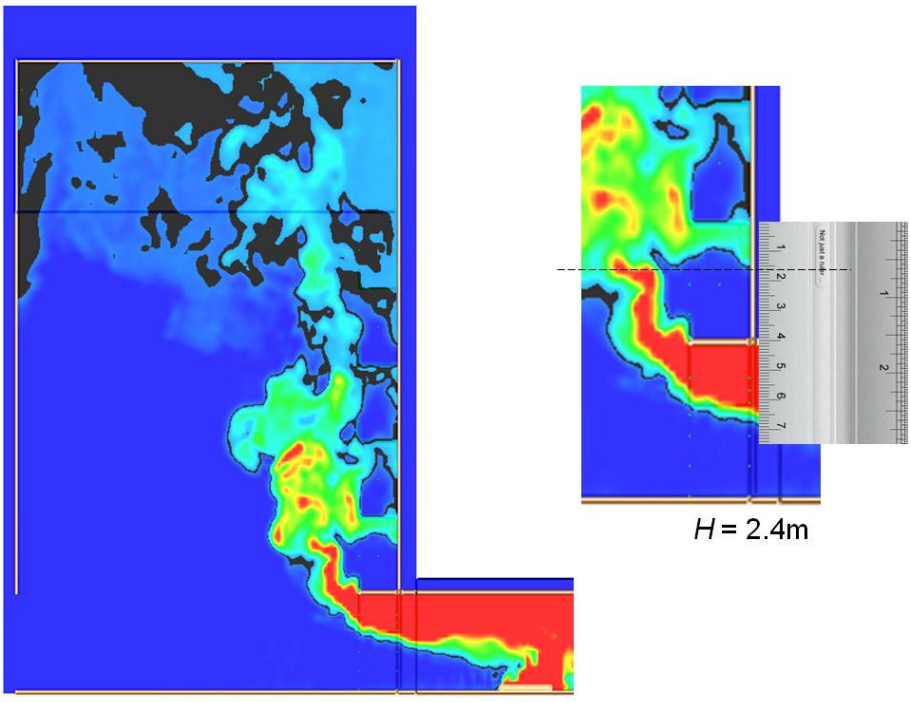

Figure D116. Smoke layer height measurement.

Full scale for 5 balcony (F39E5)

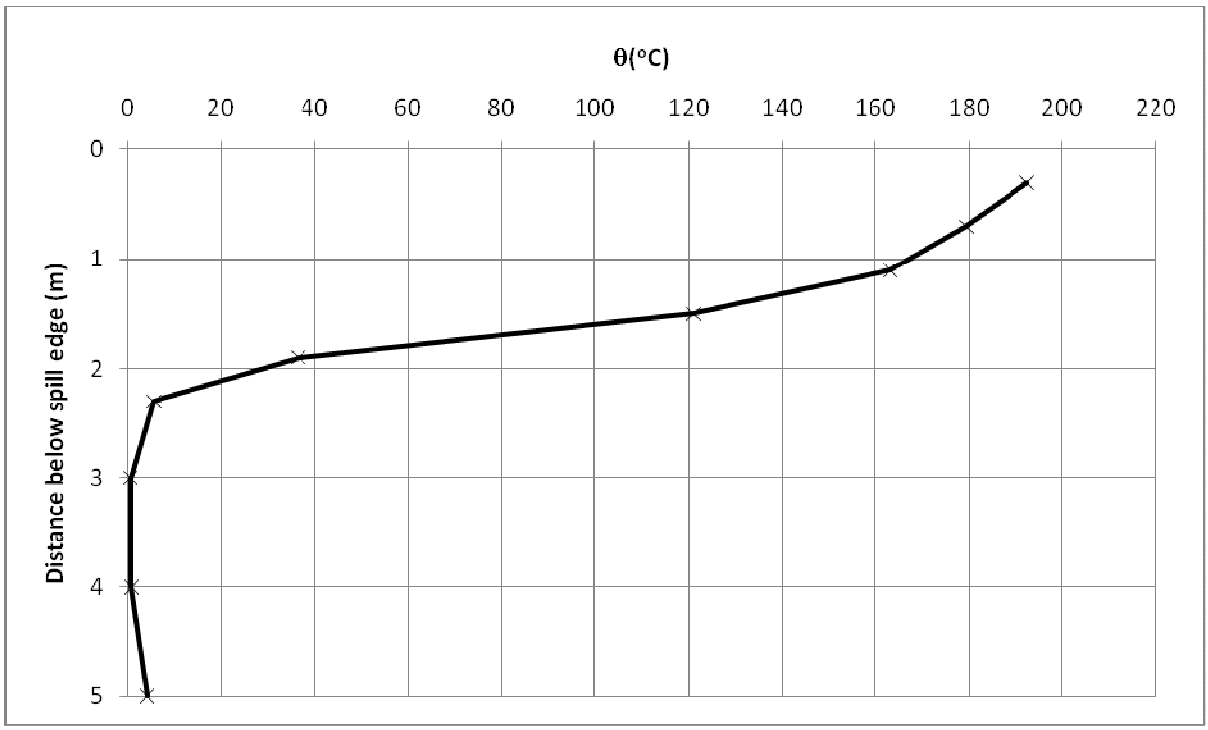

Figure D117. Temperature above ambient at the spill edge.

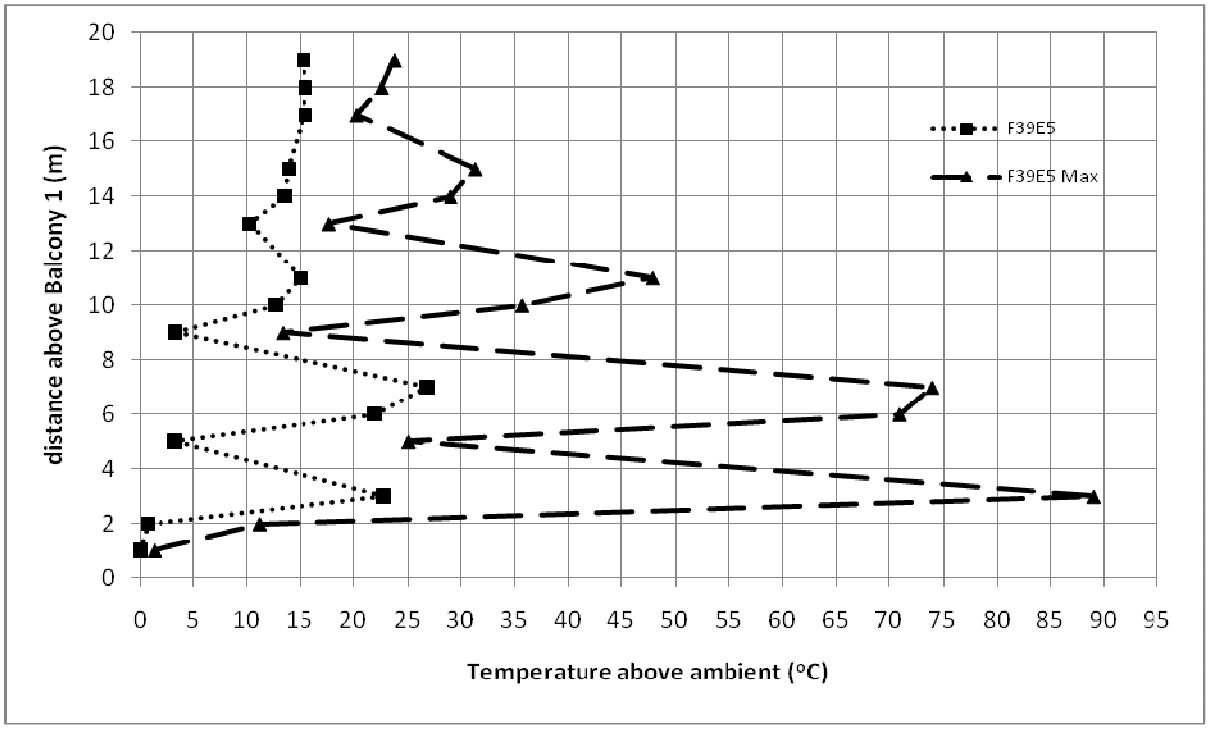

Figure D118. Temperature profiles across balcony edge.

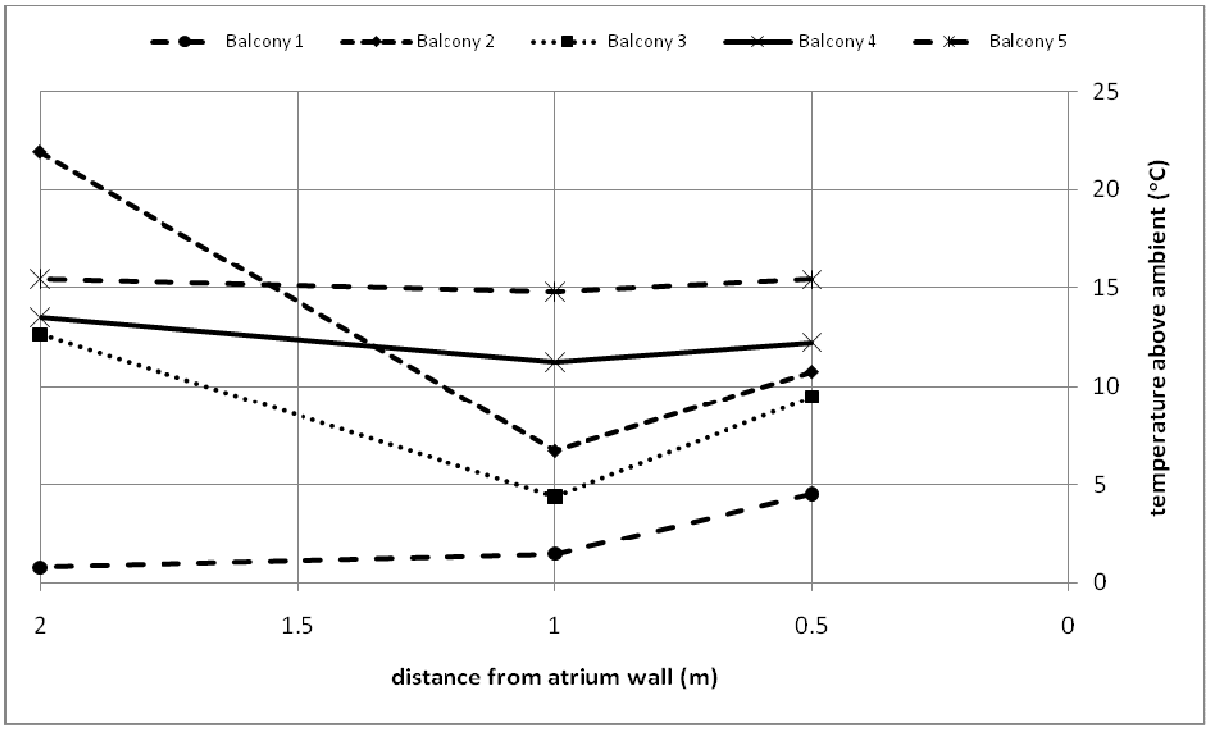

Figure D119. Temperature profiles along balcony breadth.

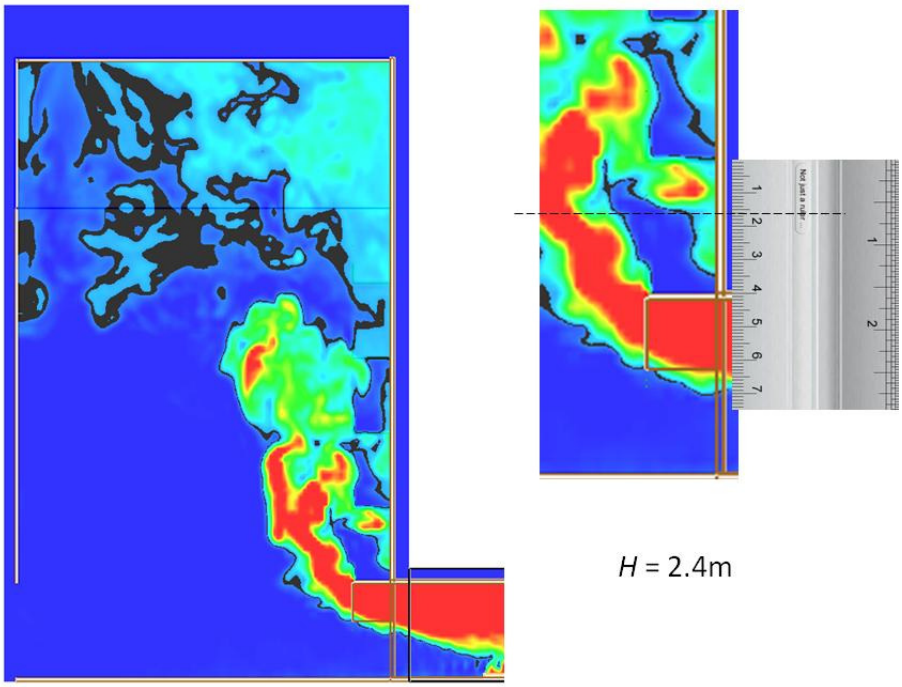

Figure D120. Smoke layer height measurement.

Full scale for 5 balcony (F40E5)

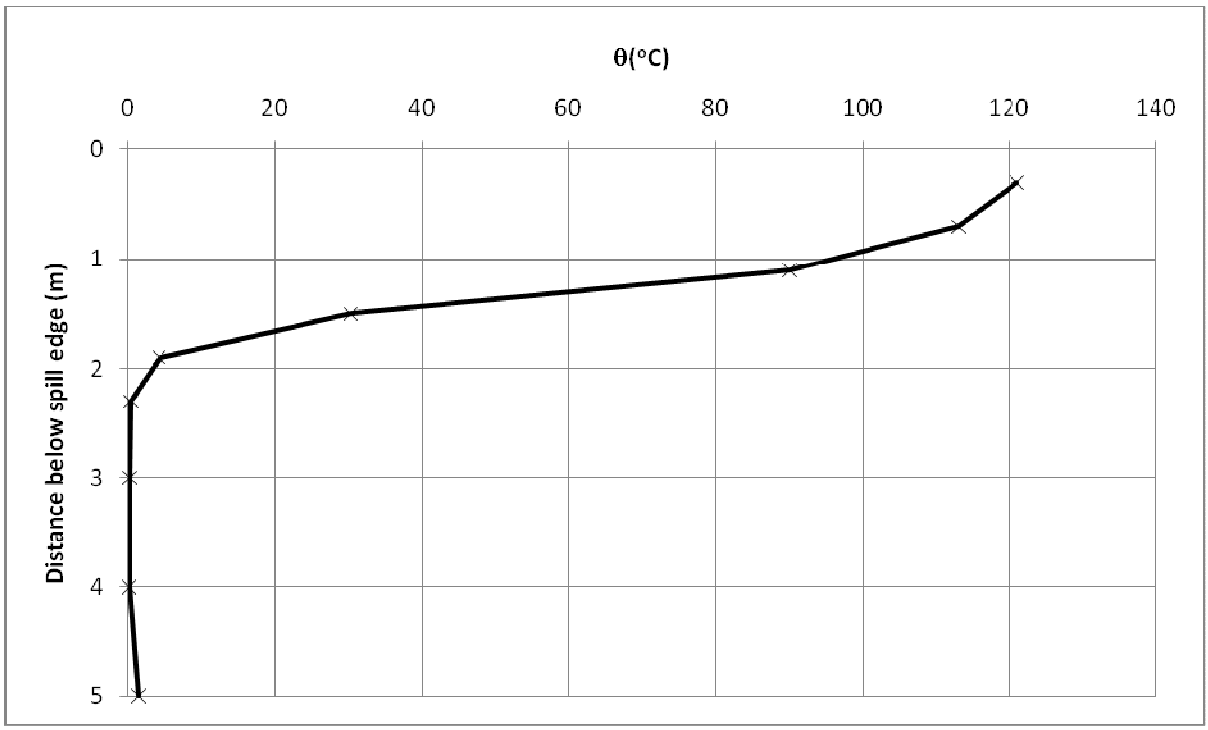

Figure D121. Temperature above ambient at the spill edge.

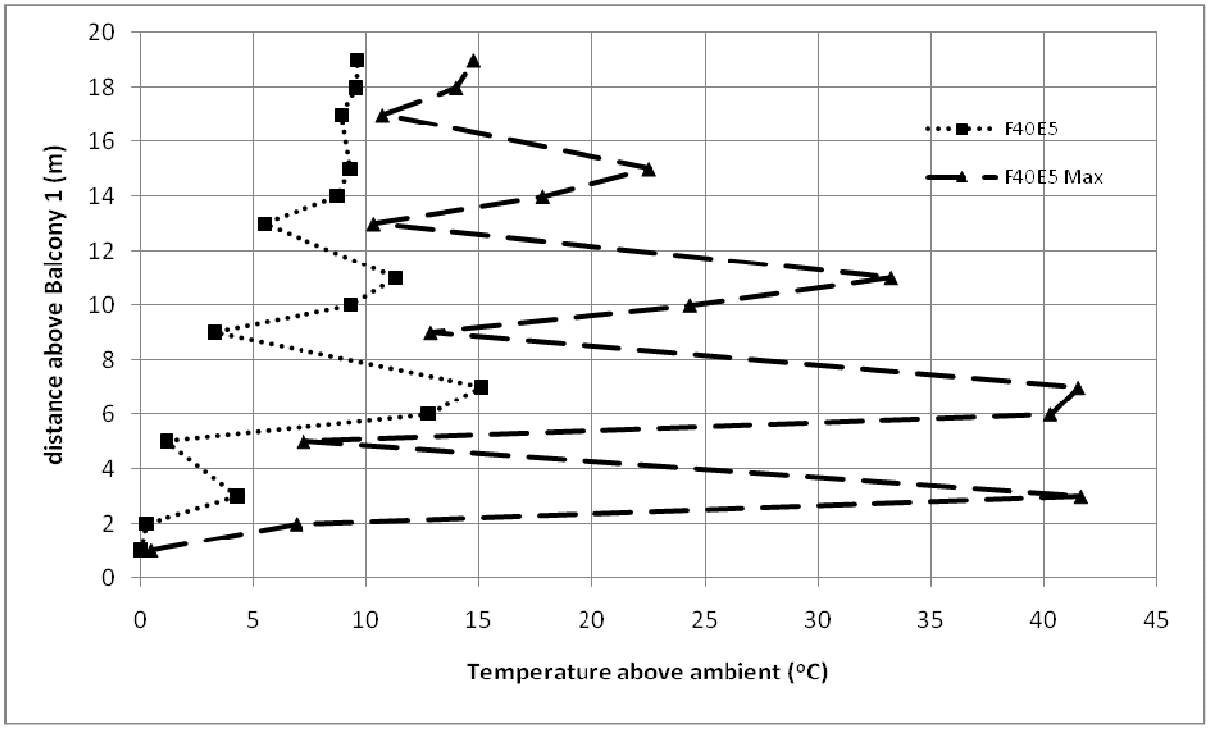

Figure D122. Temperature profiles across balcony edge.

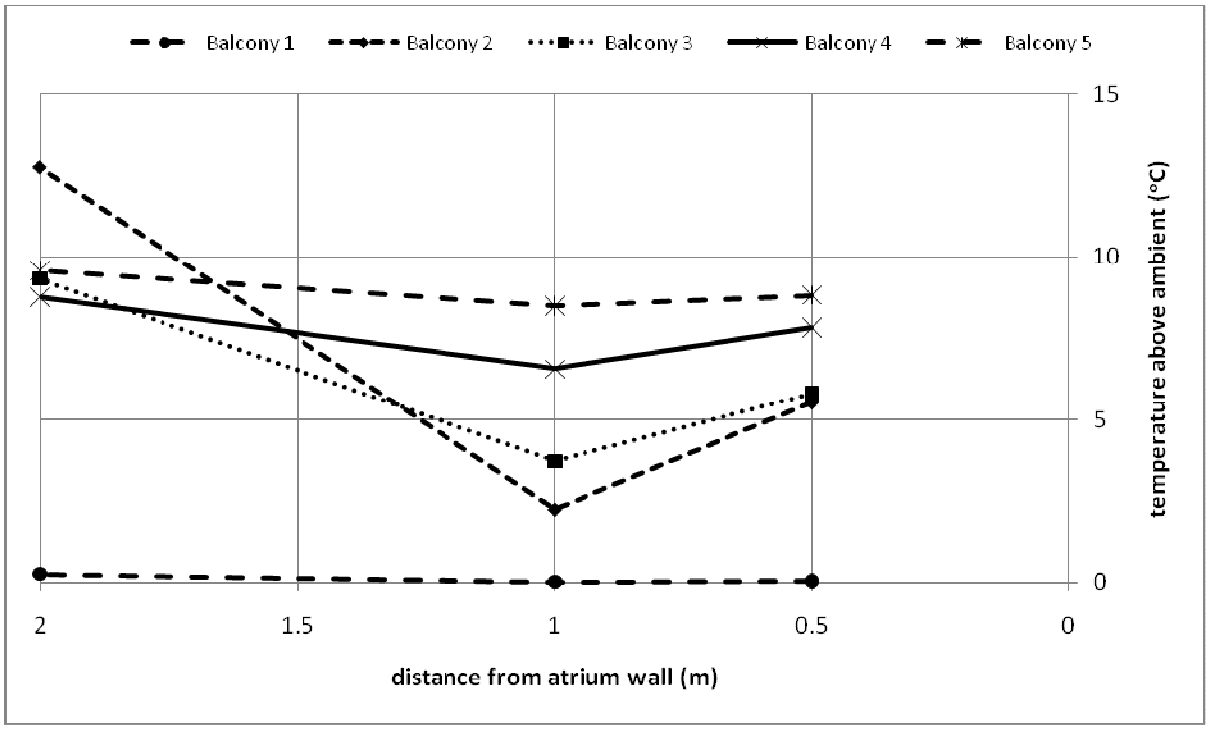

Figure D123. Temperature profiles along balcony breadth.

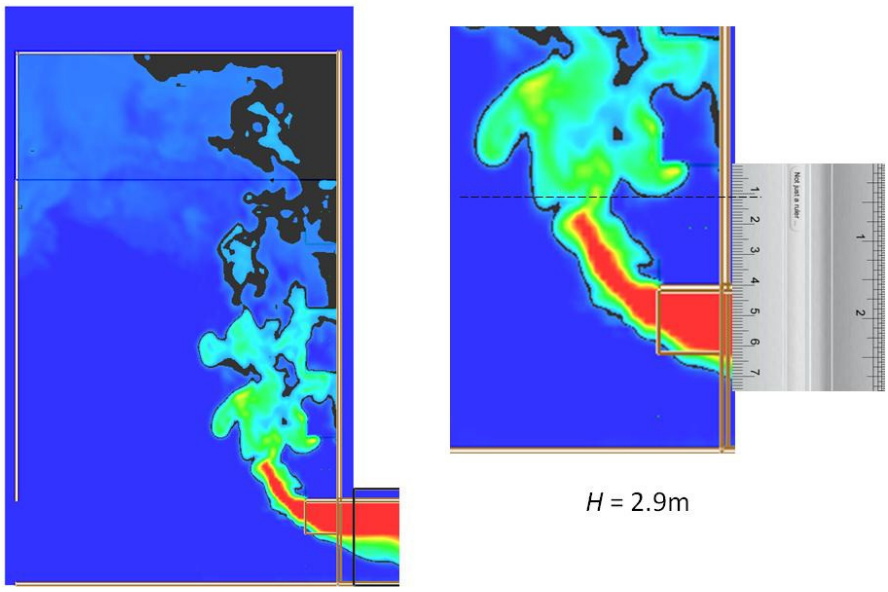

Figure D124. Smoke layer height measurement.

Full scale for 5 balcony (F41E5)

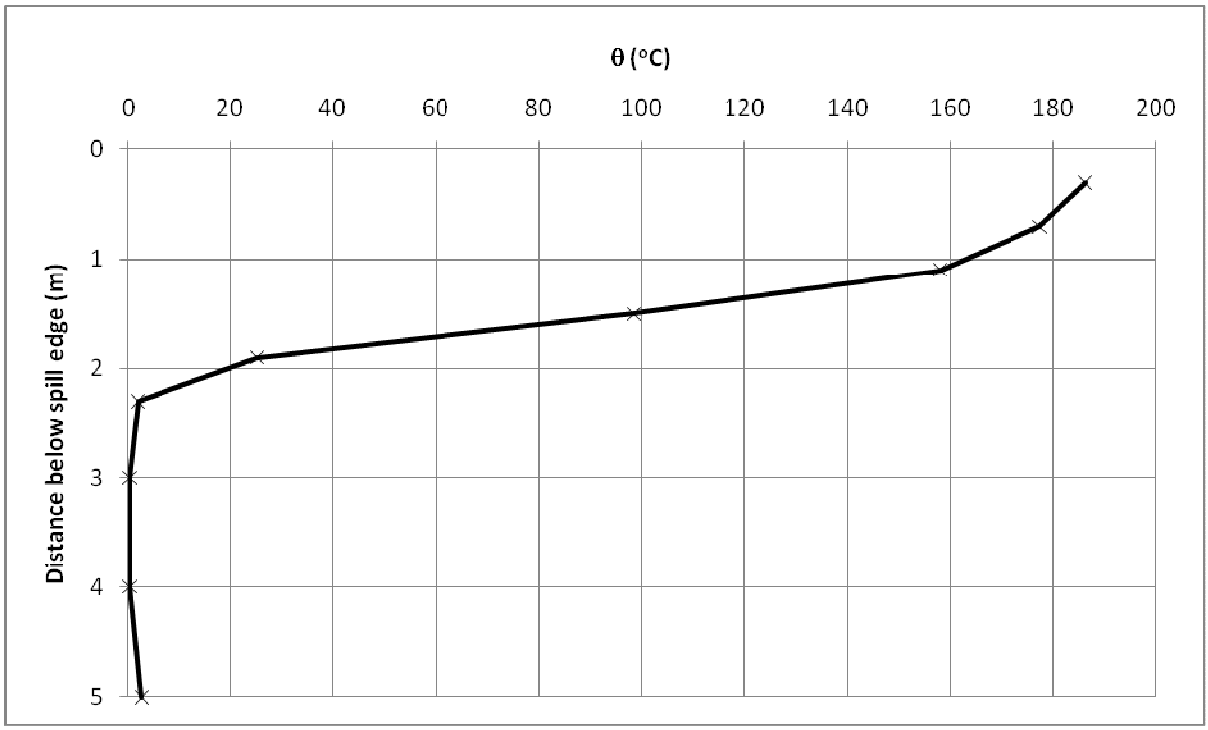

Figure D125. Temperature above ambient at the spill edge.

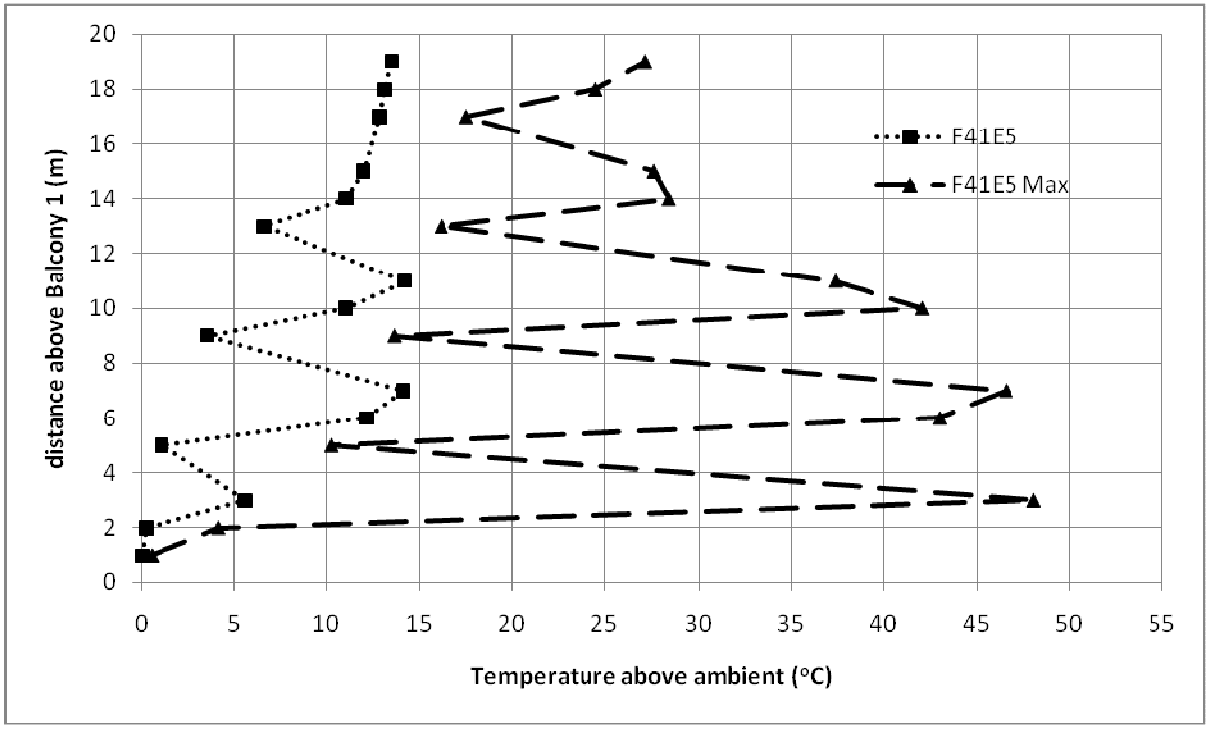

Figure D126. Temperature profiles across balcony edge.

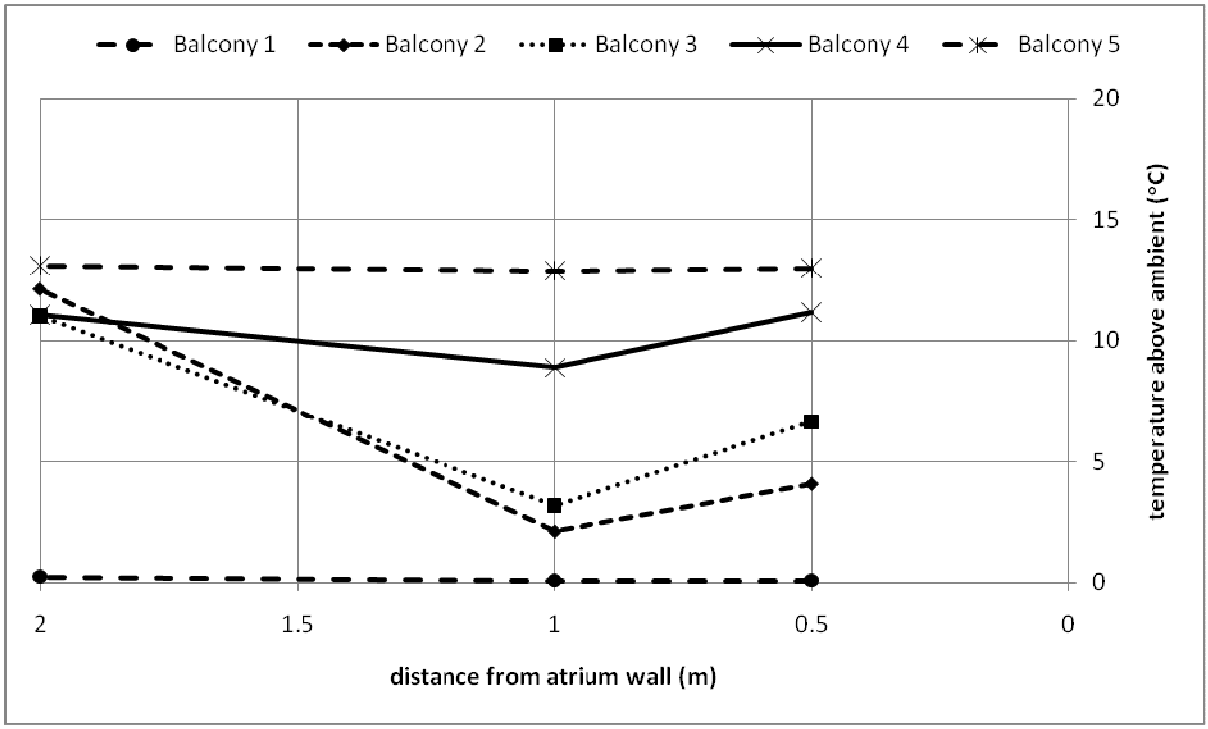

Figure D127. Temperature profiles along balcony breadth.

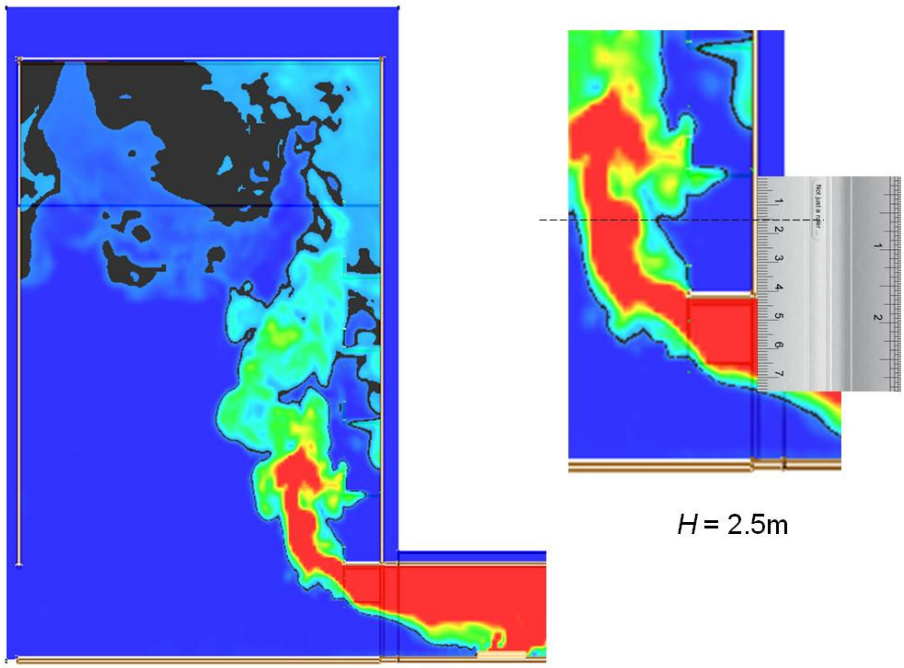

Figure D128. Smoke layer height measurement.

Full scale for 5 balcony (F42E5)

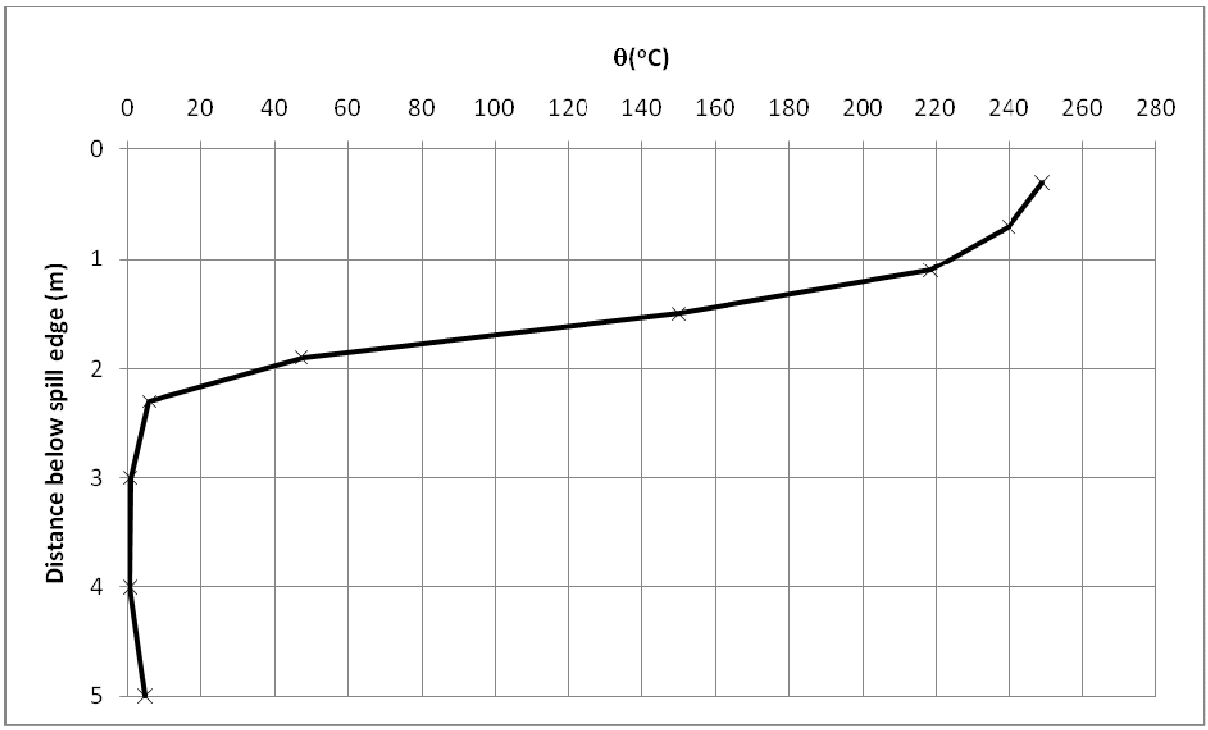

Figure D129. Temperature above ambient at the spill edge.

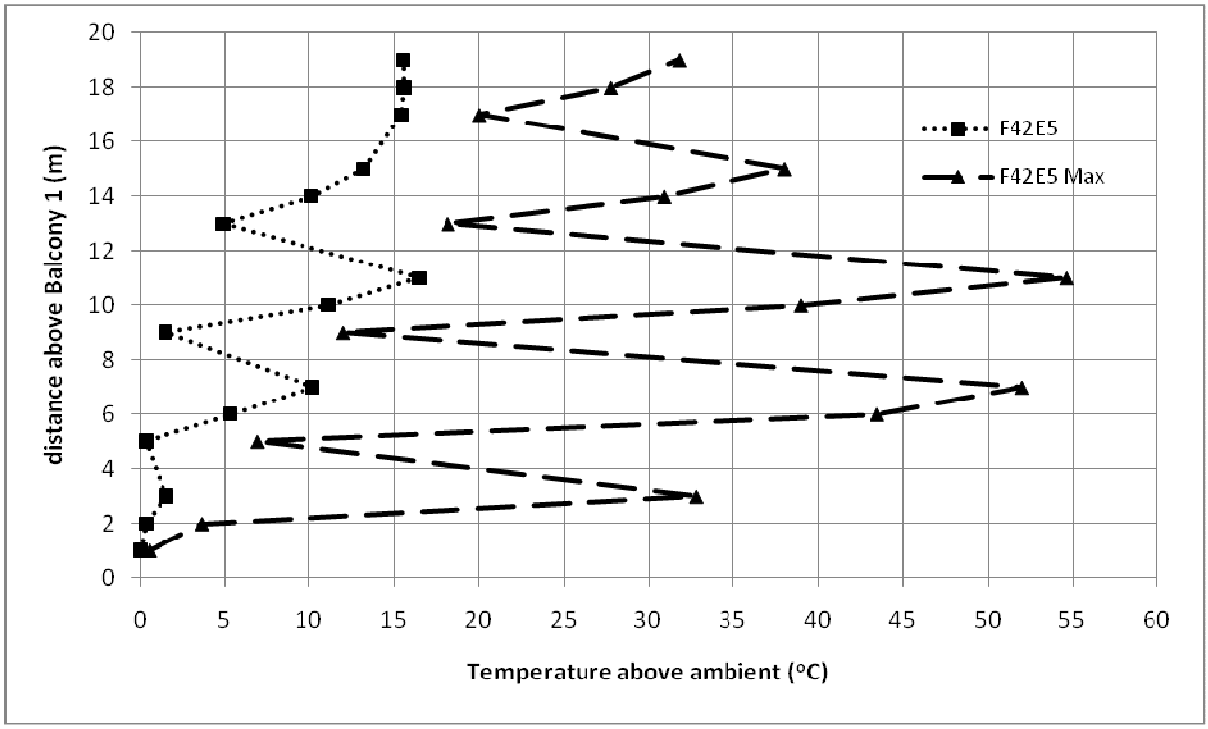

Figure D130. Temperature profiles across balcony edge.

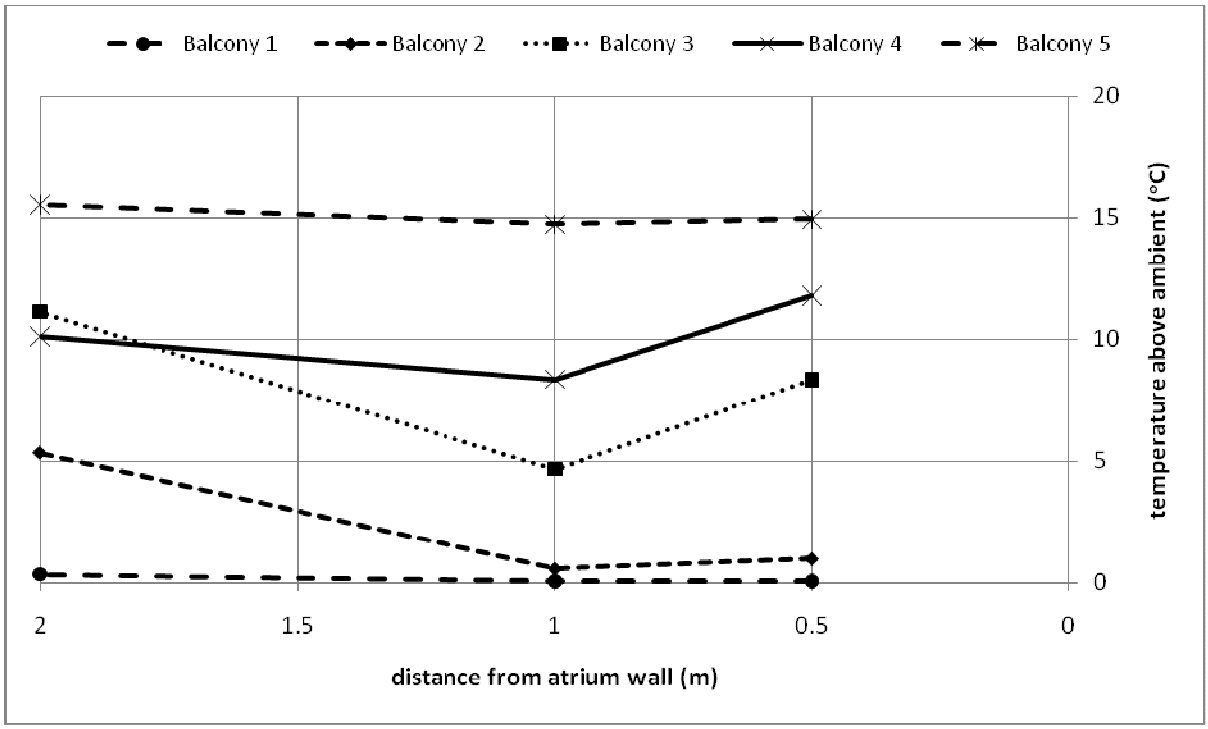

Figure D 131. Temperature profiles along balcony breadth.

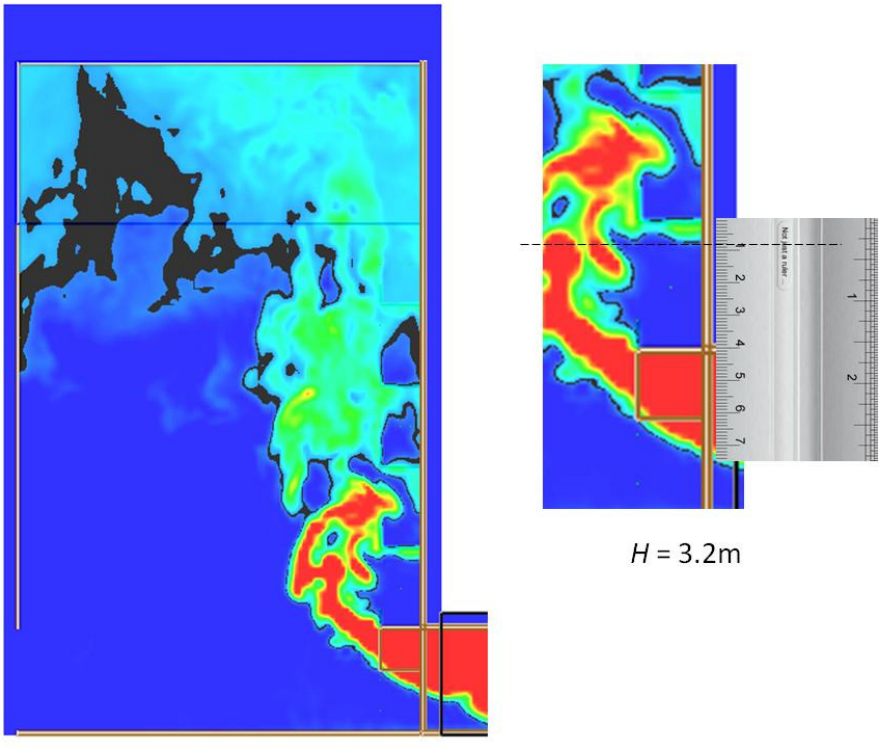

Figure D132. Smoke layer height measurement.

Full scale for 5 balcony (F43E5)

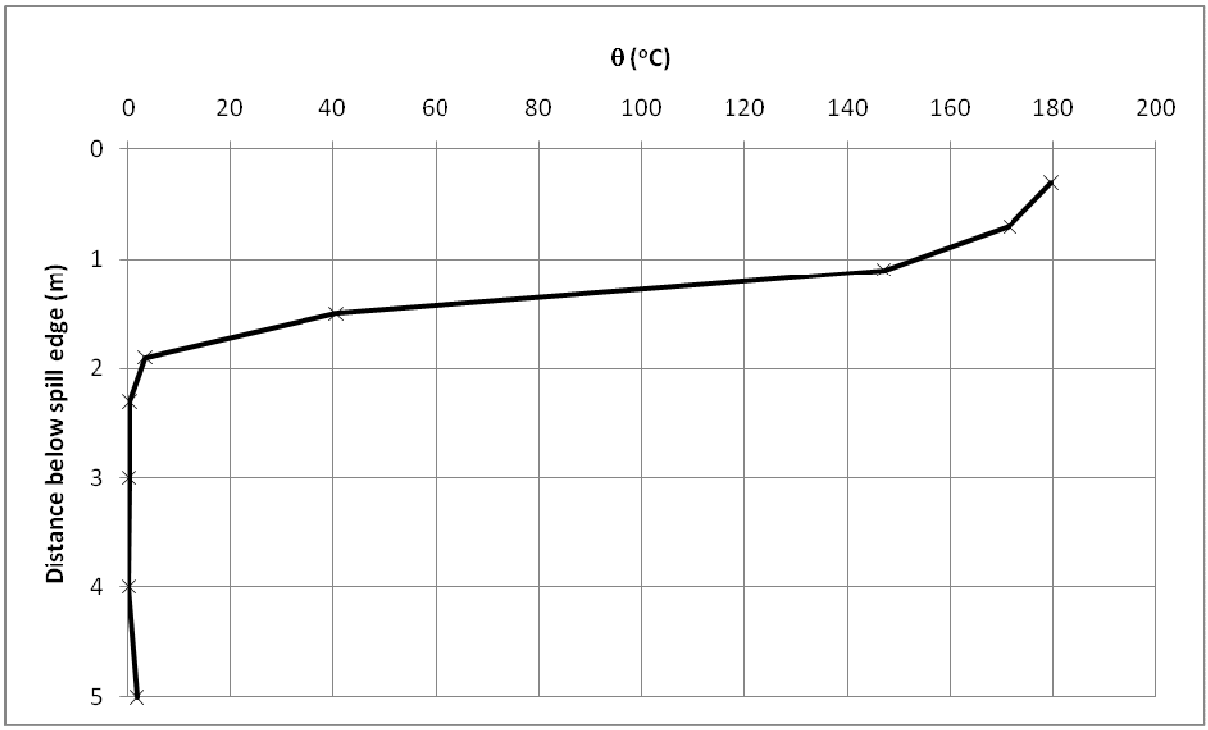

Figure D133. Temperature above ambient at the spill edge.

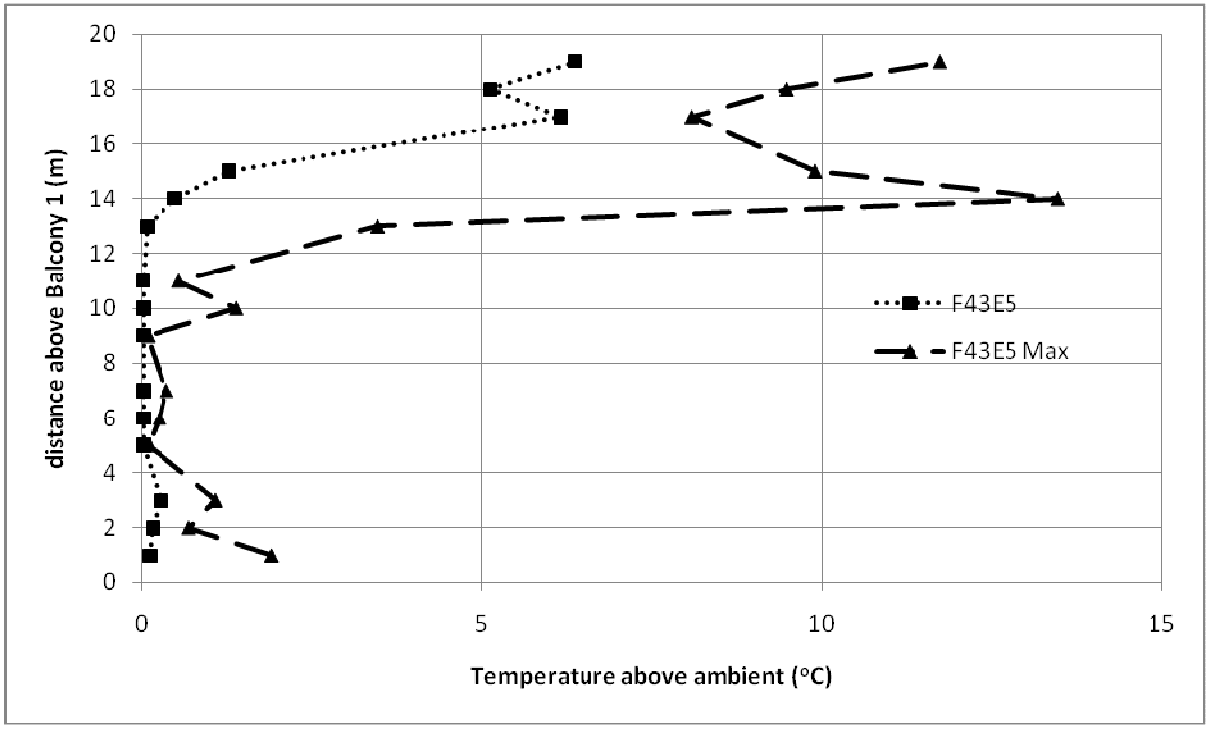

Figure D134. Temperature profiles across balcony edge.

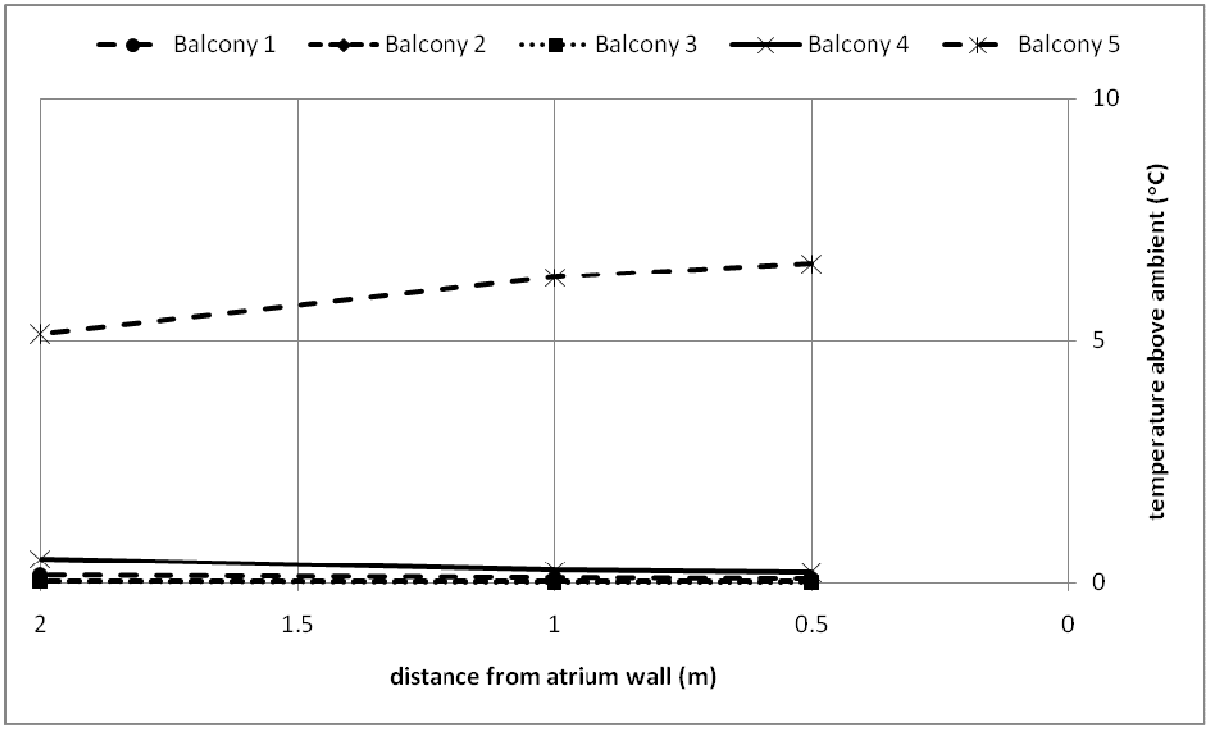

Figure D135. Temperature profiles along balcony breadth.

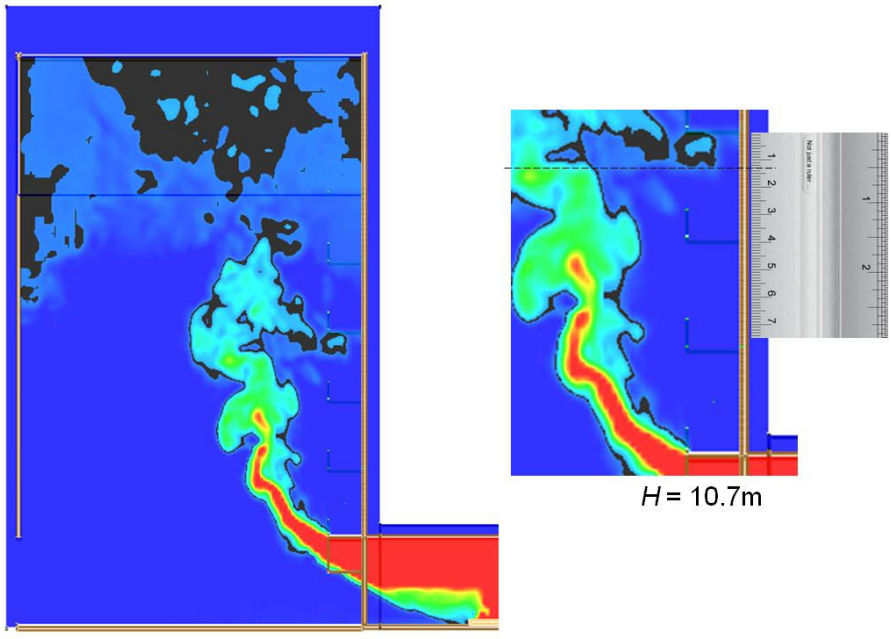

Figure D136. Smoke layer height measurement.

Full scale for 5 balcony (F44E5)

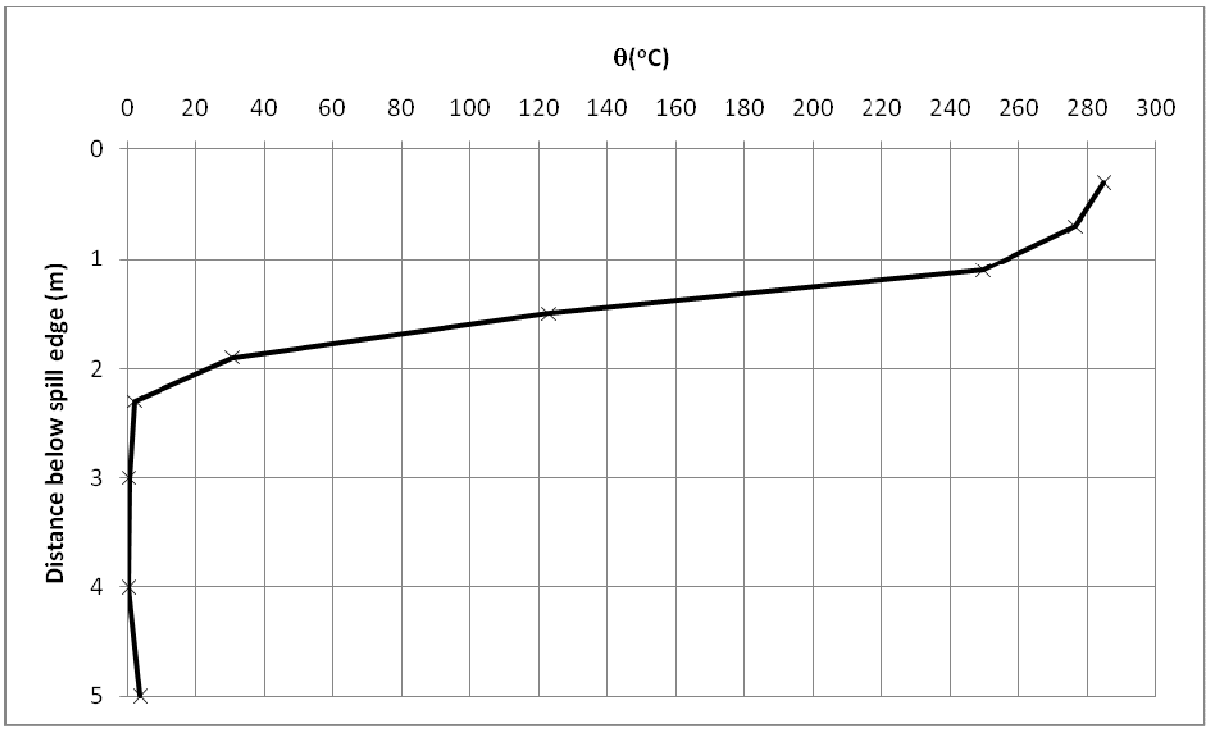

Figure D137. Temperature above ambient at the spill edge.

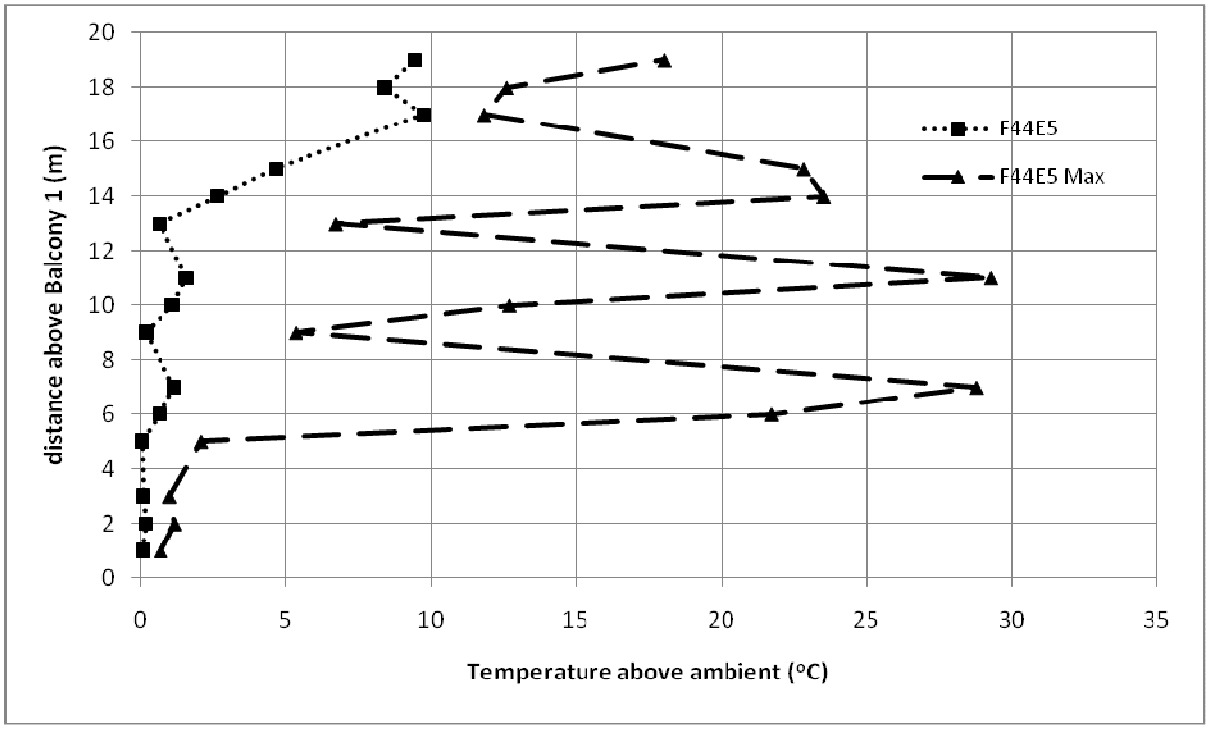

Figure D138. Temperature profiles across balcony edge.

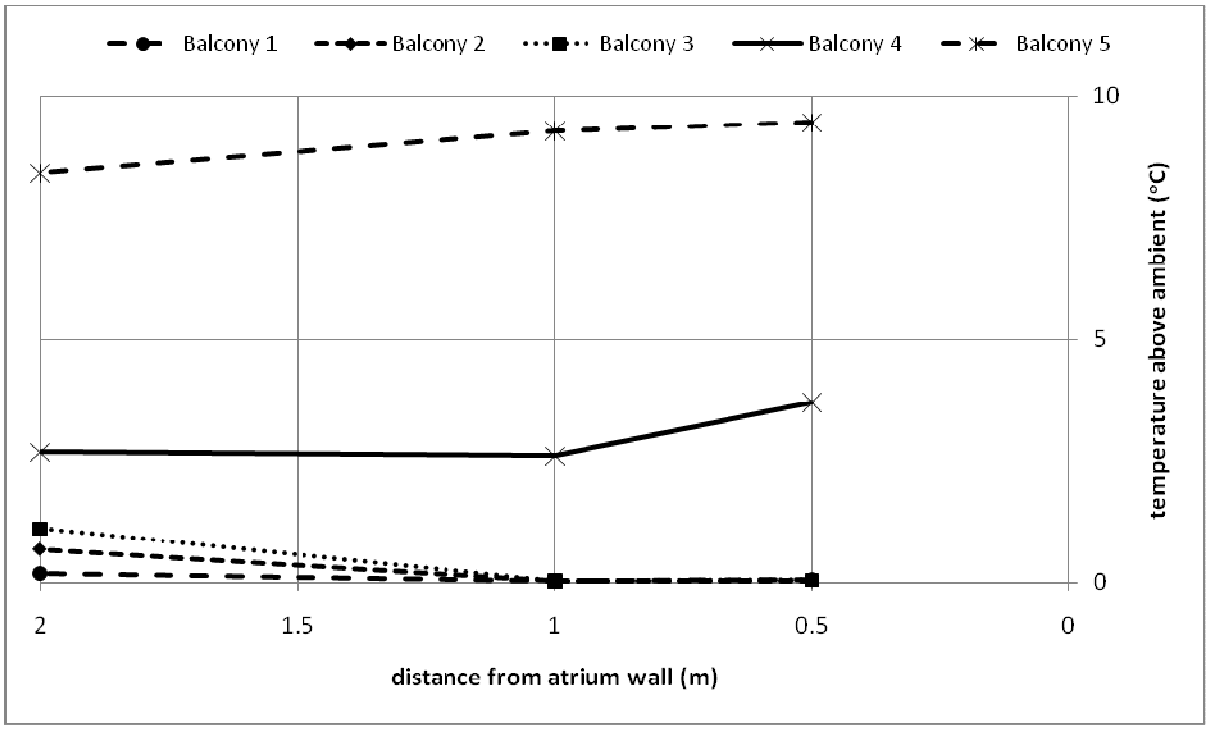

Figure D139. Temperature profiles along balcony breadth.

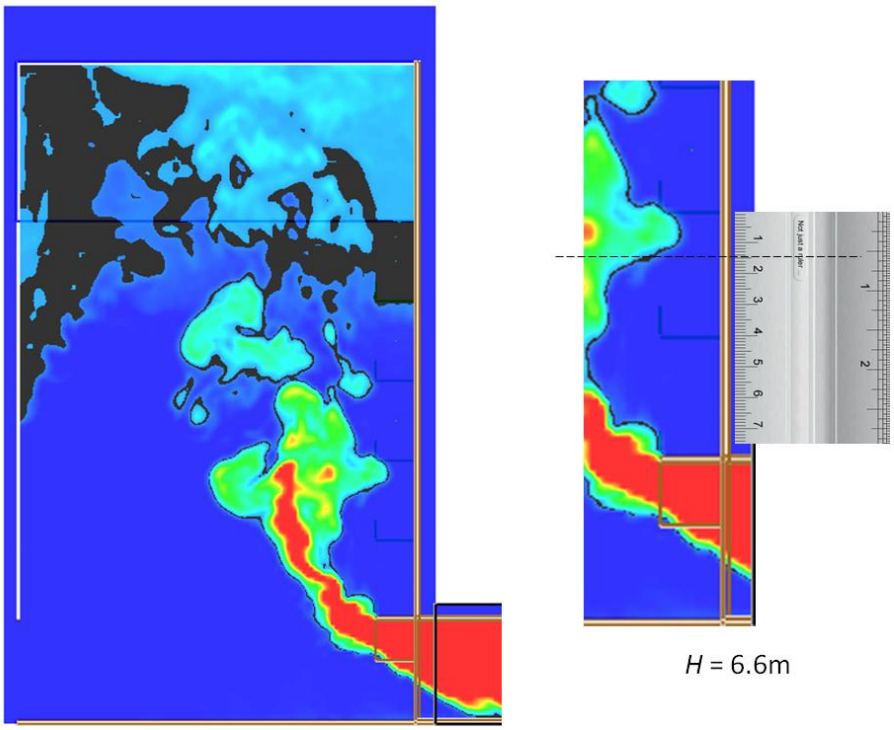

Figure D140. Smoke layer height measurement.

Full scale for 5 balcony (F45E5)

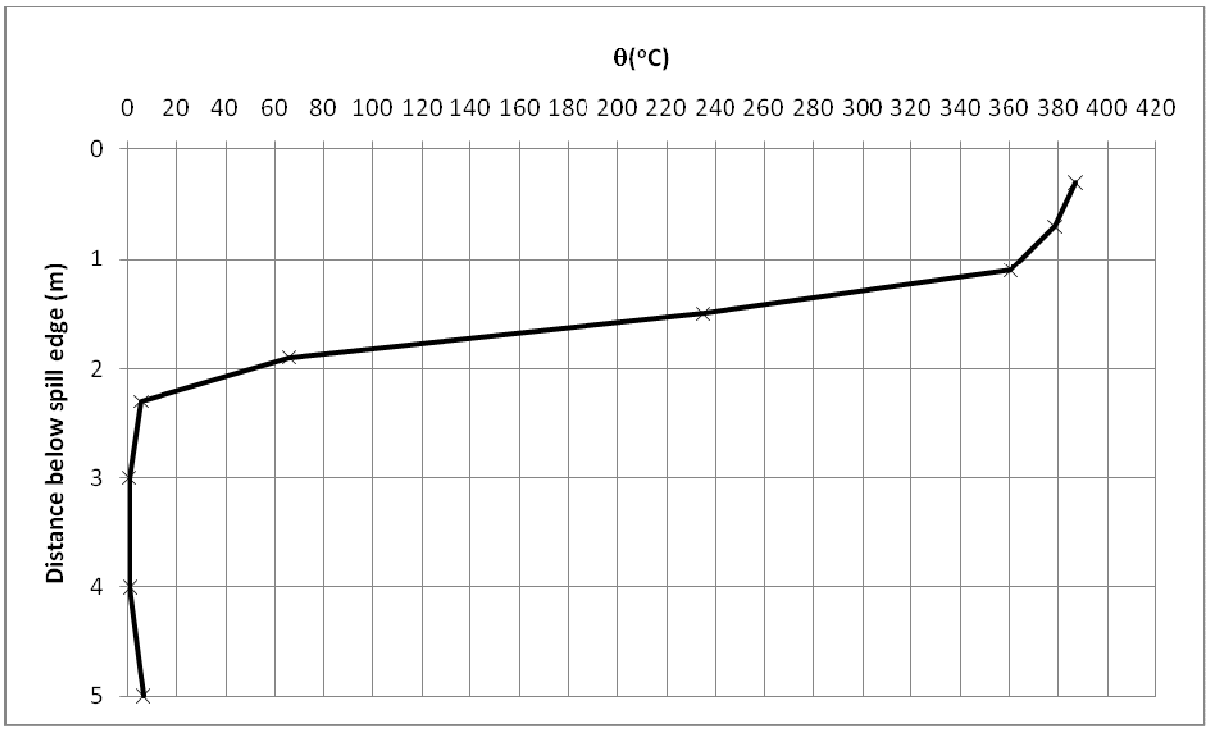

Figure D141. Temperature above ambient at the spill edge.

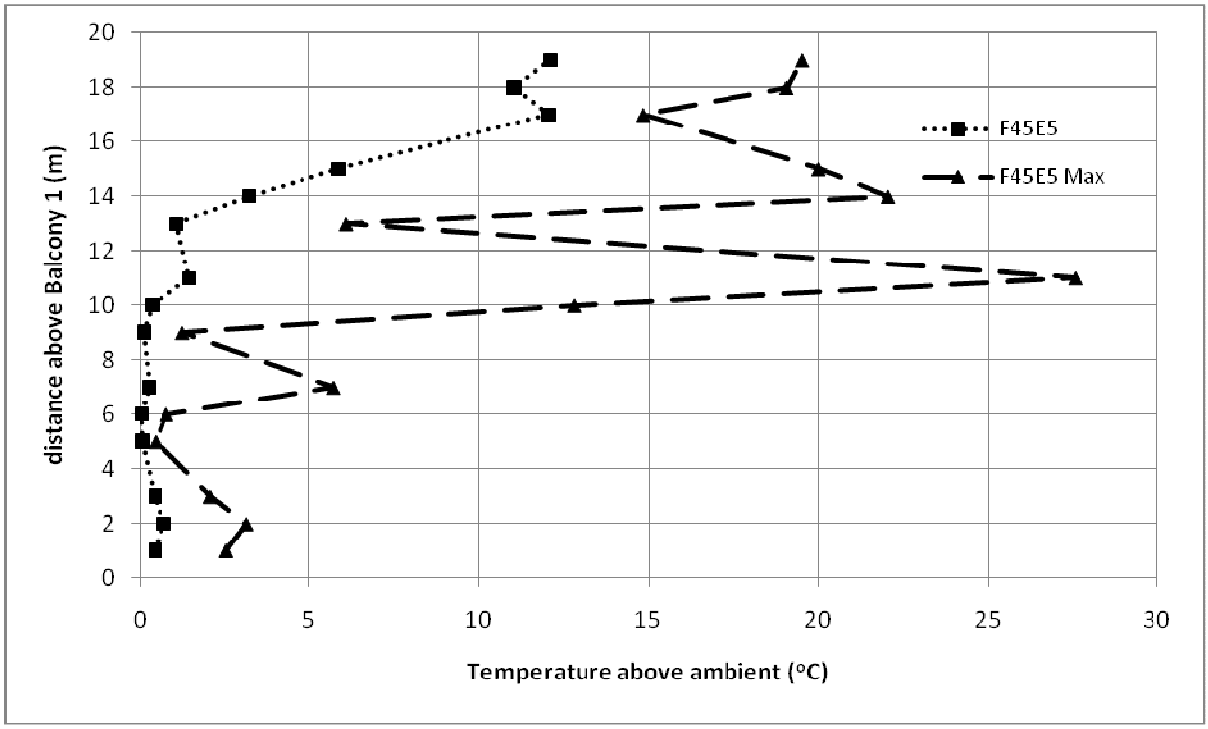

Figure D142. Temperature profiles across balcony edge.

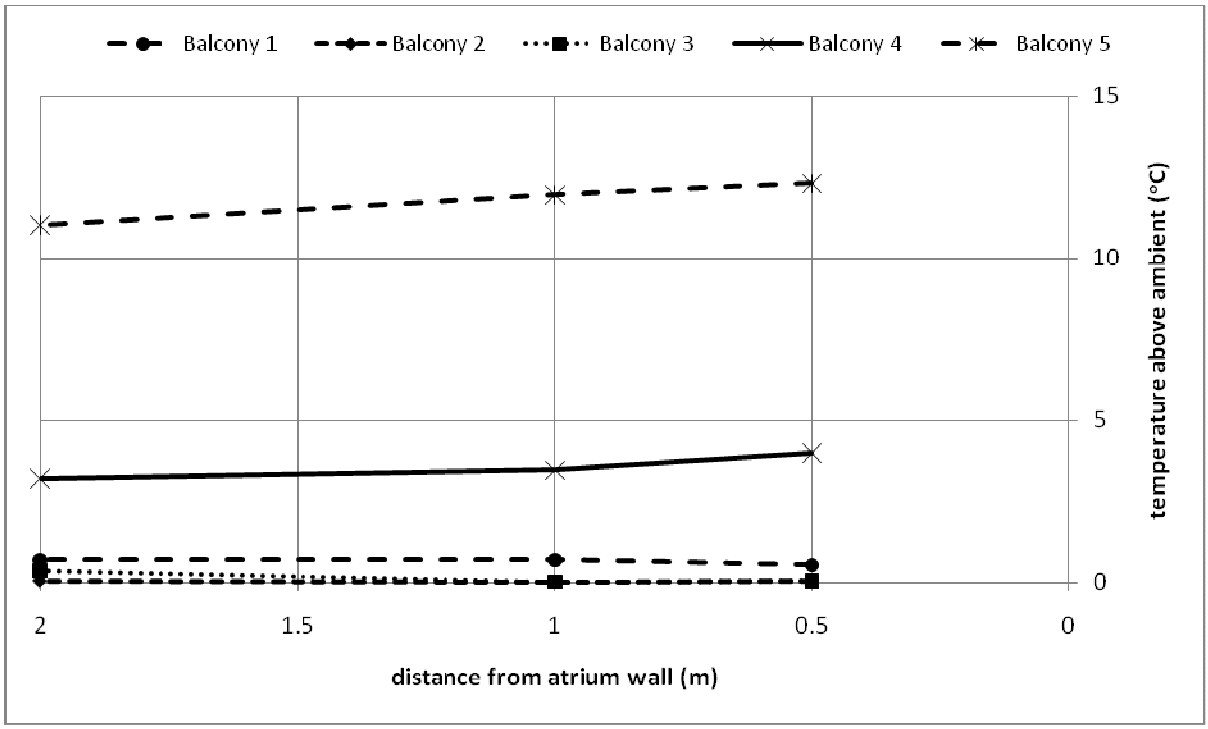

Figure D143. Temperature profiles along balcony breadth.

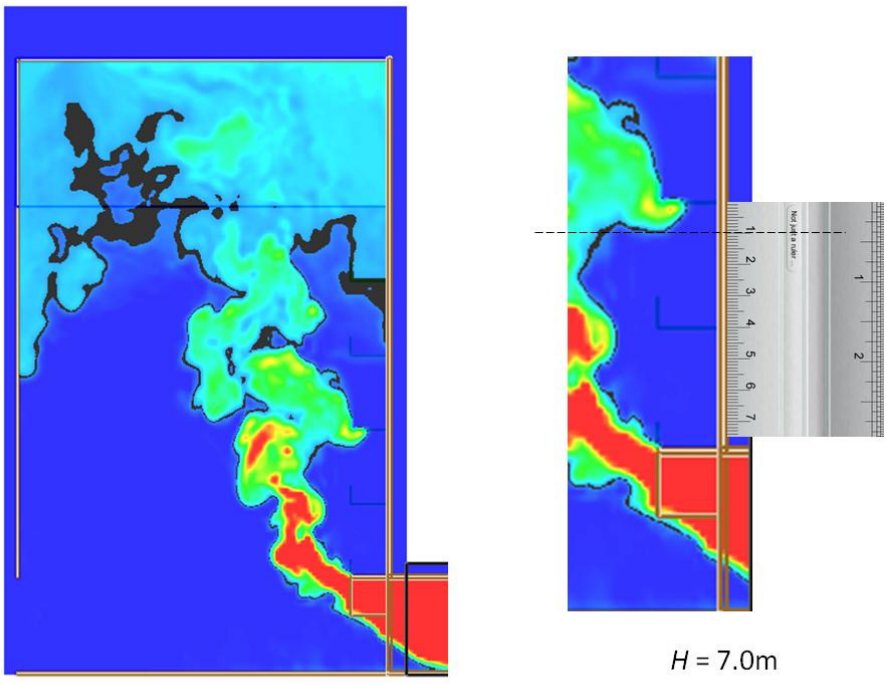

Figure D144. Smoke layer height measurement.

Full scale for 5 balcony (F55E5)

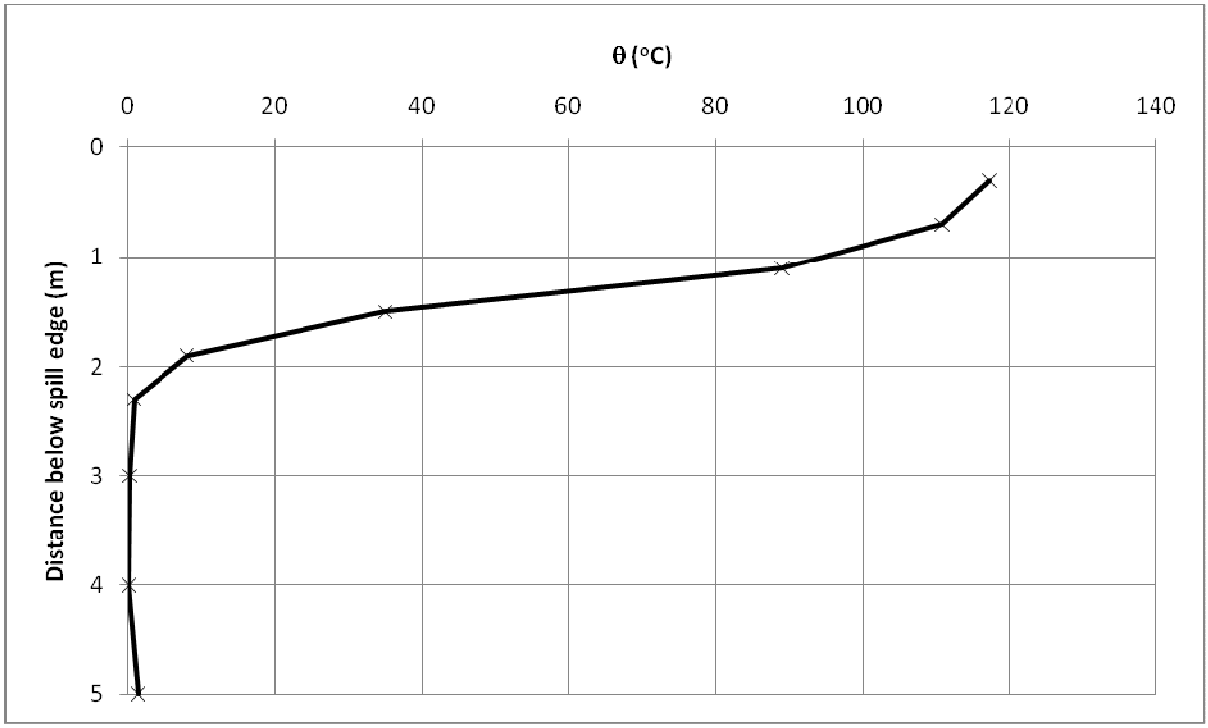

Figure D145. Temperature above ambient at the spill edge.

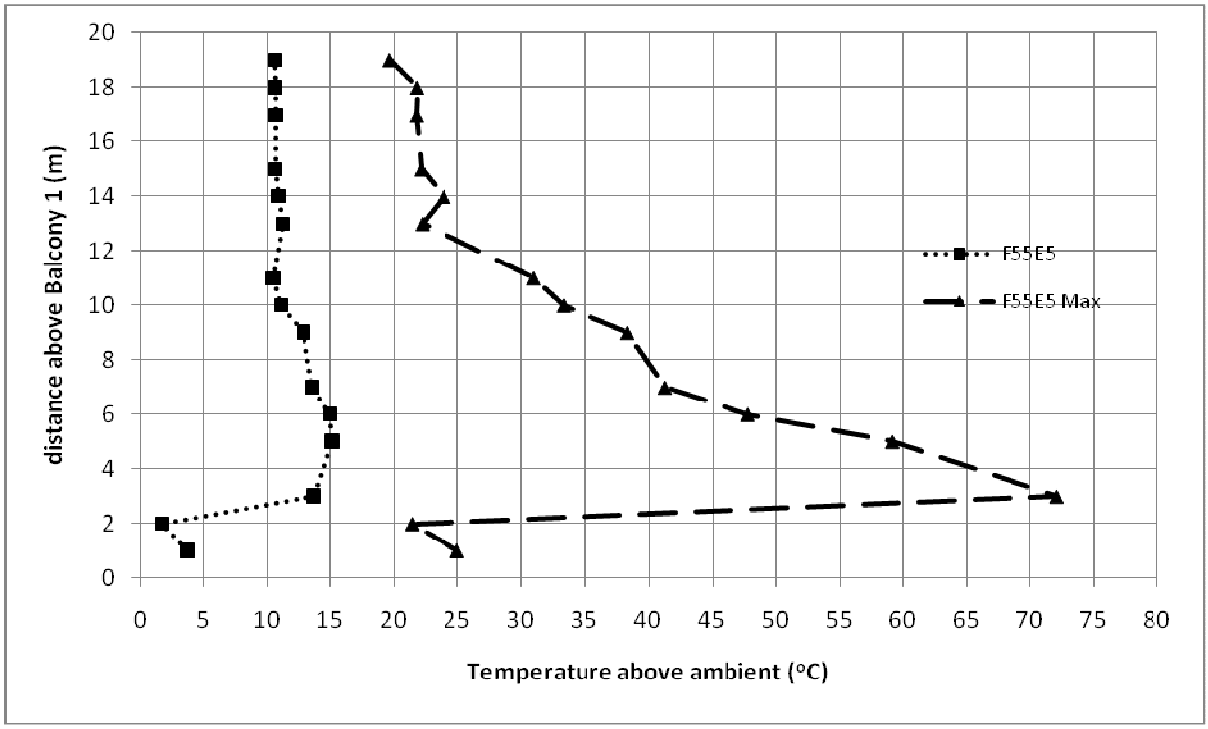

Figure D146. Temperature profiles across balcony edge.

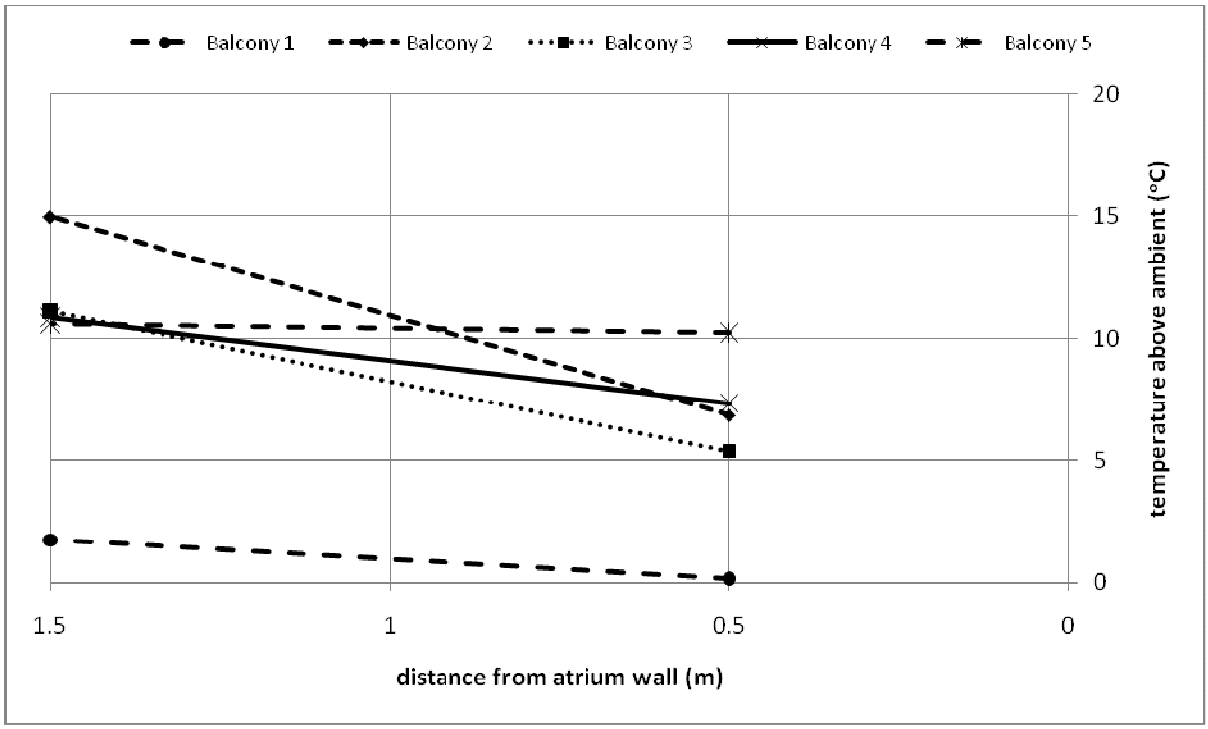

Figure D147. Temperature profiles along balcony breadth.

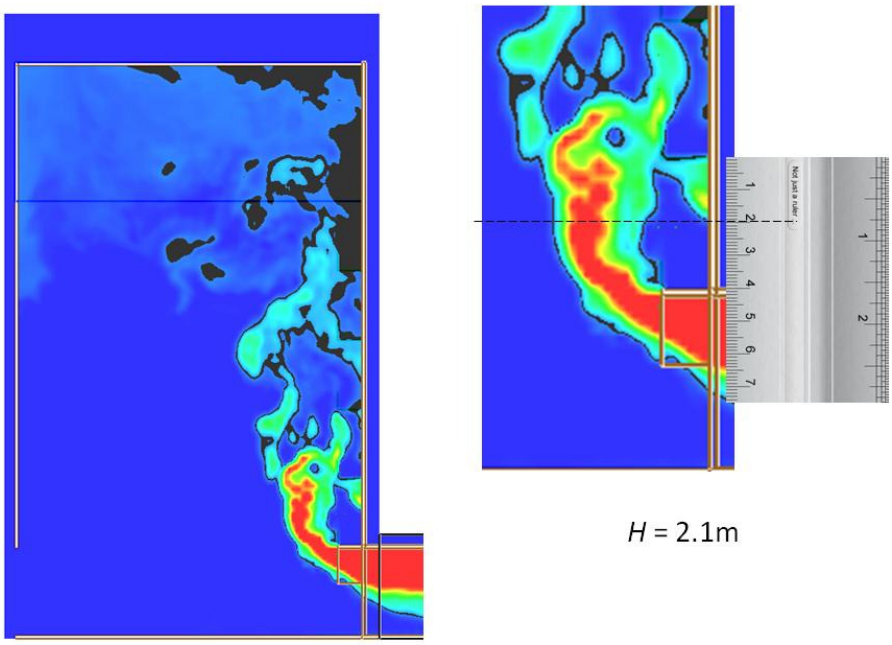

Figure D148. Smoke layer height measurement.

Full scale for 5 balcony (F56E5)

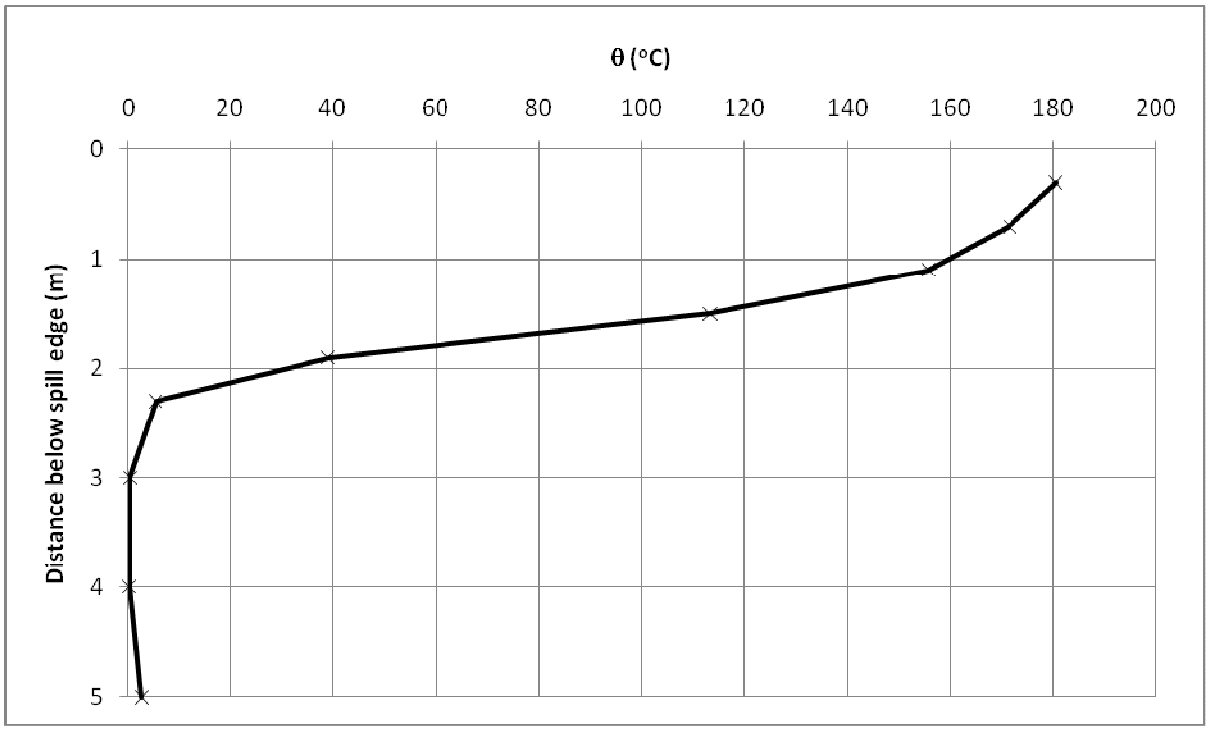

Figure D149. Temperature above ambient at the spill edge.

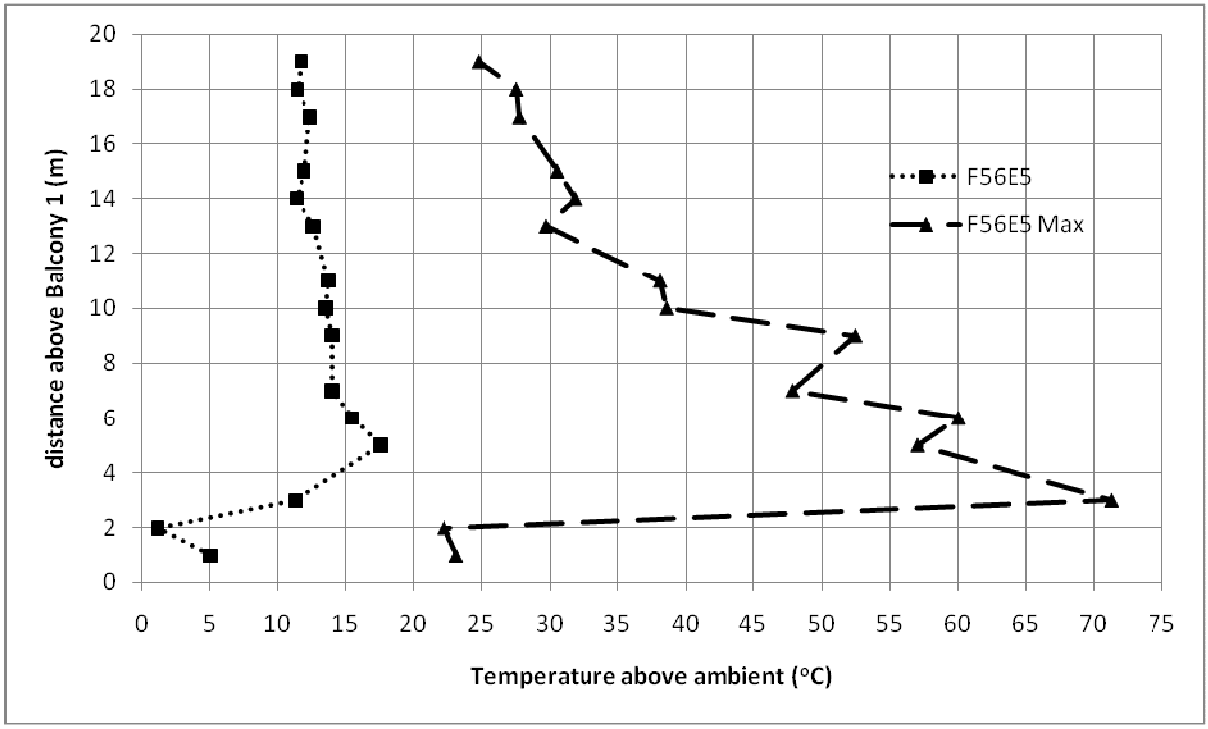

Figure D150. Temperature profiles across balcony edge.

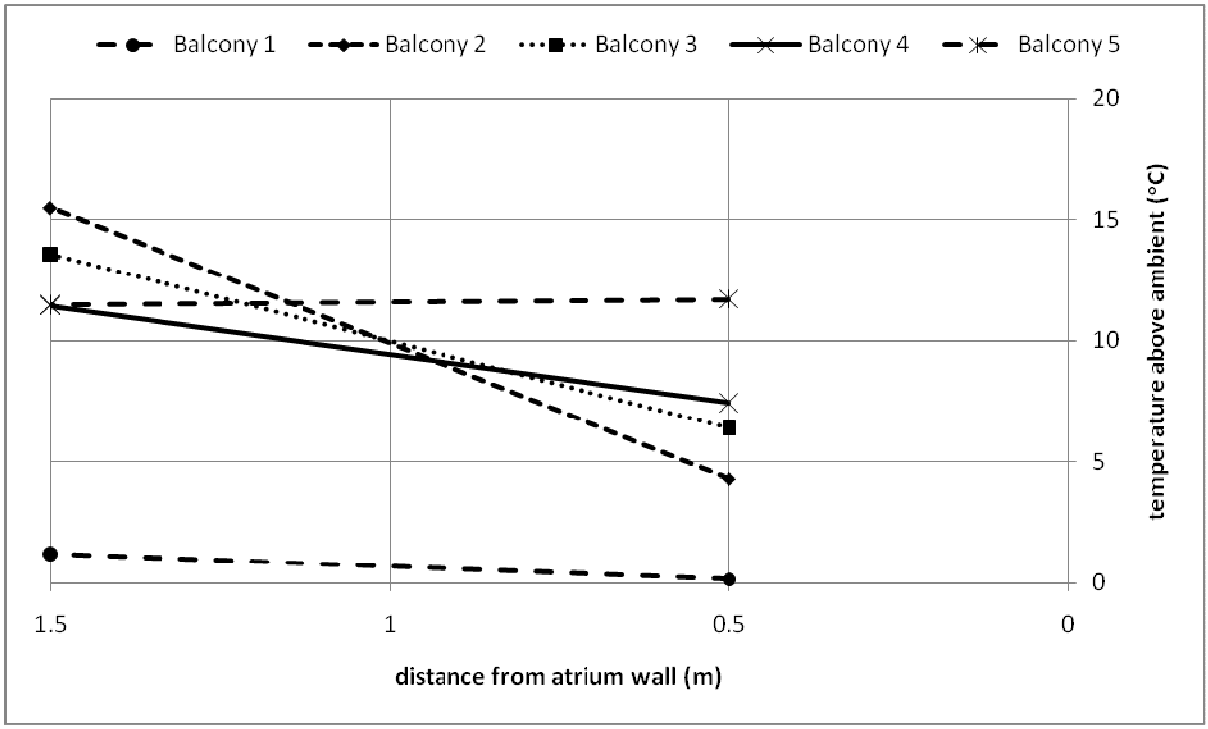

Figure D151. Temperature profiles along balcony breadth.

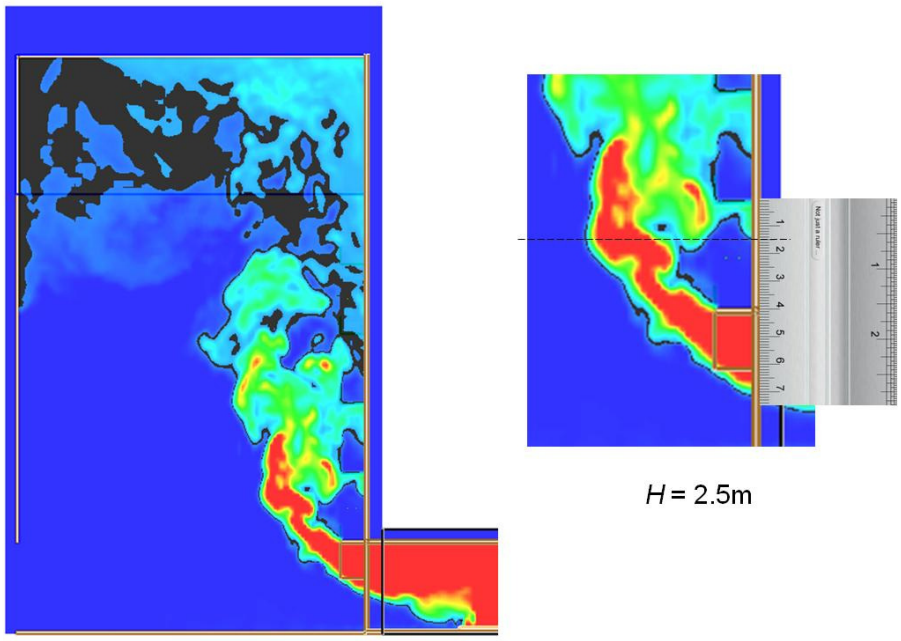

Figure D152. Smoke layer height measurement.

Full scale for 5 balcony (F57E5)

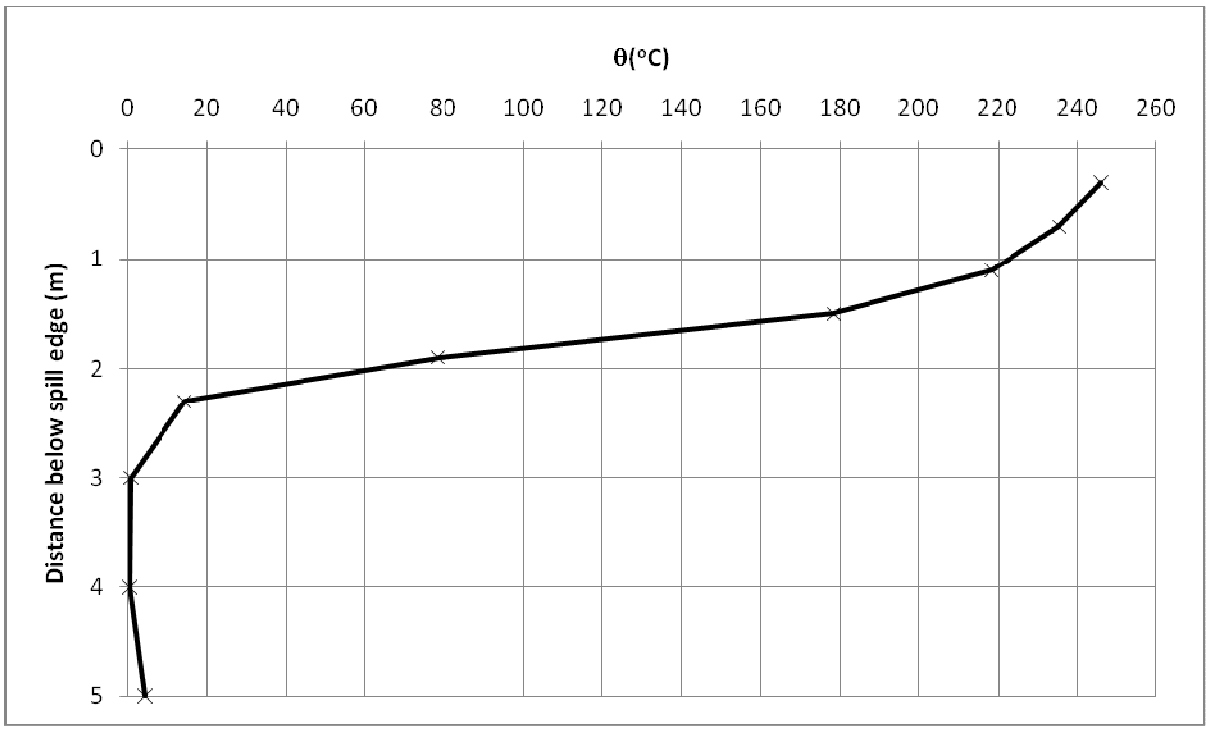

Figure D153. Temperature above ambient at the spill edge.

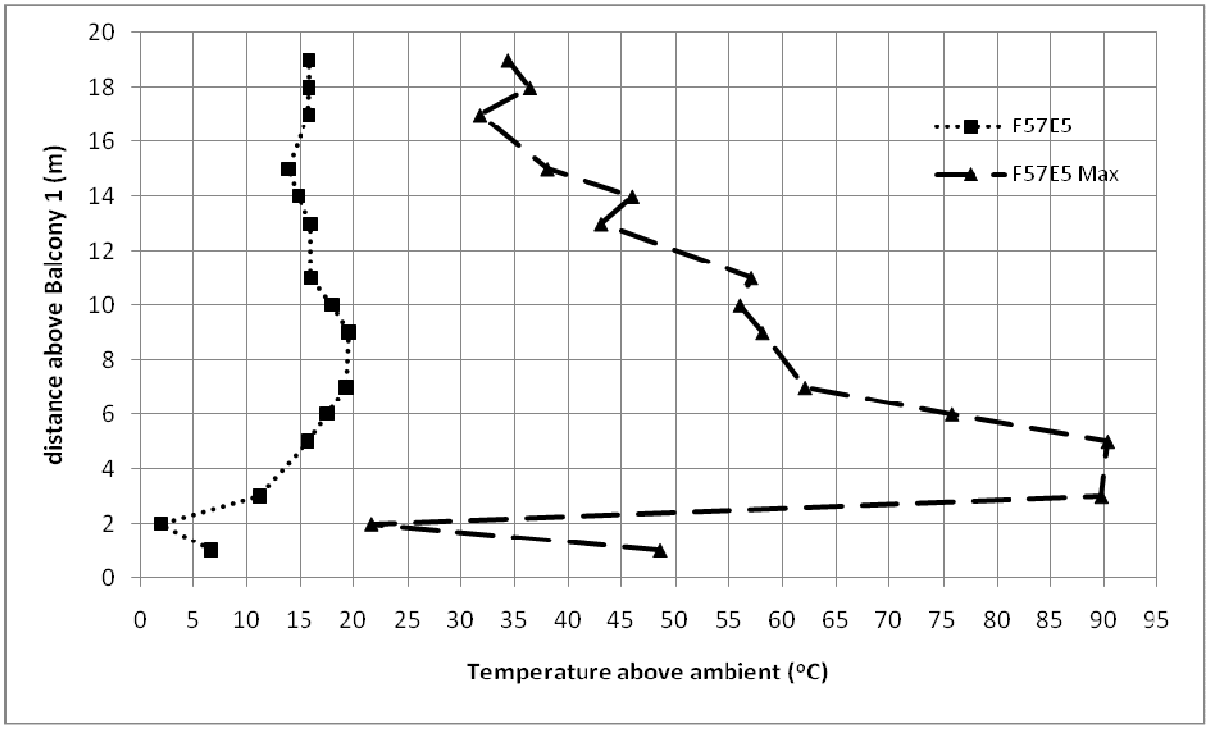

Figure D154. Temperature profiles across balcony edge.

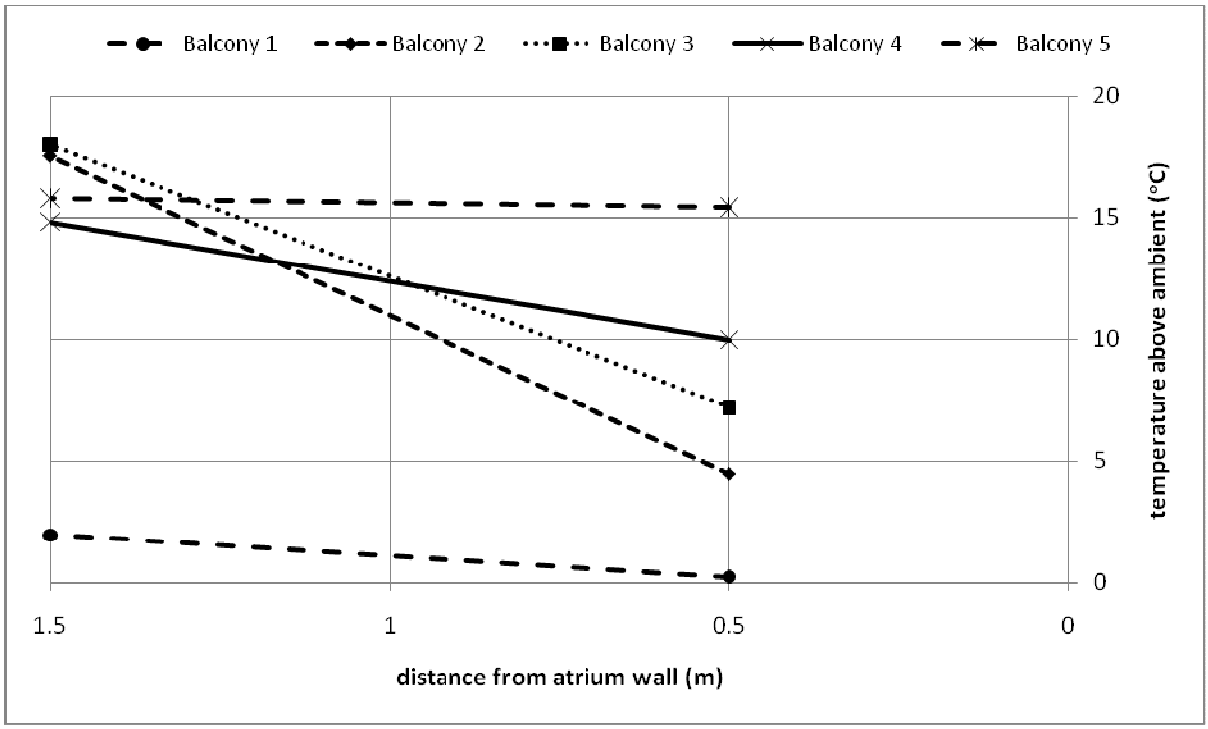

Figure D155. Temperature profiles along balcony breadth.

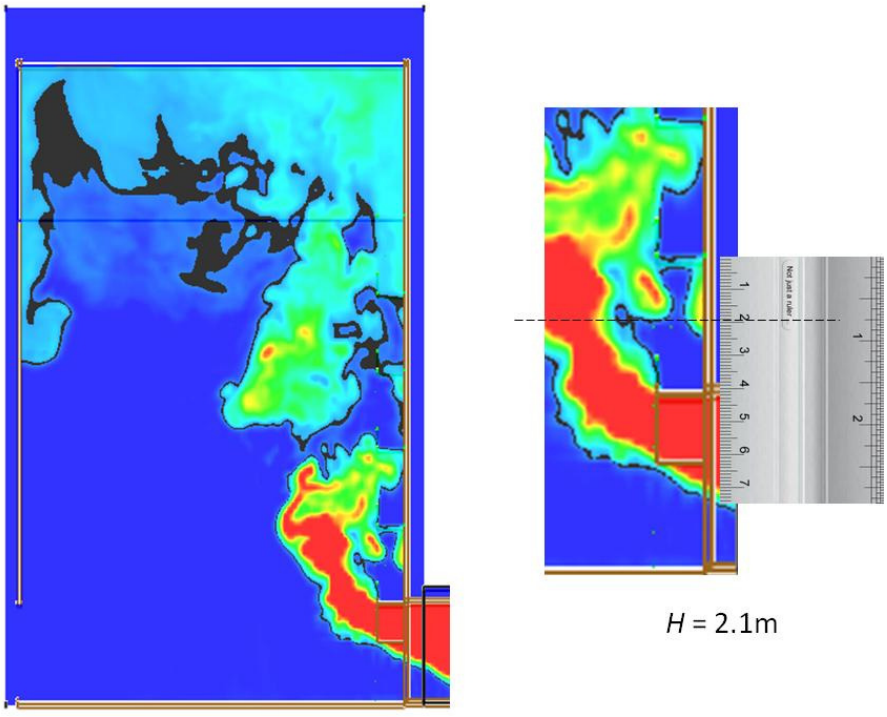

Figure D156. Smoke layer height measurement.

Full scale for 5 balcony (F58E5)

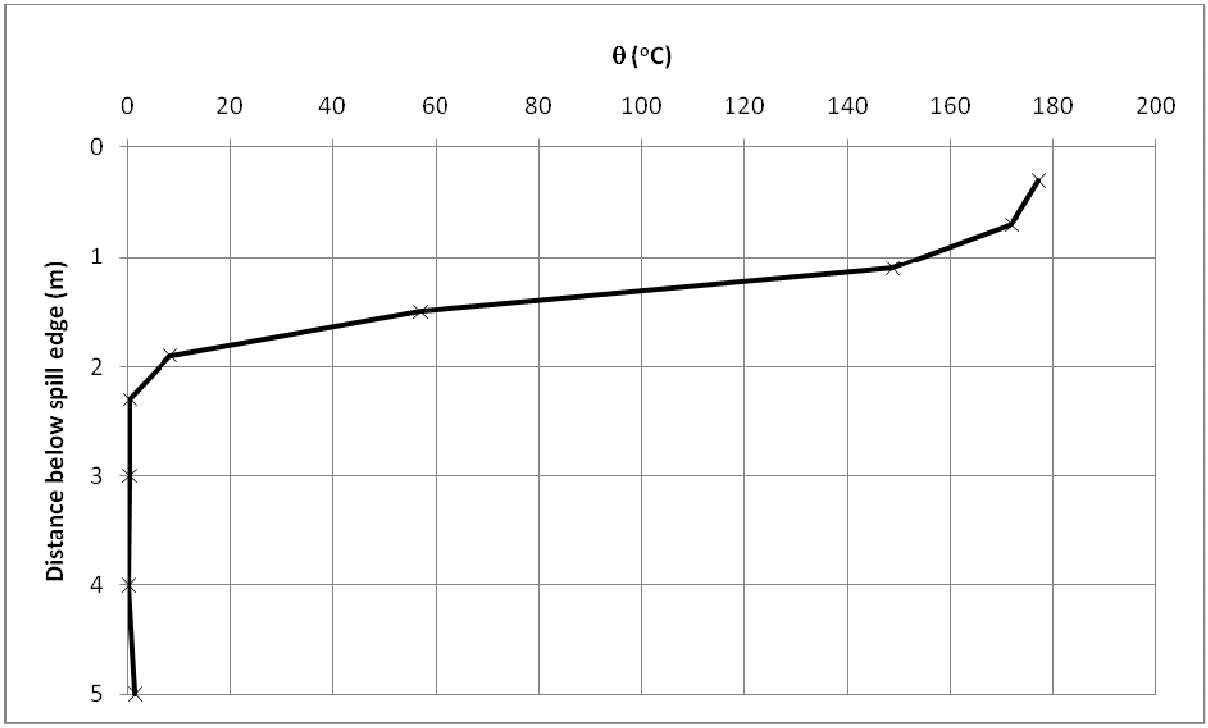

Figure D157. Temperature above ambient at the spill edge.

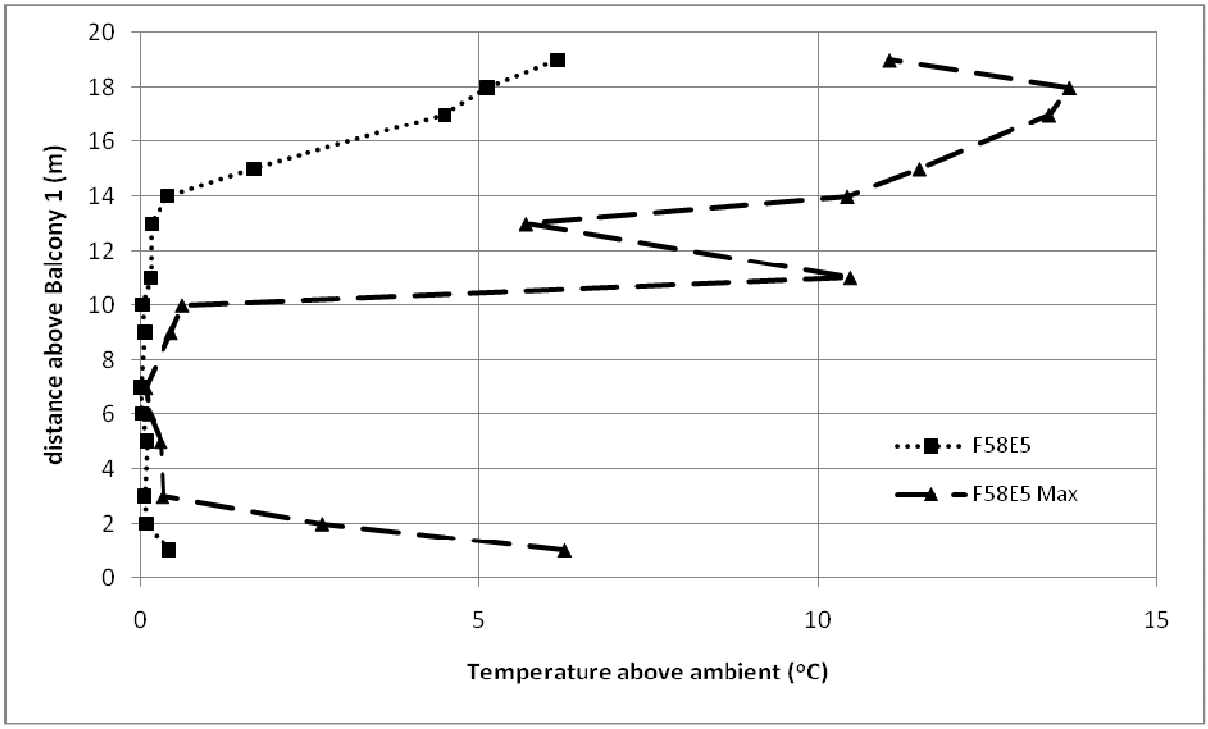

Figure D158. Temperature profiles across balcony edge.

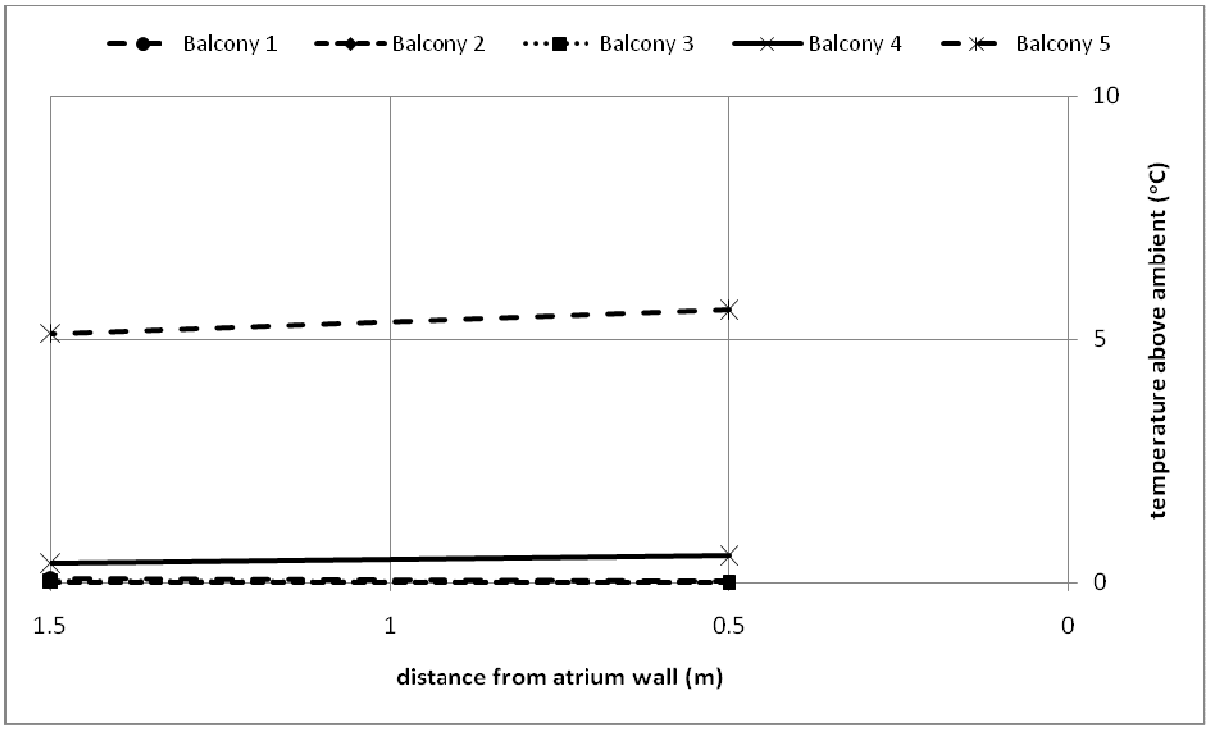

Figure D159. Temperature profiles along balcony breadth.

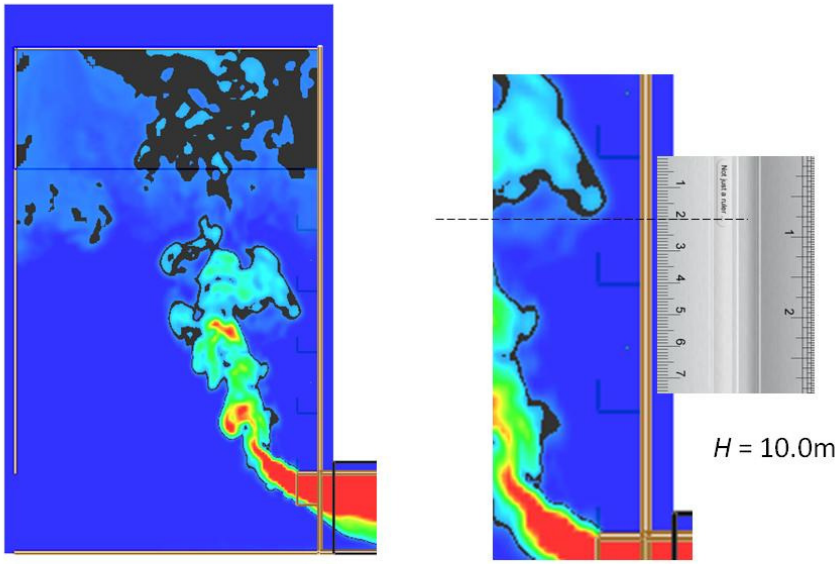

Figure D160. Smoke layer height measurement.

Full scale for 5 balcony (F59E5)

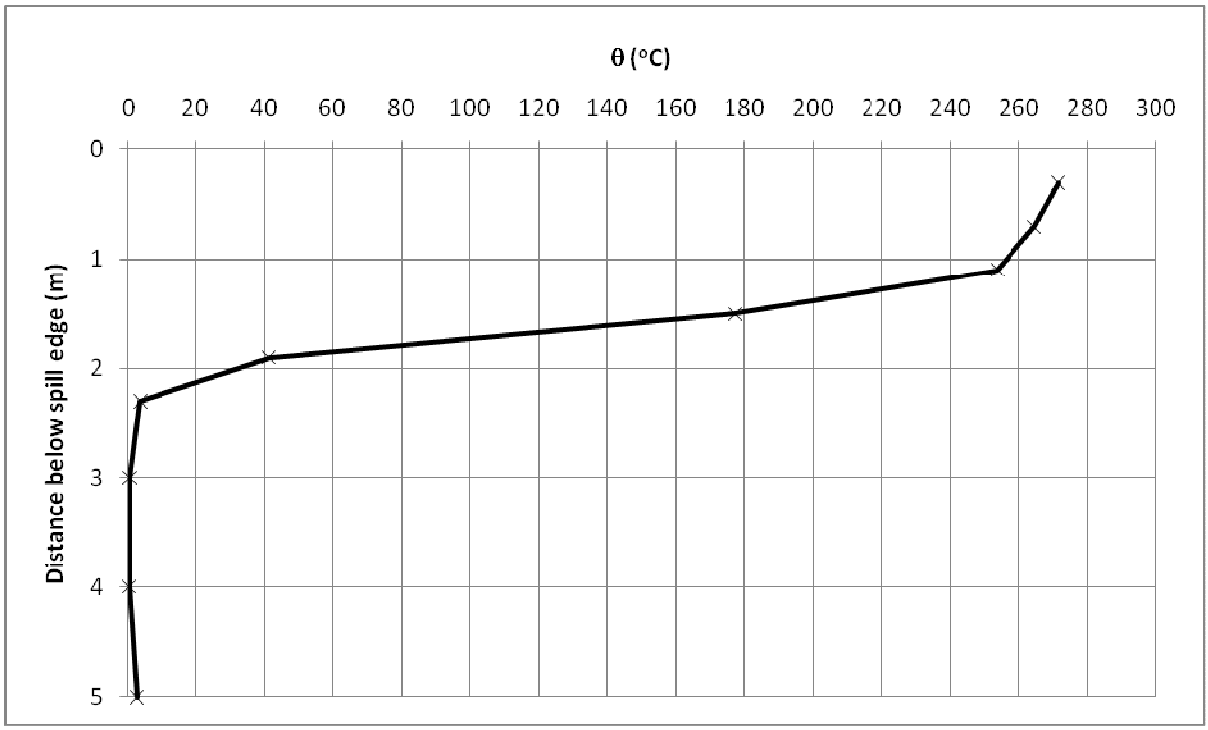

Figure D161. Temperature above ambient at the spill edge.

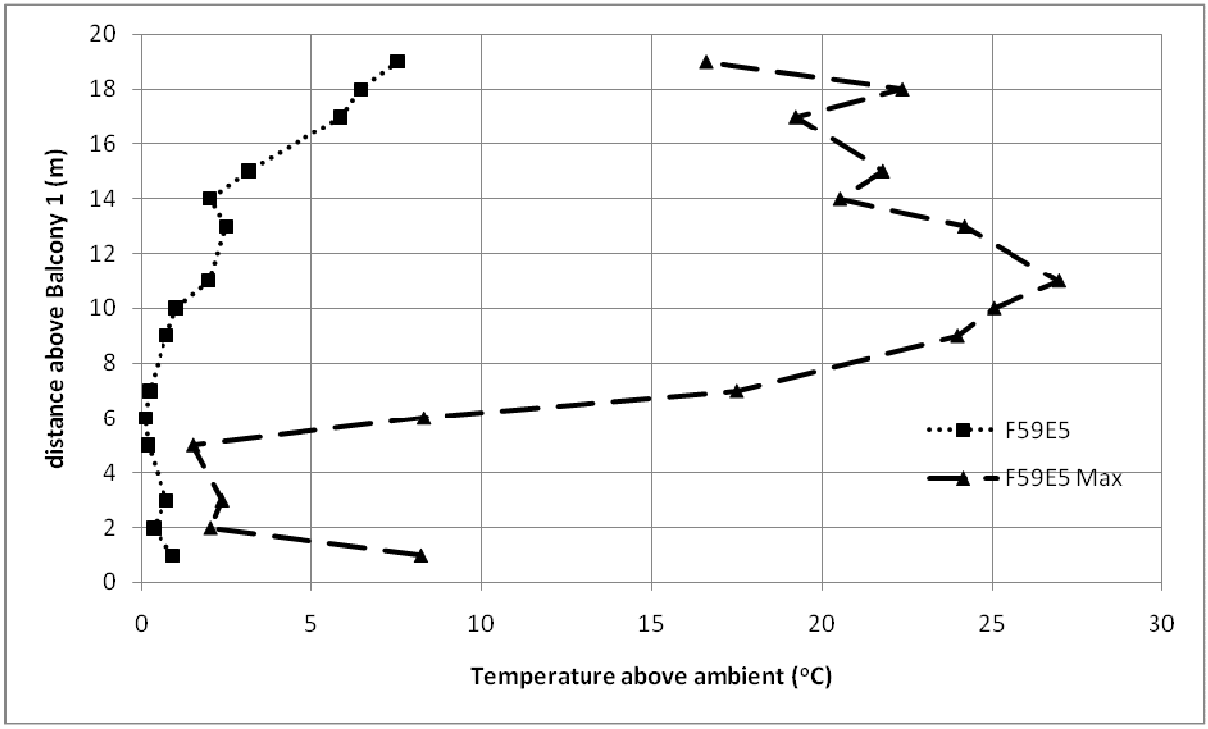

Figure D162. Temperature profiles across balcony edge.

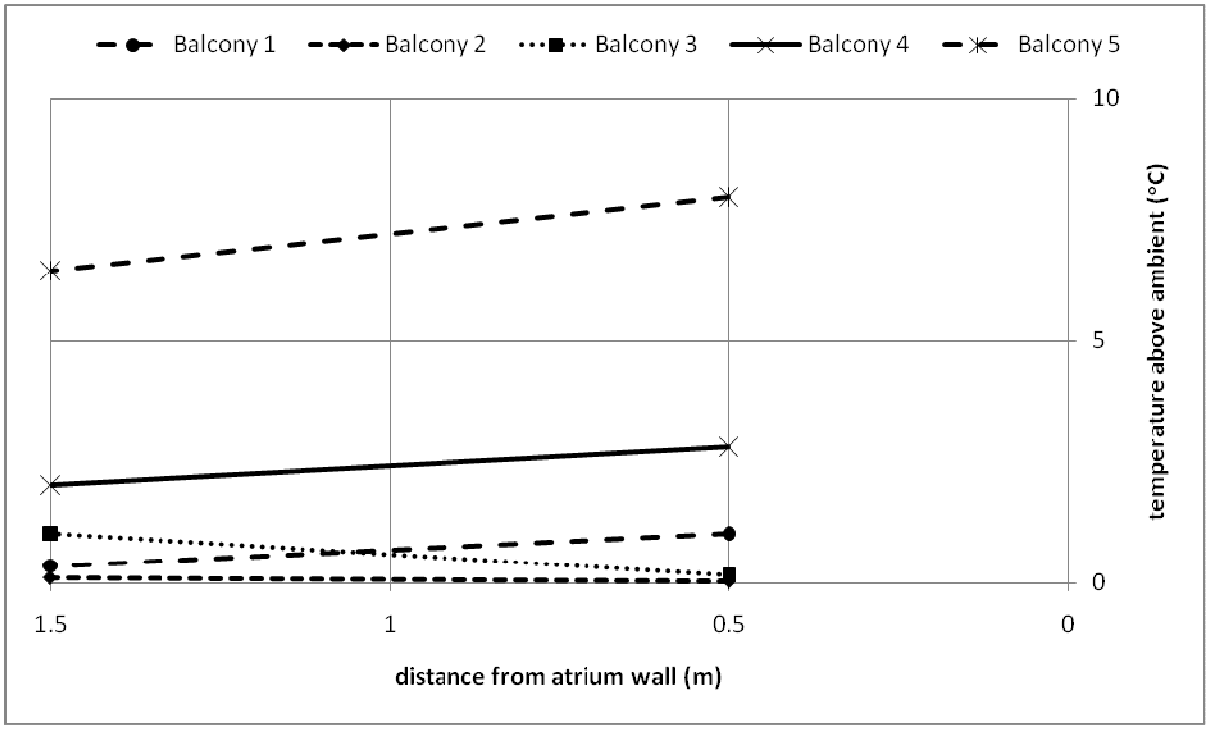

Figure D163. Temperature profiles along balcony breadth.

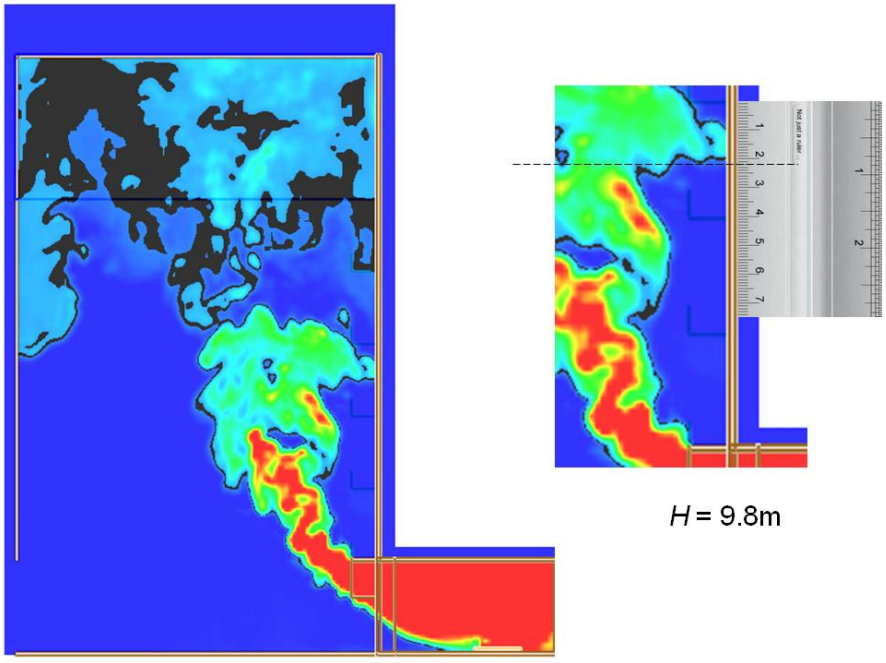

Figure D164. Smoke layer height measurement.

Full scale for 5 balcony (F60E5)

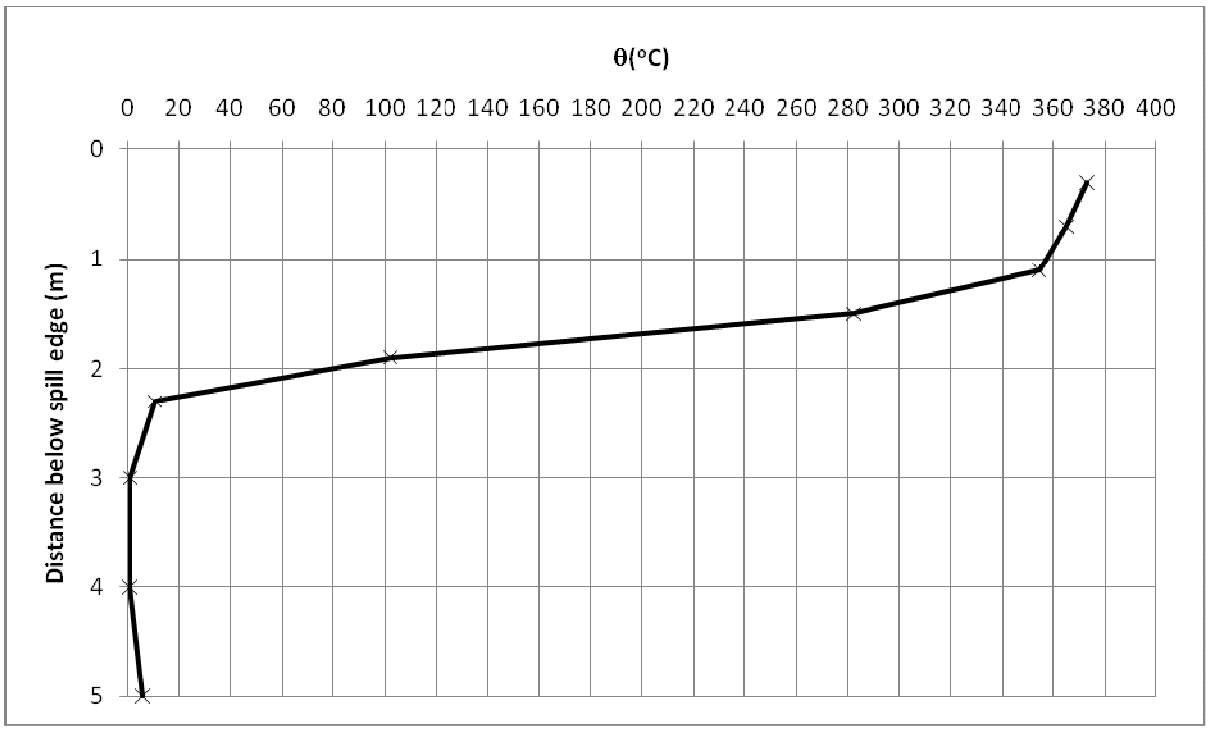

Figure D165. Temperature above ambient at the spill edge.

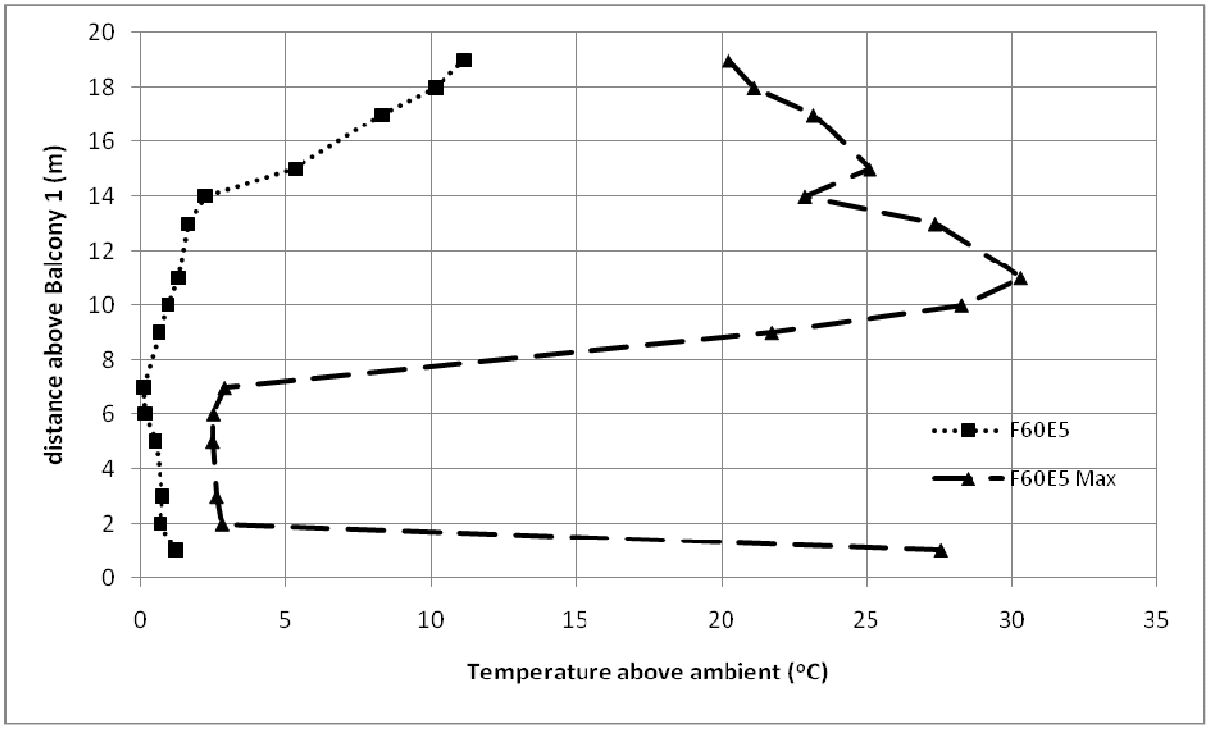

Figure D166. Temperature profiles across balcony edge.

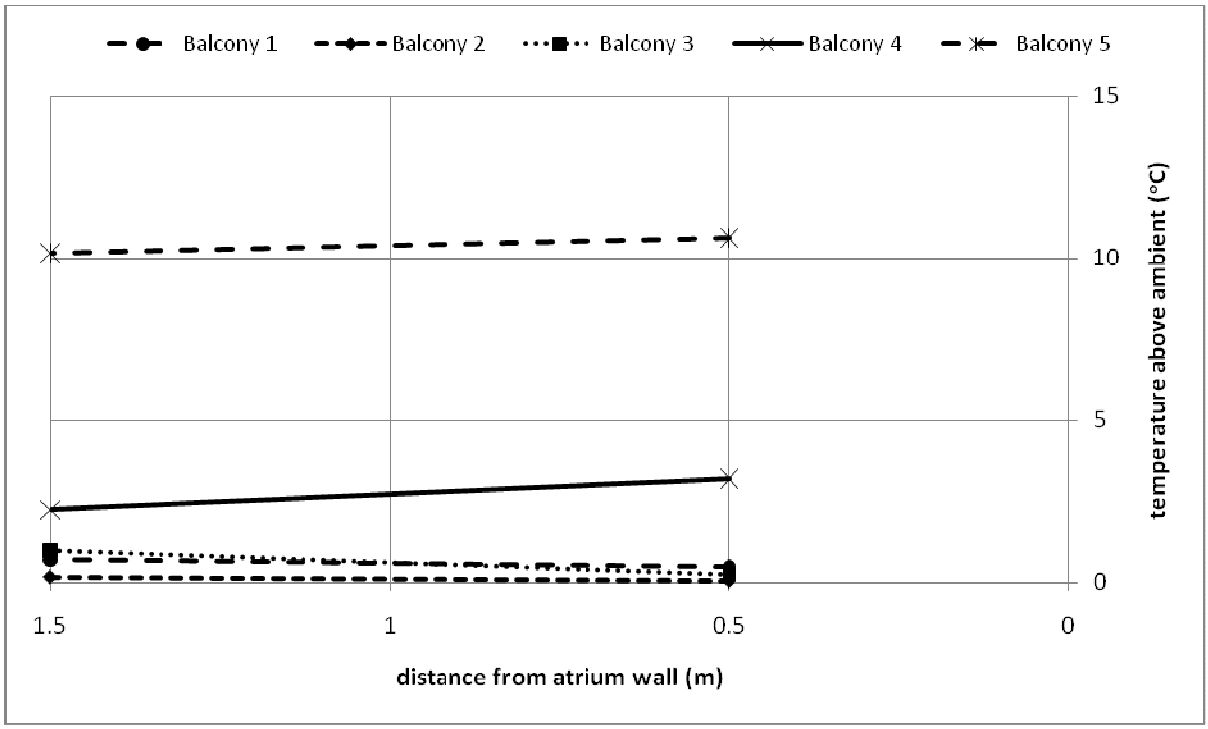

Figure D167. Temperature profiles along balcony breadth.

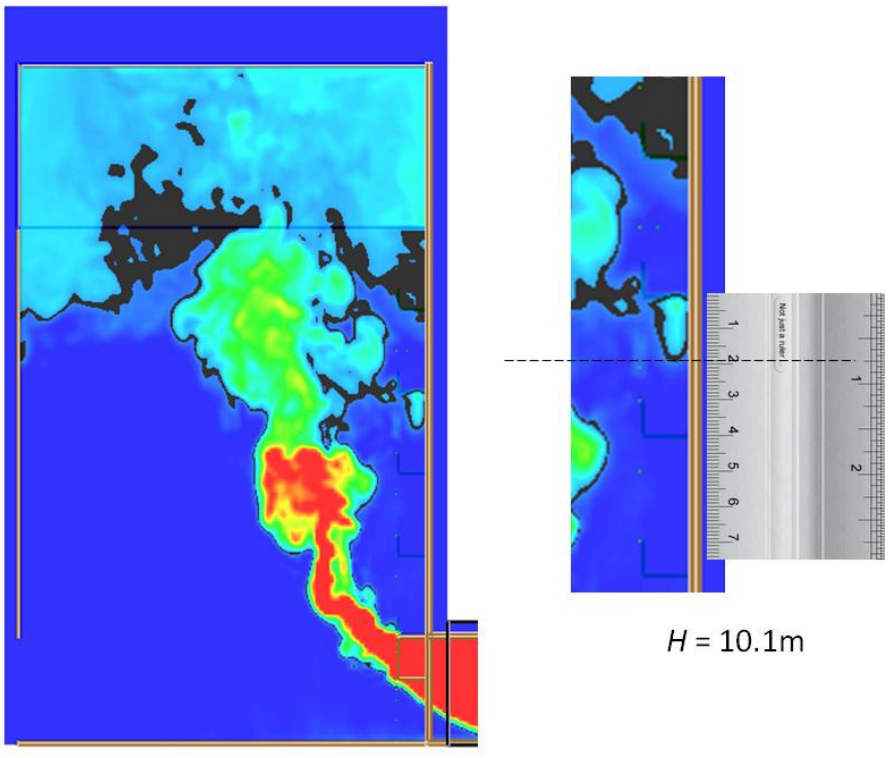

Figure D168. Smoke layer height measurement.

Comparison of Scale Model and Full-scale Model Simulation Results

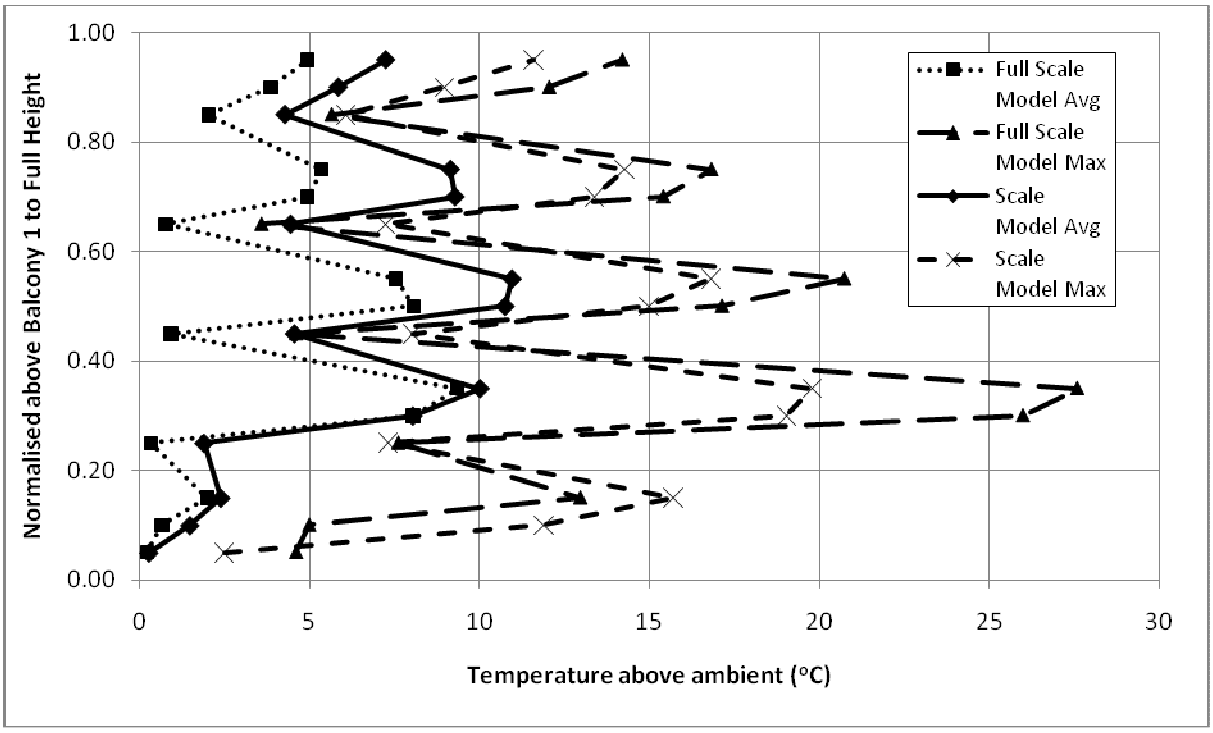

Figure E1. Comparing small scale (S01E5) and full scale (F01E5) simulation results.

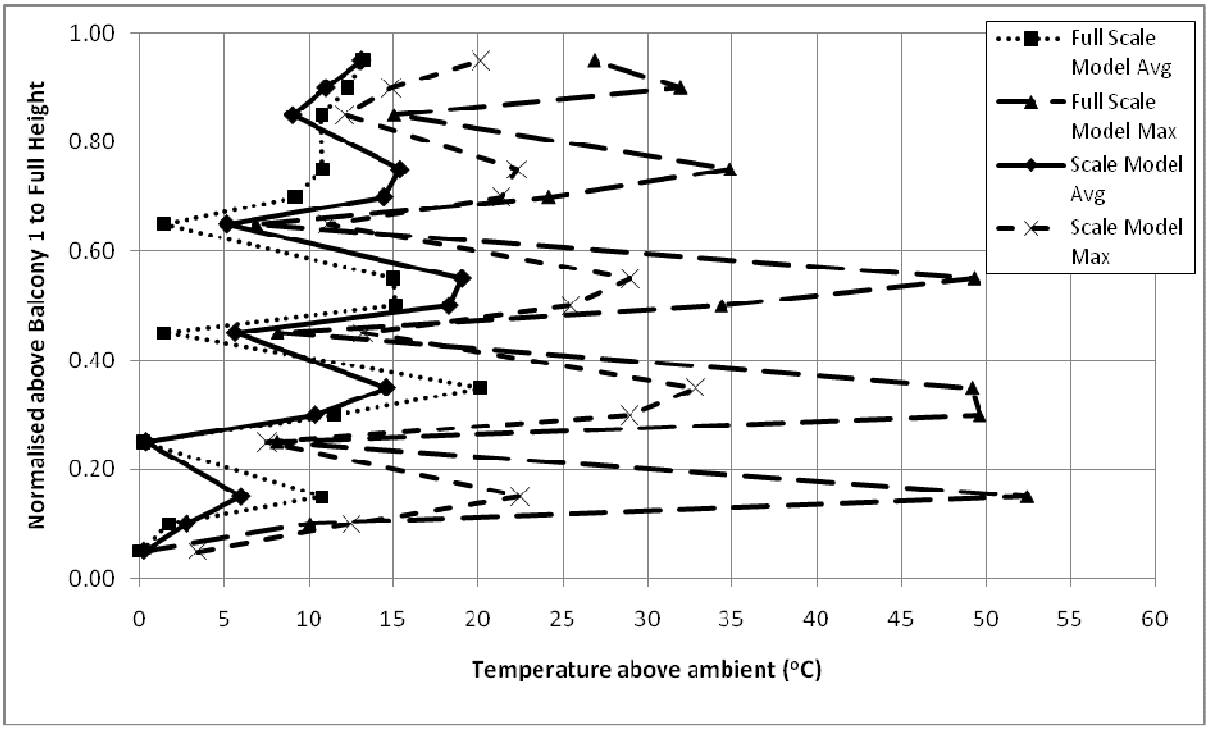

Figure E2. Comparing small scale (S03E5) and full scale (F03E5) simulation results.

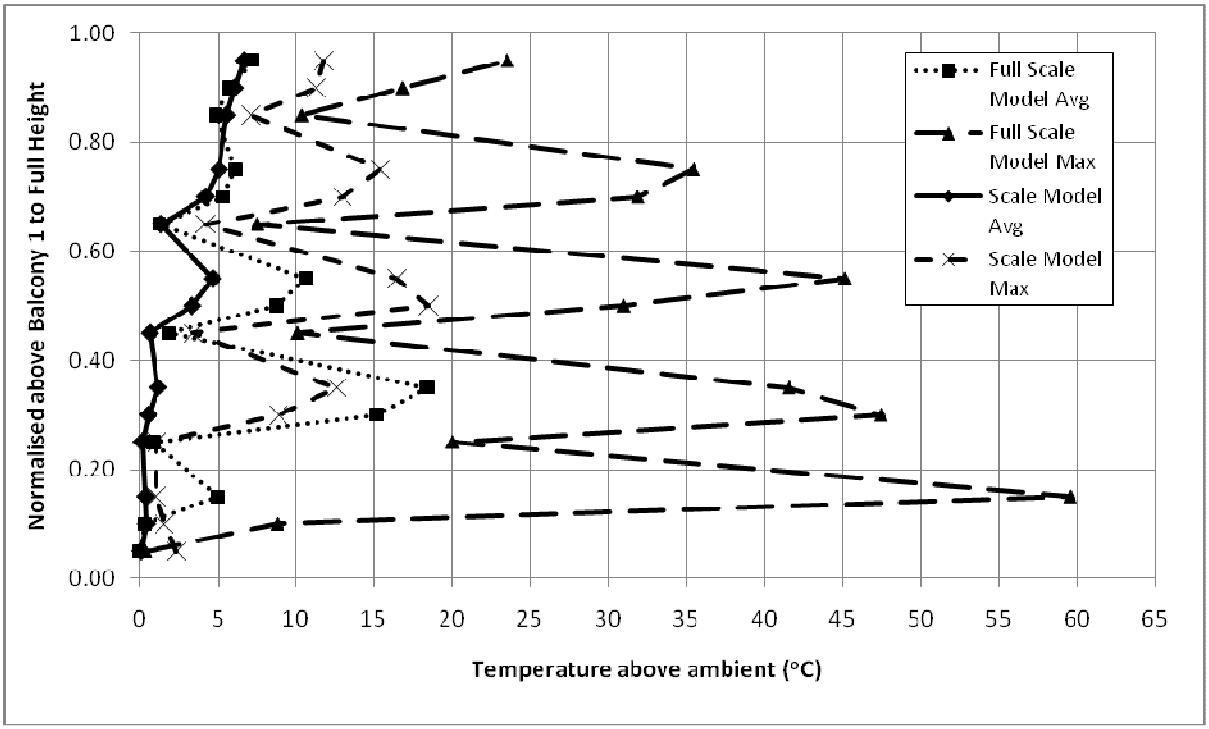

Figure E3. Comparing small scale (S08E5) and full scale (F08E5) simulation results.

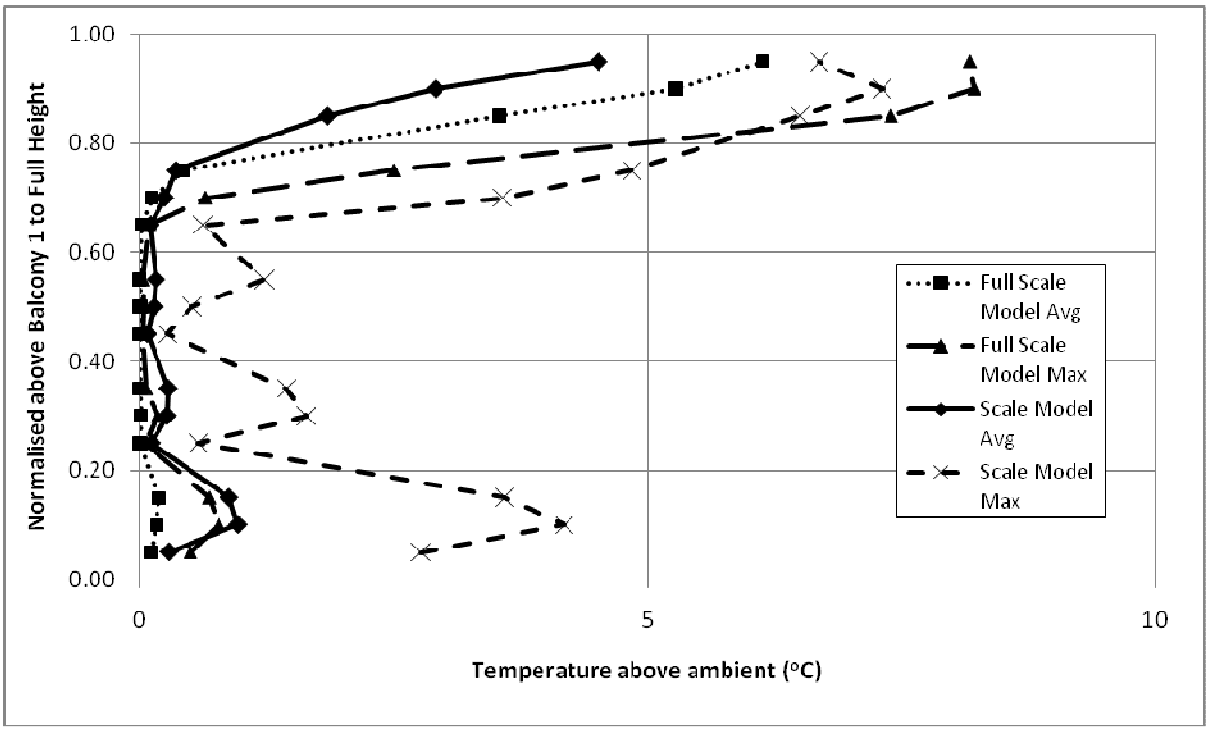

Figure E4. Comparing small scale (S13E5) and full scale (F13E5) simulation results.

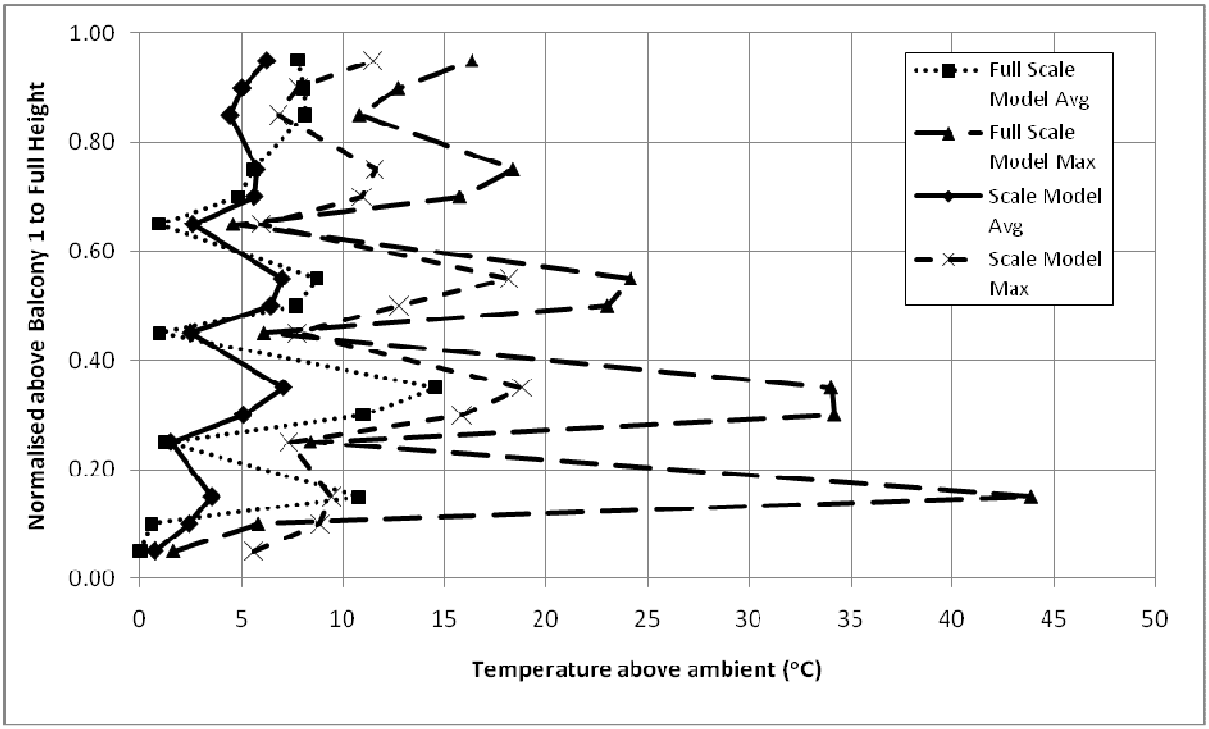

Figure E5. Comparing small scale (S19E5) and full scale (F19E5) simulation results.

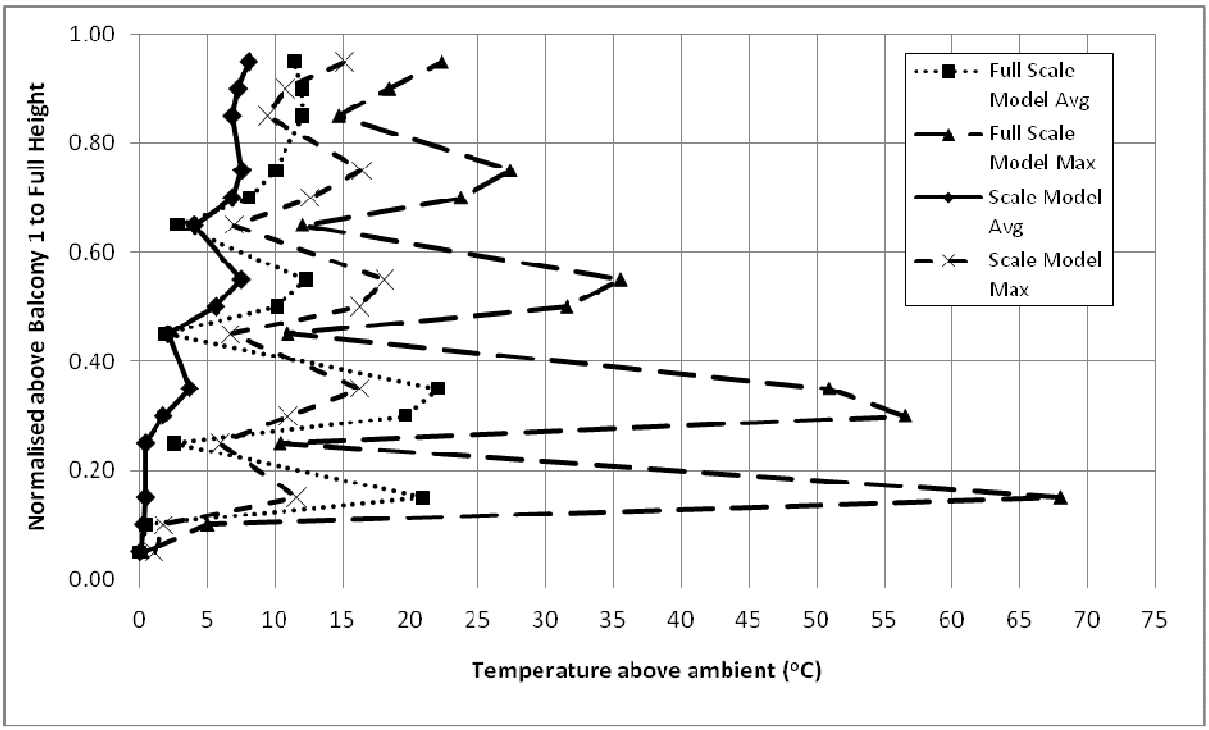

Figure E6. Comparing small scale (S23E5) and full scale (F23E5) simulation results.

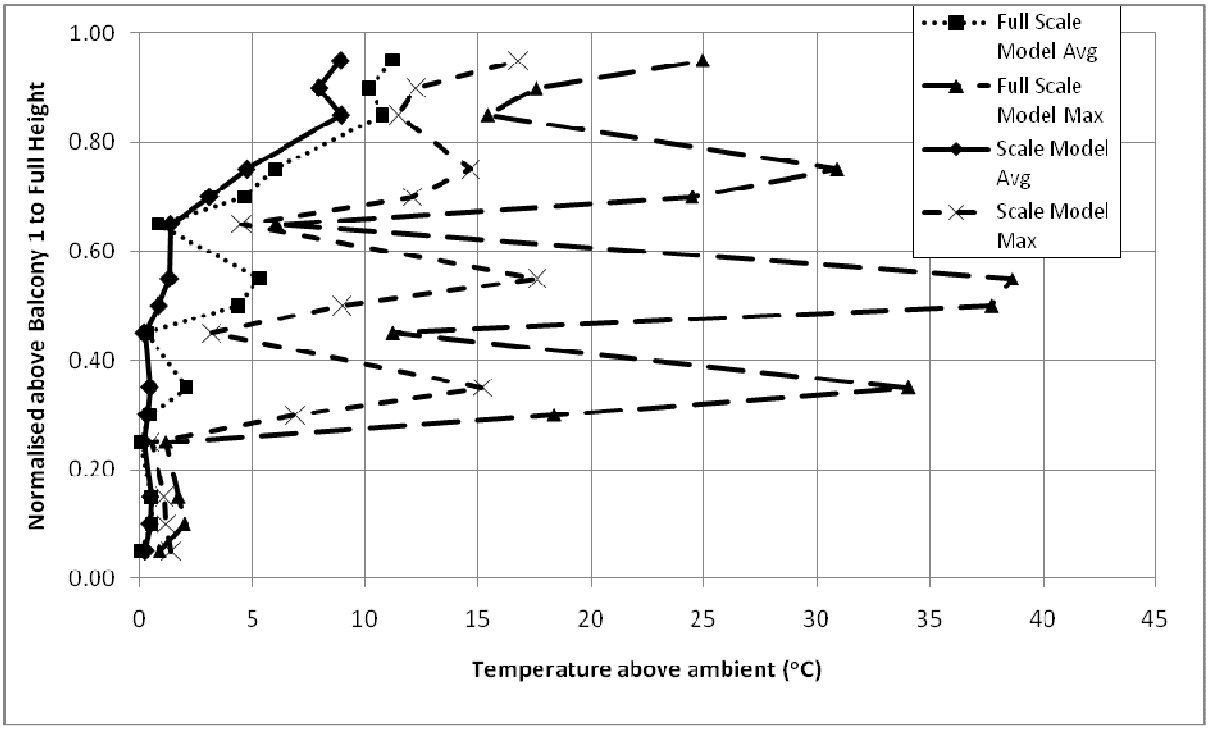

Figure E7. Comparing small scale (S27E5) and full scale (F27E5) simulation results.

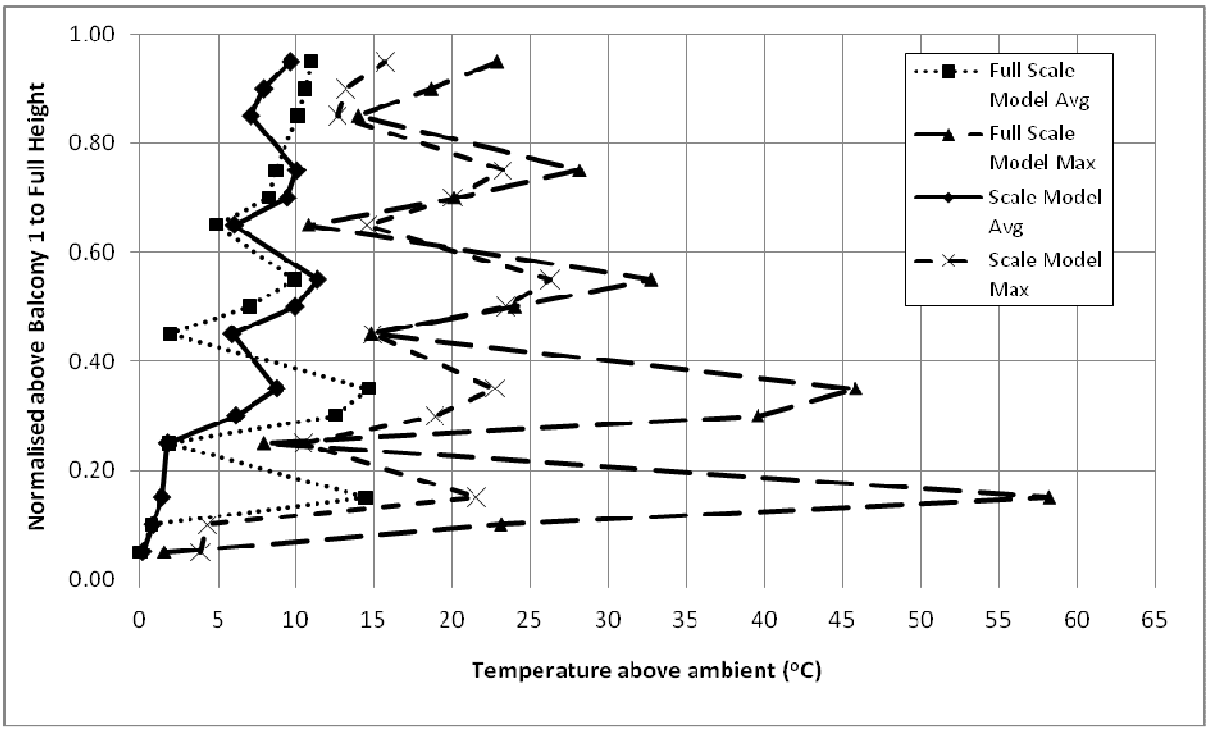

Figure E8. Comparing small scale (S38E5) and full scale (F38E5) simulation results.

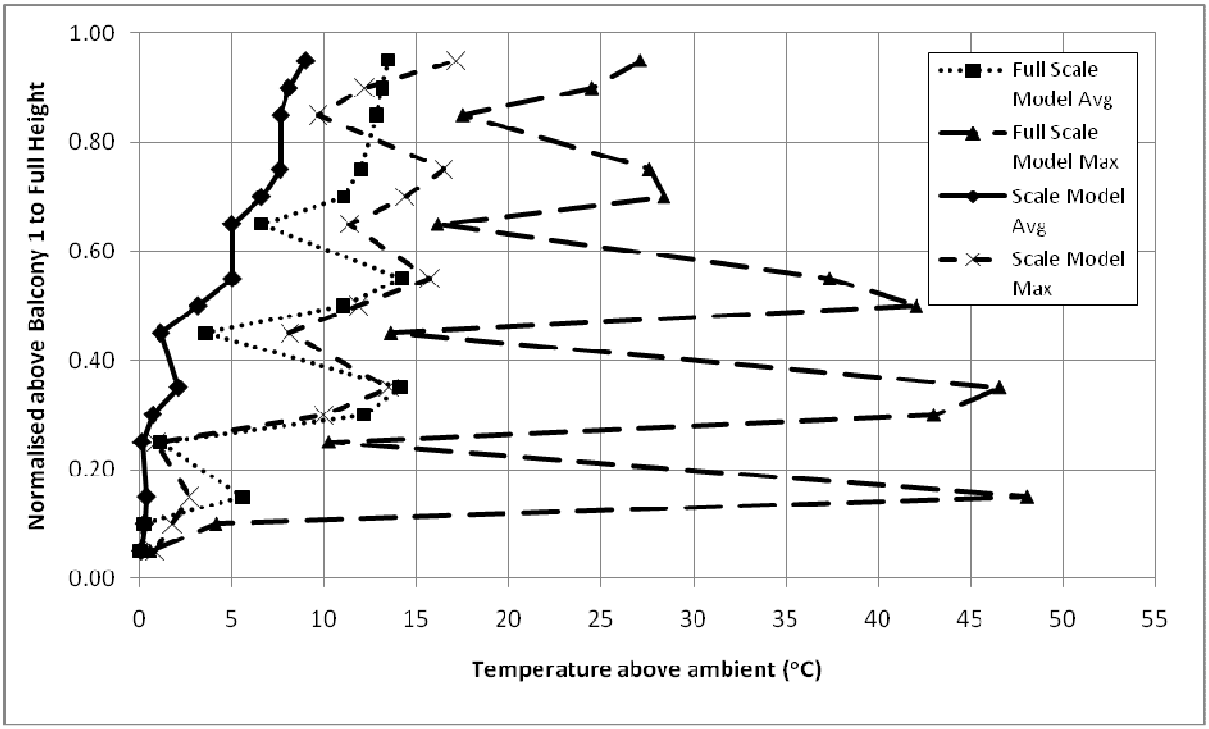

Figure E9. Comparing small scale (S41E5) and full scale (F41E5) simulation results.

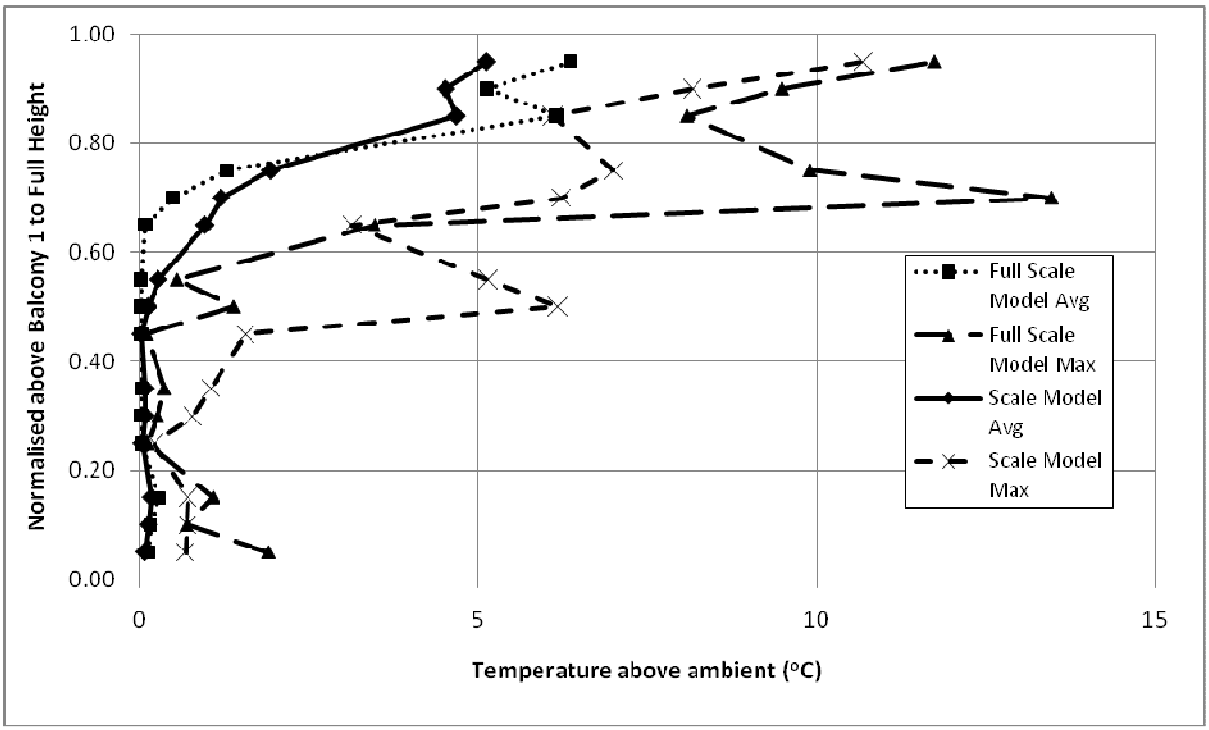

Figure E10. Comparing small scale (S43E5) and full scale (F43E5) simulation results.

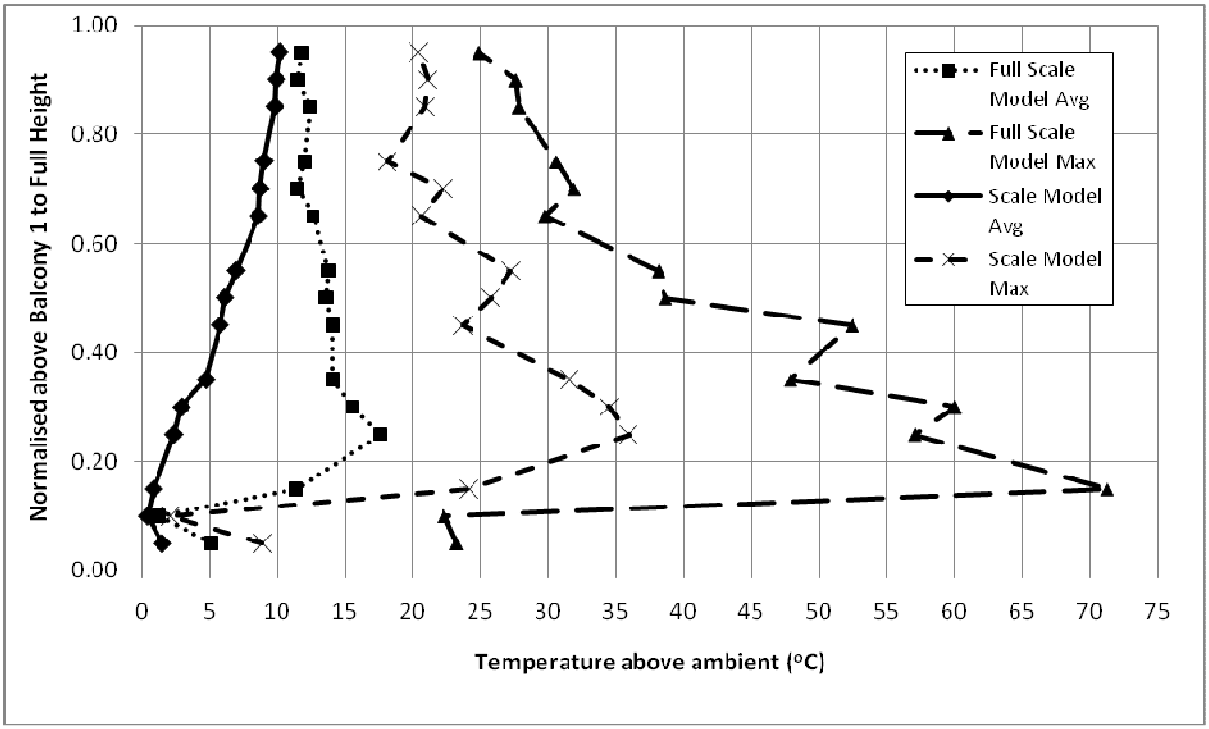

Figure E11. Comparing small scale (S56E5) and full scale (F56E5) simulation results.

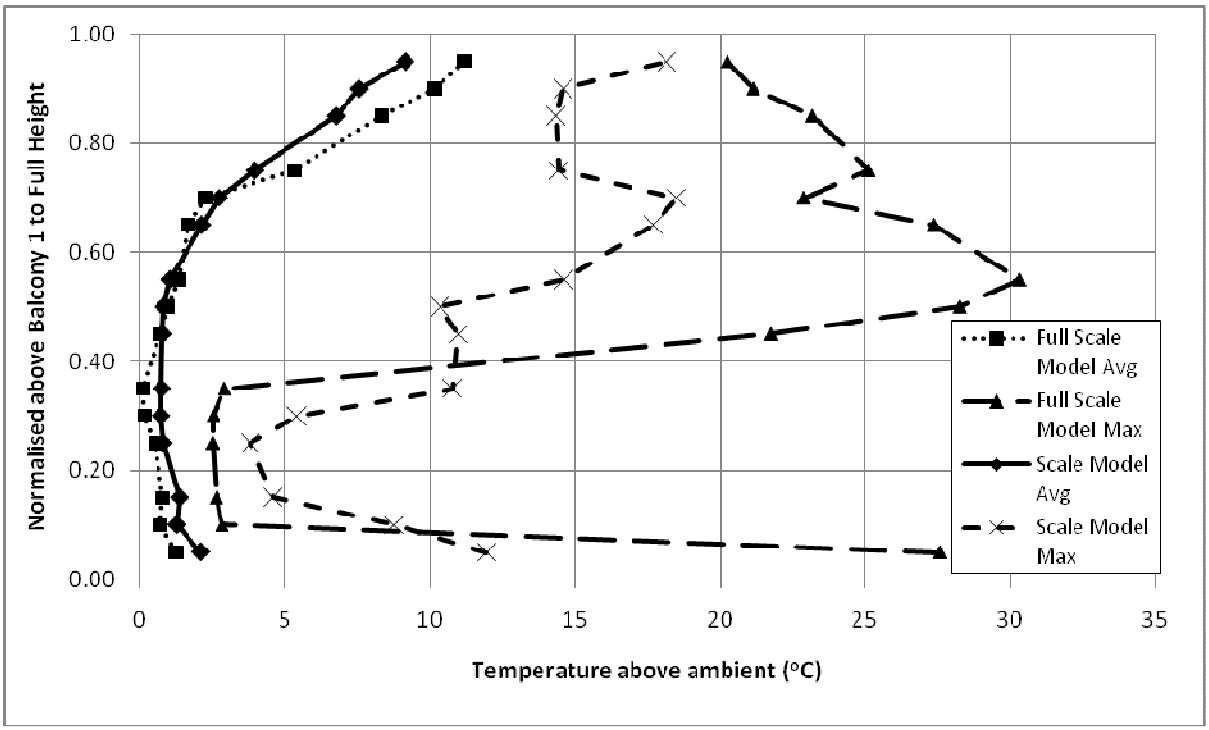

Figure E12. Comparing small scale (S60E5) and full scale (F60E5) simulation results.

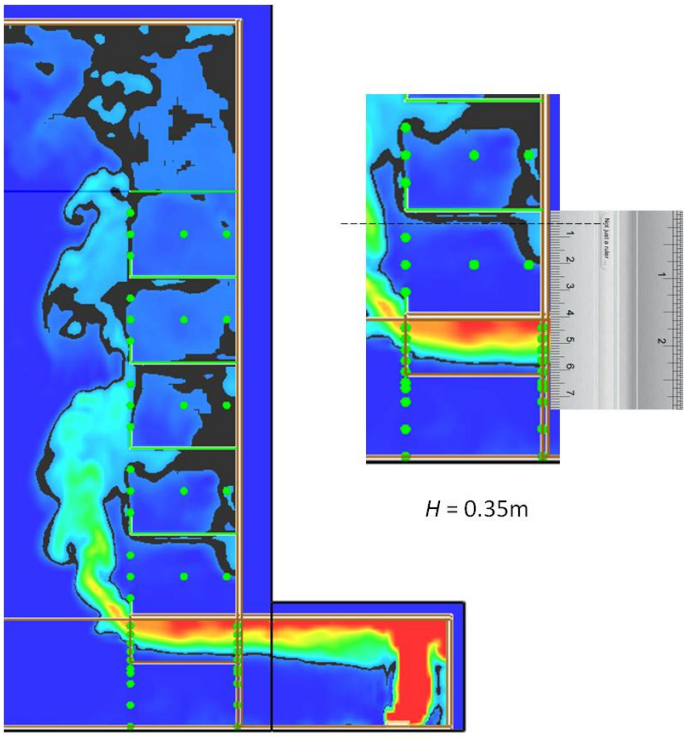

Figure E13. Smoke layer height measurement for S01E5.

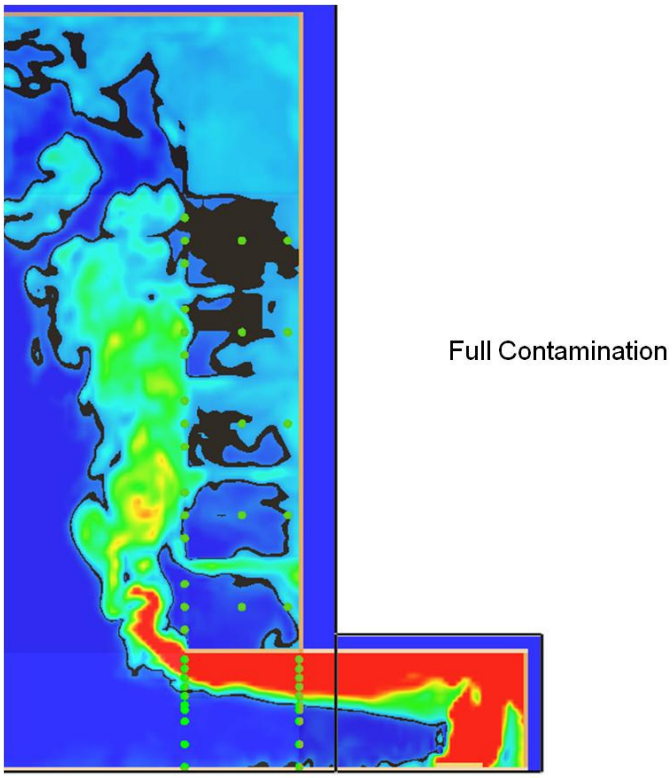

Figure E14. Smoke layer height measurement for S03E5.

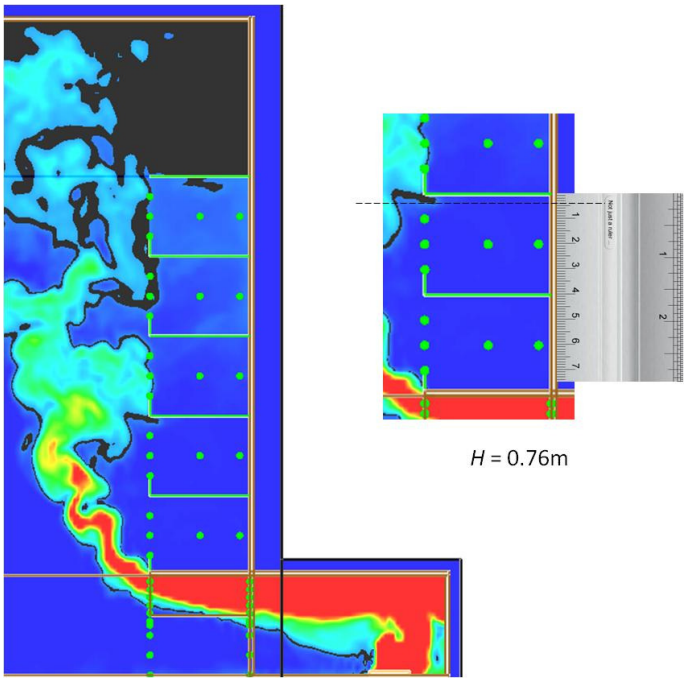

Figure E15. Smoke layer height measurement for S08E5.

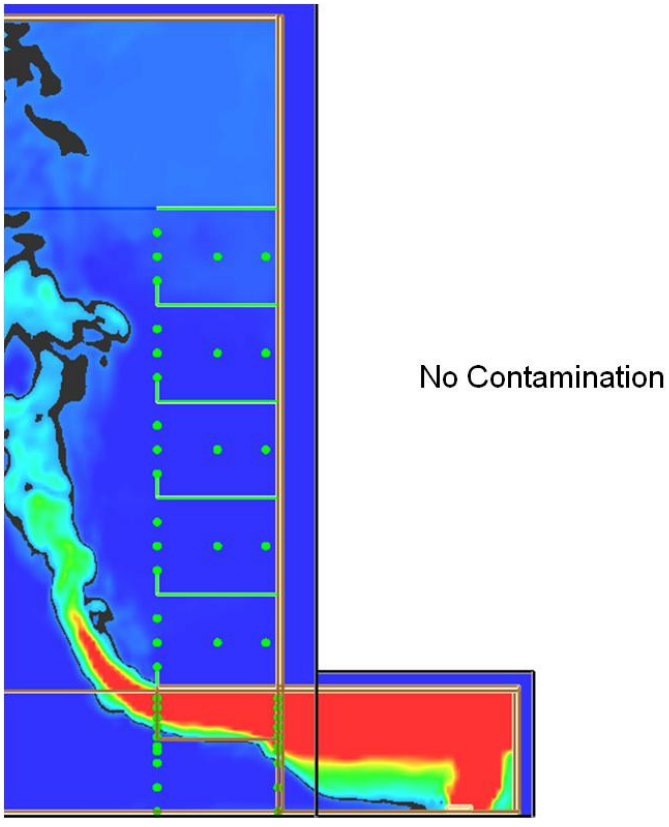

Figure E16. Smoke layer height measurement for S13E5.

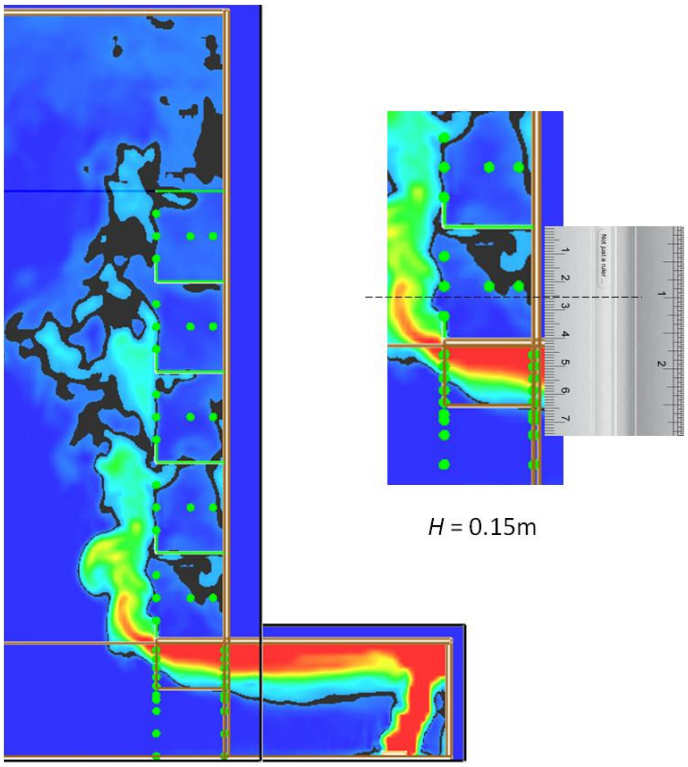

Figure E17. Smoke layer height measurement for S19E5.

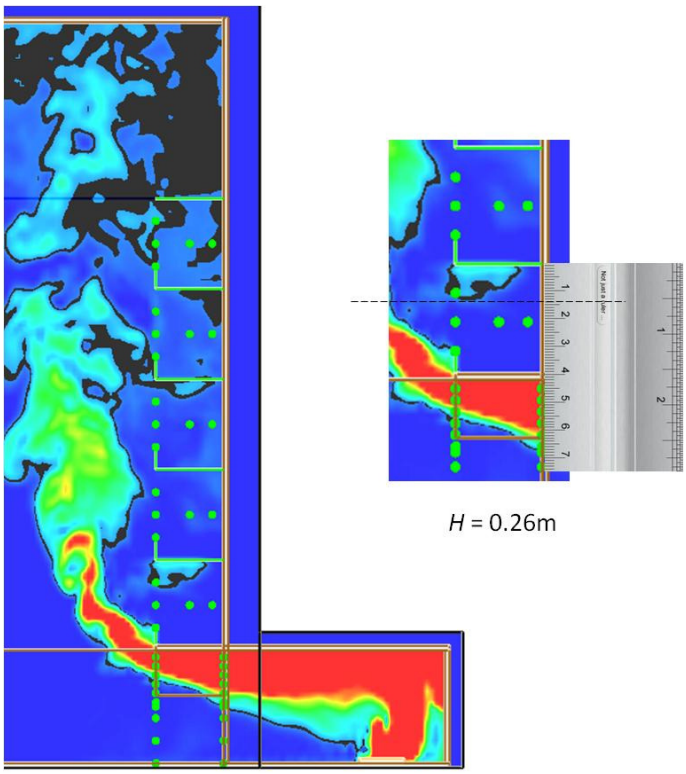

Figure E18. Smoke layer height measurement for S23E5.

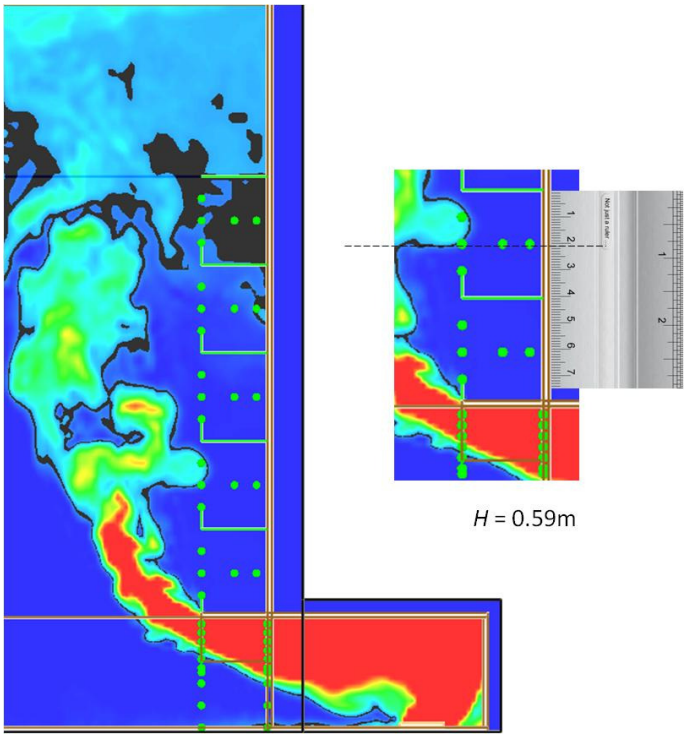

Figure E19. Smoke layer height measurement for S27E5.

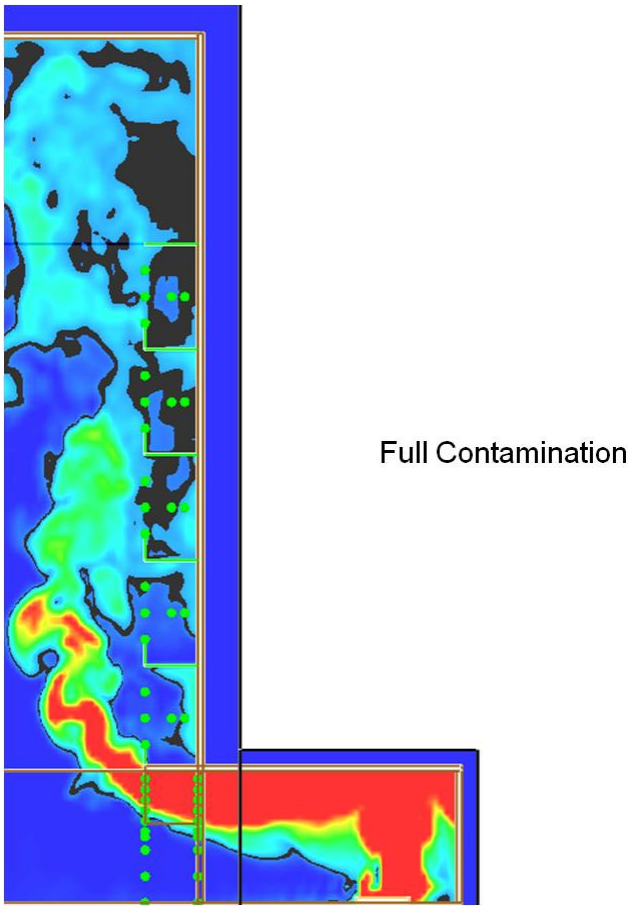

Figure E20. Smoke layer height measurement for S38E5.

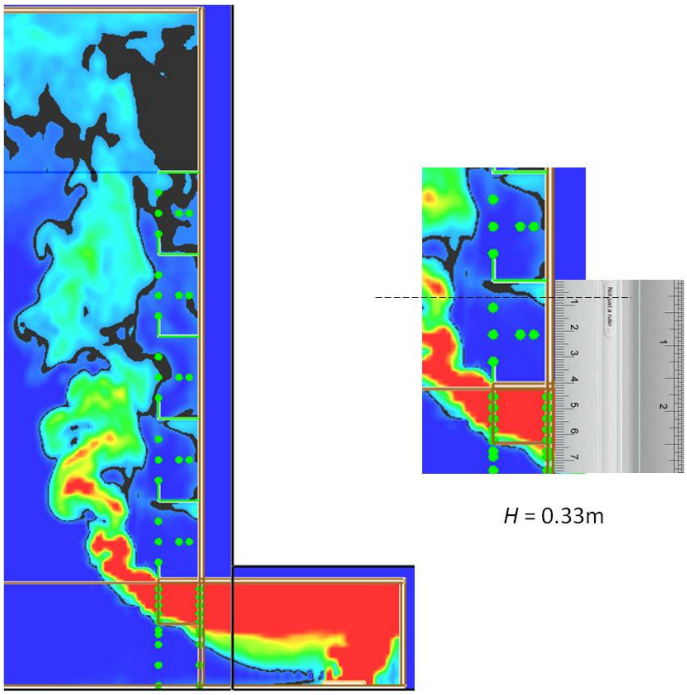

Figure E21. Smoke layer height measurement for S41E5.

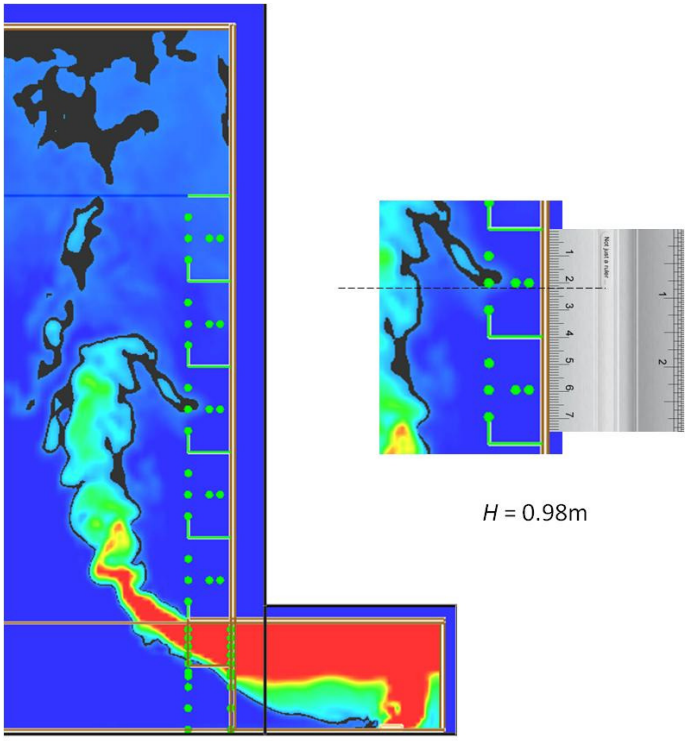

Figure E22. Smoke layer height measurement for S43E5.

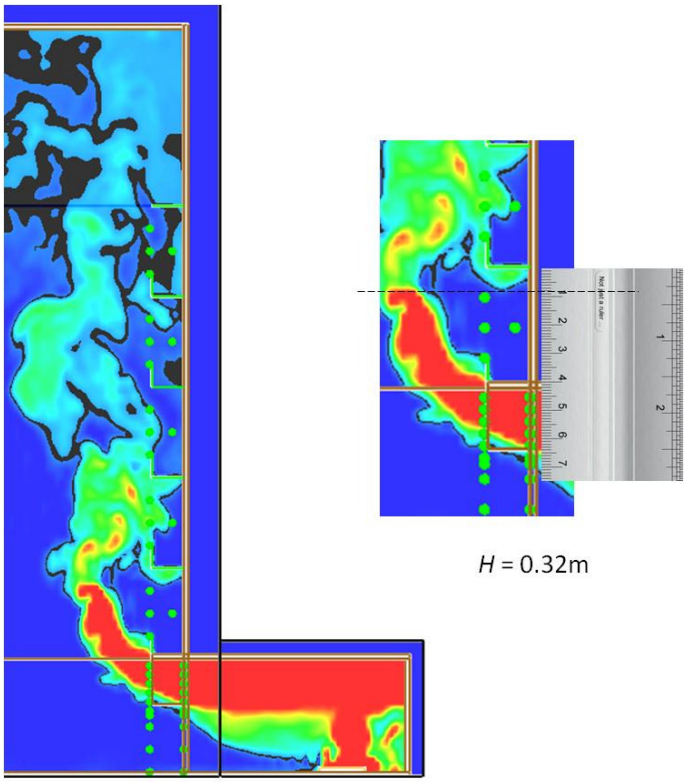

Figure E23. Smoke layer height measurement for S56E5.

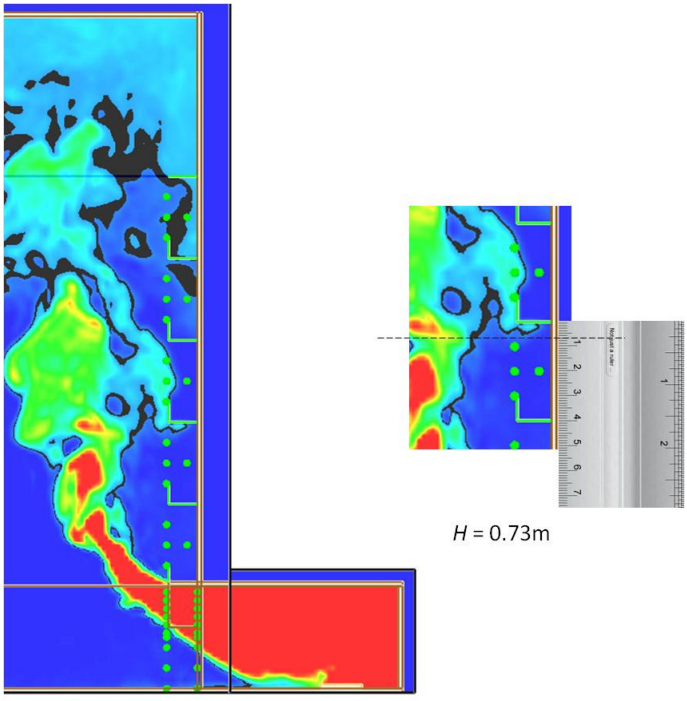

Figure E24. Smoke layer height measurement for S60E5.

Smokeview's Smoke Visualisation Output Comparison with Slice File Temperature Profile.

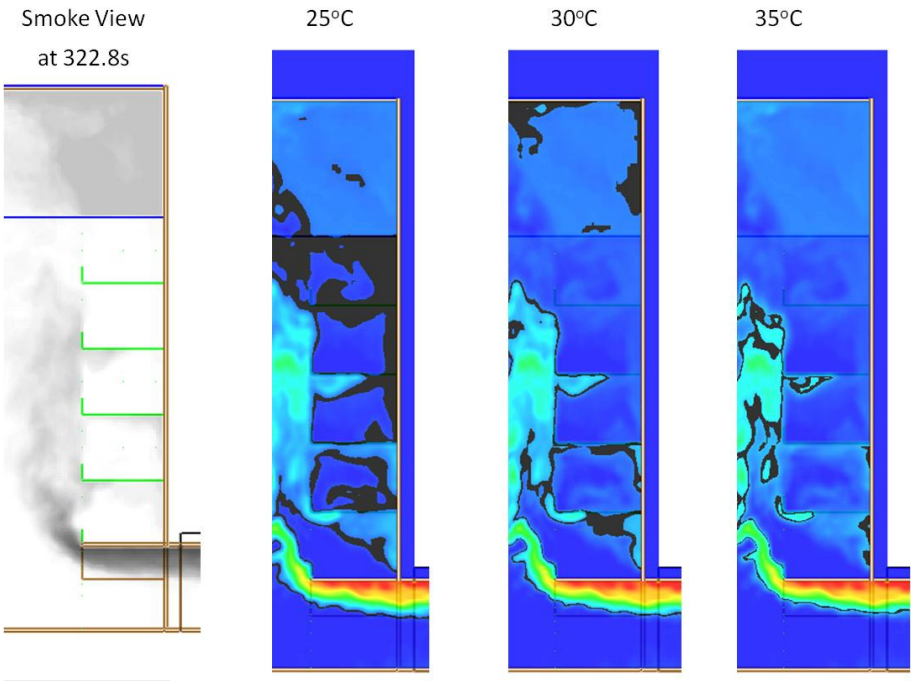

Figure F1. Smokeview and temperature profile for F01E5.

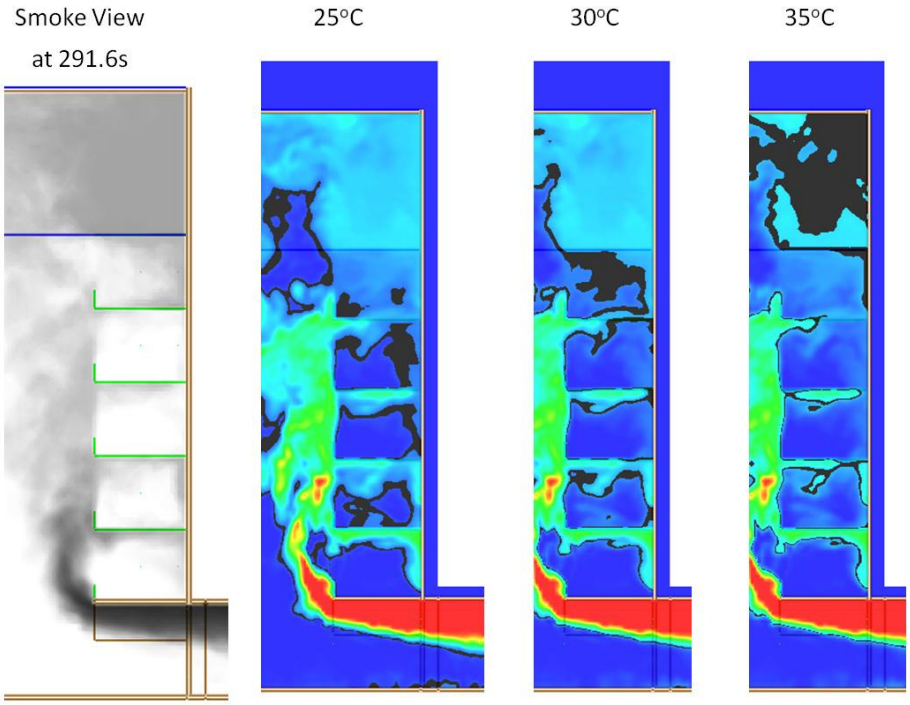

Figure F2. Smokeview and temperature profile for F03E5.

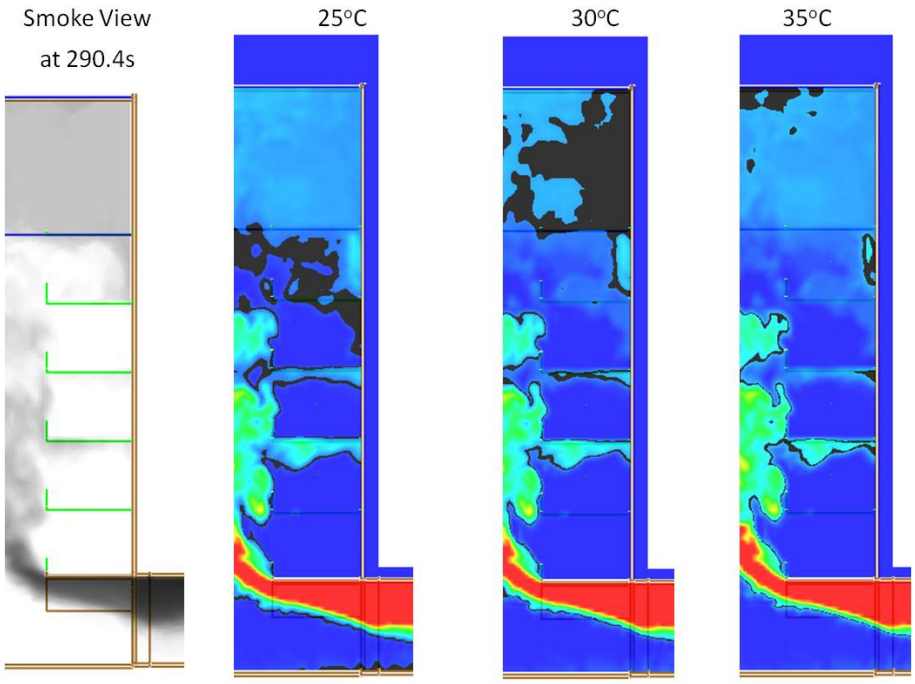

Figure F3. Smokeview and temperature profile for F08E5.

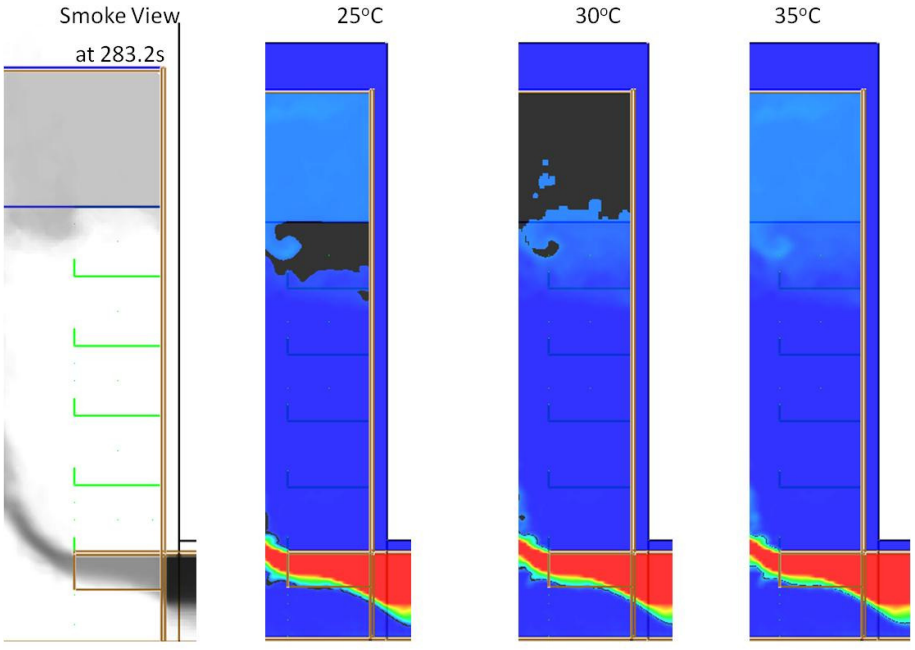

Figure F4. Smokeview and temperature profile for F13E5.

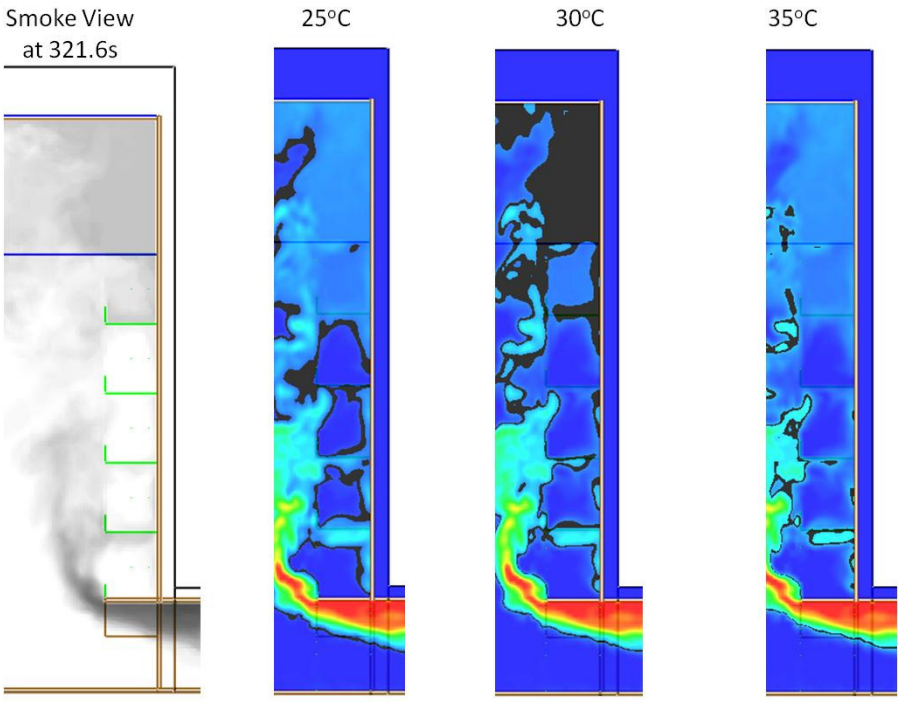

Figure F5. Smokeview and temperature profile for F19E5.

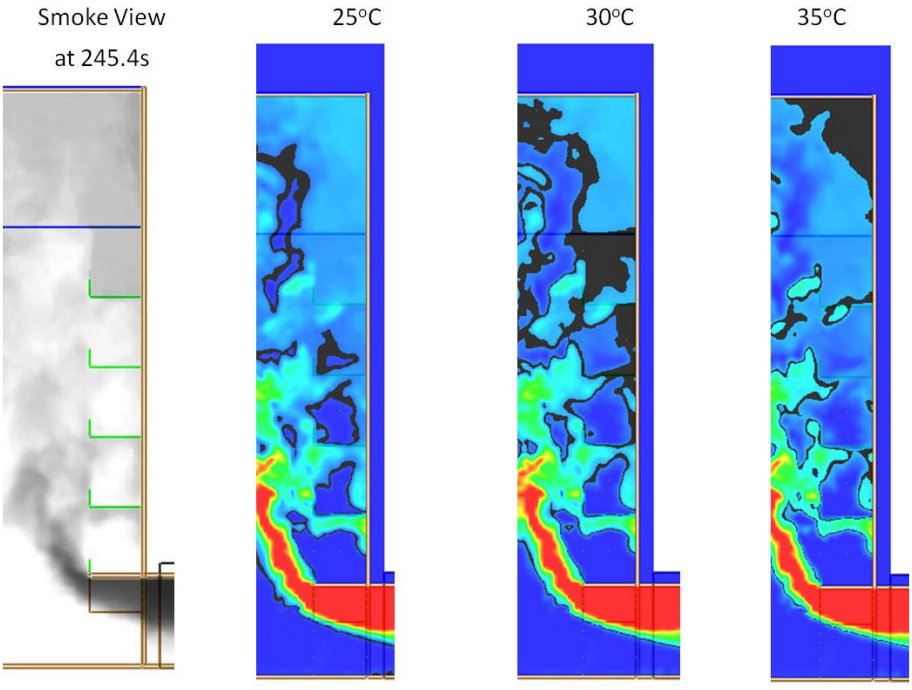

Figure F6. Smokeview and temperature profile for F23E5.

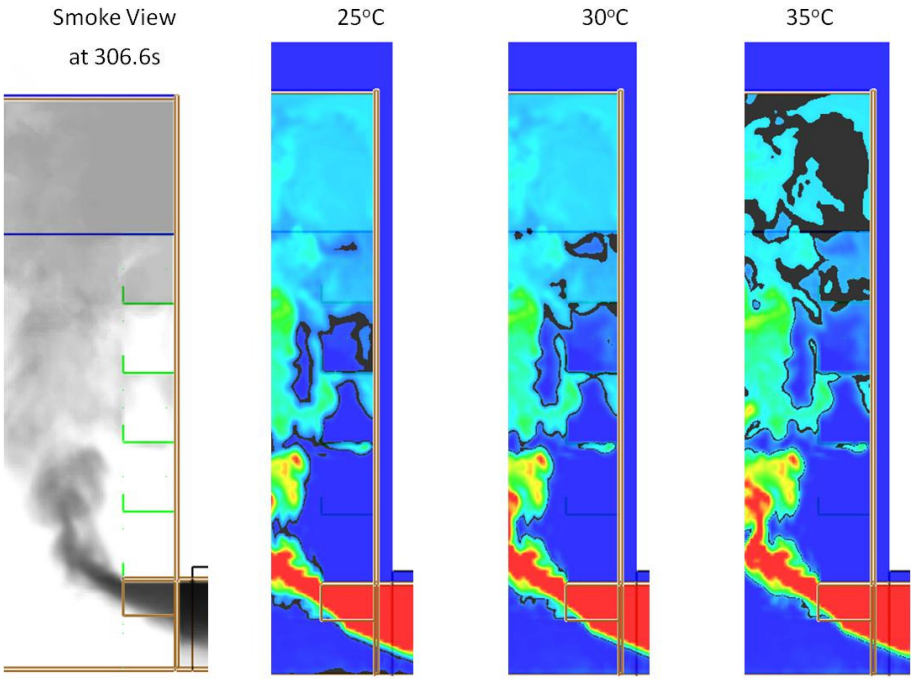

Figure F7. Smokeview and temperature profile for F27E5.

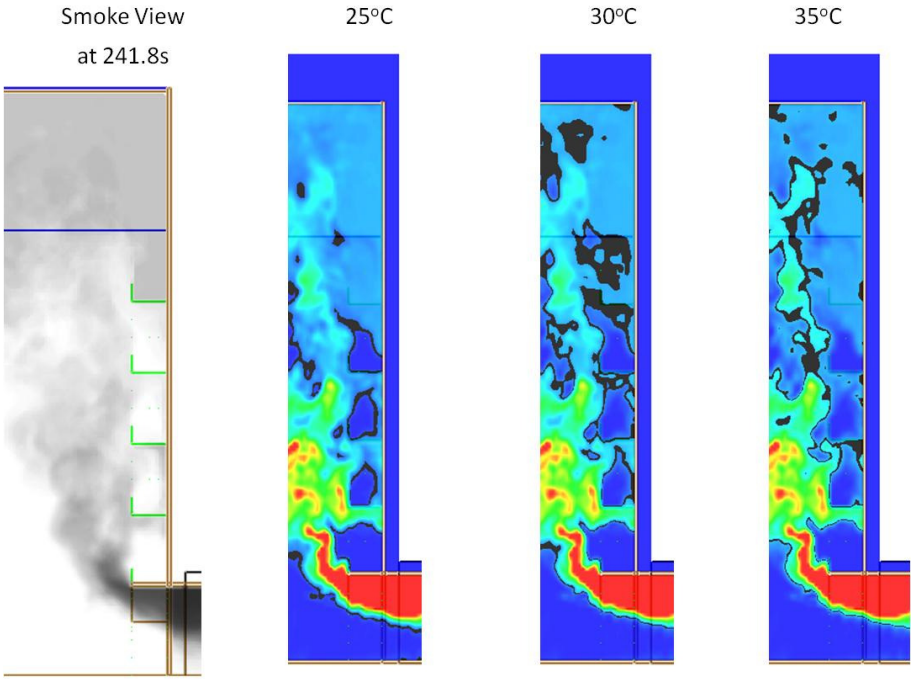

Figure F8. Smokeview and temperature profile for F38E5.

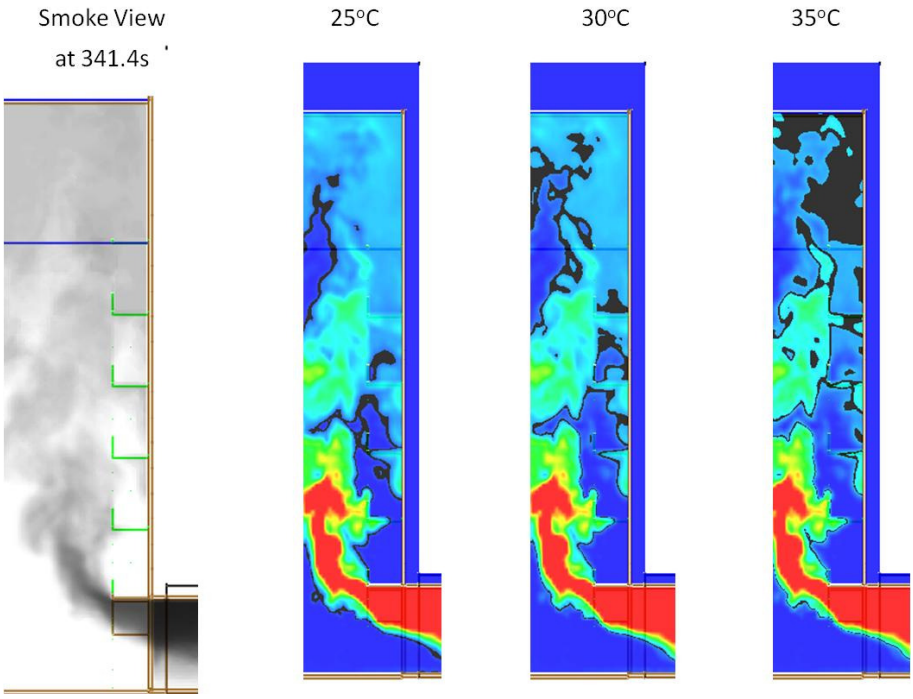

Figure F9. Smokeview and temperature profile for F41E5.

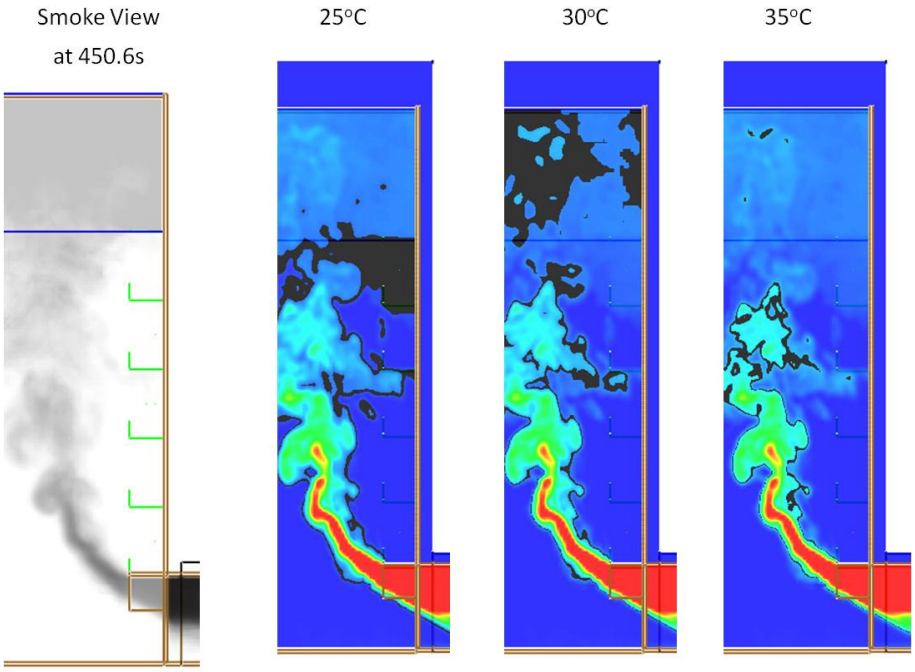

Figure F10. Smokeview and temperature profile for F43E5.

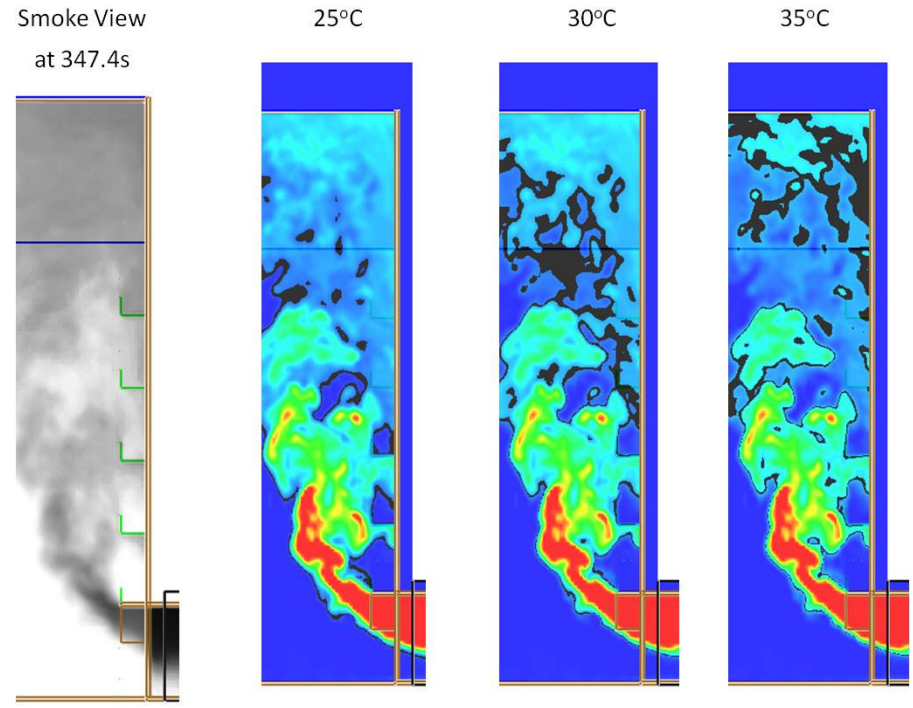

Figure F11. Smokeview and temperature profile for F56E5.

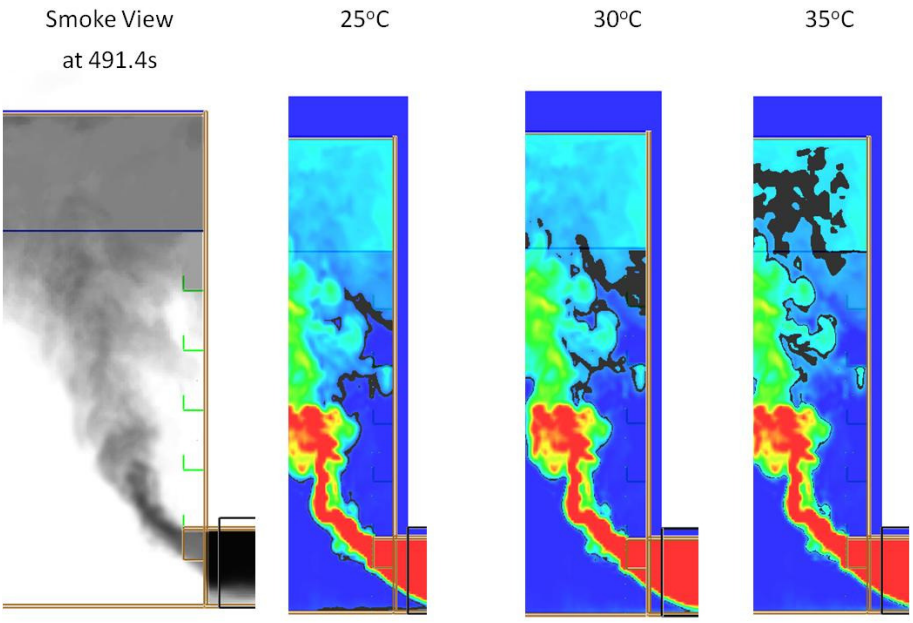

Figure F12. Smokeview and temperature profile for F60E5.

Full scale for 5 balcony (F01E5NUS)

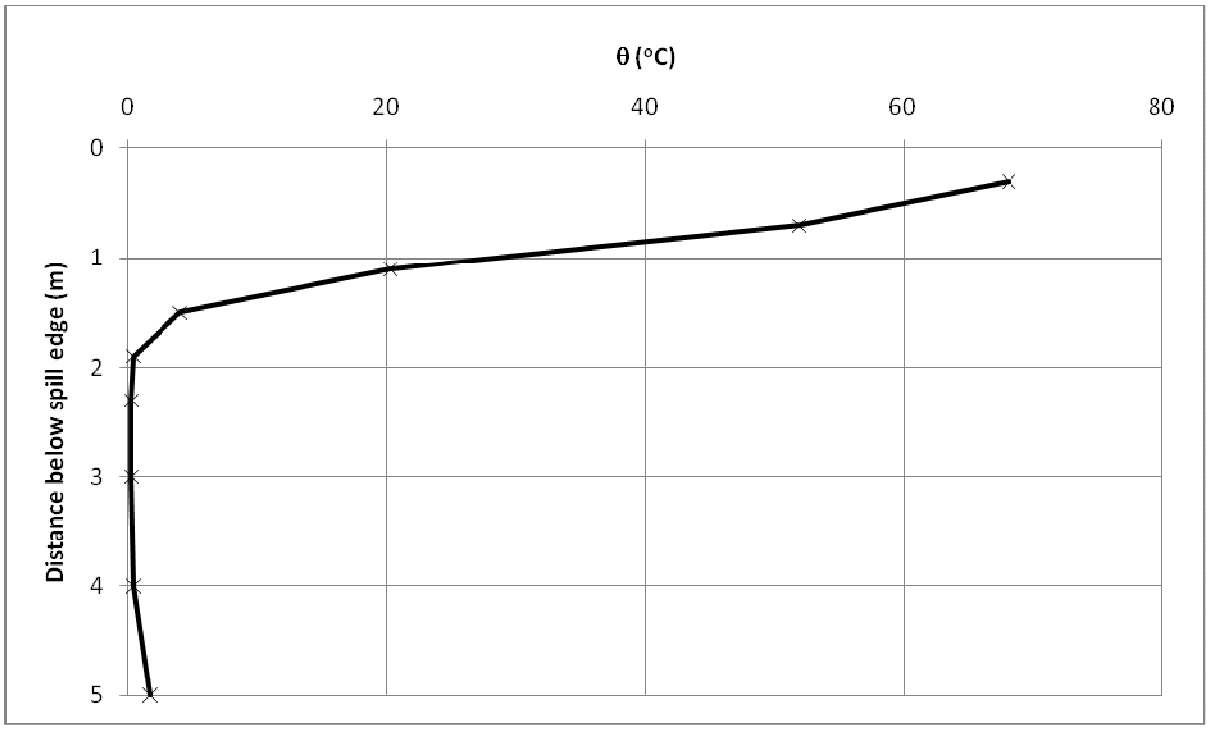

Figure G1. Temperature above ambient at the spill edge.

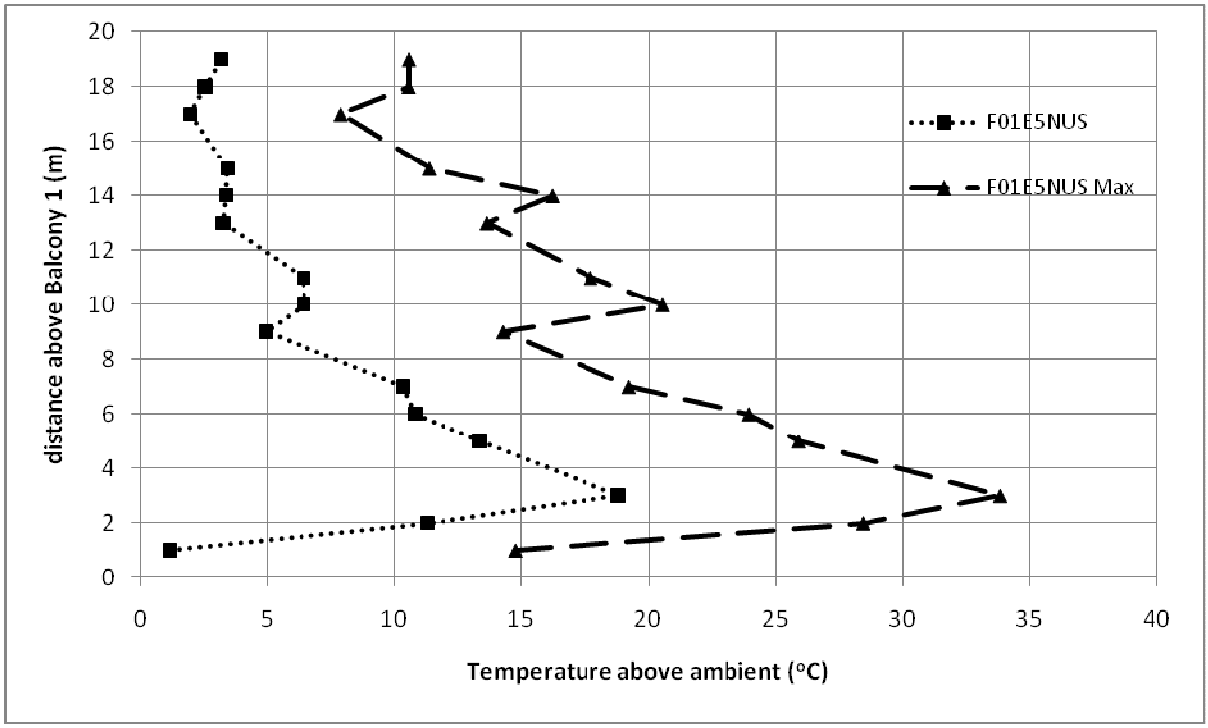

Figure G2. Temperature profiles across balcony edge.

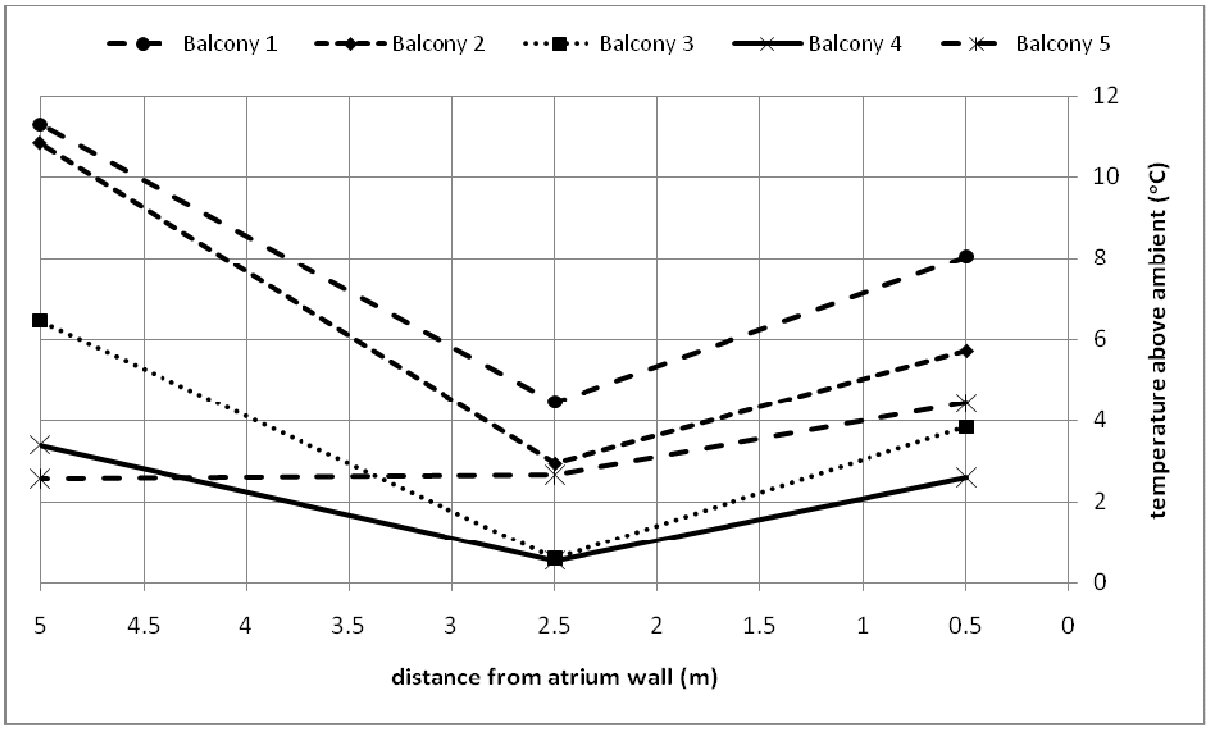

Figure G3. Temperature profiles along balcony breadth.

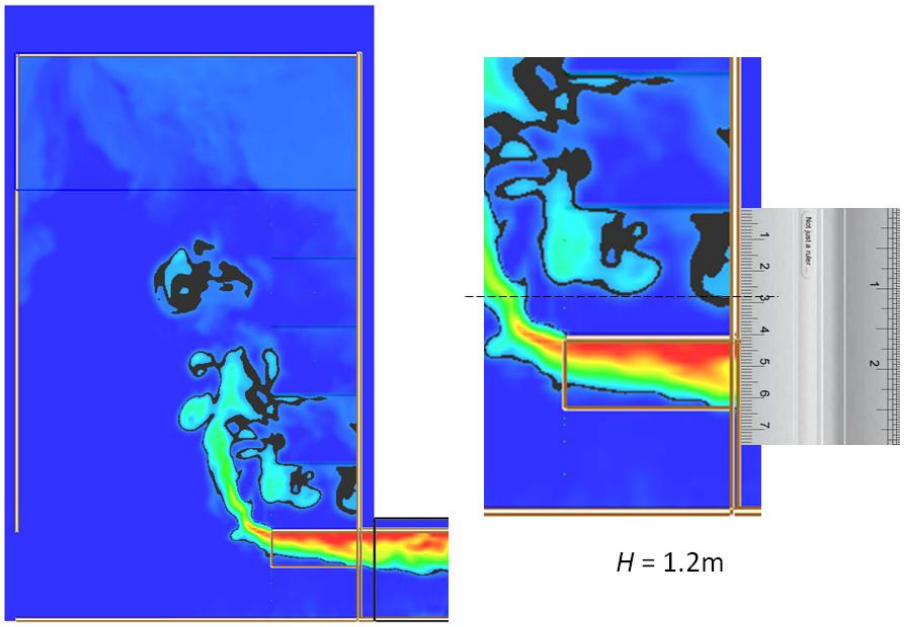

Figure G4. Smoke layer height measurement.

Full scale for 5 balcony (F03E5NUS)

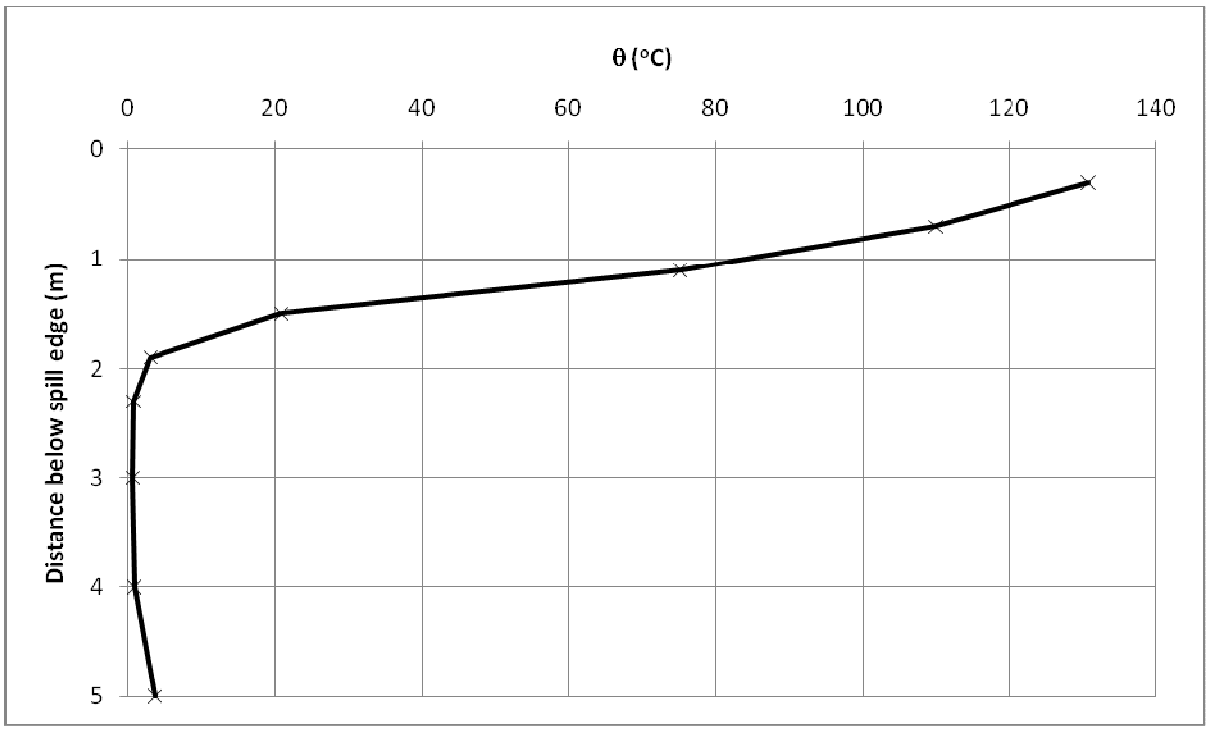

Figure G5. Temperature above ambient at the spill edge.

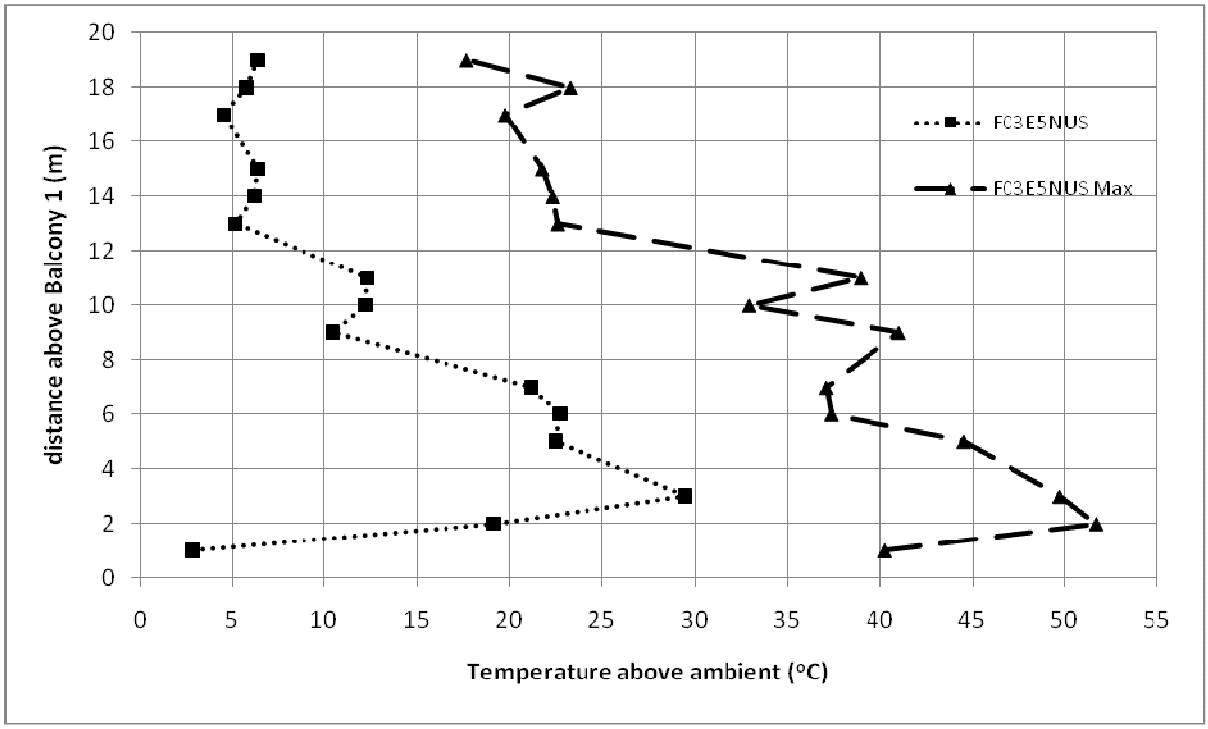

Figure G6. Temperature profiles across balcony edge.

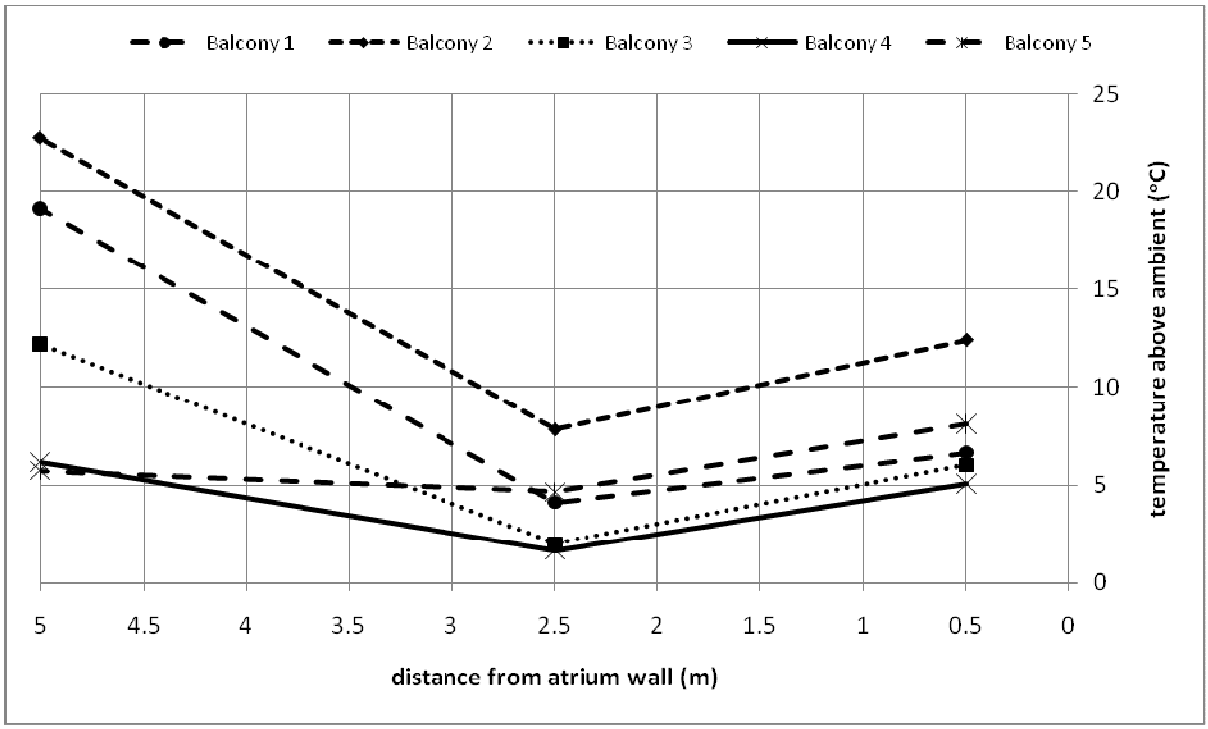

Figure G7. Temperature profiles along balcony breadth.

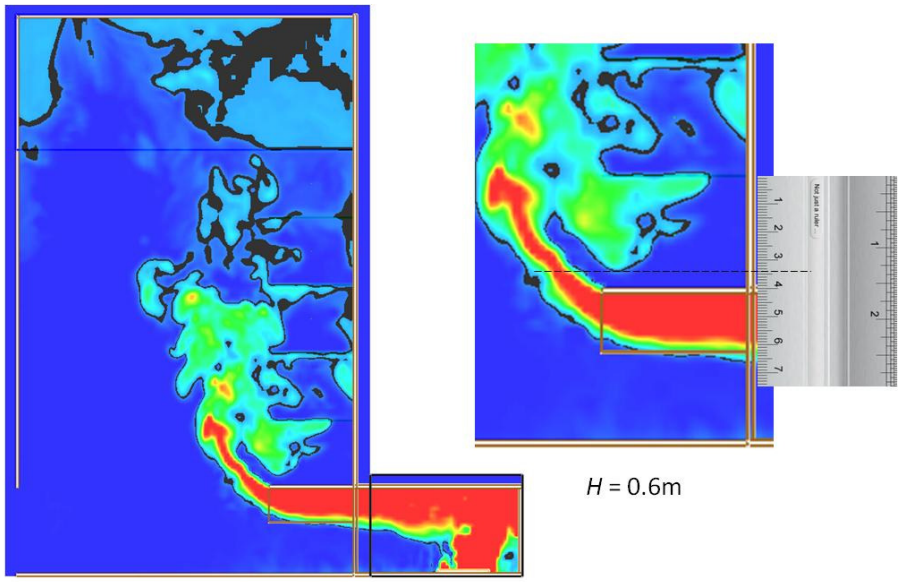

Figure G8. Smoke layer height measurement.

Full scale for 5 balcony (F08E5NUS)

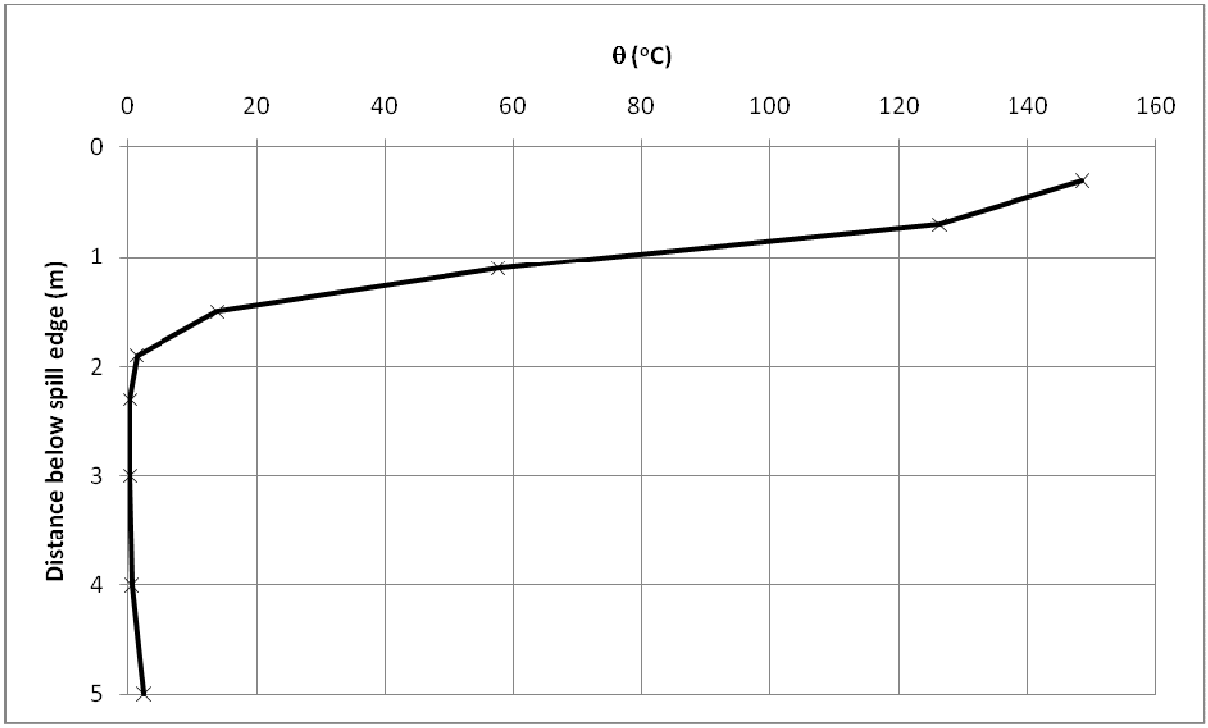

Figure G9. Temperature above ambient at the spill edge.

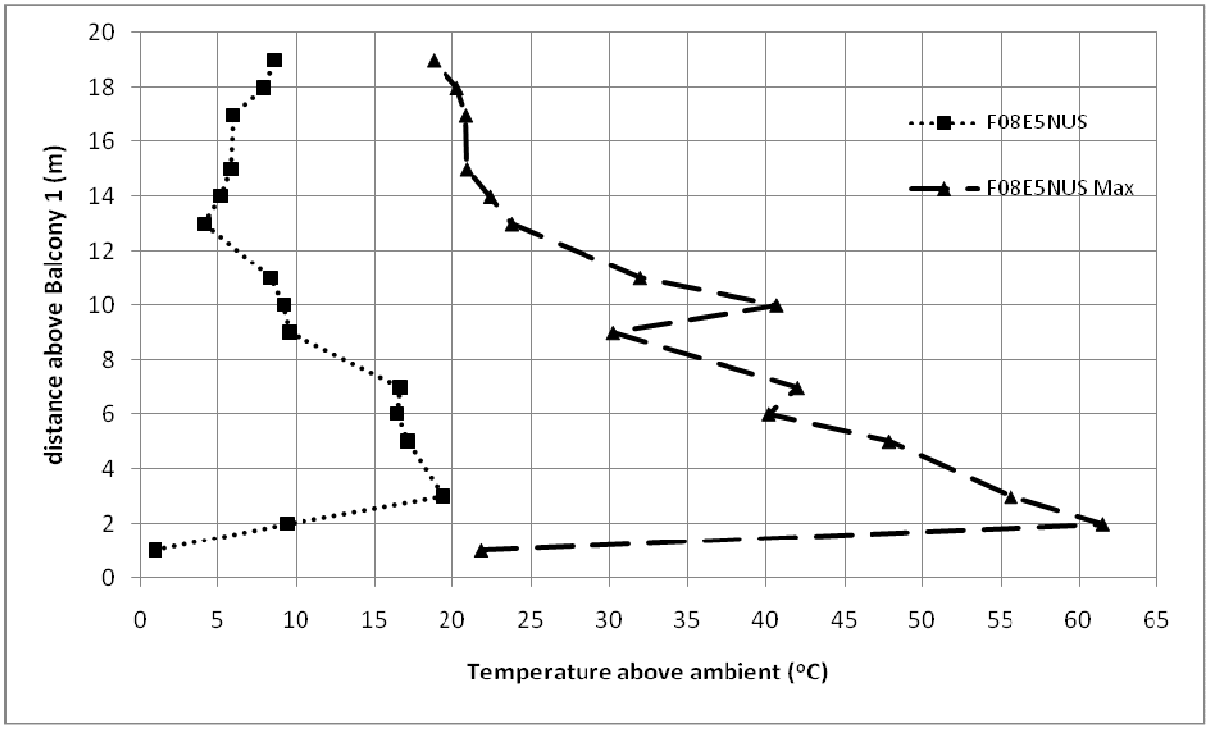

Figure G10. Temperature profiles across balcony edge.

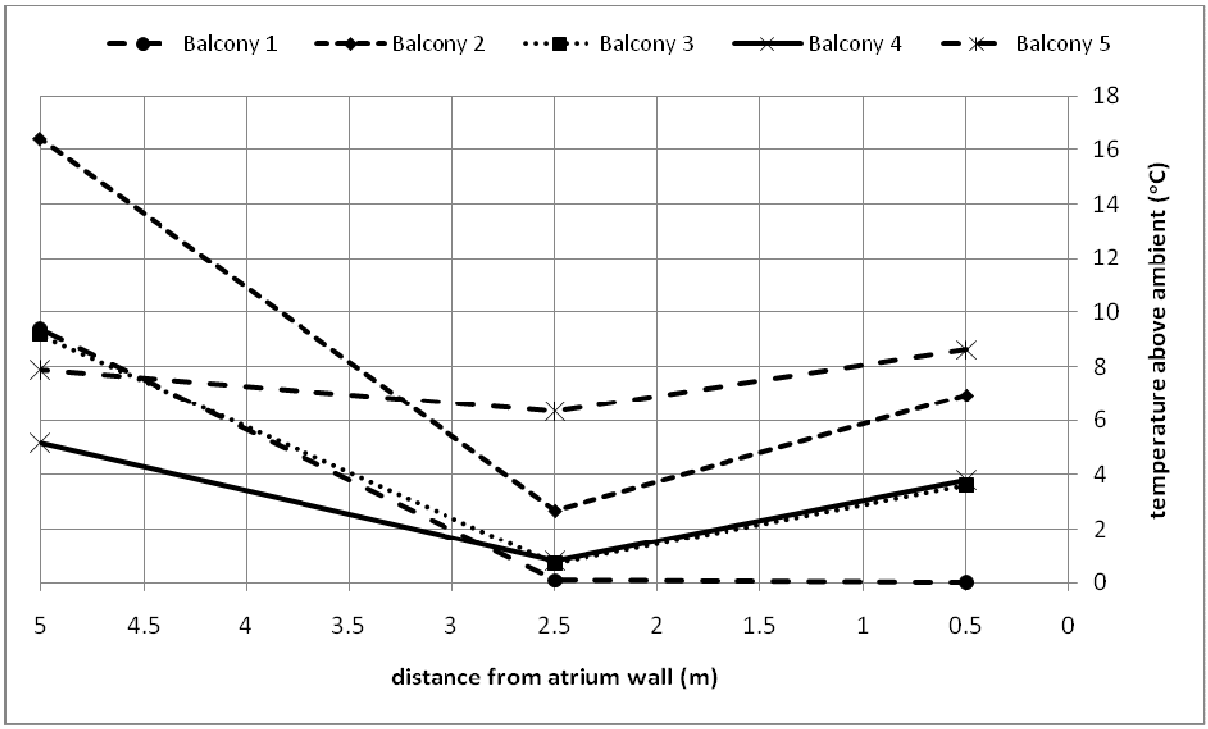

Figure G11. Temperature profiles along balcony breadth.

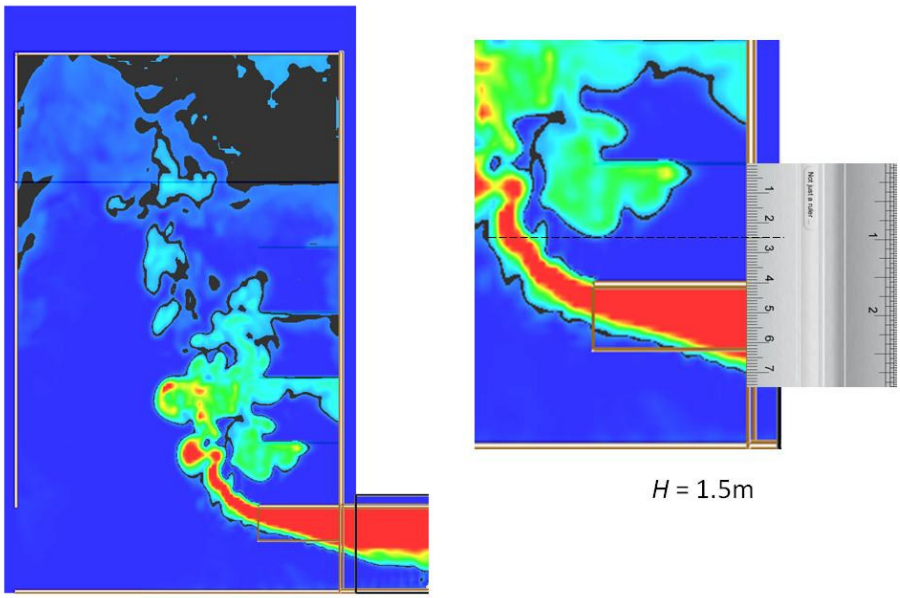

Figure G12. Smoke layer height measurement.

Full scale for 5 balcony (F13E5NUS)

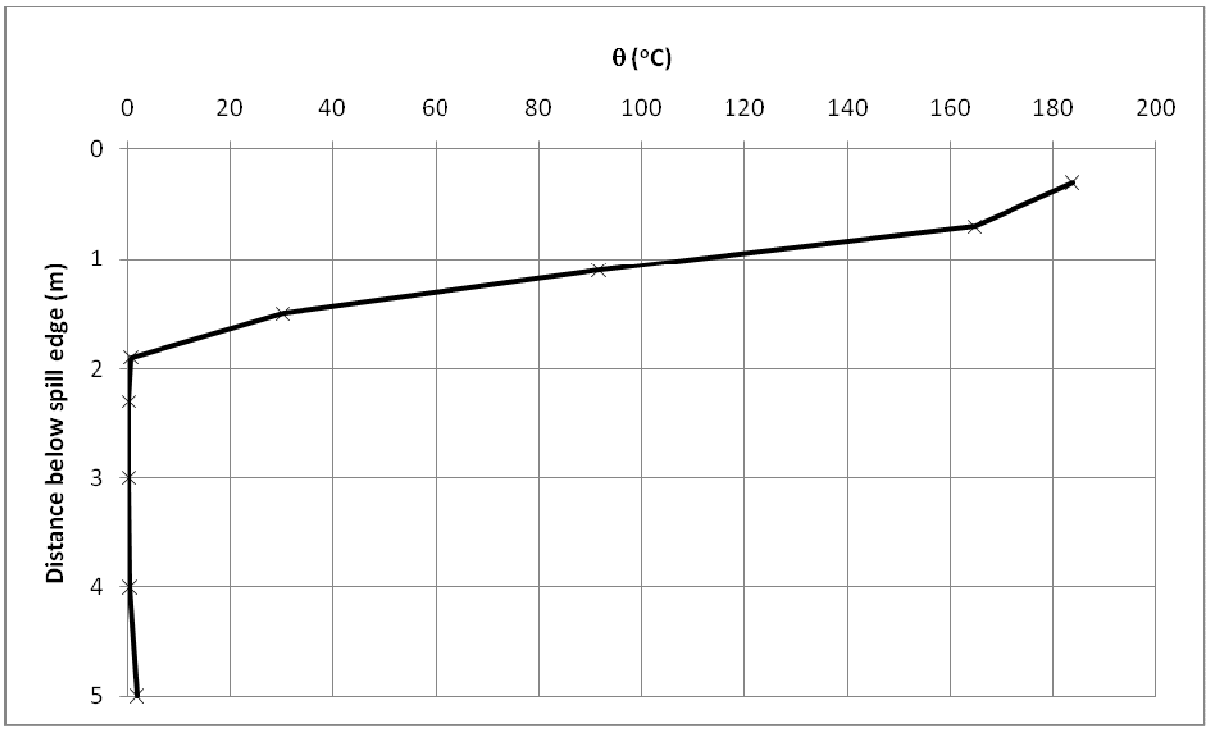

Figure G13. Temperature above ambient at the spill edge.

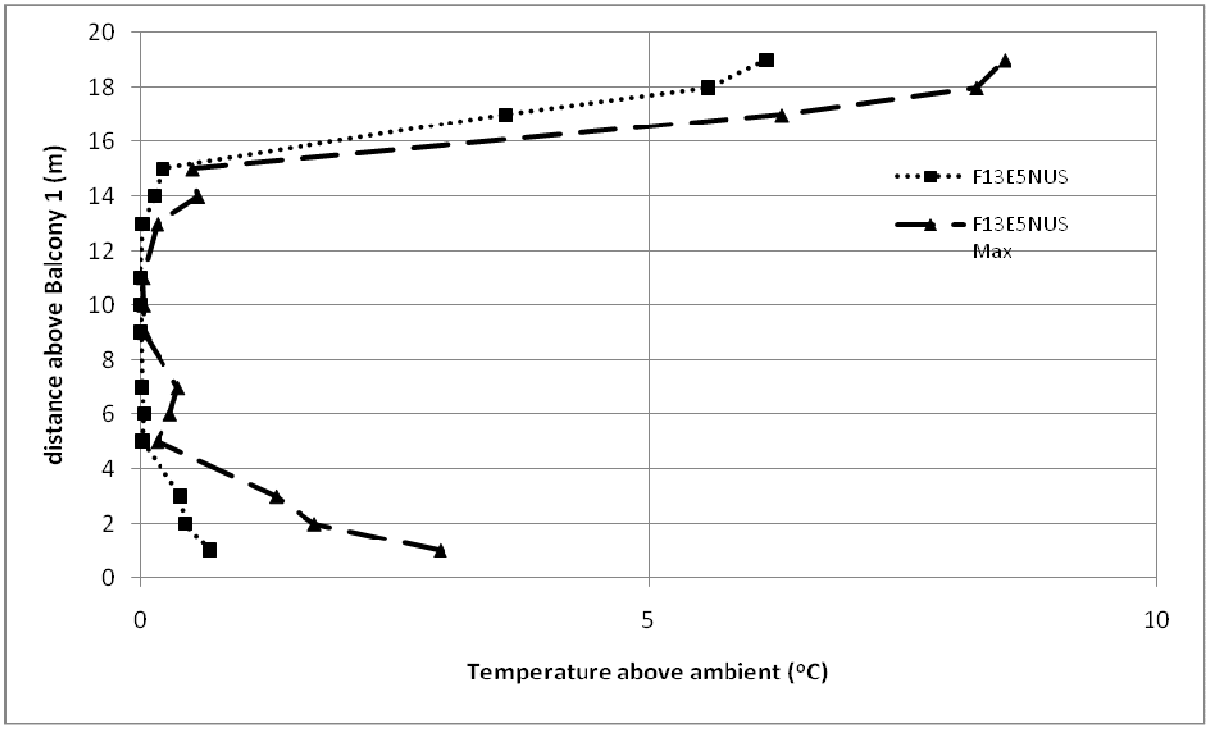

Figure G14. Temperature profiles across balcony edge.

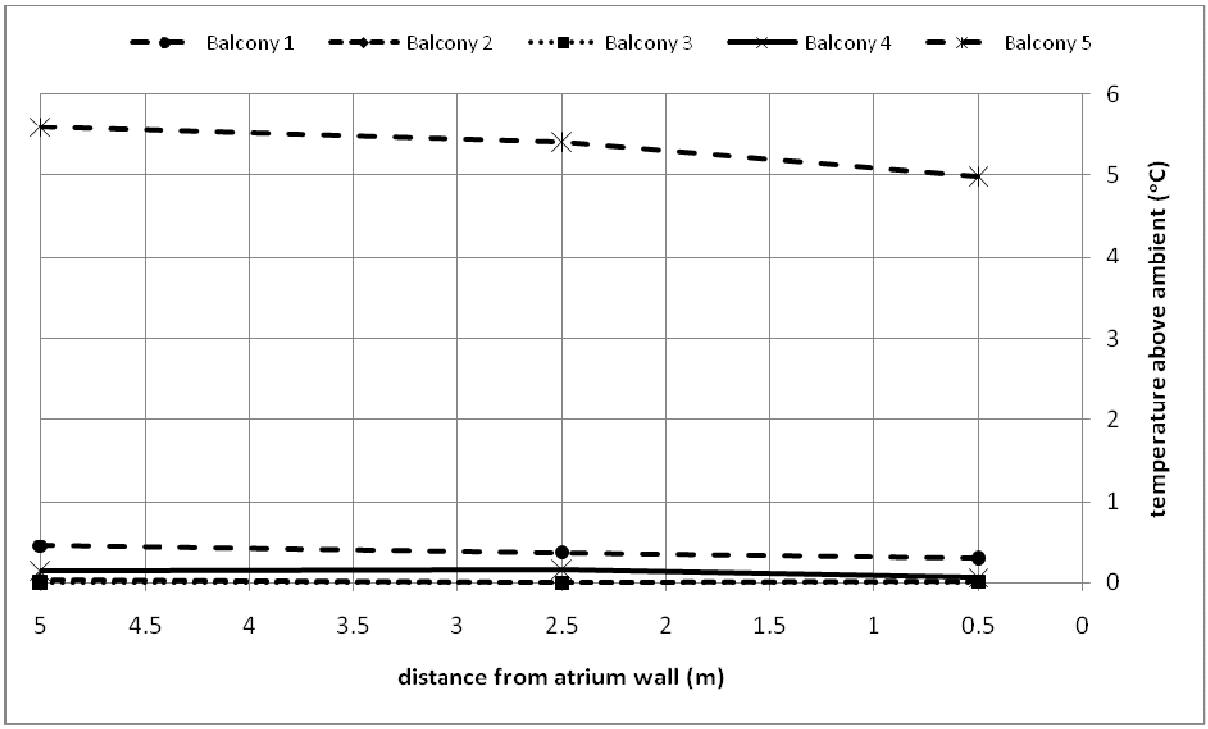

Figure G15. Temperature profiles along balcony breadth.

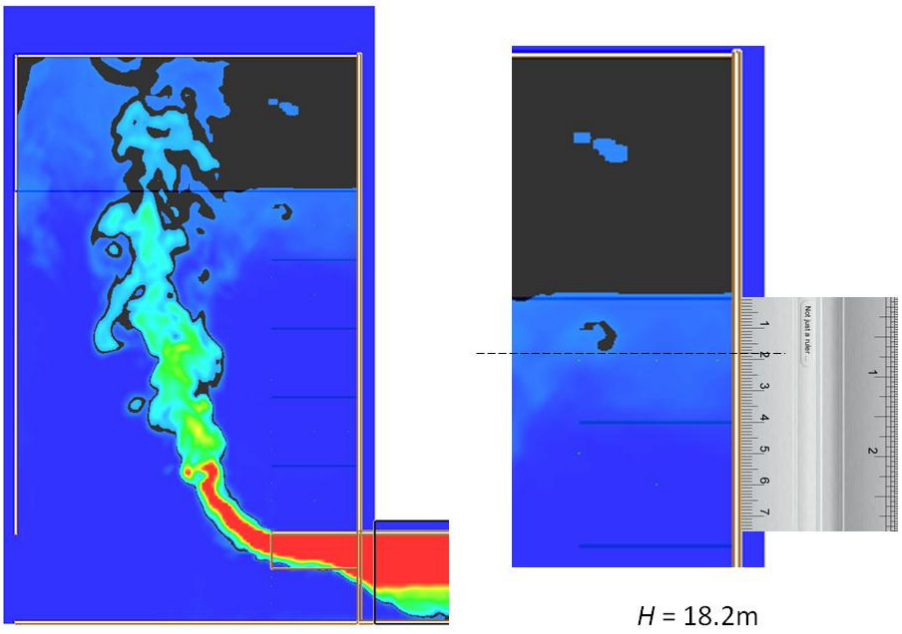

Figure G16. Smoke layer height measurement.

Full scale for 5 balcony (F19E5NUS)

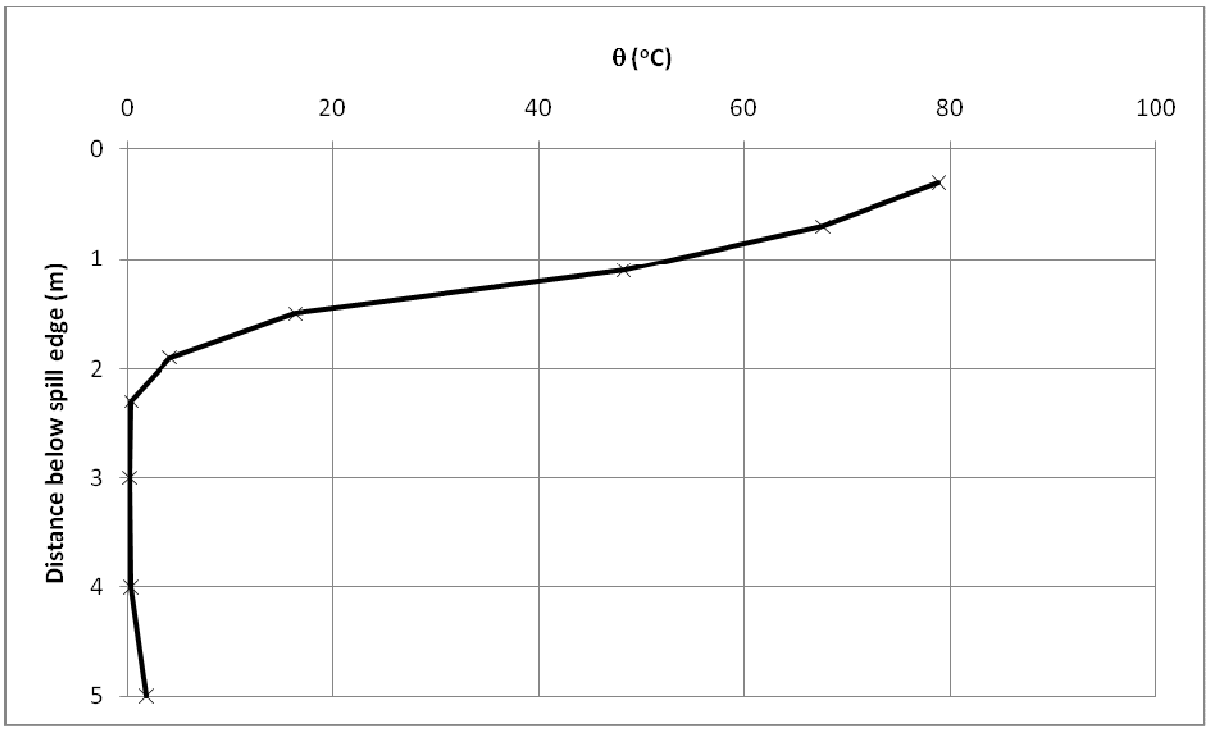

Figure G17. Temperature above ambient at the spill edge.

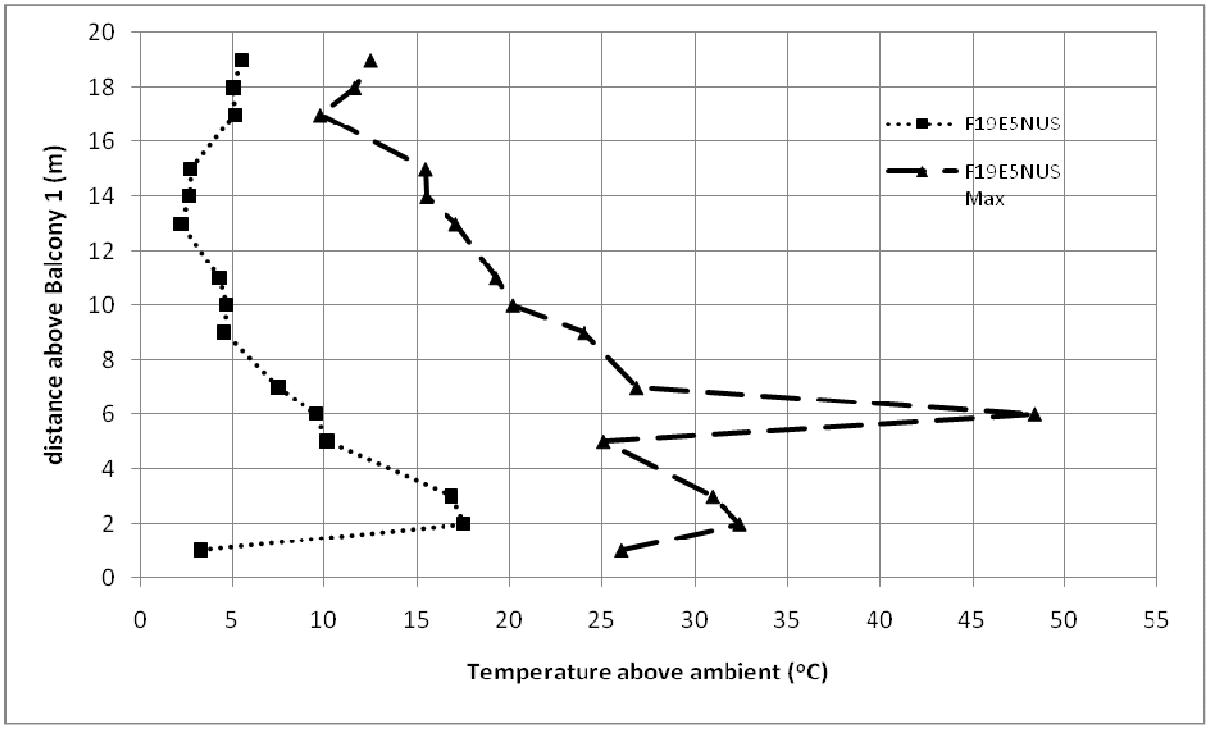

Figure G18. Temperature profiles across balcony edge.

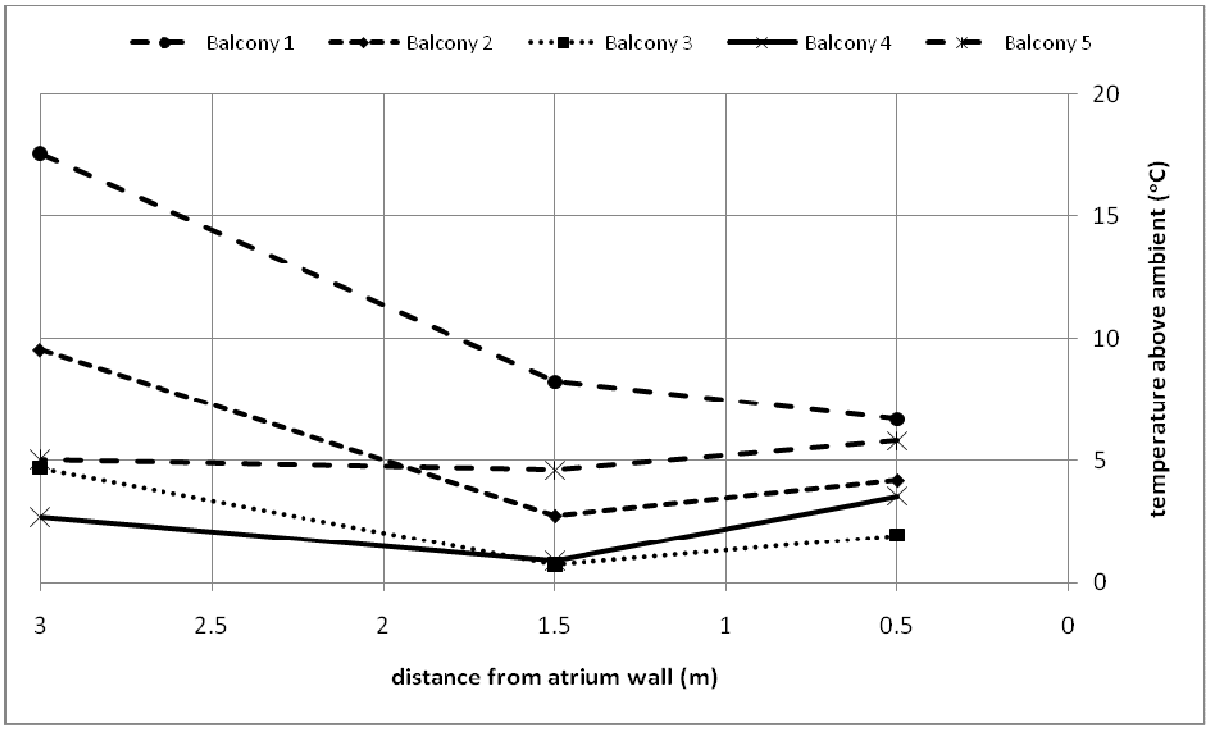

Figure G19. Temperature profiles along balcony breadth.

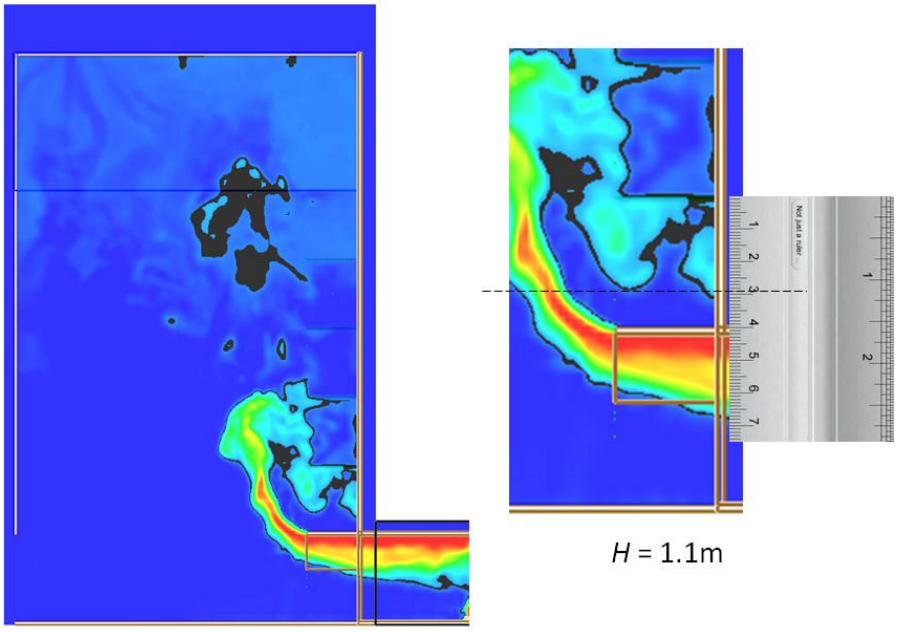

Figure G20. Smoke layer height measurement.

Full scale for 5 balcony (F23E5NUS)

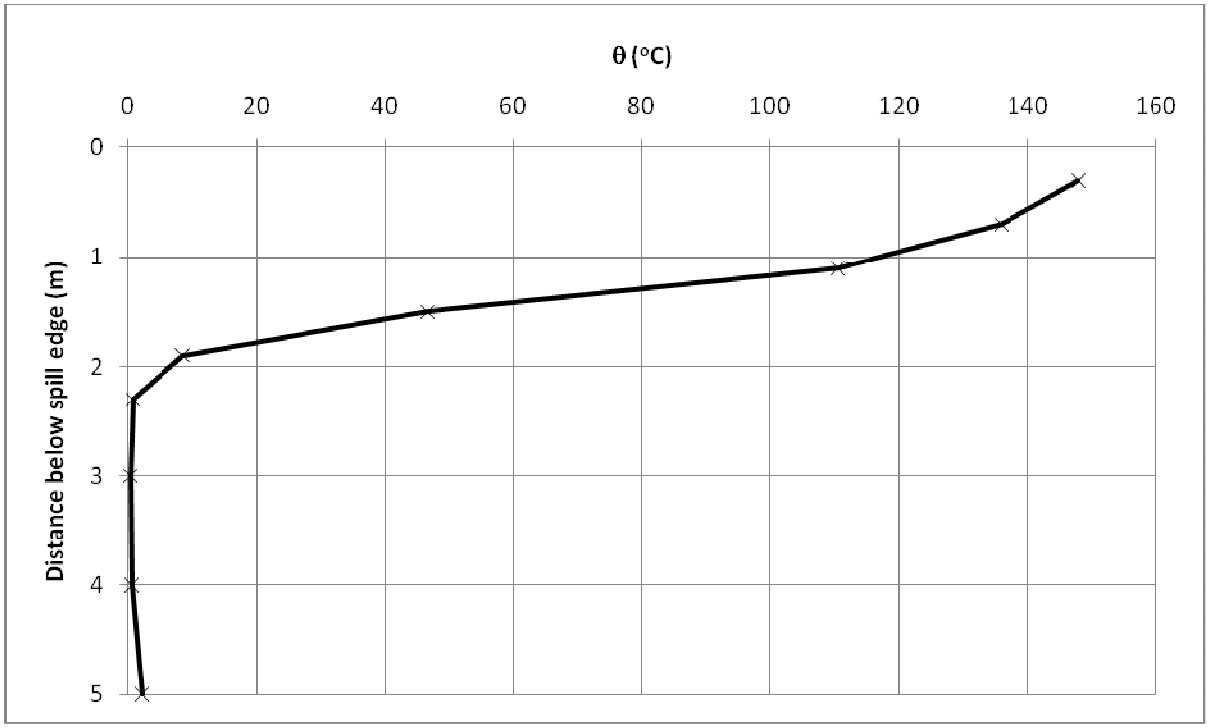

Figure G21. Temperature above ambient at the spill edge.

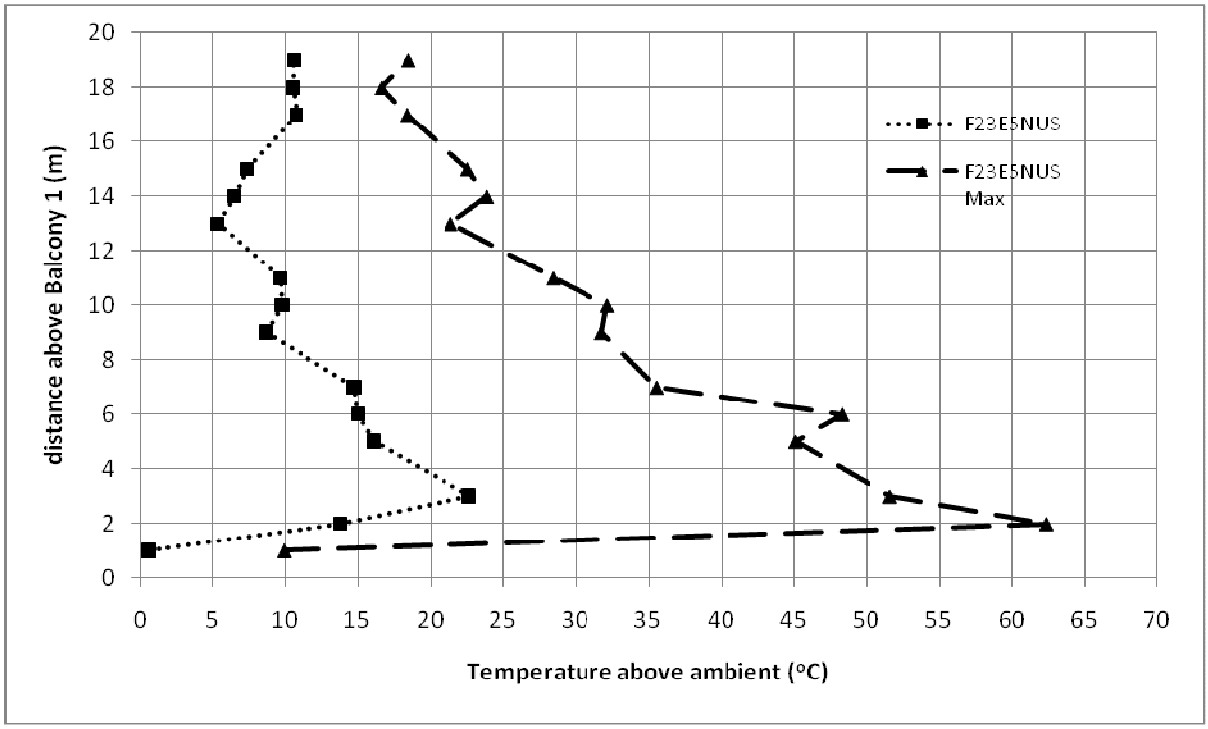

Figure G22. Temperature profiles across balcony edge.

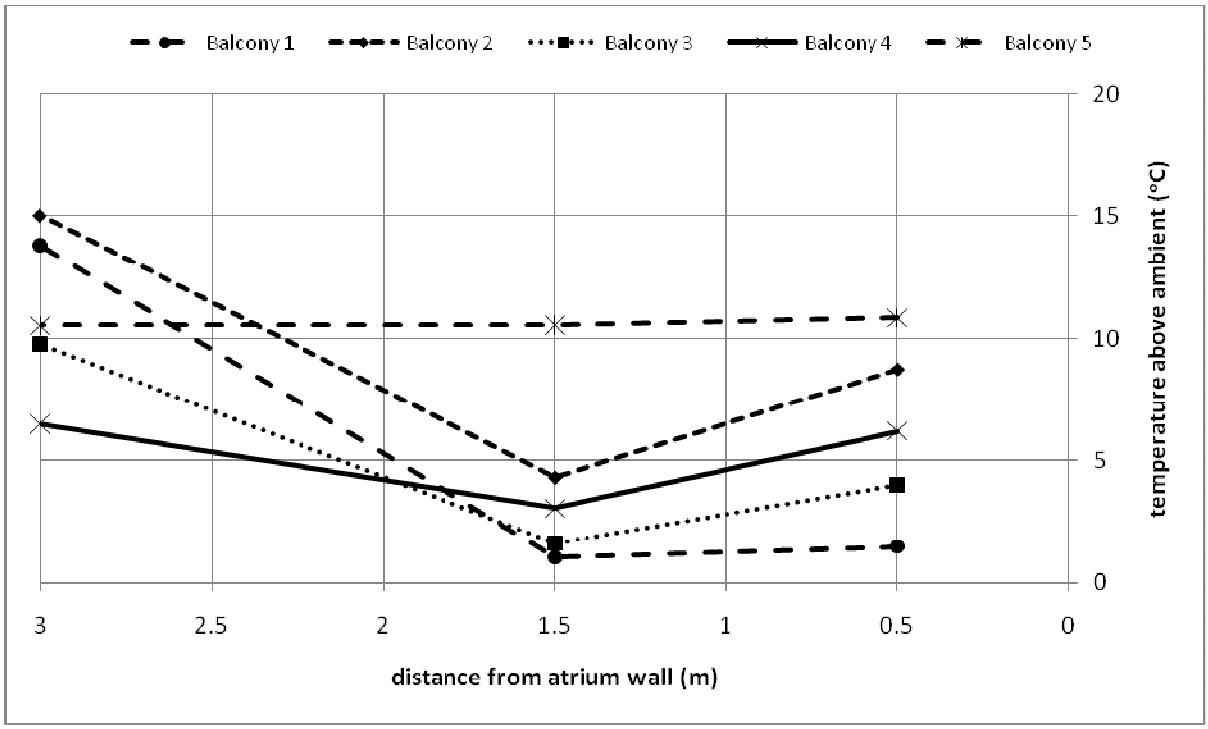

Figure G23. Temperature profiles along balcony breadth.

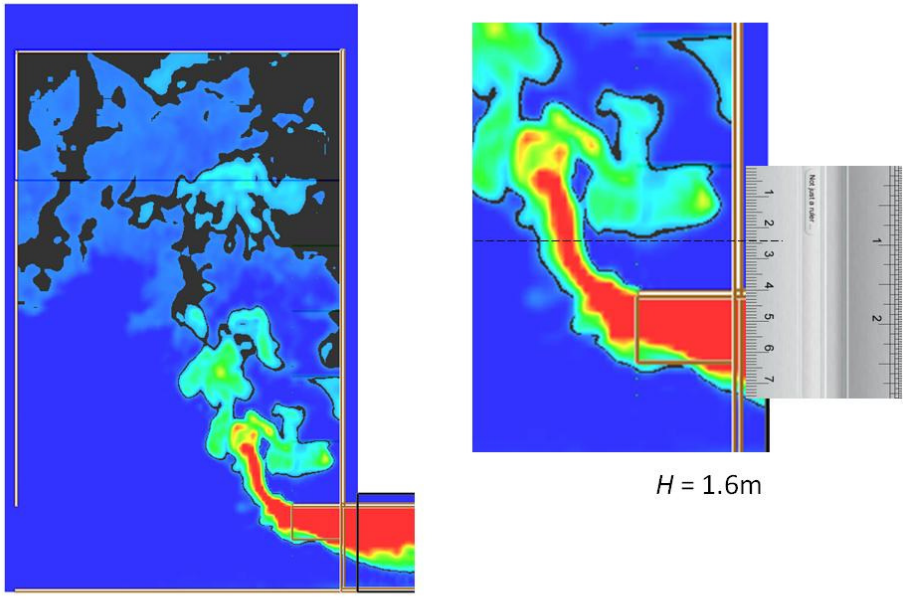

Figure G24. Smoke layer height measurement.

Full scale for 5 balcony (F27E5NUS)

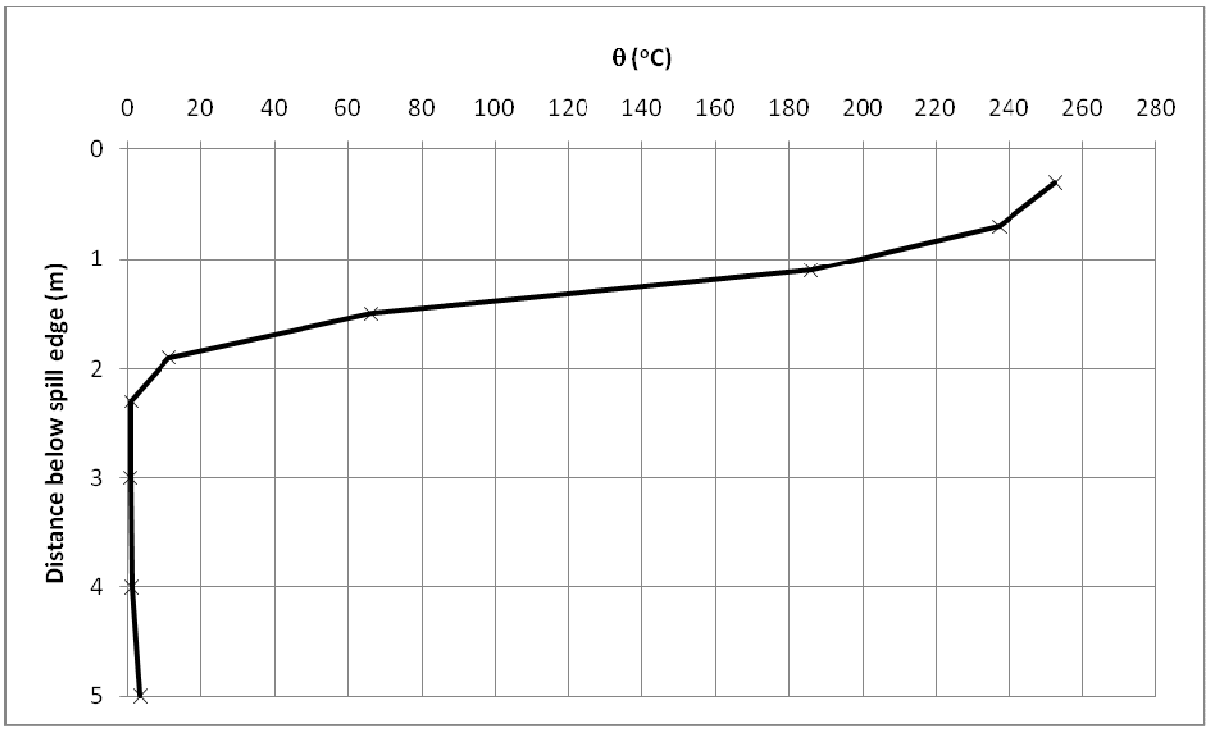

Figure G25. Temperature above ambient at the spill edge.

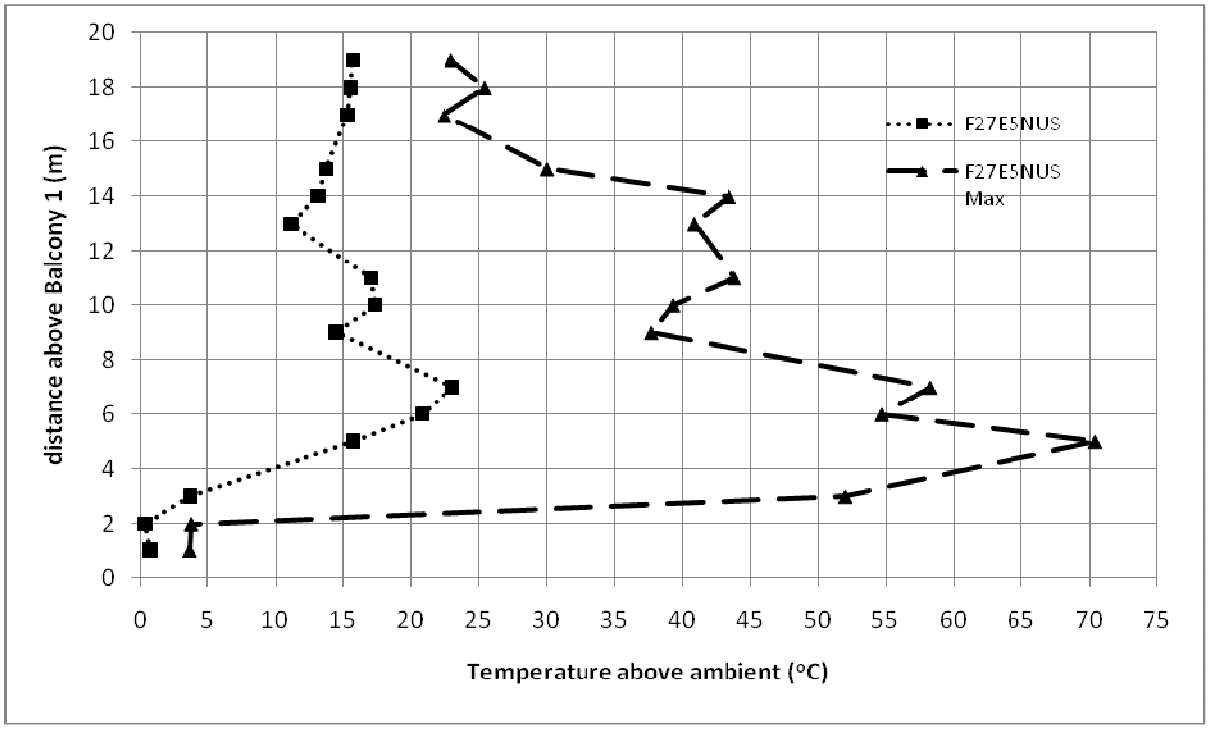

Figure G26. Temperature profiles across balcony edge.

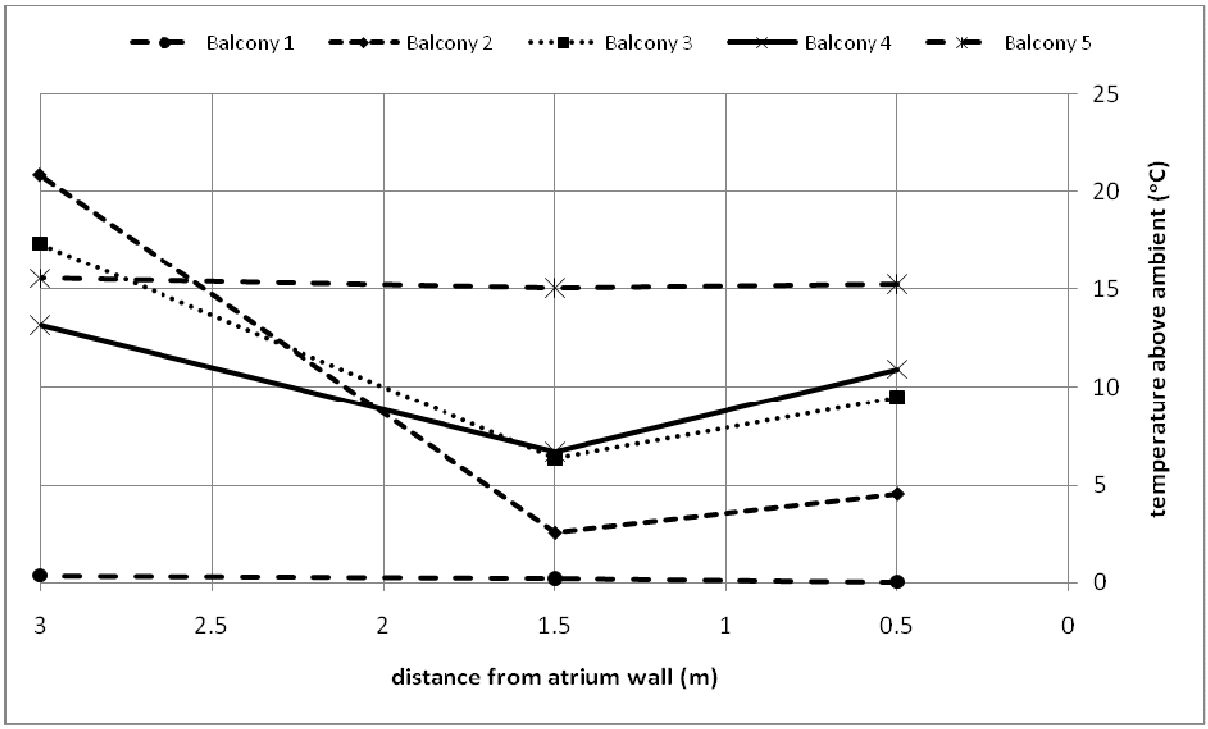

Figure G27. Temperature profiles along balcony breadth.

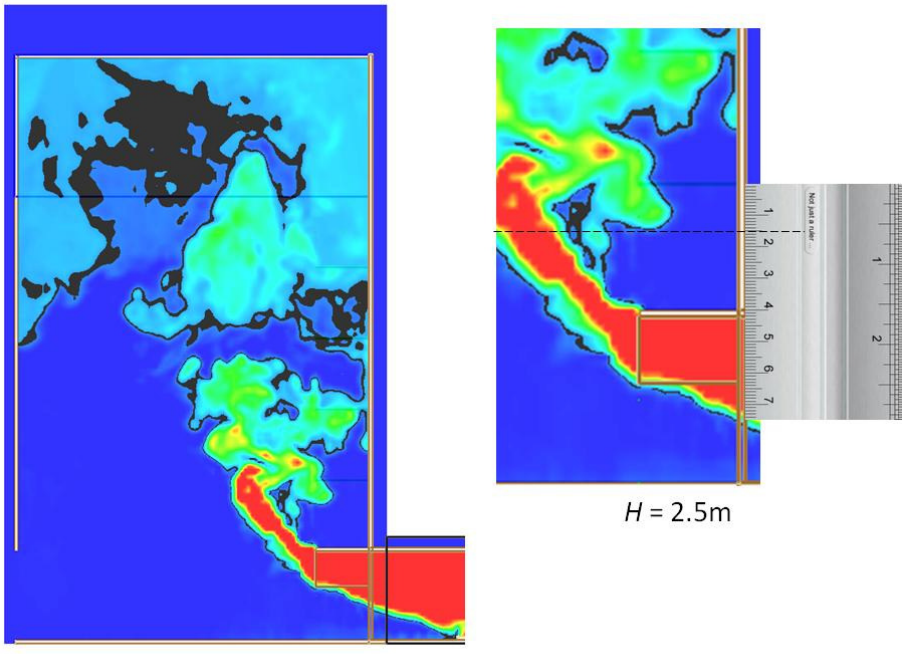

Figure G28. Smoke layer height measurement.

Full scale for 5 balcony (F38E5NUS)

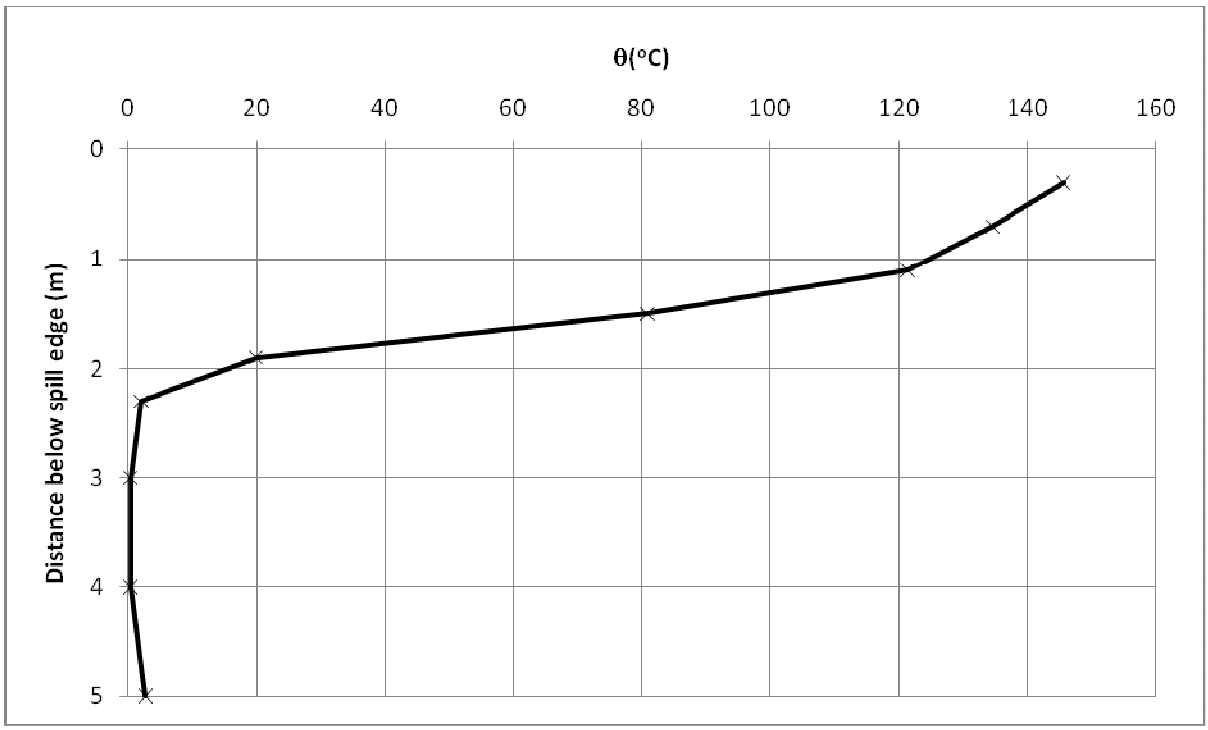

Figure G29. Temperature above ambient at the spill edge.

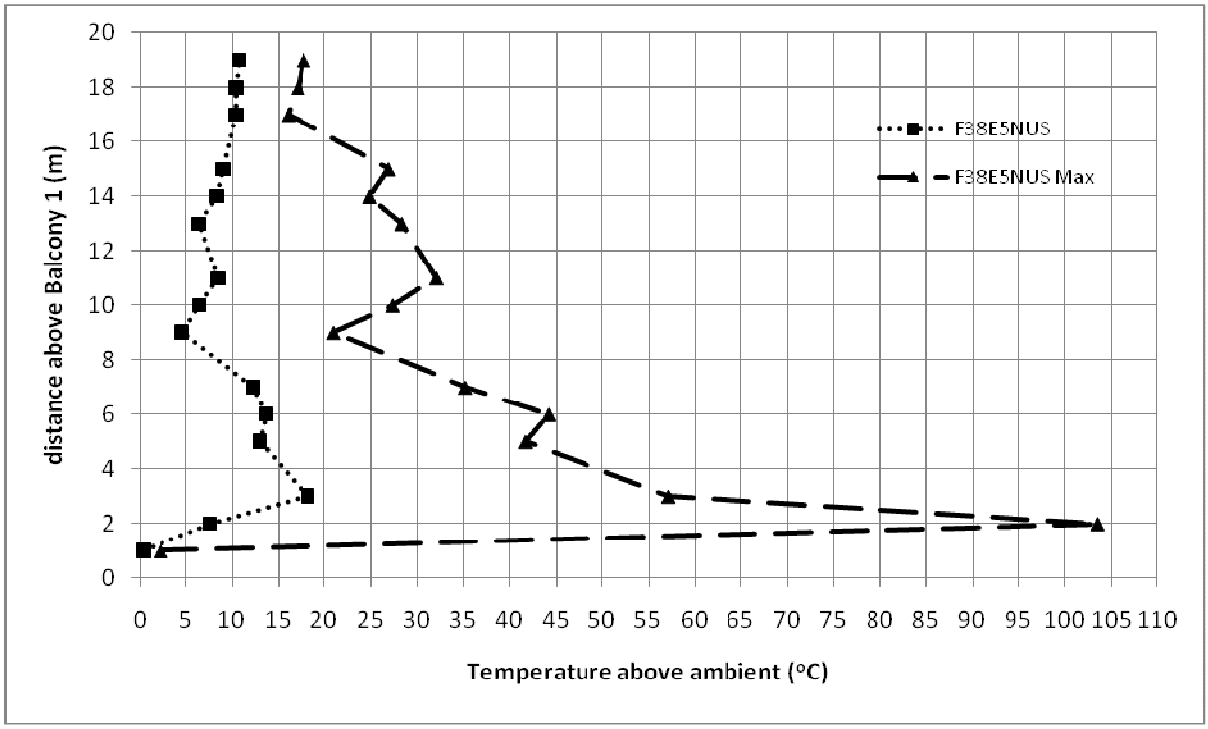

Figure G30. Temperature profiles across balcony edge.

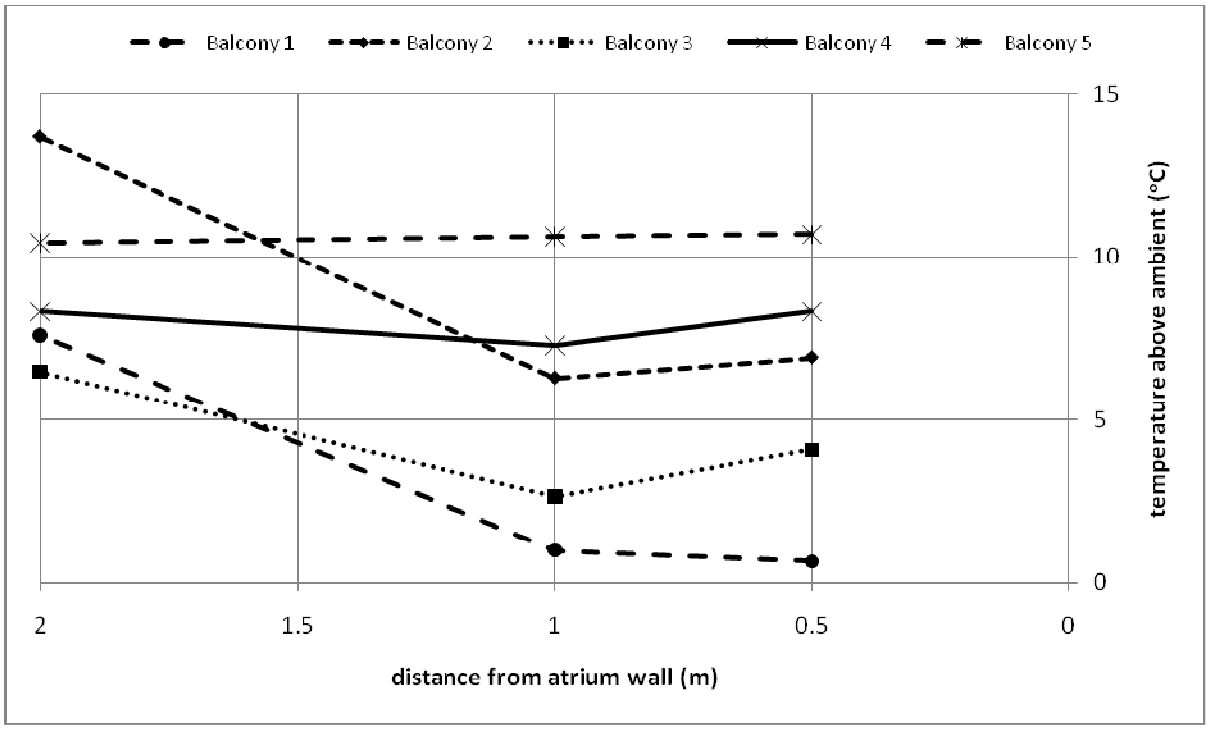

Figure G31. Temperature profiles along balcony breadth.

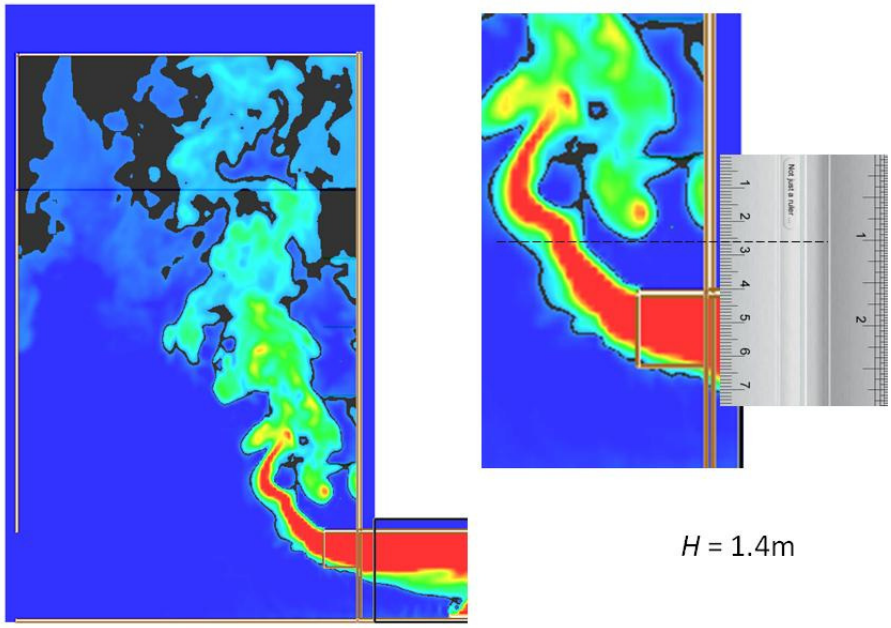

Figure G32. Smoke layer height measurement.

Full scale for 5 balcony (F41E5NUS)

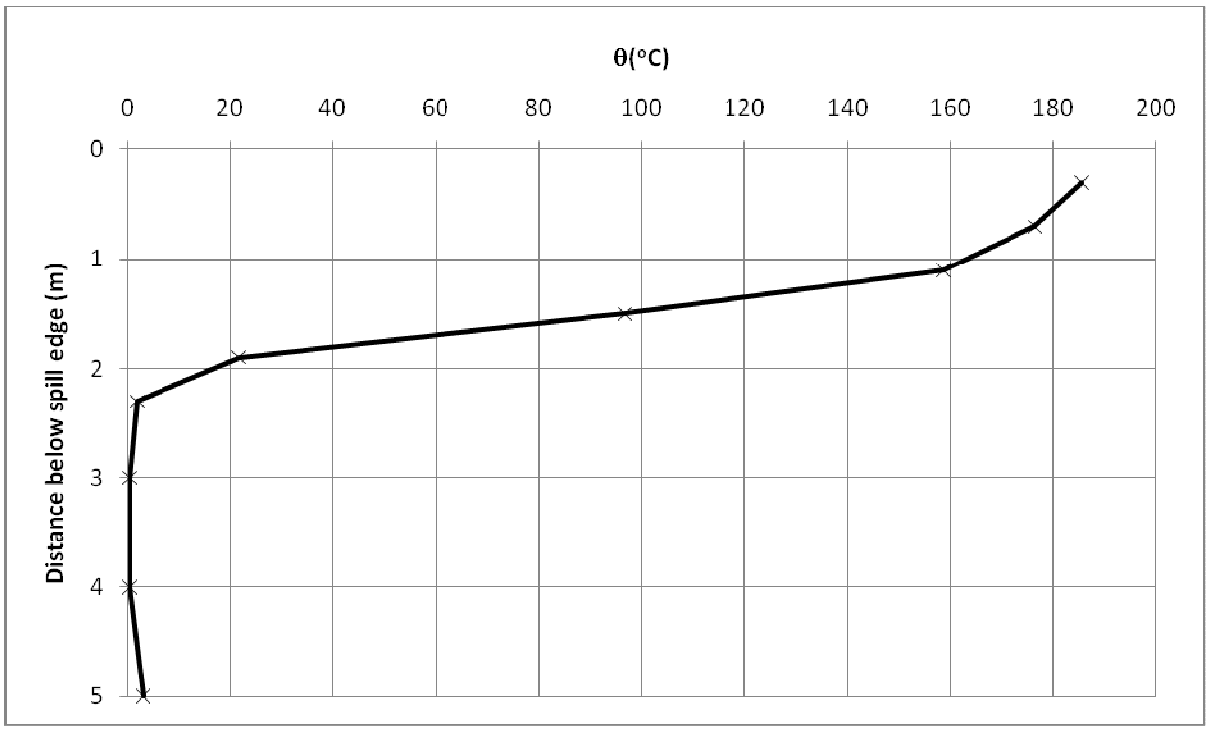

Figure G33. Temperature above ambient at the spill edge.

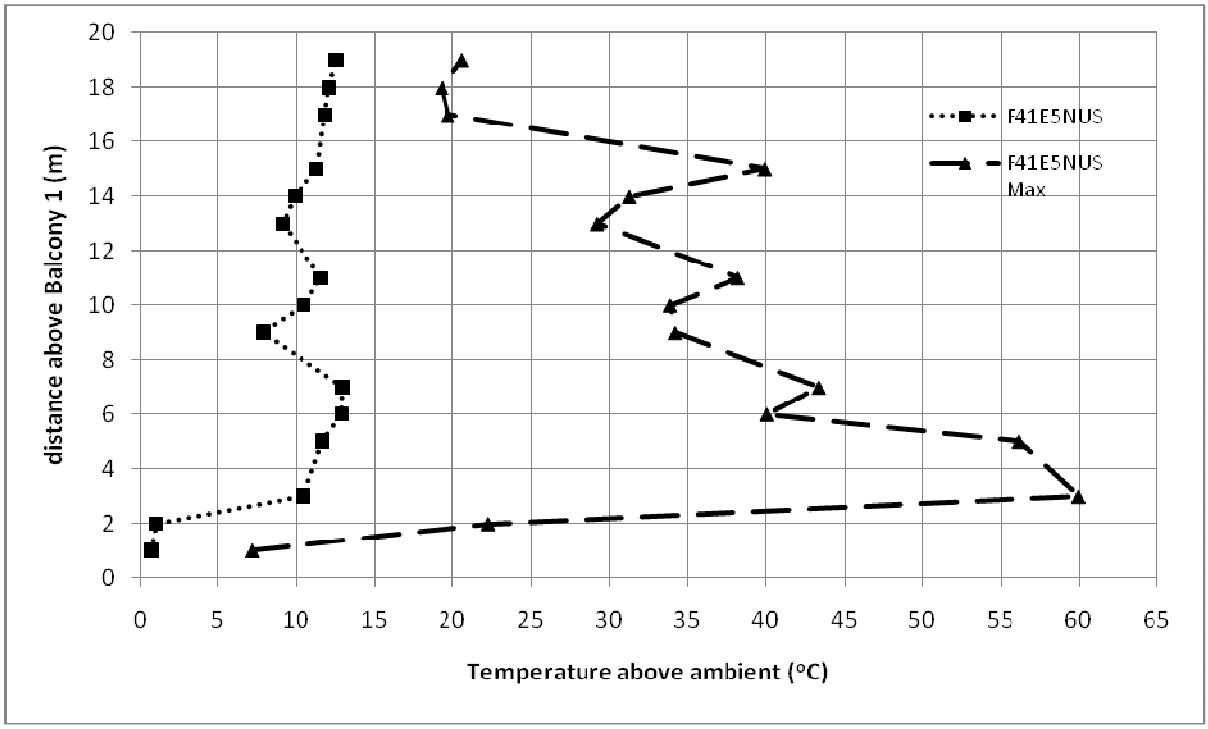

Figure G34. Temperature profiles across balcony edge.

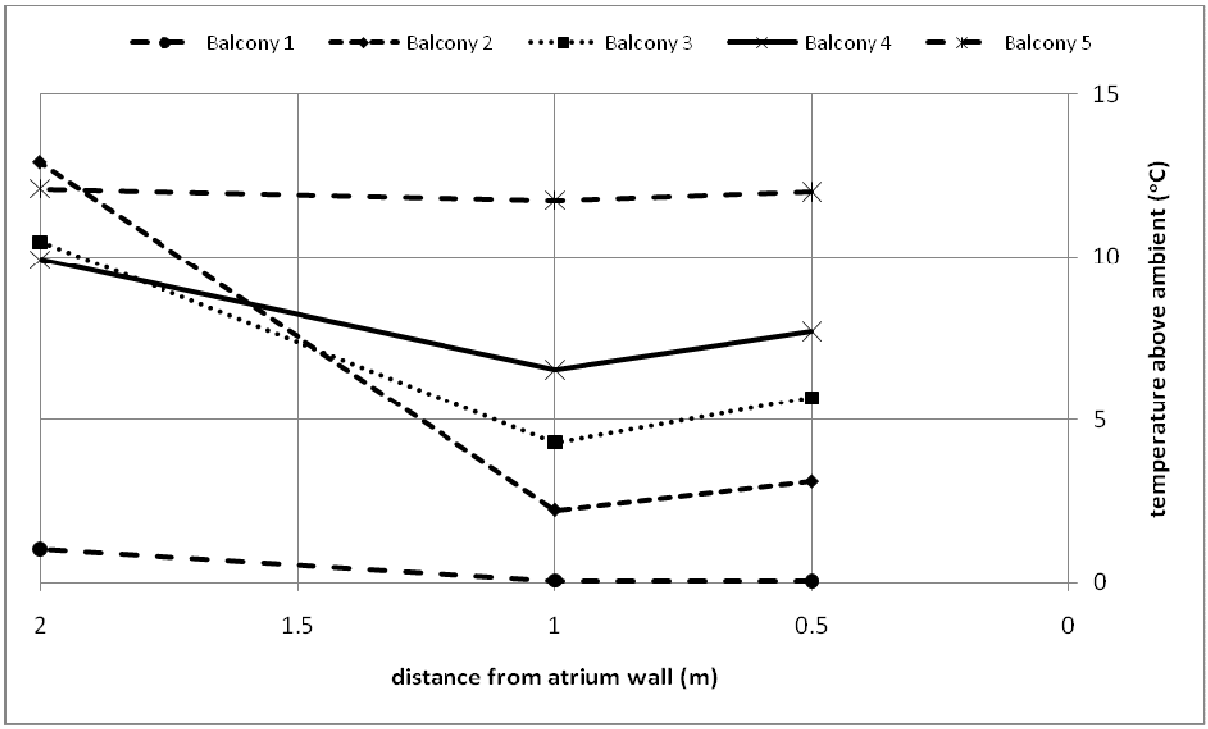

Figure G35. Temperature profiles along balcony breadth.

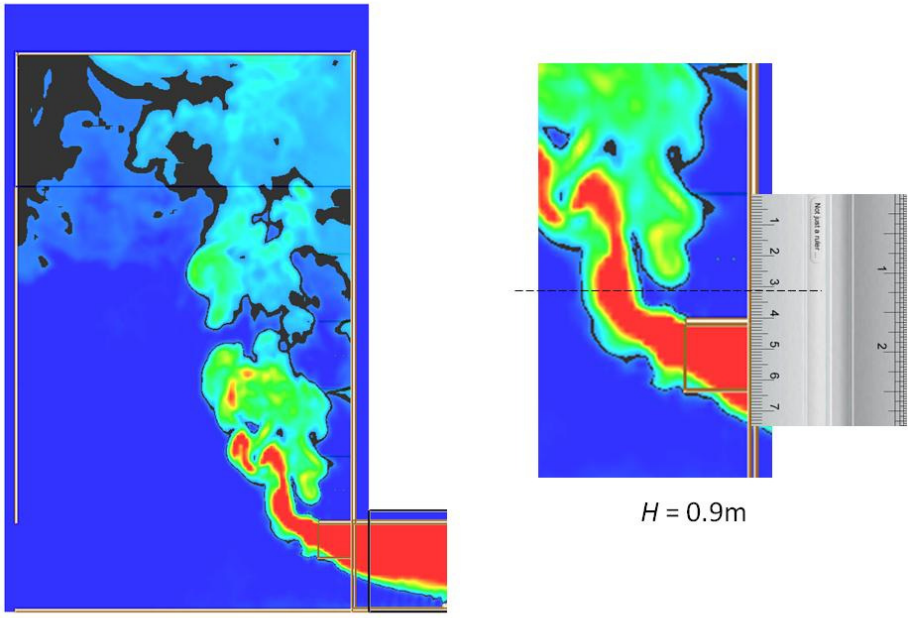

Figure G36. Smoke layer height measurement.

Full scale for 5 balcony (F43E5NUS)

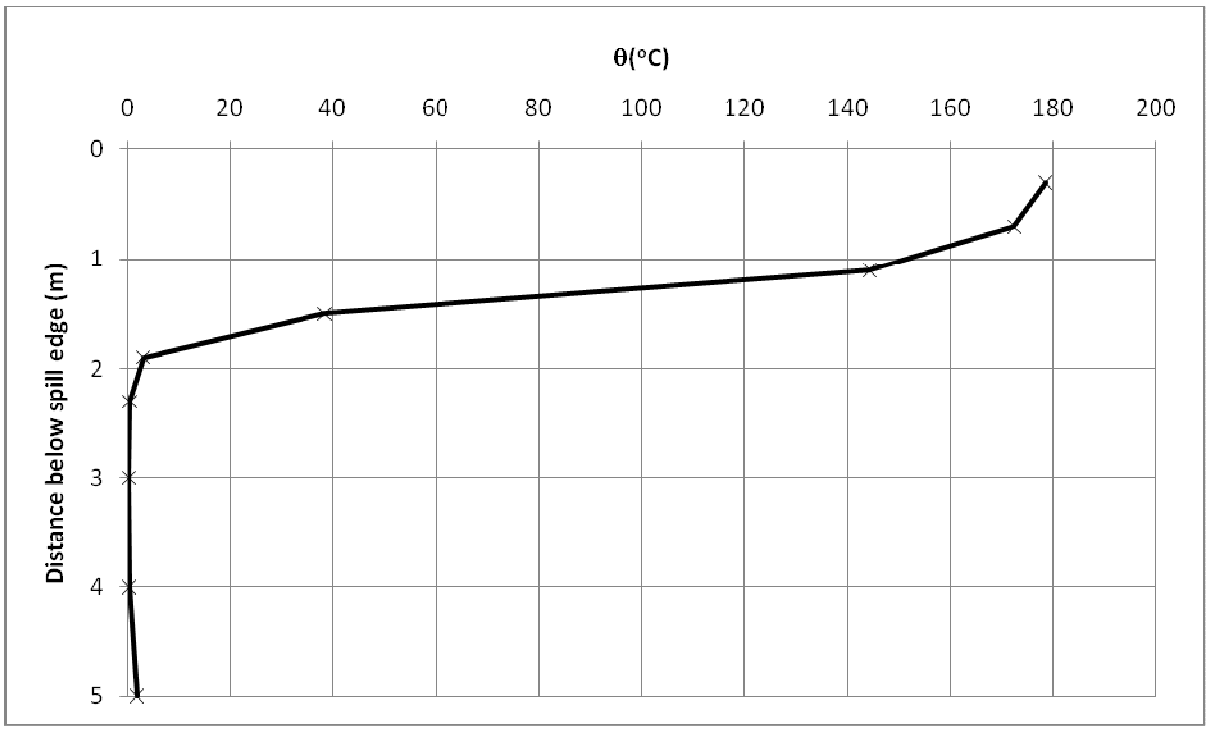

Figure G37. Temperature above ambient at the spill edge.

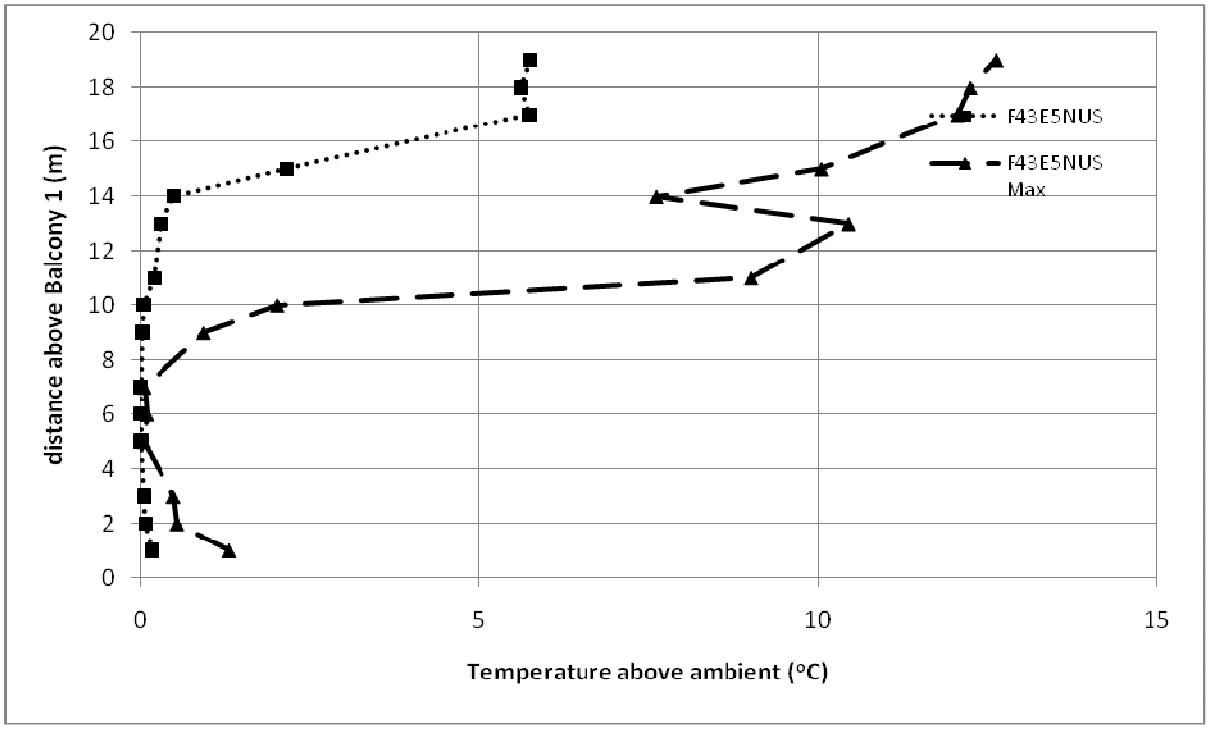

Figure G38. Temperature profiles across balcony edge.

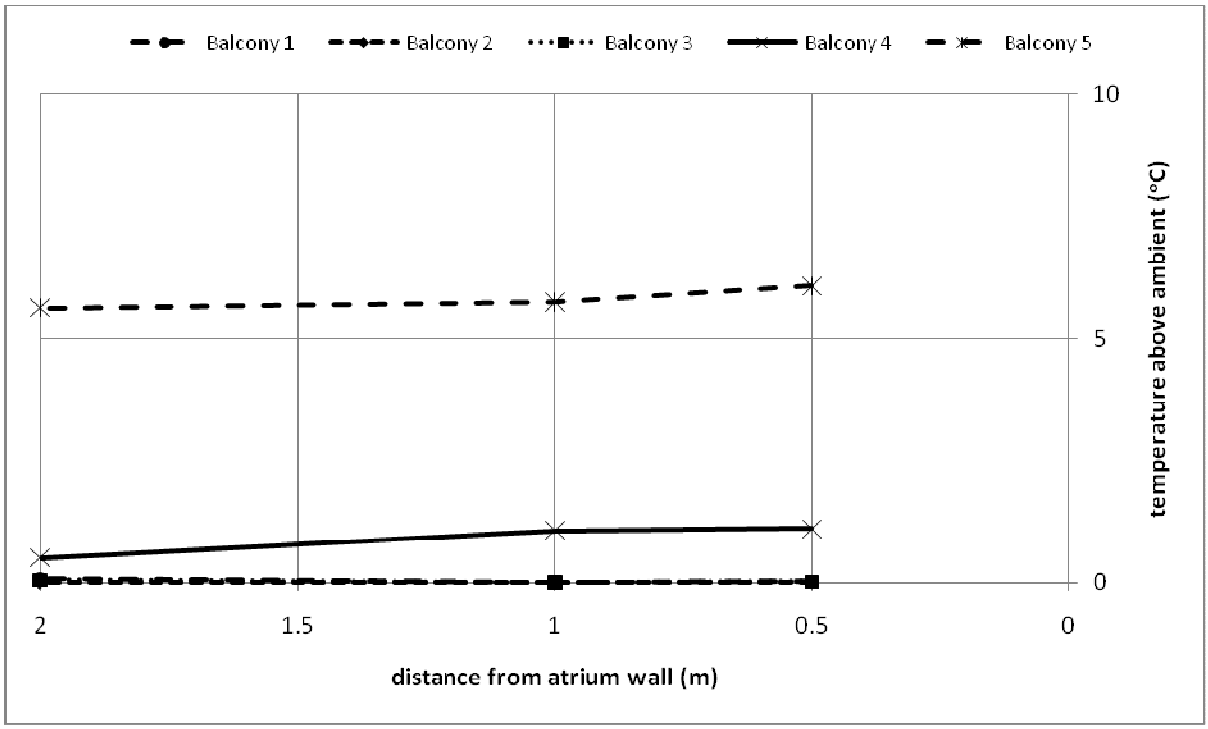

Figure G39. Temperature profiles along balcony breadth.

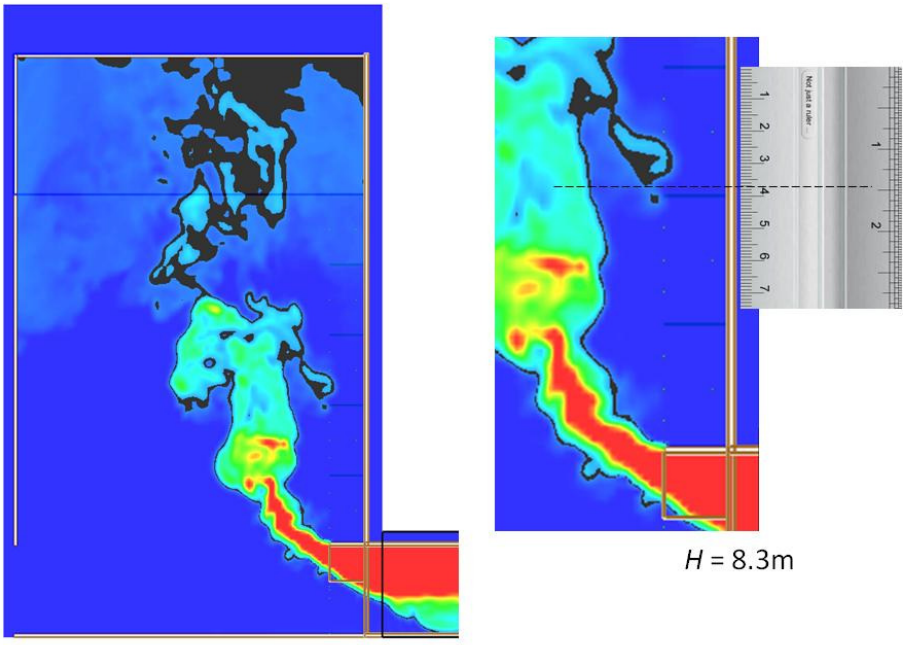

Figure G40. Smoke layer height measurement.

Full scale for 5 balcony (F56E5NUS)

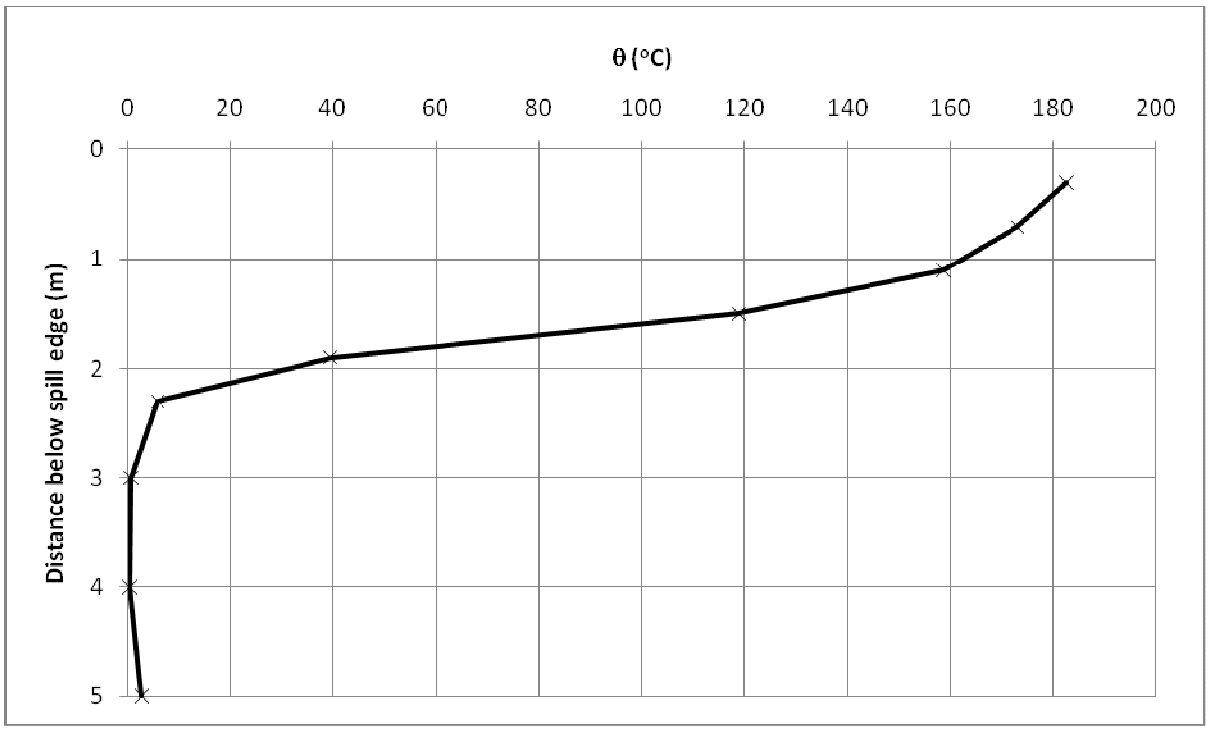

Figure G41. Temperature above ambient at the spill edge.

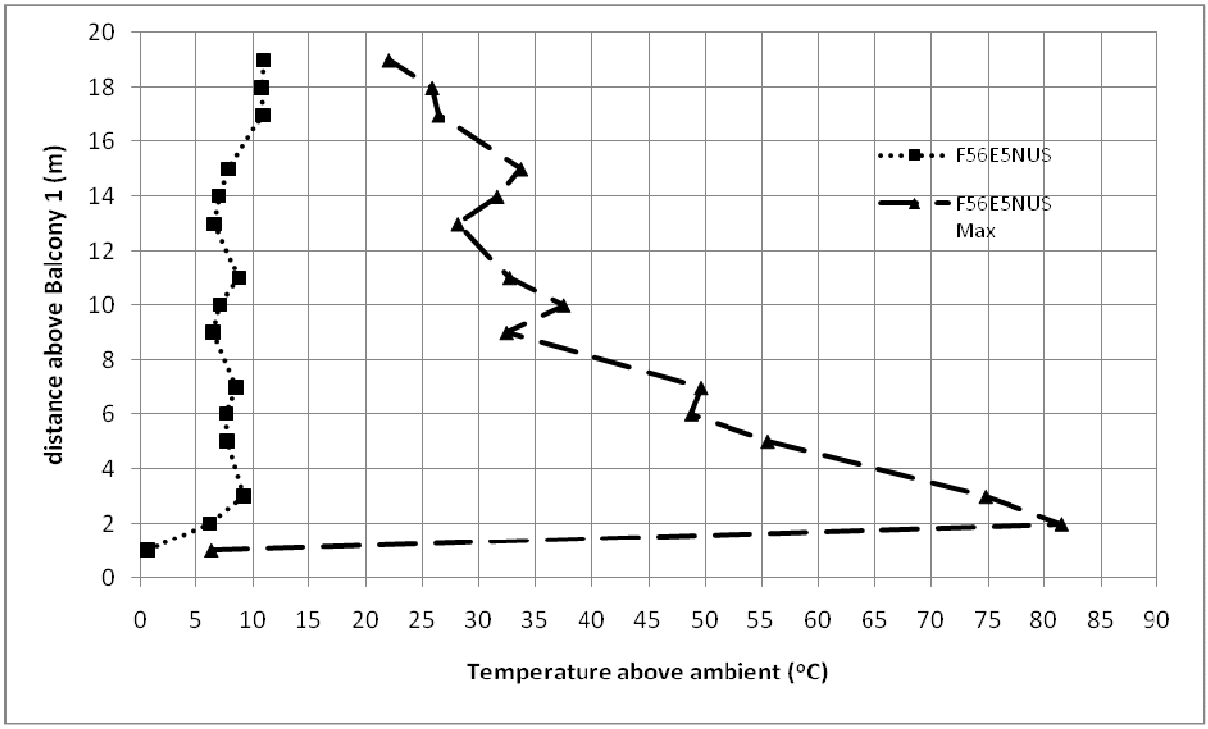

Figure G42. Temperature profiles across balcony edge.

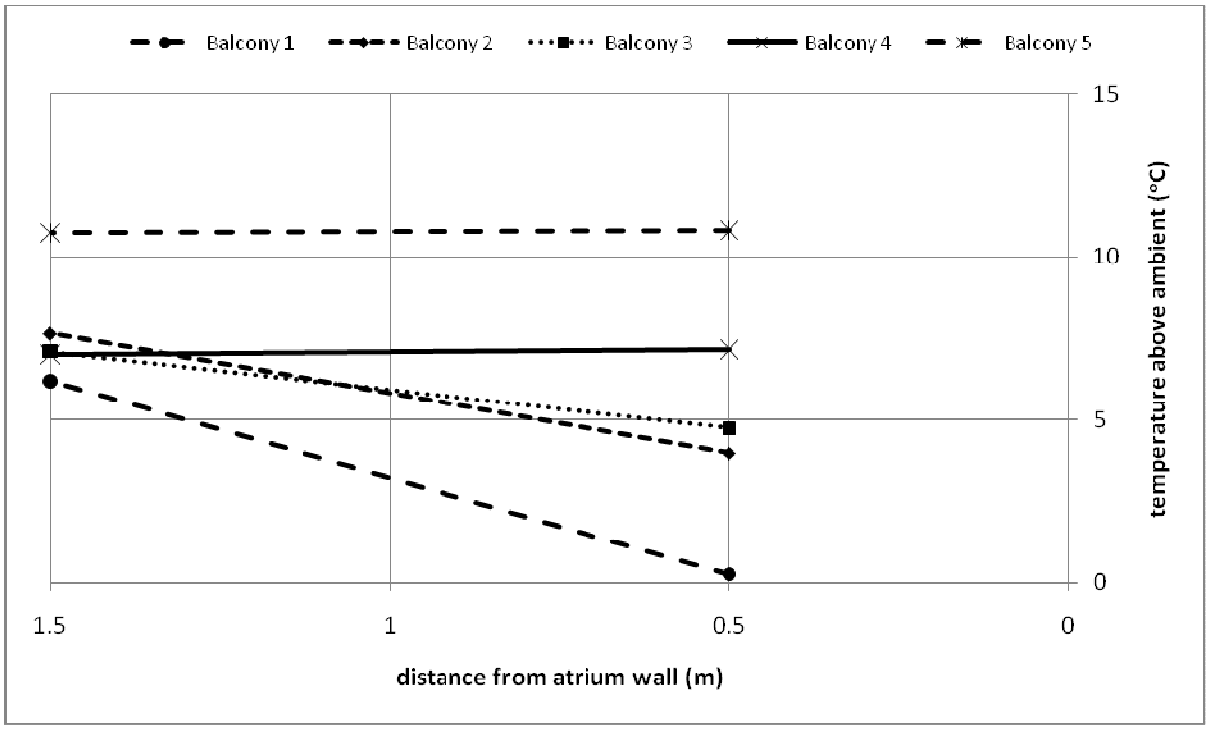

Figure G43. Temperature profiles along balcony breadth.

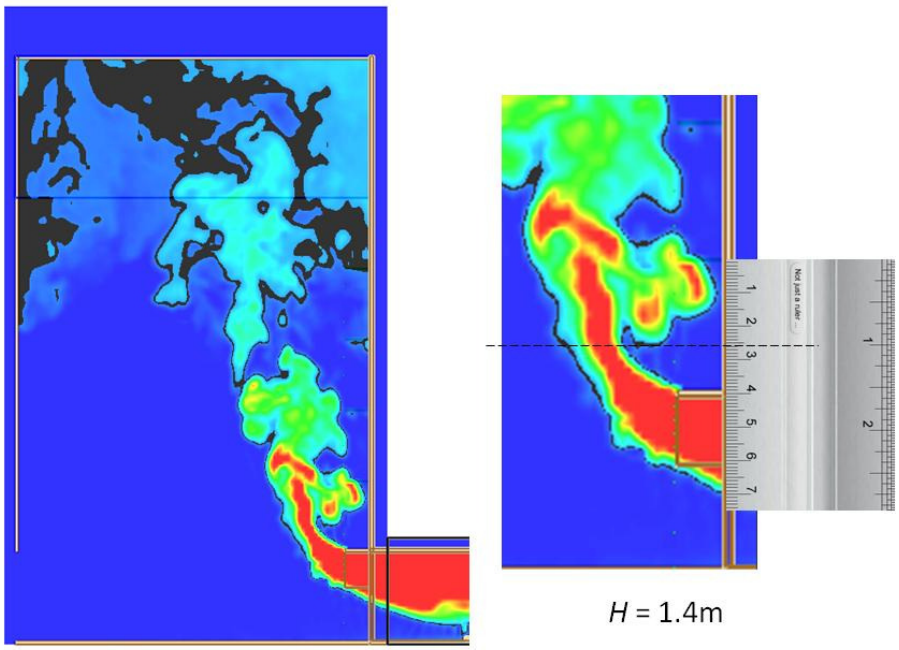

Figure G44. Smoke layer height measurement.

Full scale for 5 balcony (F60E5NUS)

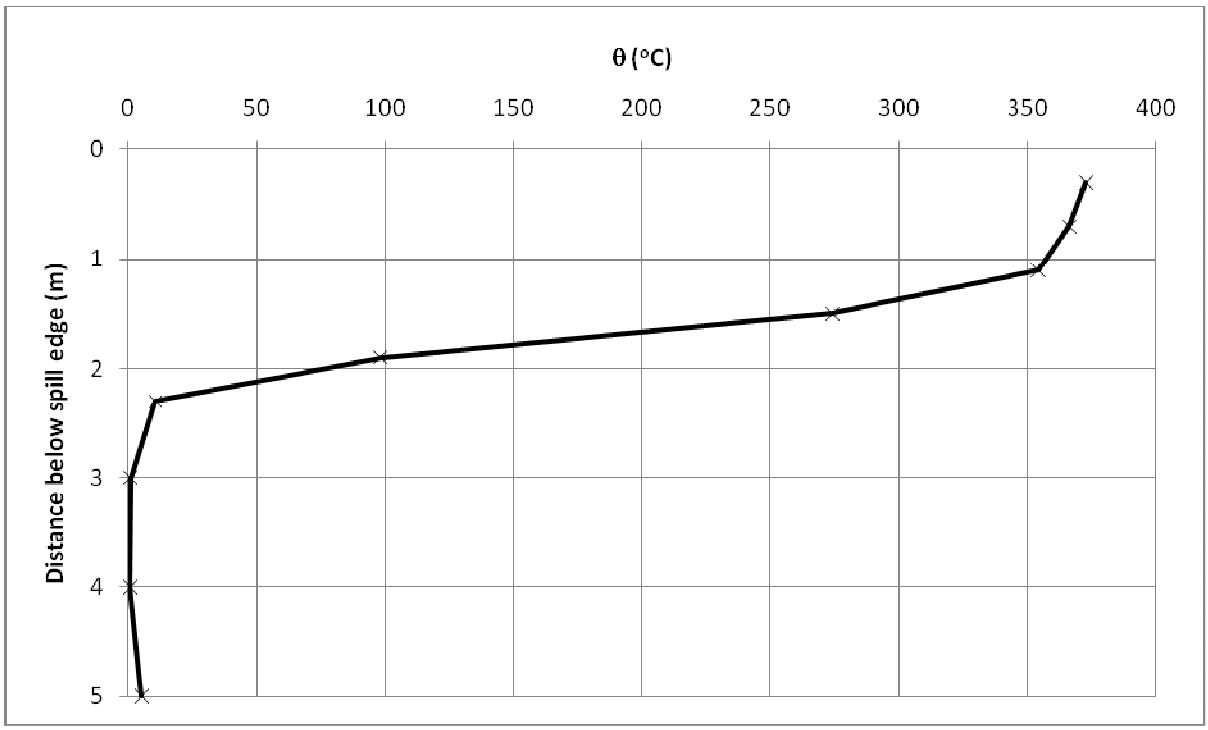

Figure G45. Temperature above ambient at the spill edge.

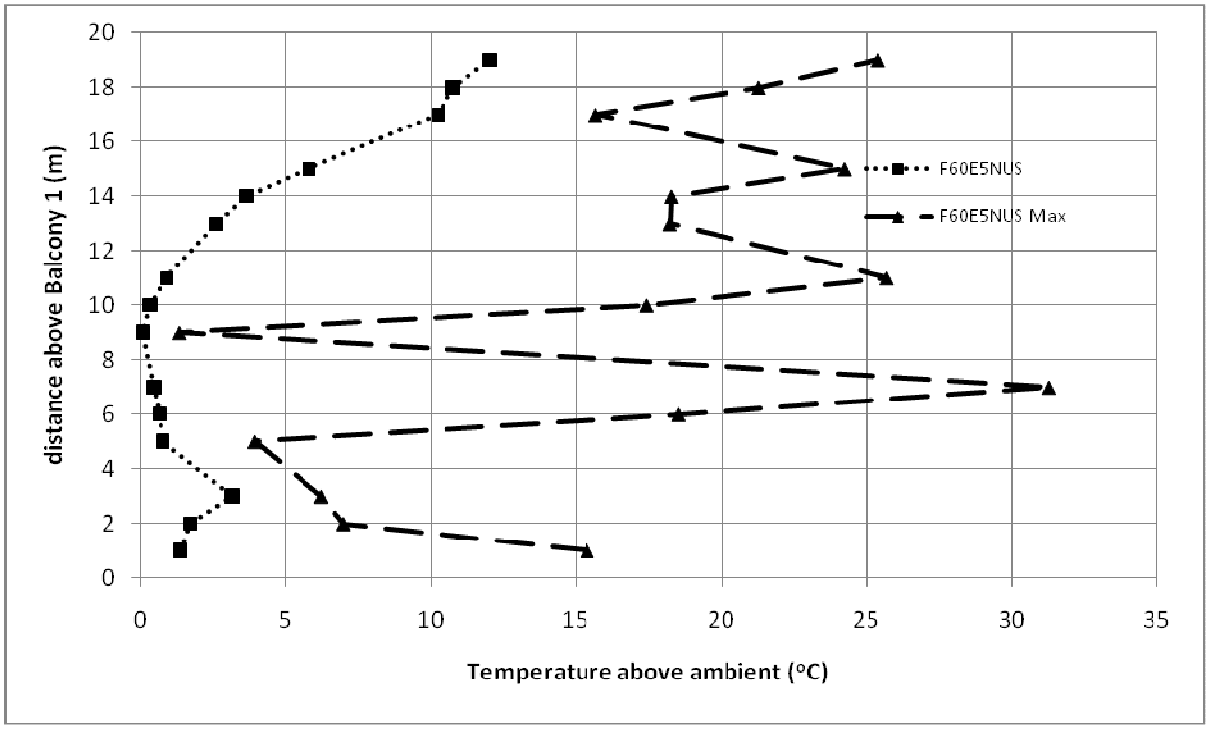

Figure G46. Temperature profiles across balcony edge.

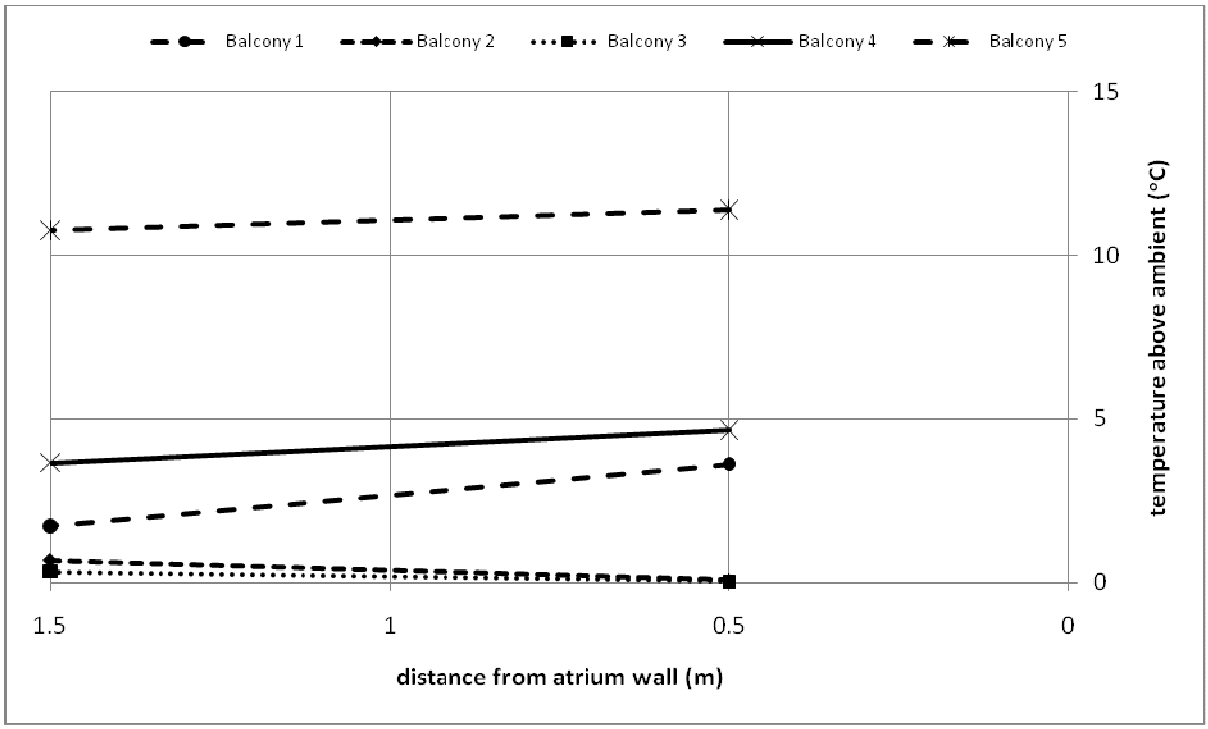

Figure G47. Temperature profiles along balcony breadth.

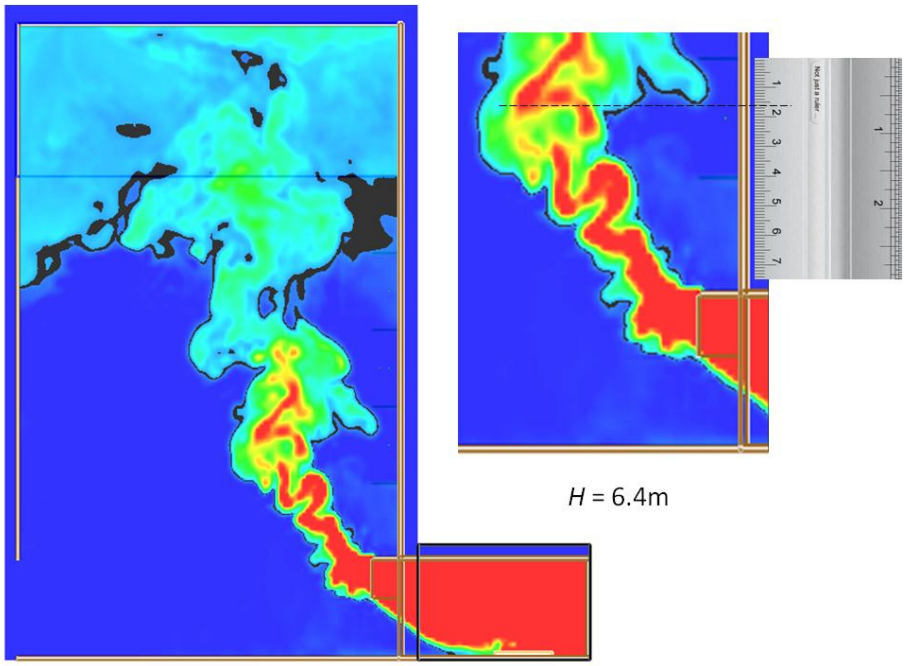

Figure G48. Smoke layer height measurement.

Comparing the Effect of Upstand on Temperature Profiles Across Balcony Edge

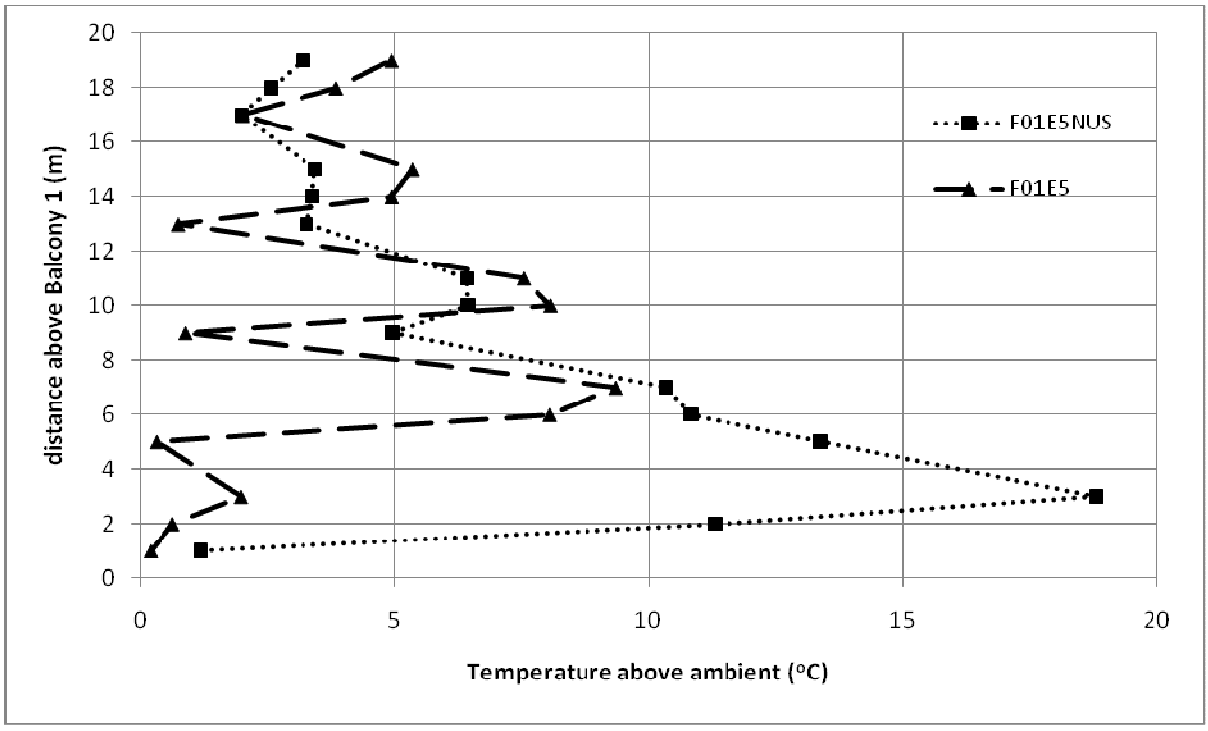

Figure H1. Comparing of F01E5 and F01E5NUS for temperature profile across balcony edge.

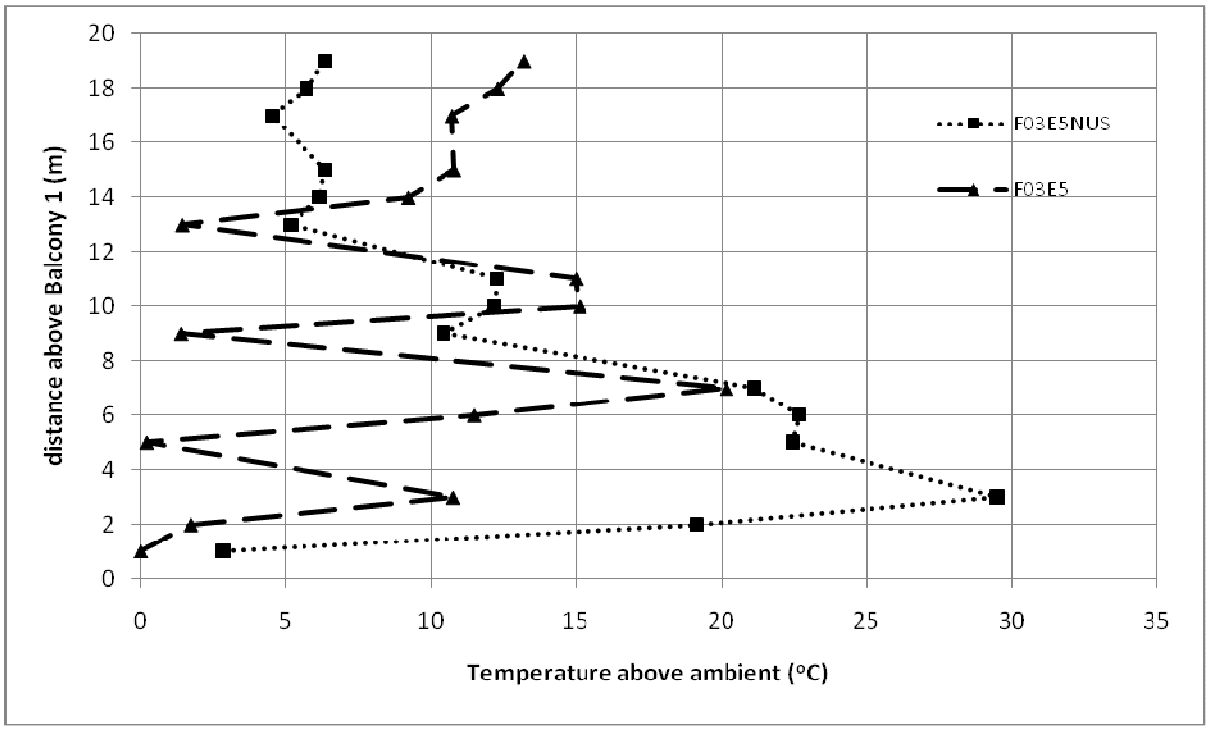

Figure H2. Comparing of F03E5 and F03E5NUS for temperature profile across balcony edge.

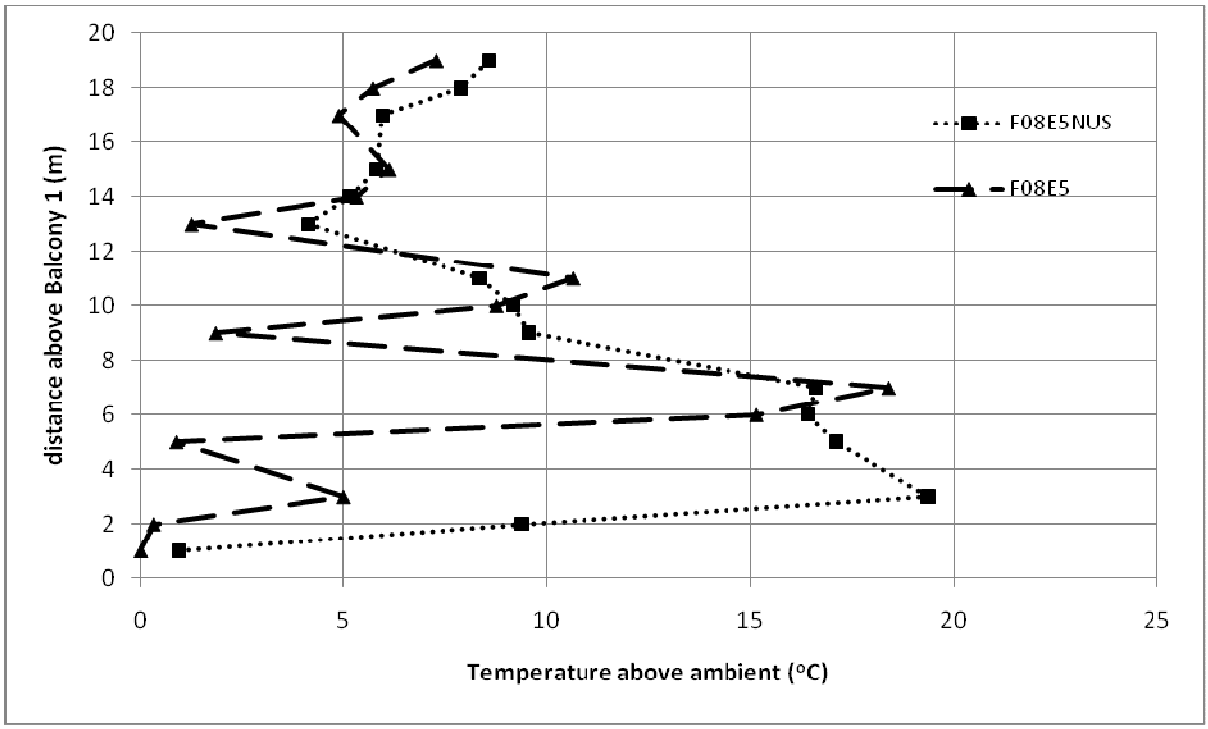

Figure H3. Comparing of F08E5 and F08E5NUS for temperature profile across balcony edge.

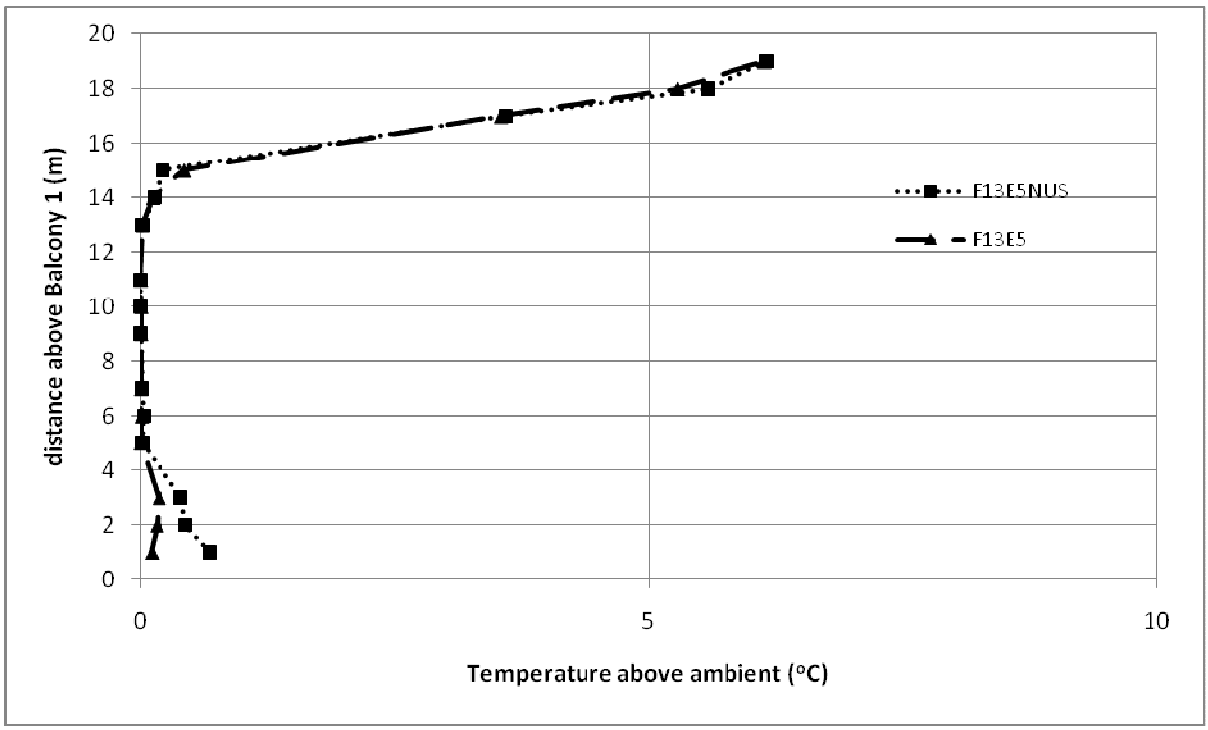

Figure H4. Comparing of F13E5 and F13E5NUS for temperature profile across balcony edge.

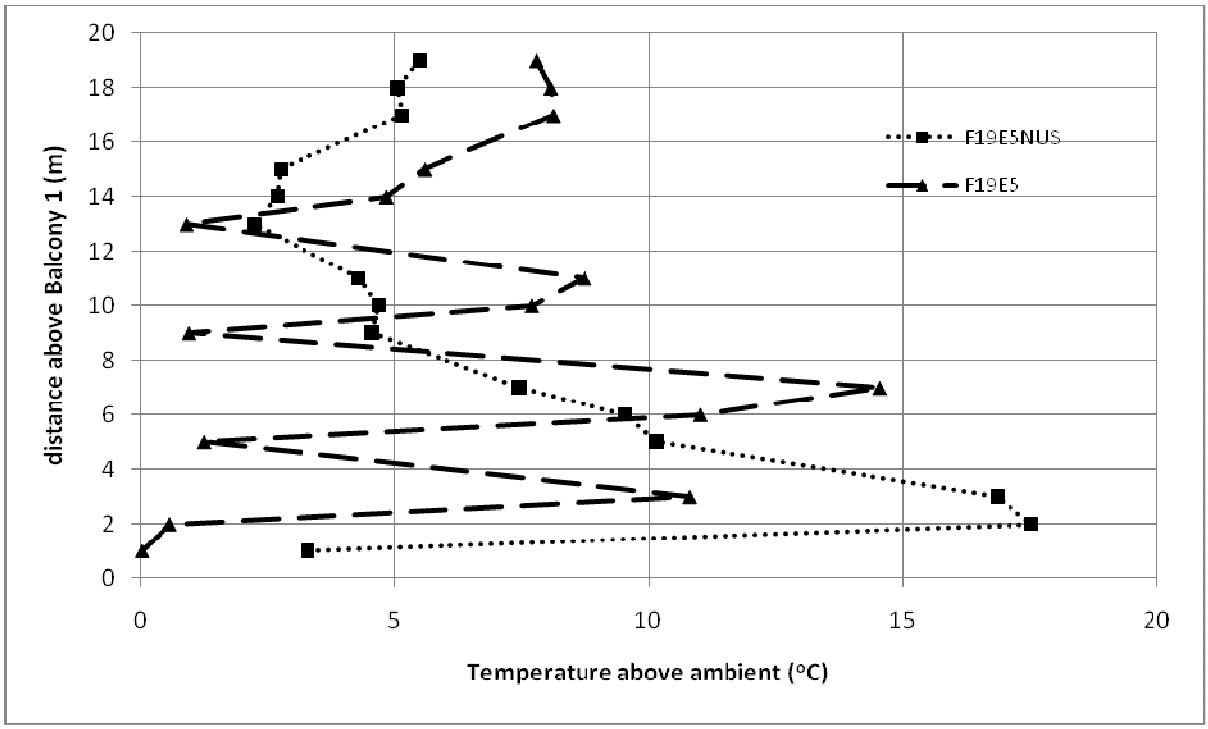

Figure H5. Comparing of F19E5 and F19E5NUS for temperature profile across balcony edge.

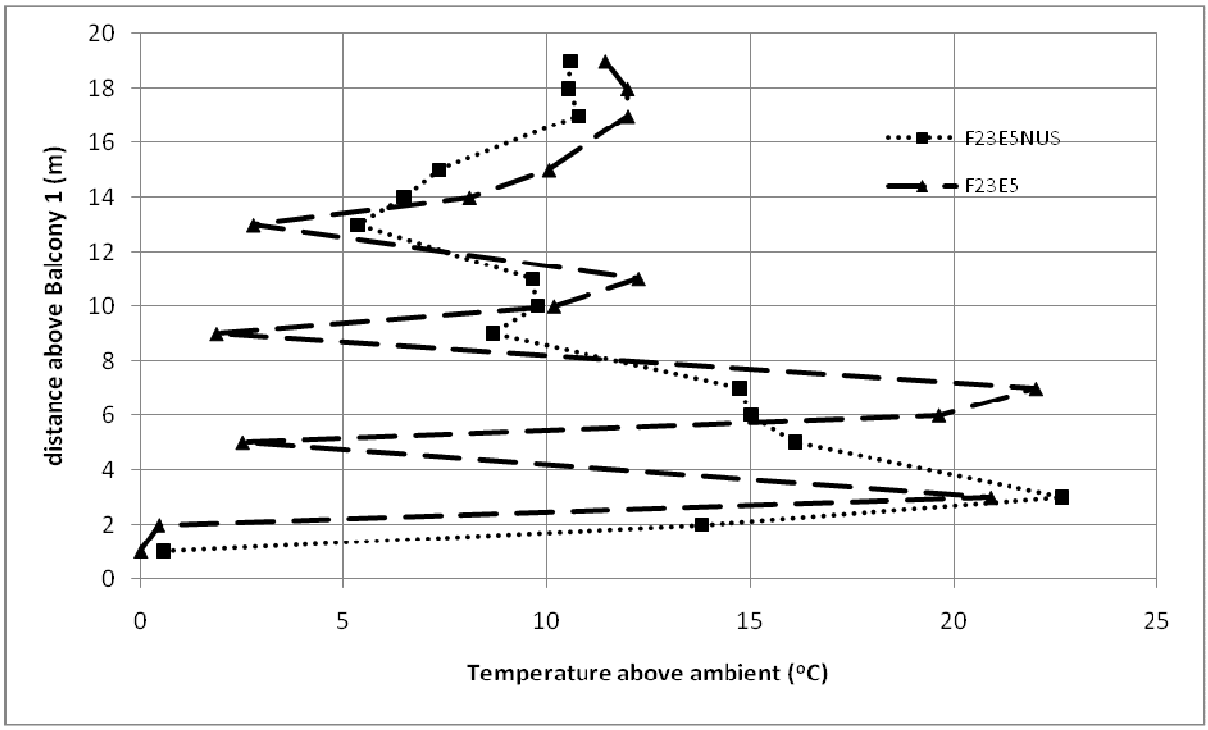

Figure H6. Comparing of F23E5 and F23E5NUS for temperature profile across balcony edge.

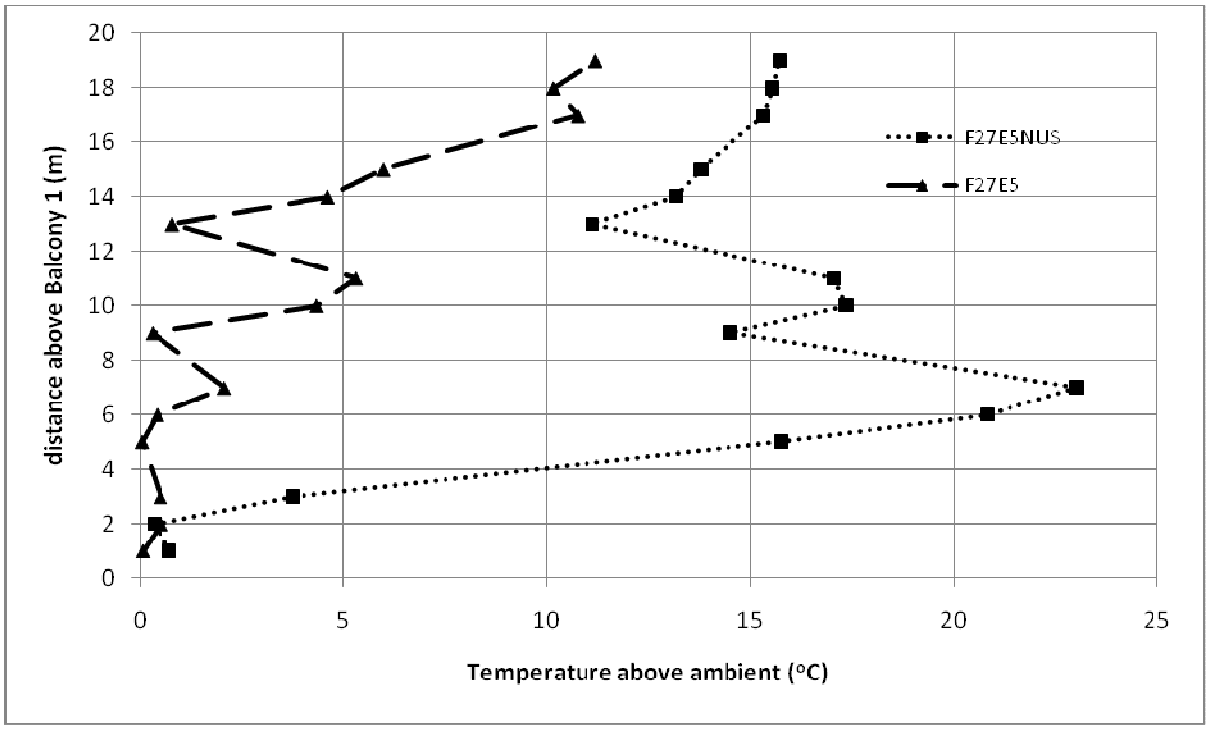

Figure H7. Comparing of F27E5 and F27E5NUS for temperature profile across balcony edge.

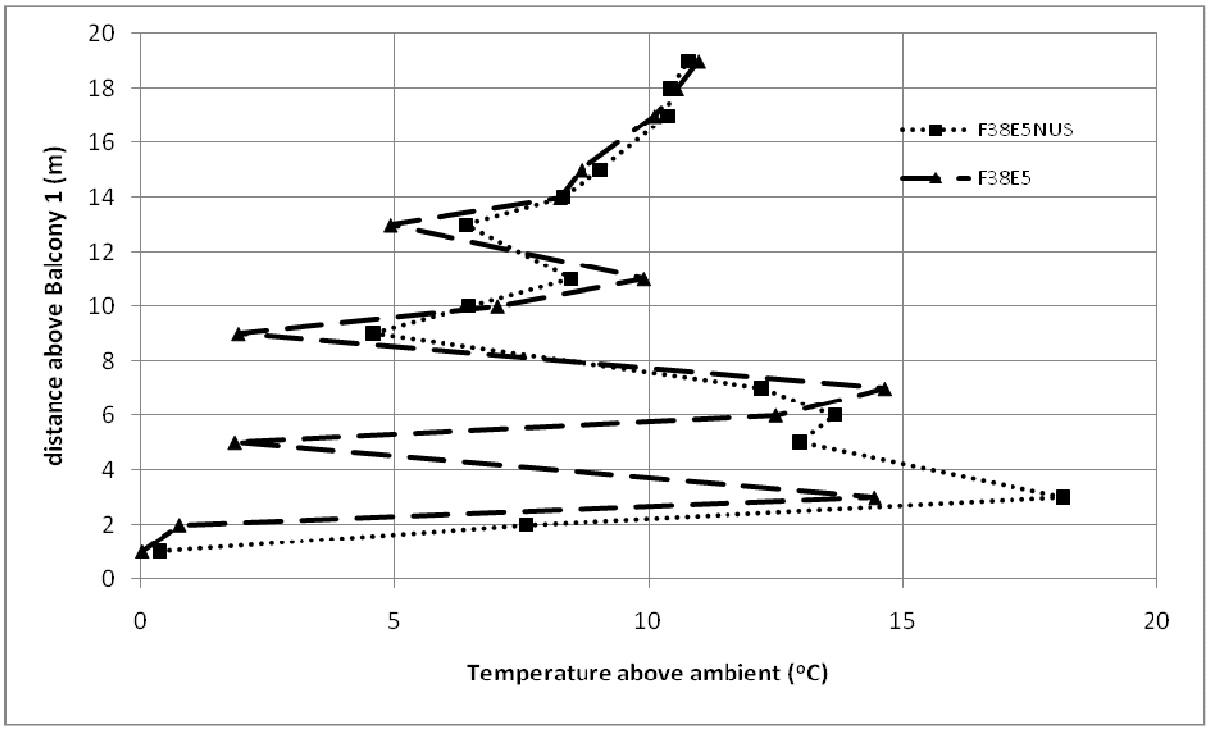

Figure H8. Comparing of F38E5 and F38E5NUS for temperature profile across balcony edge.

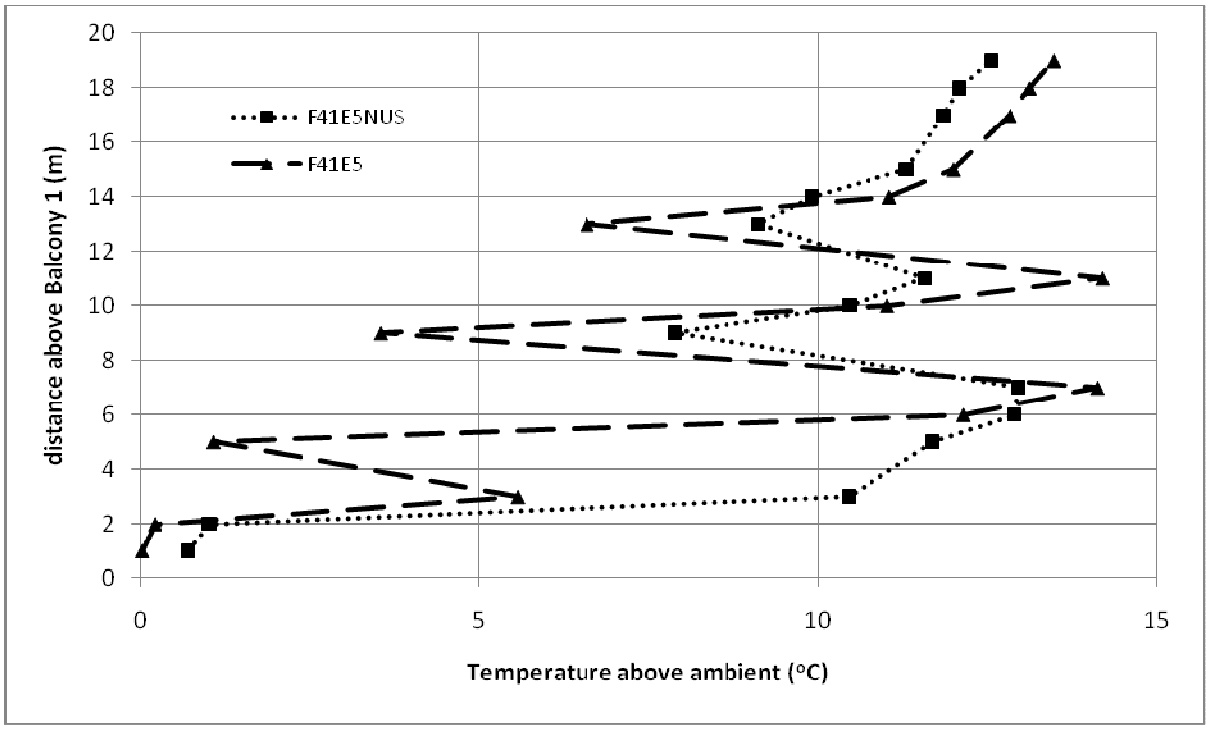

Figure H9. Comparing of F41E5 and F41E5NUS for temperature profile across balcony edge.

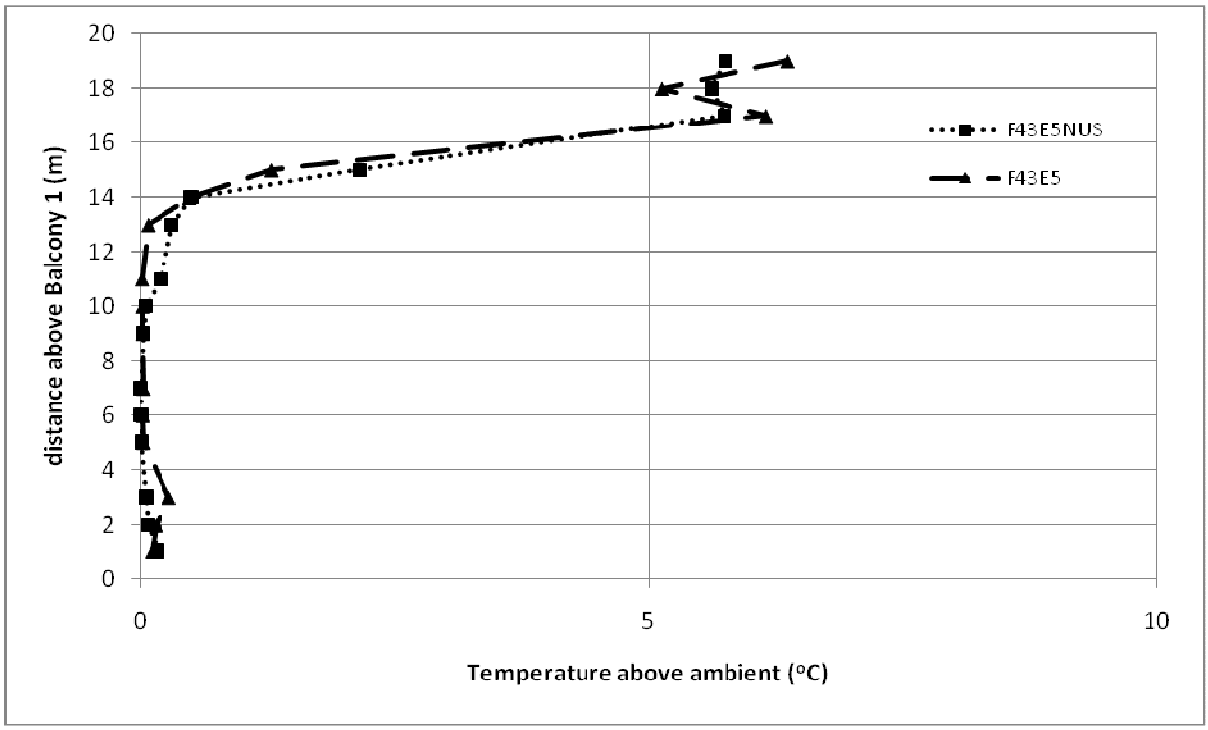

Figure H10. Comparing of F43E5 and F43E5NUS for temperature profile across balcony edge.

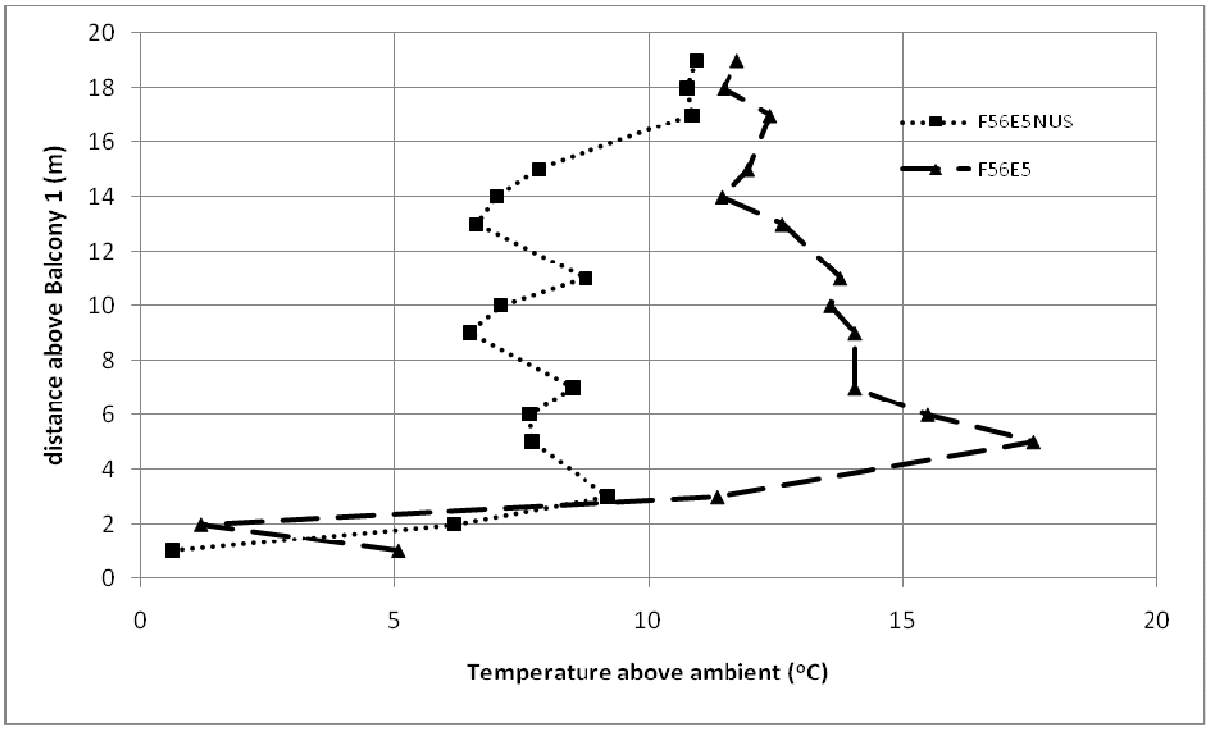

Figure H11. Comparing of F56E5 and F56E5NUS for temperature profile across balcony edge.

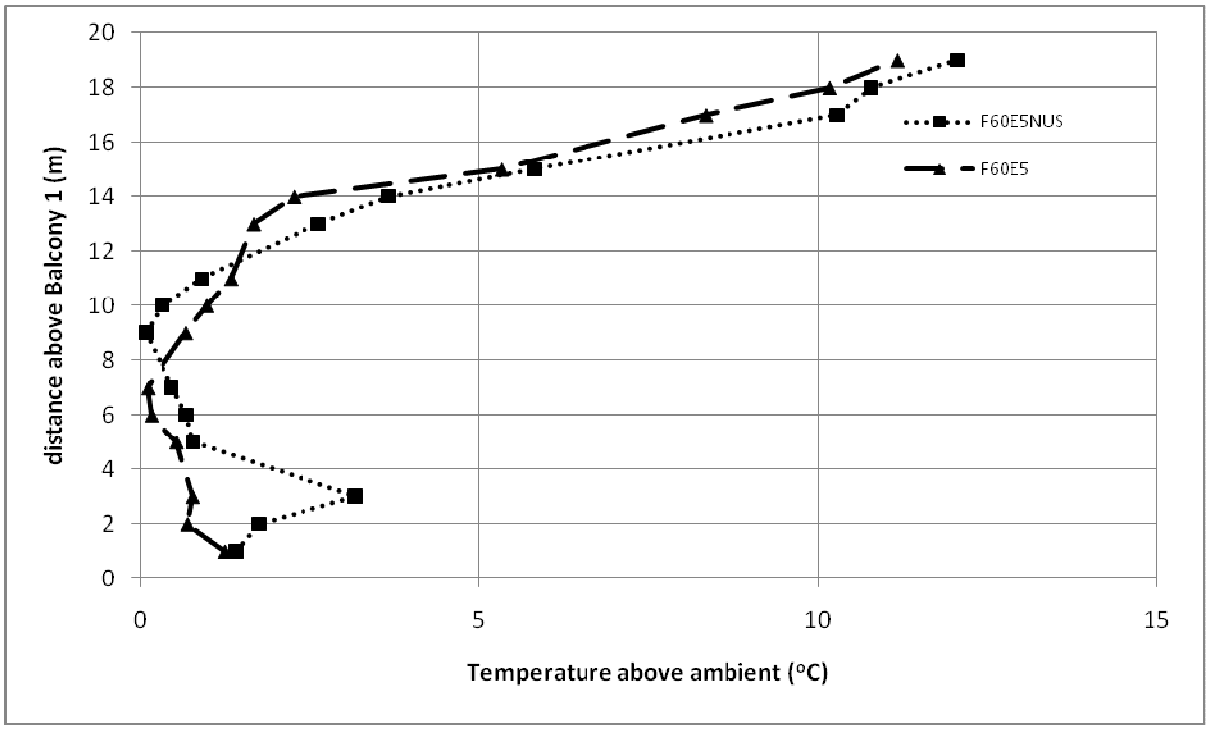

Figure H12. Comparing of F60E5 and F60E5NUS for temperature profile across balcony edge.

Simulation Result for Full-scale Seven Balcony

Full scale for 7 storey balcony (F01E7)

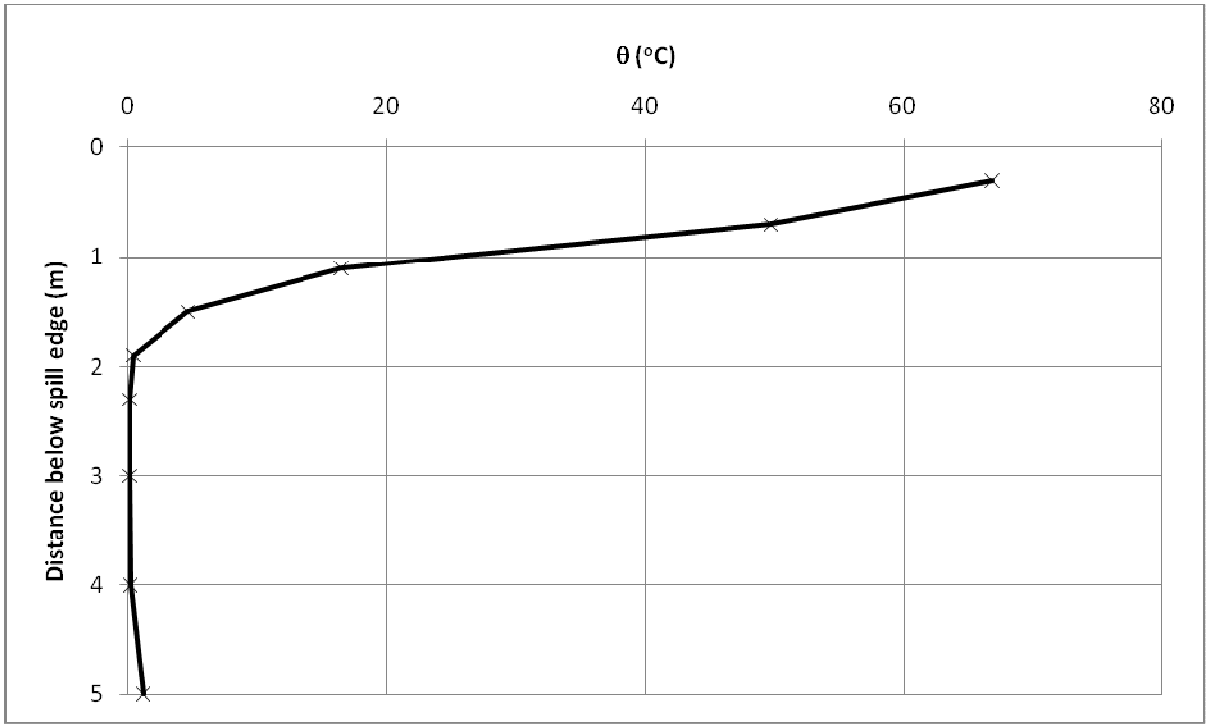

Figure I1. Temperature above ambient at the spill edge.

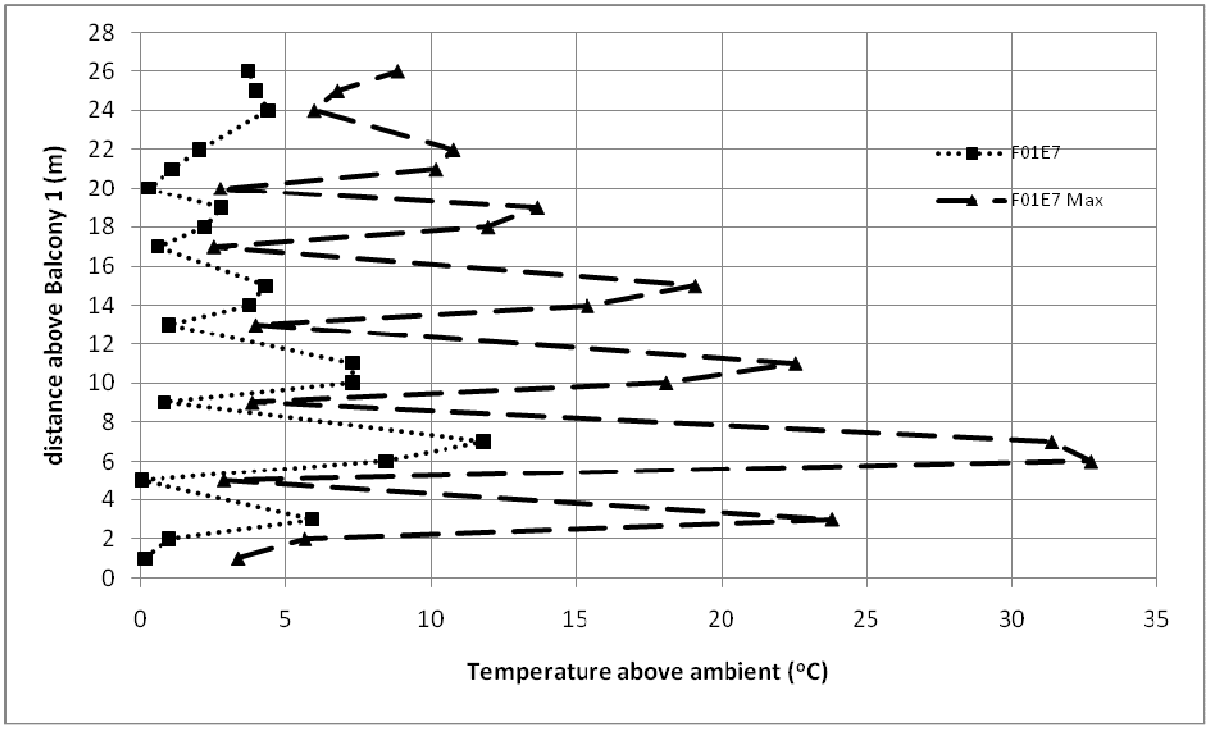

Figure I2. Temperature profiles across balcony edge.

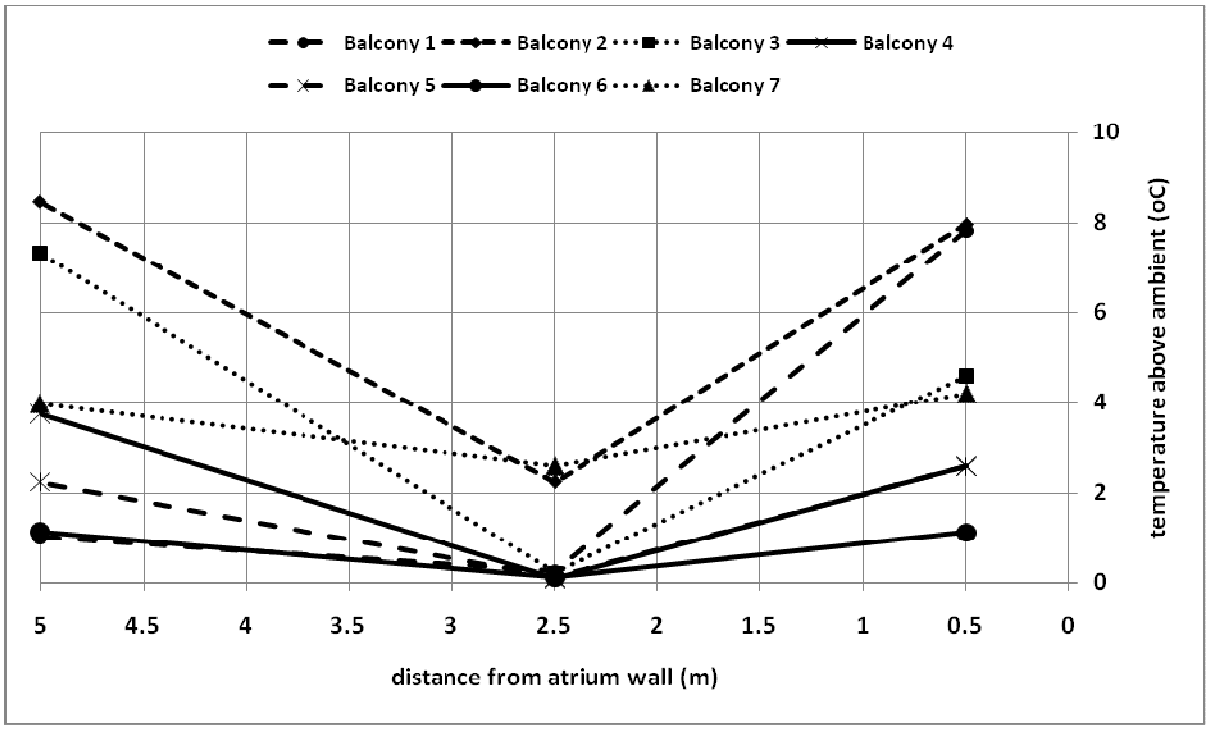

Figure I3. Temperature profiles along balcony breadth.

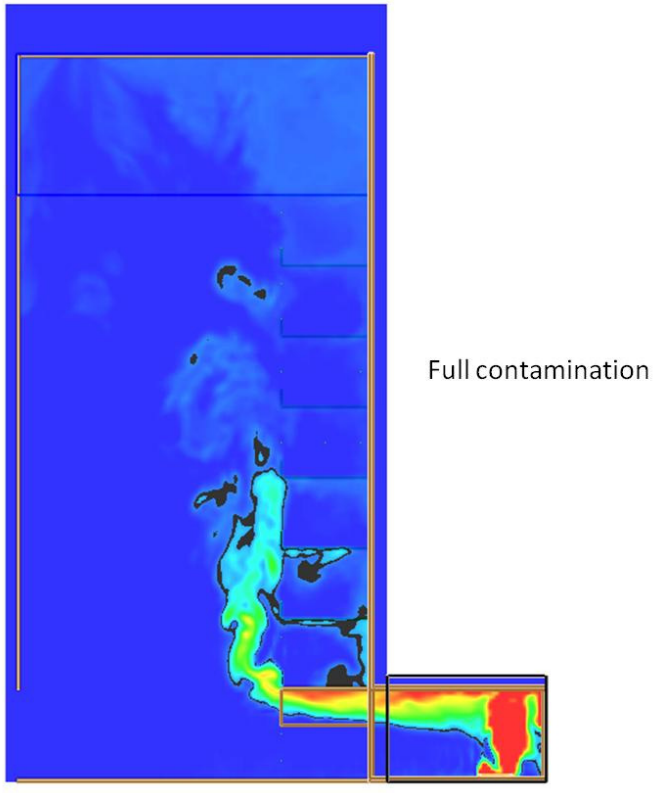

Figure I4. Smoke layer height measurement.

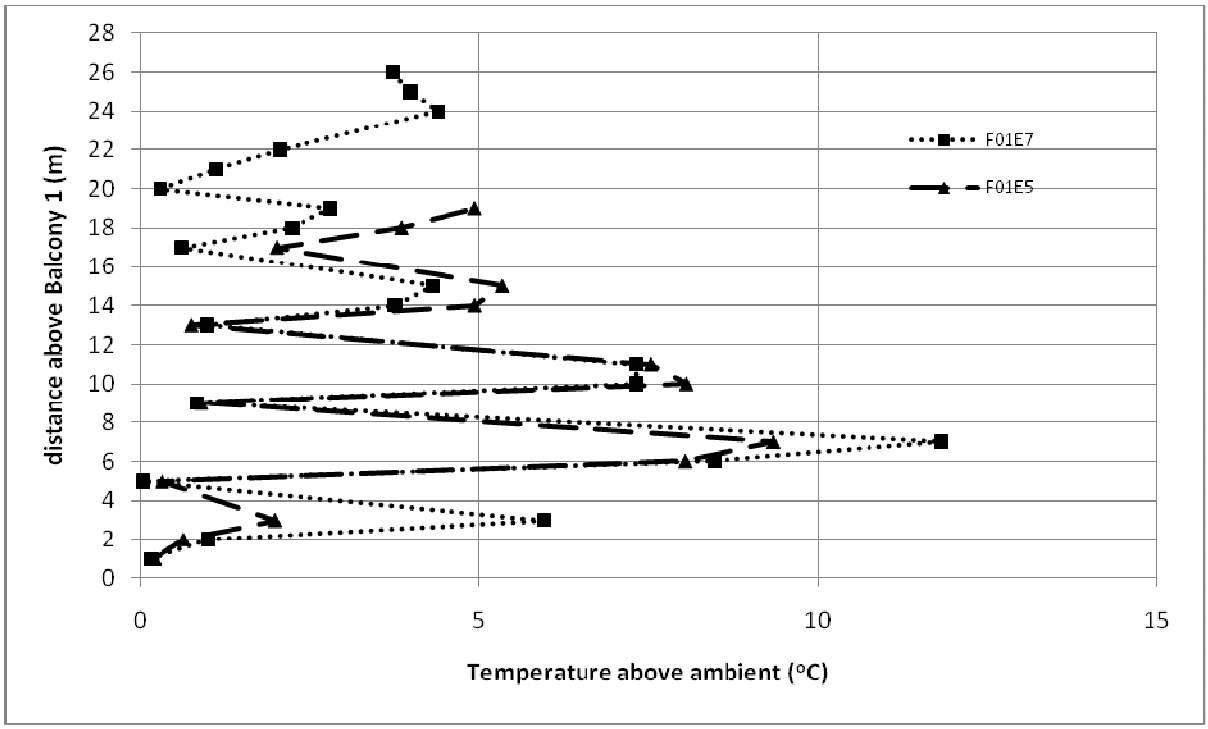

Figure I5. Comparison of seven storey balcony and five storey balcony temperature profiles along balcony edge.

Full scale for 7 storey balcony (F03E7)

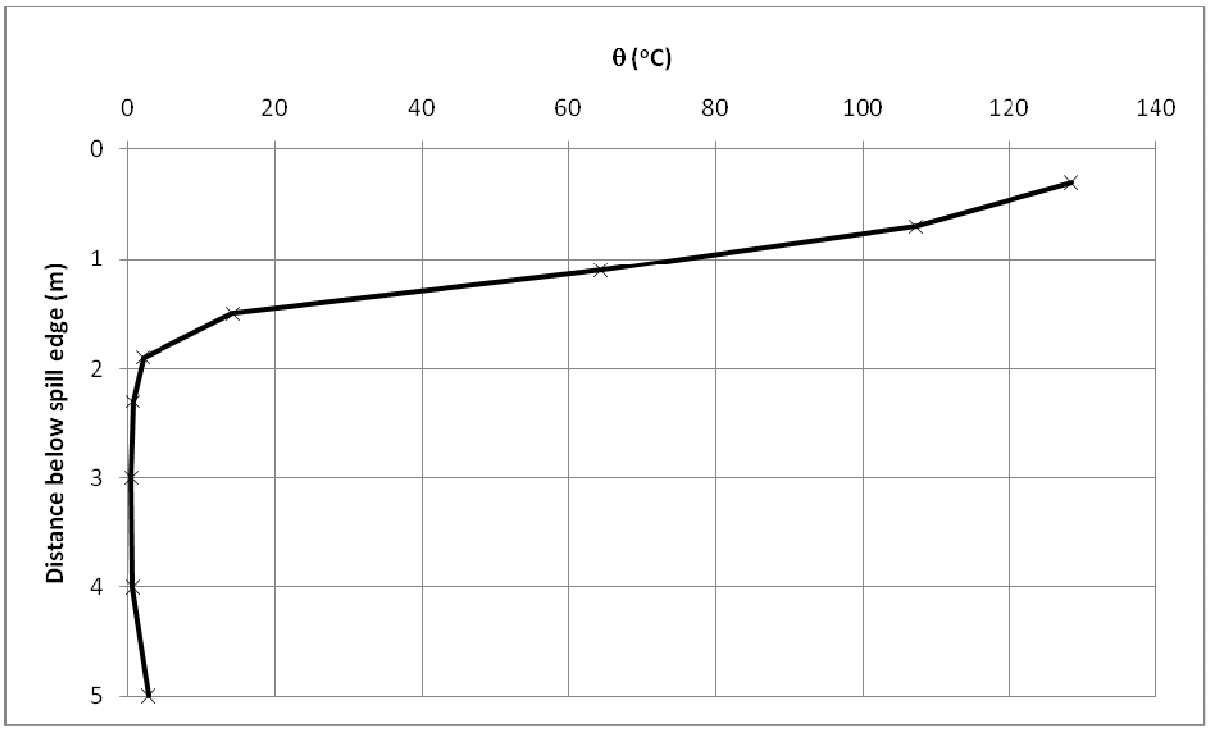

Figure I6. Temperature above ambient at the spill edge.

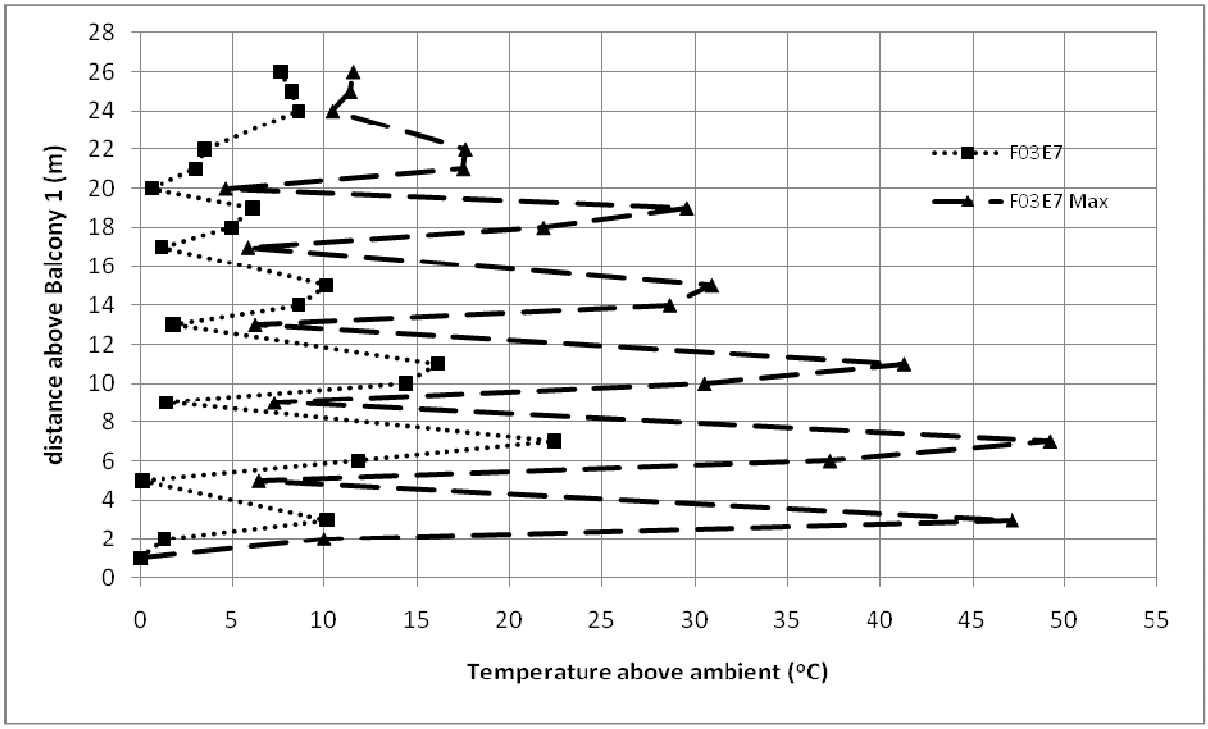

Figure I7. Temperature profiles across balcony edge.

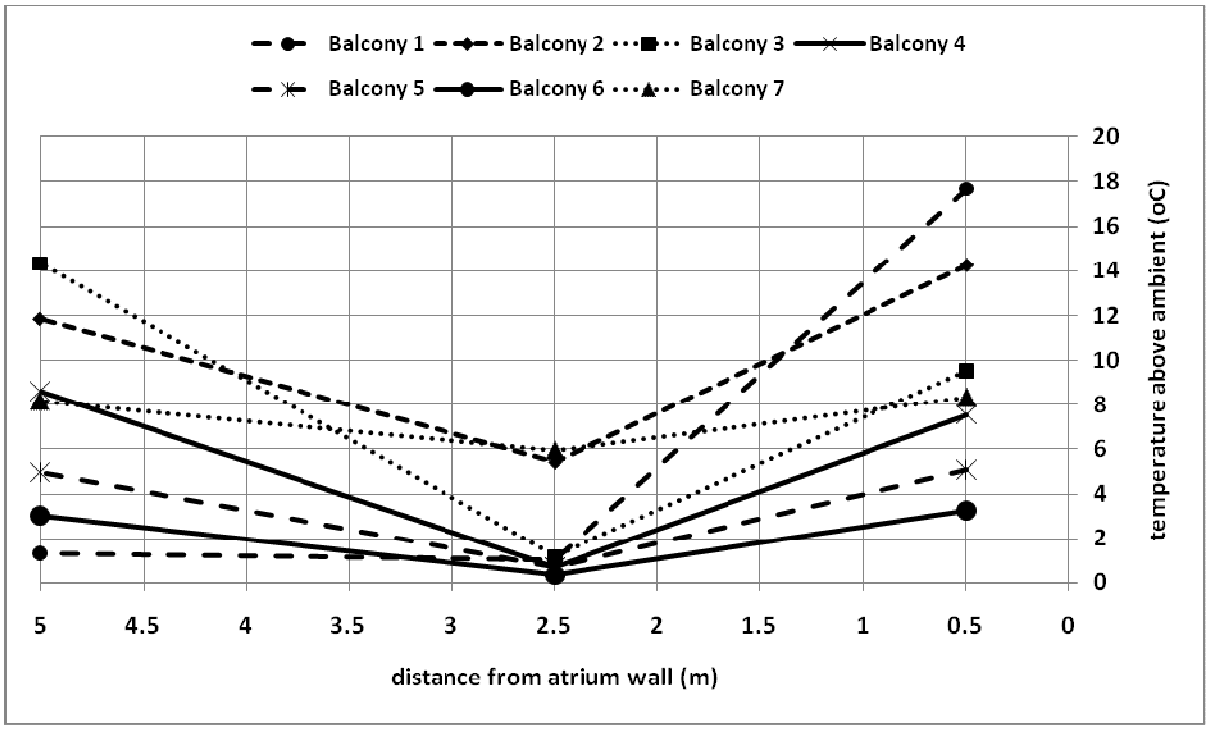

Figure I8. Temperature profiles along balcony breadth.

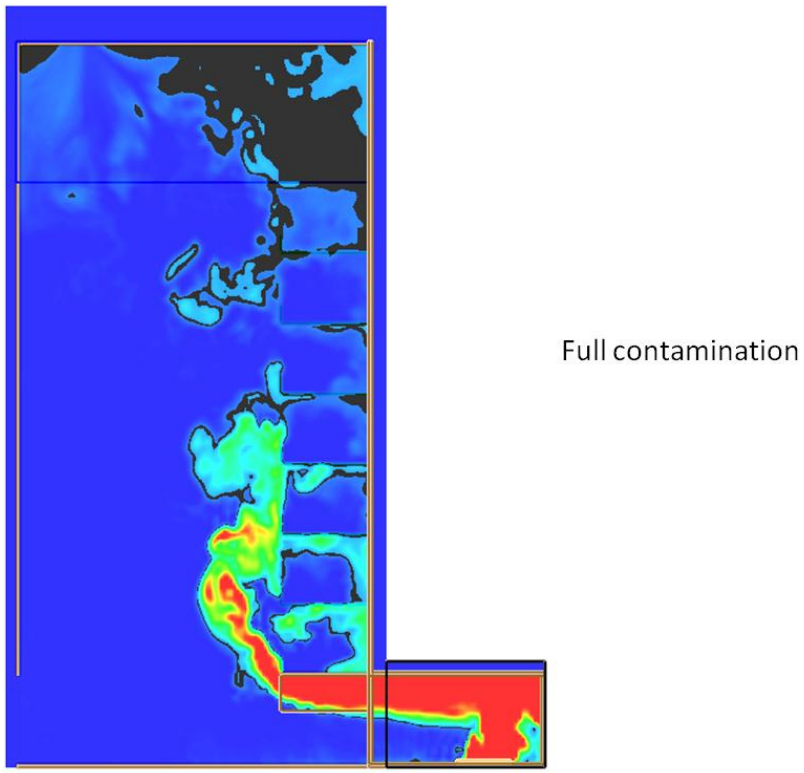

Figure I9. Smoke layer height measurement.

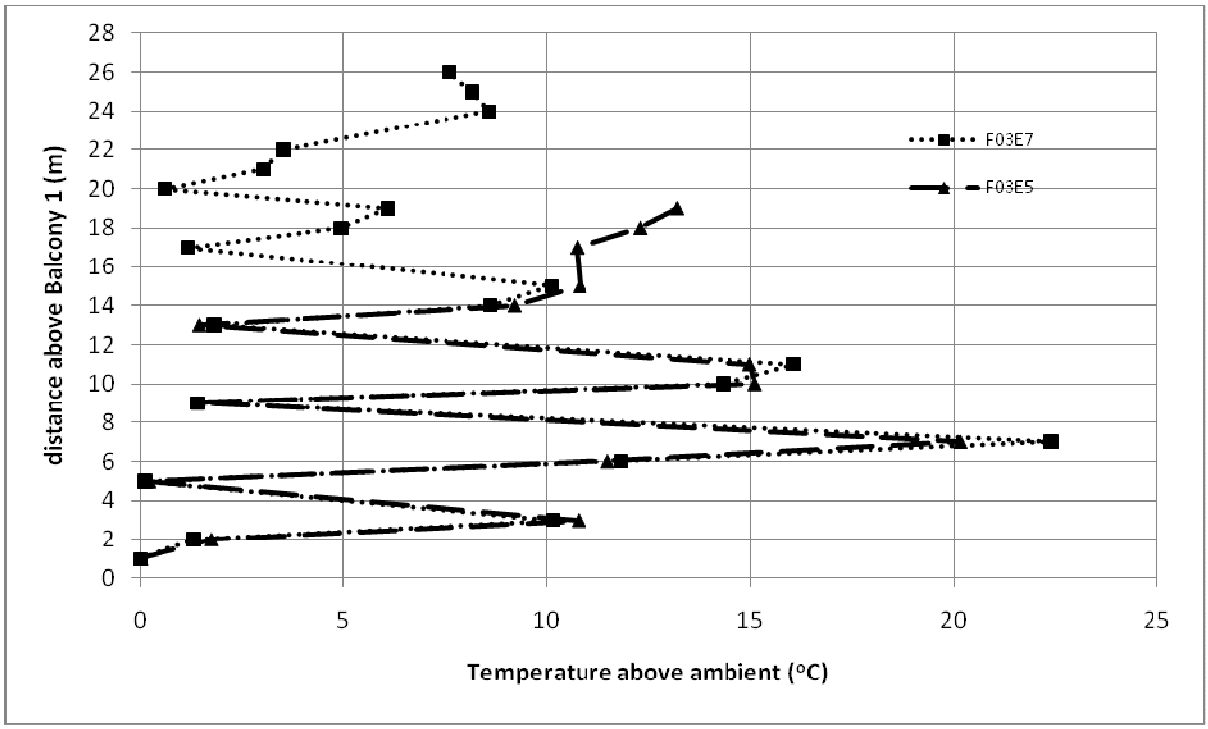

Figure I10. Comparison of seven storey balcony and five storey balcony temperature profiles along balcony edge.

Full scale for 7 storey balcony (F08E7)

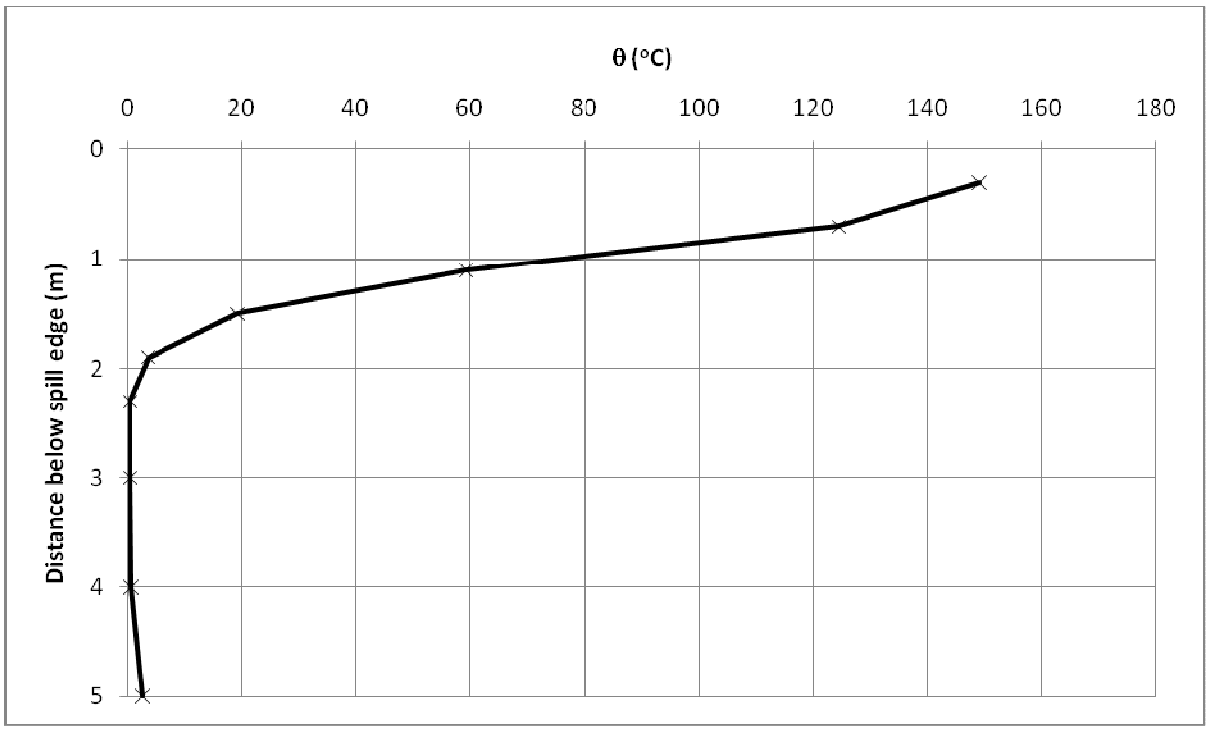

Figure I11. Temperature above ambient at the spill edge.

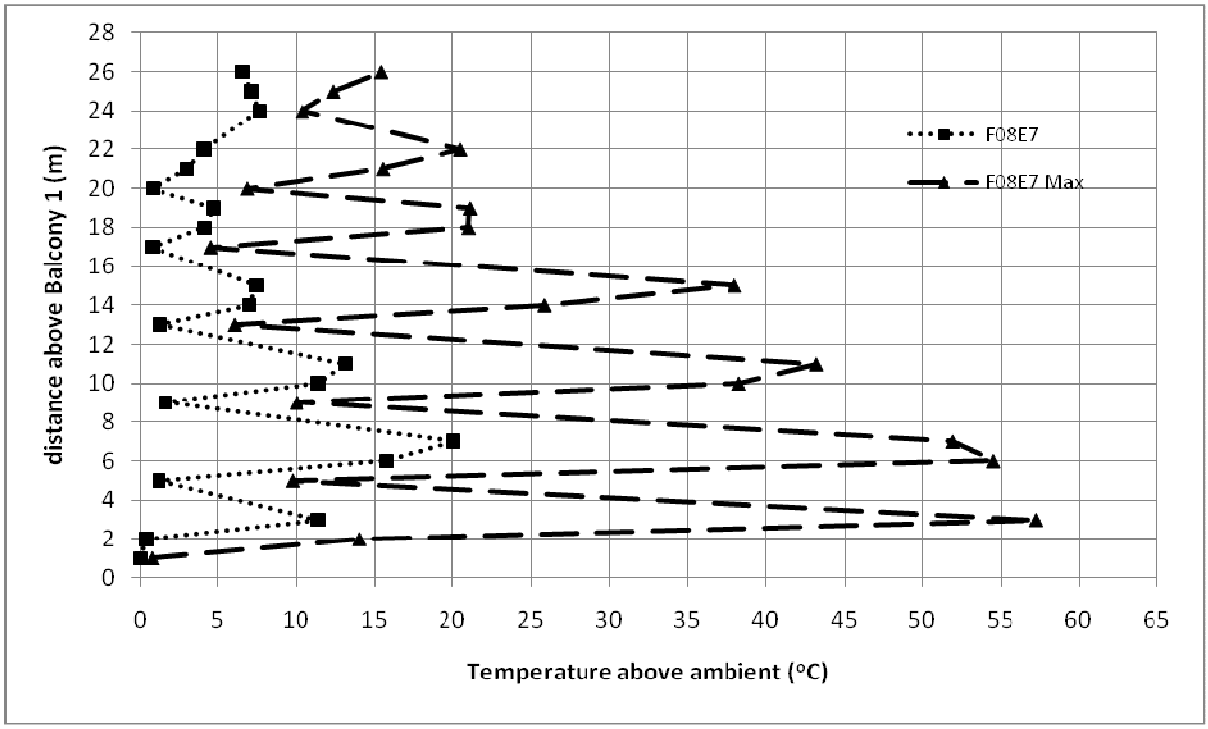

Figure I12. Temperature profiles across balcony edge.

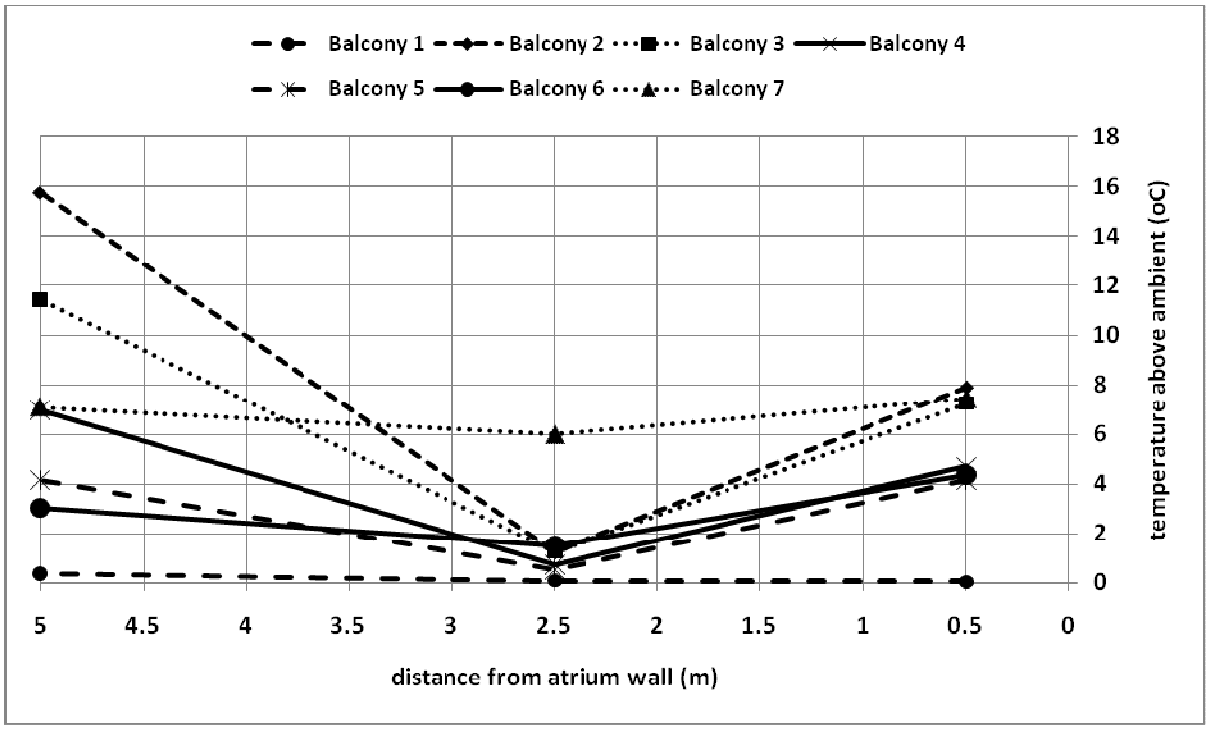

Figure I13. Temperature profiles along balcony breadth.

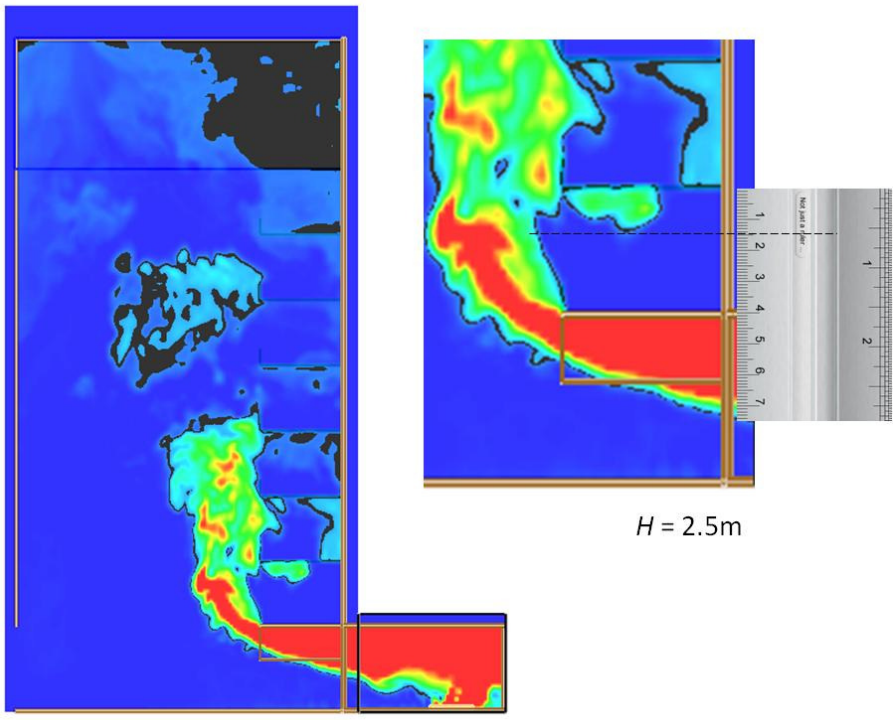

Figure I14. Smoke layer height measurement.

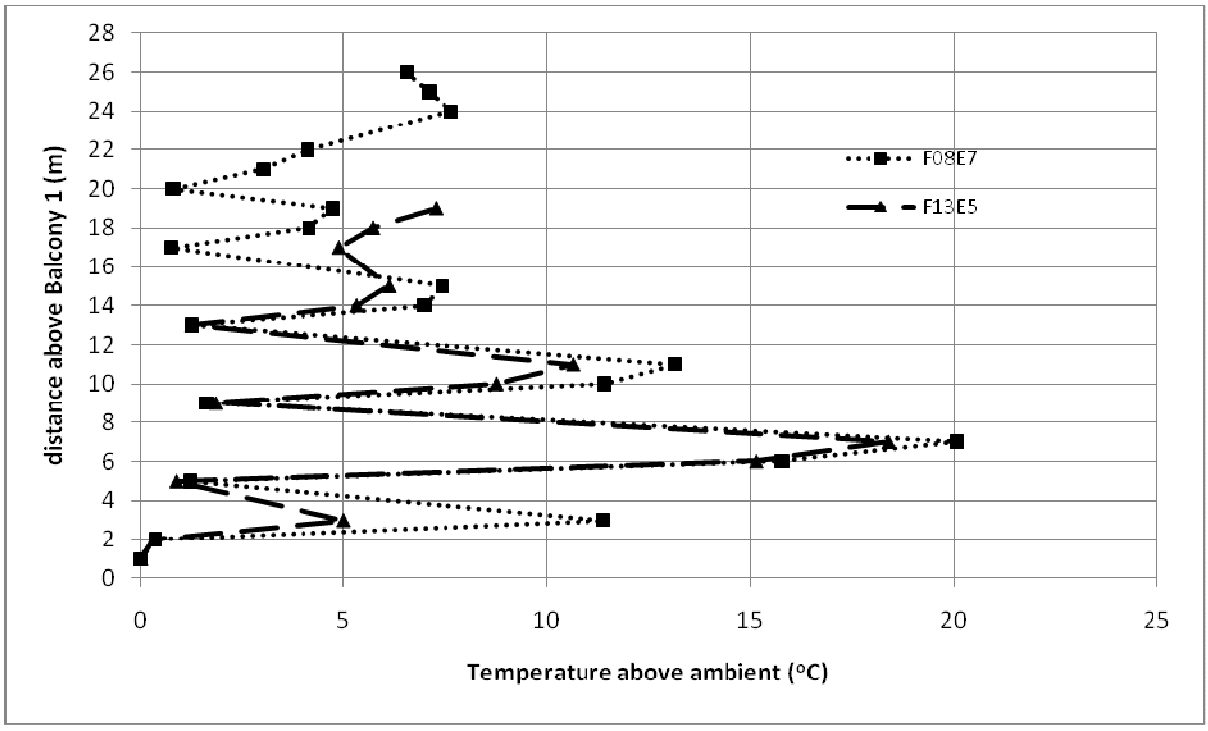

Figure I15. Comparison of seven storey balcony and five storey balcony temperature profiles along balcony edge.

Full scale for 7 storey balcony (F13E7)

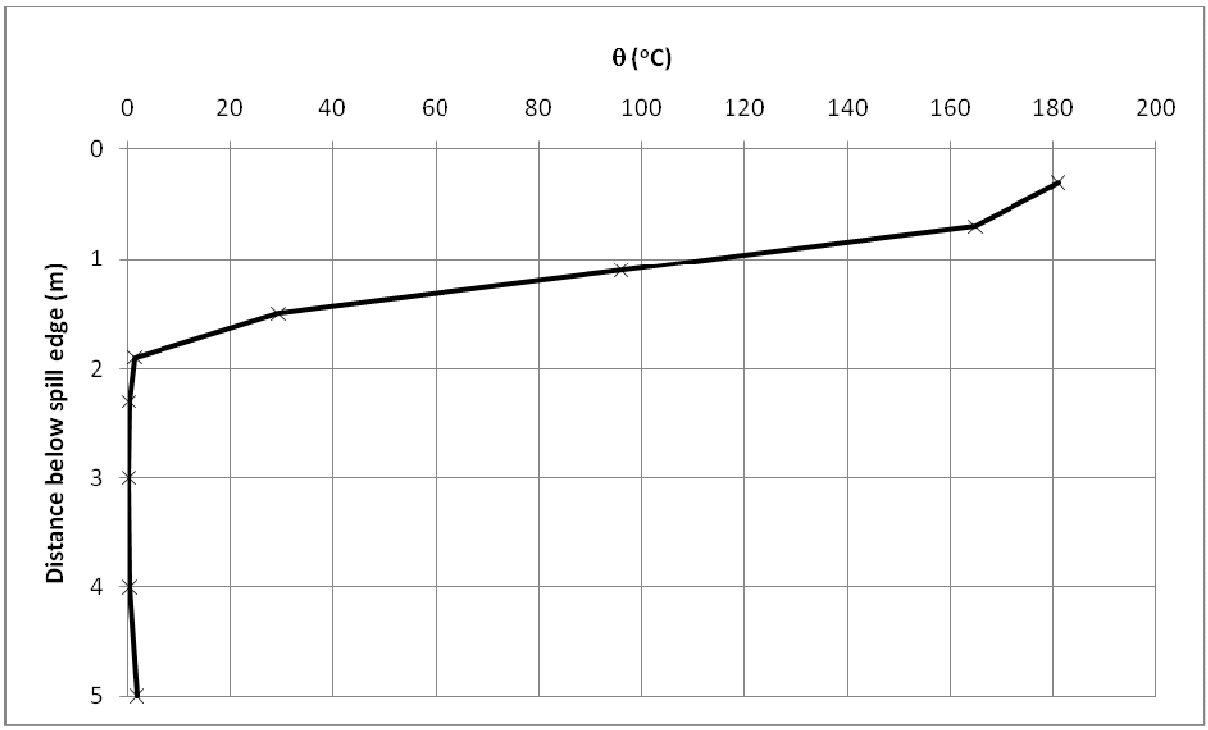

Figure I16. Temperature above ambient at the spill edge.

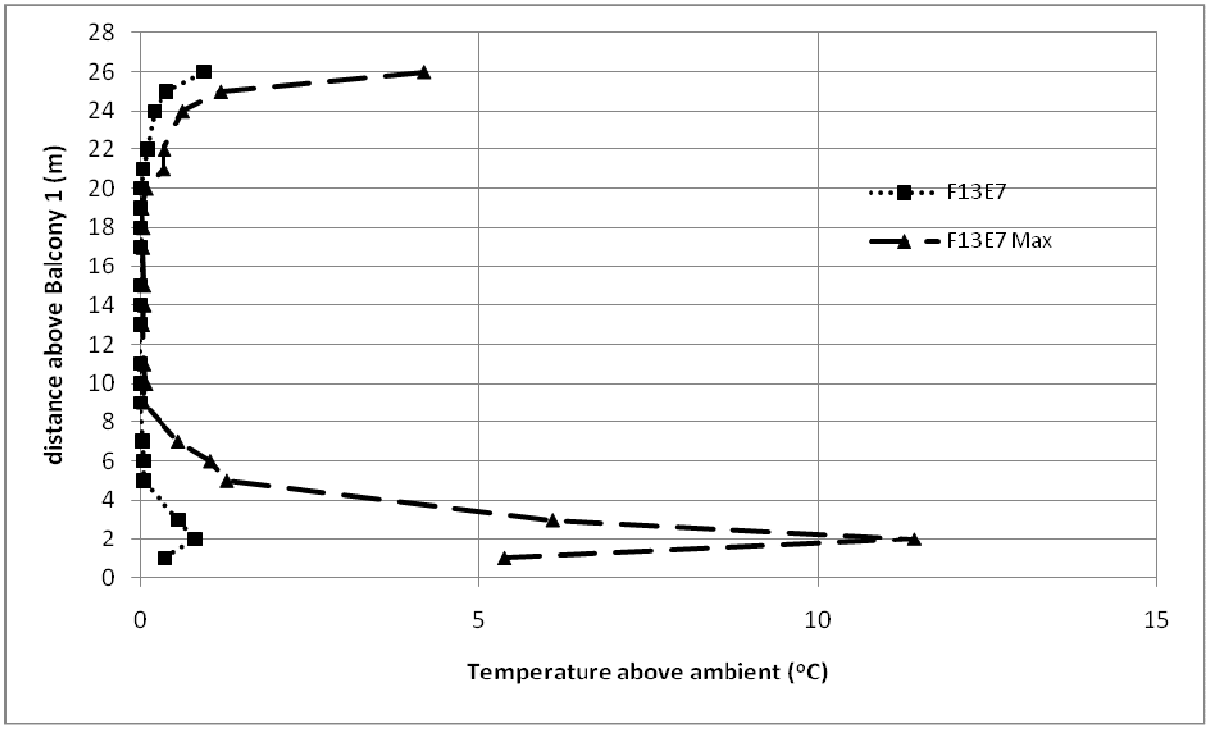

Figure I17. Temperature profiles across balcony edge.

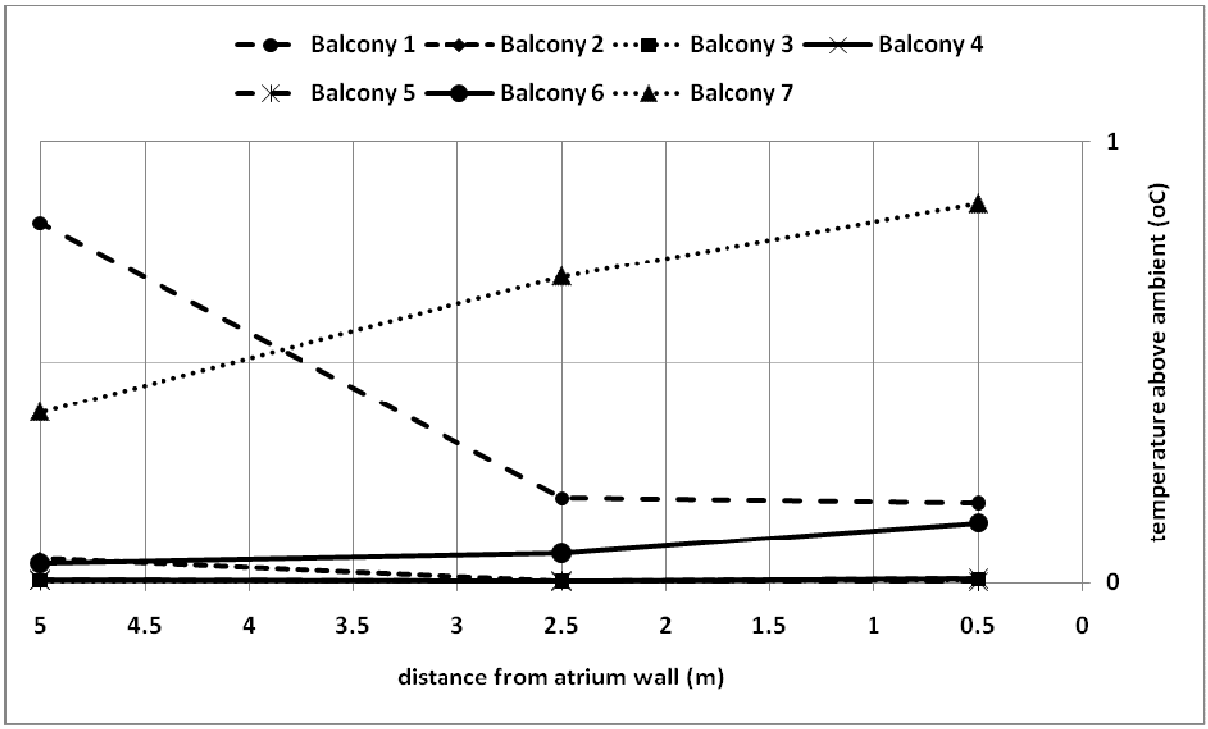

Figure I18. Temperature profiles along balcony breadth.

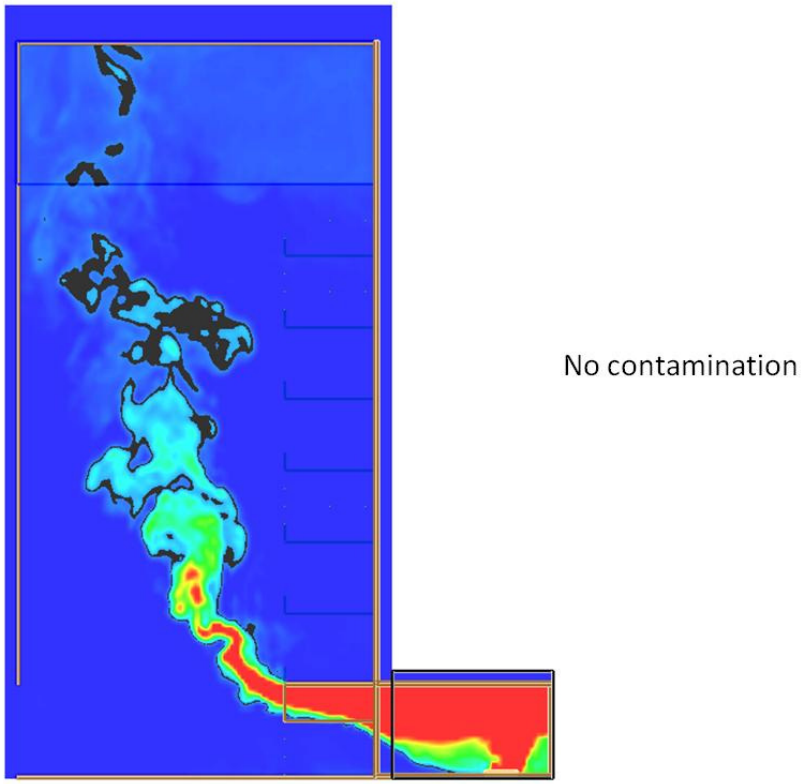

Figure I19. Smoke layer height measurement.

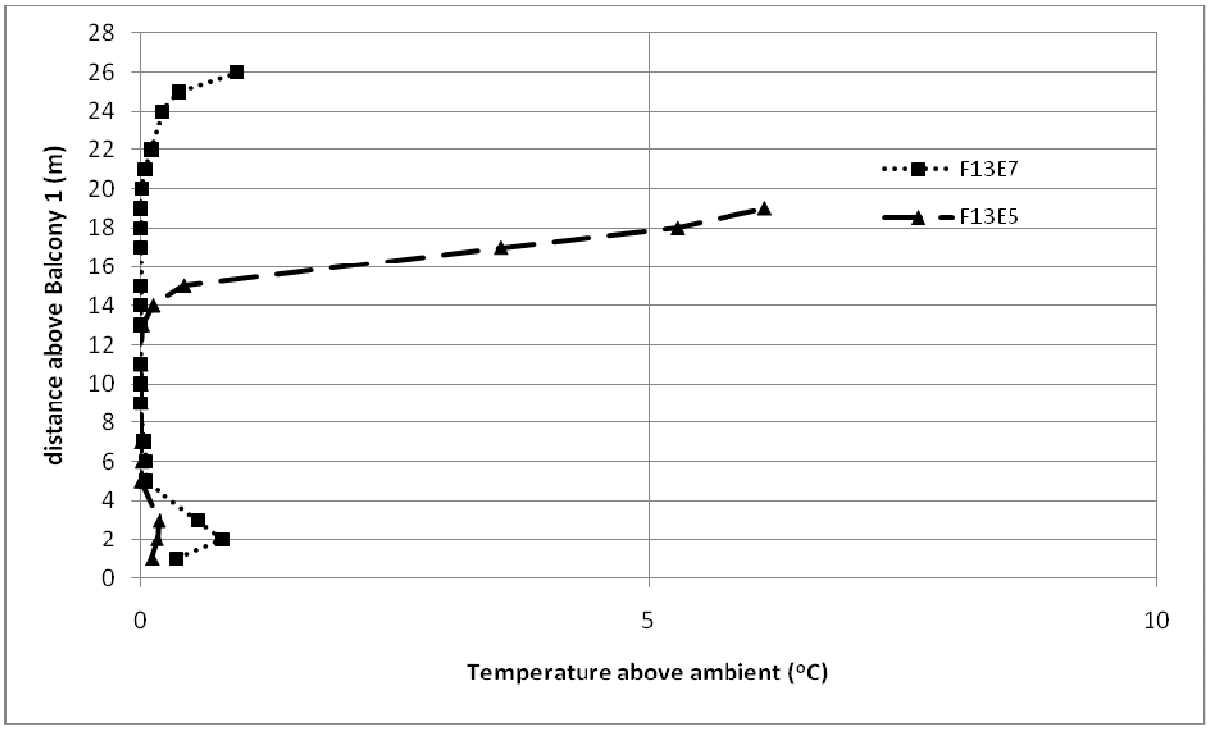

Figure I20. Comparison of seven storey balcony and five storey balcony temperature profiles along balcony edge.

Full scale for 7 storey balcony (F19E7)

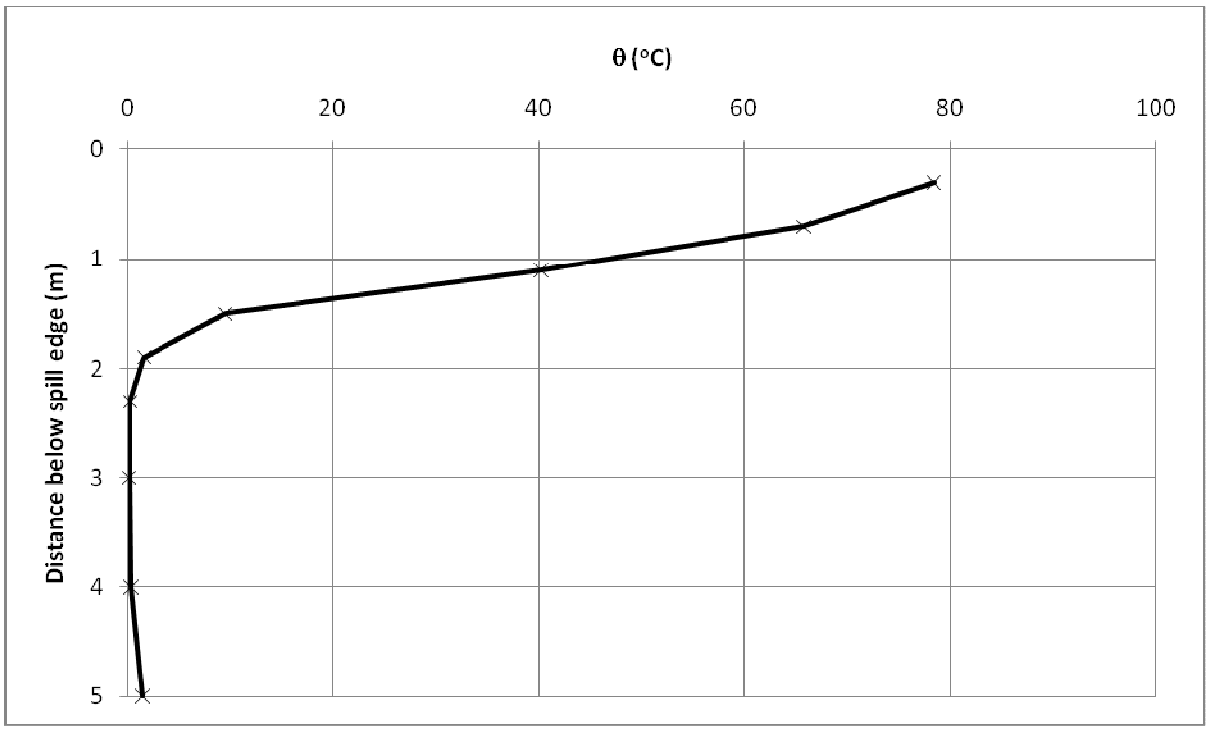

Figure I21. Temperature above ambient at the spill edge.

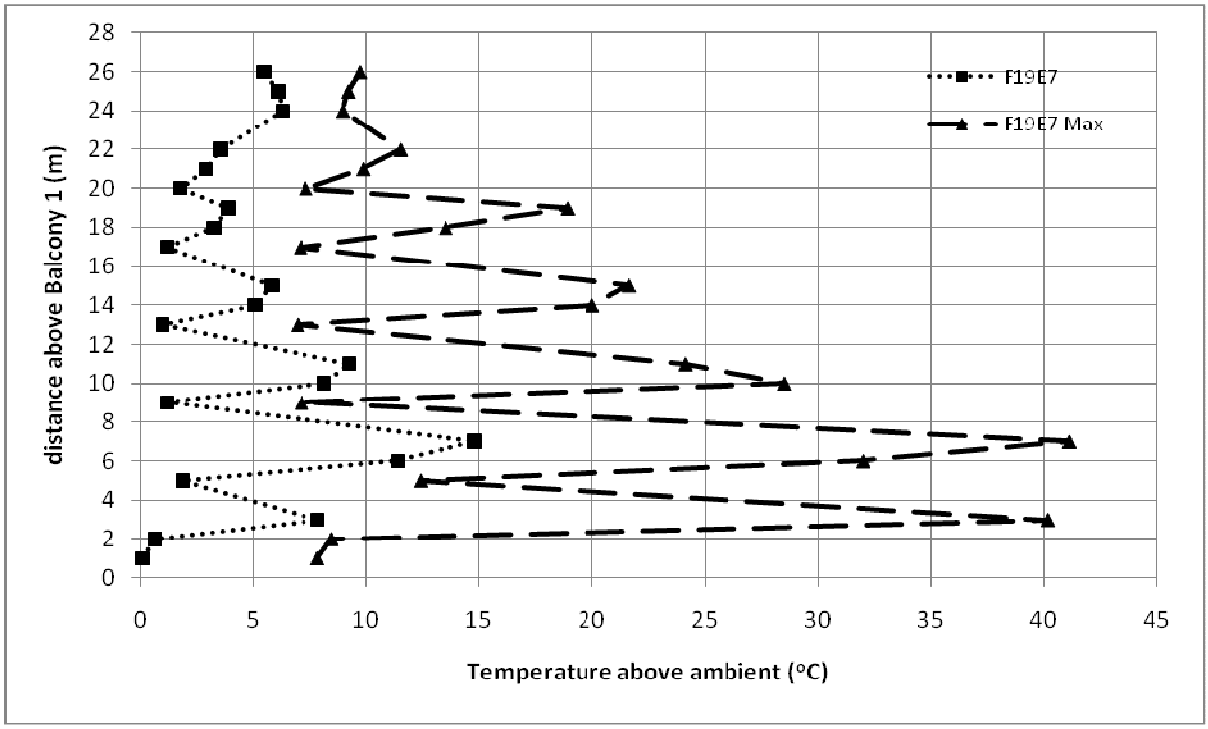

Figure I22. Temperature profiles across balcony edge.

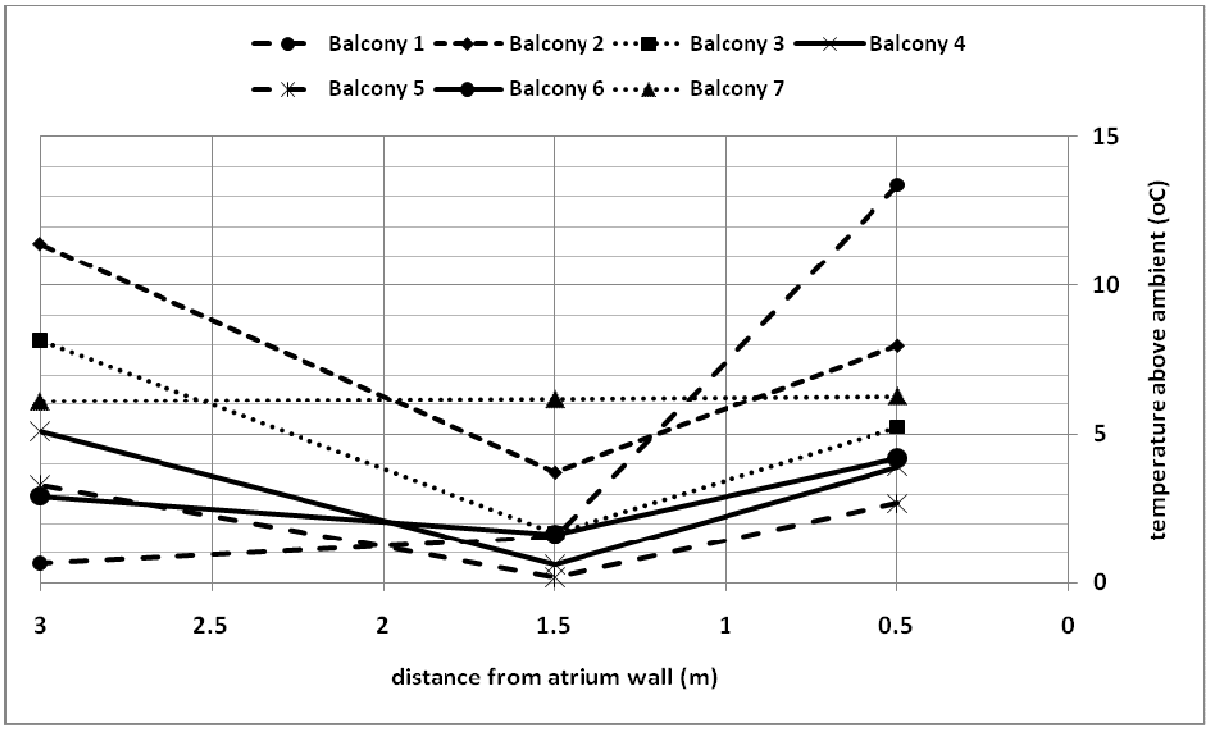

Figure I23. Temperature profiles along balcony breadth.

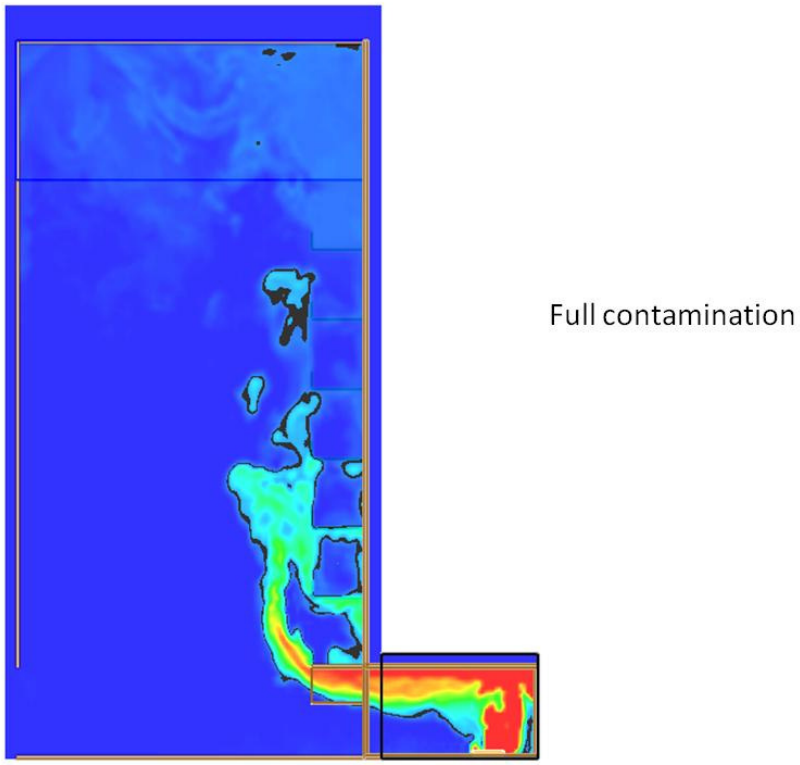

Figure I24. Smoke layer height measurement.

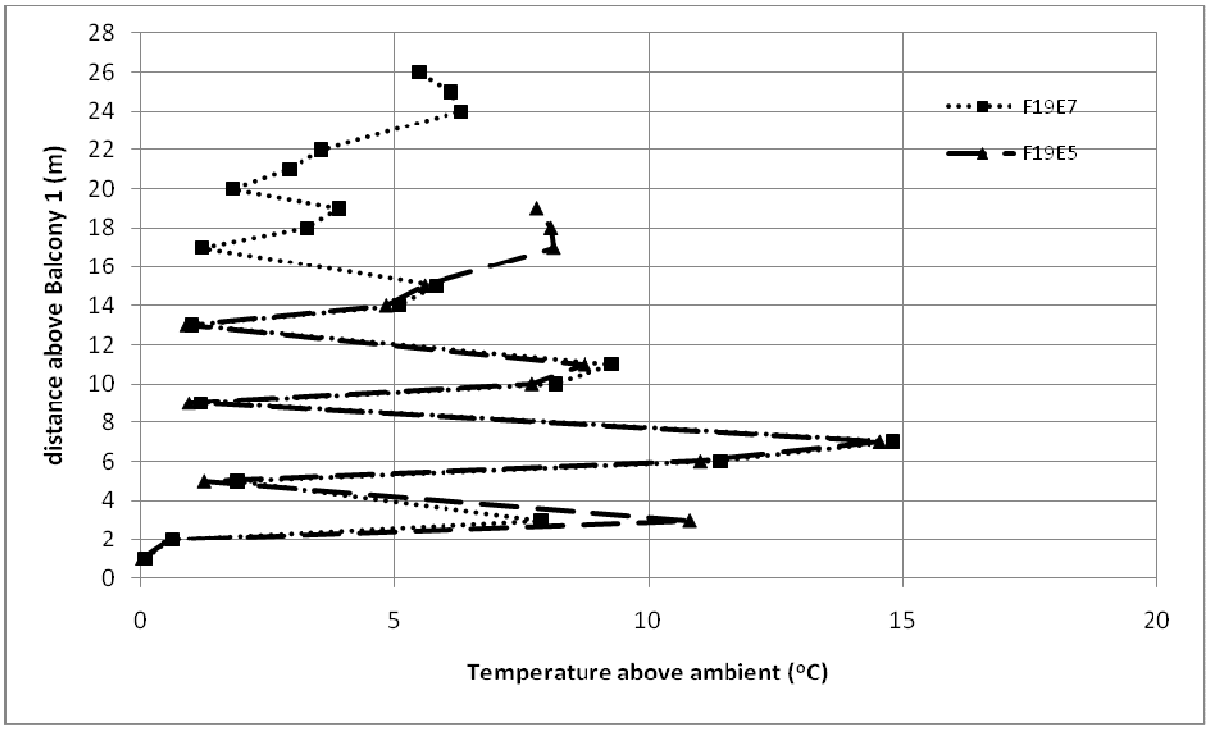

Figure I25. Comparison of seven storey balcony and five storey balcony temperature profiles along balcony edge.

Full scale for 7 storey balcony (F23E7)

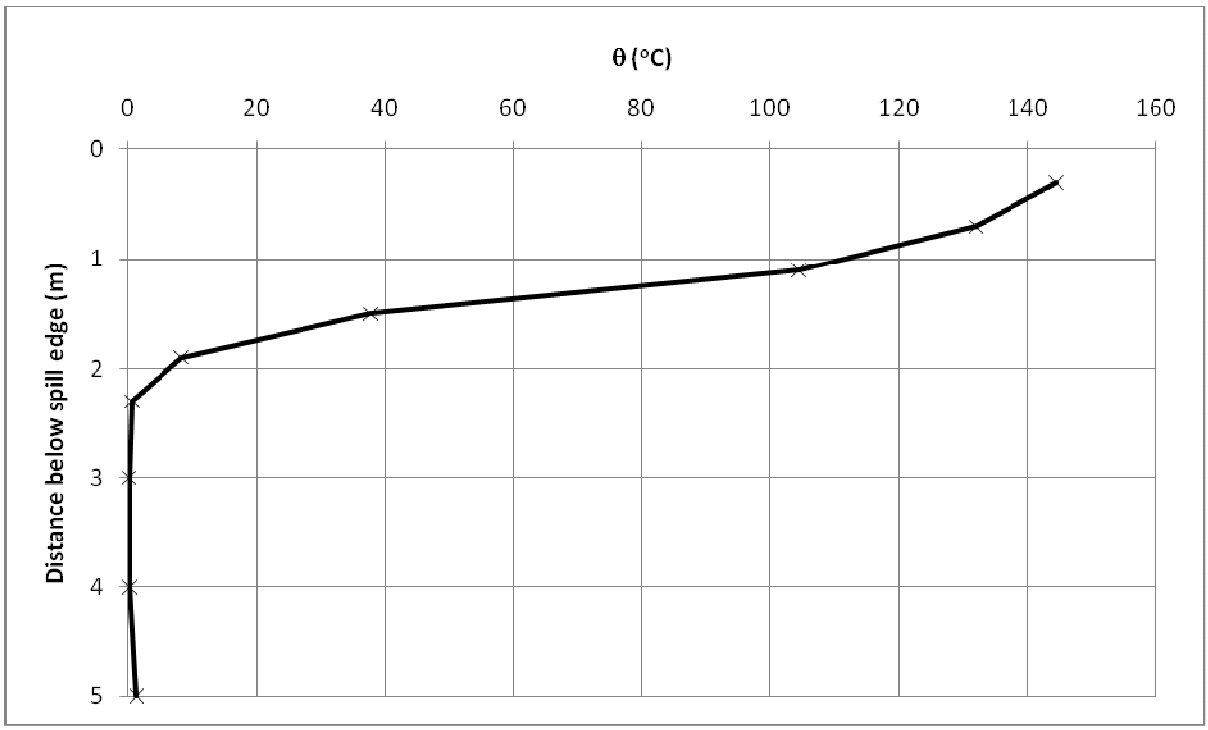

Figure I26. Temperature above ambient at the spill edge.

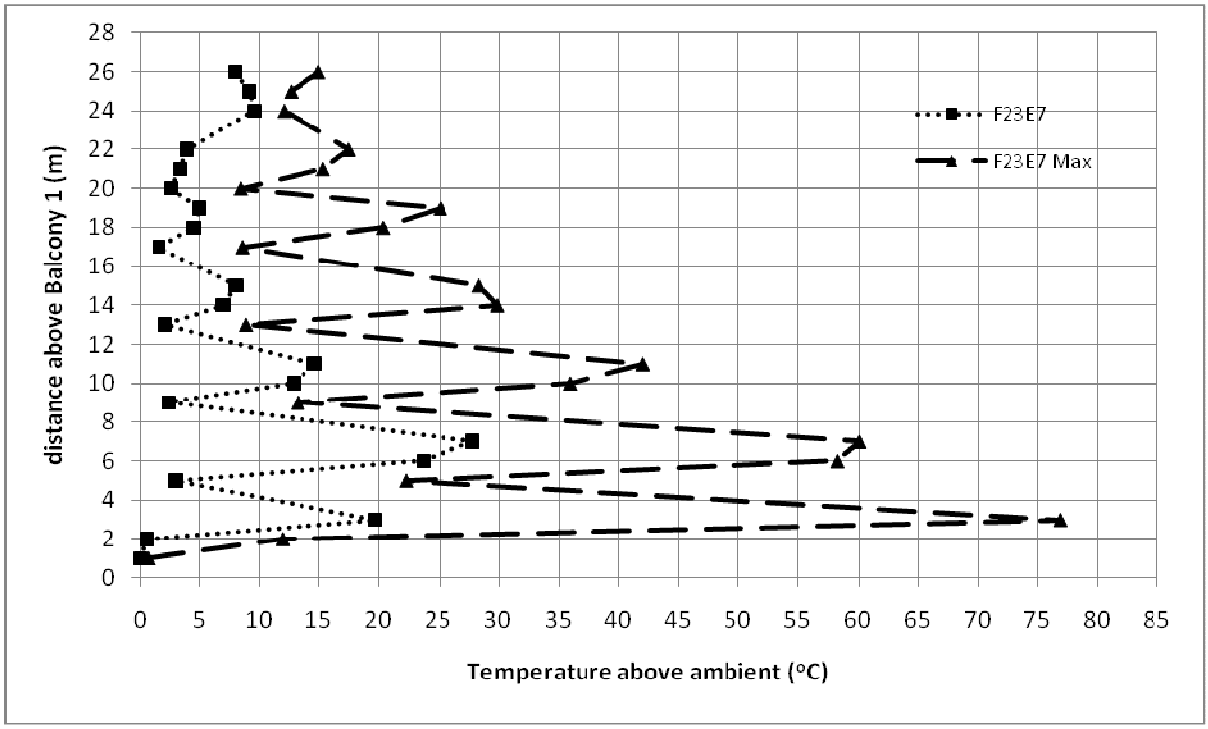

Figure I27. Temperature profiles across balcony edge.

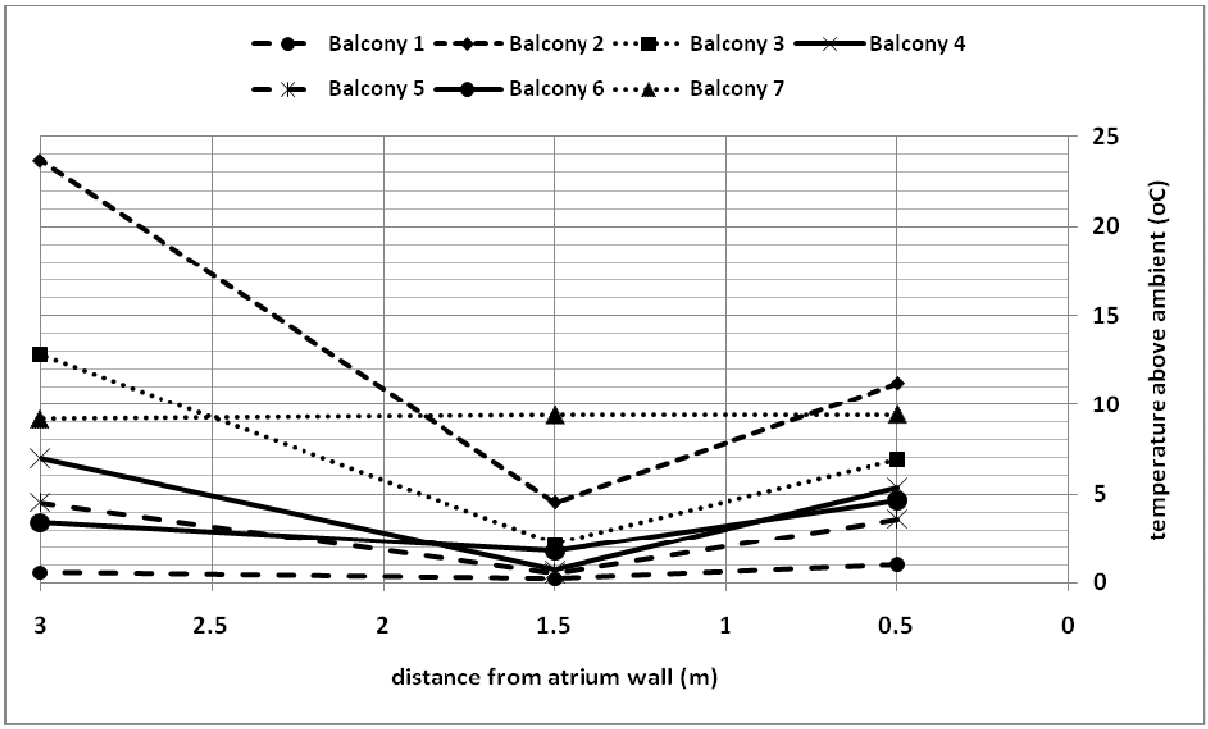

Figure I28. Temperature profiles along balcony breadth.

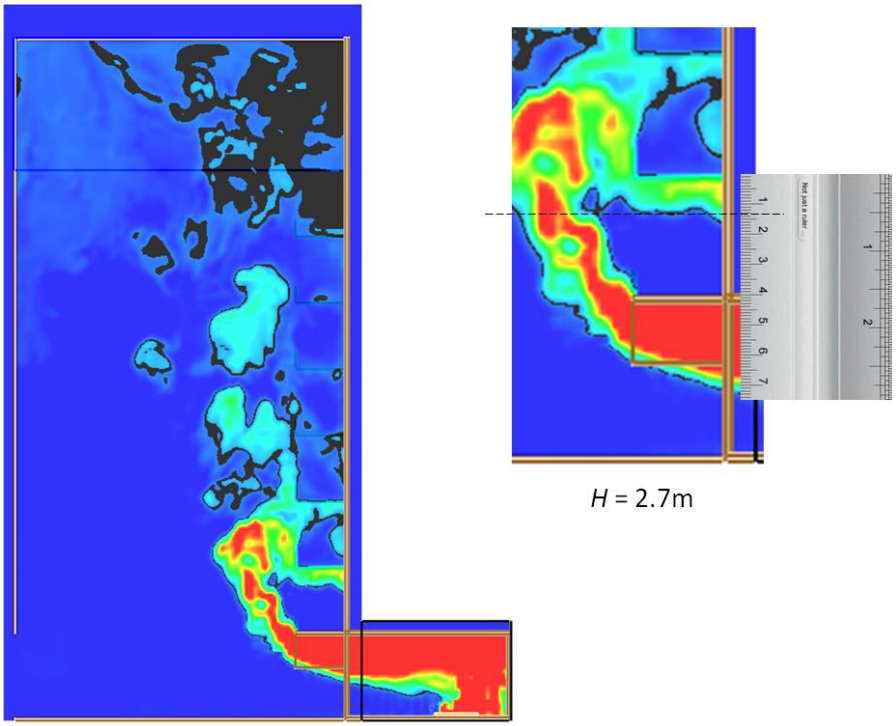

Figure I29. Smoke layer height measurement.

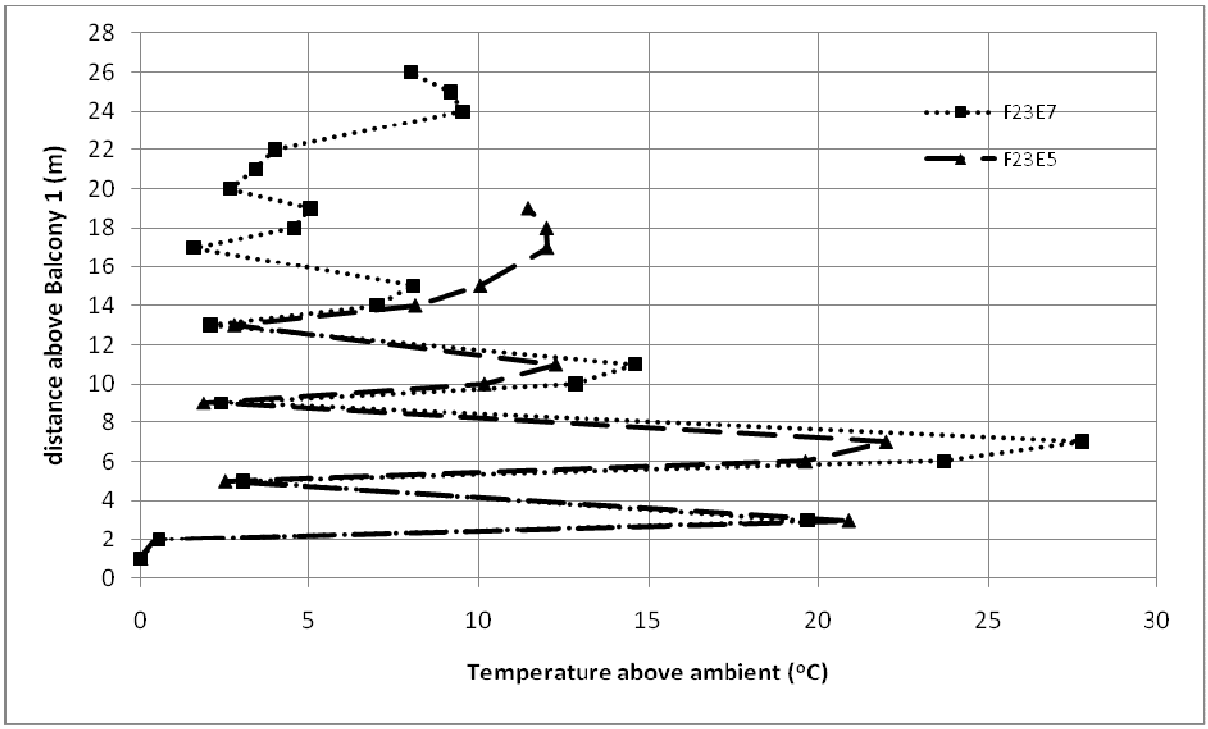

Figure I30. Comparison of seven storey balcony and five storey balcony temperature profiles along balcony edge.

Full scale for 7 storey balcony (F27E7)

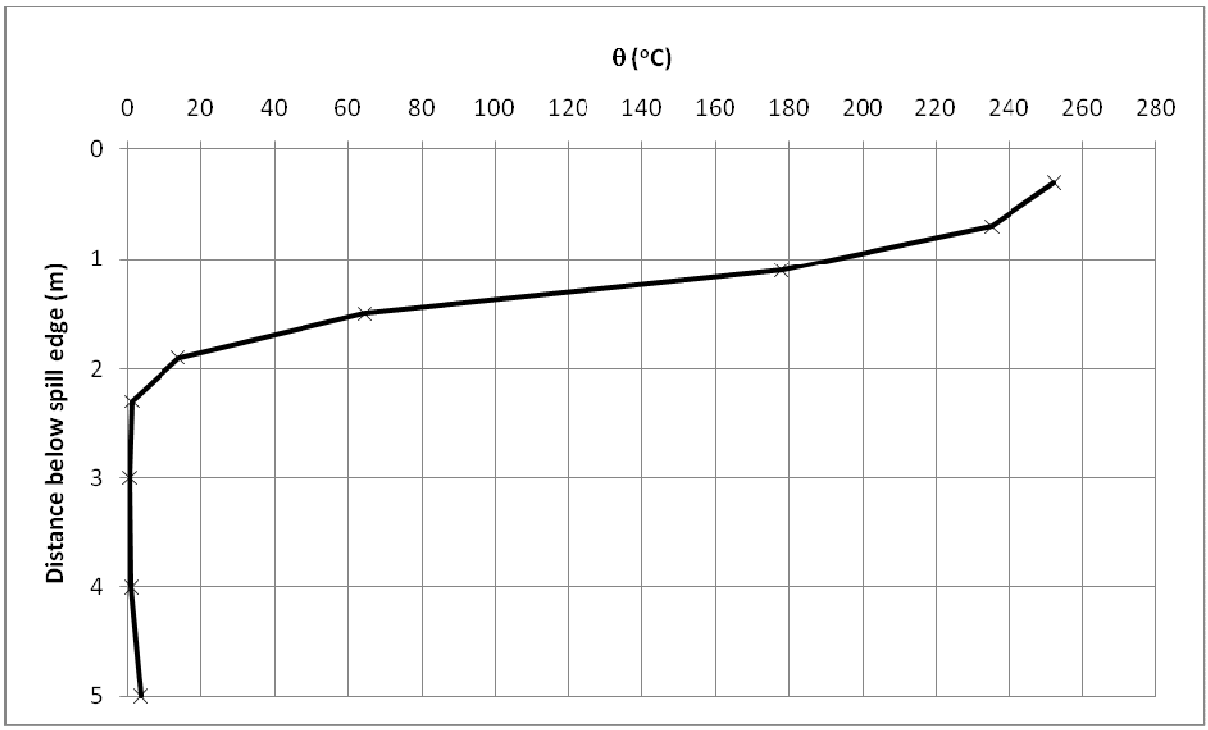

Figure I31. Temperature above ambient at the spill edge.

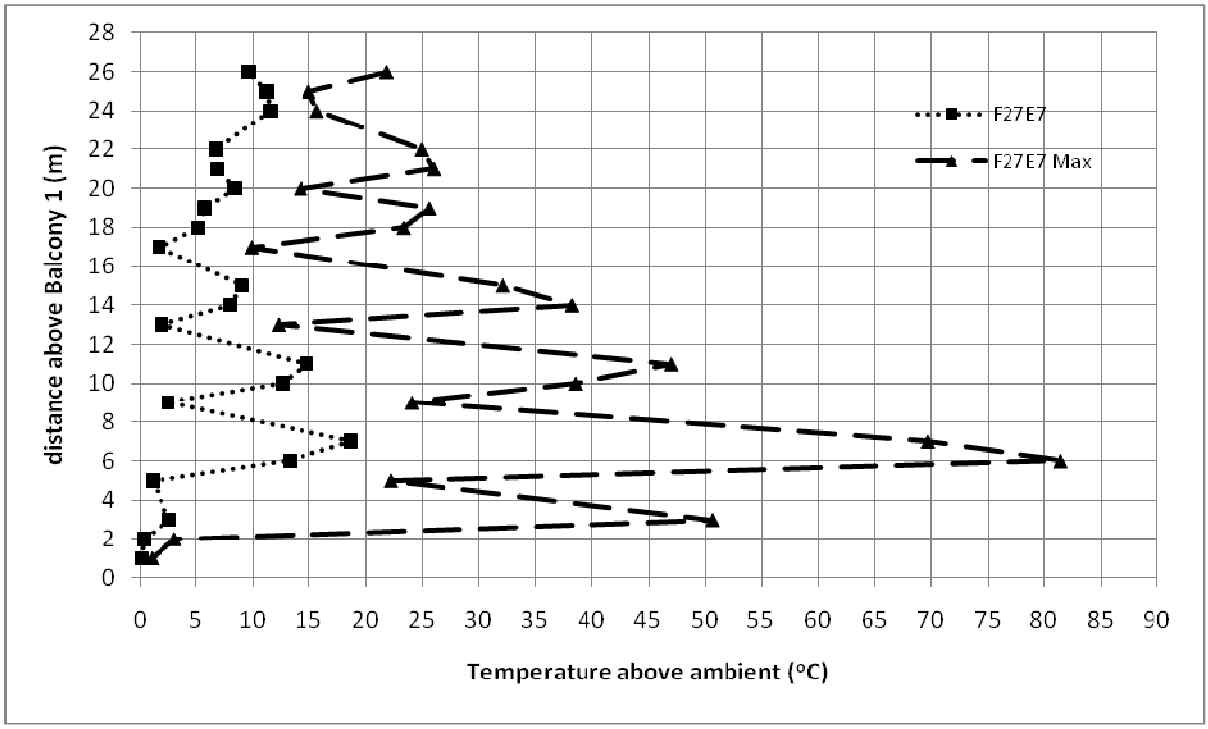

Figure I32. Temperature profiles across balcony edge.

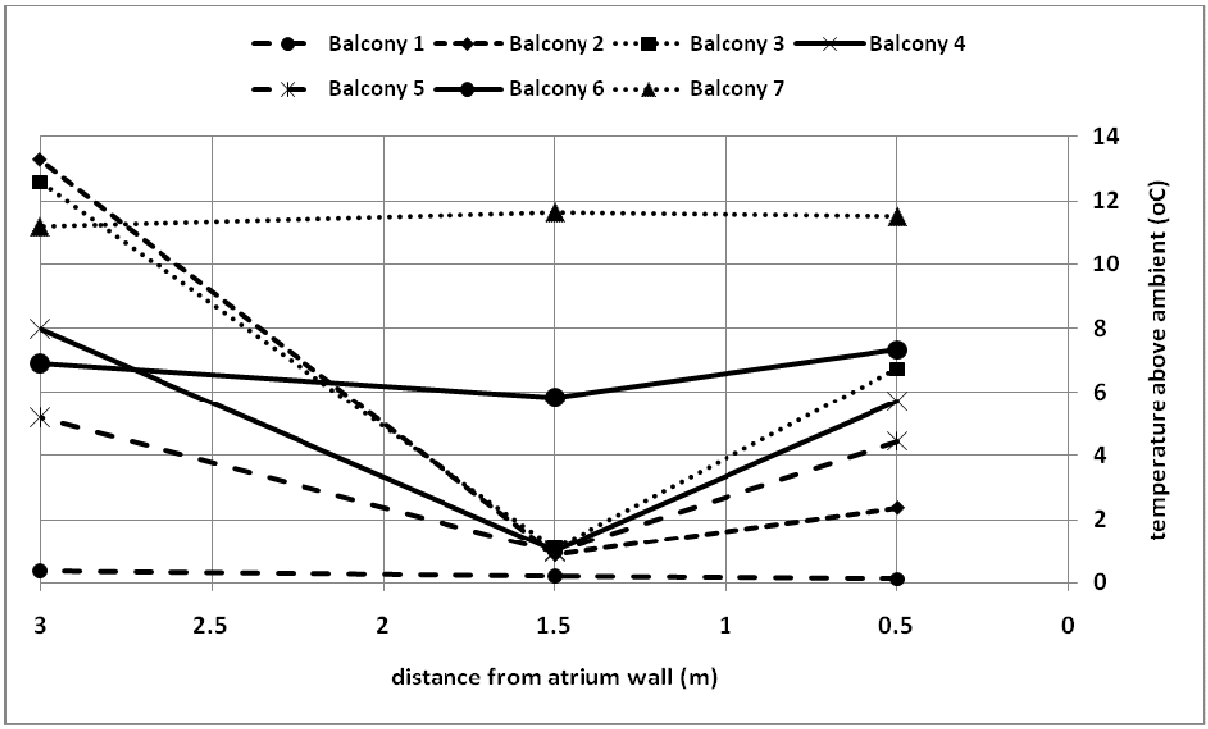

Figure I33. Temperature profiles along balcony breadth.

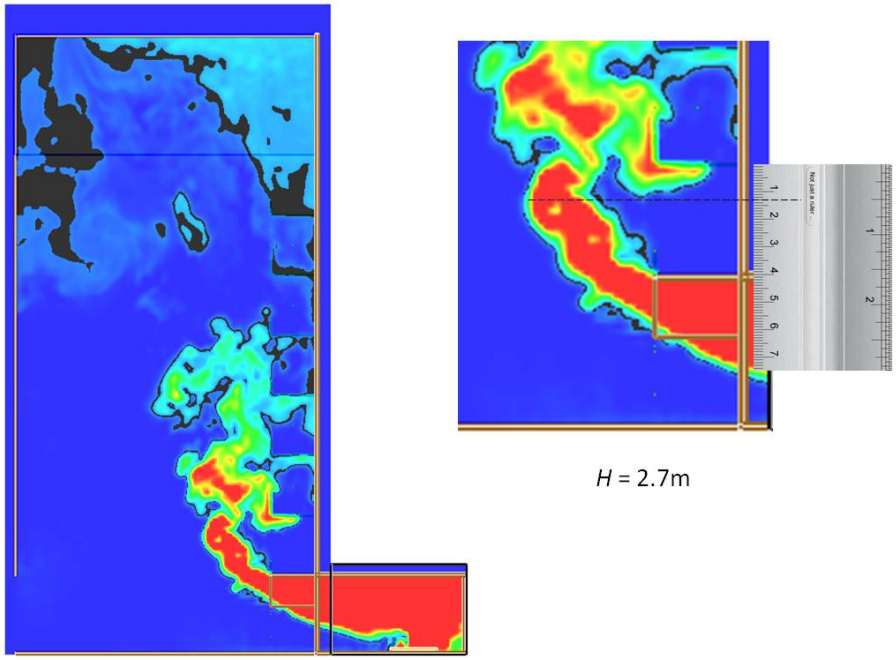

Figure I34. Smoke layer height measurement.

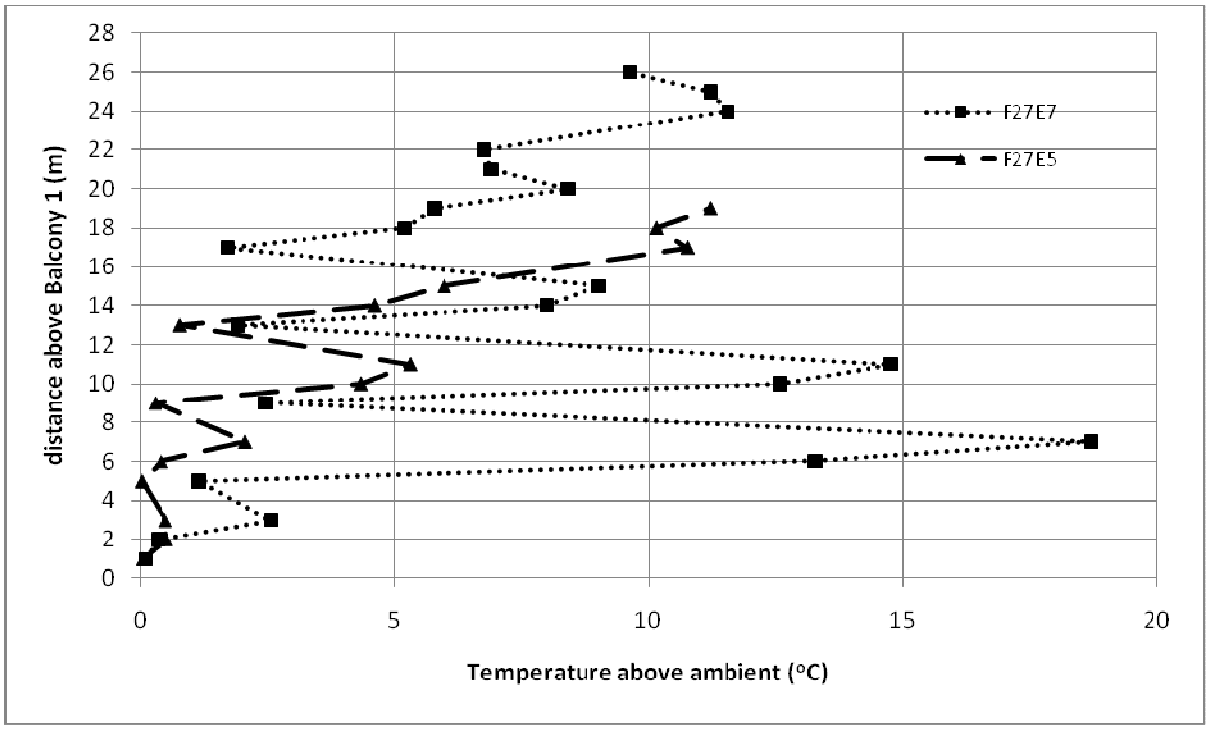

Figure I35. Comparison of seven storey balcony and five storey balcony temperature profiles along balcony edge.

Full scale for 7 storey balcony (F38E7)

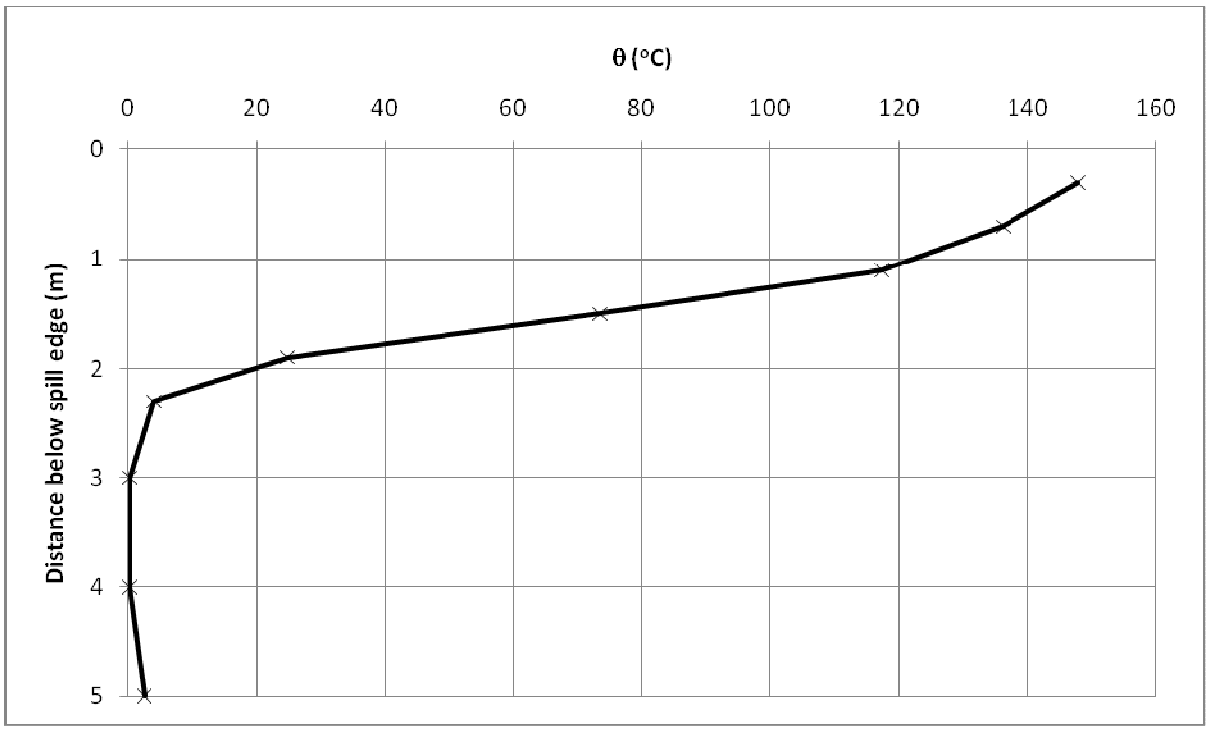

Figure I36. Temperature above ambient at the spill edge.

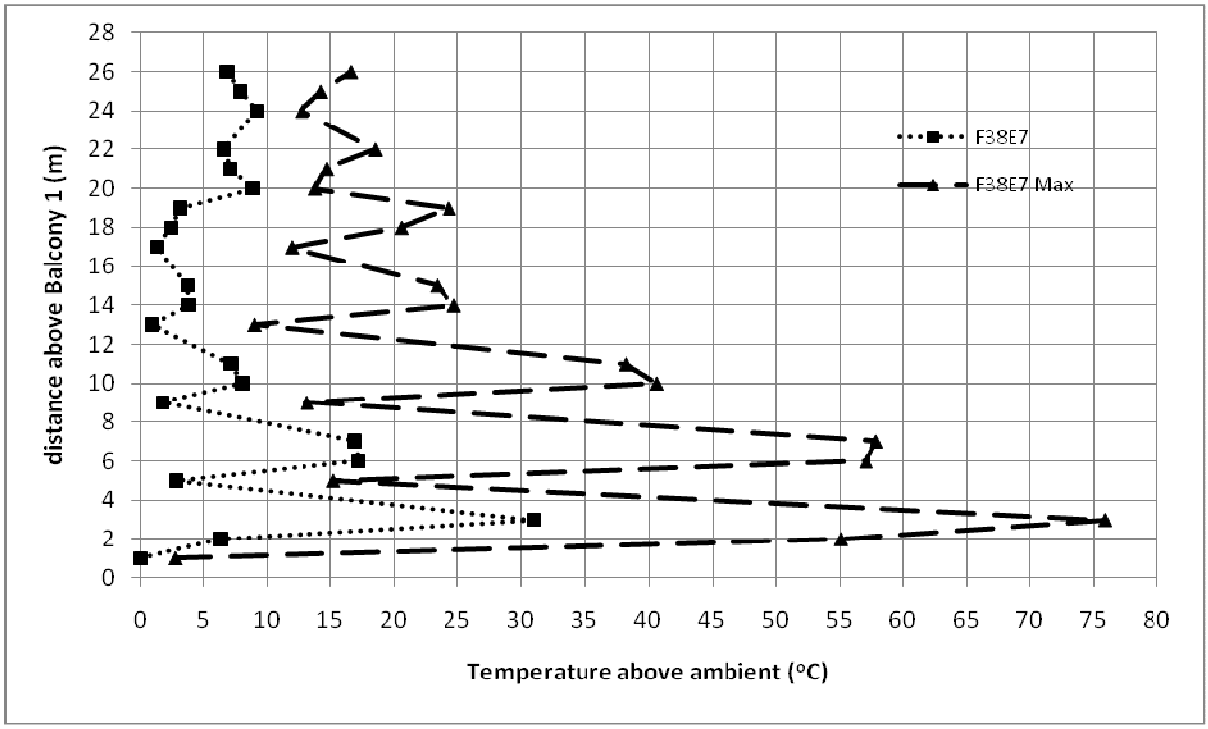

Figure I37. Temperature profiles across balcony edge.

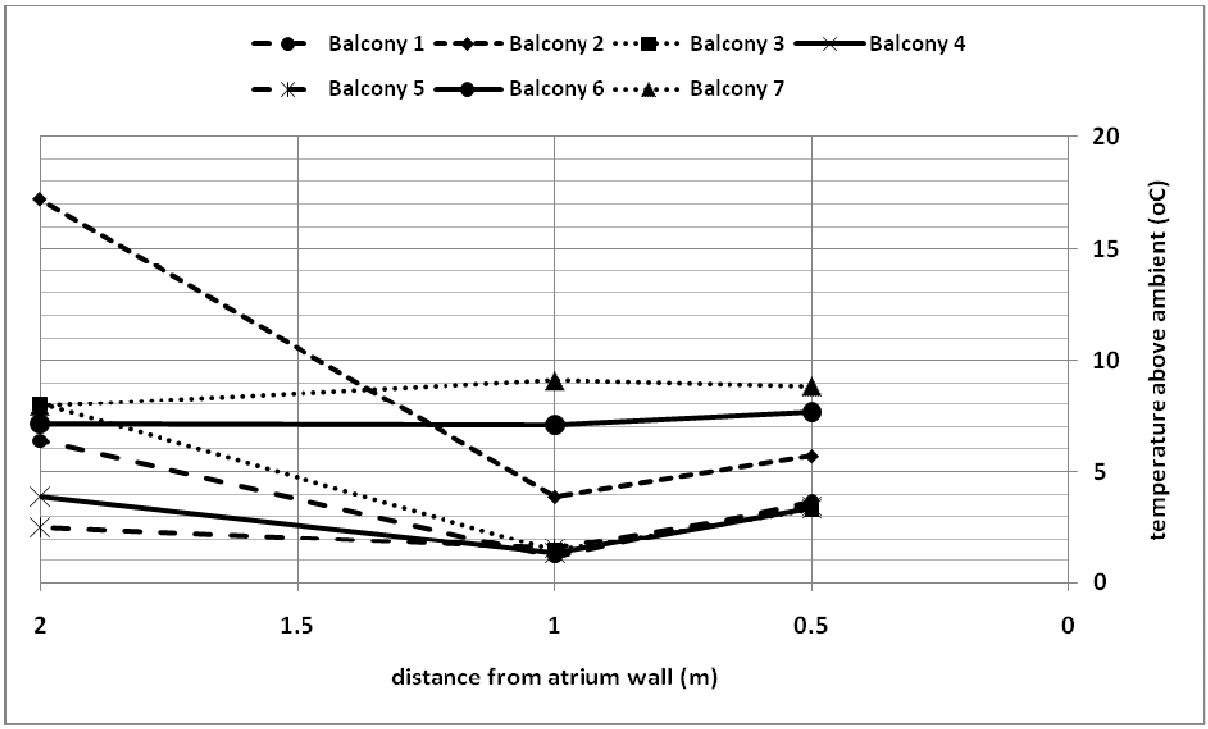

Figure I38. Temperature profiles along balcony breadth.

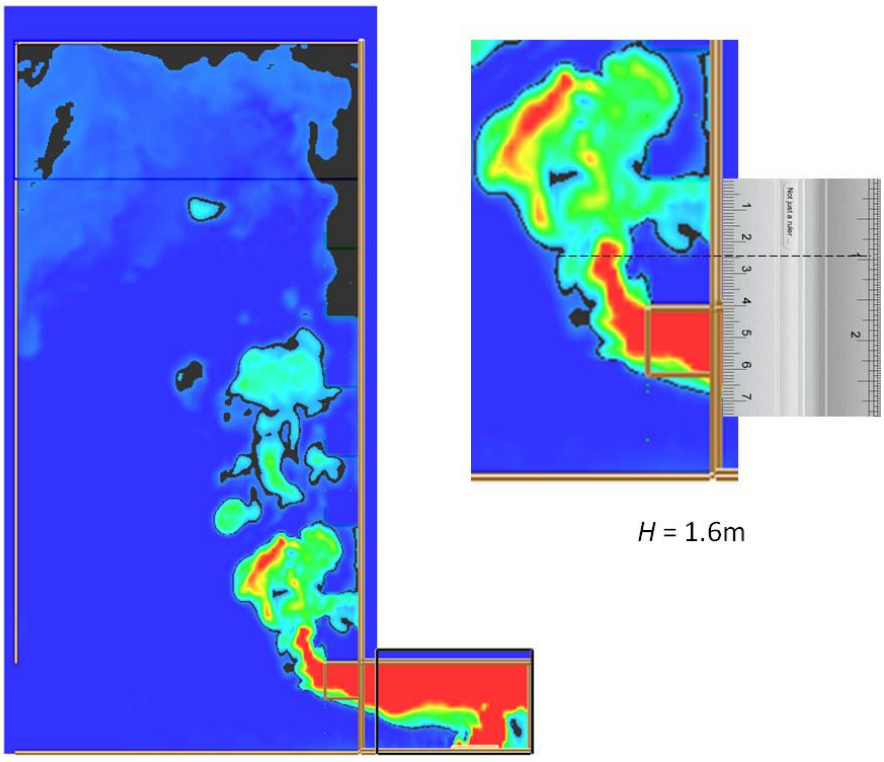

Figure I39. Smoke layer height measurement.

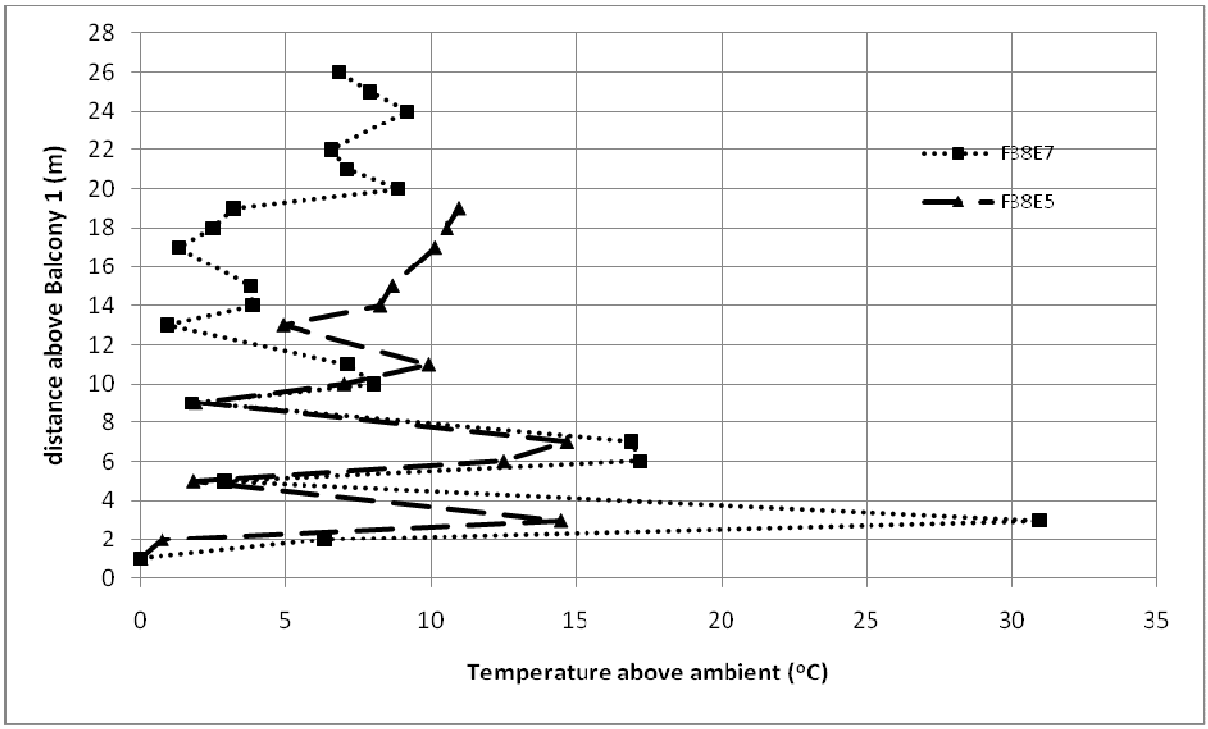

Figure I40. Comparison of seven storey balcony and five storey balcony temperature profiles along balcony edge.

Full scale for 7 storey balcony (F41E7)

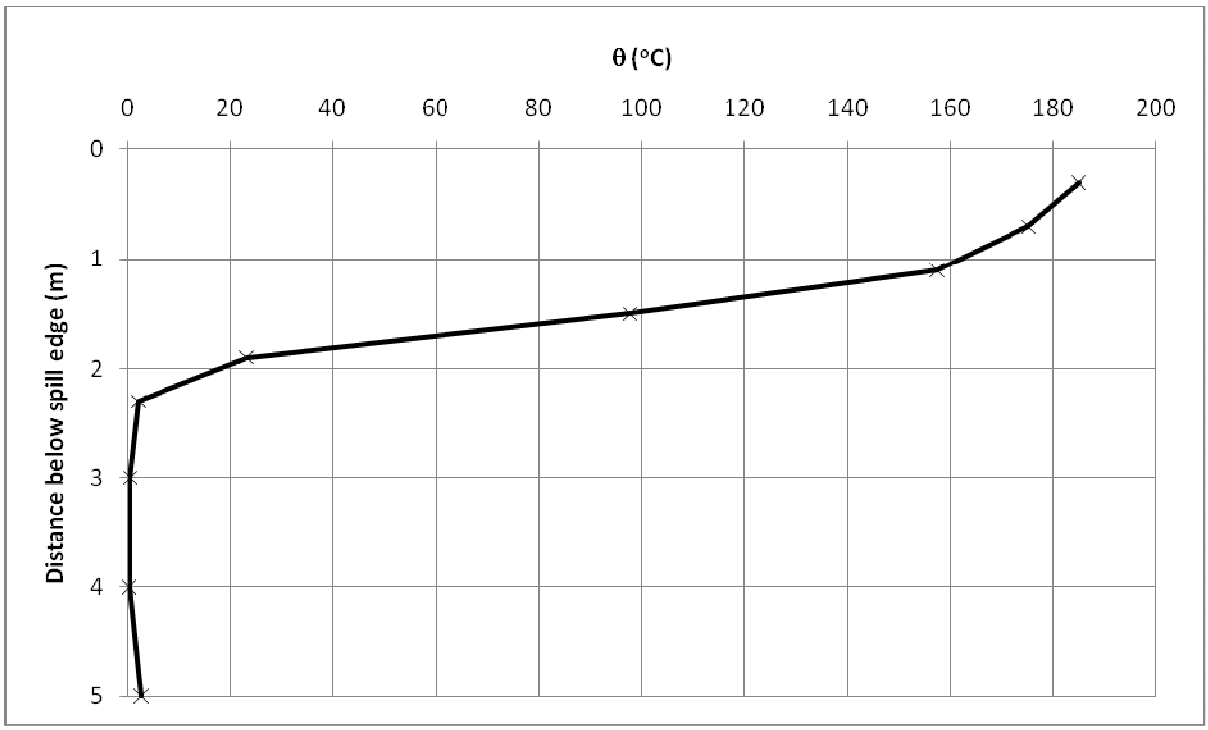

Figure I41. Temperature above ambient at the spill edge.

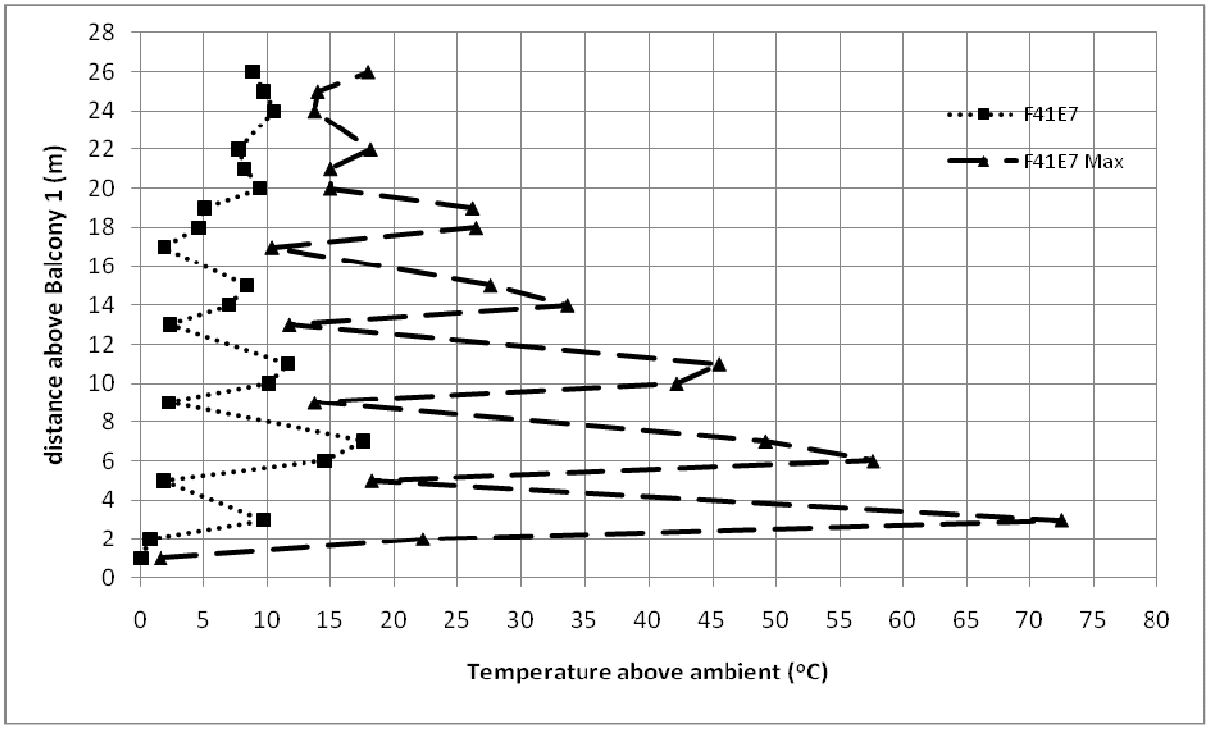

Figure I42. Temperature profiles across balcony edge.

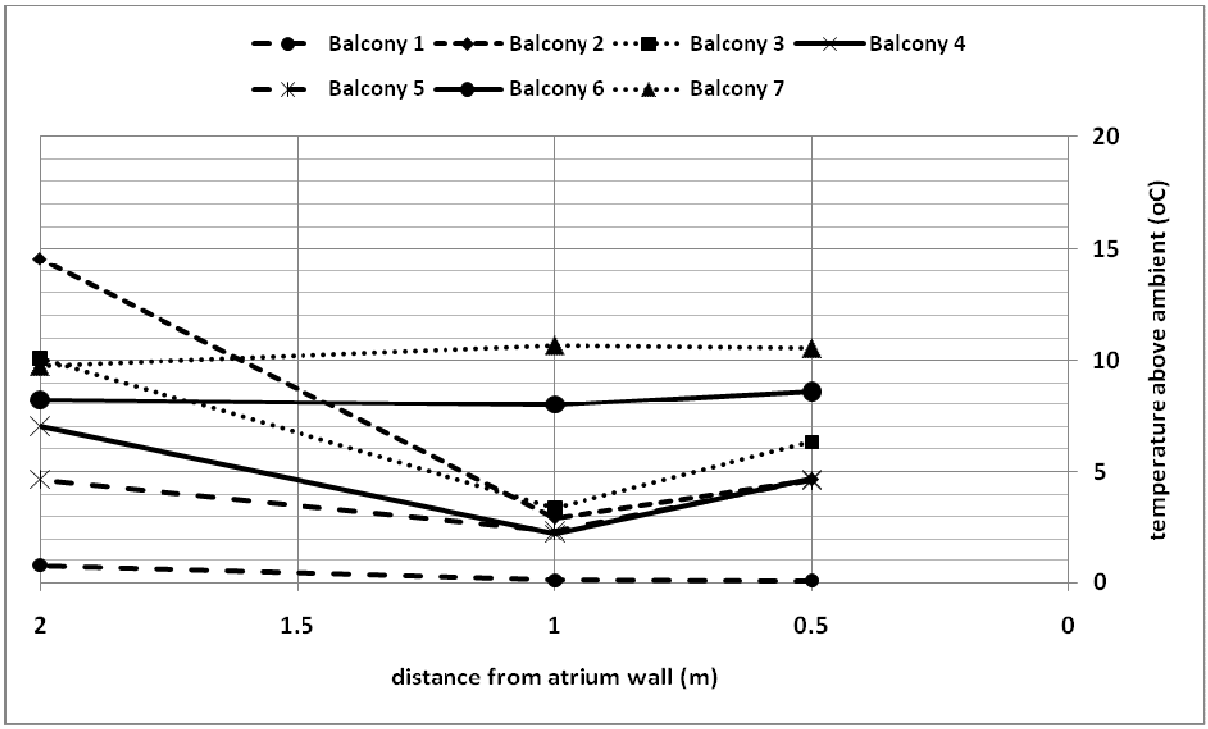

Figure I43. Temperature profiles along balcony breadth.

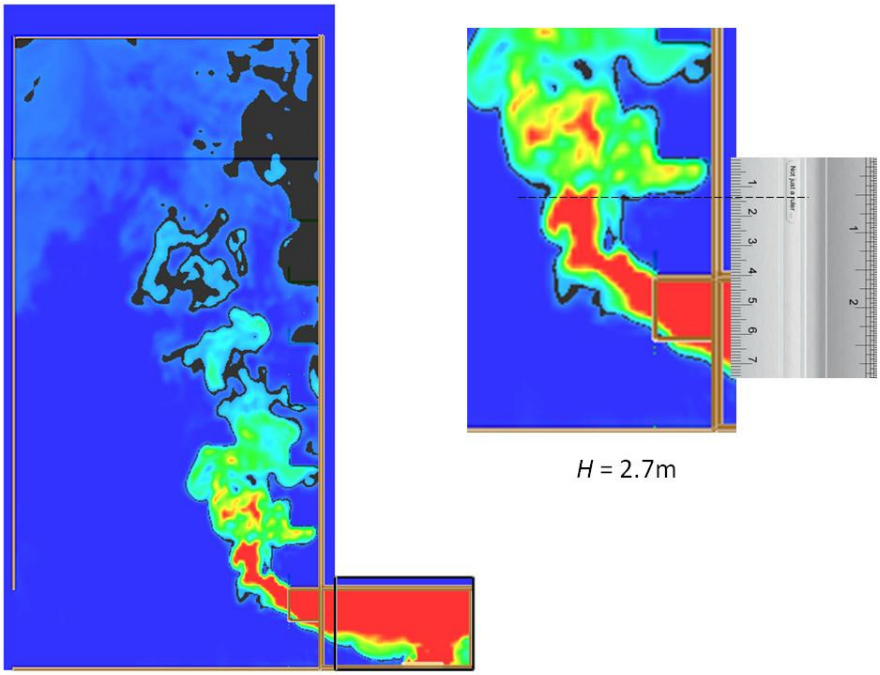

Figure I44. Smoke layer height measurement.

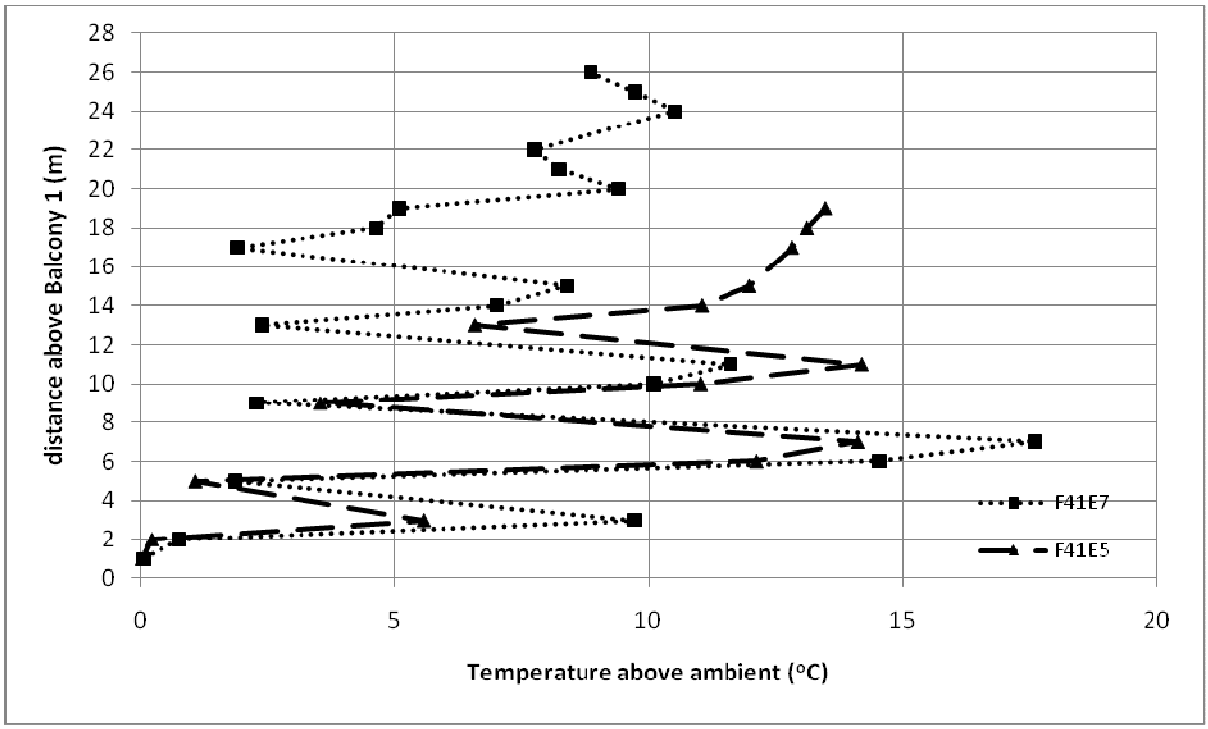

Figure I45. Comparison of seven storey balcony and five storey balcony temperature profiles along balcony edge.

Full scale for 7 storey balcony (F43E7)

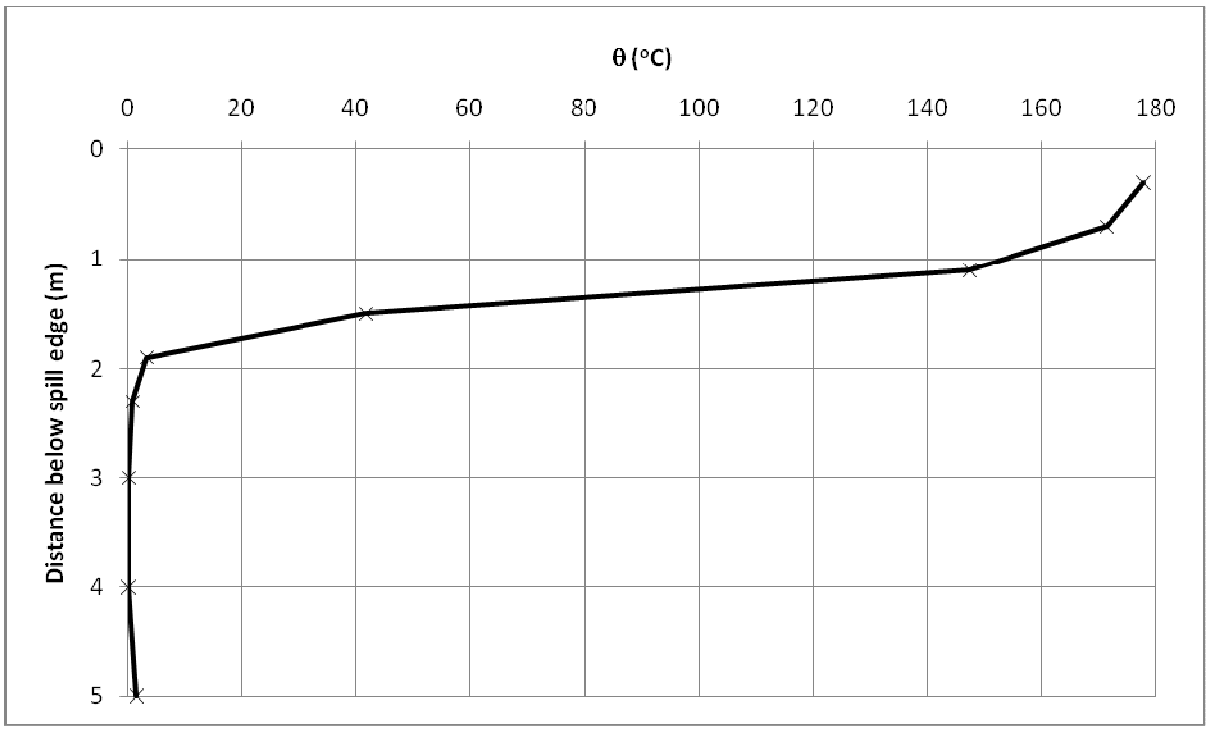

Figure I46. Temperature above ambient at the spill edge.

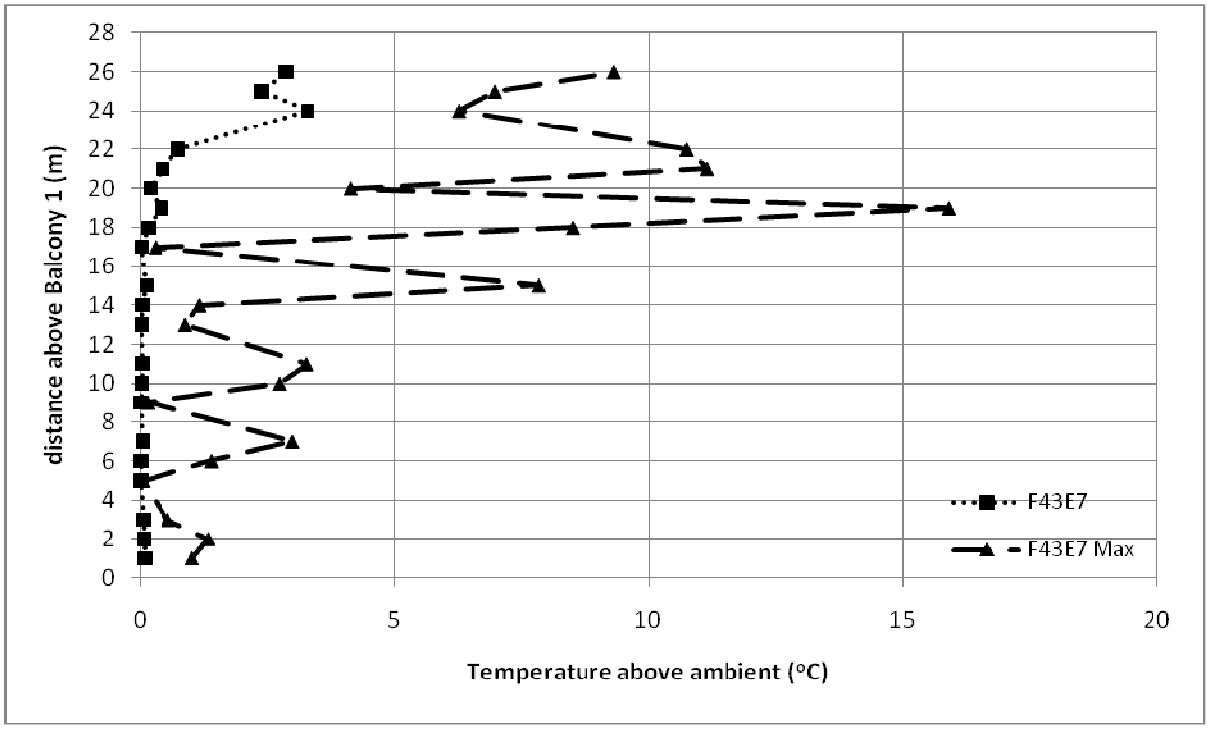

Figure I47. Temperature profiles across balcony edge.

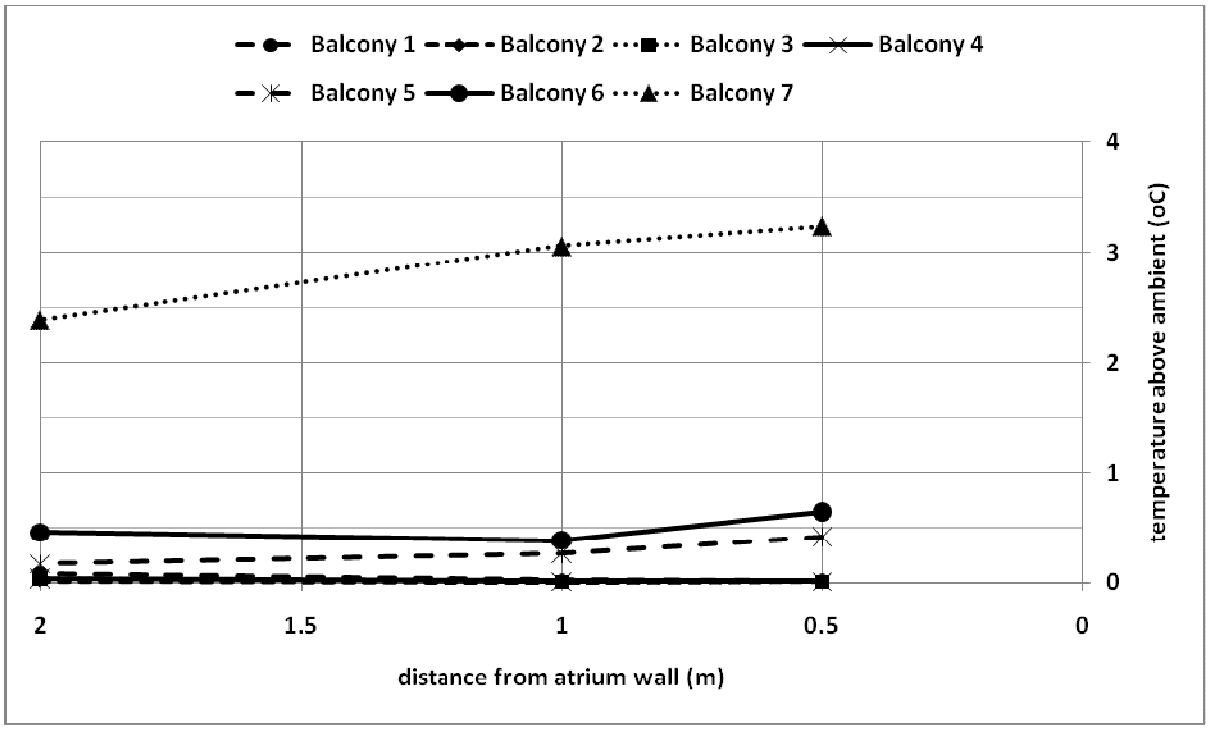

Figure I48. Temperature profiles along balcony breadth.

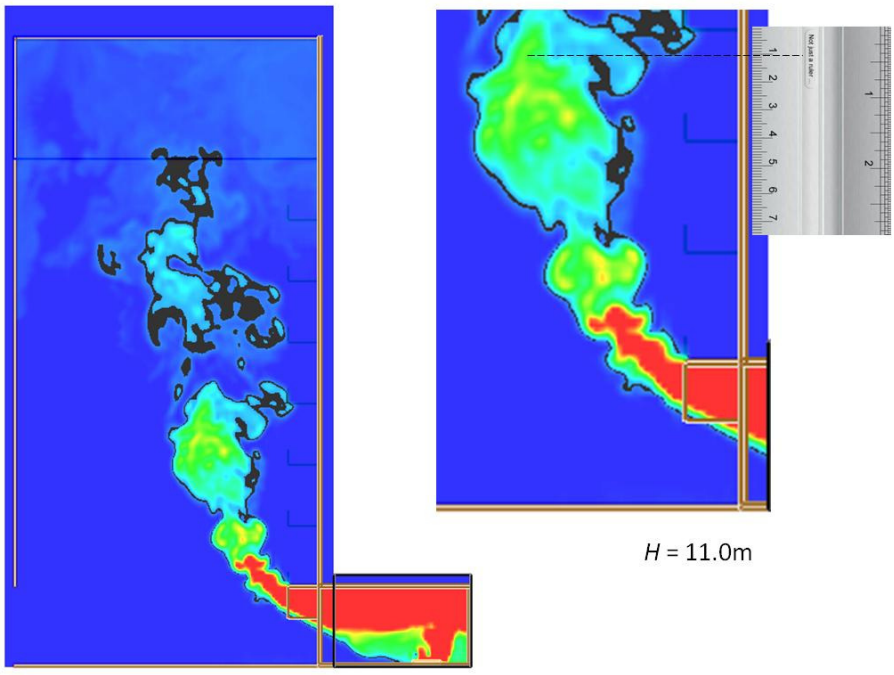

Figure I49. Smoke layer height measurement.

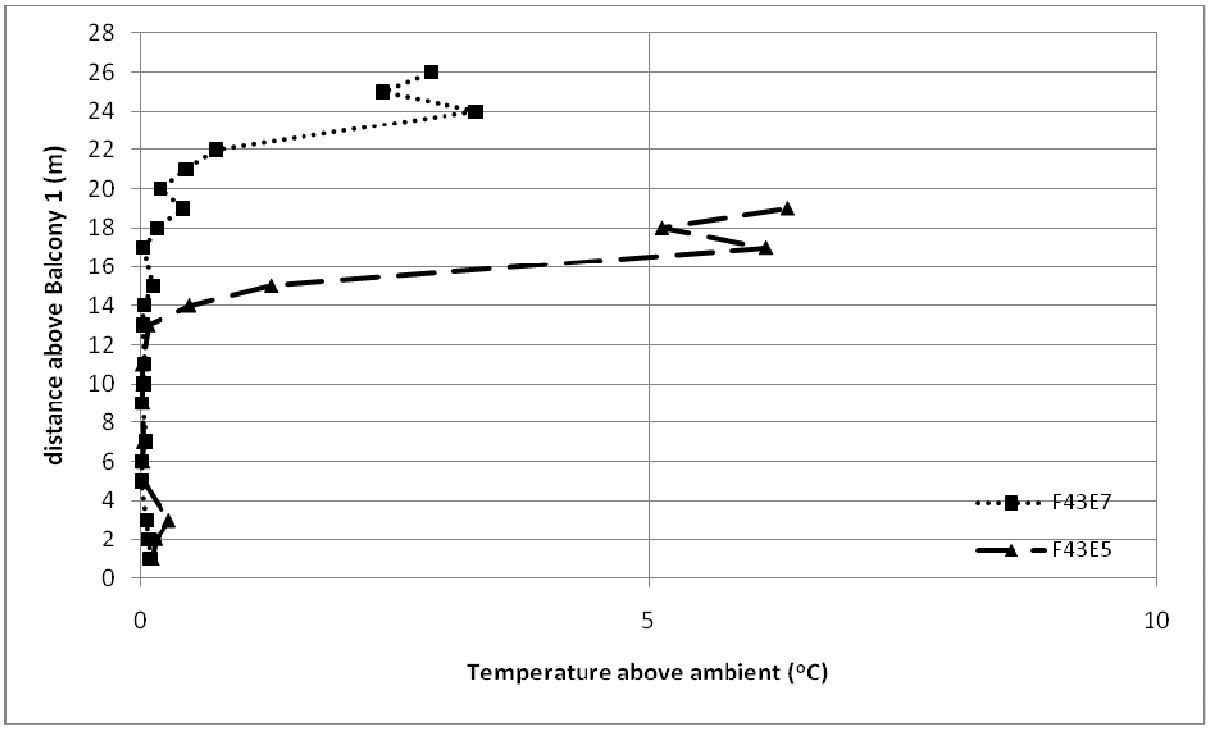

Figure I50. Comparison of seven storey balcony and five storey balcony temperature profiles along balcony edge.

Full scale for 7 storey balcony (F56E7)

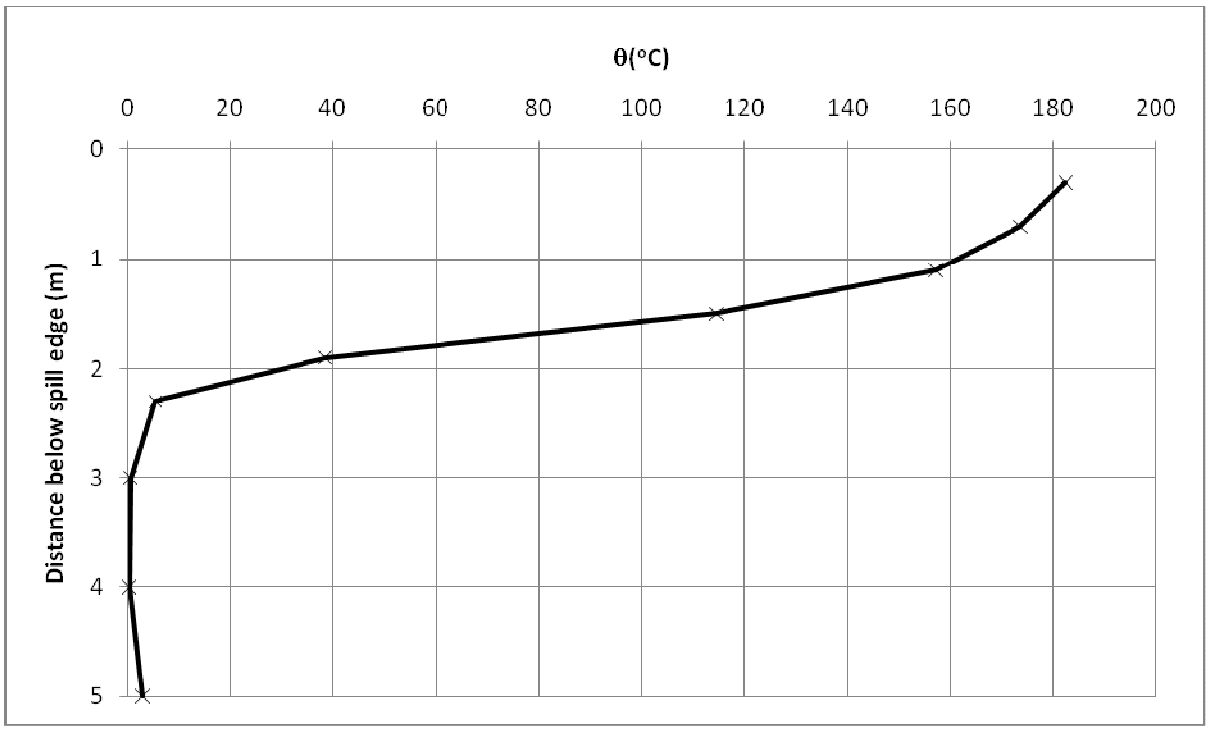

Figure I51. Temperature above ambient at the spill edge.

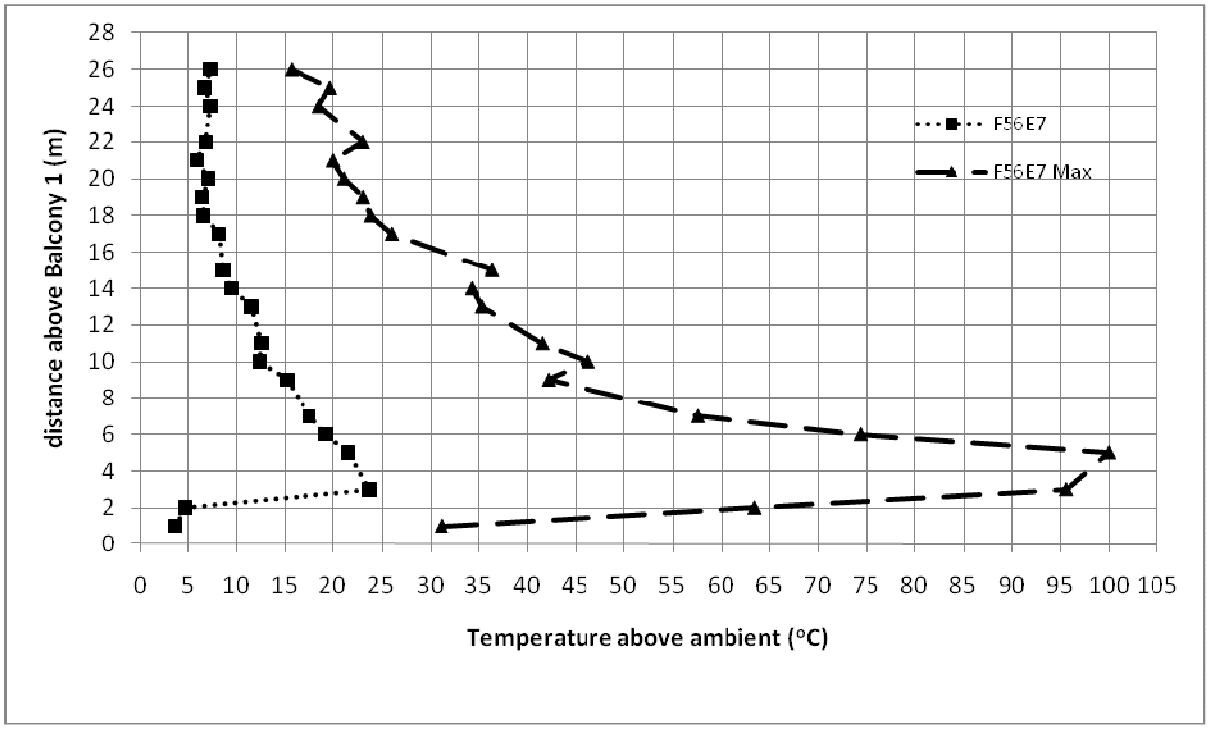

Figure I52. Temperature profiles across balcony edge.

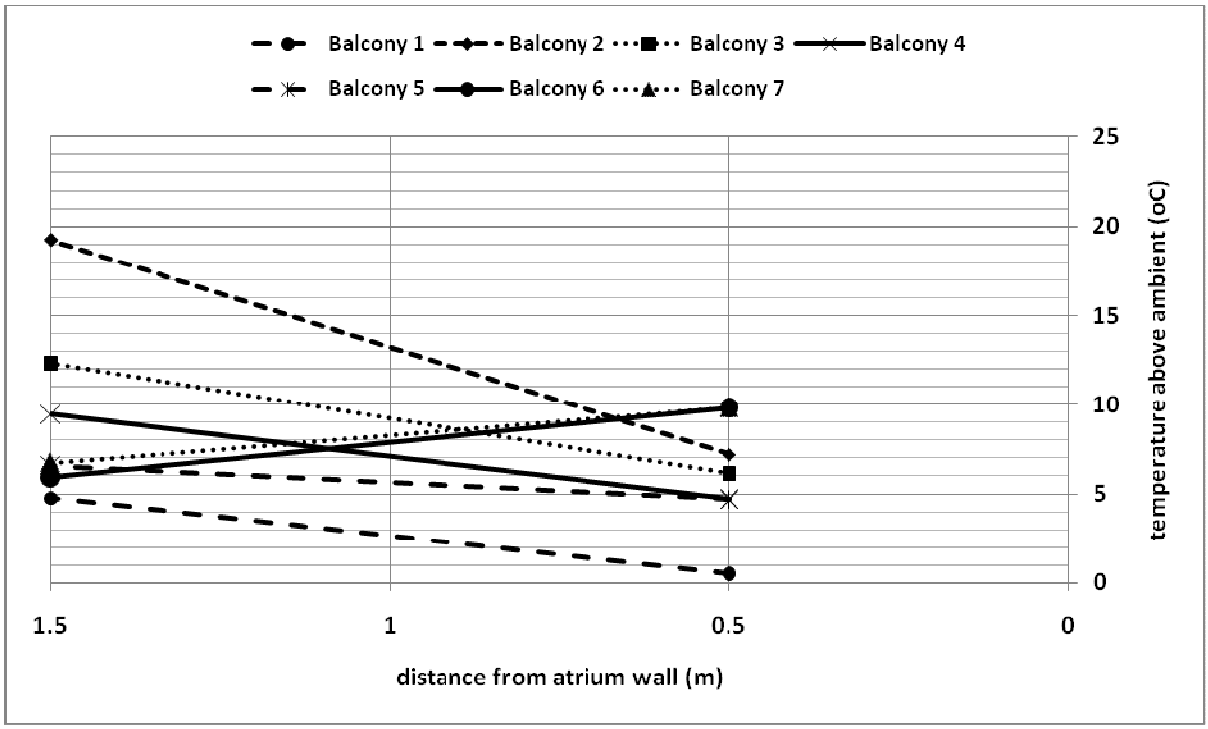

Figure I53. Temperature profiles along balcony breadth.

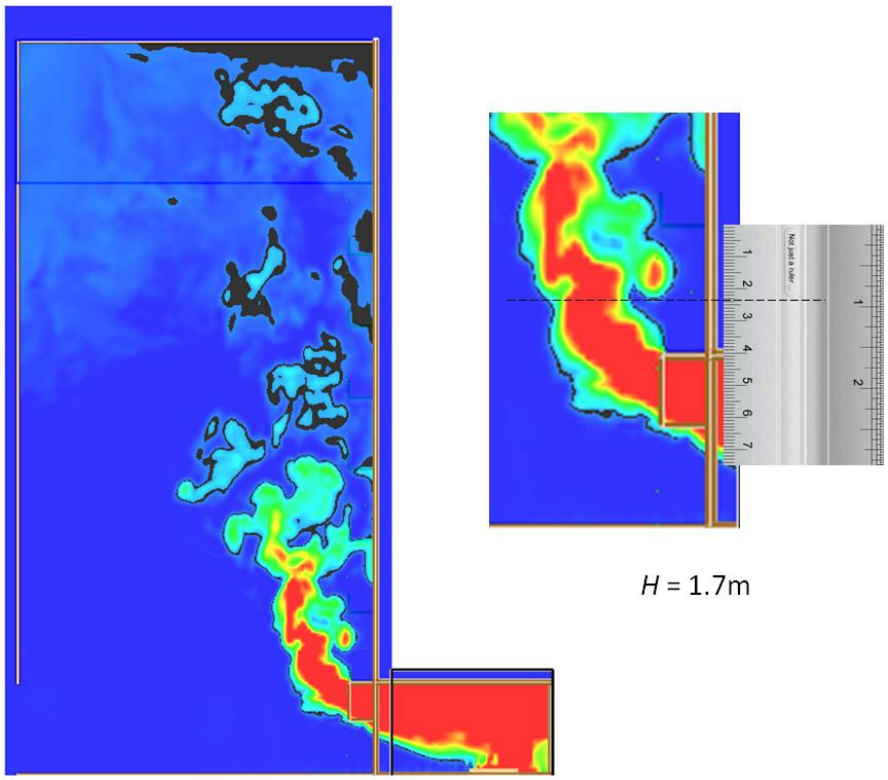

Figure I54. Smoke layer height measurement.

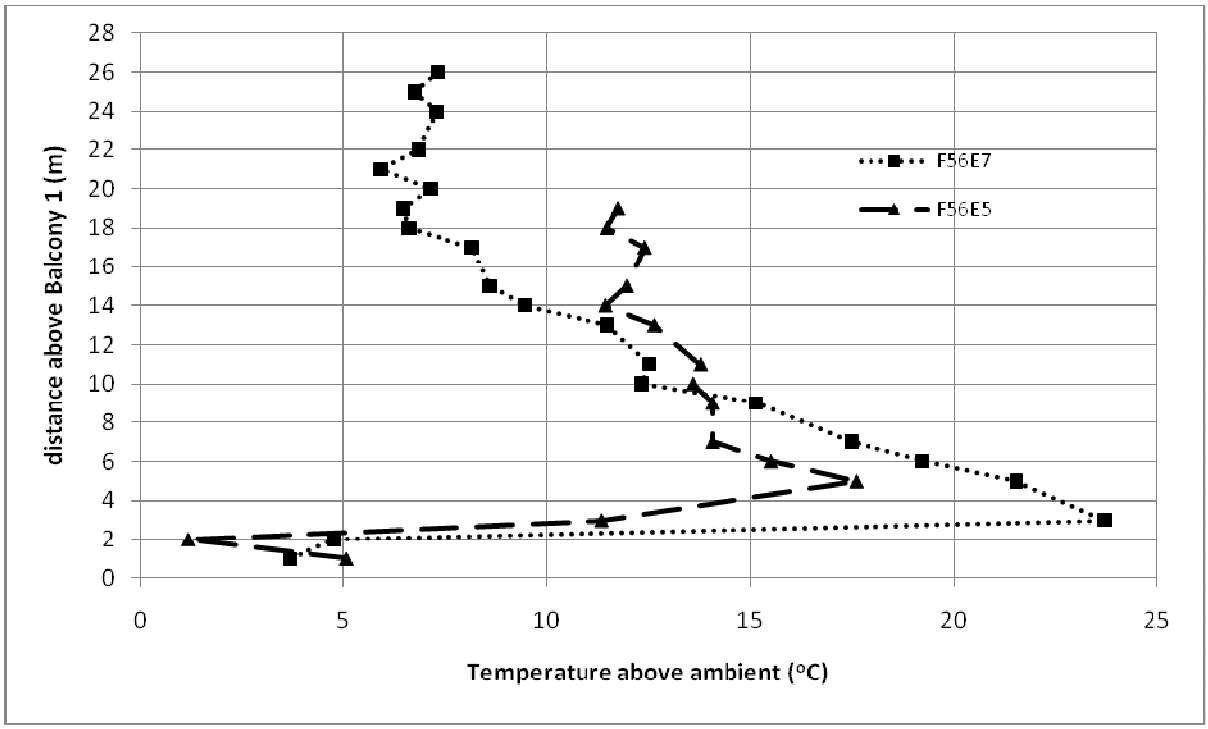

Figure I55. Comparison of seven storey balcony and five storey balcony temperature profiles along balcony edge.

Full scale for 7 storey balcony (F60E7)

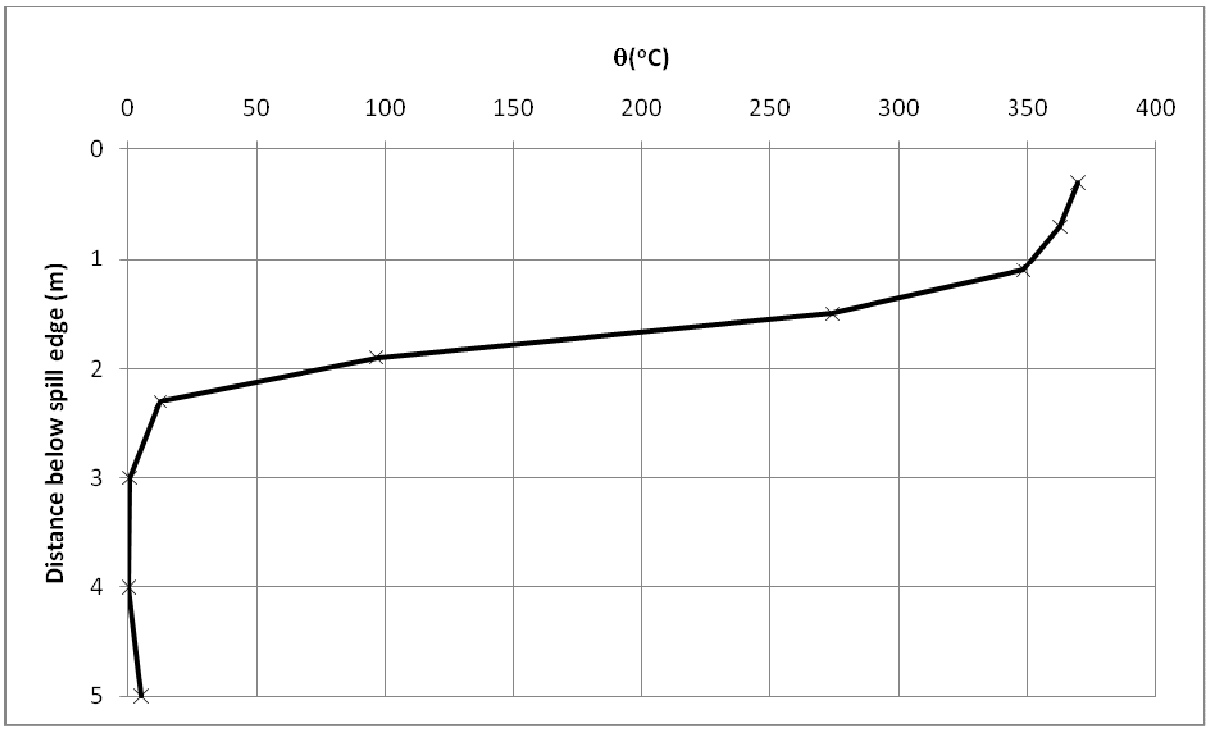

Figure I56. Temperature above ambient at the spill edge.

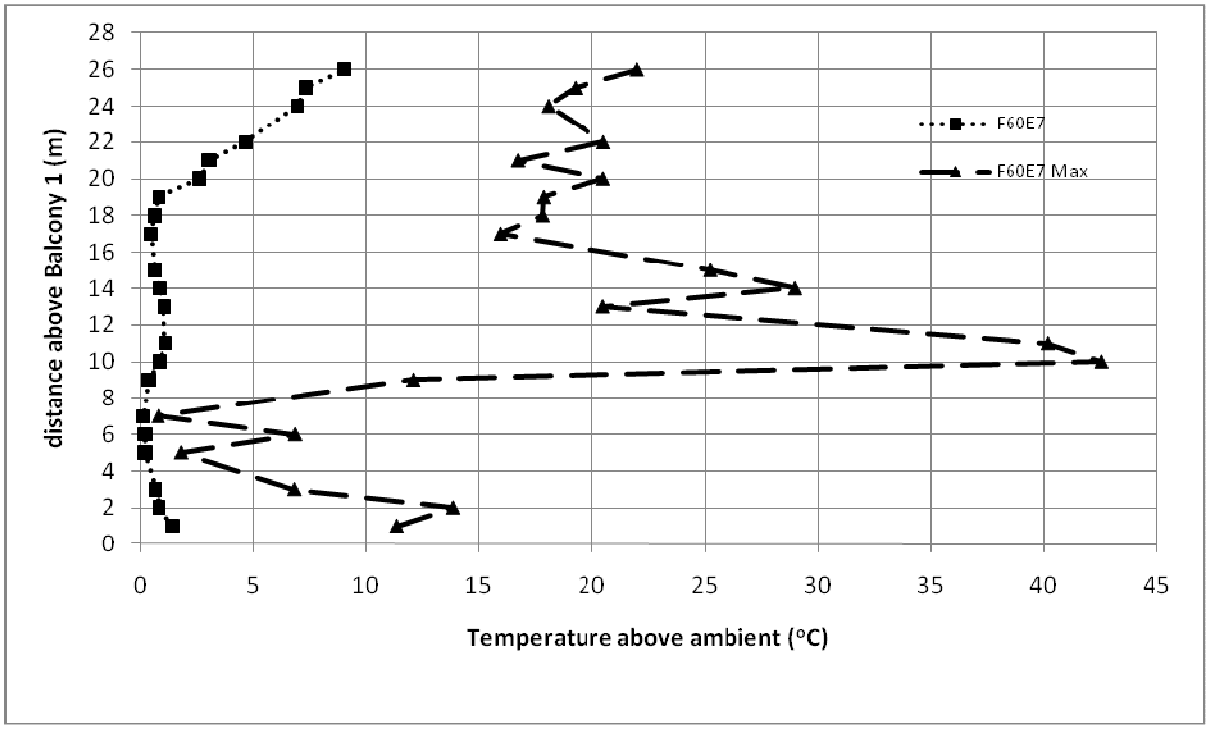

Figure I57. Temperature profiles across balcony edge.

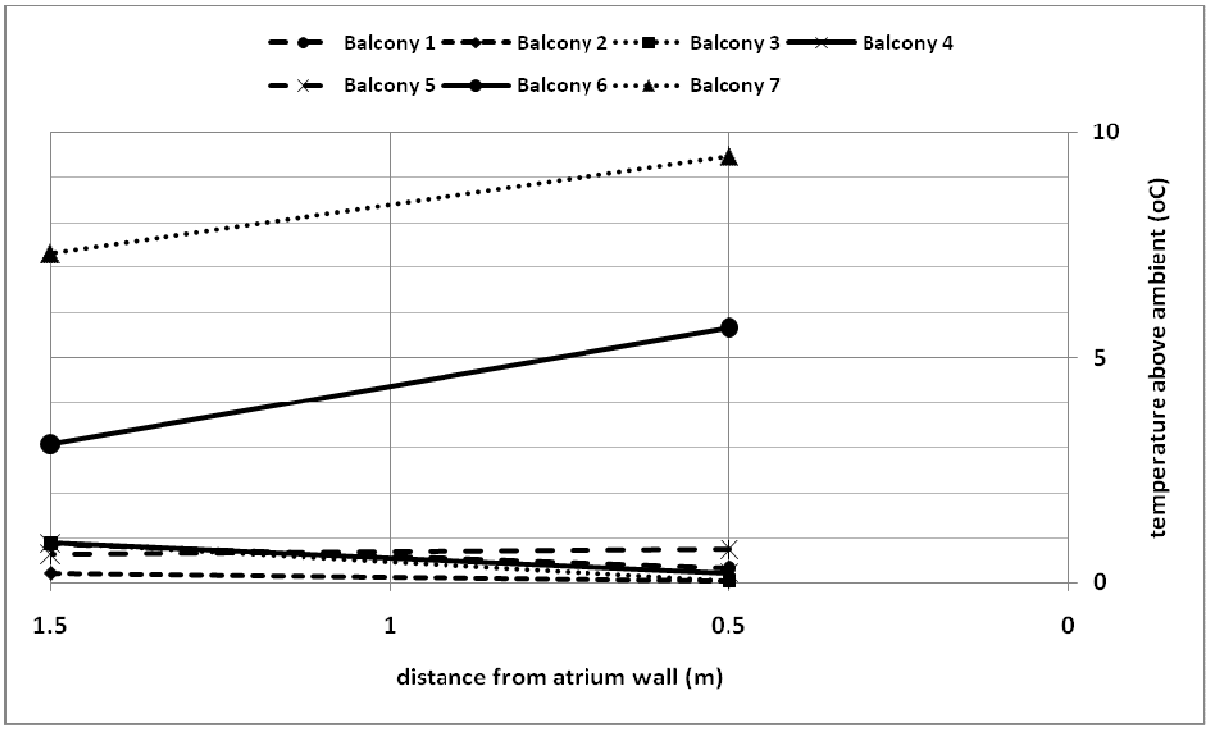

Figure I58. Temperature profiles along balcony breadth.

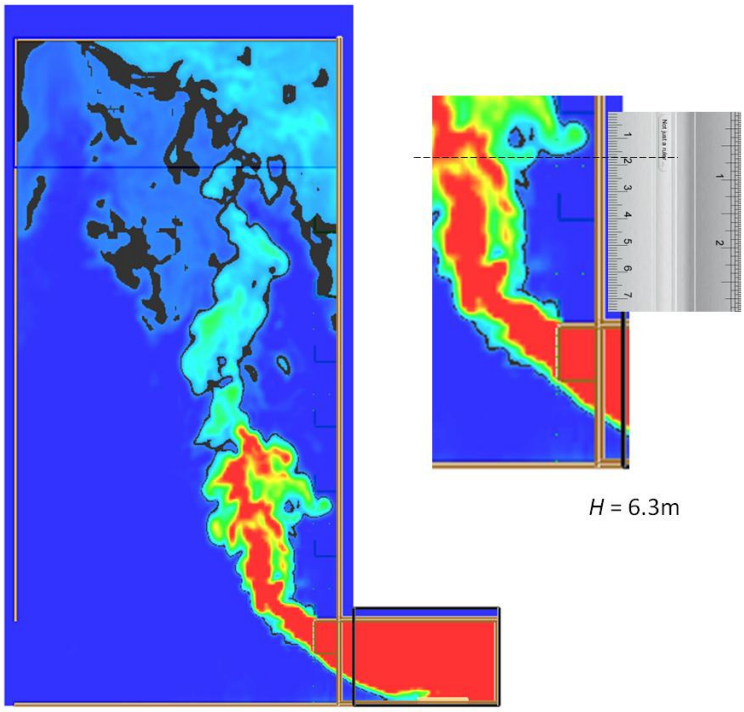

Figure I59. Smoke layer height measurement.

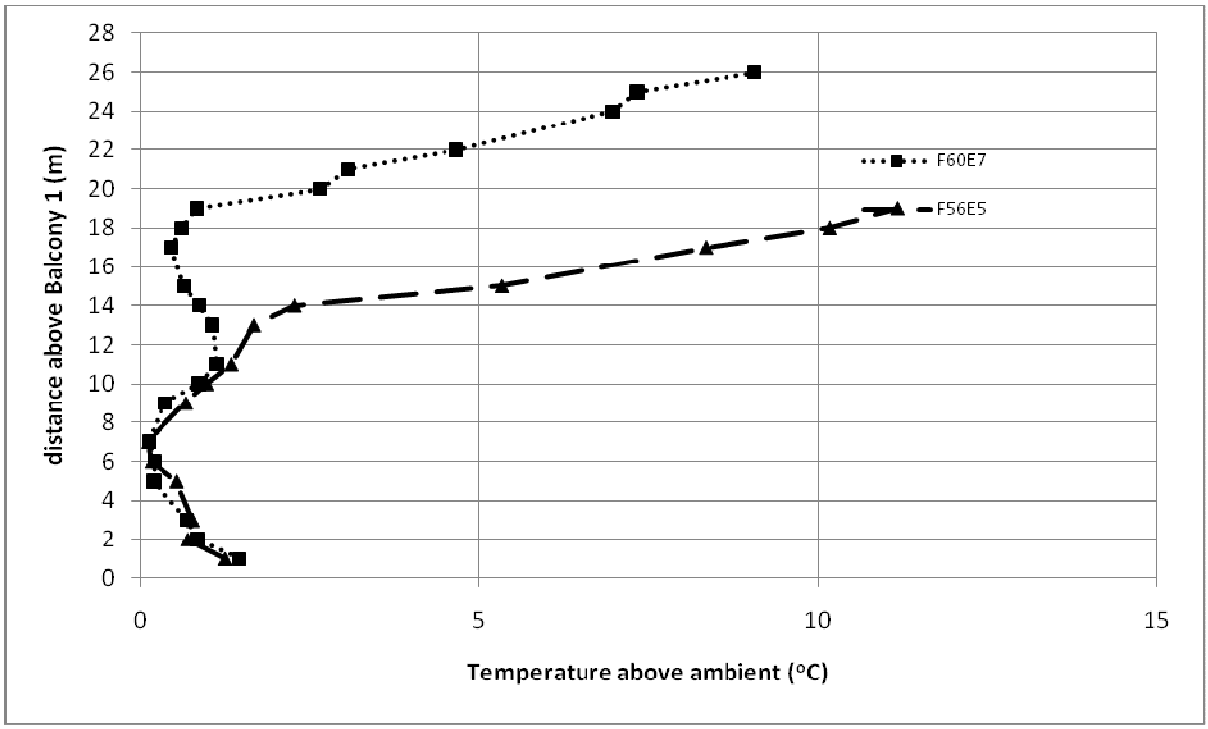

Figure I60. Comparison of seven storey balcony and five storey balcony temperature profiles along balcony edge.

Temperature Prediction for Model with 20mm Grid and Model with 10mm Core and 20mm Grid

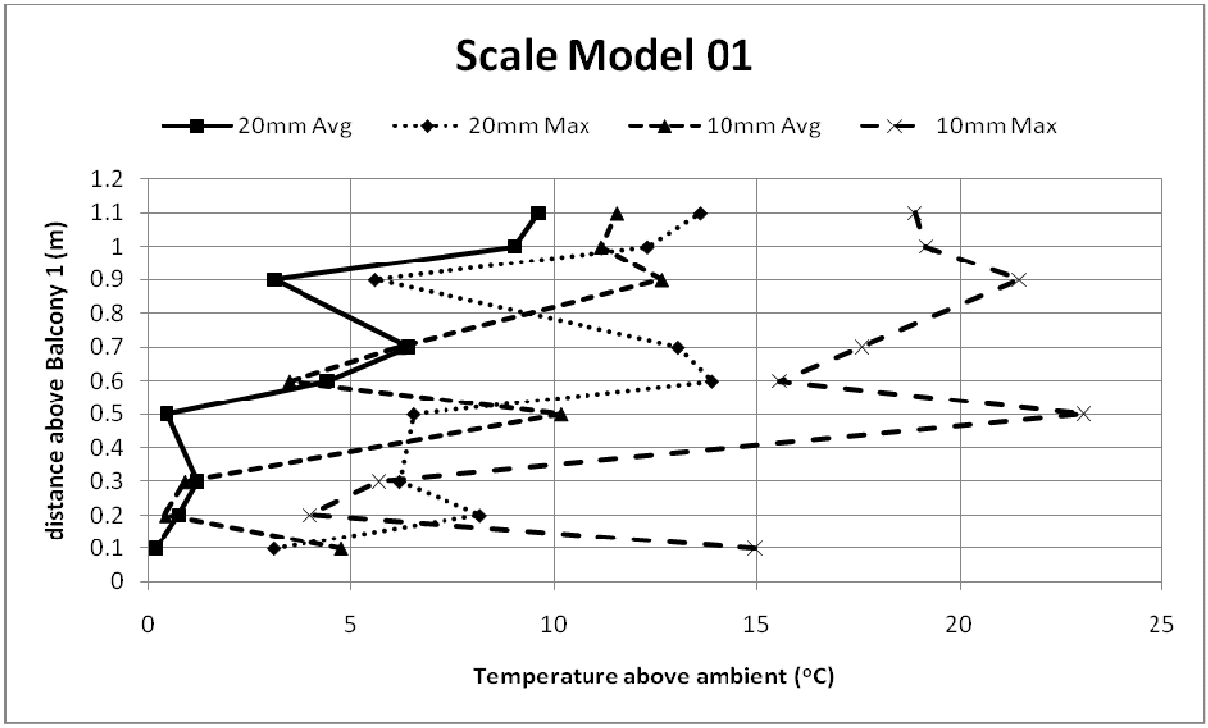

Figure J1. Comparing grid size of 20mm and 10mm core for simulation S01E.

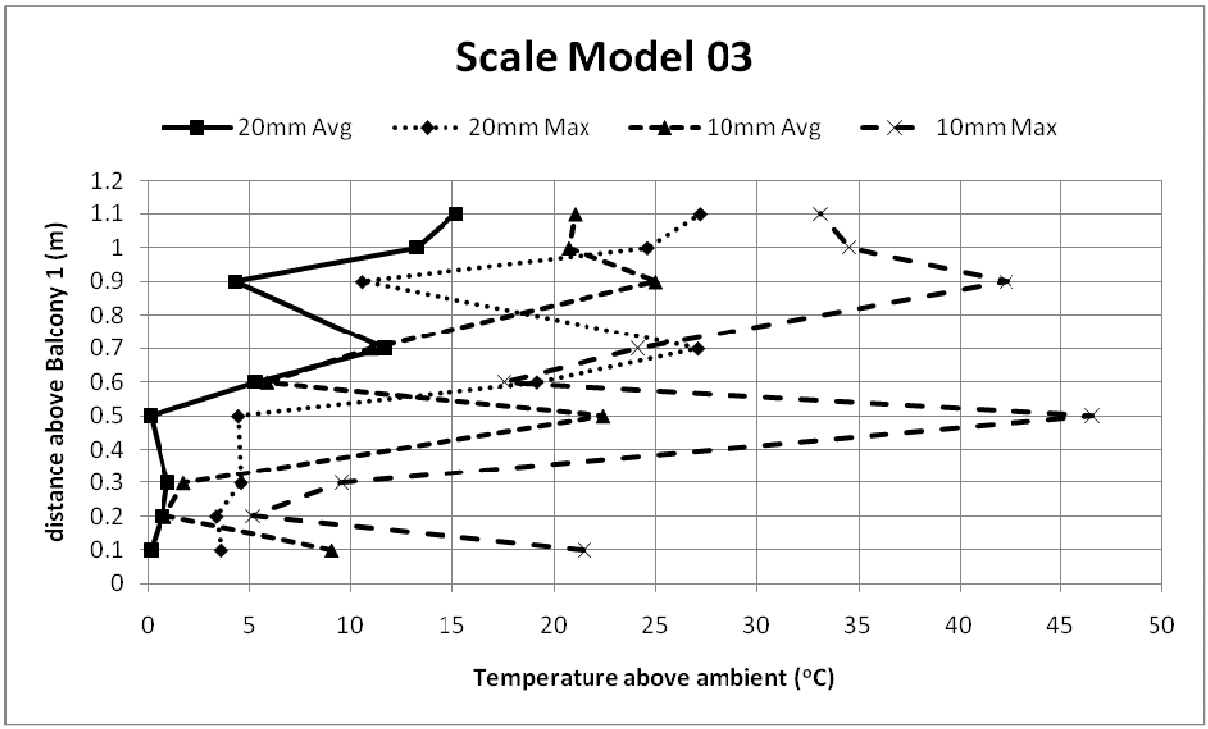

Figure J2. Comparing grid size of 20mm and 10mm core for simulation S03E.

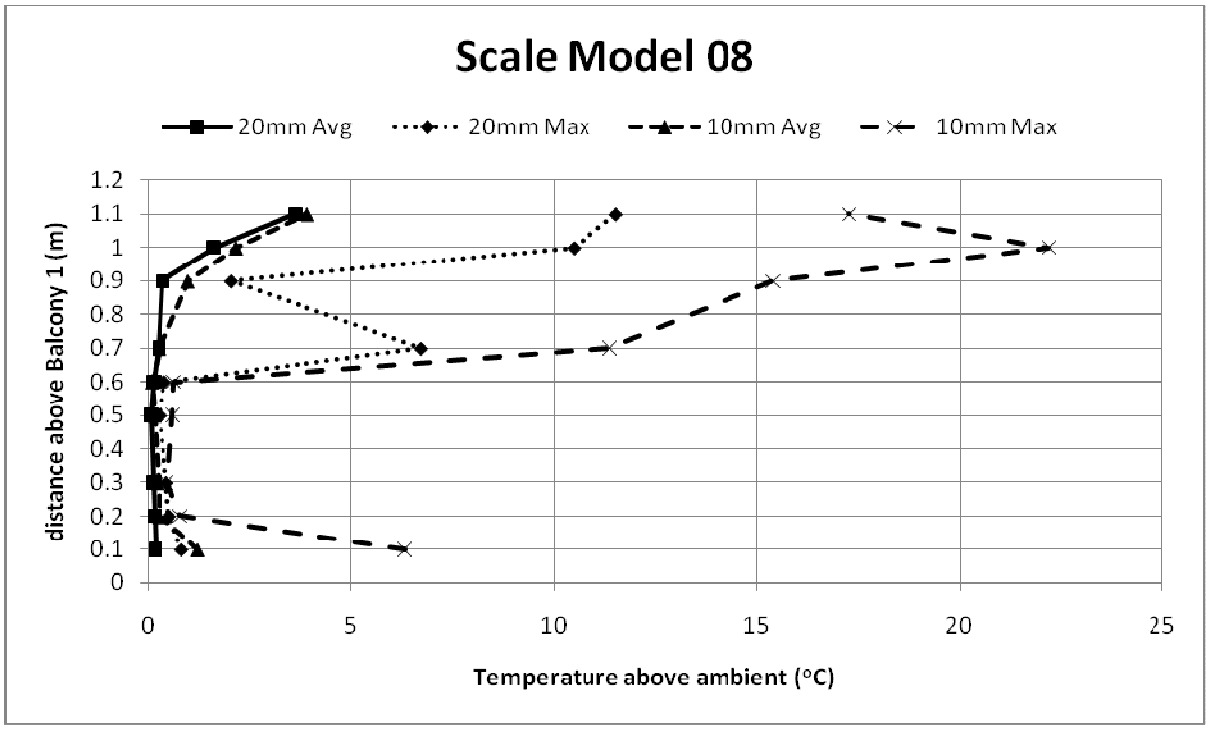

Figure J3. Comparing grid size of 20mm and 10mm core for simulation S08E.

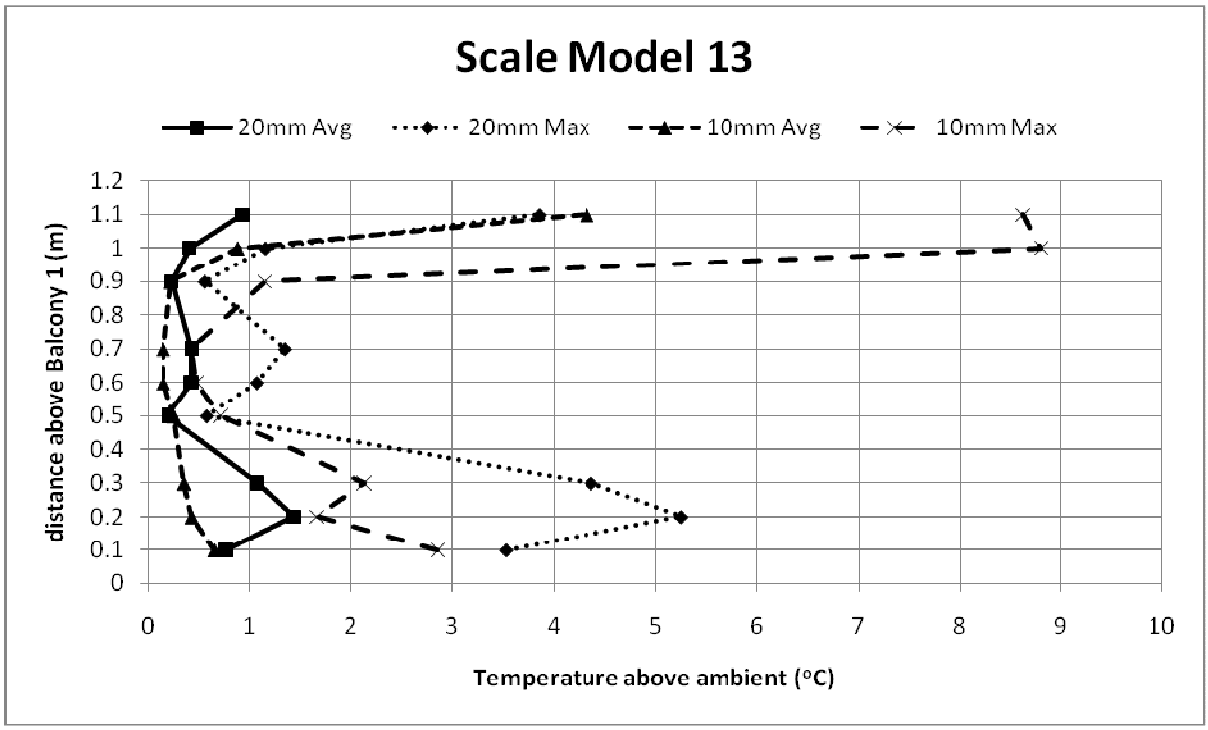

Figure J4. Comparing grid size of 20mm and 10mm core for simulation S13E.

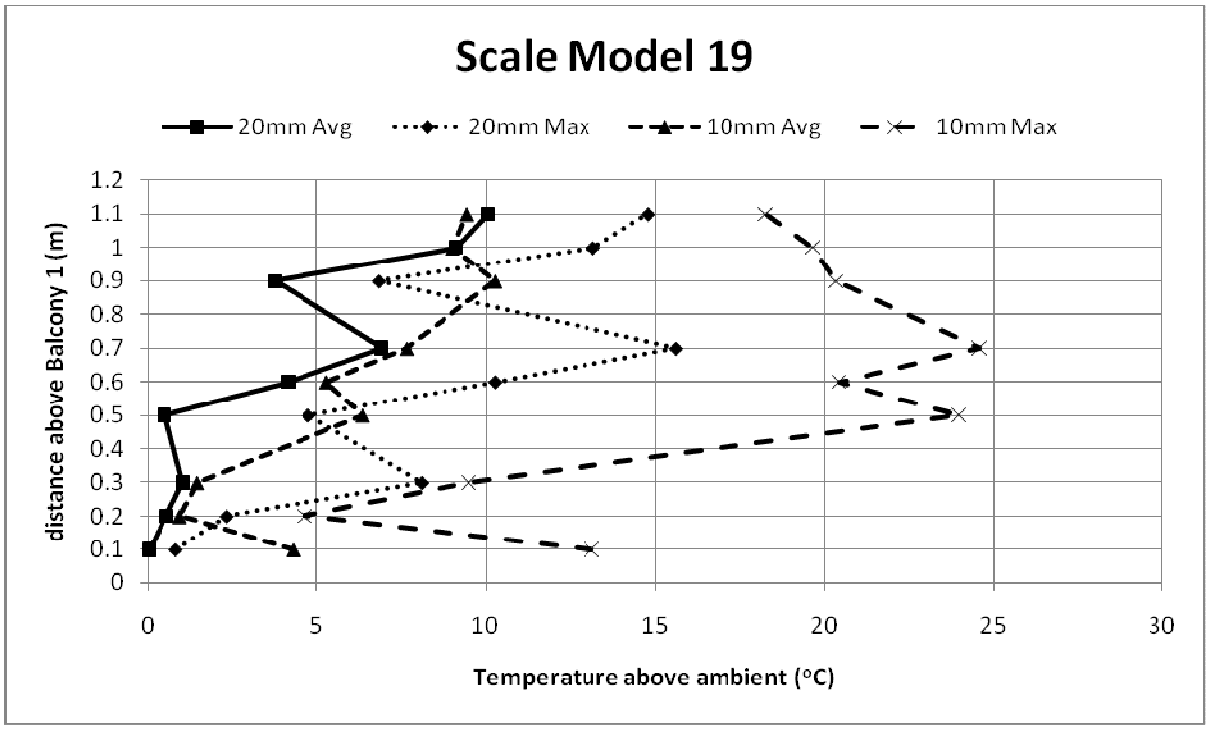

Figure J5. Comparing grid size of 20mm and 10mm core for simulation S19E.

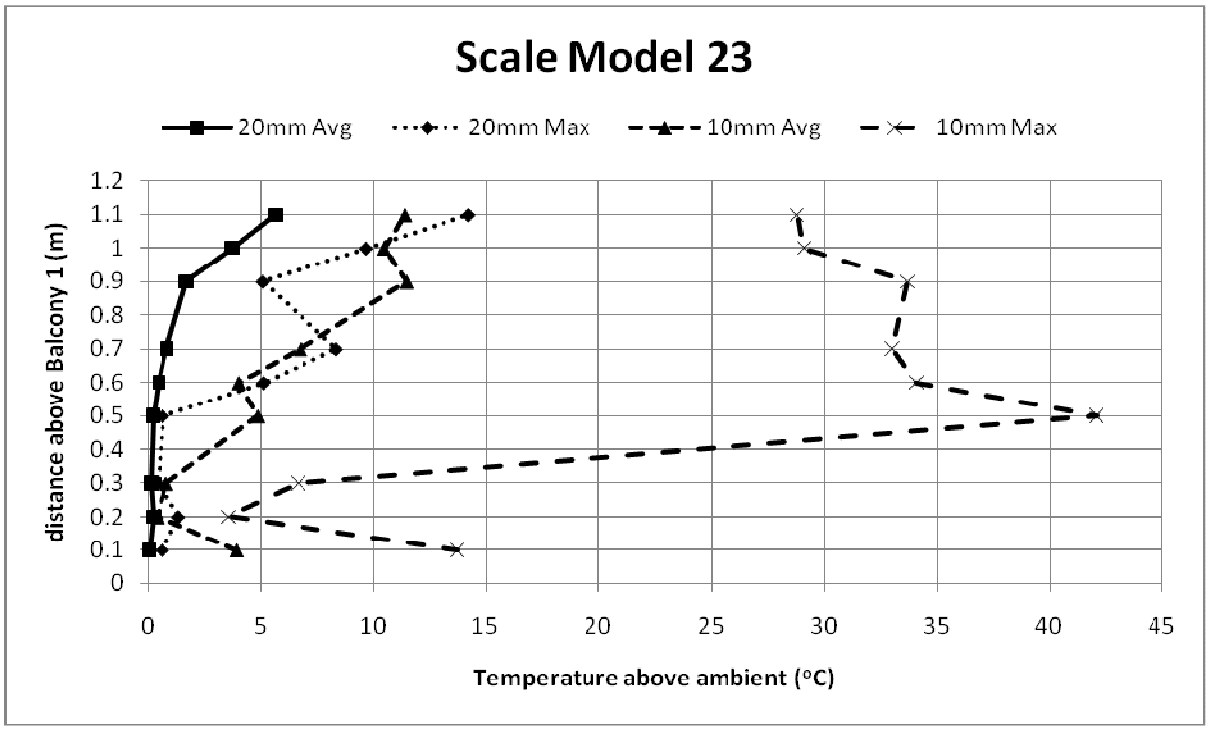

Figure J6. Comparing grid size of 20mm and 10mm core for simulation S23E.

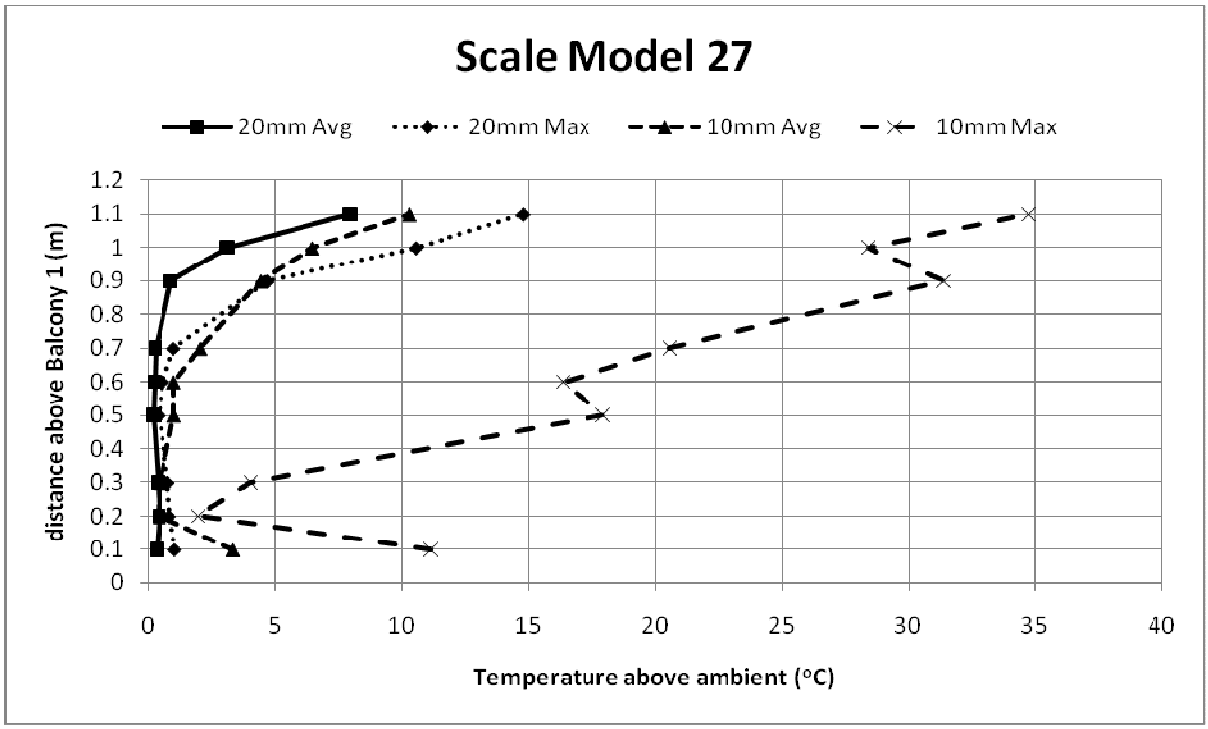

Figure J7. Comparing grid size of 20mm and 10mm core for simulation S27E.

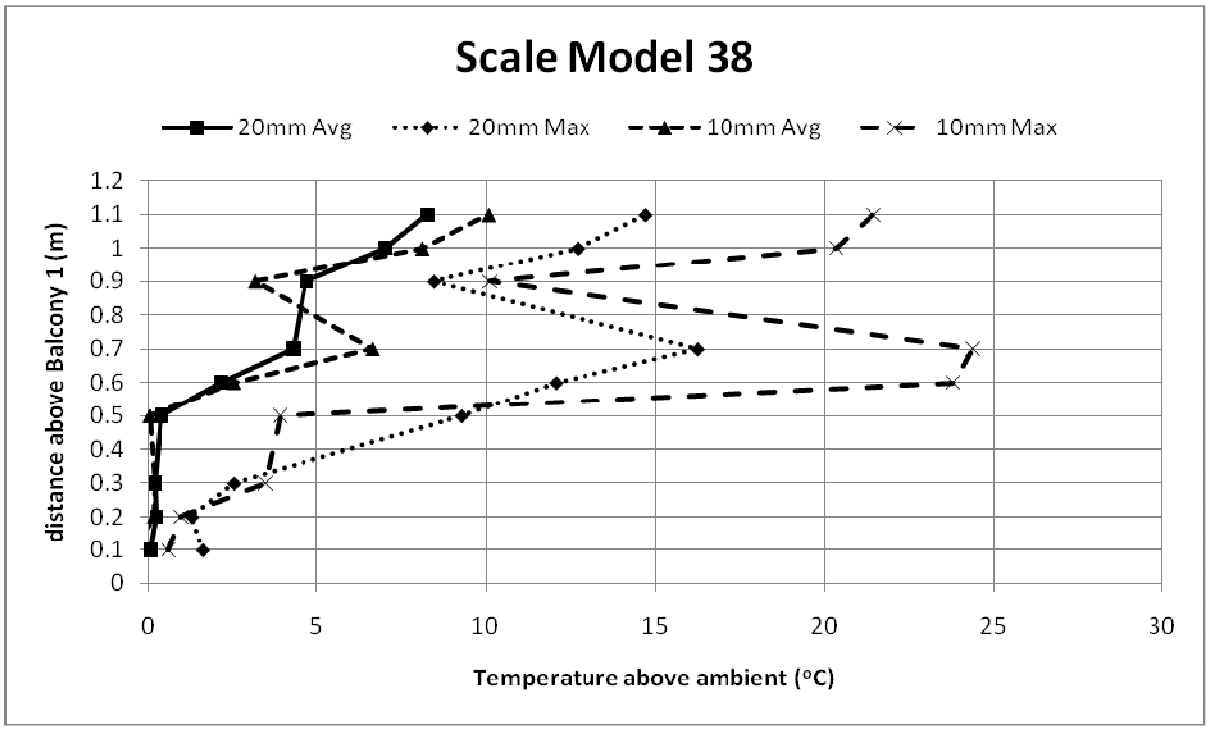

Figure J8. Comparing grid size of 20mm and 10mm core for simulation S38E.

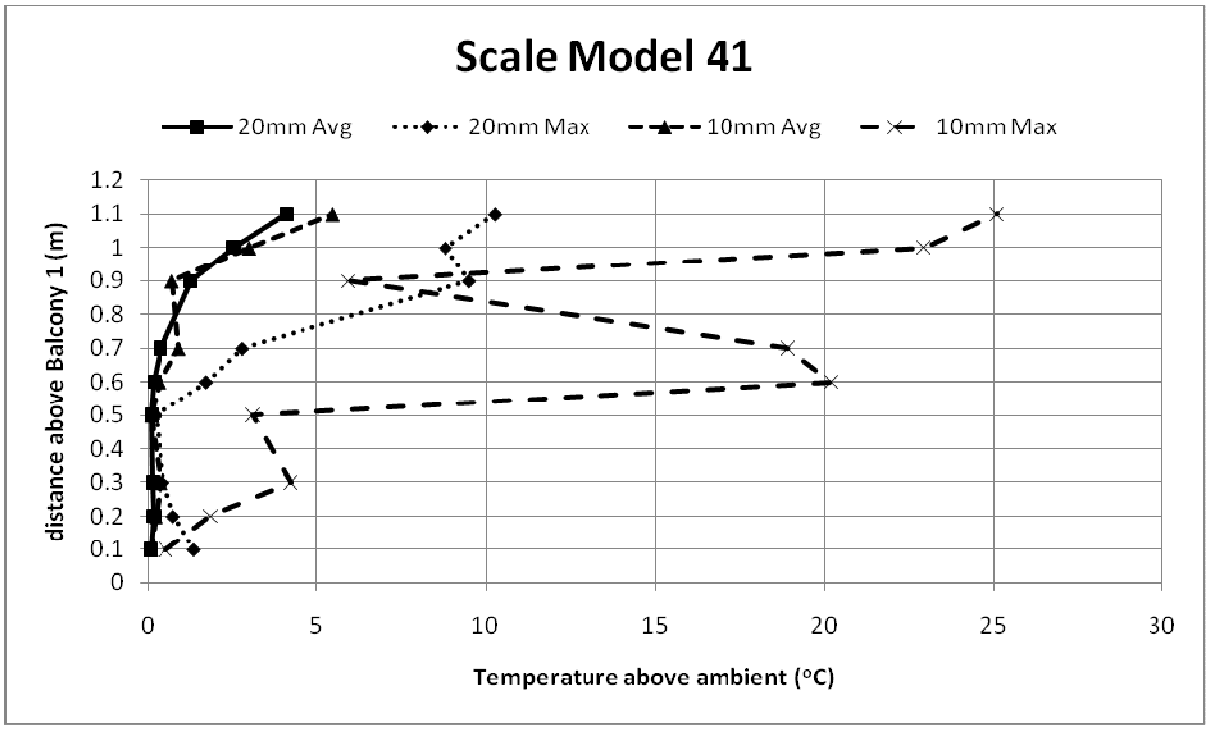

Figure J9. Comparing grid size of 20mm and 10mm core for simulation S41E.

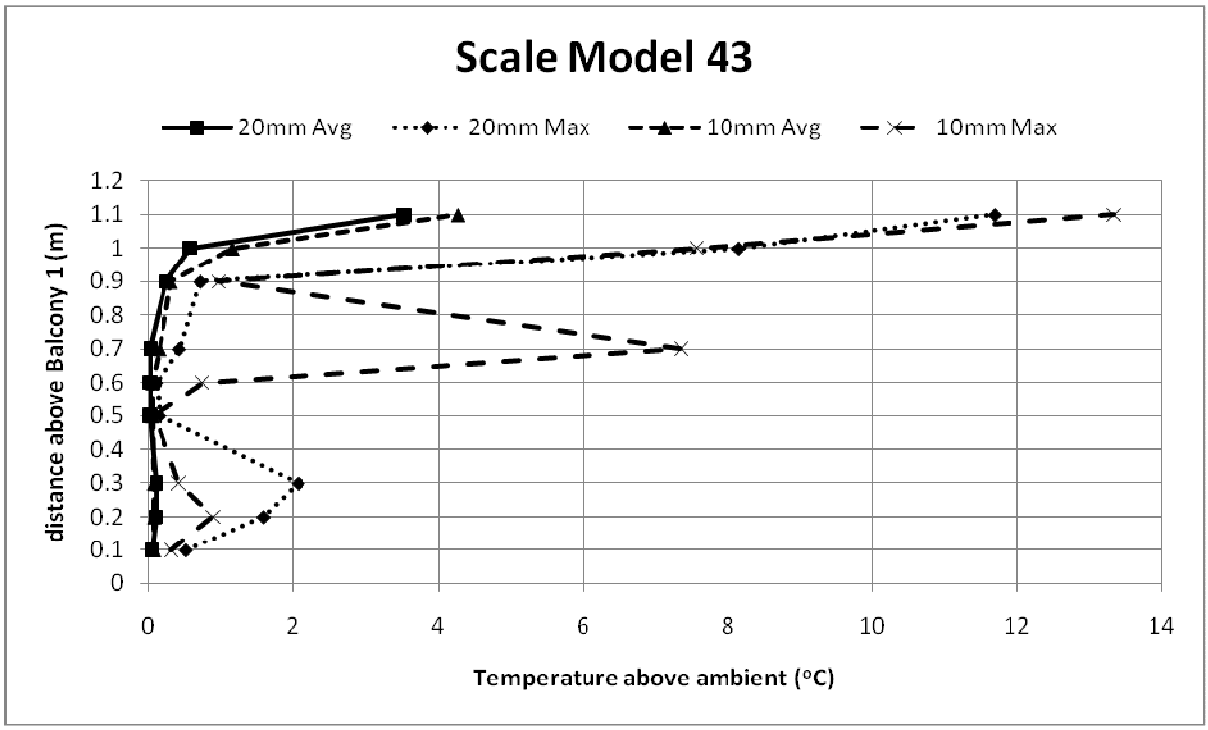

Figure J10. Comparing grid size of 20mm and 10mm core for simulation S43E.

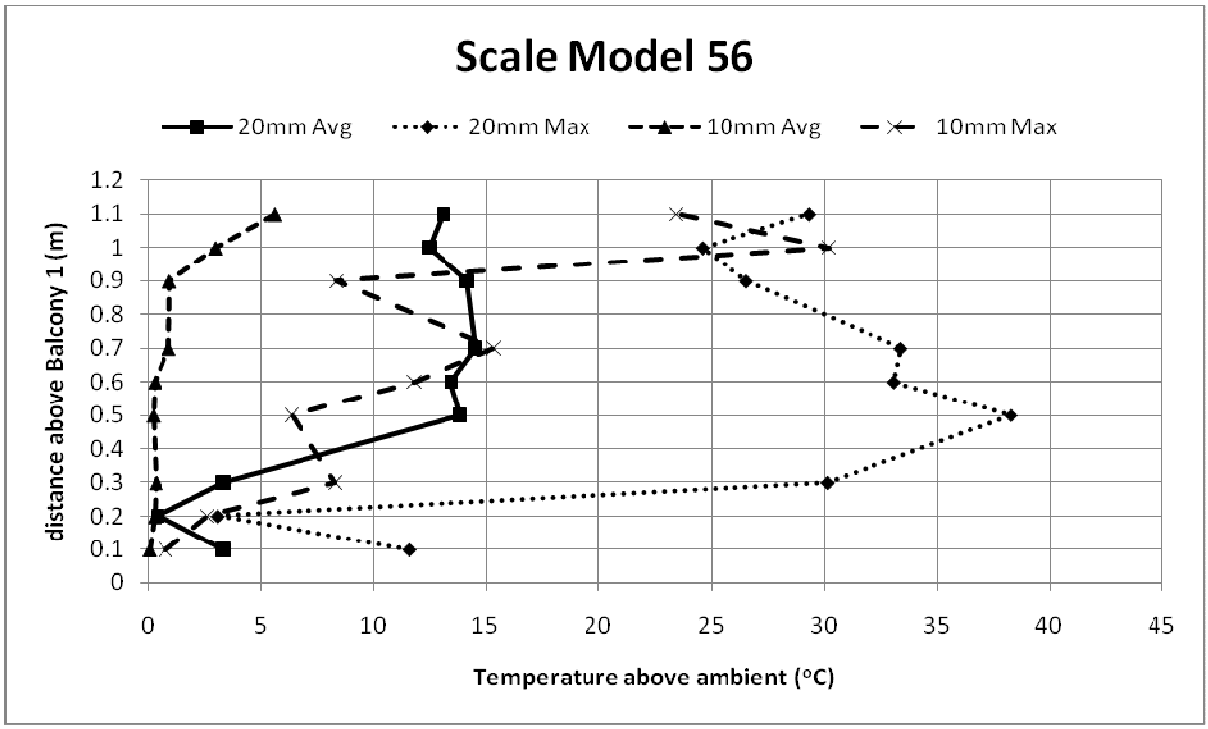

Figure J11. Comparing grid size of 20mm and 10mm core for simulation S56E.

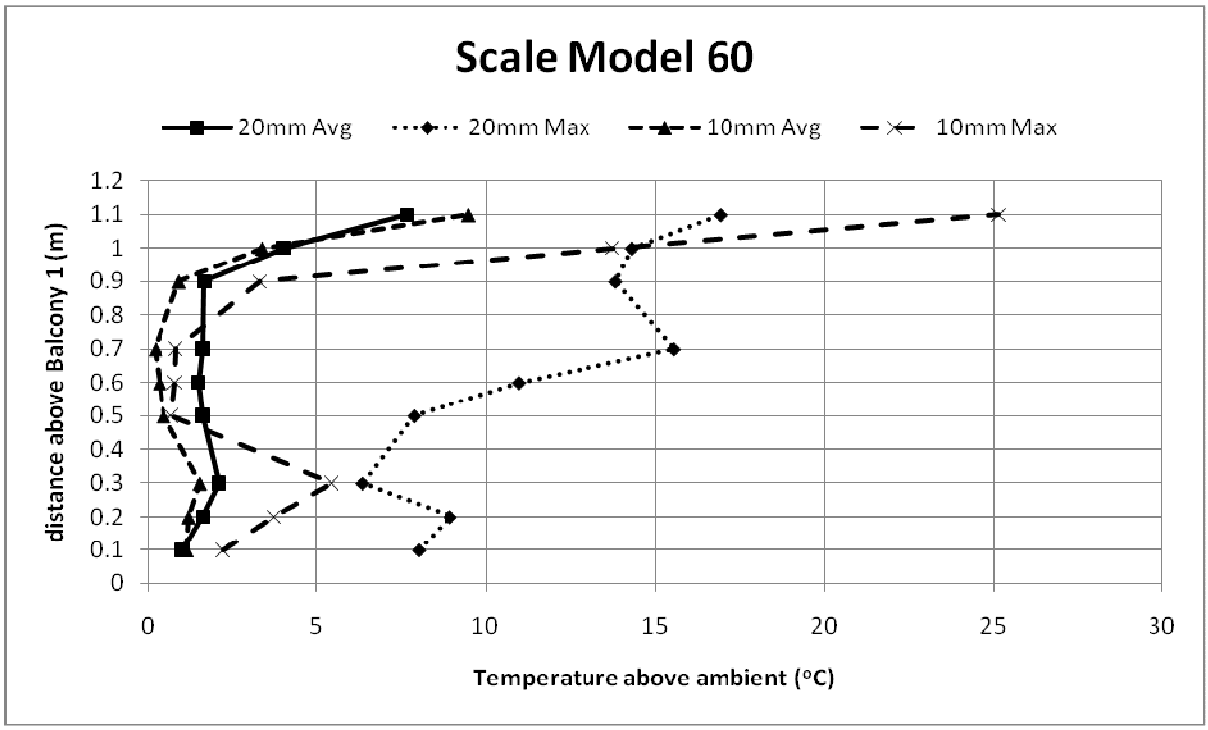

Figure J12. Comparing grid size of 20mm and 10mm core for simulation S60E.

Smoke Contamination Height and Smoke Layer Depth for Extra Large Fire Cases

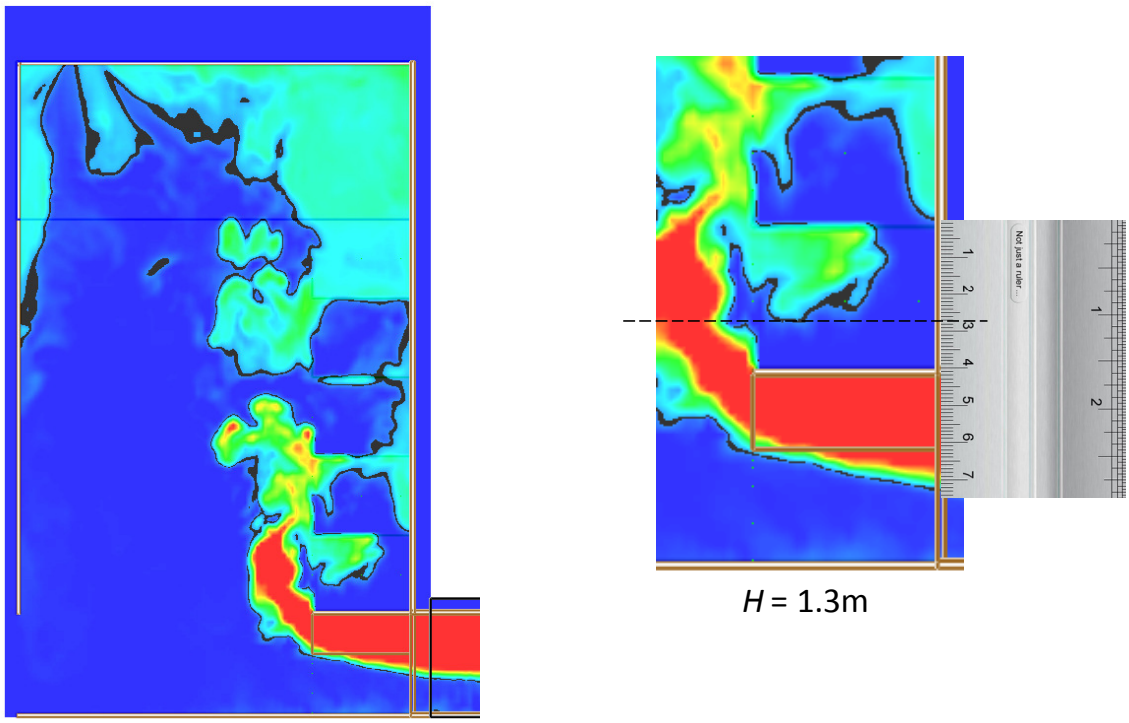

Figure K1. Smoke layer height for case F03A.

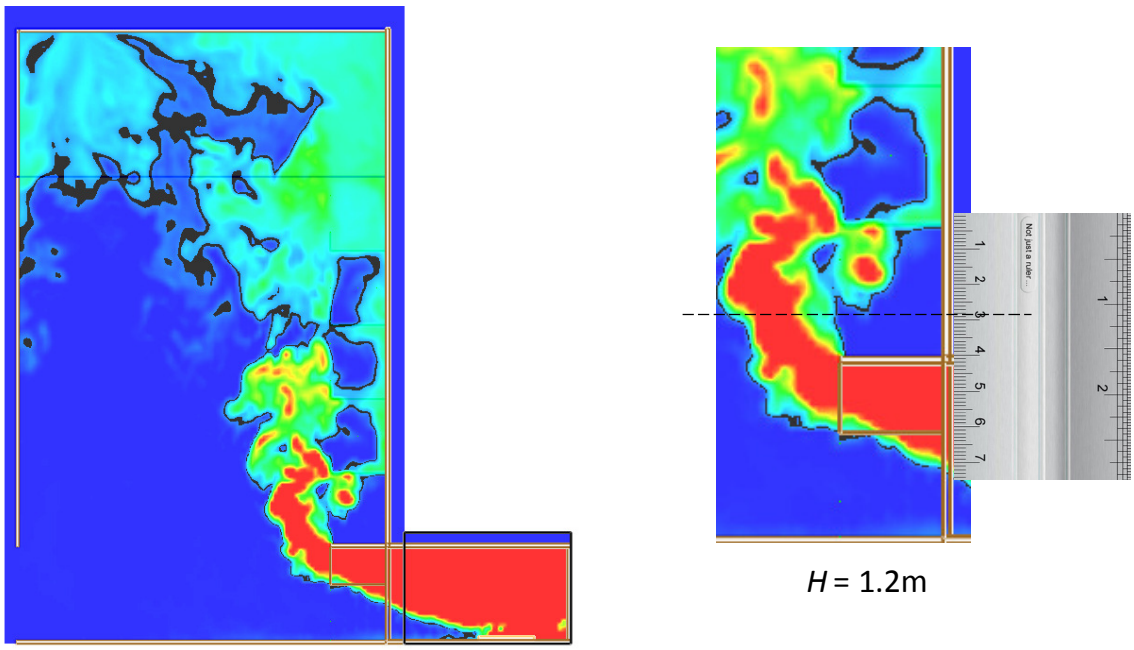

Figure K2. Smoke layer height for case F24A.

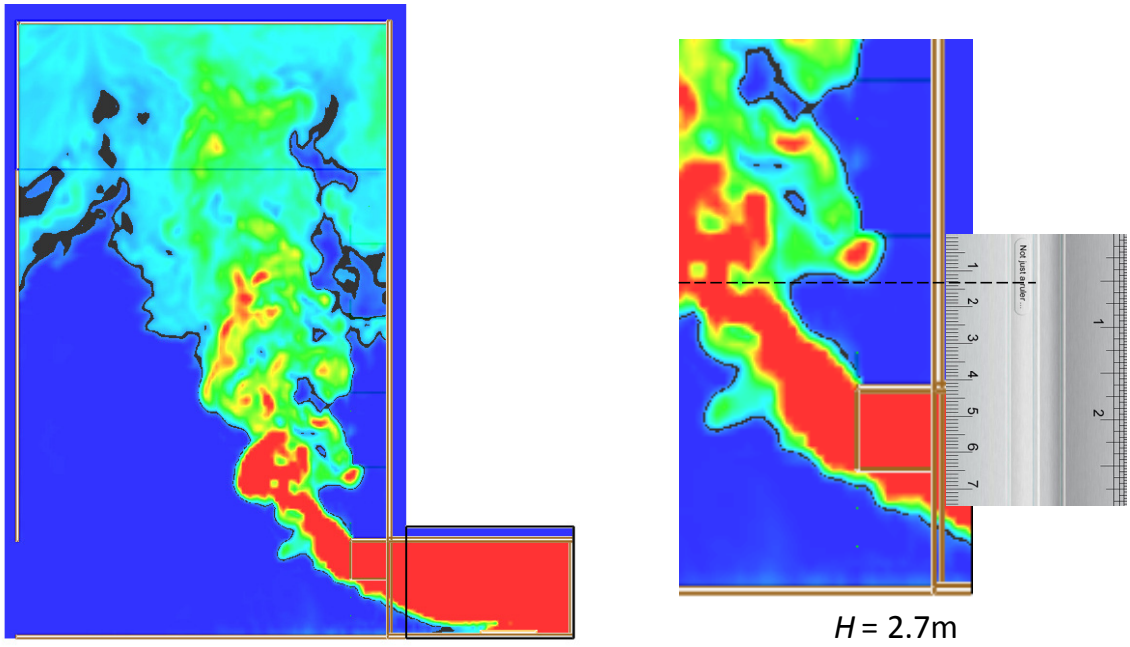

Figure K3. Smoke layer height for case F42A.

Extra Large Fire Simulation	*H* (m)	*b* (m)	*w* (m)	*d* (m)
3a	1.3	5	10	1.38
24a	1.2	3	6	1.51
42a	2.7	2	4	1.63

Table K1. Smoke layer depth at spill edge for the extra large fire.